METABOLOMICS AND DEREPLICATION STUDIES OF ENDOPHYTIC METABOLITES FROM SOME EGYPTIAN MEDICINAL PLANTS IN THE SEARCH FOR NEW POTENTIAL ANTI-CANCER AND ANTIMICROBIAL DRUGS

BY

AHMED TAWFIKE

B.Sc., M.Sc.

A THESIS PRESENTED IN THE FULFILMENT OF REQUIREMENTS FOR THE DEGREE OF DOCTOR OF PHILOSOPHY IN

INSTITUTE OF PHARMACY AND BIOMEDICAL SCIENCES

UNIVERSITY OF STRATHCLYDE

161 Cathedral Street

Glasgow

G4 0RE

United Kingdom

February 2015

This thesis is the result of the author's original research. It has been composed by the author and has not been previously submitted for examination that has led to the award of a degree.

Signed:

Date:

Dedication

I would like to dedicate this work to souls of my parents whose words of encouragement and push were ringing in my ears all the time. In the memory of my parents, a special dedication to those gave birth, raised and enclosed me. I miss them every day. To Mom and Dad I say thanks very much for every moment you scarified for me. Hope Allah blesses you.

Acknowledgements

I would like to express my deep gratitude to Dr. Ruangelie Edrada-Ebel, my first research supervisor, for her patient guidance, enthusiastic encouragement and useful critiques of this research work. I would also like to thank Dr. David Watson, my second research supervisor, for his advice and encouragement. My grateful thanks are also extended to Dr. Rothwelle Tate for his help in doing the molecular biological procedures, to Ms. Carol Clements, who did the antimicrobial assays, to Mrs. Louise Young and Ms. Grainne Abbott for cytotoxicity assays.

I would like to express my very great appreciation to our collaborators from Laboratoire de Biologie Moléculaire et Cellulaire du Cancer (LBMCC), Luxembourg, Professor Mark Diederich, Dr. Mark Schumacher and Dr. Richard Sawadogo for accomplishment of anti-cancer assays.

I would also like to extend my thanks to the staff members of MS and NMR laboratories in SIPBS, Dr. Tong Zhang and Dr. Gavin Blackburn for their lessons in running the mass and NMR experiments.

I am particularly grateful for my students Fatma Al-Lawati, Yasir Jarad and Muhammad Romli who contributed in some of this work. I would like to offer my special thanks to my colleagues, my dear lab mates, Dr. Christina Viegelmann, Enitome Bafor, Nurkhalida Kamal, Dr. Lynsey McIntyre, Noor Wini Binti Mazlan, Nashwa Tawfike, Haitham Ali, Weqas Alotaibi, Kirsty Black, Daniela de Paula and Catherine Dowdells. Their help and advices were greatly appreciated.

I would like to extend my appreciation to sector of missions, ministry of higher education in Egypt for sponsoring my PhD scholarship.

Finally, I wish to thank my family specially my parents who prayed for me and advised me a lot in all my life. My lovely wife, Hayam Ibrahim, for cheering me up and stood by me through the good as well as bad times, my new baby Fares who lights my life, my sister Nashwa and my brother Eslam for their support and encouragement throughout my study.

Table of Contents

Publication

Ahmed F Tawfike, Christina Viegelmann, RuAngelie Edrada-Ebel. (2013) **Metabolomics and Dereplication Strategies in Natural Products.** *Springer protocols,* book title: Metabolomics Tools for Natural Product Discovery: Methods and Protocols, series: Methods in Molecular Biology, **2013**, v1055, p227-244.

Ahmed F Tawfike, Rothwelle Tate, Marc Schumacher, Marc Diederich, Ruangelie Edrada-Ebel. (2014) **Metabolomic Tools to Assess the Chemistry and Bioactivity of Endophytic *Aspergillus* Strains.** *Fungal diversity Journal* 2015. (Under revision)

Ahmed F. Tawfike, Carol Clements, Louise Young, Richard Sawadogo, Marc Diederich, Ruangelie Edrada-Ebel. (2014) **Metabolites profiling and dereplication studies of *Curvularia* sp. endophyte, from the leaves of *Terminalia laxiflora* Combretaceae.** *Journal of Natural Products* 2015. (Under revision)

Metabolomics and Dereplication studies of endophytic metabolites from some Egyptian medicinal plants in the search for new potential anticancers. Poster published in Metabomeeting 2012, Manchester, UK and Metabolomics 2014 in Tsuruka, Japan.

Metabolomics and Dereplication strategies in natural products discovery. Oral presentation in Bionat II 2011, Alexandria, Egypt; Biocom 2012, Cadiz, Spain and Metabolomics 2013, Glasgow, UK.

Abstract

Endophytes are microbes that inhabit living, internal tissues of plants without causing any immediate, apparent negative effects. Endophytic fungi associated with medicinal plants represent a potential source of novel chemistry and biology. This study involved isolation of three endophytic fungal strains from two Egyptian medicinal plants, *Terminalia laxiflora* and *Markhamia platicalyx*. Identification of the strains has been achieved through molecular biological methods. Metabolomic profiling, using 2D-NMR and HR-ESIFTMS were done at different stages of the growth phase for both solid and liquid culture media. Dereplication studies were accomplished by utilizing the MZmine 2.10 software with aid of the AntiBase and DNP databases. The optimized method in terms of media, incubation time, and maximum production of bioactive compounds were taken into account for the scale-up. The chemometric analysis using SIMCA-P v13 software was accomplished to compare the active and inactive extracts and/or fractions in order to highlight the bioactive metabolites at earlier stages. The bioassay-guided fractionation was established using flash chromatography that employed BUCHI®, Biotage® and Reveleris® flash systems. The cytotoxicity of extracts, fractions and the isolated compounds was tested against both chronic myelogenous leukemia (K562) and prostate cancer (PC3) cell lines. The antimicrobial activity was investigated against *Trypanosoma brucei* and *Mycobacterium marinum* ATCCBAA 535. This work led to isolation of three new natural compounds and 34 known endophytic metabolites from *Aspergillus aculeatus*, *A. flocculus* and *Curvularia sp.* The isolated fungal compounds were elucidated using 1D and 2D-NMR experiments and HR-ESIFTMS with aid of DNP databases. Secalonic acids D, B, F and C from *A. aculeatus*; phomaligol A, p-hydroxybenzaldehyde, 4-hydroxyphenyl-methoxy-acetic acid, mellein derivatives like mellein, *trans*-4-hydroxymellein and 5-hydroxymellien and diorcinol from *A. flocculus*; dipeptide (N-acetyl-phenylalanine-L-phenylalanine) from *Curvularia sp*., were the most significant bioactive metabolites. Metabolomics has been shown to be a powerful facilitator in the discovery of natural products, which are considered an excellent source for novel leads, and even more, as a means to highlight novel targets.

Chapter 1: Introduction

1. Introduction

1.1. General Introduction

Natural products have been considered as a rich source of compounds that have played an important role in preserving human health. Several important drugs in the market have been developed and derivatised from natural sources. Through structural modification of these natural products, appropriate drugs have been synthesized to improve efficacy and safety. The search for improved antibiotics, antioxidants and anticancer compounds is an important pipeline in the discovery of modern drugs. The large structural diversity of natural products along with their biological activity have served as "lead" compounds by molecular modification to improve their therapeutic potential. On the other hand, many natural compounds in the drug market have not undergone any chemical modification which is, a proof to the distinguished ability of microorganisms to synthesize drug-like molecules e.g. Taxol. Since the possibility to release a compound without any chemical modification is a unique property of natural compounds over all other sources of chemical diversity, this initiates efforts to discover more new compounds.

1.2. Cancer and natural products

Cancer is a condition where fast reproducing malignant cells are able to invade and destroy surrounding healthy tissue and organs. As published in 2010, cancer was the number one cause of mortality and the number of cancer deaths exceeded that of cardiovascular disease in the U.S (Aggarwal et al., 2009). Current estimates from Cancer Research UK indicate that 14.1 million cases of cancer were diagnosed in 2012, with 8.2 million deaths worldwide. It is important to mention that 60 % of currently used anticancer drugs are from natural sources, including plants and microorganisms of marine and terrestrial (Cragg, 2005); (Newman, 2003). The first plant derived compounds (Fig.1) were the vinca alkaloids e.g. vincristine and vinblastine which were isolated from *Catharanthus roseus*, family Apocyanaceae. Recently, semisynthetic derivatives of vinca

alkaloid like vinorelbine and vindesine are used in combination with other anticancer drugs for treatment of some types of cancer like leukaemia, lymophoma, testicular cancer, breast and lung cancer (Gueritte, 2005). Semisynthetic derivatives of podophyllotoxin (etoposide and teniposide) are two of the historical anticancer drugs that were isolated from *Podophyllum* species (*P. peltatum* and *P. emodii*). They are clinically active analogues used in the treatment of lymphoma, bronchial and testicular cancers (Lee, 2005). However, they were dropped from further drug development due to their toxicity and lack of efficacy. Paclitaxel (taxol®) was the first billion dollar anticancer drug, isolated from the Yew tree (*Taxus brevifolia* family Taxaceae), which is used in the treatment of breast and ovarian cancer (Schiff, 1980). One of the most important additions to anticancer natural products are topotecan, which is used in ovarian cancer therapy and irinotecan for the treatment of colorectal cancer. Both are derived from camptothecin which was isolated from *Camptotheca acuminata*, family Nyssaceae (Rahier, 2005). Another anticancer natural compound in clinical use is homoharringtonine, isolated from *Cephalotaxus harringtonia* family Cephalotaxaceae, that is used in combination with harringtonine (which is one CH_2 group less than homoharringtonine) in treatment of leukemia (Itokawa, 2005).

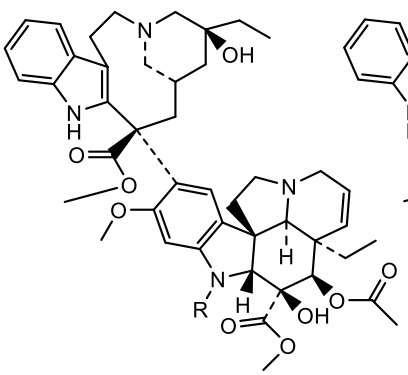

Vinblastine R = CH_3
Vincristine R= CHO

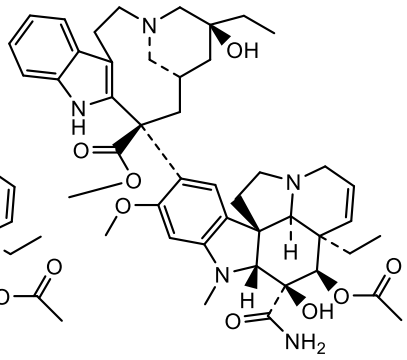

Vindesine

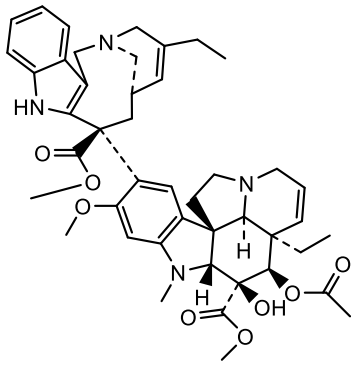

Vinorelbine

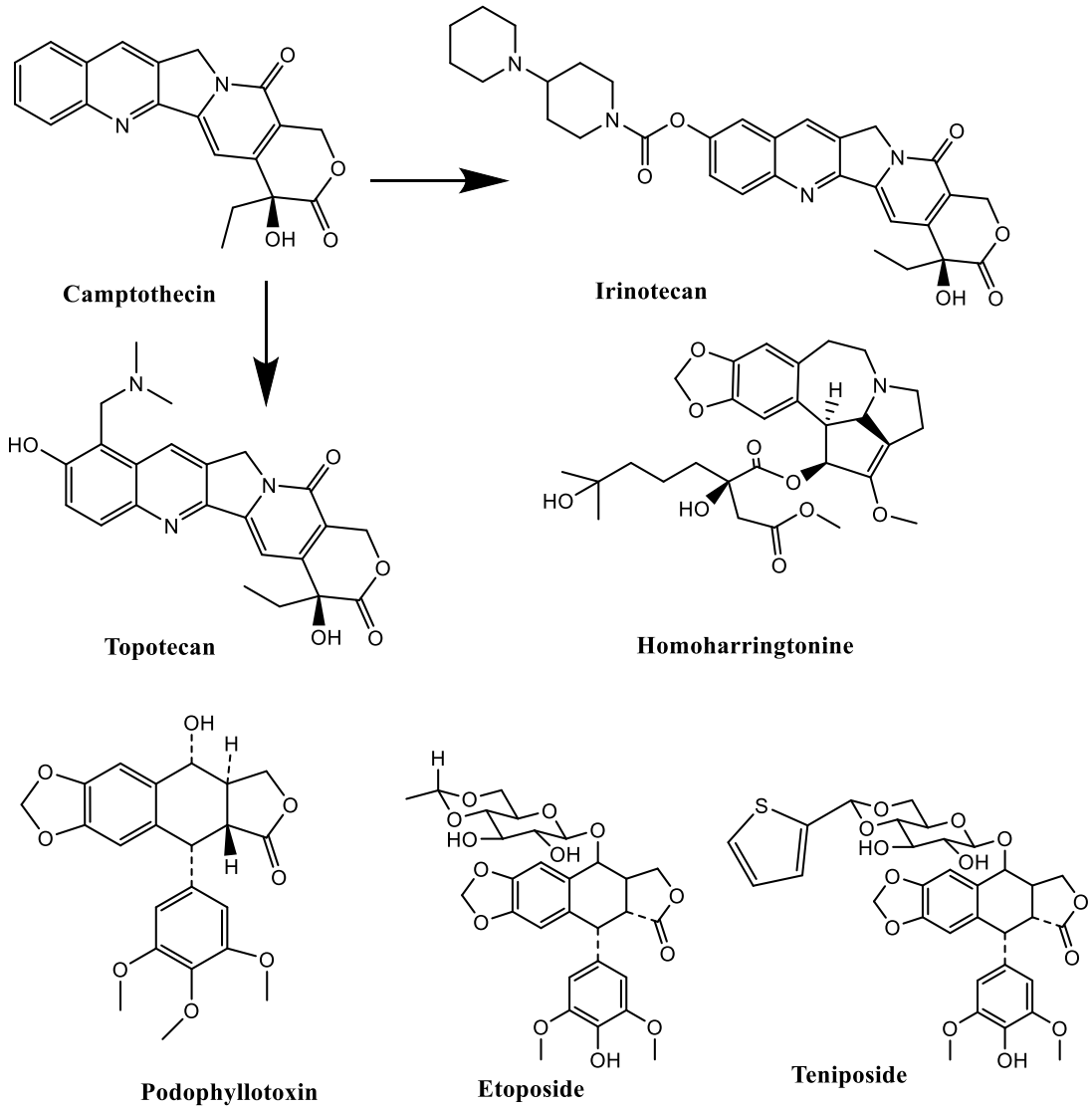

Fig.1 First plant derived compounds used as anticancer

To date, more than thirty natural products are in clinical development for the treatment of several kinds of cancer (Fig.2). For example, ixabepilone which was isolated from the endophytic myxobacterium *Sorangium cellulosum* (Lee, 2008), romidepsin (FR901228) from the endophyte *Chromobacterium violaceum (Ueda, 1994)* were approved by the US food and drug administration (FDA) for non-Hodgkin T-cell lymphoma and was described as a histone deacetylase inhibitor which also induced tumor suppressor gene transcription, apoptosis and cell differentiation (Glaser, 2007) (Bayes, 2007a). Moreover, ECO-4601 from the gram positive bacterium *Micromonospora* sp. (Gourdeau, 2007) was found to

inhibit CNS tumor cell lines. Other anticancer natural products in clinical development are the combretastatins, which were isolated from *Combretum caffrum*, family Combretaceae. Species of *Combretum* and *Terminalia* from the family Combretaceae are used in African and Indian traditional medicine for the treatment of cancer. Combretastatin A4 is among the most known anticancer compound, that causes vascular cessation and subsequent tumour necrosis (Li, 2002) (Pinney, 2005). Curcumin from the dried rhizomes of *Curcuma longa*, a compound present in food products, was considered a good initial lead compound to drug discovery. Curcumin has exhibited antitumor activity but its development into an anticancer drug was not successful due to its low potency and reduced bioavailability (Mosley, 2007).

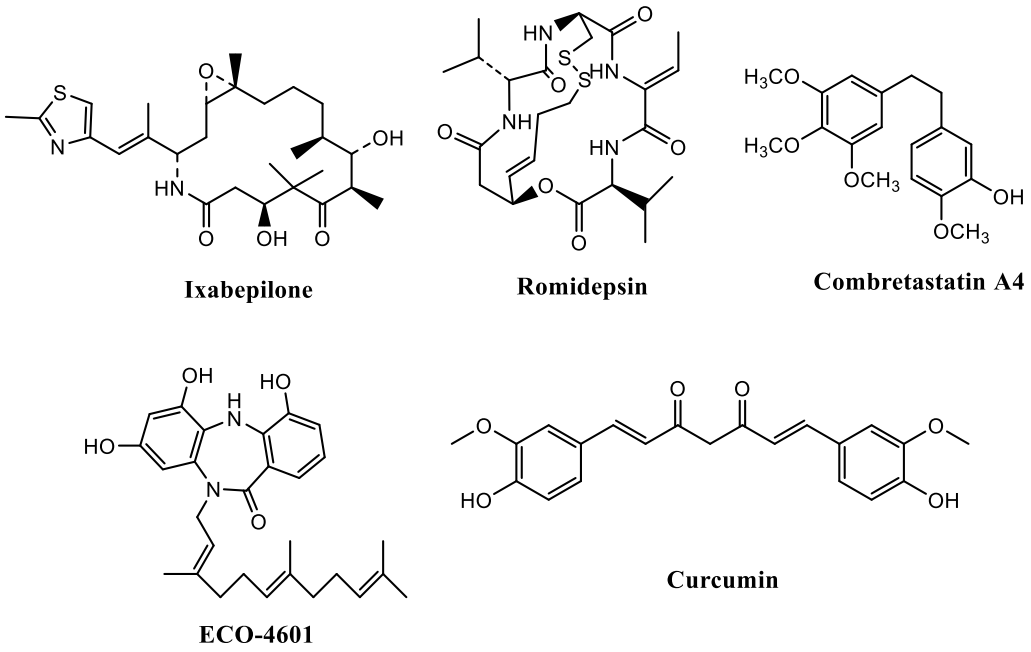

Fig.2 Plant derived anticancer compounds in clinical development

Some anticancer natural products are in preclinical development (Fig.3) and examples of these products are betulinic acid, a lupane-type triterpene found in *Betula* sp. family Betulaceae (Cichewitz, 2004), olomucine, isolated from *Raphanus sativus* L. Family Brassicaceae (Newman, 2002) and β-lapachone, a naphthaquinone derivative from *Tabebuia* sp. family Bignoniaceae (Ravelo, 2004).

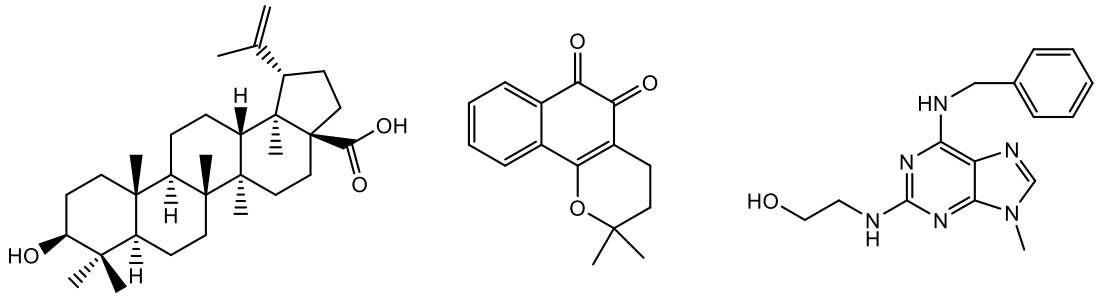

Betulinic acid **β-lapachone** **Olomucine**

Fig.3 Plant derived anticancer compounds in preclinical developments

1.3. Human African trypanosomiasis (HAT)

Human African trypanosomiasis, or sleeping sickness, is a vector-borne parasitic disease. Trypanosomiasis or trypanosomosis is provoked by parasitic protozoan trypanosomes of the genus *Trypanosoma*. *Trypanosoma brucei rhodesiense* and *T. b. gambiense* cause human sleeping sickness (HAT) and *T. b. brucei* (which is morphologically and biochemically indistinguishable from the two other subspecies), *T. congolense* and *T. vivax* cause nagana in livestock (cattle, sheep and goats). They are transmitted by tsetse fly (*Glossina* genus) which have acquired their infection from human beings or from animals harbouring the human pathogenic parasites (WHO, 1998). Sleeping sickness is endemic in thirty African countries threatening over 60 million people. Now, it has reached epidemic proportions in some countries, such as Angola, southern Sudan, Uganda and the Democratic Republic of Congo. Nearly 45,000 cases of HAT were reported in 1999 but the World Health Organization estimated that the actual number of cases is between 300,000 and 500,000 who are inhabitants of difficult to access or rural areas. Only three to four million people at risk of infection are under investigation with regular examination or access to health centres while many of the affected populations live in isolated areas with inadequate access to suitable health services (Barrett, 1999). Human African Trypanosomiasis affects the central nerveuos system . It has two stages: the first is the haemolymphatic stage which lasts for one to three weeks, followed by the chronic stage in which trypanosomes cross the blood–brain barrier to invade the central nervous system

resulting to chronic meningo-encephalitis and eventually leads to encephalopathy. Symptoms in the first stage include fever, headaches, joint pains and itching which are very often misinterpreted as influenza or malaria. The chronic phase includes psychatric disorder, seizures, coma and death (Enanga et al., 2002).

1.4. Chemotherapeutic antitrypanosomal compounds

Current chemotherapeutic drugs are very restricted and far from the appropriate treatment. There are only four approved drugs for HAT, were established years ago which include suramin, pentamidine, melarsoprol and eflornithine (Fig.4). Other molecules such as homidium, isometamidium, and diminazene aceturate are used in animal infections. Only melarsoprol and eflornithine, are able to cross the blood–brain barrier, and can be used for latter stages. Moreover, eflornithine is only active against *T. b. gambiense* infection (Gastellu-Etchegorry and Legros, 1999). The mechanisms of action of these products remain incompletely understood except for eflornithine, which inhibits the polyamine biosynthetic pathway (Buguet et al., 2003). All these drugs have to be taken by injection over long time thus requiring medical facilities and specialized staff that often do not exist in rural areas. Adverse effects are severe and sometimes life threatening. There are also increasing reports of treatment failures, particularly with melarsoprol (Brun et al., 2001, Legros et al., 1999). Furthermore, availability of the aforementioned drugs has not always been guaranteed as drug companies periodically stop their production because of lack of effectiveness (Hoet et al., 2004). Therefore, there is an urgent requisite for new molecules against sleeping sickness, which are safe, effective, cheap and easy-to-administer, and for new leads with novel mechanisms of action.

Second stage drugs

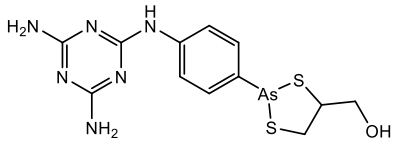

Melarsoprol

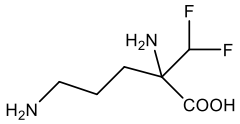

Eflornithine

First stage drugs

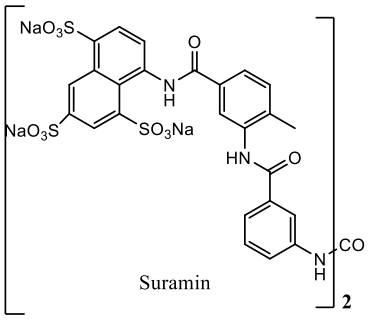

Suramin

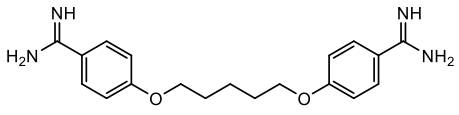

Pentamidine

Fig.4 Approved drugs for the first and second stage HAT

1.5. Tuberculosis

Tuberculosis or TB (tubercle bacillus) is a fatal infectious disease caused by various strains of mycobacteria, typically *Mycobacterium tuberculosis* a Gram-positive, acid-fast bacillus. Tuberculosis commonly attacks the pulmonary system, but can also affect other parts of the body. Approximately 33 % of world population is infected with *Mycobacterium tuberculosis* that might have risk for development of vigorous tuberculosis. Approximately 8.8 million people are diagnosed with active tuberculosis that causes 1.6 million deaths per year (van den Boogaard et al., 2009). The current first-line treatment for TB is a multidrug regimen consisting of rifampicin, isoniazid, pyrazinamide, and ethambutol (RHZE). It must be administrated for at least 6 months to reach high cure rates. These drugs can cure tuberculosis successfully when drug resistance is not observed. Nevertheless, there is high treatment failure rate in multi-drug resistant tuberculosis (MDR-TB) leading to rifampicin and isoniazid resistance and extensively drug resistant tuberculosis (XDR-TB) which is resistant to any drug of either fluoroquinolones or aminoglycoside types in addition to those defined under MDR-TB. The second-line drugs used in the treatment of MDR-TB have

many side effects, and require a long treatment period that limit their usage (Jacobson et al., 2010). Discovery of new drugs is essential in order to overcome the resistance to MDR-TB and XDR-TB drugs, the current treatment regimens can be shorten and latent TB will be treated in patients, who are infected with the bacteria but have not developed any symptoms of the disease.

1.6. Endophytes

Endophytes are microbes that inhabit living, internal tissues of plants without causing any immediate, apparent negative effects (Newman, 2003). Endophytic fungi had previously been unobserved as potential sources of bioactive metabolites. This was most likely due to the absence of any visible sign of fungal colonisation on the host plant (Blunt, 2006). However, it has been later realised that plants may contain countless, previously unnoticed and unrealized numbers of these microorganisms known as endophytes. This has driven an international scientific attempt to isolate endophytic fungi and to study their secondary metabolites. Scientists have since discovered that endophytes may be considered an important area for discovery of new natural products. Each individual plant from about 300,000 higher plant species that exist on earth is thought to be host to one or more endophytes (Strobel, 2004a). Moreover, endophytes associated with plants are considered to have an infinite undisclosed reservoir of metabolic diversity. Advanced methods in cultivation and dereplication procedures have provided access to a rich source of novel drug leads having the advantage of optimizing efficient production at higher yields under low cost through large scale cultivation of the microorganisms. Furthermore, beside investigation of endophytes for their biologically active natural compounds, which might prove to be suitable for specific medicinal application, a field of major interest is to study these secondary metabolites in search of novel anticancer and antimicrobial agents. In many cases endophytic fungi might be involved in the biosynthesis of plant natural products, but they might be also the producers themselves of several other groups of new pharmacologically active and structurally diverse secondary metabolites (Arnold, 2007). It was found that the majority of endophytic species were identified to

belong to the ascomycete and deuteromycete classes of fungi.

1.7. Endophyte-host interaction

It is thought that endophyte-plant relationship may have evolved at the same time that higher plants were found millions of years ago (Bayes, 2007b). This is supported by the fact that endophytes have been detected in fossilised tissues of plants (Mosley, 2007). It is reasonable therefore, that due to these long-held associations, that some endophytes may have developed genetic systems permitting the transmission of genetic information between themselves and higher plants as well as vice versa. In an endophyte-host interaction, nutrition is the minimum contribution that the plant could provide (Bayes, 2007b). These interactions provide metabolites essential for plant growth to support its life cycle as well as self-defence (Metz, 2000, Strobel, 2004b). Moreover, plants afford spatial structure, protection from dehydration, nutrients, photosynthesis and in the case of vertical-transmission, spreading to the next generation of hosts (Clay, 1988, Rudgers, 2004). Studies showed that endophytes are more likely to be mutualistic when reproducing vertically (systemic) by growing into seeds and more antagonistic to the host when transmitted horizontally (non-systemic) via spores (Schardl, 1991, Saikkonen, 1998). Endophytes gain support from the mutual interaction with their host plants mainly by helping the hosts to increase their resistance to herbivores which has been identified as an "acquired plant defences" (Carroll, 1988, Schulz, 1999, Clay, 1988, Faeth, 2002). The in vitro models clearly established the antioxidant potency of extracts of mangrove plants and their associated endophytic fungi, which aids in understanding the mutualistic association of plant and endophyte against various biotic and abiotic stresses (Ravindran et al., 2012).

Endophytes also increase host fitness, strength and competitive abilities, by increasing nutrient uptake, germination success, resistance to dehydration, resistance to seed predators, tolerance to heavy metal presence, tolerance to high salinity, and growth rate by evolving biochemical pathways to produce plant growth hormones. Moreover, endophytes are able to promote the biological degradation of the dead host plant that starts the vital steps of nutrient recycling

(Tan, 2001, Strobel, 2002a, Zhang, 2006).

1.8. Metabolomics

Metabolomics is the technology designed to provide general qualitative and quantitative profile of metabolites in organisms exposed to different conditions. Plants and microorganisms produce a large number of metabolites with different activities and behaviours against stress conditions. Metabolomics provides extra information to analyse these complex relationships and explore the production of natural products in the search for novel compounds. Metabolomics provide the holistic overview of the biochemical status of biological systems (Rochfort, 2005). Metabolomics is relatively a new field of 'omics', espousing to a systematic biological approach, with the goal of qualitatively and quantitatively analysing all metabolites contained in an organism at a specific time and under specific influence (Tawfike et al., 2013). The metabolome is the complete set of small molecules found in a cell, tissue or organism at a certain point in time. Metabolomics is considered as a functional approach in monitoring gene function and identifying the biochemical status of an organism (Yuliana et al., 2011).

1.9. Metabolomics applications and techniques

Metabolomics is applied in many aspects of natural drug discoveries, particularly in bioactivity screening to improve dereplication and identification procedures. Fast dereplication of known compounds and identification of lead bioactive metabolites is important in the primary stages of metabolomics profiling prior to an intensive isolation work. Different analytical techniques are applied followed by multivariate data analysis (MVDA) to minimize the redundant analysis in isolation steps of active compounds from the natural source (Hall, 2006). Metabolomics has also been used to evaluate the bioavailability, toxicity and efficacy of natural compounds. The advance approach in standard analysis is to associate metabolic profile to bioactivity directly on the workflow; consequently, the activity of the individual compounds could be measured separately. The use of metabolomics is a good means to guide the isolation of compounds, as well as to help improve the productivity of downstream fermentation methods (Yuliana et

al., 2011). Metabolomics provide statistical and computational tools to this standard approach of rapid HPLC fractionation, which would identify the active entities at an earlier stage. The goal of HPLC fractionation is to obtain the maximum purity of active components which, however, is not achievable in the initial chromatographic isolation work (Tawfike et al., 2013). With metabolomics tools, it will be possible to refer to the active components at the first fractionation step as well as identify the functional groups involve in the bioactivity which would be present in a series of fractions as shown by the bioactivity screening results. This can be chemometrically achieved by such NMR-metabolomics/PCA (principal component analysis) software like ALICE (Tawfike et al., 2013). The use of metabolomics will help in determining which fractions will go first for purification work, which should save time and resources in isolating the target compounds. Metabolomics is used for quality control of the natural products and isolates to monitor the different metabolic profile between individuals e.g. detection of the herbal adulteration with similar species but with low levels of the active compounds (Yuliana et al., 2011). Metabolomics can also be used to monitor environmental alterations during growth and harvesting, post harvesting treatment, extraction and method of isolation, all of which can affect the efficacy of natural products. Metabolomics might help to get a better view of the mode of action of herbal or natural products and lead to the possibility of gaining proof of their pharmacological activity over different batches. This is based on considering the bulk of chemical constituents rather than focusing on certain individual components or groups of compounds (Yuliana et al., 2013). Metabolomics can be used to detect biomarkers and/or precursors to dereplicate the biosynthesis of the natural product at different development stages of their biological source as well as simultaneously screen for the bioactivity. By using combinations of different analytical methods, the bioassay-guided isolation route is getting short and rapid dereplication of known activities is delivered (Ebada et al., 2008). MACROS (MacIntyre et al, 2014) have been developed to efficiently detect the production of interesting secondary metabolites during the cultivation and production processes. This would assist in maintaining or enhancing biosynthesis of the desired compounds (Abdelmohsen et al., 2014). These algorithms are coupled to

differential expression analysis software like SIEVE and Mzmine, web-based software developed by VTT (Technical Research Centre of Finland, which can then integrate the results to an in-house database that includes MarinLit and Antibase to further identify microbial secondary metabolites (Tawfike et al., 2013).

Metabolomics has become a significant tool in systems biology and permits obtaining insights into the potential of natural isolates for synthesis of substantial quantities of the desired new agents, and monitor the control of the environment within fermentation systems in a rational way to select a promising metabolome.

1.10. *Aspergillus* endophyte

Aspergillus is one of the most popular and common endophytic fungi found to be associated with natural sources either marine or terrestrial habitat. *Aspergillus* is belonging to Ascomycetes fungi that are found in most of terrestrials and plants from the arctic tundra to tropics (A. Elizabeth, 2007, Huang et al., 2008).

1.10.1. Anticancer secondary metabolites from *Aspergillus* endophyte

Taxol (**1**), is one of the most well-known anticancer compounds isolated from natural source, a diterpenoid first isolated from the bark of *Taxus brevifolia* Nutt. (Wani et al., 1971), and is still mainly extracted from the bark of yews. However, this method cannot meet the increasing demand for taxol on the market because yews grow very slowly and are rare and endangered species belonging to first-level conservation (Kean et al., 2007). Recently, increasing efforts have been made to develop alternative means of taxol production, such as using complete chemical synthesis and semi-synthesis and the *Taxus* spp. plant cell culture. Since 1993, observations of taxol-producing fungi, *Taxomyces andreanae* and *Pestalotiopsis microspora*, have been reported, demonstrating that microorganisms can produce taxol (Stierle et al., 1993, Strobel et al., 1996, Zhou et al., 2007). So far, more than 30 taxol-producing fungi have been reported globally, most of these endophytes of *Taxus* spp. belong to ascomycetes and imperfect fungi (Ji et al., 2006). Recently, *Aspergillus candidus* MD3, an

endophytic taxol-producing fungus has been successfully isolated from the inner bark of *Taxus* x *media* (hybrid of *Taxus baccata* x *Taxus cuspidate*) (Zhang et al., 2009b). HD86-9 is a new variant of taxol-producing endophytic fungi from *Taxus cuspidata*, and it was named *Aspergillus niger* var. taxi (Zhao et al., 2009). In addition, *Aspergillus niger*, an endophyte isolated from the inner bark of a *Taxus chinensis* tree, was used as an elicitor to stimulate the Taxol (paclitaxel) production in the cell suspension culture of *Taxus chinensis*. The elicitation resulted in a more than two-fold increase in the Taxol yield and about a six-fold increase in total secretion (Wang et al., 2001).

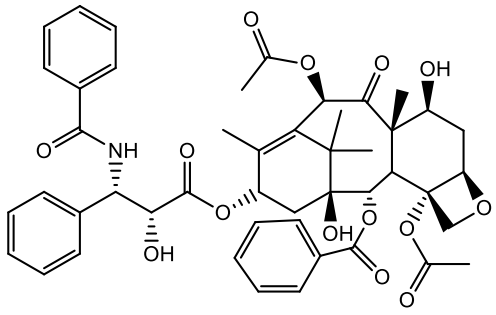

1

Other anticancer metabolites have been isolated from different species of *Aspergillus endophyte* e.g. Terpeptin A (**2**) and B (**3**), two new members of the indolic enamides, along with three known compounds were identified from a strain of *Aspergillus* sp. (w-6), an endophytic fungus associated with *Acanthus ilicifolius*. They exhibited moderate cytotoxicity against the carcinomic human alveolar basal epithelial A-549 cell line (Lin et al., 2008).

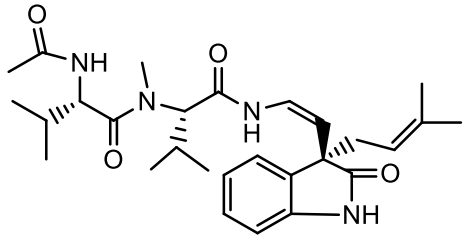

2

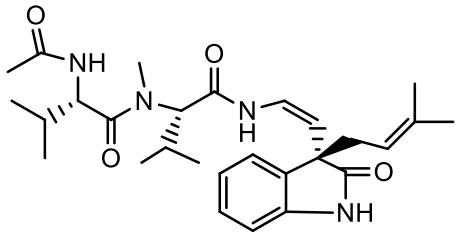

3

Aspergillus niger MA-132, an endophytic fungus obtained from the fresh tissue of the marine mangrove plant *Avicennia marinafrom* from which eight new α-

pyrone derivatives were isolated, namely, nigerapyrones A-E (**4-8**) and nigerapyrones F-H (**9-11**), along with two known congeners, asnipyrones B (**12**) and A (**13**). Nigerapyrone E (**8**) showed cytotoxicities against SW1990, MDA-MB-231, and A549 cell lines. This compound also showed weak or moderate activity against MCF-7, HepG2, Du145 and NCI-H460 cell lines. Nigerapyrone B (**5**) showed selective activity against the HepG2, asnipyrone A (**13**) showed activity against the A549 cell line and nigerapyrone D (**7**) showed moderate or weak activity against the MCF-7, HepG2, and A549 cell lines (Liu et al., 2011). *Aspergillus tubingensis* was one of 49 endophytic fungi obtained from Dragon's blood materials of *Dracaena* sp. They has been investigated for their antimicrobial and antitumor activity against six pathogenic microbes and five tumor cells. *Aspergillus tubingensis* showed activity against *S. aurues* and *C. albicans*. Moreover, inhibition percentages against different cancer cell lines were 60-80% against breast cancer cells MCF7, 40-60% for ovarian cancer cells and 10-20% for a human embryonic kidney cells 293-T (Cui et al., 2011).

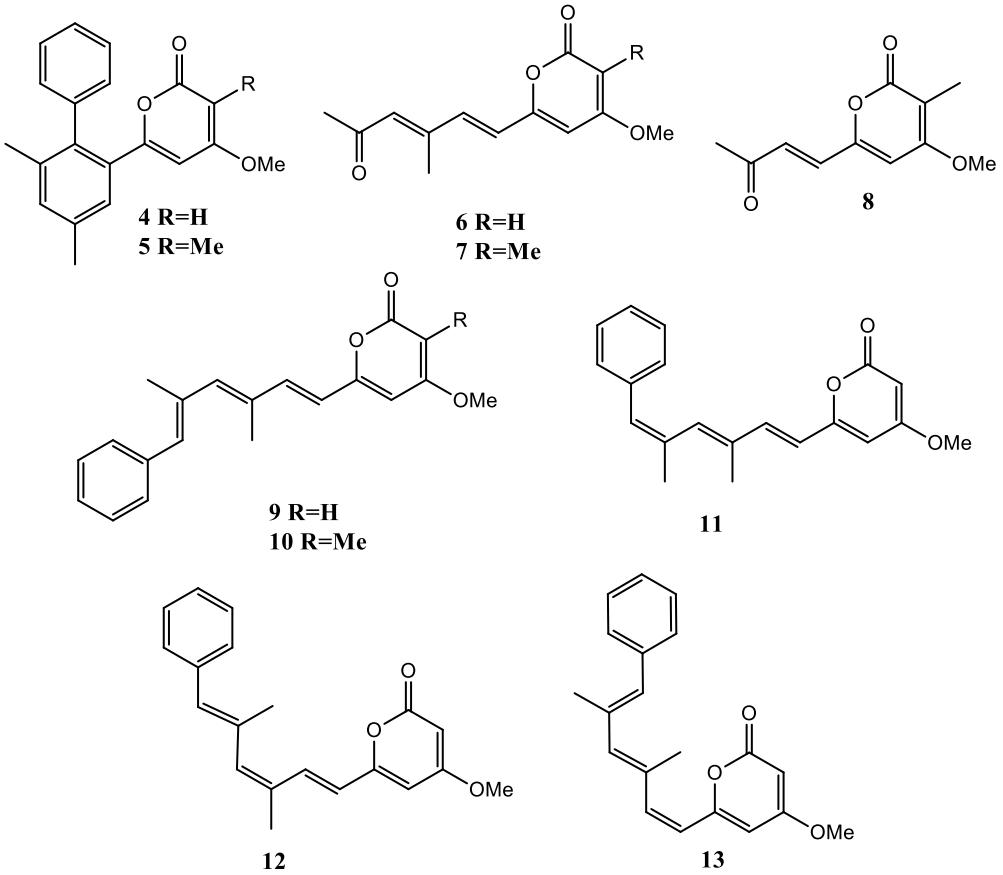

Aspergillus niger IFB-E003, an endophyte in *Cyndon dactylon*, gave four known compounds. These naphtho-γ-pyrone compounds are rubrofusarin B (**14**), fonsecinone A (**15**), asperpyrone B (**16**) and aurasperone A (**17**). Rubrofusarin B was shown to be cytotoxic to the colon cancer cell line SW1116 and aurasperone had an inhibitory effect on XO (xanthine oxidase) (Song et al., 2004). Moreover, Aspernigerin (**18**), was isolated from the same endophyte, is a novel cytotoxic alkaloid against the tumor cell lines nasopharynyeal epidermoid KB, cervical carcinoma Hela, and colorectal carcinoma SW1116 (Shen et al., 2006). 9-deacetoxyfumigaclavine C (**19**) was isolated from the culture of *Aspergillus fumigatus* from stem of *Cynodon dactylon*, showed selectively potent cytotoxicity against human leukemia cells (K562) (Ge et al., 2009).

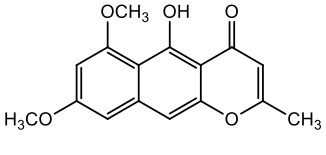

14

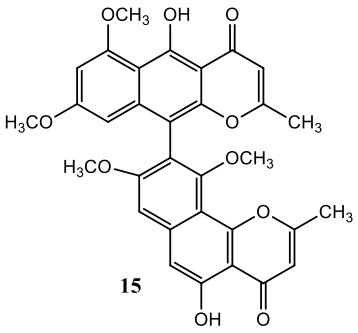

15

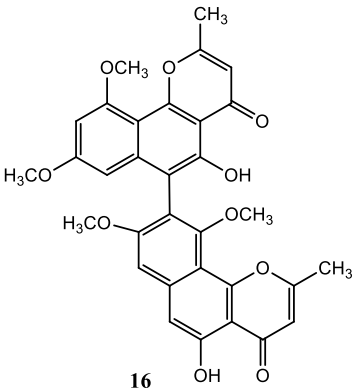

16

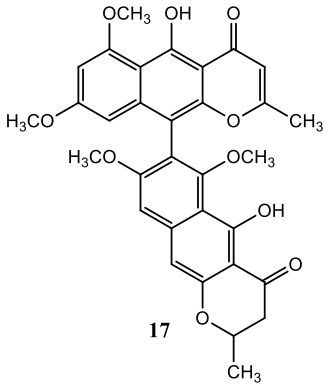

17

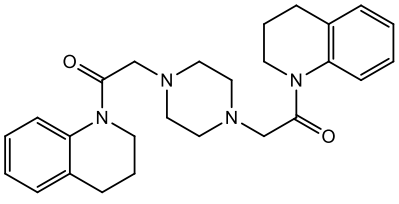

18

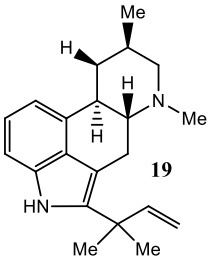

19

A culture extract of *Aspergillus flavipes*, an endophytic fungus associated with *Acanthus ilicifolius*, gave upon fractionation five new cytochalasins, Z16–Z20 (**20**-**24**), and three known ones, (**25**-**27**). Cytochalasin Z17 (**21**) and rosellichalasin (**27**) showed cytotoxic activities against A-549 cell lines (human alveolar epithelial cells) with IC_{50} values of 5.6 and 7.9 μM, respectively (Lin et al., 2009). Z17 (**21**), was isolated from the liquid culture of the endophytic fungus *Aspergillus terreus* IFB-E030 from stem of *Artemisia annua* L. (Asteraceae), had moderate cytotoxicity against human nasopharyngeal epidermoid tumor KB cell line with an IC_{50} value of 26.2 μM (Zhang et al., 2010).

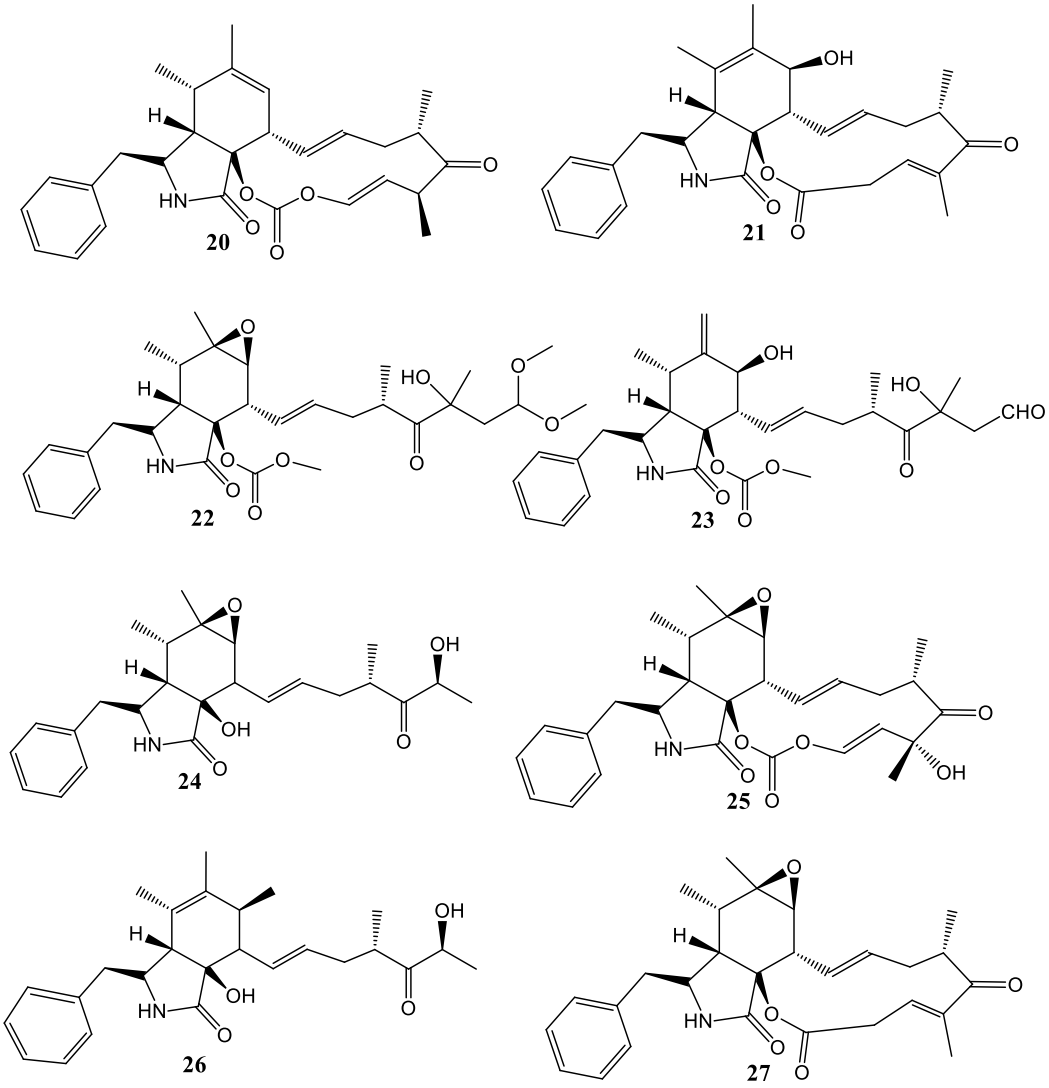

Rubasperone D (**28**) a new dimeric naphtho-γ-pyrones with known monomeric

naphtho-γ-pyrones TMC-256 A1 (**29**), were isolated from the mangrove endophytic fungus *Aspergillus tubingensis* from the radix of *Pongamia pinnata* from the South China Sea in Guangxi Province, P. R. China, showed mild cytotoxicity activity against MCF-7, MDA-MB-435, Hep3B, Huh7, SNB19, and U87 MG (Huang et al., 2011).

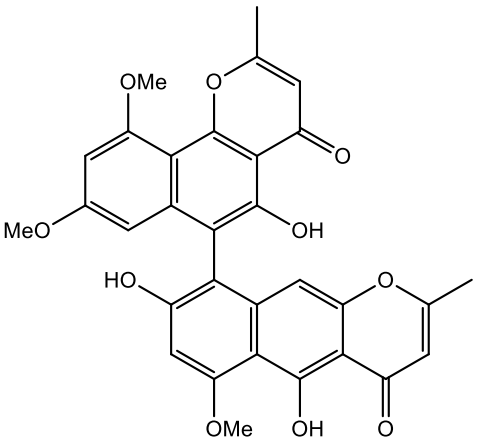

28

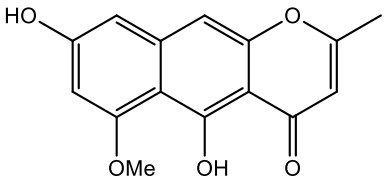

29

A new application for *Aspergillus ochraceus* ATCC 1009 resting cells, which is biotransformation of Sch-642305 to yield three new derivatives (**30**-**32**), compound (30), showed antimicrobial activity against Gram-negative bacteria. Furthermore, while all derivatives showed cytotoxic activity against various cancer cell lines, compound (**31**) achieved an IC_{50} of 4 nM against human myelogenous leukemia K 562, compared to 20 nM for the parent Sch-642305 (Adelin et al., 2011).

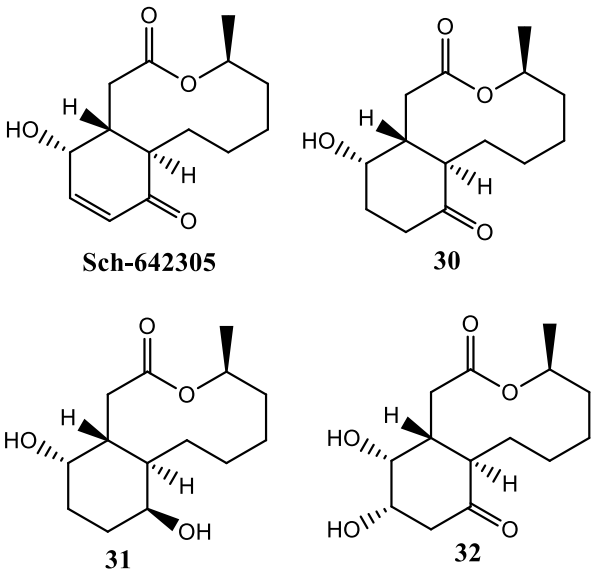

One uncommon thiophene compound (**33**), together with anhydrojavanicin (**34**), 8-O-methylbostrycoidin (**35**), 8-O-methyljavanicin (**36**), botryosphaerone D (**37**), 6-ethyl-5-hydroxy-3,7-dimethoxynaphthoquinone (**38**), 3β,5α-dihydroxy-(22E,24R)-ergosta-7,22-dien-6-one (**39**), 3β,5α,14α-trihydroxy-(22E,24R)-ergosta-7, 22-dien-6-one (**40**), NGA0187 (**41**) and beauvericin (**42**), were isolated from the mangrove endophytic fungus *Aspergillus terreus* (No. GX7-3B). Compounds **34**, **35**, **41** and **42** showed obvious inhibiting actions against α-acetylcholinesterase (AChE). Moreover, compounds **39** and **42** exhibited strong or moderate cytotoxic activities against MCF-7, A549, Hela and KB cell lines with IC_{50} values 4.98 and 2.02 (MCF-7), 1.95 and 0.82 (A549), 0.68 and 1.14 (Hela), and 1.50 and 1.10 μM (KB), respectively (Deng et al., 2013).

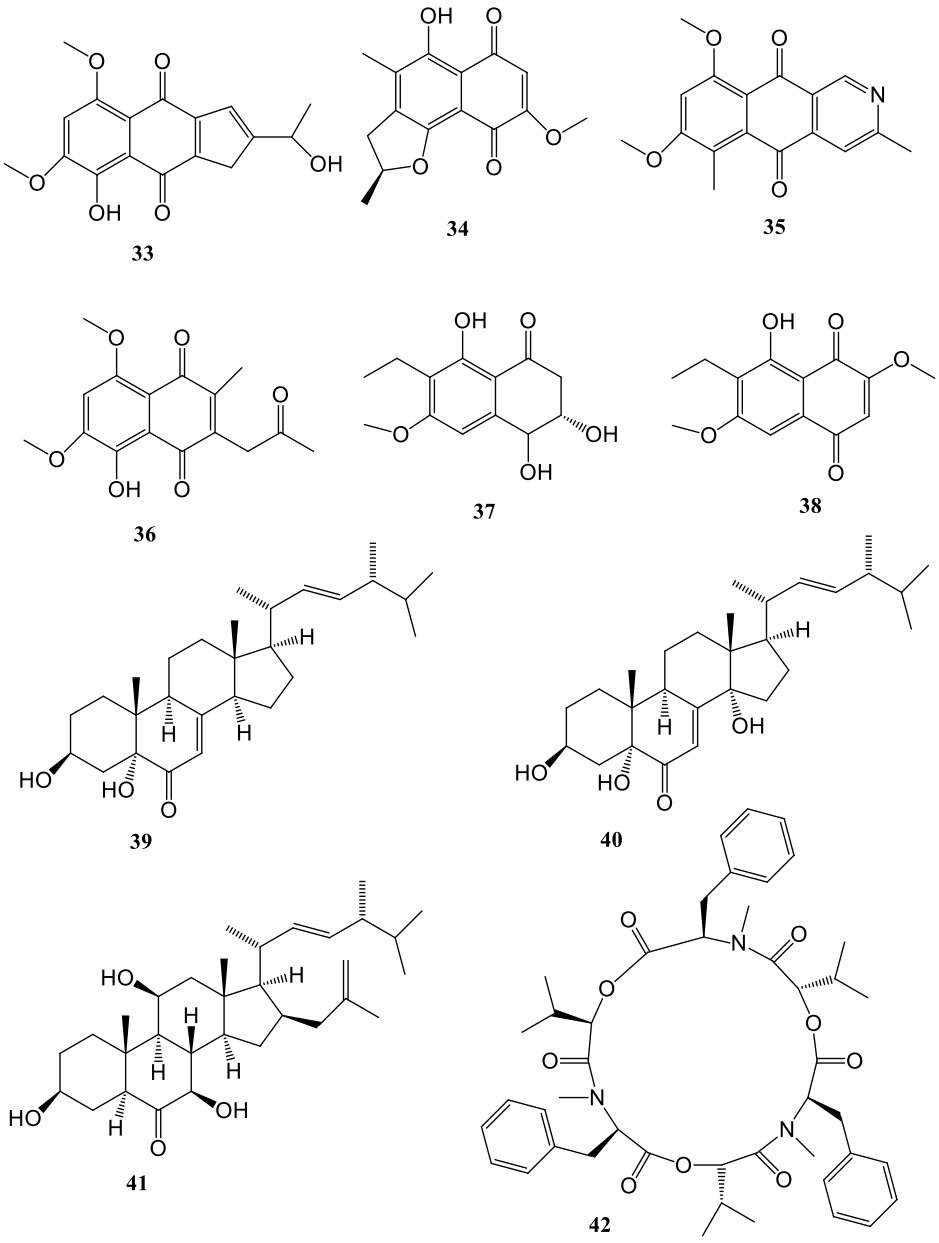

Four new quinazolinone alkaloids (**43-46**) were isolated from the mangrove-derived endophytic fungus *Aspergillus nidulans* MA-143. All the compounds exhibited potent brine shrimp toxicity with LD_{50} values of 1.27, 2.11, 4.95 and 3.42 μM, respectively (An et al., 2013). Malformin A1 (**47**), was characterized from extract of *Aspergillus niger*, an endophytic fungus from the Chinese liverwort *Heteroscyphus tener* (Steph.) Schiffn. Malformin A1 exhibited significant cytotoxic activities against the human A2780, H1688, K562, M231, PC3 cell lines in vitro with IC_{50} values of 0.14, 1.02, 0.13, 0.45, 0.14 μM, respectively (Li et al., 2013).

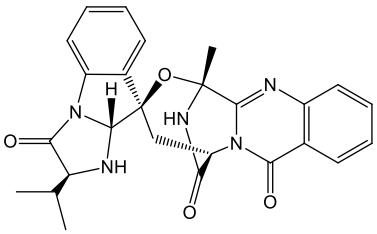

43

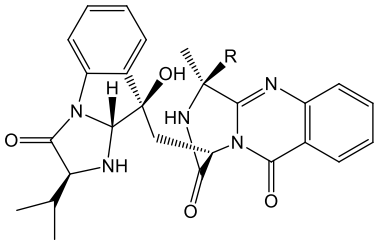

44 R=H
45 R=OH

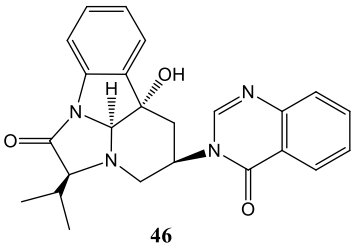

46

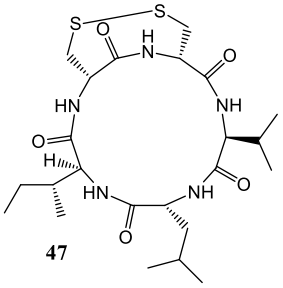

47

The endophytic fungi *Aspergillus fumigatus* sp. isolate R7 was found to produce Fumiquinazoline-F (**48**) and Fumiquinazoline-D (**49**) which exhibited a strong cytotoxic activity in brine shrimp assay and also a further activity against the Gram-positive *Bacillus subtilis* (12, 15 mm), *Staphylococcus aureus* (12, 15 mm) and fungi (*C. albicans* [11, 11 mm] and *M. miehi* [12, 13 mm]) (Shaaban et al., 2013).

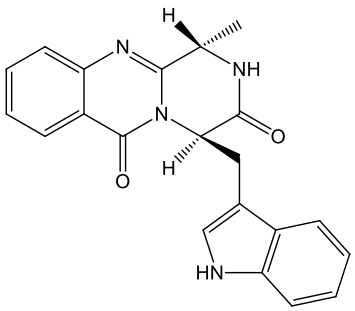

48

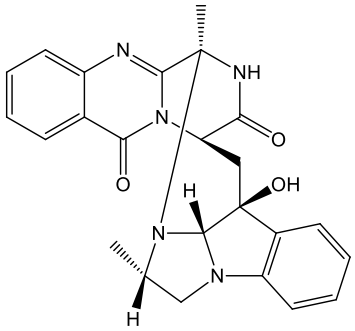

49

Nigerasterols A and B (**50** and **51**, respectively) represent the first 5,9-epidioxy-sterol compounds of marine origin, and they displayed potent activity against tumor cell lines HL60 and A549 in a preliminary bioassay, isolated form the culture extract of *Aspergillus niger* MA-132, an endophytic fungus isolated from

a fresh healthy sample of the mangrove plant *Avicennia marina* (Deng et al., 2013).

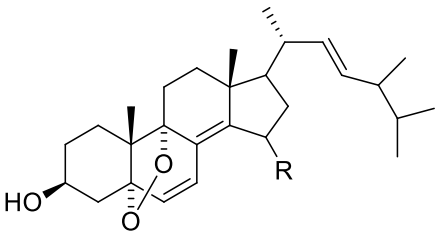

50 R=H
51 R=OH

The endophytic fungus *Aspergillus terreus* MHL-P22, residing in the fresh leaves of *Malus halliana,* produced two new furandiones named asperterone B (**52**) and C (**53**) from the liquid culture. Compounds (**52)** and (**53)** exhibited moderate cytotoxic activities against human colorectal carcinoma SW1116 cells with IC_{50} values of 57.5 and 71.0 µM, respectively (Gu and Qiao, 2012).

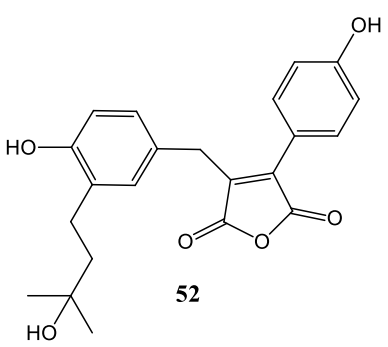

52

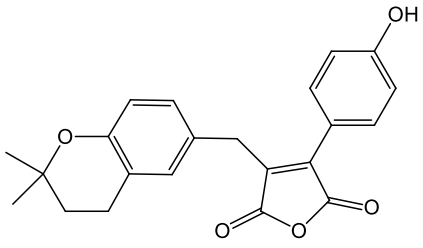

53

Compound KL4 (**54**), isolated from *Aspergillus* spp. endophyte coming from the seeds of *Gloriosa superba*, was found to possess potency comparable to standard anticancer agents Mitomycin-C and 5-FU when tested against six cancer cell lines, viz., A-549, HEP-2, MCF-7, OVCAR-5, THP-1, and CV-1. It also showed a significant antimicrobial activity against *Saccharomyces cerevisiae* (MTCC 172), *Candida albicans* (MTCC 3018), and *Cryptococcus gastricus* (MTCC 1715) (Budhiraja et al., 2013).

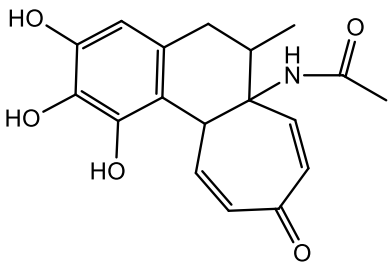

54

Aspergillus niger PN2 an endophytic fungus, was isolated from the healthy tissues of *Taxus baccata*, showed ability to produce lovastatin in much high quantity. The isolated fungal lovastatin exhibited a strong cytotoxic activity in vitro culture of tested human cancer cells (HeLa and HepG2) by apoptotic assay (Raghunath et al., 2012).

1.10.2. Antimicrobial secondary metabolite from *Aspergillus* endophyte

The bioassay-guided fractionation of the cultural extract of endophytic fungus *Aspergillus fumigatus* CY018 isolated from leaves of *Cynodon dactylon* gave a new metabolite, named asperfumoid (**55**) together with other four known metabolites. Fumigaclavine C (**69)**, fumitremorgin C (**56**), physcion (**57**) and helvolic acid (**58**) inhibited *C. albicans* with MICs of 75.0, 31.5, 62.5, 125.0 and 31.5 μg/mL, respectively (Liu et al., 2004).

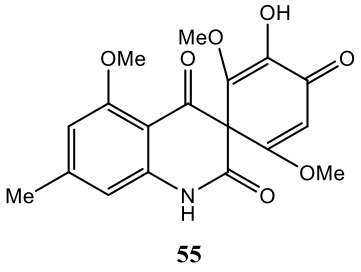

55

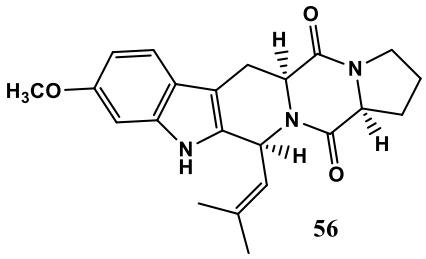

56

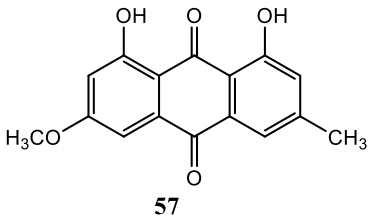

57

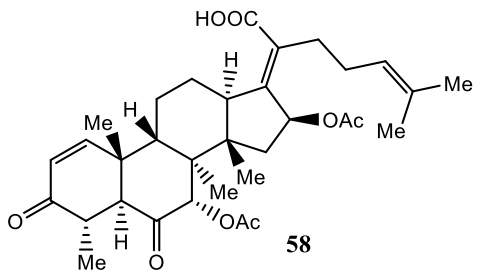

58

Aspergillus fumigatus Fresenius, an endophytic fungus isolated from *Juniperus communis* L. Horstmann was found to be a novel source of the anticancer pro-drug deoxypodophyllotoxin (**59**). It has displayed antimicrobial activity against Gram-positive bacterium *S. aureus* subsp. *aureus* (DSM 799), and Gram-negative bacteria K. *pneumoniae* subsp. *ozaenae* (DSM 681), *P. aeruginosa* (DSM 1128) except for *E. coli* (DSM 682) which was not at all susceptible to either podophyllotoxin or the fungal deoxypodophyllotoxin at the concentrations tested (Kusari et al., 2009). *Aspergillus clavatonanicus*, an endophytic fungus of *Taxus mairei*, when grown in surface culture, the fungus produced clavatol (**60**) (2',4'-dihydroxy-3',5'-dimethylacetophenone) and patulin (**61**) (2-hydroxy-3,7-dioxabicyclo [4.3.0]nona-5,9-dien-8-one), both exhibited inhibitory activity in vitro against several plant pathogenic fungi, i.e., *Botrytis cinerea*, *Didymella bryoniae*, *Fusarium oxysporum* sp. *cucumerinum*, *Rhizoctonia solani*, and *Pythium ultimum* (Zhang et al., 2008a).

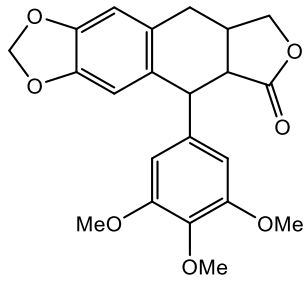

59

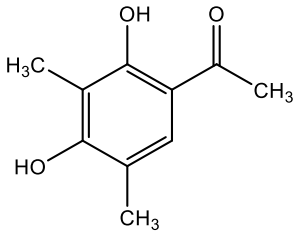

60

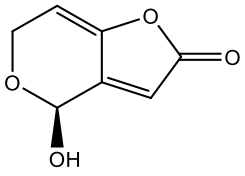

61

Endophytic fungi (strain number: CY725) identified as *Aspergillus* sp., isolated from the medicinal herb *Cynodon dactylon* (Poaceae), was the most active endophyte against *Helicobacter pylori*. Helvolic acid (**58**), monomethylsulochrin (**62**), ergosterol (**63**) and 3b-hydroxy-5a, 8a-epidioxy- ergosta-6,22-diene (**64**) were isolated and have corresponding MICs of 8.0, 10.0, 20.0 and 30.0 µg/mL, respectively. Helvolic acid was also inhibitory to the growth of *Sarcina lutea*, *Staphylococcus aureus* and *Candida albicans* with MICs of 15.0, 20.0 and 30.0 µg/mL, respectively (Li et al., 2005).

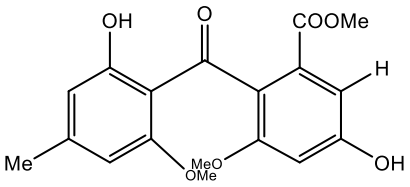

62

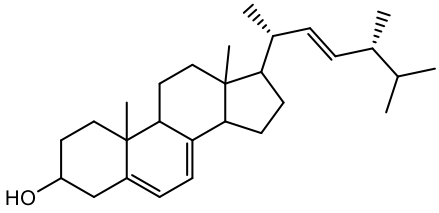

63

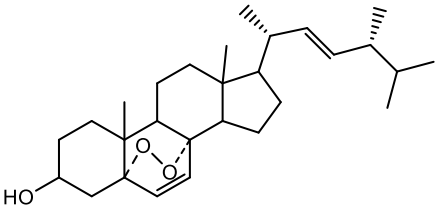

64

Aspergillus fumigatus LN-4, an endophytic fungus isolated from the stem bark of *Melia azedarach*, produced thirty-nine fungal metabolites including two new alkaloids, 12β-hydroxy-13α-methoxyverruculogen TR-2 (**65**) and 3-hydroxyfumiquinazoline A (**68**). Sixteen compounds displayed potent antifungal activities, four of them, 12β-hydroxy-13α-methoxyverruculogen TR-2 (**65**), fumitremorgin B (**66**), verruculogen (**67**), and helvolic acid (**58**), showed antifungal activities with MIC values of 6.25−50 μg/mL, which were comparable to the two positive controls carbendazim and hymexazol. Compounds **66** and **67** exhibited significant toxicities toward brime shrimps and displayed the best antifeedant activity against armyworm larvae (Li et al., 2012b).

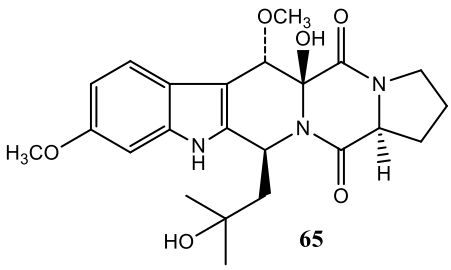

65

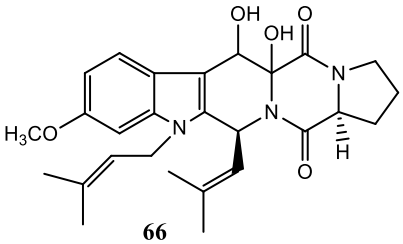

66

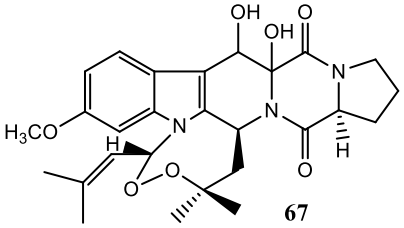

67

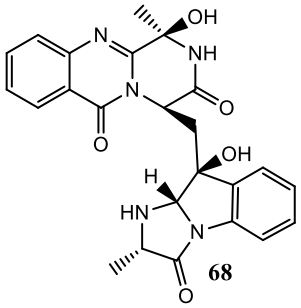

68

Aspergillus niger is one of thirteen different endophytes isolated from *Tabebuia aregntea*. Screening of the cultural extract showing that *Aspergillus niger* yielded saponins, phenolic compounds, anthraquinones, steroids, cardiac glycosides and tannins. The fungal culture of *A. niger* showed the strongest antioxidant capacity, having the highest levels of phenolics and significant antimicrobial activity against an array of pathogenic fungi and bacteria (Sadananda et al., 2011). The alkaloids, fumigaclavine C (**69**) and pseurotin A (**70**), were obtained from endophytic fungus *Aspergillus* sp. EJC08 isolated from medical plant *Bauhinia guianensis*. Both exhibited broad-spectrum antibacterial activity (Pinheiro et al., 2013). Asperterpenoid A (**71**), a novel sesterterpenoid with a new carbon skeleton, has been isolated from a mangrove endophytic fungus *Aspergillus* sp.16-5c., exhibited strong inhibitory activity against *Mycobacterium tuberculosis* protein tyrosine phosphatase B (mPTPB) with an IC_{50} value of 2.2 μM (Huang et al., 2013).

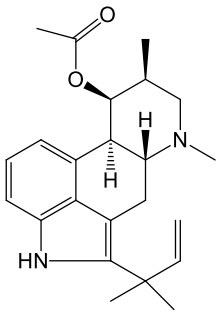

69

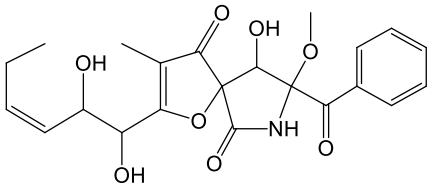

70

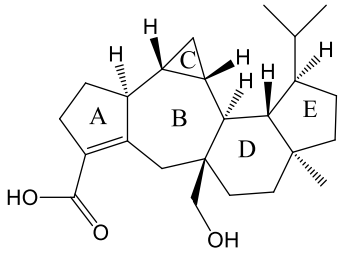

71

The anti-phytopathogenic activity of the isolated indolyl diketopiperazines, isolated from the endophytic fungus *Aspergillus tamarii* in *Ficus carica* L., proposes that *A. tamari* could guard the host by producing the bioactive metabolites. They were identified as fumitremorgin B (**66**), verruculogen (**67**), fumitremorgin C (**56**), cyclotryprostatins B (**72**), tryprostatin A (**73**) and tryprostatin B (**74**) (Zhang et al., 2012). Furthermore, compounds (**66**, **67**, **56** and **72**) and fumiquinazoline J (**75**) were also isolated from the EtOAc extract of the culture of an endophytic fungus, *Aspergillus fumigatus* isolated from the root of *Astragalus membranaceus*. The purified compounds were tested for their antifungal and antibacterial properties towards the tested microorganisms (Gram-positive, negative bacteria and fungi). Compounds (**66, 56)** showed potent antibacterial and antifungal activities with MICs of 4–64 µg/mL. Moreover, compound (**67, 72)** inhibited the growth of bacteria and fungi with MICs of 1–32 µg/mL. It was significant that the activity of compound (**75)** was close to that of gentamicin and was stronger than that of nystatin, present antifungal drugs (Zhou et al., 2013).

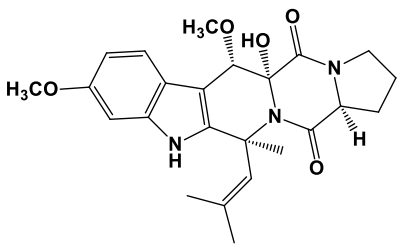

72

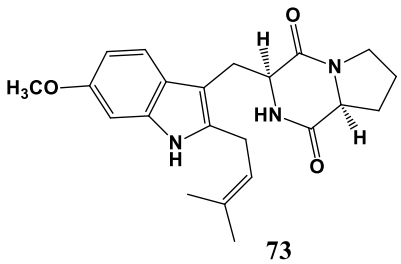

73

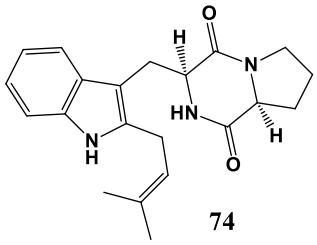

74

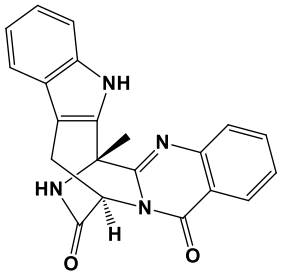

75

Aspergillus aculeatus, was one of nine bioactive fungal endophytes isolated from *Garcinia* species, showed anti-TB, antiplasmodium, antioxidant and anti-proliferation against human small-cell lung cancer cell (NCI-H187) (Phongpaichit et al., 2007). Aspergillumarins A and B (**76, 77**), two new dihydroisocoumarin derivatives, were isolated from the culture broth of a marine-derived fungus *Aspergillus* sp., which was isolated from the fresh leaf of the mangrove tree *Bruguiera gymnorrhiza* collected from the South China Sea. Compounds (**76, 77**) showed weak antibacterial activity against *Staphylococcus aureus* and *Bacillus subtilis* at a concentration of 50 µg/mL (Li et al., 2012a). The five compounds: pseurotin A (**70**), 14-norpseurotin A (**78**), FD-838 (**79**), and pseurotin D (**80**), and fumoquinone B (**81**), were isolated from *Aspergillus* sp. strain F1544 which was isolated from a mature leaf of *Guapira standleyana* (Nyctaginaceae). All compounds showed good antileishmanial and moderate anticancer activities (Martinez-Luis et al., 2012).

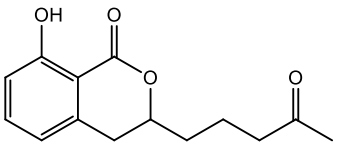

76

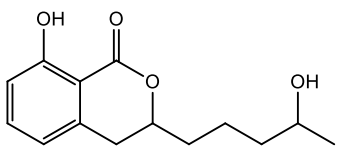

77

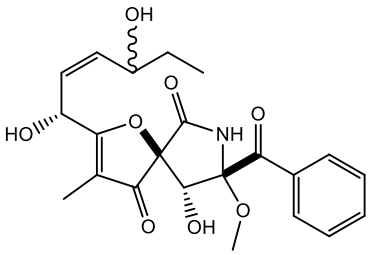

78

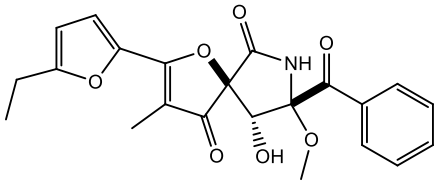

79

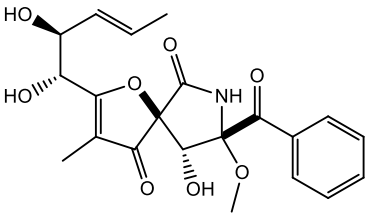

80

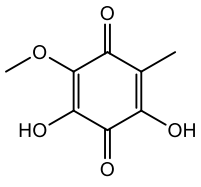

81

2-phenylethanol was characterized from the cultural extract of *Aspergillus niger*. 2-phenylethanol is an important constituent of rose oil constituting about 4.06% of rose oil. The rose oil industry is the major identified deligence for its application in perfumery, flavouring, ointments, and pharmaceuticals including various herbal products. Besides this, the other commercial applications of phenylethanol include its use in antiseptics, disinfectants, antimicrobials and preservative in pharmaceuticals (Wani et al., 2010).

The mycelial extract of *Aspergillus* sp. from *Writhtia tinctoria* displayed maximum antibacterial activity against *Pseudomonas fluorescens* and *P. aeruginosa* and was subjected to instrumental analyses which indicated the presence of alkaloids (Sunkar and Nachiyar, 2011). *Aspergillus versicolor*, one of 39 endophytic filamentous fungi from coffee plants (*Coffea arabica* and *C. robusta*), has antimicrobial activity toward *Salmonella choleraesuis* (CBMAI 484), *Staphylococcus aureus* (CBMAI 485), *Pseudomonas aeruginosa* (CBMAI 489) and four different *Escherichia coli* serotypes (Sette et al., 2006). The ethyl

acetate extract of *Aspergillus* sp. isolated from *Ficus carica* showed significant antimicrobial activity against *Pseudomonas aeruginosa* as test organism (Prabavathy and Nachiyar, 2011). The crude extracts of *Aspergillus* sp. JPY1, *Aspergillus* sp. JPY2, *Aspergillus niger*, endophytes associated with *Salvadora oleoides* Decne, exhibited the maximum activity against three pathogenic *Aspergilli sp* (Dhankhar et al., 2013). *Aspergillus* sp., together with other 24 endophytic fungi were isolated from nineteen plant from different areas in Panama, was tested for anti-parasite activity and it showed > 70 % inhibition toward *Leishmania donovani* (Martinez-Luis et al., 2011).

1.11. *Curvularia* sp.

Curvularia is also belonging to the ascomycetes. However, it is not very popular like *Aspergillus*. The genus *Curvularia* contains some 35 species, which are mostly subtropical, and tropical plant parasites. *Curvularia* endophyte is another example for the biodiversity and a good source of some bioactive metabolites.

1.11.1. Anticancer secondary metabolites from *Curvularia* sp.

Libertellenone G (**82**) and libertellenone H (**83**) two diterpenoids *(Lu et al., 2013)* with other three metabolites cytochalasin Z24 (**84**), cytochalasin Z25 (**85**) and cytochalasin Z26 (**86**), were extracted from fungus *Curvularia*. The compounds possessed a significant anti-tumor activity (Liu et al., 2013).

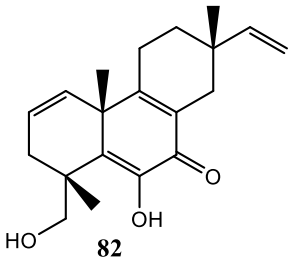

82

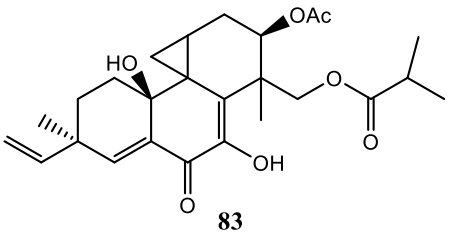

83

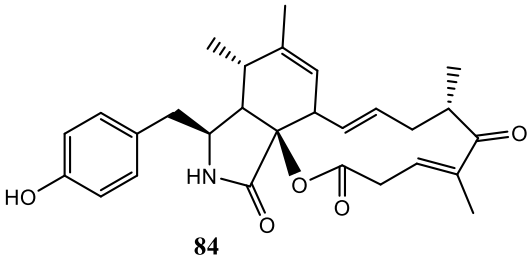

84

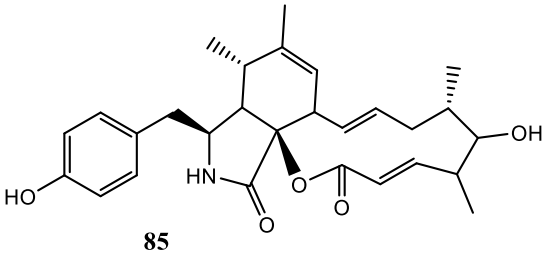

85

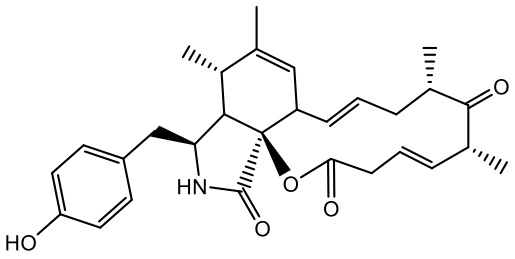

86

The crude extract from *Curvularia inaequalis* strain HS-FG-257 exhibited cytotoxicity against certain tumor cell lines. Fractionations lead to isolation of two new antitumor constituents, curvularone A (**87**) and 4-hydroxyradianthin (**88**) (Pang et al., 2013).

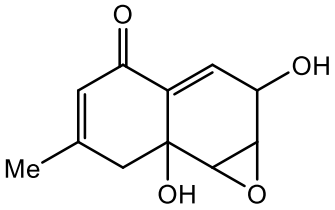

87

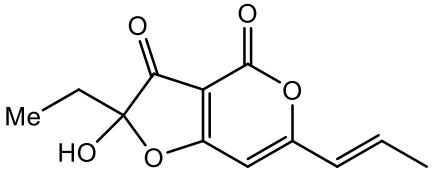

88

Apralactone (**89**), a novel macrolide as well as some known metabolites (**90**-**105**) were characterized from the culture extract of the marine fungus *Curvularia* sp. (strain no. 768), isolated from the red alga *Acanthophora spicifera*. Apralactone A (**89**), (+)-(10E,15R)-10,11-dehydrocurvularin (**90**), (+)-(10E,15R)-13-hydroxy-10,11-dehydrocurvularin (**100**), (+)-(11S,15R)-11-hydroxycurvularin (**101**), and

(+)-(11R,15R)-11-hydroxycurvularin (**102**) were found to be cytotoxic towards human tumor cell lines with mean IC_{50} values in the range of 1.25 to 30.06 μM (Greve et al., 2008).

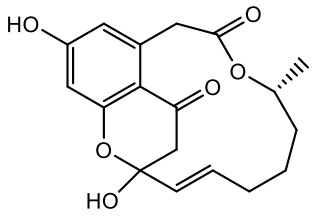

89

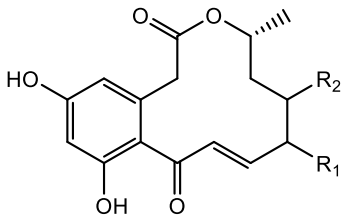

90 R_1=H, R_2=H
100 R_1=OH, R_2= H
101 R_1=H, R_2=OH

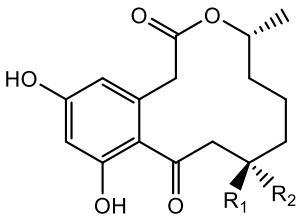

102 R_1=H, R_2=OH
103 R_1=OH, R_2=H

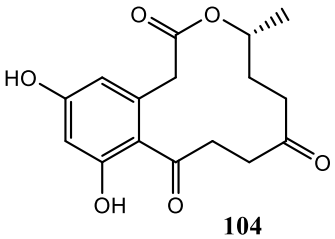

104

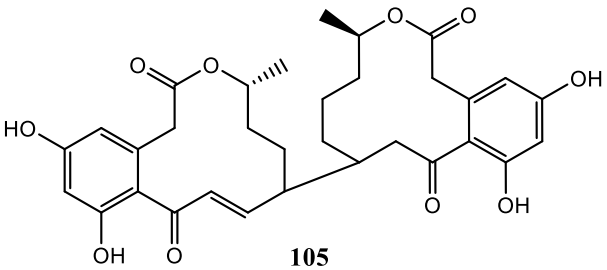

105

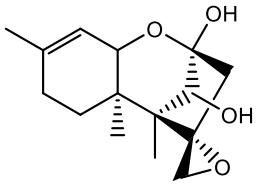

106

A new cell growth inhibitor, curvularol (**106**), was isolated from the fermentation broth of *Curvularia* sp. RK97-F166, inhibited cell cycle progression of normal rat kidney (NRK) cells in G1 phase at 150 ng/mL, induced the morphological reversion of srcts-transformed NRK cells at 100 ng/mL, and inhibited protein synthesis the same as cycloheximide (Honda et al., 2001). Harveynone (**107**), isolated from the culture of *C. harveyi* IFO 30129, which at 3.2-12.5 μg/mL inhibited cell division of sea urchin egg (Kawazu et al., 1991).

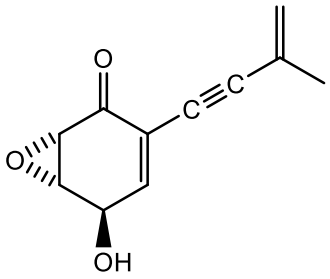

107

1.11.2. Antimicrobial secondary metabolites from *Curvularia* sp.

Two new curvularin-type macrolides, curvulone A (**108**) and B (**109**), and two known ones (**110**, **111**) of the rare 15R series have been characterized from the fungus *Curvularia* sp., which has been isolated from the marine algae *Gracilaria folifera*, were biologically active against fungal, bacterial and algal test organisms (Dai et al., 2010).

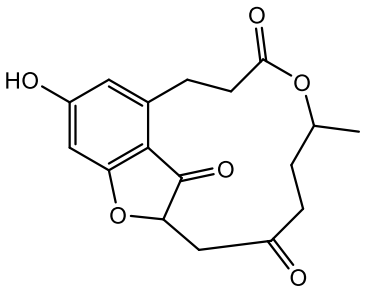

108

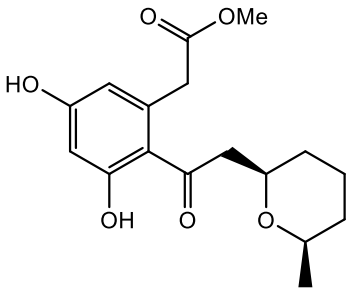

109

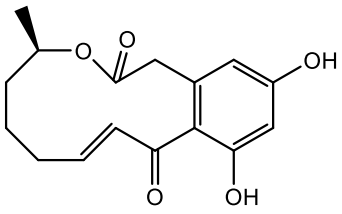

110

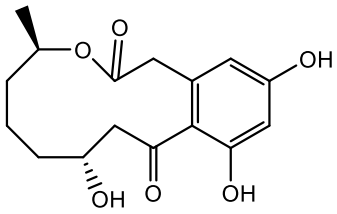

111

The major compounds from the culture extract of *Curvularia oryzae* MTCC 2605 were purified by silica gel column chromatography and elucidated to be 11-α-methoxycurvularin (**112**) and (S)-5-ethyl-8, 8-dimethylnonanal (**113**) by NMR and Mass spectral data. 11-α-methoxycurvularin showed a significant activity against bacteria, fungi and 4th instar *Spodoptera litura* larvae (Busi et al., 2009).

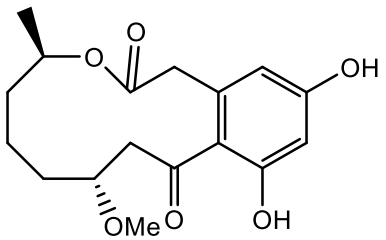

112

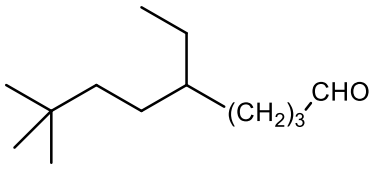

113

1.12. Cytotoxic natural products and other recently reported metabolites from the plants under investigation.

1.12.1. Genus *Terminalia*

Species of *Terminalia* belonging to family Combretaceae, are common in Egypt and other subtropical and tropical regions. The fruit is used traditionally in the leather tanning manufacturing and folk medicine, fruit extract possesses purgative, laxative, diuretic and astringent properties.

Table 1: Bioactive secondry metabolites from *Terminalia* species

Plant species	Name/ structure	References
T. ivorensis	Ivorenoside A (114) Ivorenoside B (115) 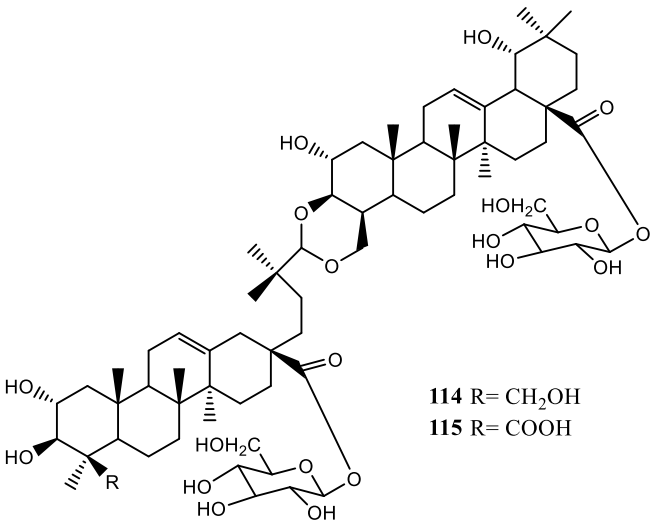 **114** R= CH_2OH **115** R= COOH Ivorengenin A (116)	**Anticancer** (Ponou et al., 2010, Ponou, 2010, Ponou et al., 2011)

	Ivorengenin B (117) 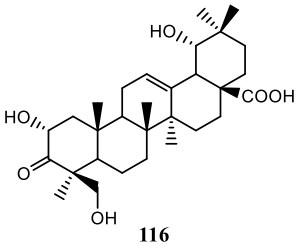 116 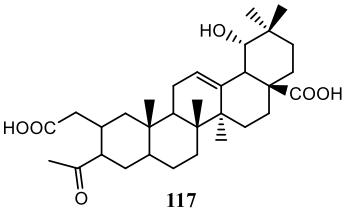 117	
	(118) 3,3'-di-O-methylellagic acid; (**119)** 2-Hydroxy-3,7,8 trimethoxychromeno [5,4,3-cde]chromene-5,10-dione; (**120)** Progallin A; (**121)** 3,3',4-O-Trimethyl-4'-O-β-D-glucopyranosylellagicacid; (**122)** Punicalagin; (**123)** Punicalin. 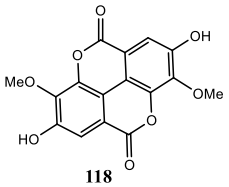 118 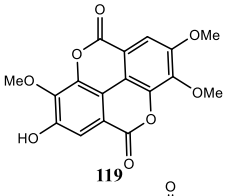 119 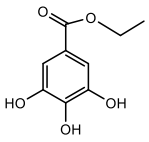 120 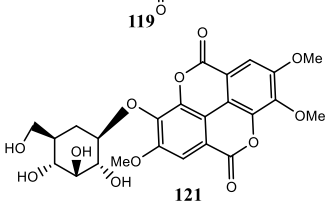 121 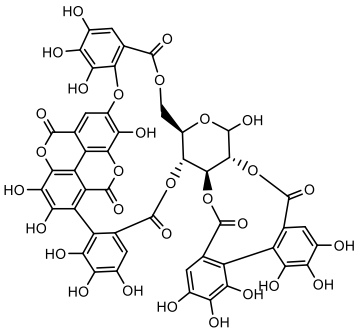 122 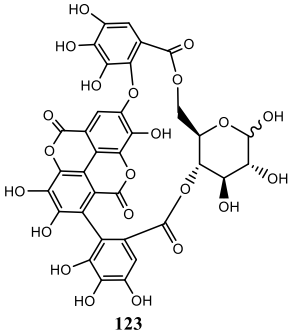 123	**anti-inflammatory, antioxidant and anti-HIV activities** (Adiko et al., 2013)
T. fagifolia	isoliquiritigenin-4-methyl-ether (**124**) isoliquiritigenin-4'-methyl-ether (**125**) 1-(2'-hydroxy-4',6'-dimethoxyphenyl)- 3-(3"-methoxy-4"-hydroxyphenyl)-propane (**126**) 23-(3",4"-di-*O*-methyl)-galloylarjunglucoside II (**127**) 23-(3",4",5"-tri-*O*-methyl)-galloylarjunglucoside II (**128**)	**Anticancer** (Garcez et al., 2006)

	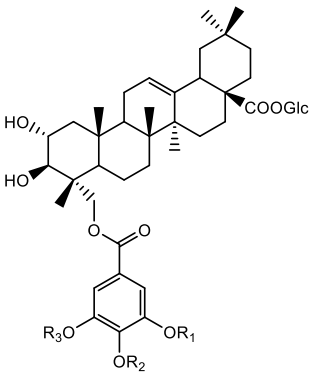 **126 R1=R2=Me, R3=H** **127 R1=R2=R3=Me** 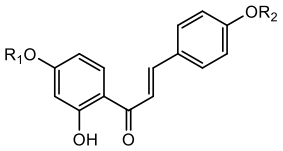 **124 R1=H, R2=Me** **125 R1=Me, R2=H** 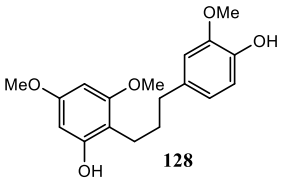 **128**	
T. calcicola	Termicalcicolanone A (**129**) Termicalcicolanone B (**130**) 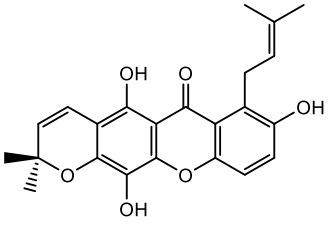 **129** 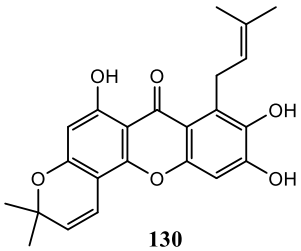 **130**	**Anticancer** (Cao et al., 2007)
T. Laxiflora	Gallic acid (**131**), flavogallic acid (**132**), terchebulin (**133**) and ellagic acid (**134**)	**Antiacne, antibacterial and antioxidant** (Muddathir et al., 2013) **Nematicidal activity** (Nguyen et al., 2013)

	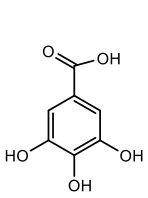 **131** 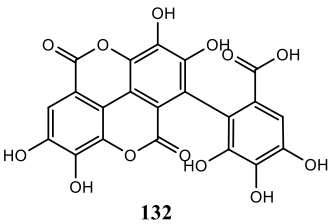 **132** 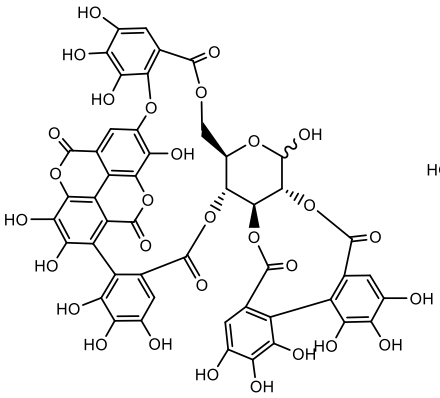 **133** 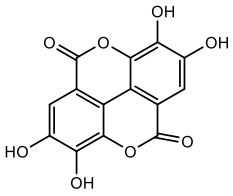 **134**	
T. chebula	Nine phenolic compounds, including two phenolic carboxylic acids (**135**, **136**), seven hydrolysable tannins (**137-143**), eight triterpenoids, including four oleanane-type triterpene acids (**144-147**) and four of their glucosides (**148-151**). 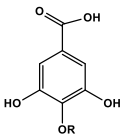 **135 R=H** **136 R=Me** 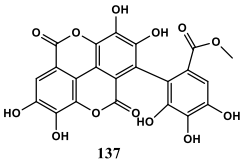 **137** 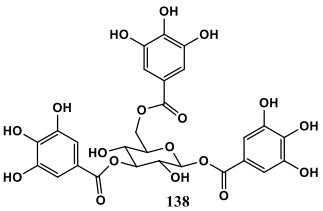 **138** 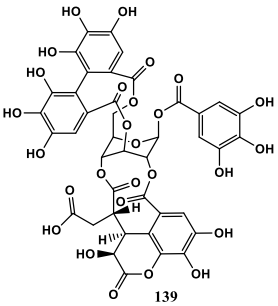 **139**	**Anticancer, anti-inflammatory and anti-oxidant** (Manosroi et al., 2013, Tokura and Kagawa, 1995, Lee et al., 1995) **Anti-bacterial** (Bag et al., 2013) **Anti-mutagenic, chemo-preventive** (Pellati et al., 2013) **Radio-protective** (Dixit et al.,

	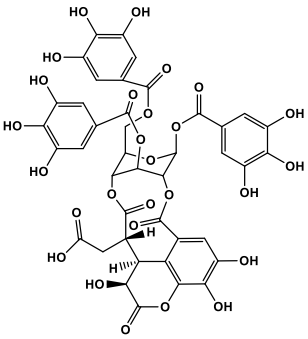 140 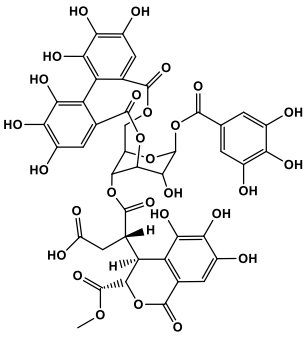 141 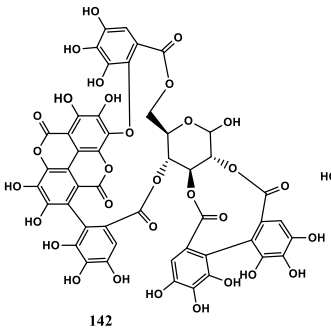 142 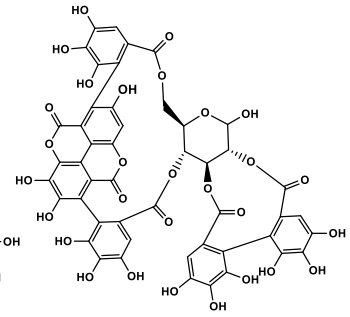 143 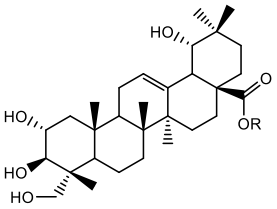 144 R=H 148 R=Glc 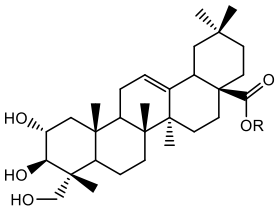 145R=H 149 R=Glc 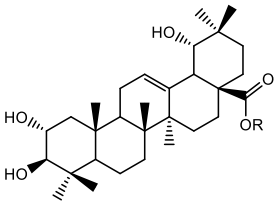 146 R=H 150 R=Glc 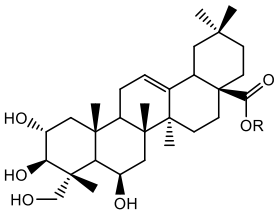 147 R=H 151 R=Glc Olean-12-en-28-oic acid, 2,19-dihydroxy-3-oxo-,4-O-(6-deoxy-α-L-mannopyranosyl)-β-D-glucopyranosyl ester, (2α,19α)- (9CI) (**152**) and 4H-1-Benzopyran-4-one, 2-[4-[(3-O-β-D-galactopyranosyl-β-D-glucopyranosyl)oxy]-2-methoxyphenyl]-2,3-dihydro-5,7-dimethoxy-, (2S)- (**153**).	2013) **antifungal and antifeedant** (Srivastava and Srivastava, 2004, Chouksey and Srivastava, 2001)

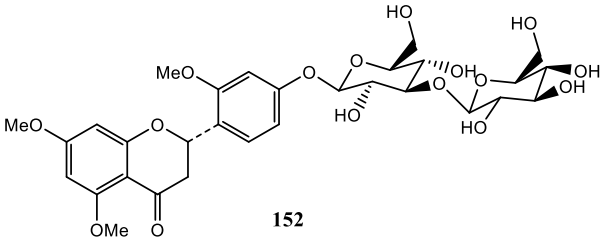

152

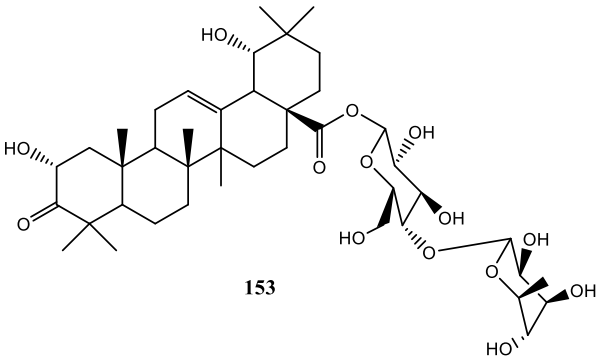

153

2α,19α-dihydroxy-3-oxo-olean-12-en-28-oic acid-28-O-β-D-glucopyranoside (**154**) and chebulanin (**155**)

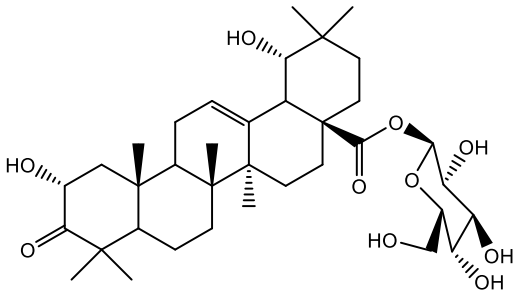

154

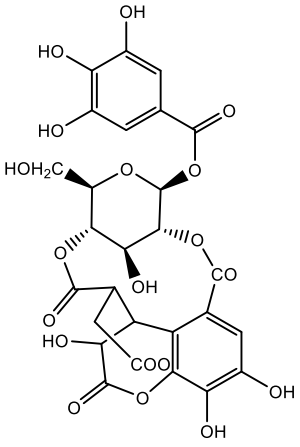

155

T. arjuna	A new fatty alcohol (E)-3,5,7,16 tetramethylheptadeca-2-en-1-ol (**156**), luteoline (**157**), arjunolic acid (**158**), ursolic acid (**159**), casuarinin (**160**) and arjunin (**161**) 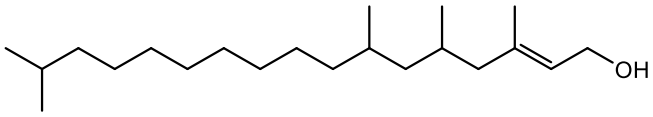 **156** 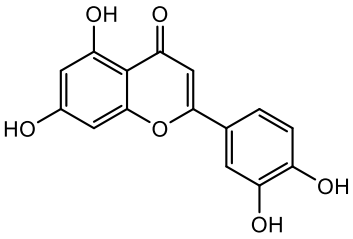 **157** 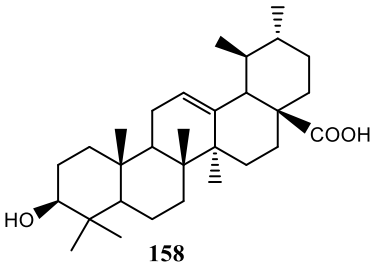 **158** 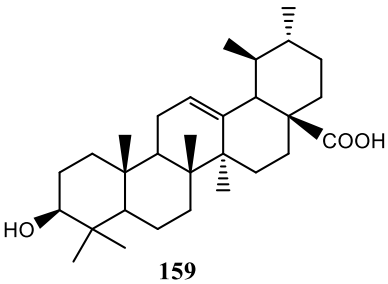 **159**	**Anti-leishmanial** (Ross et al., 2013) **Anticancer** (Pettit et al., 1996, Ramesh et al., 2012, Biswas et al., 2010, Kuo et al., 2005, Kandil and Nassar, 1998)

	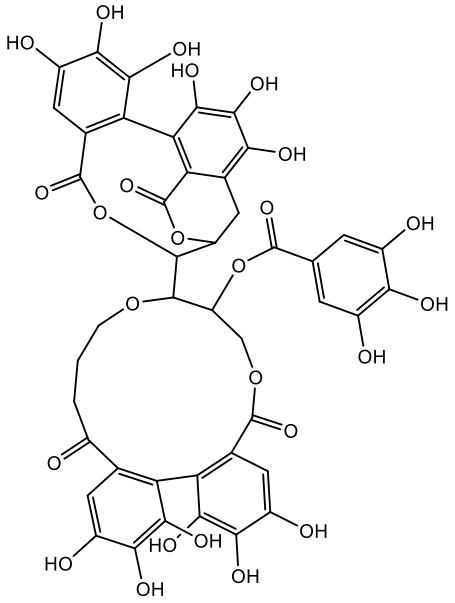 **160** 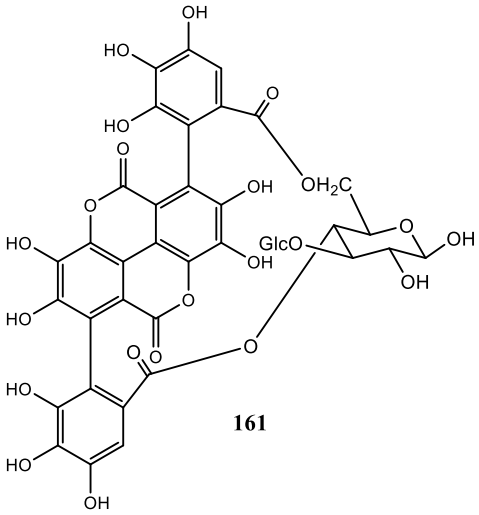 **161**	
T. brownii	β-sitosterol (**162**), stigmasterol (**163**), monogynol A (**164**), betulinic acid (**165**) and arjungenin (**166**)	**Antifungal and anti-bacterial** (Opiyo et al., 2011).

	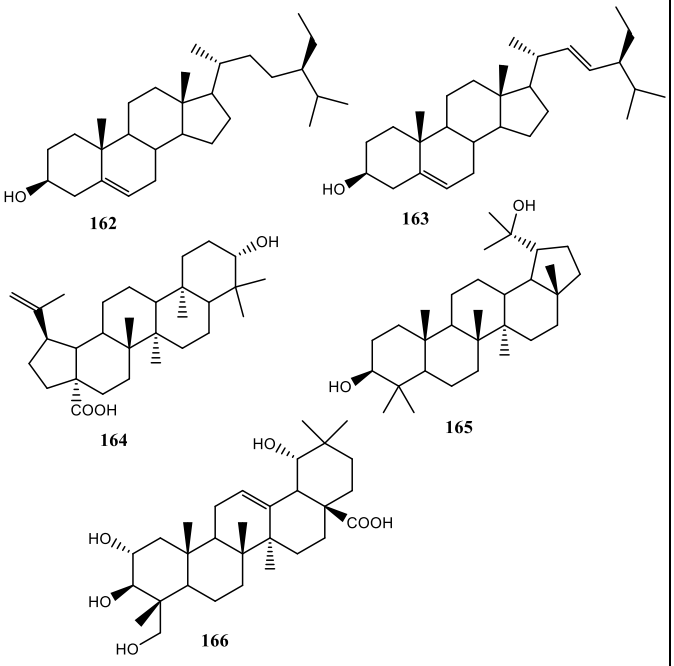	
T. tropophylla	New oleanane-type triterpenoid saponin (**167**) 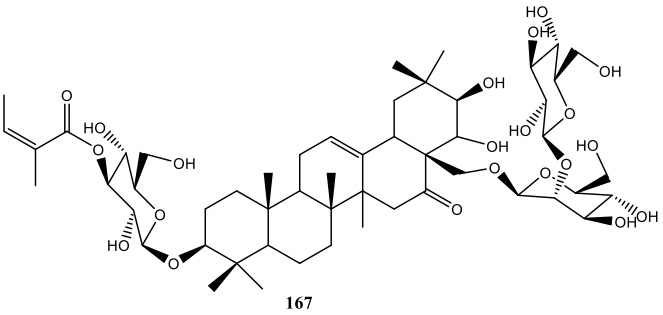	**Anti-proliferative** (Cao et al., 2009)
T. bellerica	7-O-α-L-rhamnopyranoside (**168**), termilignan (**169**) and thannilignan (**170**) 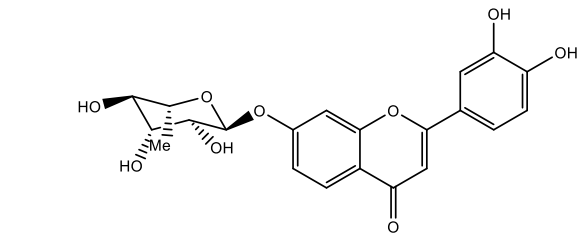 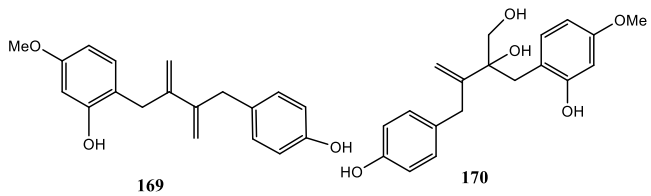	**Anti-microbial** (Asati et al., 2008) **anti-HIV-1, antimalarial, and antifungal** (Valsaraj et al., 1997)

T. sericea	Termilignan B (**171**), anolignan B (**172**) 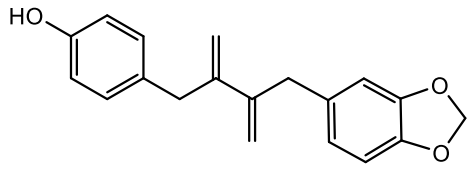 **171** 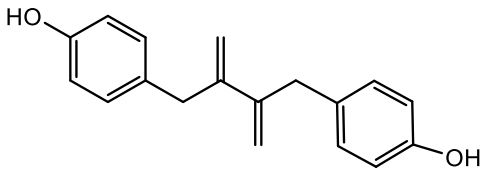 **172**	**Anti-microbial and anti-inflammatory** (Eldeen et al., 2008),(Eldeen et al., 2006)
T. superba	(7S,8R,7'R,8'S)-4'-hydroxy-4-methoxy-7,7'-epoxylignan (**173**) and meso-(rel 7S,8R,7'R,8'S)-4,4'-dimethoxy-7,7'-epoxylignan (**174**) 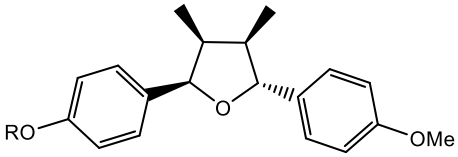 **173** R=H **174** R=Me	**α-Glucosidase inhibitor** (Wansi et al., 2007)
T. glaucescens	Glaucinoic acid (2α,3β,19α,24-tetrahydroxyolean-12-en-30-oic acid) (**175**) 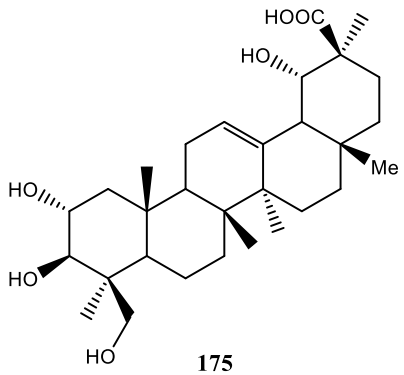 **175**	**β-glucuronidase inhibitor** (Atta ur et al., 2005)
T. myriocarpa	Flavogallonic acid methyl ester (**176**)	**Hepato-protective** (Marzouk et al., 2002)

	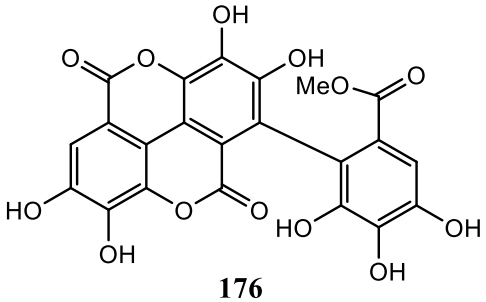 **176**	
T. alata	2α,19α-dihydroxyolean-12-en-28-Me ester-3β-O-rutinoside (**177**) 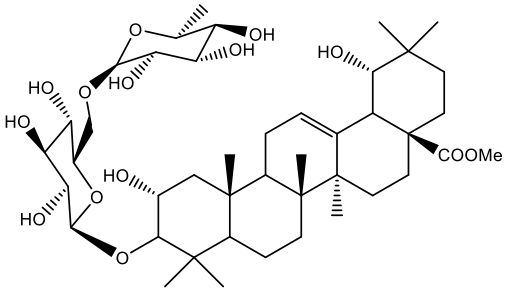 **177**	**Anti-microbial** (Srivastava et al., 2000)
T. calamansanai	2-O-galloylpunicalin (**178**) and sanguiin H-4 (**179**) 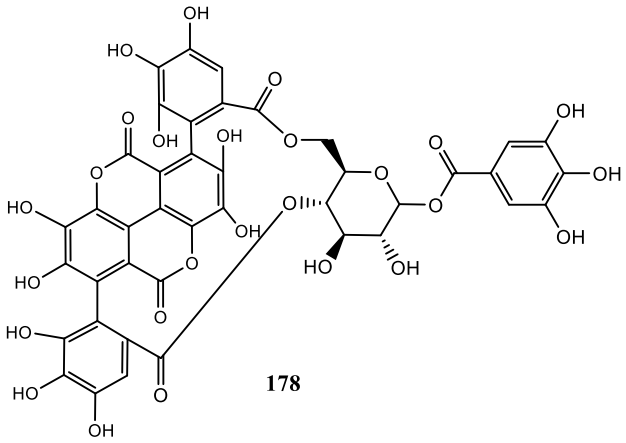 **178** 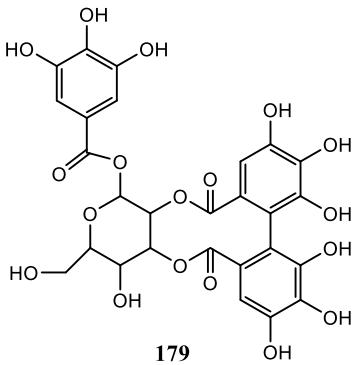 **179**	**Antitumor** (Chen et al., 2009)

T. catappa	Punicalagin (**122**)	**Antitumor** (Chen and Li, 2006)
T. macroptera	Punicacortein C (**180**) 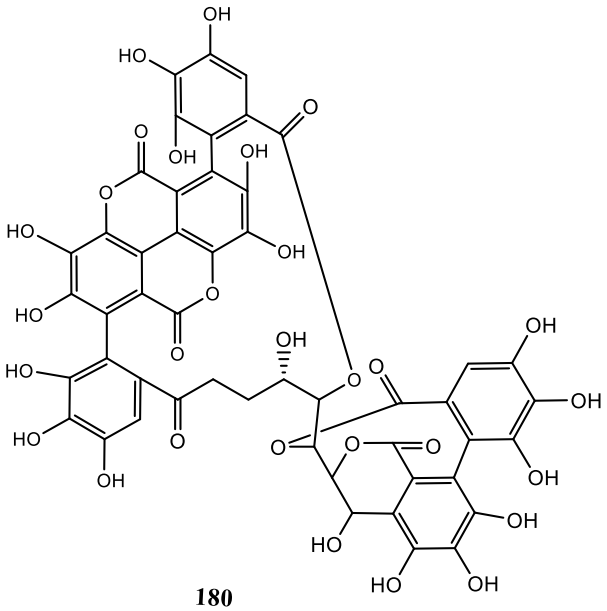 **180**	**Cytotoxic** (Conrad et al., 2001)

1.12.2. Genus *Markhamia*

Markhamia roots are used to treat backaches, pains, and to reduce stomach gas. Other uses that were reported in the literature like treatment for scrofula, hookworm, snakebites and convulsions in children; and boiled roots, bark and leaves used as an inhalant.

Table 2: Bioactive secondry metabolites from *Markhamia* species

Plant species	Name/Structure	References
M. tomentosa	2-acetylnaphtho[2,3-b]furan-4,9-dione (**181**) and 2-acetyl-6-methoxynaphtho[2,3-b]furan-4, 9-dione (**182**)	**Anticancer and Anti-protozoal** (Tantangmo et al., 2010)

	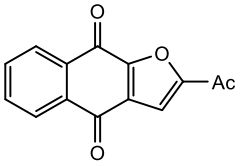 **181** 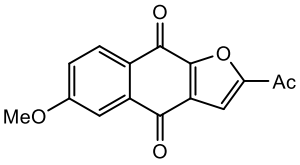 **182**	
M. obtusifolia (Baker) Sprague	Pomolic acid (**183**) 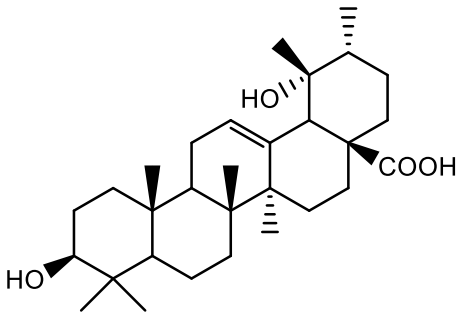 **183**	**Anti-candida** (Nchu et al., 2010)
M. lutea	musambins A-C (**184**, **186** and **188** resp.) and their 3-O-xyloside derivatives (**185**, **187** and **189** resp.)	**Antiparasitic and mild cytotoxic** (Lacroix et al., 2009) **Antiviral** (Kernan et al., 1998)

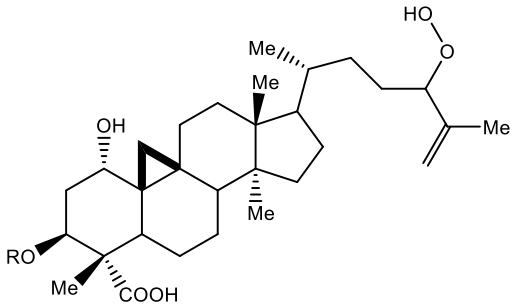

184 R=H
185 R=Xy

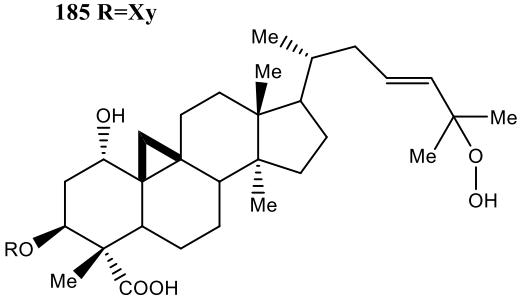

186 R=H
187 R=Xy

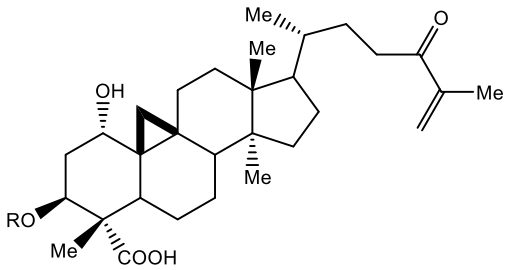

188 R=H
189 R=Xy

Lutoside A (**190**), lutoside B (**191**), lutoside C (**192**), verbascoside (**193**) and isoverbascoside (**194**).

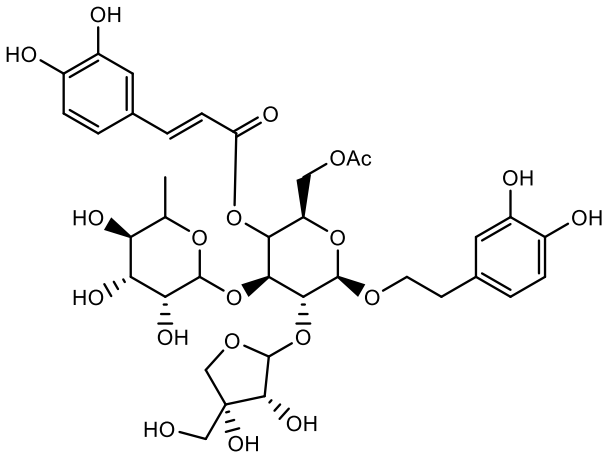

190

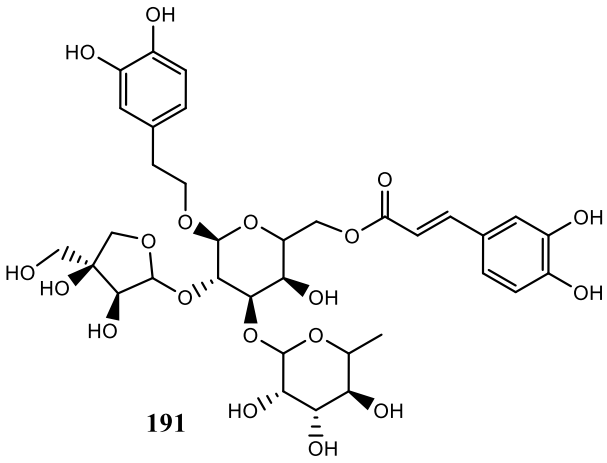

191

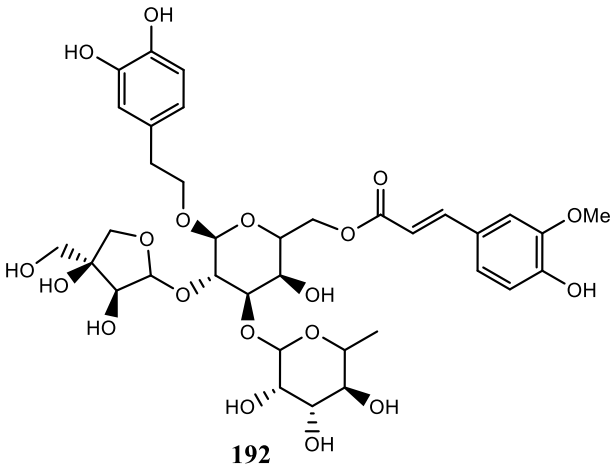

192

	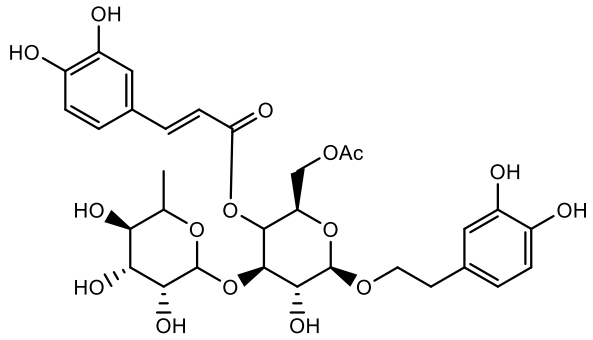 **193** 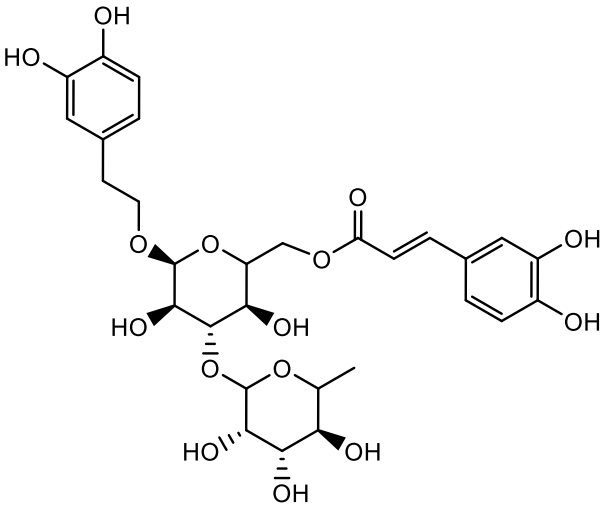 **194**	
M. zanzibarica	γ-Sitosterol (**195**) 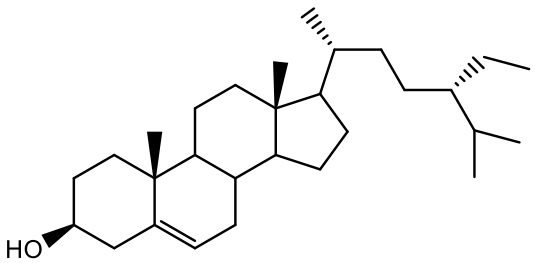 **195**	**Cytotoxic** (Khan and Mlungwana, 1999)
M. hildebrandtii	Three naphthoquinone derivatives are lapachol (**196**), 2-isopropenylfurano-1,4-naphthoquinone (**197**), and dehydro-α-lapachone (**198**)	**Antitumor** (Chen and Lee, 1986)

	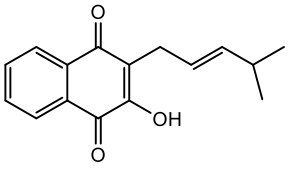 **196** 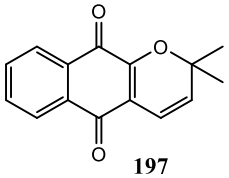 **197** 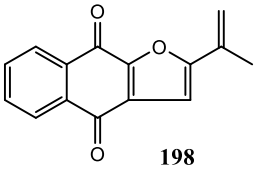 **198**	

1.13. Hypothesis and Aim of this Project

Hypothesis: Application of metabolomics studies in the discovery of bioactive endophytic metabolites mainly in the bioactive screening where rapid dereplication of known compounds and identification of lead bioactive metabolites is important. This included different analytical techniques followed by multivariate data analysis (MVDA) to prioritise the extracts and/or fractions that will go for further fractionantion and minimize the redundant analysis in isolation steps of active compounds from the endophytic fungi, which reduce the chance of re-isolating of known metabolites.

The ultimate aim of this study is to find novel potential anticancer and/or antimicrobial compounds isolated from endophytic fungi of some important Egyptian medicinal plants, which can be later cultivated and fermented to produce the active secondary metabolites at a larger scale. Endophytes from Egyptian medicinal plants of various diverse habitats will be explored and screened for anti-cancer and/or antimicrobial activity. HPLC-HRFTMS and NMR dereplication studies were used to identify novel chemical entities in quick and efficient manner. This brings targeted-isolation work on the biologically active compounds with the aim of deciding if activity is due to known compounds or new chemical entities. Metabolomics tools will aid in optimizing the cultivation media that produce the largest quantity of the bioactive metabolites and choosing the extracts and/or fractions will be submitted for further fractionation work. Bioassay guided fractionation will sort the fractions and/or pure compounds according to their activities. ESI-HRMS, 1D and 2D NMR spectroscopic techniques will be employed to elucidate the purified compounds from the three endophytes *Aspergillus aculeatus, A. flocculus* and *Curvularia* sp.

Chapter 2: Materials and Methods

2. Materials and methods

2.1. Materials

2.1.1 Plant materials

Plant samples were collected from Zohriya Botanical Garden in Al-Zamalek Island under the Cairo Tower, Giza, Egypt. The plants in the whole garden were identified by Dr. Therese L. Yousef, senior expert - Orman Garden, Eng. Mervat A. Hasan, herbarium curator - Orman Garden and Eng. Mamdooh M. Shokary, executive manager, Zohriya Garden. Fresh plant materials including stems and leaves from each plant species (Table 3) were cut a day before isolation of fungal strains, kept in tightly closed plastic bags under 4° C and transported to Strathclyde institute of pharmacy and biomedical science, Glasgow, UK for the isolation work.

2.1.2 Pure fungal strains isolated from the selected plants

Table 3: List of the endophytic fungal strains isolated from different organs of the collected plant samples and their corresponding plant materials.

Fungal strain	**Plant part**	**Plant name/Voucher specimen** (Orman Garden herbarium)
Drac-Froz F1	Leaf	*Dracaena dermensis* Family Agavaceae Voucher specimen: 290
Drac-Froz F2		
Drac-Mid		
Markh-Stem F1	Stem	*Markhamia platycalyx* Family Bignoniaceae Voucher specimen: 633
Markh-Stem F2		
Markh-Stem F3a		
Markh-Stem F3b		

Markh-leaves	Leaf	
Markh-flowers	Flower	
Syz-Stem F1	Stem	*Eugenia uniflora* Family Myrtaceae Voucher specimen: 340
Syz-Stem F2		
Syz-leaves	Leaf	
Tab-leaves F1a	Leaf	*Tabebuia argentea* Family Bignoniaceae Voucher specimen: 805
Tab-leaves F1b		
Tab-leaves F2		
Ter-yl-F1a	Leaf	*Terminalia laxiflora* Family Combretaceae Voucher specimen: 822
Ter-yl-F1b		
Ter-Al-F1		
Ter-Al-F2		
Ter-st-F1	Stem	
Ter-st-F2		

2.1.3 Media

2.1.3.1. Composition of malt agar (MA) medium

MA medium was used for short-term storage of fungal cultures or fresh seeding for preparation of liquid cultures.

Agar-Agar	15.0 g
Malt extract	15.0 g
Distilled water	To 1000 ml
PH	7.4 - 7.8 (adjusted with NaOH/HCl)

For the isolation of endophytic fungi from plant tissues, chloramphenicol or streptomycin (0.2or 0.1 g, respectively) were added to the medium to suppress bacterial growth.

2.1.3.2. Composition of Wickerham medium for liquid cultures

Yeast extract	3.0 g
Malt extract	3.0 g
Peptone	5.0 g
Glucose	10.0 g
Distilled water	to 1000 mL
pH	7.2 - 7.4 (adjusted with NaOH/HCl)

2.1.3.3. Composition of rice medium for solid cultures

Rice	100 g
Distilled water	100 ml

Water was added to the rice and kept overnight then autoclaved.

2.1.4 Chemicals

2.1.4.1. General laboratory chemicals

Acetic acid	Acros Organic
Anisaldehyde (4-methoxybenzaldehyde)	Acros Organic
Butanol	Merck
Concentrated sulphuric acid	Fisher scientific
Dimethylsulfoxide	Euriso-Top
Formic acid	VWR
Isopropyl alcohol	Fisher scientific
Potasium hydroxide	Sigma
Glacial acetic acid	Alfa Aesar

Diphenyl boryloxyethanolamine	Fluka-sigma
Polyethylene glycol 400	Fisher scientific

2.1.4.2. Chemicals for culture media

Agar-agar	Oxoid
Chloramphenicol	Acros Organics
Glucose	Fisons
Malt extract	Oxoid
NaCl	VWR
Peptone	Fisher scientific
Streptomycin	Sigma
Yeast extract	Oxoid

2.1.4.3. Chemicals for PCR

RED Extract-N-Amp™ Plant PCR Kit	Sigma
GenElute™ Gel extraction kit	Sigma

2.1.4.4. Chemicals for agarose gel electrophoresis

Agarose	Serva
Tris/Borate/EDTA (TBE) buffer	Merck
Ethidium bromide	Serva
Standards	NEB

2.1.5 Chromatography

2.1.5.1. Stationary phase

Pre-coated TLC plates, Silica Gel 60 F254, layer thickness 0.2 mm	Merck
Pre-coated TLC plates , RP-18, F254 S, layer thickness 0.25 mm	Merck
Pre-coated TLC plates, Cellulose	Merck
Sephadex LH 20, 0.25 - 0.1 mm mesh size	Merck

Diaion HP20	Supelco, USA

2.1.5.2. Spray reagents

The reagents were stored in amber-colored bottles and kept refrigerated until use. TLC was used to monitor the identity of each of the fractions and the qualitative purity of the isolated compounds. It was also utilized to optimize the solvent system that would be applied for column chromatography.

Anisaldehyde/H_2SO_4 Spray Reagent

Methanol	85 mL
Glacial acetic acid	10 mL
Conc. H_2SO_4	5 mL (added slowly)
Anisaldehyde	0.5 mL

Naturstoff reagent for flavonoids

Solution A: 1 % diphenyl boryloxyethanolamine in methanol.
Solution B: 5 % polyethylene glycol 400 in ethanol.

Ferric chloride reagent (1 % in ethanol) for phenolic compounds

2.1.6 Solvents

2.1.6.1. Normal grade solvents

Acetone	Sigma Aldrich
Dichloromethane	Fisher scientific
Ethyl acetate	Fisher scientific
n- N-hexane	Fisher scientific
Butanol	Sigma Aldrich

Methanol	Sigma Aldrich

2.1.6.2. HPLC grade solvents

Acetonitrile	HPLC grade (Fisher scientific)
Methanol	HPLC grade (Fisher scientific)
Pure grade water	distilled and heavy metals free water obtained by passing distilled water through Purite Ltd. Select Neptune filter

2.1.6.3. Solvents for NMR

Acetone-d_6	Euriso-Top
Chloroform-d_6	Euriso-Top
DMSO-d_6	Euriso-Top

2.2. Equipment

2.2.1. General Equipment

The analytical miller (model: IKA A11 Basic) was purchased from IKA, Germany. Two rotary evaporators (model no: R-110 and R-3) were from BÜCHI, Switzerland. The centrifuge used was Force 7 from Fisher Scientific. The Ultrawave sonicator was from Scientific Laboratory Supplies, Ltd. The UV lamp (UVGL-55 Handheld UV Lamp) was purchased from UVP, Cambridge, UK. The heat gun HL 2010 E Type 3482 was the product of Steinel, USA. The Stuart® block heater SBH 130D/3 was from Bibby Scientific Ltd., Staffordshire, UK. The freeze dryer (model: Christ Alpha 2-4) was from Martin Christ Gefriertrocknunsanlagen GmbH, Germany. The optical rotations of the compounds were measured on a 341 Polarimeter from PerkinElmer, Inc., USA.

2.2.2. Microbiology Equipment

The laminar flow hood (BioMAT2) was purchased from Medical Air Technology, UK. The stand incubator (Incu-160S) used for agar plates was from SciQuip Ltd., Shropshire. The homogenizer (IKA T18 Basic Ultra-Turrax) and handheld homogenizer (Ultra-Turrax T8) came from IKA Labortechnik, Germany.

2.2.3. Liquid Chromatography – Mass Spectrometry Instruments

The High Pressure Liquid Chromatography was carried out using Dionex UltiMate3000-ThermoScientific Exactive system instrument, Germany. Separated compounds were passed on UV detectors and a Finnigan LTQ HRESI-MS spectrometer. Another HPLC-MS system was used for some of the later analyses was the Accela HPLC system coupled to an Exactive mass spectrometer (Thermo Scientific, Germany). The low-resolution mass spectrometry system was a Finnigan LCQ-Deca coupled to an HPLC (series 1100) from Hewlett Packard. Fragmentation was performed on a Finnigan Surveyor system coupled to a Thermo-Finnigan LTQ Orbitrap (Thermo Scientific, Germany).

2.2.4. Gas Chromatography- Mass Spectrometry Instruments

The high-resolution GC-MS at SIPBS is a Focus GC coupled to a DSQ II from Thermo Scientific, Germany. The column, InertCap 1MS (ID: 0.25 mm, length: 30 m, df: 0.25 μm) was purchased from GL Sciences Inc., Japan. The low-resolution GC-MS used at the Department of Pure and Applied Chemistry is a Thermo Finnigan Polaris Q with Trace GC. The column used was an Agilent DB5-ms UI (ID: 0.25 mm, length: 30 m, df: 0.25 μm).

2.2.5. Nuclear Magnetic Resonance Instruments

The Nuclear Magnetic Resonance spectroscopy machine JNM-LA400 model was from JEOL, Japan and the magnet NMR AS400 model EUR0034 came from Oxford Instruments, England. The NMR has a Pulse-Field Gradient "Autotune"TM probe 40TH5AT/FG broadband high sensitivity probe for 5mm tubes. It has FG coils, 2H lock channel and can operate at various temperatures.
An AVANCE-III 600 instrument with a 14.1 T Bruker UltraShield magnet from the Department of Pure and Applied Chemistry was also used. It has a 24 position autosampler, 3 channel console, is DQD and Waveform-equipped and can use

either a BBO-z-ATMA-[31P-183W/1H] probe or a TBI-z-[1H, 13C, 31P-15N] probe.

DMSO and $CDCl_3$ Shigemi® tubes and Wilmad® NMR capillary tubes were purchased from Sigma-Aldrich Inc., USA.

2.2.6. Medium pressure Liquid Chromatography Equipment

Medium pressure liquid chromatography (MPLC) or flash chromatography is a separation technique in which pressure is applied to elute the sample through the column at a faster rate and to get better separation (Roge et al., 2011). The solvent system and the column to be used were selected following thin layer chromatography so the targeted band or the compound of interest had an Rf value of 0.4 on the TLC plate.

The BÜCHI MPLC instrument was the Sepacore Purification System, consisting of two C-601 pump modules and the C-615 pump manager (BÜCHI, Switzerland). This allowed binary solvent gradients with flow rates of 2.5 to 250 mL/min. The columns and the column stand were purchased from VersaFlash/Supelco, Sigma-Aldrich, Germany. The fraction collector (CF2) was from Spectrum Labs. The Reveleris® Flash Forward system of Grace Davison Discovery Sciences (Illinois, United States) was also used for flash chromatography. This system was characterized by having two detectors, an evaporative light scattering detector (ELSD) and a UV detector (wavelength range: 200-500 nm). This guaranteed greater sensitivity and the detection of all peaks and not only the UV-active compounds. The system consisted of four independent channels so up to four solvents can be used in a binary gradient during a single run. The flow rate could range from 4 to 200 mL/min and was automatically adjusted if the pressure became too high. The fraction collector was built into the system and the trays recognised by the software in order to reduce errors. In addition, the chromatogram could be saved and printed. Another system, the Biotage® IsoleraTM Spektra One Flash Purification System ISO-1SV, a product of Biotage, Uppsala, Sweden, was also used. This had a UV detector (wavelength range: 200-400 nm) but did not have an ELSD. Again, the Biotage had four solvent channels allowing four solvents to be used in a binary

gradient during a single run. Biotage® SNAP cartridges were used which permitted the loading of samples onto frits before being placed into the column. This was suitable for samples insoluble in the starting solvent system.

2.2.7. TLC Plates

The normal phase thin layer chromatography plates (TLC silica gel 60 F254), reverse phase TLC plates (TLC silica gel 60 RP-18 F254S) and preparative TLC plates (TLC silica gel 60 F254 on 20x20 cm aluminium sheets) were from Merck KGaA, Germany.

2.2.8. Software

LC-MS and GC-MS spectra were viewed using Thermo Xcalibur 2.1 (Thermo Scientific, Germany). To convert the raw data into separate positive and negative ionisation files, a program called msconvert from ProteoWizard (pwiz) was used. The files were then imported to the data mining software, MZmine 2.10.

The databases used for the identification of compounds were the Dictionary of Natural Products (DNP) 2012 and AntiMarin 2012, a combination of Antibase and MarinLit. MestReNova (MNova) 2.8 by Mestrelab Research, S.L, (Santiago de Compostela, Spain) was used to process all NMR data. SIMCA 13 (Umetrics AB, Umeå, Sweden) was used for multivariate data analysis.

2.3. Taxonomy of Identified fungal strains

2.3.1. Aspergillus aculeatus

The fungus was isolated from fresh young leaves of *Terminalia laxiflora* (Combretaceae).

Kingdom:	Fungi
Phylum:	Ascomycota
Class:	Eurotiomycetes
Subclass:	Eurotiomycetidae
Order:	Eurotiales
Family:	Trichocomaceae

Genus:	*Aspergillus*
Species:	*A. aculeatus*

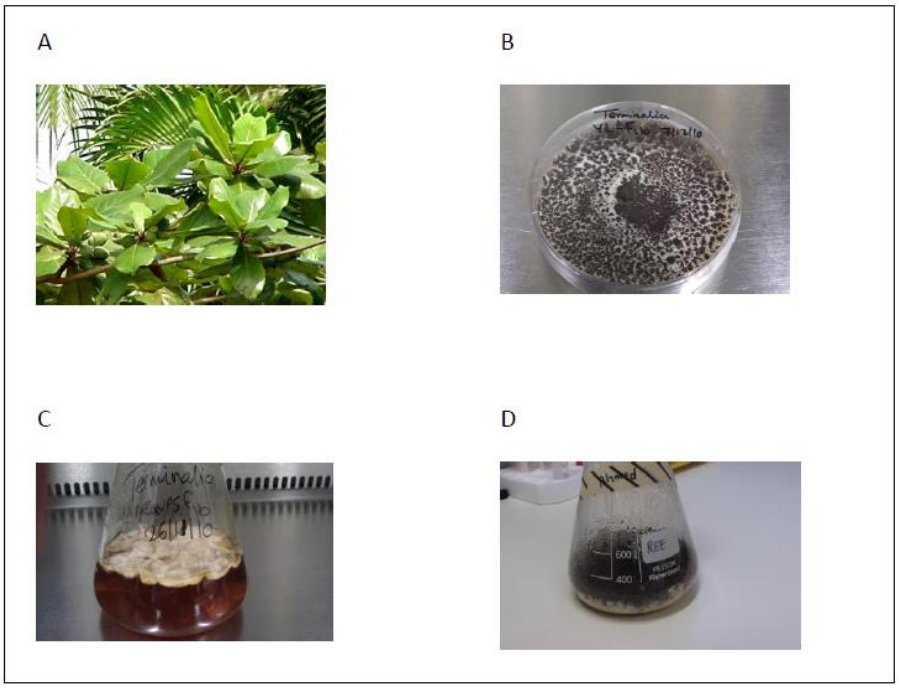

Fig.5 A: *Terminalia laxiflora* leaves, B*: Asperagillus aculeatus* on MA plate C: Liquid culture in Wickerham medium, D: Solid rice culture

2.3.2. Curvularia sp.

The fungus isolated from the fresh adult leaves of *Terminalia laxiflora* (Combretaceae).

Kingdom:	Fungi
Phylum:	Ascomycota
Class:	Euascomycetes
Order:	Pleosporales
Family:	Pleosporaceae
Genus:	*Curvularia*
Species:	*Curvularia* sp.

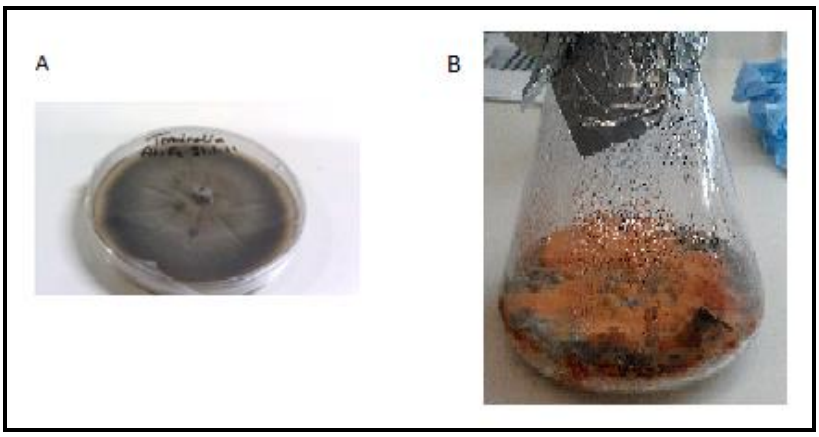

Fig.6 A: *Curvularia* sp. on MA plate B: Rice culture of *Curvularia* sp.

2.3.3. Aspergillus oryzae

The fungus was isolated from the fresh leaves of *Dracaena dermensis* (Agavaceae), *Terminalia laxiflora* (Combretaceae) and *Tabebuia argentea* (Bignoniaceae).

Kingdom:	Fungi
Division:	Ascomycota
Class:	Eurotiomycetes
Order:	Eurotiales
Family:	Trichocomaceae
Genus:	*Aspergillus*
Species:	*A. oryzae*

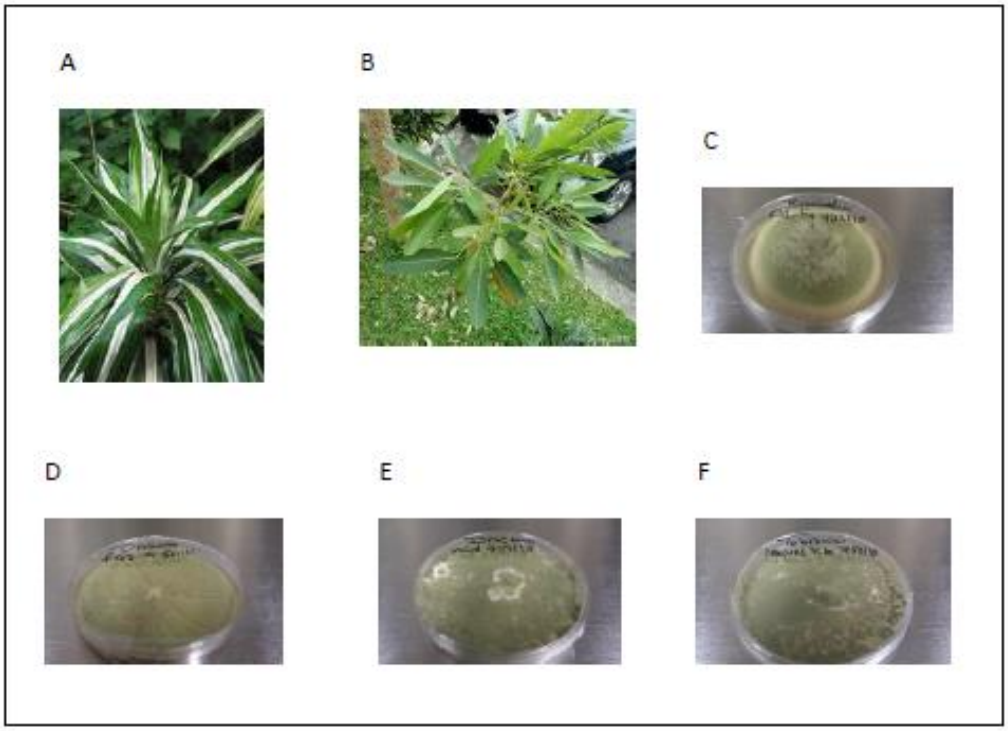

Fig.7 A: *Dracaena dermensis*, B: *Tabebuia argentea*, C: *A. oryzae* from *T. laxiflora*, D: *A. oryzae* from *Dracaena* Frozen leaves, E: *A. oryzae* from *Dracaena* midrib, F: *A. oryzae* from *Tabebuia* leaves

2.3.4. Aspergillus flocculus

The fungus was isolated from the fresh stem of *Markhamia platycalyx* family Bignoniaceae.

Kingdom:	Fungi
Phylum:	Ascomycota
Class:	Eurotiomycetes
Subclass:	Eurotiomycetidae
Order:	Eurotiales
Family:	Trichocomaceae
Genus:	*Aspergillus*
Species:	*A. flocculus*

Fig.8 A: *Markhamia platycalyx* B: *A. flocculus* MA plate C: Liquid broth culture, D: Rice solid culture

2.3.5. Syncephalastrum racemosum

The fungus was isolated from the fresh stem of *Markhamia platycalyx* family Bignoniaceae.

Kingdom:	Fungi
Phylum:	Zygomycota
Subphylum:	Mucoromycotina
Class:	Zygomycetes
Order:	Mucorales
Family:	Syncephalastraceae
Genus:	*Syncephalastrum*
Species:	*S. racemosum*

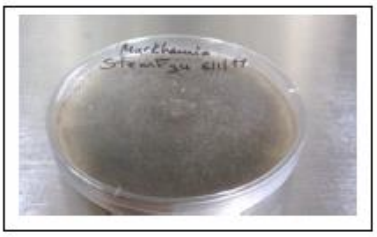

Fig.9 *S. racemosum* on MA plate

2.4. Methodology

2.4.1. Collection of plant material and purification of the fungal strain

Egyptian medicinal plants, with emphasis on unexplored associated endophytes, have been collected and identified taxonomically by a botanist Dr. Therese L. Yousef, senior expert at Orman Garden, Giza, Egypt where the voucher specimens are there. Plant materials were cut into small pieces, washed with sterilized demineralized water, then thoroughly surface sterilized with 70% isopropanol for 1-2 minutes and ultimately air dried under a laminar flow hood. This is done in order to eliminate surface contaminating microbes. With a sterile scalpel, outer tissues were removed from the plant samples and the inner tissues were carefully dissected under sterile conditions and laid over malt agar (MA) plates containing chloramphenicol, in order to prevent the bacterial growth. After 3-4 weeks of incubation at 30°C, hyphal tips of the fungi were removed and transferred to fresh MA medium. Plates are prepared in duplicates to eliminate the possibility of contamination. Pure strains were isolated by repeated inoculation.

2.4.2. Cultivation of pure fungal strains

2.4.2.1. Cultivation for short-term storage

Fungi were grown on MA medium at 27-30°C for 14 days. Cultures were stored at 4º C for a maximum period of 6 months, and then re-inoculated onto fresh media.

2.4.3. Identification of fungal strain

Fungal species were identified using molecular biological techniques through DNA extraction, amplification by PCR, and finally sequencing using primers ITS1, ITS4, β-tubulins and specifically designed primers AT1F, AT1R for Ascomycetes e.g. *Aspergillus* sp. and *Zygomycetes* primers e.g. V9D and LS266 from Eurofins Genomics™.

2.4.3.1. DNA extraction

A piece of 0.5 cm^2 was cut from the fungal culture in the MA plate and freeze-dried in 2ml tube. 100 µL of rapid lysis solution from Sigma REDExtract-N-Amp™ Plant PCR Kit was then added followed by incubation for 10 min at 95℃, sometimes vortex with glass beads and/or mixing using a mixer mill was required. 100 µL of dilution solution was added after heating for neutralization.

2.4.3.2. DNA amplification

DNA amplification was done by using a polymerase chain reaction (PCR) in which Sigma REDExtract-N-Amp™ Plant PCR Kit's polymerase and different primers were used. 4 µL of DNA template was added to 46 µL from the polymerase master mixture which consisted of 25 µL REDExtract-N-Amp™ Plant PCR solution, 3 µL of each primer (10 pmol / µL each) and 18 µL RNA free water. The 50 µL solution sample was then subjected to the PCR reaction.

Ascomycetes Primers: e.g. ITS and β-tubulin

ITS1: (5'-TCCGTAGGTGAACCTGCGG-3')
ITS4: (5'-TCCTCCGCTTATTGATATGC-3')
Bt2a: (5'-GGTAACCAAATCGGTGCTGCTTTC-3')
Bt2b: (5'-ACCCTCAGTGTAGTGACCCTTGGC-3')

Primers specifically designed to differentiate between Aspergillus flavus and A. oryzae

AT1-For: (5'-GCCATCTTTCCTCCTTCTCTCTTC-3')
AT1-Rev: (5'-TCGAAGGCATTGAGACATACCAG-3')

Zygomycetes Primers

V9D: (5'-TTAAGTCCCTGCCCTTTGTA-3')

LS266 (5'-GCATTCCCAAACAACTCGACTC-3')

PCR protocol

Initial denaturation was done at 95°C for 15 mins followed by denaturation at 95 °C for 1 min then annealing at 56°C for 0.5 min Or at 62℃ for 0.5 min for β-tubulin primers. Extension process was accomplished at 72°C for 1 min followed by final extension at 72°C for 10 mins. Steps, except initial denaturation and final extension, were repeated 35 times.

Touchdown PCR protocol

Initial denaturation was done at 95 °C for 15min followed by denaturation at 95°C for 1 min then annealing started at 68°C reaching 56°C for 0.5 min for 12 cycles then 56°C for rest of cycles. Extension process was at 72°C for 1 min followed by final extension at 72 °C for 10min. Steps, except initial denaturation, intial annealing and final extension, were repeated 35 times.

2.4.3.3. DNA electrophoresis

15µL of the PCR product and 6µL of DNA size marker HyperLadder™ II (Bioline, UK) were applied to each well of the agarose gel, covered with TBE buffer and allowed to run for 45 min at 60 V. the agarose gel consisted of 0.5 gm agar in 50 mL TBE buffer and stained with 2µL ethidium bromide.

2.4.3.4. Purification of the DNA product

After electrophoresis, the gel was transferred into the UV-transluminator to confirm that the PCR has been successfully carried out and the PCR products had the right size of about 550 bp by comparing them with the DNA ladder. The band was precisely excised from the gel and placed into an Eppendorf tube. The PCR product was isolated from the gel slice using sigma GenElute™ Gel Extraction Kit according to manufacturer's protocol. Three-gel volume of the solubilisation solution was added to the gel and heated at 50-60℃ for 15 min., one gel volume

of isopropanol was added for the precipitation of the DNA. The solution then was applied to the binding column followed by spinning at 13,000 rpm for 1 min. Then washing solution was added to get rid of any impurities followed by spinning at 13,000 rpm. Finally, the collection tube was changed and elution solution was added, followed by spinning to elute the DNA from the column. The DNA concentration was determined using Nano drop 2000 and the PCR product was stored at -20 °C until sequencing.

2.4.3.5. DNA sequencing

30ng of PCR product was added to 3.2pmol primer, 8µL big dye and 20µL RNA free water. Then subjected to PCR reaction commenced with intial denaturation at 96 °C for 1 min then 35 cycles of denaturation at 96 °C for 10 seconds, annealing at 50 °C for 5 seconds followed by extension at 60 °C for 4 mins. The products were stored at 8 °C and then submitted to Dr. Rothwelle Tate for direct sequencing in the sequencing laboratory, SIPBS, Strathclyde University, UK. The next step was the alignment of these sequences through Clustalw® and Boxshade® websites. BLAST search of the FASTA sequence was performed with the option "nr", including GenBank, RefSeq Nucleotides, EMBL, DDBJ and PDB sequences on the BLAST homepage, NCBI, Bethesda, USA.

2.4.4. Fungal Extraction

2.4.4.1. Small scale extraction for screening, metabolomics profiling and dereplication

A plate of each fungal species was transferred into 250 ml flask, then macerated with ethyl acetate and left overnight followed by homogenization and filtration. The precipitate was then macerated with ethyl acetate and filtered (3x200 mL). The filtrate is then dried under vacuum, suspended in 200 mL H_2O and partitioned by adding EtOAc (3 × 200 mL) in a separating funnel. H_2O soluble portion was concentrated and then passed over HP-20 column using methanol as eluant. Methanol and ethyl acetate soluble portions were concentrated, 1mg of each extract was subjected to MS analysis and 5 mg to 10 mg to NMR analysis

for metabolomics profiling and dereplication studies using Dictionary of natural products (DNP version 6.1) and a microbial secondary metabolites database (Antibase version 12.0.2). A sample of 1mg/mL concentration of each fungal extract was prepared in duplicate to be sent to Fondation de Recherche Cancer et Sang, Luxembourg for bioassays against prostate (PC3) and chronic myelogenous leukaemia (K562) cancer cell lines. Another set of samples of concentration 1 mg/100 µL DMSO was sent to Ms. Carol Clements at the Strathclyde Institute for Drug Research (SIDR) to be tested against *Trypanosome brucei brucei.* The purified compounds were prepared in 1mg concentration and sent to Mrs. Louise Young and Ms. Carol Clements at SIDR for bioassay against the same cancer cell lines, *T. b. brucei* and *Mycobacterium marinum.*

2.4.4.2. Cultivation for large scale extraction

Fresh fungal cultures were transferred into Erlenmeyer flasks (1L each) containing 500 mL of Wickerham medium for liquid cultures or 100 g rice for solid cultures (Fig.10). The cultures were then incubated at room temperature as stand cultures for 7, 15 and 30 days. Medium scale cultivation was carried out using 20 and 10 one-L Erlenmeyer flasks for liquid and solid rice cultures, respectively. Moreover, large-scale cultivation was carried out using 20 one-L Erlenmeyer flasks for rice cultures.

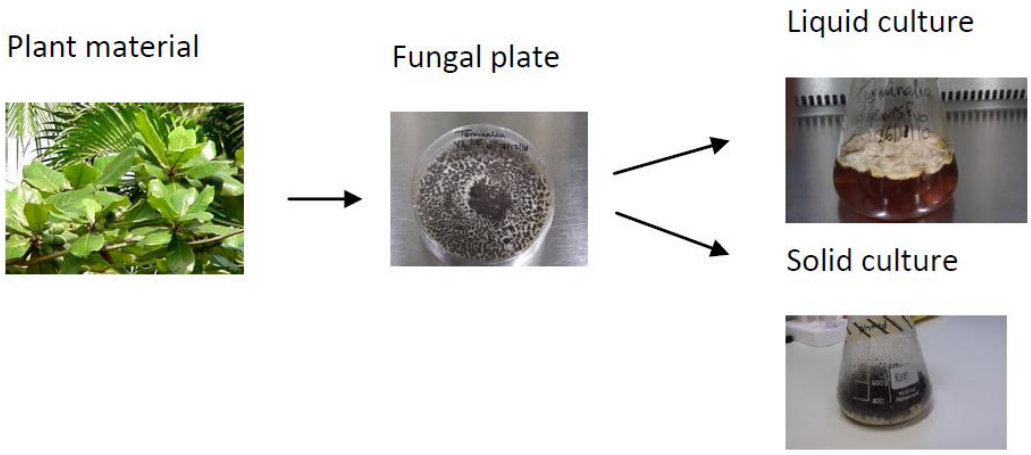

Fig.10 Cultivation for large-scale extraction

2.4.4.3. Extraction of fungal liquid culture

250 mL EtOAc was added to Erlenmeyer flasks containing 500mL culture medium and left overnight to stop cell growth. Culture media and mycelia were then homogenized in the Ultraturrax for 10 min for cell destruction, followed by vacuum filtration using a Buchner funnel. The mycelium residue was discarded while EtOAc culture filtrates were collected, pooled, dried under vacuum, suspended in 200mL H_2O and extracted with EtOAc (3 x 200 mL) using a separating funnel. The pooled EtOAc extracts were then concentrated under pressure with a rotary evaporator. The water phase was passed through a HP-20 using MeOH as eluent (Fig.11).

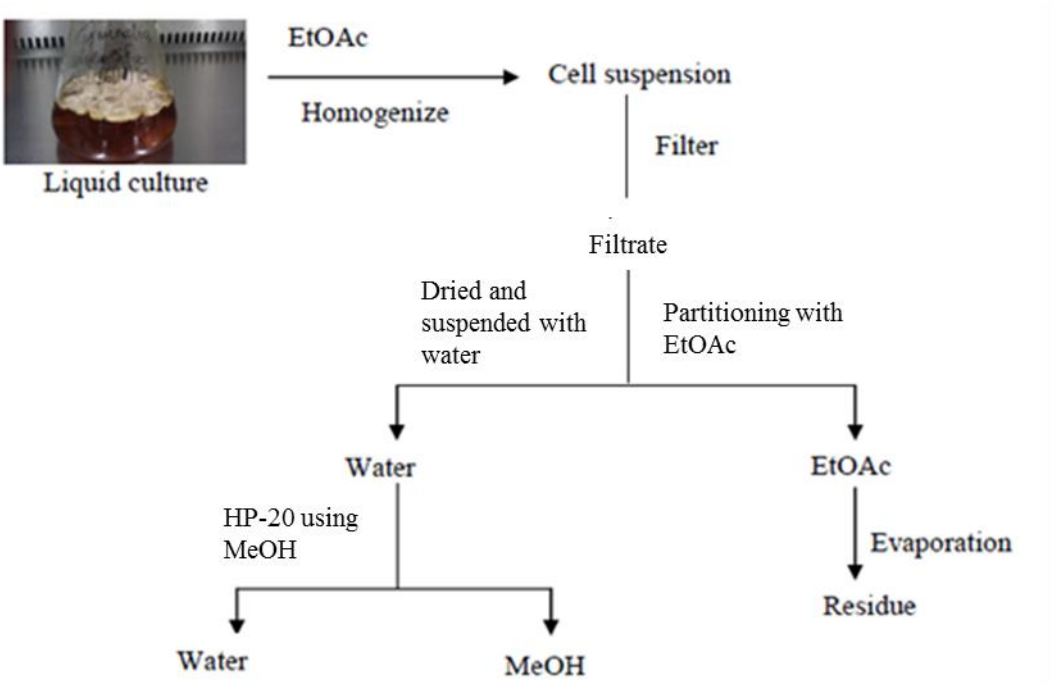

Fig.11 Extraction of fungal liquid culture

2.4.4.4. Extraction of solid rice culture

250mL EtOAc were added to the cultures and left overnight. Culture media were then cut into pieces to allow complete maceration and left for 3–5 days. Then

filtration was done followed by repeated extraction with EtOAc until exhaustion. The combined EtOAc extracts were evaporated under vacuum, suspended in 200mL H_2O and partitioned by adding EtOAc (3x200 mL) in a separating funnel. The pooled EtOAc extracts were then taken to dryness under vacuum (Fig.12).

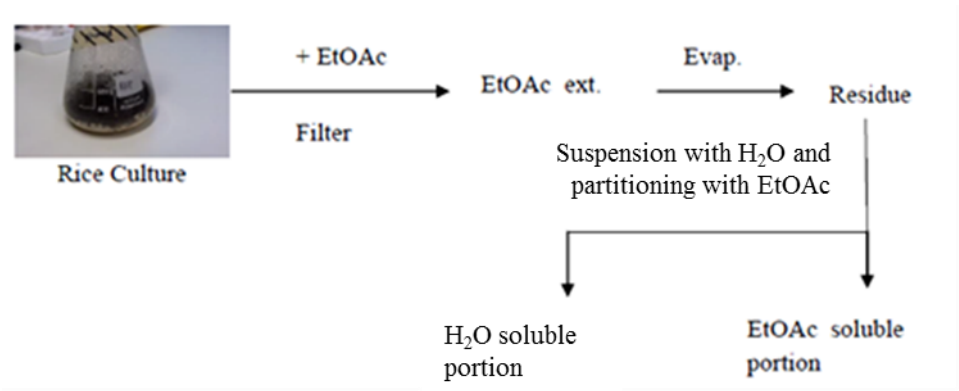

Fig.12 Extraction of solid rice culture

2.4.5. Metabolomics profiling and dereplication of extracts using NMR and HRFTLCMS

2.4.5.1. NMR Analysis

All Fungal extracts were subjected to 1D and 2D NMR spectroscopic analysis on the aforementioned Jeol-LA400 FT-NMR spectrometer. 600 µL of deuterated solvent, which was $CDCl_3$, DMSO or $(CD_3)_2CO$, added to the dried sample of concentration 8 mg to 10 mg in 5 mm NMR tube. Nuclear Magnetic Resonance (NMR) spectroscopy is an analytical chemistry technique used in quality control and research for determining the content and purity of a sample as well as its molecular structure. For example, NMR can quantitatively analyse mixtures containing known compounds. For unknown compounds, NMR can be used either to match against spectral libraries or to elucidate the basic structure directly. In order to achieve the desired results, varieties of NMR techniques were done e.g. 1D and 2D according to the complexity of the structure. The principle behind NMR is that many nuclei have spin and all nuclei are electrically charged. If an external magnetic field is applied, magnetic nuclei absorb and re-emit electromagnetic (EM) energy at a specific wavelength corresponds to radio

frequancies. The transfer of energy can be translated in order to give NMR spectrum.

2.4.5.2. LC-HRFTMS Analysis

Fungal extracts were dried and dissolved in 50:50 H_2O: MeOH HPLC-grade, to make a concentration of 1mg/mL and subjected to high resolution LC-FTMS ThermoScientific Exactive coupled to a Dionex UltiMate 3000 HPLC system. The samples were eluted through a C-18 column (ACE) with a length of 75mm, internal diameter of 3.0 mm and silica particle size 5 µm. Using a mobile phase of 0.1% formic acid of HPLC-grade water (solvent A) and acetonitrile (solvent B) and a flow rate of 300µL/min. Gradient elution was employed, commencing with 10% B for 5 minutes, which was increased to 100% B over 30 minutes and for another 5 minutes before decreasing to 10% B in the next minute. The column was then equilibrated with 10% B for 4 minutes until end of the run.

2.4.5.3. Mass Spectral Data Processing and Metabolomic Profiling

Mass spectral data can be processed using differential expression analysis software like MZmine 2.10. MZmine is a free ware and can be downloaded through http://mzmine.sourceforge.net/. The peaks in the solvent blank and blank medium were detected using the chromatogram builder. Mass detection was performed using the exact mass detector with a noise level set at 1.00E2. The peaks were filtered using FTML shoulder peaks filter using a mass resolution of 50,000 and the Gaussian peak model. The chromatogram builder used the highest data point function. The minimum time span was set at 2.0 seconds, and the minimum height and *m/z* tolerance were 1.00E4 and 0.001, respectively. Chromatogram deconvolution was then performed to detect the individual peaks. The baseline cut-off method (minimum peak height: 1.00E4, minimum peak duration: 0:02, baseline level 1.00E1) was applied. The spectra were first time filtered to 2 - 35min using the crop filter. Chromatogram building and deconvolution then followed, while the noise and baseline levels were set higher (noise level: 1.00E5, minimum time span: 0:10, minimum height: 1.00E5, and *m/z*

tolerance: 0.001, baseline level: 1.00E3). Isotopes were also identified using the isotopic peaks grouper (*m/z* tolerance: 0.050, RT tolerance: 0.05, monotonic shape, maximum charge: 1, and representative isotope: most intense). The duplicate peaks were filtered out using the duplicate peak filter *(m/z* tolerance: 0.050, RT tolerance: 0:05 seconds, requiring the same identification). An adduct search was performed for Na-H, K-H and NH_3 (RT tolerance: 0:10, *m/z* tolerance: 0.100, max adduct peak height: 20%) and a complex search was performed for both the positive and negative modes of ionization (RT tolerance: 0:10, *m/z* tolerance: 0.100, max complex peak height: 20%) (Tawfike et al., 2013).

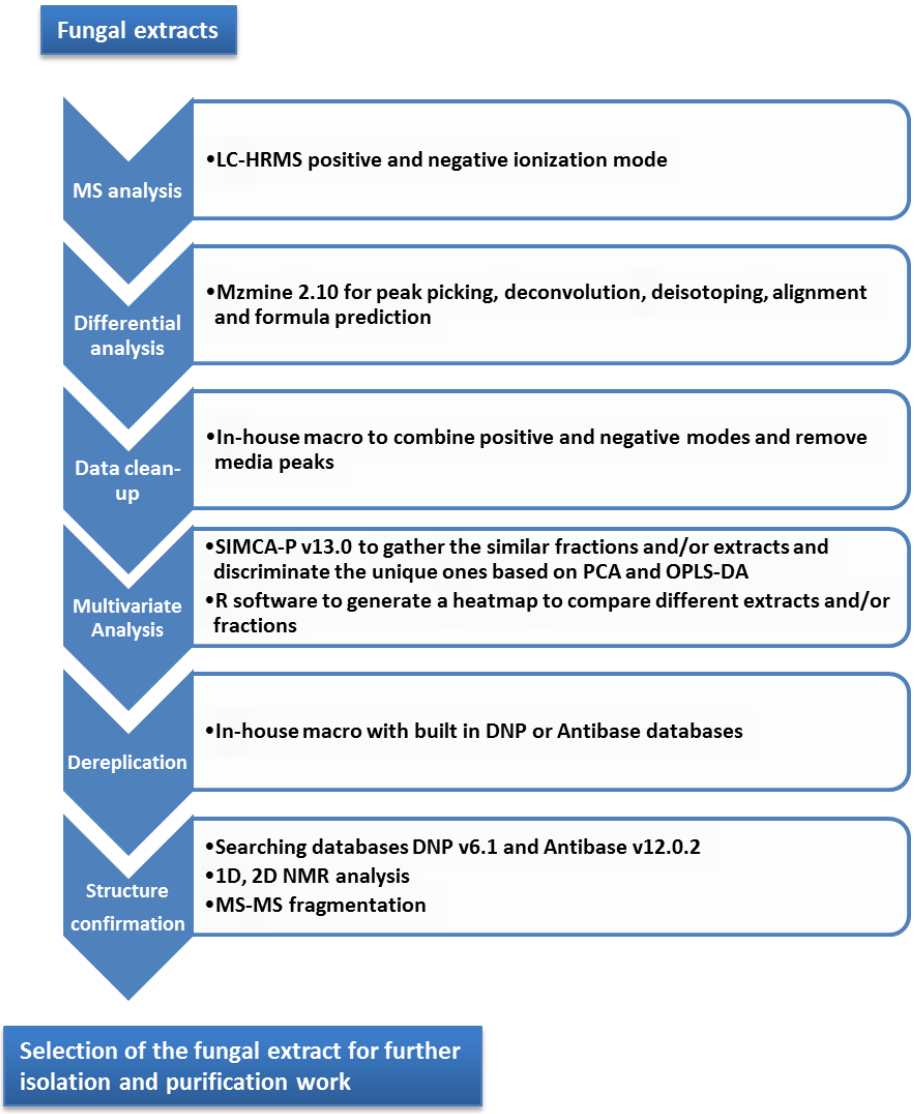

Fig.13 Metabolomics and dereplication work flow

Finally, the peak lists of the solvent blank, media blank and the extracts were aligned using the join aligner parameters set at *m/z* tolerance: 0.100, weight for *m/z*: 70, RT tolerance type: Absolute, RT tolerance: 0:30, Relative RT tolerance: 15%, Weight for RT: 10. This required same charge state, same ID State, compare isotope pattern, and isotope pattern score threshold level: 65%. The peaks from the blank media and solvent were then subtracted from those of the extracts, and the remaining peaks were compared to the Antibase version 12.0.2 for identification through a custom database-searching tool as demonstrated in Figure (13). Positive and negative data were then exported as a CSV files for further clean up. The CSV files were then imported into in-house macro written on Excel (Macintyre et al., 2014) which enabled both positive and negative modes to be merged for further statistical data analysis. Excel macros were used to subtract the background peaks and to combine positive and negative ionization mode data files generated by MZmine. Peaks originating from the culture medium were extracted. By applying an algorithm to calculate the intensity of each *m/z* in both fungal extracts and medium extracts, ion peaks originating from the medium were subtracted while features with peak intensity 20 times greater in the samples than in the medium were retained. Fungal extracts were grouped according to their culture media and this data clean-up step was carried out for each culture medium used (Macintyre et al., 2014). The Excel macro was written also to enable the dereplication of each *m/z* ion peak with compounds in the customized database (using RT and *m/z* threshold of ±3 ppm) which provided details on the recognized identities of all metabolites in each fungal extract and sequentially sorted the number of remaining unknowns for each extract. The macro was then utilized to identify the top 20 features (ranked by peak intensity) and corresponding recognized identities in each sample by creating a list for each extract. Hits from Antibase database were accessed using ChemBioFinder version 13 (PerkinElmer Informatics, Cambridge, UK) in order to find the structure. The data was then converted into a CSV file and exported to SIMCA-P V 13.0 (Umetrics, Umeå, Sweden). The data set was further analysed using SIMCA-P V 13.0 employing the supervised statistical analysis method OPLS-DA and

principal component analysis (PCA) with Pareto scaling (Macintyre et al., 2014).

2.4.6. General chromatographic methods

Chromatography refers to any separation method in which the compounds in a mixture are partitioned between stationary phase and mobile phase. The partitioning occurs because sample components have different affinities for the stationary and mobile phases. Therefore, compounds are eluted at different rates.

2.4.6.1. Diaion HP-20 Column

Diaion HP-20 is a polyaromatic adsorbent resin for hydrophobic compounds. Water-soluble components of liquid cultivation media should be removed using HP-20 column chromatography. The presence of media components can mask the NMR peaks of the interesting compounds. Approximately 400 cm^3 of HP-20 was covered in analytical grade methanol and poured into the column, which was plugged with cotton that had been previously soaked in methanol, until the column was half-full. More methanol was added and the HP-20 was activated for three hours. The methanol was then drained from the column. A cotton pledger was placed above the HP-20. Fresh methanol was run through the column to wash it. The washing was collected and run through the column a second time. The column was then washed with pure-grade water twice. Pure-grade water was then poured and the column was equilibrated overnight. The dried extract was reconstituted in 20 mL methanol and 20 mL acetone. The flasks were sonicated to aid in the dissolution of the sample. The sample was mixed thoroughly with enough Celite and placed in the fume hood to dry. The Celite containing the adsorbed extract was loaded at the top of the column. Purified sand was added to reduce the caking of the Celite. Cotton was placed above the Celite. The polar molecules including media components were eluted first using 100% pure-grade water until exhaustion followed by 100% methanol (HPLC grade) to elute the semi-polar and non-polar molecules. 250 mL of 50:50 acetone: methanol (HPLC grade), followed by two additional runs of 100% methanol were used to wash the column. Two mL of each portion was collected for LC-HRFTMS analysis. The methanol soluble portion was then dried and placed in the desiccator prior to

weighing and further fractionation.

2.4.6.2. Sephadex® LH-20 Chromatography

Sephadex® LH-20 is a hydroxypropylated dextran that has both hydrophilic and lipophilic properties. It is a kind of size exclusion chromatography, which makes use of molecular sieving to separate the analytes. The compounds are separated according to its molecular size. No compounds greater than 4000 Da are retained. It is useful in separating lipids, steroids, and low molecular weight peptides. Sephadex® LH-20 was suspended in methanol and poured into the column. It was then allowed to settle overnight. The sample was carefully pipetted onto the top of the Sephadex® and small amounts of mobile phase were added until the sample had been adsorbed into the Sephadex®. A larger volume of solvent was then poured into the column. Once all the bands had been eluted and the column washed, the collected fractions were analysed and pooled using TLC. The pooled fractions were subjected for NMR and LC-HRFTMS.

2.4.6.3. Adsorption Chromatography using Silica Gel

Silica gel is the widely used stationary phase for adsorption chromatography. The OH-bounded surface of the silica gel interacts with the compounds. The less polar compounds do not interact strongly with these hydroxyl groups and thus elute much faster from the column. Silica gel was suspended in the most non-polar component of the mobile phase and left overnight to be activated. The slurry was then poured into the column and the silica was left to settle. The column was then equilibrated with the desired mobile phase. As with the Sephadex column, the sample was gently applied along the inside of the column so that it would flow down the glass and would not disturb the settled silica. Small amounts of the mobile phase were added until the mobile phase above the silica was colourless, indicating that the sample had been adsorbed into the silica. A larger quantity of mobile phase was poured into the column. After the collection of all the bands and the washing of the column, the fractions were pooled according to their TLC chromatograms and subjected for NMR and LC-HRFTMS analysis.

2.4.6.4. Thin layer chromatography (TLC)

Thin layer chromatography (TLC) can be used as a qualitative analytical tool for the identification of a compound based on its Rf value. It is also used to determine the purity of a sample and to estimate the number of compounds present in an extract, and even to decide on a suitable solvent system for flash chromatography. It can also be used as a preparative technique to purify compounds. TLC plates were pre-coated with silica gel 60 F254 (layer thickness 0.2 mm) which is the stationary phase and the eluents (mobile phase) were the following:

For polar compounds EtOAc: Formic acid: H_2O (85:10:5)
For semi-polar compounds EtOAc: MeOH (90:10) or DCM: MeOH (95:5) and DCM/EtOAc (70:30)
For non-polar compounds n-hexane: EtOAc (70:30), (50:50) and (30:70)

Reversed phase TLC plates were pre-coated with RP18 silica gel and used for the polar compounds with eluents MeOH: H_2O (70:30, 50:50 and 30:70). Tha sample spotted at 1 cm from the edge and allowed to run with the desired mobile phase until reaching the solvent front at 0.5 cm from the top. The bands on TLC plates were visualized under UV lamp at 254 and 366 nm, followed by spraying with anisaldehyde/H_2SO_4 with subsequent heating at 110℃.

For preparative TLC the samples were spotted in a band 2 cm above the bottom edge of the plate. The TLC chamber contained 40 mL of the mobile phase. Prior to the elution of the plates, mobile phase was allowed to run in tissue paper that was placed inside the chamber, thus will equilibrate the chamber with the solvent faster. In addition, this will prevent the solvent front from evaporation from the plate as it rises. Therefore, the velocity of the solvent front was not decreased and the solvent front would not be concave in shape. Moreover, the plates can be run several times to improve resolution (Stevens, 1969). The bands were viewed

under UV light and marked with pencil. The bands were cut out of the plates and the compounds were re-dissolved in acetone.

2.4.6.5. Medium pressure liquid chromatography (MPLC)

MPLC is a type of column chromatography in which a medium pressure was provided through a pump to move the mobile phase with the analytes through the stationary phase packed in the column. MPLC was used for the preliminary separation of the compounds from the plant and fungal extracts and individual fractions. The mobile phase was a combination of MeOH and H_2O applied in a gradient manner on a reversed phase silica gel (RP18). This was applied mainly for the plant extracts.

Pump	Buchi pump manager C-615
MPLC program	0-5 min (5 % MeOH)
	5-30 min (5-100 % MeOH)
	30-40 min(100 % MeOH)
Column	Versapak C18 (spherical)
	23x53 mm (flow rate 10 mL/min) and 40x150 mm (flow rate 100mL/min)

The fungal extracts and/or fractions were fractionated on normal silica gel columns with a gradient elution system employing n-hexane and EtOAc as following:

Pump	Buchi pump manager C-615
MPLC program	0-5 min (5 % EtOAc)
	5-30 min (5-100 % EtOAc)
	30-40 min(100 % EtOAc)
Column	Versapak normal silica (spherical, 20-45 µm)

23x53 mm (flow rate 10 mL/min) and
40x150 mm (flow rate 100mL/min)

2.4.6.6. Flash chromatography

Flash column chromatography was performed either on Biotage-Isolera One 1.5.2 and/or Grace-Reveleris flash setup equipped with prepacked cartridges for 250mg to 1g fractions. Separation was carried out by an isocratic or gradient solvent system that is either MeOH/H_2O elution system to fractionate the polar fractions on a reversed phase silica or EtOAc/Hexan or EtOAc/DCM system for the non-polar fractions on normal phase silica. All solvents used for chromatography were of analytical grade. Pre-packed columns were for normal phase either (Si60) or reversed phase C18 that was run under pressure of less than 5 bars at not more than 100 mL/min flow rate.

2.4.7. Chromatographic isolation of the pure compounds from 7-days rice culture extract of *A. aculeatus*

The ethyl acetate extract (72 gm) of 7-days rice culture was dried under vacuum, dissolved in 10% aqueous MeOH and partitioned in a separating funnel with n-hexane in order to get rid of fats. The MeOH soluble portion (18 gm) of the EtOAc extract was then dried and applied to MPLC fractionation using a normal silica gel column of 100 g bed weight, 40 mm internal diameter, 150 mm length, 20-45 µm spherical silica gel particles and n-hexane/EtOAc gradient elution system with a flow rate of 100 mL/min. The gradient system started with 0% EtOAc for 10 minutes and then reached to 100% EtOAc in the next 45 minutes. This was followed by a second run to elute the highly polar compounds using EtOAc/MeOH gradient system which started with 0% MeOH reaching 30% in 20 minutes. 74 fractions (each of 100 mL volume) were concentrated and subjected to TLC to pool the similar fractions. This resulted in 25 pooled-fractions, which were submitted for bioactivity assays. The active fractions were selected for further fractionation work. Fractions F28-29, F35-37, F42 and F46 were fractionated mainly using conventional column either silica gel or sephadex LH-

20. F28-29 (514 mg) was applied on conventional silica gel column (25 mm x 460 mm) using isocratic eluents employing CH_2Cl_2 and MeOH at a ratio of 98: 2. This was then followed by purification of the resulted sub-fraction F29-51 (112 mg) using the same silica gel column and CH_2CL_2/MeOH (97:3) as elution system to give F110-114 (9 mg) which corresponded to compound AA2 (nymphasterol). Moreover, F35-37 (101 mg) was fractionated by the same column and elution system used for F28-29 to give F6 (13 mg) which is compound AA1 (egrosterol peroxide). F42 (81 mg) and F46 (185 mg) were fractionated on sephadex LH-20 column (10 mm x 460 mm) with isocratic elution system CH_2Cl_2/MeOH (1:1) to yield fractions F18-20 (3 mg) and F88-97 (11 mg) which corresponded to compounds AA3 (dihydro-dinaphtho-furandione) and AA4 (cirtic acid) respectively. Furthermore, F43-45 (400 mg) was applied on Biotage silica cartridge SNAP 25 g (29 mm (ID) x 78 mm (L)) with isocratic/gradient elution system of CH_2Cl_2/MeOH. The run commenced with 0% MeOH for 3 minutes, then reached 5% in the next 15 minutes and remained at 5% for another 5 minutes. This was followed by gradient elution from 5% to 30% MeOH in 10 minutes. The sub-fractions eluted from F43-45 were pooled according to the TLC plates. Sub-fraction F75-79 (14 mg) corresponded to compound AA6 (homogenistic acid). While sub-fraction F11-14 (61 mg) was subjected to fractionation using Biotage silica cartridge (SNAP 10 g, 20 mm x 60 mm) with isocratic elution system CH_2Cl_2/MeOH (98:2) for 45 minutes which resulted in elution of fractions F74-78 (9 mg) equivalent for compounds AA5 (secalonic acid F). Moreover, the pooled sub-fractions F18-52 (51 mg) were evaporated, dissolved in 100% CH_2CL_2 and precipitated by adding MeOH to give a precipitate (16 mg) which is compound AA7 (secalonic acid D). While the soluble portion, a mixture of compound AA8 (6 mg) and AA9 (5 mg), was concentrated and applied to preparative TLC fractionation. Using normal silica gel 60 F254 TLC plate (20 x 20 cm) and solvent system of CH_2Cl_2/MeOH (98:2) which resulted in two bands at 0.55 and 0.64 Rf values for compounds AA8 and AA9 which corresponded to secalonic acid C and B respectively. F76-78 (1.2 g) was fractionated on Biotage silica cartridge (SNAP 25 g) using isocratic/gradient elution system employing CH_2Cl_2/MeOH started at ratio 98:2 for 30 minutes and

reached 70:30 in the next 15 minutes. The resulted sub-fractions were pooled according to TLC. Pooled sub-fractions F29-32 (53 mg) and F46-60 (117 mg) were concentrated and purified using Biotage silica cartridge (SNAP 10 g) with isocratic elution system of EtOAc/MeOH (95:5) for 40 minutes run to give F4 (16 mg) and F34-63 (11 mg) which are equivalent for compound AA11 (JBIR 75) and AA10 (uridine), respectively. Eleven pure compounds were isolated and purified as shown in the isolation scheme (Fig.14).

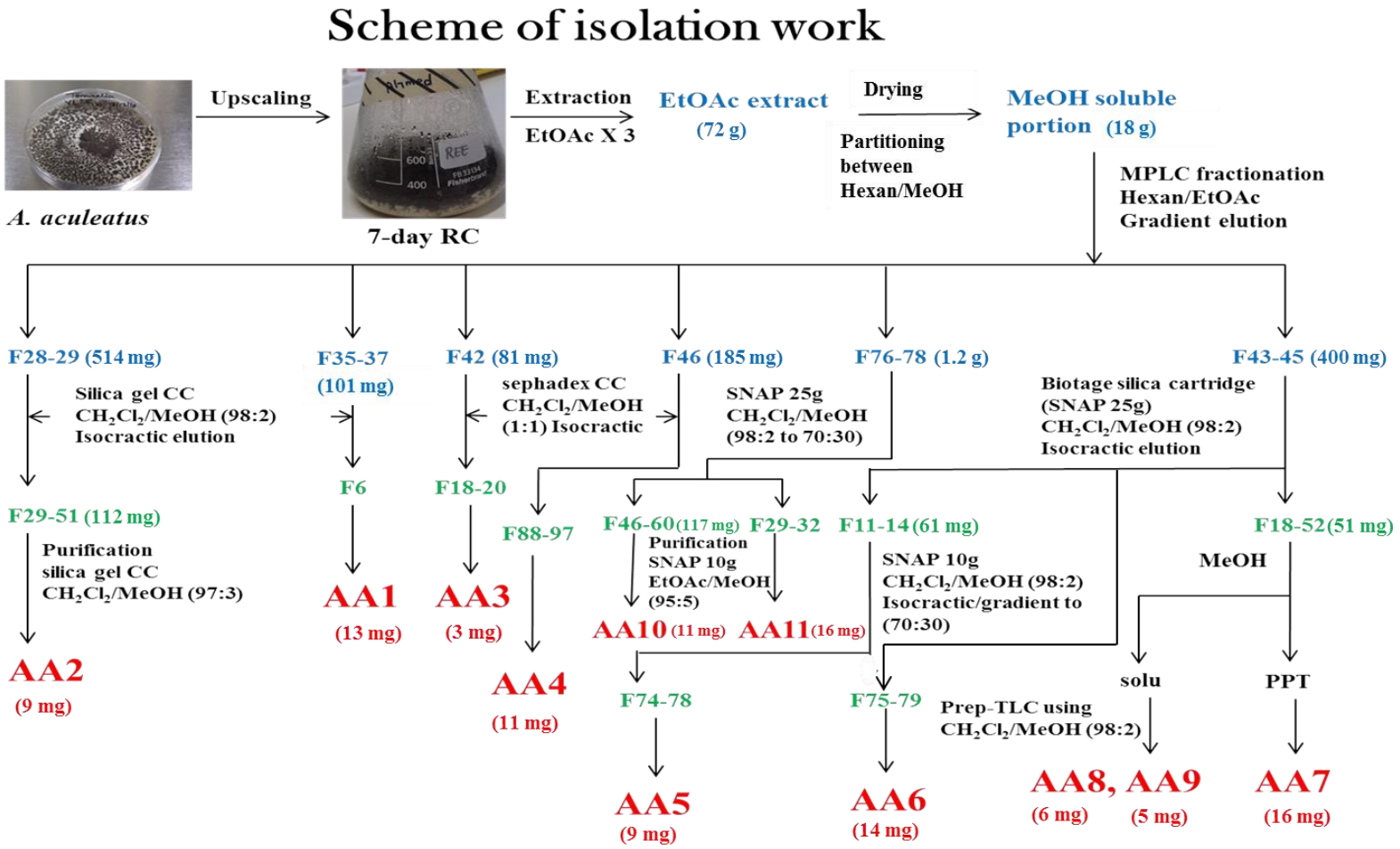

Fig.14 the isolation scheme for 7-day rice culture extract of *A. aculeatus*

2.4.8. Chromatographic isolation of the pure compounds from 30 days rice culture extract of *A. flocculus*

Compounds AF1 (Dihydroaspyrone) and AF2 (Unknown polyketide) were isolated from the small scale batch of 30-days rice culture of *A. flocculus* which employed 2 x 1L Erlenmeyer flasks in the preliminary study while the rest of the compounds were isolated from the medium scale batch of 30-days rice culture employing 10 x 1L Erlenmeyer flasks. The ethyl acetate extract (6 g) of small-scale 30-days rice culture of *A. flocculus* was divided into two portions. The first portion (2.3 g) was subjected to MPLC fractionation using VersaPack silica gel column (23 x 110 mL) at a flow rate of 15 mL/min and n-hexane/EtOAc as mobile phase with gradient elution starting at 100% n-hexane and reaching to 100% EtOAc in 2.1 hours run. The MPLC fractionation led to isolation of 253 fraction 50 mL each. Fractions were subjected to TLC where similar fractions were pooled and dried for further analysis. Fraction MPLC-24 (16 mg) eluted with 80% EtOAc was equivalent for compound AF1 (Dihydroaspyrone). In order to compare two different isolation methods, which may yield variant isolated compounds, the second portion (3.6 g) of EtOAc extract was subjected to size exclusion chromatographic separation on Sephadex LH-20 column (25mm x 510mm) with 100% methanol as mobile phase. 11 fractions resulted, evaporated and subjected to TLC. In accordance to the NF-κB inhibition activity, fraction Seph-5 (500 mg) was selected for further fractionation work on MPLC using VersaPack C18 silica gel column (23 x 53 mm). Flow rate was at 10 mL/min and H_2O/MeOH was used as mobile phase at gradient elution starting at 100% H_2O reaching to 100% MeOH for 60 minutes, which led to the isolation of 12 sub-fractions. The sub-fractions were evaporated and subjected to LC-HRMS and NMR analysis. Sub-fraction M6 (12 mg) eluted with 70% MeOH was corresponding to compound AF2 (unknown polyketide).

The EtOAc extract of the medium scale batch of 30-days rice culture (30 g) was dried and reconstituted in MeOH which was slowly evaporated that allowed the precipitation of Kojic acid crystals (AF4) (4.8 g) which was further purified by decantation. The rest of the MeOH extract (25 g) was dried under vacuum,

dissolved in 10% aqueous MeOH and partitioned with n-hexane in a separating funnel as a defatting step. The n-hexane soluble layer was concentrated and subjected to further fractionation on silica gel open column (19 mm x 46 mm) using DCM/EtOAc (90:10) as eluent to give compounds AF6 (ergosterol) 8 mg, AF7 (ergosterol peroxide) 7 mg and AF8 (campesterol) 9 mg. While the methanol soluble portion (5.1 g) was fractionated on a Grace flash chromatography instrument using silica gel cartridge 80g (186 mm (L) x 32 mm (ID), 40µm particle size) with n-hexane and EtOAc as mobile phase on gradient elution started at 100% n-hexane reaching to 100% EtOAc in 2 hours 15 minutes. This was followed by another run, to elute the highly polar compounds, employing EtOAc/MeOH as a gradient elution system started at 0% MeOH reaching 30% MeOH in 20 minutes. 135 fractions were eluted from the first run while the second run yielded 265 fractions. The fractions were collected in 20 mL volume each, evaporated under nitrogen and pooled in accordance to TLC. 20 pooled-fractions were resulted from both runs, evaporated and subjected for further analysis. Fraction F11-19 (216 mg) was further fractionated using Grace Silica cartridge 12g (82 mm x 22 mm) with isocratic elution system employing n-hexane/CH_2Cl_2 at ratio (65:35) in 55 minutes run. This resulted in isolation of compounds AF16a and AF16b in a mixture (11mg) which equivalent for botryoisocoumarin A and mellein respectively. Fraction F53-71 (157 mg) was applied on Grace silica cartridge 12g (82 mm x 22 mm) with isocratic elution system employing n-hexane/CH_2Cl_2/EtOAc at ratio (70:20:10) in 65 minutes run which gave instantaneously 71 sub-fractions. The sub-fractions have pooled according to TLC and yielded 13 pooled sub-fractions. Sub-fraction F40-53 (40 mg) was further purified on Biotage silica cartridge SNAP 10 g (20 mm x 60 mm) using n-hexane/CH_2Cl_2/EtOAc at ratio (70:20:10) in 60 minutes run to give compound AF13 (cis-4-hydroxymellein) 13 mg and AF14 (trans-4-hydroxymellein) 15 mg. While sub-fraction F18-28 (49 mg) was subjected to further fractionation on preparative normal silica gel 60 F254 TLC plates (20 x 20 cm) using n-hexane/CH_2CL_2/EtOAc at ratio (70:10:20). This yielded a band at Rf value 0.8 corresponding to compound AF9 (unknown steroid) 4 mg. Fraction F72-89 (479 mg) was fractionated using Grace silica cartridge 12g (82 mm x 22

mm) with isocratic elution system employing n-hexane/CH_2Cl_2/EtOAc at ratio (70:20:10) in 62 minutes run which gave instantly 92 sub-fractions. Sub-fractions F41-47 (60 mg) and F32-40 (53 mg) were applied on Biotage silica cartridge SNAP 10 g (20 mm x 60 mm) using n-hexane/CH_2Cl_2/EtOAc at ratio (70:20:10) in 45 minutes run to give compounds AF11 (10 mg) and AF17 (12 mg) equivalent for 3-hydroxymellein and diorcinol respectively, from F41-47. While F32-40 yielded compound AF15 corresponded to 5-hydroxymellein. Fraction F90-135 (2.7 g) was subjected to fractionation using Grace Silica cartridge 40 g (122 mm x 27 mm) with isocratic/gradient elution system employing CH_2Cl_2/MeOH commenced with 0% MeOH reaching to 3% MeOH in 5 min that remained for 20 min isocratic elution. Followed by gradient elution started at 3% MeOH to 30% in the next 20 mins. This resulted in 74 fractions, which evaporated and pooled according to TLC to give 15 sub-fractions. Sub-fraction F16-43 (500 mg) was applied on Biotage silica cartridge SNAP 25g (29 mm x 78 mm) to be fractionated using n-hexane/CH_2Cl_2/EtOAc at ratio 70:20:10 for 30 minutes followed by EtOAc/MeOH gradient elution system started at 0% MeOH reaching to 30% in 20 minutes. This resulted in elution of F113-117 (189 mg) corresponded to AF5 (7-O-acetyl kojic acid), F2-19 (12 mg) which corresponded to compound AF22 (methyl 2-(4-hydroxyphenyl) acetate) and F108-112 (51 mg). F108-112 was subjected to fractionation using preparative TLC using n-hexane/CH_2Cl_2/EtOAc (70:20:10) for three cycles which resulted in isolation of three bands at Rf values 0.8, 0.7 and 0.3 equivalent for compounds AF19 (7 mg), AF20 (5mg) and AF3 (11 mg) corresponded to phomaligol A, phomaligol A-2 epimer and dihydropenicillic acid respectively. Sub-fraction F51-66 (1.5 g) was fractionated using Grace Silica cartridge 40 g (122 mm x 27 mm) with gradient elution system employing CH_2Cl_2/EtOAc, started by 0% EtOAc reaching 100% in 55 minutes and followed by another run using gradient elution system EtOAc/MeOH started at 0% MeOH to 30% in 20 minutes. This resulted in elution of F2-8 (61 mg) which has been purified using preparative TLC with n-hexane/EtOAc at ratio 70:30 as a mobile phase. This resulted in separation of compound AF21 (8 mg) equivalent for p-hydroxy benzaldehyde; F17-37 (520 mg) that has been subjected to fractionation using Grace silica cartridge 12 g (82

mm x 22 mm) with isocratic/gradient elution system employing CH_2Cl_2/MeOH. The run commenced with 0% MeOH reaching to 3% in 5 minute, remained at 3% MeOH for another 25 minutes and followed by gradient elution started at 3% MeOH reaching to 20 % in 15 minutes run. This led to isolation of F36-37 (15 mg) which, was a mixture of compounds AF23a (2-hydroxyphenyl acetic acid) and AF23b (4-hydroxyphenyl acetic acid); F33-35 (170 mg) was purified using preparative TLC with mobile phase CH_2Cl_2/MeOH at ratio 95:5 three cycles to give a band at Rf value 0.7. The band was corresponded to compound AF18 (17 mg) equivalent to 4, 5-dihydroxymellien. The isolation work has been illustrated in the scheme (Fig.15).

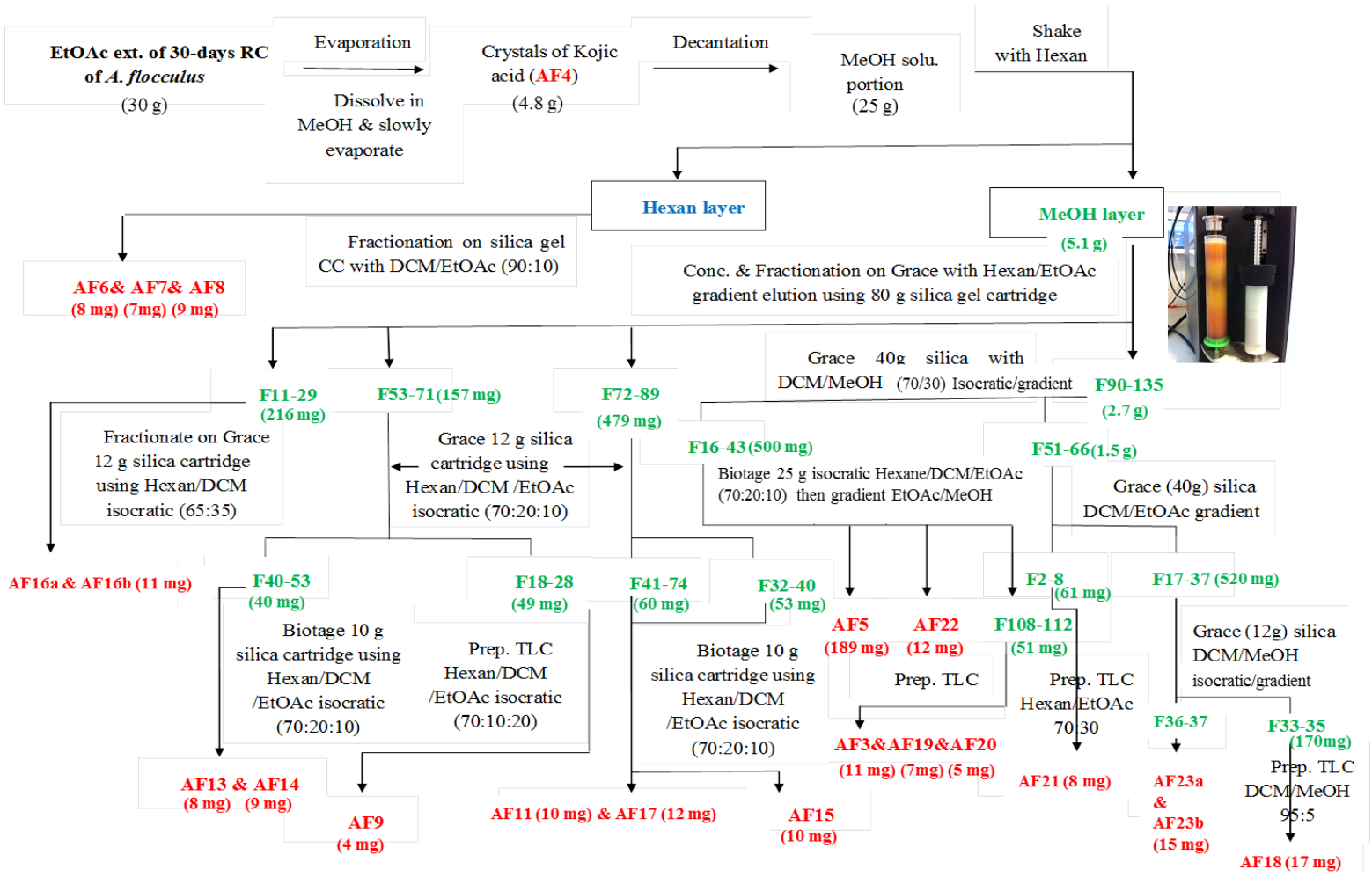

Fig.15 The isolation scheme for the medium upscaled 30-days rice culture extract of *A. flocculus*

2.4.9. Chromatographic isolation of the pure compounds from 30 days rice culture extract of *Curvularia* sp.

The rice culture of *Curvularia* sp. was extracted using EtOAc (3 x 200mL). The EtOAc extract was evaporated, dissolved in 10% aqueous MeOH and defatted by partitioning with n-hexane in a separating funnel. The MeOH soluble portion (2 gm) was then dried and fractionated on Biotage C18 silica gel cartridge SNAP 60g (85 mm x 37 mm) using 0.1 % formic acid in water and 0.1 % formic acid in acetonitrile as solvents. A step-wise gradient elution was employed by commencing with 100 % water reaching to 50 % acetonitrile in 70 minutes followed by another 20 minutes to 100 % acetonitrile with flow rate at 12 mL/min. The fractions were concentrated, pooled according to TLC and UV chromatogram (Fig.16). F87-95 equivalent for compound CV6 (11 mg) eluted at 30% acetonitrile and corresponded to N-acetyl-phenylalanine. While F116-130 and F131-139 equivalent to compounds CV5 and CV4, eluted at 45% and 50% acetonitrile respectively, corresponded to unknown di- and tri-peptides.

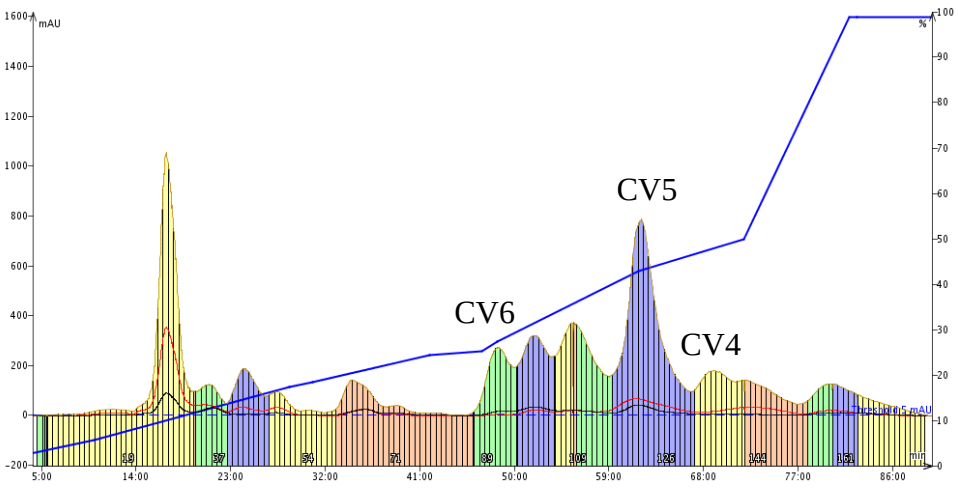

Fig.16 UV chromatogram for fractions from rice culture extract of *Curvularia* sp.

2.4.10. Biological assays

2.4.10.1. Cell culture and treatment

The in vitro growth inhibitory ability of the extracts, fractions and pure compounds were determined on different cell lines including Human Philadelphia chromosome-positive chronic myelogenous leukemia cells (K562) and prostate

cancer cells (PC3). The cell lines were purchased from Deutsche SammLung für Mikroorganismen und Zellkulturen (DSMZ, Braunschweig, Germany) and cultured in RPMI 1640 medium (Lonza, Verviers, Belgium) supplemented with 10% fetal calf serum (FCS) (Hyclone, Perbio, Erembodegem, Belgium) and 1% (v/v) antibiotic– antimycotic (Lonza, BioWhittaker™, Verviers, Belgium) at 37℃, in a 5% CO2, humidified atmosphere. Human recombinant TNFa (PeproTech, Rocky Hill, NJ, USA) was resuspended in a phosphate buffer salt (PBS) 1X sterile solution containing 0.5% bovine serum albumin (MP Biomedicals, Asse-Relegem, Belgium) to reach a final concentration of 10µg/mL (Schumacher et al., 2010).

2.4.10.2. Transient transfection and luciferase reporter gene assay

Transient transfections of K562 cells were performed as previously described (Duvoix et al., 2004). Briefly, 5 µg of luciferase reporter gene construct containing five repeats of a consensus NF-κB site (Stratagene, Huissen, Netherlands) and 5 µg Renilla luciferase plasmid (Promega, Leiden, Netherlands) was used for each pulse. Following electroporation, the cells were resuspended in growth medium (RPMI/FCS 10%) and incubated at 37 °C and 5% CO2. 20 h after transfection, the cells were harvested and resuspended in growth medium (RPMI/FCS 0.1%) to a final concentration of 106 cells/mL and treated for 2 h with or without the natural compound. The cells were then challenged with 20 ng/mL TNFα for 6 h. 75 µl Dual-Glo™ Luciferase Reagent (Promega) were added to the cells for a 10 min incubation at 22 °C before luciferase activity was measured. Then, 75 µl Dual-Glo™ Stop and Glo1 Reagent (Promega) were added for 10 min at 22 °C in order to assay Renilla activity. Luciferase and Renilla (Promega) activities were measured using an Orion microplate luminometer (Berthold, Pforzheim, Germany) by integrating light emission for 10 s. The results are expressed as a ratio of arbitrary units of firefly luciferase activity normalized to Renilla luciferase activity (Schumacher et al., 2010).

2.4.10.3. In vitro cytotoxic assay (viability assay)

The cell lines were maintained in continuous culture in a humid atmosphere at 37 °C and 5% CO_2 in RPMI 1640 medium supplemented with penicillin, streptomycin, gentamicin, L-glutamine, and fetal calf serum. Potential mycoplasm contaminations were checked twice per month. For the assay, 24-well plates were seeded with 500 µL of cell suspension containing more or less 2 x 10^5 cells/mL. Cells were treated with natural compounds at different concentrations (in the range between 0.1 up to 100 µM). After 24 h incubation, the cells were transferred to 96-well microplates and assayed for the CellTiter-Glo® Luminescent Cell Viability Assay to determine the number of viable cells in culture, based on quantification of the ATP present. Each condition was carried out in triplicate. The results correspond to an average of three independent experiments ± SD (Schumacher et al., 2010).

2.4.10.4. Alamar blue assay to determine drug sensitivity of African trypanosomes in vitro

Bioassays for antitrypanosomal activity were carried out against the blood stream form of *Trypanosoma brucei brucei* (S427) using a modification of the microplate Alamar blue assay to determine drug sensitivity of African trypanosomes (Räz et al., 1997). Test compounds were prepared as 10 mg/mL stock solutions in 100% DMSO. The samples were initially screened at a concentration of 20µg/mL and then minimum inhibitory concentration (MIC) determinations were determined for the active compounds. MICs were carried out in 96-well microplates. The compounds were tested in duplicate over a concentration range of 0.2–100 µg/mL in HMI-9 medium (10% FBS) at a final well volume of 200µL. DMSO at a concentration range of 0.001–1% and suramin over a concentration range of 0.8–100 µM were included as negative and positive controls. A well without bacteria was included as a sterility check. Trypanosomes were counted using a haemocytometer and the suspension adjusted to (3 x 104) trypanosomes/mL in HMI-9 medium to provide the microplate inocula of 100µL/well. The microplates were incubated at 37ºC in a humidified 5% CO2 atmosphere for 48 hours. Thereafter 10% alamar blue™ was added to each well and the microplates were incubated for a further 20 hours. Fluorescence was determined using a microplate

fluorometer at an excitation wavelength of 560 nm and an emission wavelength of 590 nm. Percentages of control values were calculated and the MIC was determined as the lowest compound concentration with <5 % of the control values.

2.4.10.5. Antimicrobial assay - M. marinum ATCC.BAA535

A modification of the microplate Alamar blue method for susceptibility testing of fast growing species of *Mycobacterium* was used (Collins and Franzblau, 1997, Franzblau et al., 1998). *M. marinum* resembles *M. tuberculosis*; however, it is less dangerous to humans and faster growing, so it is the model used in screening for anti-mycobacterial activity. *Mycobacterium marinum* ATCC.BAA535 from the thawed stock cryoculture was streaked onto Columbia (5% horse blood) agar slopes and incubated at 31ºC for 5 days. A loopful of the culture was then transferred into 10 mL of sterile 0.9% NaCl containing glass beads. The suspension was mixed and allowed to settle. 1 mL of the supernatant was added to 10 mL sterile MHB (Mueller Hinton broth) saline that had been used to zero the turbidity meter. The turbidity of the solution was adjusted to be the same as a 0.5 McFarland standard. A few drops of Tween 80 0.02% were filter sterilized and added to homogenise the suspension. This was then shaken and the inoculum diluted 1 in 10 with cation adjusted Mueller Hinton Broth for use in the assay. Samples were dissolved in a sufficient quantity of DMSO to reach a concentration of 10 mg/mL or 1 mg/100 µL. For the initial screen, the 10 mg/mL stock solutions of the samples were diluted ten times to 1000 µg/mL using MHB. Twenty microlitres of each extract were placed in each well and 80 µL of MHB was added to each. DMSO was included as the negative control at a concentration range of 1 to 0.002% and gentamycin was included as the positive control at a range of 100 to 0.78 µg/mL. One hundred microlitres of the bacterial suspension were added to the wells. The plates were sealed and incubated at 31ºC for 5 days before the addition of 10µl of Alamar blue. The plates were again sealed and incubated at the same temperature for 24 hours after which fluorescence was determined using the Wallac Victor microplate reader in fluorescence mode (Excitation 530nm; Emission 590nm). The results were calculated as percentages

of control values.

The MICs of the active samples were determined following the same procedure; however, the final concentrations of the test solutions in the 96-well plate ranged from 100 to 0.17 μg/mL. MIC assays were only performed on samples having sufficient activity (>90% inhibition); thus, where no MIC was available the % inhibition was reported.

Chapter 3: Results

3. Results

3.1. Plant materials, isolated endophytes and biological activity

Five endophytic fungi were isolated from four plant species (Table 4) collected from Al-Zohrya gardens, Zamalek, Cairo, Egypt. Four out of the five endophytes belonged to Ascomycota, which included *Aspergillus aculeatus, Curvularia sp., A. oryzae* and *A. flocculus*, isolated from four Egyptian medicinal plants *Terminalia laxiflora, Dracaena deremensis, Tabebuia argentea* and *Markhamia platycalyx,* respectively. The endophytes were identified using molecular biology procedures by comparison of the isolated DNA sequence with those found in the gene bank. All of them showed 100% similarity, using a PCR program previously described by Rychlik and co-workers (Rychlik et al., 1990). For *A. flocculus* which only showed 93% similarity, a touchdown PCR (Don et al., 1991) was employed. The touchdown PCR was used since impurities (DNA from other sources) were found. Thus, the primers avoided amplifying nonspecific sequences. By increasing the annealing temperature, only very specific base pairing between the primer and the DNA template was allowed. The primers used were ITS and β-tubulin which are used in the identification of the Ascomycetes. Moreover, specially designed primers AT1-F and AT1-R were used for *A. oryzae* due to the very close similarity in DNA sequence to *A. flavus*. Only one endophyte was found to belong to Zygomycota that is *Syncephalastrum racemosum,* isolated from stem of *M. platycalyx*. *S. racemosum* was identified using an ITS primer and Zygomycota primers V9D and LS266 employing the previously described PCR program (Rychlik et al., 1990).

The isolated endophytes showed a remarkable anticancer activity against prostate cancer (PC3) and/or chronic myelogenous leukemia (K562) cell lines except for *Curvularia sp.* (code: Ter-AL-F2a) which exhibited no significant anticancer activity against both cancer cell lines. In addition, *S. racemosum* (code: Markh-ST-F3a, F3b) showed a remarkable activity against *Trypanosoma brucei brucei*. The biological activity is discussed in more details in section (3.2.4).

Table 4: Plant materials, isolated endophytes and biological activity. The species highlighted were subjected for further metabolomics and fractionation work

Plant species /Part	Fungi isolated (Code)	PCR program (% Similarity)	Primers	Bioactivity of Fungal Extract
Terminalia laxiflora **(Combretaceae) Leaves**	***Aspergillus aculeatus*** (Ter-YL-F1B)	Regular 100%	ITS1, ITS4	Prostate cancer cell line (PC-3) Chronic myelogenous leukemia (K562)
	***Curvularia* sp.** (Ter-AL- F2a)	Regular 100%	ITS1, ITS4	
	Aspergillus oryzae (Ter-AL-F2b)	Regular 100%	ITS1, ITS4 BT2a, BT2b AT1F, AT1R	Prostate cancer cell line (PC-3)
Dracaena deremensis **(Agavaceae) Leaves**	*Aspergillus oryzae* (Drac-MID, FROZ-F1)	Regular 100%	ITS1, ITS4 BT2a, BT2b AT1F, AT1R	Prostate cancer cell line (PC-3)
Tabebuia argentea **(Bignoniaceae) Leaves**	*Aspergillus oryzae* (Tab-leaves F1a, F1b)	Regular 100%	ITS1, ITS4 BT2a, BT2b AT1F, AT1R	Prostate cancer cell line (PC-3) Chronic myelogenous leukemia (K562)
Markhamia platycalyx **(Bignoniceae) Stem**	***Aspergillus flocculosus*** or *A.ochraceopetaliformis* (Markh-ST-F1, F2)	Touch down 100%	ITS1, ITS4	Prostate cancer cell line (PC-3)
	Syncephalastrum racemosum (Markh-ST-F3a)	93%	ITS1, ITS4 V9D, LS266	Anti-trypanosomal

3.2. Metabolomic and Dereplication studies for Aspergillus aculeatus

3.2.1. Dereplication studies using NMR spectroscopy

The [1]HNMR spectra of *A. aculeatus* extracts (Fig.17 and 18) showed that the rice culture extract exhibiting more resolved peaks in the aromatic region with the presence of broad peak around 12 ppm indicating the presence of a hydrogen-bound phenolic moiety as those found in flavonoids or anthraquinones (Fig.18).

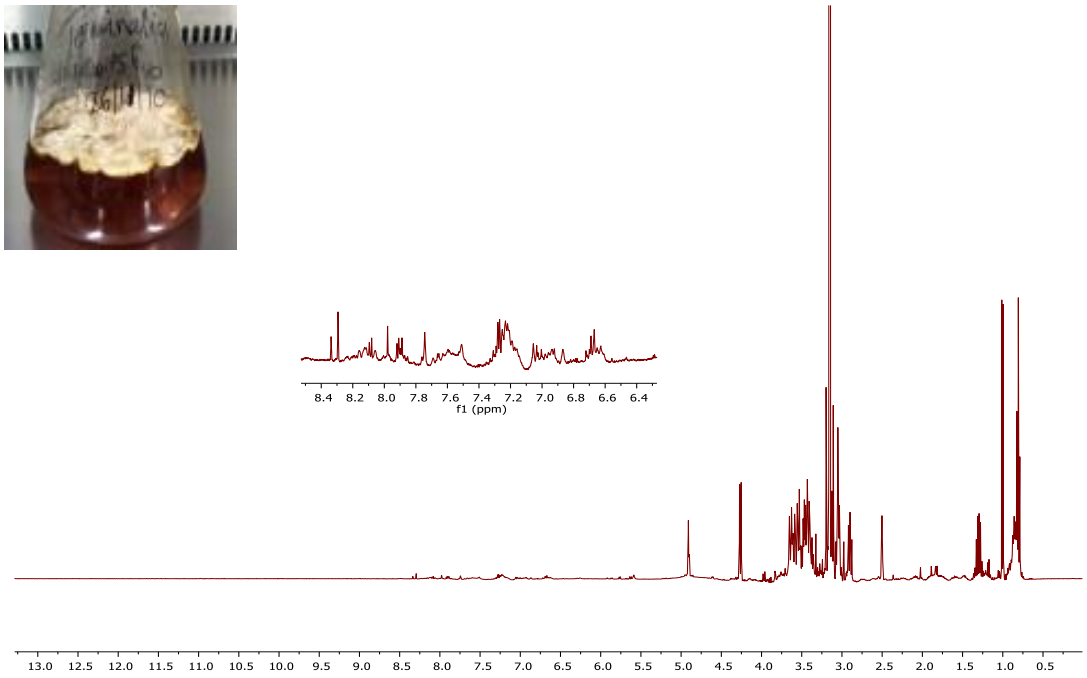

Fig.17 [1]HNMR spectrum of small scale LC extract of *A.aculeatus*

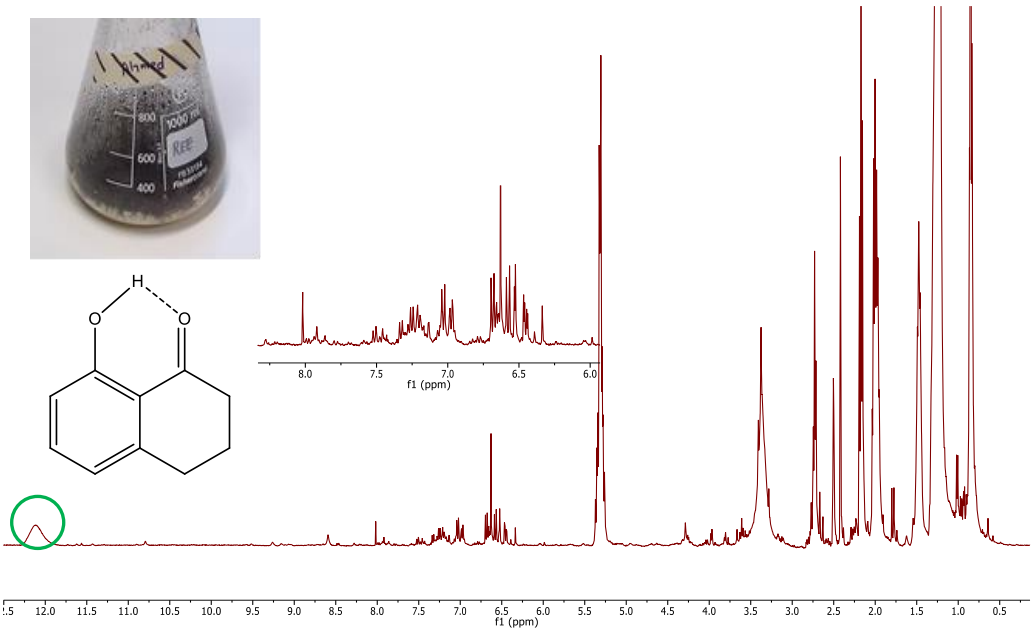

Fig.18 [1]HNMR spectrum of small scale RC extract of *A.aculeatus*

3.2.2. Dereplication studies using MZmine

The total ion chromatogram of both rice and liquid culture extracts of *A. aculeatus* have been subjected to a metabolomics workflow which included data processing in MZmine 2.10. This included peak detection and deconvolution using the local minimum search algorithm for deisotoping, alignment, gap filling, adduct and complex searching, molecular formula prediction and finally customized database search tools, employing Antibase and/or Dictionary of Natural products (DNP) databases, for dereplicating the afforded metabolites in both the rice (RC) and liquid culture (LC) extracts. Comparison of the total ion chromatogram of both RC and LC extracts of *A. aculeatus* showed the presence of more peaks in the RC extract (Fig.19). The scatter plot (Fig.20) of RC extract against LC extract, showed more metabolites in the RC side of the diagonal, which was represented by the increase in density of the blue dots below the diagonal. This confirmed that the RC produced more metabolites than the LC of *A. aculeatus.* The comparison showed the similarity and differences in the produced metabolites between both extracts. The only limitation of MZmine 2.10 was that the positive and negative ionization mode could not be combined. Hence a CSV file for each mode was exported from the MZmine and imported simultaneously into a macro written in excel which enable the combination of both modes, allowed further clean up and database searching (Macintyre et al. 2014). Searching the Antibase® and/or Dictionary of Natural Products (DNP) databases for the metabolites found in the RC and LC extracts of *A. aculeatus* as well as the ethyl acetate and BuOH extracts of *Terminalia* leaves, from which the endophyte was isolated, showed that most of the isolated metabolites have been previously identified in the dereplication table (Table 5). Some of the metabolites produced by the endophyte were also found at very small intensities in EtOAc and/or BuOH extracts of *Terminalia* leaves. For example the metabolites of ion peaks at *m/z* (retention time in minutes) 436.198 $[M+H]^+$ (9.95 min), 381.155 $[M+H]^+$ (10.18 min), 180.102 $[M+H]^+$ (4.33 min) and 405.229 $[M+H]^+$ equivalent for neoxaline, dinaphtho[2,1-b:1',2'-d] furan-5,9-dion, phenylalanine-N-Me and phalarine respectively as shown in dereplication table (5). Neoxaline has been

isolated previously from *Aspergillus japonicus* (Hirano et al. 1979), Dinaphtho [2,1-b:1',2'-d] furan-5,9-dion was produced by *Sphaeropsidales* sp. ((Bode and Zeeck 2000) and phalarine was characterized from the extract of *Phalaris coerulescens* plant. The intensity of the peak height of the produced metabolites was used for the initial screening purpose in order to dereplicate the most predominant metabolites in each extract where peak area gave false positive results because of the broad peaks came from some impurities or unionized metabolites. However, the peak area of the produced metabolites was used to compare the amount of certain metabolites produced in some or all extracts as shown in table (6). In this table, the peak area of the produced metabolites previously described in (Table 5) was shown, confirmed that metabolites produced at higher concentration in the fungal extracts were found at lower concentration in the plant extracts. This confirmed two facts, first the endophyte can produce the same plant metabolites in larger quantities with advantageous of sustainability and the second is allocation of the fungal metabolites in the plant extracts is a proof of the biological source of the endophyte. Moreover, the metabolites at corresponding ion peak *m/z* 436.198 $[M+H]^+$ and 478.270 $[M+H]^+$ eluted at 9.95 and 11.01 min equivalent for neoxaline and paraherquamide E respectively, produced at more concentration by the LC extract. While metabolites at *m/z* (retention time) 639.171 $[M+H]^+$ (19.22 min) ,235.119 $[M+H]^+$ (3.21 min), 381.155 $[M+H]^+$ (9.57 min), 180.102 $[M+H]^+$ (4.33 min) and 405.229 $[M+H]^+$ (9.00 min) equivalent for secalonic acid D, JBIR-75, dinaphtho [2,1-b:1',2'-d] furan-5,9-dion, phenylalanine-N-Me and phalarine respectively, were found at larger quantities in 7-days RC extract. This indicated that 7-days RC extract was richer with the metabolites than other fungal extracts. The corresponding ion peak at *m/z* 475.325 eluted at 37.42 min was found to be undescribed in the literature however MZmine was able to find the predicted molecular formula which was $C_{25}H_{46}O_8$. Furthermore, heatmap of the RC extracts over R 2.15.2 software (Fig.21) showed a significant difference in the produced metabolites, represented by the blue lines, between RC 7-days and RC 30-days extracts. This was an indication of the variance in the chemical profile between the two extracts that may be reflected upon the biological activity. Moreover, 15-

days RC extract showed lower abundance of the produced metabolites than both 7 and 30-days RC extracts. This indicated that 15-days RC was an intermediate stage in which the metabolites were produced in 7-days culture, consumed by the fungi in the 15-days culture to produce other secondary metabolites in 30-days culture as a survival mechanism.

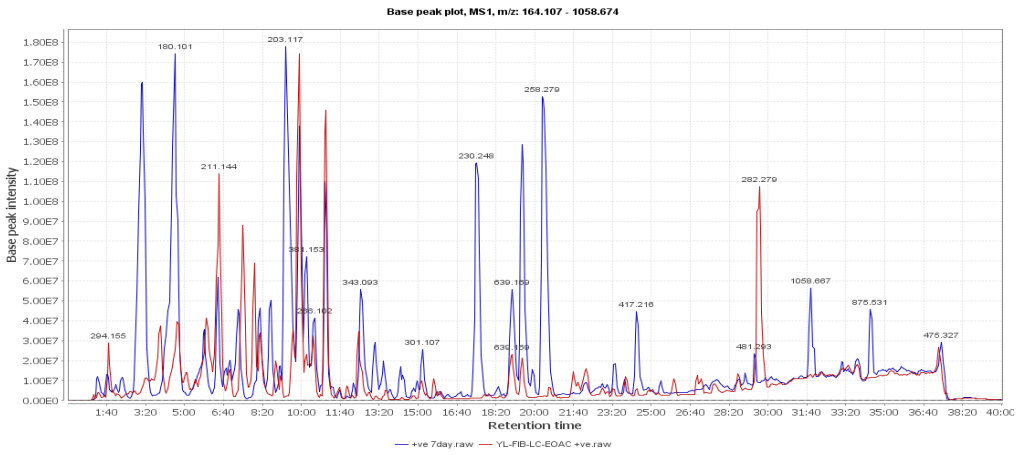

Fig.19 TIC of both RC (●) and LC (●)

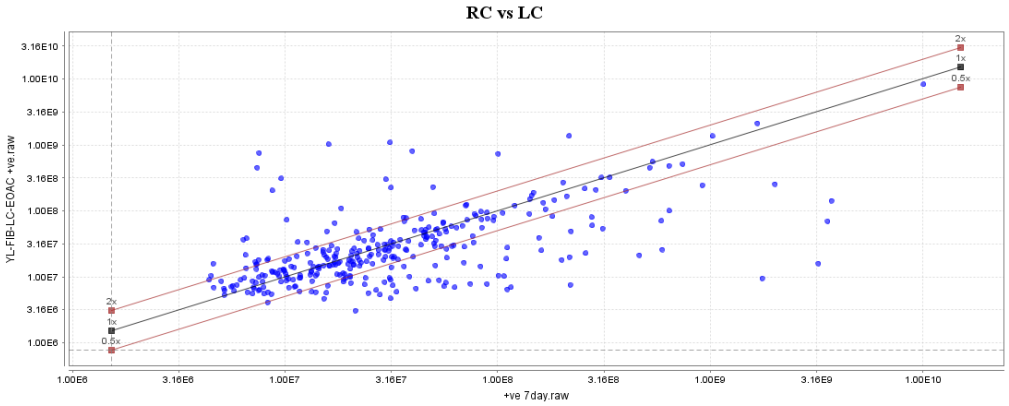

Fig.20 Scatter plot of RC (X-axis) and LC (Y-axis)

Table 5: Dereplication table for *A. aculeatus* extracts which includes mass to charge ratio (*m/z*), retention time (RT), formula, name and source of the detected metabolites in liquid culture fungal extract (LC), 7 days, 15 days, 30 days rice culture (RC) fungal extracts, butanol extract (BuOH ext.) and ethyl acetate extract (EtOAc ext.) of plant leaves. The highlighted rows represented the metabolites, which were found at lower intensities in the extracts of the source plant. The extracts were compared according to the peak height of the produced metabolites. All metabolites represented by $[M+H]^+$

row *m/z*	row RT	Formula/ Name	LC	BuOH plant ext.	EtOAC plant ext.	RC-7days	RC-15days	RC-30days
203.118	9.39	$C_{12}H_{14}N_2O$ Nb-Acetyl-tryptamine	1.89E+07	0	0	2.97E+09	7.66E+06	4.89E+07
180.102	4.33	$C_{10}H_{13}NO_2$ Phenyl-alanine-N-Me	1.37E+08	9.83E+03	5.45E+03	2.05E+09	6.27E+06	6.83E+07
235.119	3.21	$C_{11}H_{14}N_4O_2$ JBIR-75 *Aspergillus* sp. fS14	7.11E+07	0	0	1.93E+09	3.03E+07	6.75E+08
475.326	36.46	$C_{25}H_{46}O_8$	2.31E+09	7.49E+02	0.00E+00	1.76E+09	1.78E+09	1.77E+08
639.171	19.22	$C_{32}H_{30}O_{14}$ Secalonic acid D *A. aculeatus*	6.28E+08	0	0	1.57E+09	4.88E+07	1.48E+08
436.198	9.95	$C_{22}H_{29}NO_8$ Neoxaline *A. japonicus*	2.28E+09	0	6.96E+02	1.05E+09	9.49E+07	5.13E+08
340.259	8.19		5.05E+08	0	0	8.75E+08	1.18E+09	9.86E+08
381.155	9.57	$C_{19}H_{24}O_8$ Dinaphtho[2,1-b:1',2'-d] furan-5,9-dione *Sphaero-psidales sp.*	1.95E+05	2.85E+02	1.96E+03	7.24E+08	3.48E+06	4.96E+07
343.092	12.46		2.49E+08	0	0	7.02E+08	3.30E+07	3.45E+08
478.27	11.01	$C_{28}H_{35}N_3O_4$ Paraherquamide E *A. aculeatus*	1.38E+09	0	0	6.34E+08	5.22E+07	1.67E+08
405.229	9.00	$C_{23}H_{32}O_6$ Phalarine *Pharalis coerulescens*	2.45E+04	4.61E+03	2.02E+03	5.83E+08	3.49E+04	3.17E+05

Table 6: Peak area of the metabolites produced by *A. aculeatus* extracts including liquid culture fungal extract (LC), 7 days, 30 days rice culture (RC) fungal extracts, butanol extract (BuOH ext.) and ethyl acetate extract (EtOAc ext.) of plant leaves. The highlighted rows represented the metabolites produced at lower concentration in the plant extracts. All metabolites represented by $[M+H]^+$

row *m/z*	row RT	LC	BuOH ext.	EtOAc ext.	RC-7days	RC-15days	RC-30days
203.118	9.39	1.89E+07	0	0	2.97E+09	7.67E+06	4.89E+07
258.279	20.6	5.49E+06	0	0	1.84E+09	3.26E+07	1.20E+10
475.325	37.42	3.89E+08	1.54E+03	0	1.16E+09	1.12E+09	1.54E+09
235.119	3.21	7.11E+07	0	0	1.93E+09	3.03E+07	6.75E+08
639.171	19.22	6.28E+08	0	0	1.57E+09	4.88E+07	1.48E+08
180.102	4.33	1.37E+08	9.83E+03	5.45E+03	2.05E+09	6.27E+06	6.83E+07
436.198	9.95	2.28E+09	0	6.96E+02	1.05E+09	9.49E+07	5.13E+08
230.248	18.11	1.15E+07	0	0	1.10E+09	1.85E+07	8.46E+08
478.27	11.01	1.38E+09	0	0	6.34E+08	5.22E+07	1.67E+08
405.229	9.00	2.45E+04	4.61E+03	2.02E+03	5.83E+08	3.49E+04	3.17E+05
381.155	9.57	1.95E+05	2.85E+02	1.96E+03	7.24E+08	3.49E+06	4.96E+07
340.259	8.19	5.05E+08	0.00E+00	0.00E+00	8.75E+08	1.18E+09	9.86E+08

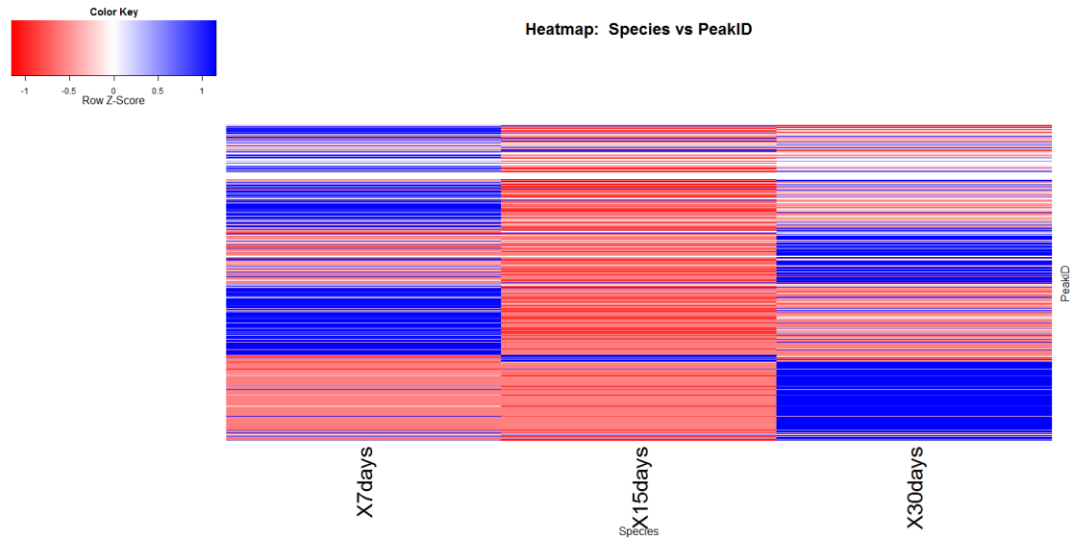

Fig.21 Heatmap for rice culture extracts of *A. aculeatus* in which the blue lines represented the produced metabolites

3.2.3. Metabolomic study using SIMCA-P$^+$

3.2.3.1. A.aculeatus extracts vs Terminalia leaves extracts

Chemometric analysis of different culture extracts of *A. aculeatus* and the EtOAc extract of *Terminalia* leaves on the SIMCA-P$^+$ software discriminated the 7- and 30-days RC extracts from each other and from other fungal and plant extracts as

shown in the PCA score plot (Fig. 22) which was indicative of the unique nature of the metabolites of both extracts. The PCA loading plot (Fig. 23) showed the outlier metabolites expected to be belonging to each of the extracts. The 7-days extract of *A. aculeatus* showed a significant anticancer activity over other extracts when tested against prostate cancer cell line (PC3) and leukaemia cell lines (K562). While the 15-days RC extract showed moderate activity. All other extracts including 30-days RC showed no activity against both cancer cell lines. The OPLS-DA score plot (Fig. 24) showed outlying of both 7-days and 15-days RC extracts. The OPLS-DA loading plot (Fig.25) showed the putative metabolites belonging to the 7-days RC extract which were synonymous to those exhibited in the PCA loading plot. These metabolites corresponded to ion peaks at *m/z* (retention time) 203.118 (9.38 min), 639.171 (18.55 min), 379.141 (10.18), 191.020 (1.94 min) and 235.119 (3.20 min), which were described in the dereplication table (Table 7) as N-acetyl-tryptamine, secalonic acid, dinaphthofurandione, citric acid and JBIR-75, respectively. The dereplication table (Table 7) has been accomplished by searching DNP databases built in the excel written macro (Macintyre et al., 2014) using both positive and negative modes in order to compare the top hit predominant metabolites between the very active 7-days extract and other inactive extracts. The comparison showed that metabolites with corresponding ion peaks at *m/z* 203.118, 379.141 and 405.229 eluted at 9.38, 10.18 and 9.00 minutes identified as N-acetyl-tryptamine, dinaphthofurandione and phalarine, respectively, were found at a higher concentration in the 7-days rice culture extracts. This may indicate that these metabolites may be responsible for the activity of the 7-days rice culture extract.

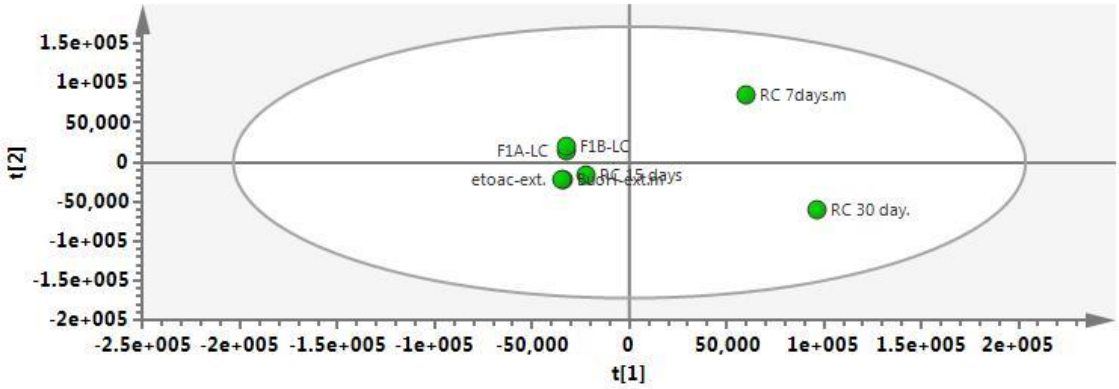

Fig.22 PCA score plot of *A. aculeatus* and *Terminalia* leaves extracts

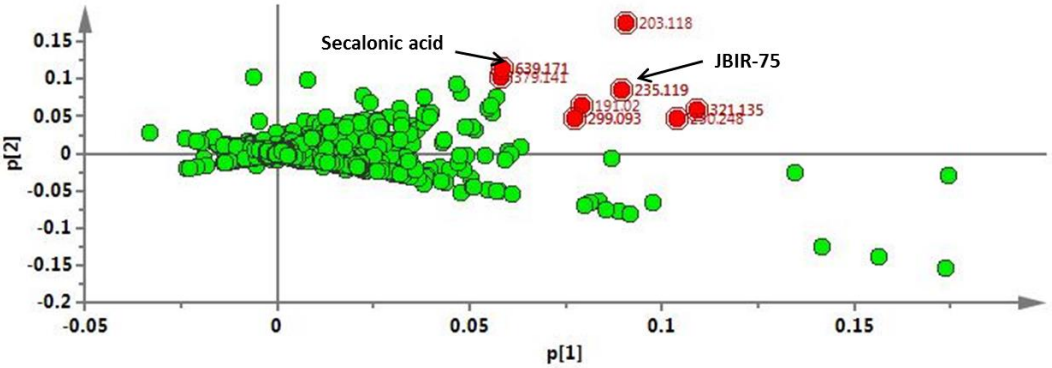

Fig.23 PCA loading plot of *A. aculeatus* and *Terminalia* leaves extracts showing the outlier metabolites belonged to 7-days RC extract (●)

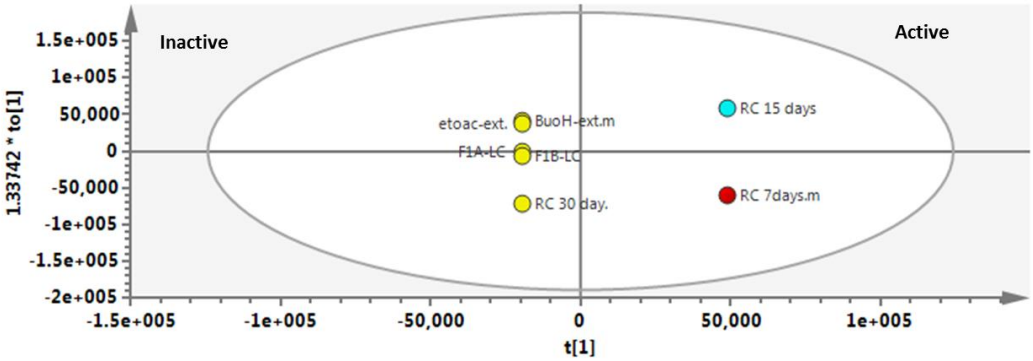

Fig.24 OPLS-DA score plot of *A. aculeatus* and *Terminalia* leaves different extracts. (●) Active fractions (●) moderately active (●) Inactive fractions

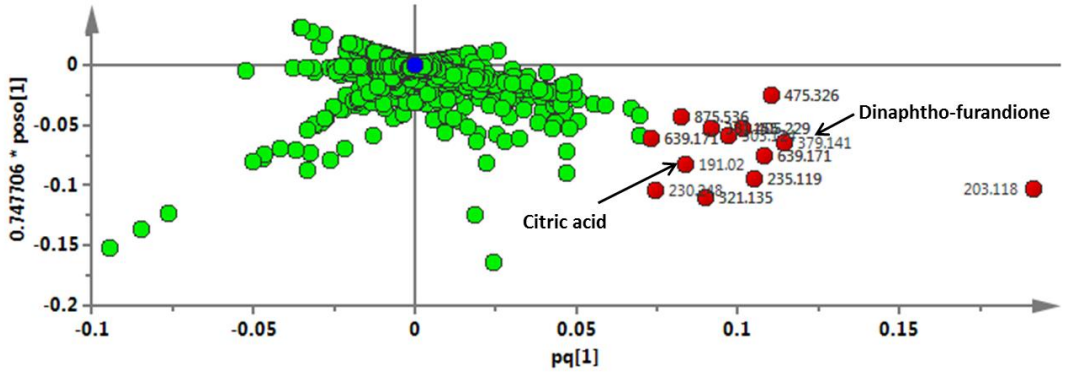

Fig.25 OPLS-DA loading plot of *A. aculeatus* and *Terminalia* leaves different extracts. (●) the putative metabolites predicted to belong to 7-days RC extracts

Table 7: Dereplication table prepared using macro-database involving both negative and positive modes**.** The comparison based on peak height intensity. The table included mass to charge ratio (*m/z*), retention time (RT), polarity, molecular formula, name and source of the detected metabolites in liquid culture fungal extract (LC), 7 days, 30 days rice culture (RC) fungal extracts and ethyl acetate extract (EtOAc ext.) of plant leaves.

m/z	Rt	Polarity	Formula/Name	LC	EtOAc ext.	RC-7days	RC-30-days
203.1179	9.39	P	$C_{12}H_{14}N_2O$ Nb-Acetyl-tryptamine	1.31E+06	0	2.63E+08	4.10E+06
235.1189	3.21	P	$C_{11}H_{14}N_4O_2$ JBIR-75 *Aspergillus* sp. fS14	3.93E+06	0	1.09E+08	4.06E+07
321.1349	9.43	N	$C_{17}H_{22}O_6$ Tubiporone *Tubipora musica*	1.35E+06	1.23E+04	1.08E+08	6.84E+07
436.198	9.95	P	$C_{23}H_{25}N_5O_4$ Neoxaline *A. japonicus*	1.86E+08	3.03E+02	9.71E+07	5.12E+07
379.1406	10.18	N	$C_{19}H_{24}O_8$ Dinaphtho[2,1-b:1',2'-d] furan-5,9-dione *Sphaeropsidales* sp.	6.46E+04	1.66E+03	9.52E+07	4.88E+06
478.2705	11.00	P	$C_{28}H_{35}N_3O_4$ Paraherquamide E *A. aculeatus*	1.47E+08	0	7.97E+07	1.93E+07
191.0201	1.94	N	$C_6H_8O_7$ Citric acid	8.02E+06	1.36E+04	7.47E+07	3.55E+07
365.1249	7.31	N		3.13E+05	9.60E+02	7.28E+07	1.42E+08

405.2291	9.00	P	$C_{23}H_{32}O_6$ Phalarine *Phalaris coerulescens*	7.41E+03	4.77E+02	7.27E+07	4.73E+04
303.1244	13.08	N		2.25E+04	0	6.48E+07	1.22E+07
299.0932	15.07	N	$C_{18}H_{12}N_4O$ plakinidine C	1.77E+07	9.38E+01	5.97E+07	4.60E+07
639.1713	18.55	P	$C_{32}H_{30}O_{14}$ secalonic acid D *A. aculeatus*	2.23E+06	0	5.15E+07	1.45E+07

3.2.3.2. MPLC fractions of 7-days RC extracts

The most active 7-days rice culture extract was subjected to fractionation using MPLC. The MPLC fractions of 7-days rice culture extract were sent to chemometric analysis using SIMCA-P^+ software. The PCA score plot (Fig.26) showed the outlier MPLC fractions for the 7-days rice culture extract of *A. aculeatus* while the PCA loading plot (Fig.27) showed the discriminated metabolites, which are unique to these fractions. The putative metabolites obtained in (Fig.27) were similar to that obtained from the OPLS-DA loading plot (Fig.25) which confirmed the validity of the previous metabolomics model used in comparison of the active with the inactive fungal extracts and showed the relation between the discriminated metabolites and the exhibited bioactivity. The active fractions, resulted from the bioassay-guided fractionation of the 7-days RC extract, were compared to the inactive fractions to help in early prediction of the unique metabolites that could be responsible for the bioactivity. The OPLS-DA score plot (Fig.28) showed outlying and clustering of fractions 47-50 and 51-56, which indicated the same unique bioactive metabolites shown in the OPLS-DA loading plot (Fig.29). Both fractions were active against K562 cancer cell line while fraction 76, which was also active against K562, found to be discriminated in the other side of the OPLS-DA score plot (Fig.28) which indicated to its characteristic metabolites. Fractions 15-25, 26, 30-32 and 40-41, were active against PC3 cancer cell line, and so grouped together in OPLS-DA score plot (Fig.28) however fraction 40-41 was found to be distinctive in the PCA analysis (Fig.26) which indicated to its distinguishing metabolites. The loading scatter plot

(Fig.29) showed the putative metabolites related to the active fractions of 7-days RC extract of *A. aculeatus*. They were represented by corresponding ion peak *m/z* 639.171 $[M+H]^+$, 191.020 $[M-H]^+$, 235.119 $[M+H]^+$ and 379.141 $[M-H]^+$ which were identified (Table 7) as secalonic acid, citric acid, JBIR 75 and Dinaphtho[2,1-b:1',2'-d]furan-5,9-dione, respectively. The S-line plot (Fig.30) sorted the structure of the isolated metabolites which were identical to the putative metabolites detected during the dereplication study and were predicted to be responsible for the anticancer activity of the active extracts and/or fractions. Moreover, presence of the citric acid among the putative metabolites as well as the isolated metabolites indicated its importance as a precursor and/or a biomarker in the biosynthetic pathway of the secalonic acid compounds as shown in discussion section (4.2). Secalonic acid was the major anticancer compound in 7-days rice culture extract of *A.aculeatus*. The compounds have been isolated using the chromatographic methods as described in section (2.4.7) and the structures were elucidated using HRESI-MS, MS-MS and 1D, 2D-NMR as shown in result section (3.2.5).

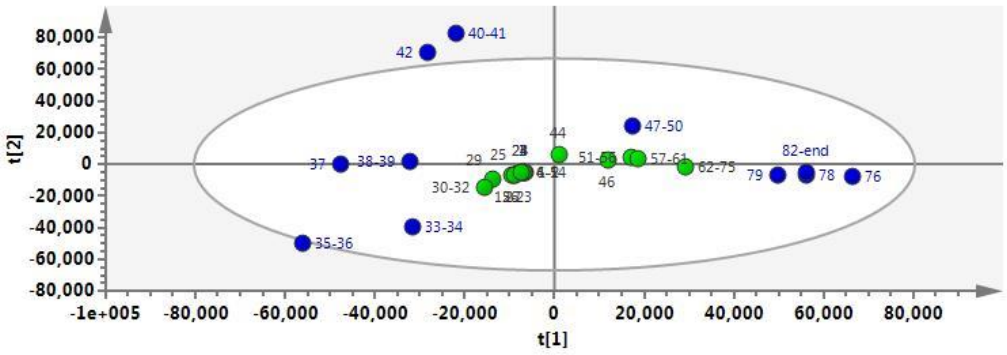

Fig.26 PCA score plot of the fractions of 7-day RC extract of *A. aculeatus* showing the discriminated fractions (●)

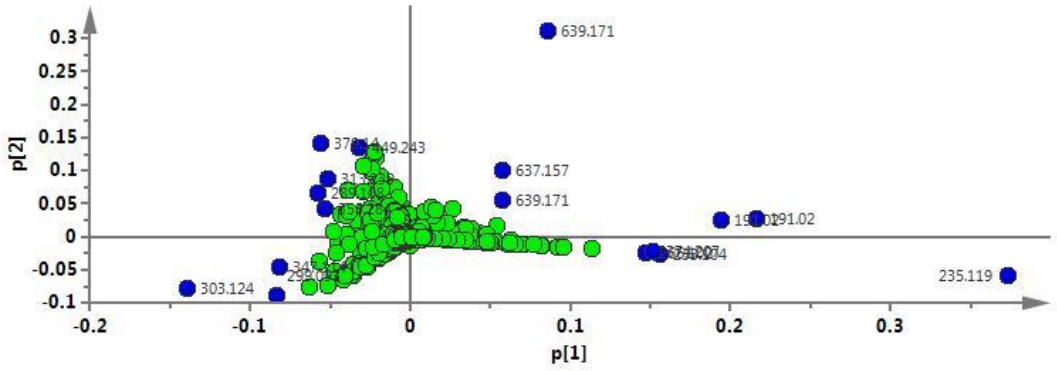

Fig.27 PCA loading plot of the fractions of 7-day RC extract of *A. aculeatus* showing the discriminated metabolites (●)

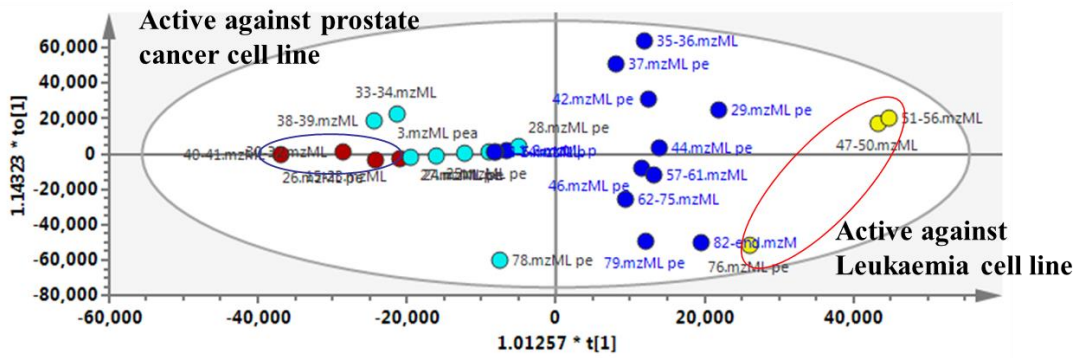

Fig.28 OPLS-DA Score plot of the active vs inactive fractions of 7-day RC extract of A. aculeatus (●) Active against K562 (●) Active against PC3 (●) Active against both (●) Inactive

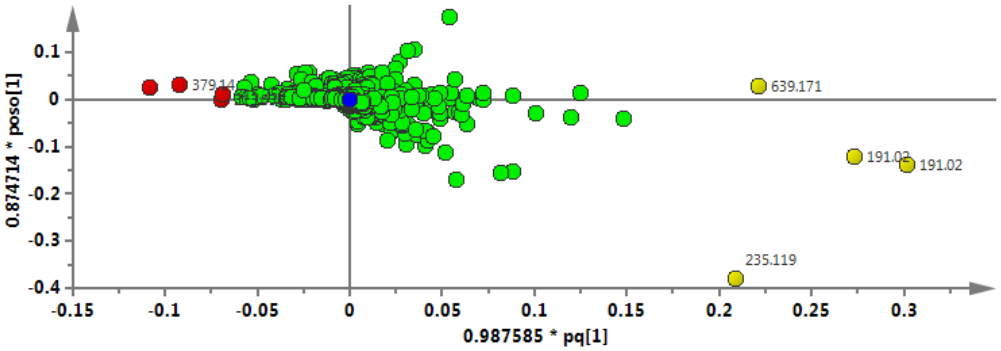

Fig.29 OPLS-DA loading scatter plot of the active vs inactive fractions of 7-day RC extract of *A. aculeatus* showing the expected metabolites of the active fractions (●) active against K562 (●) active against PC3

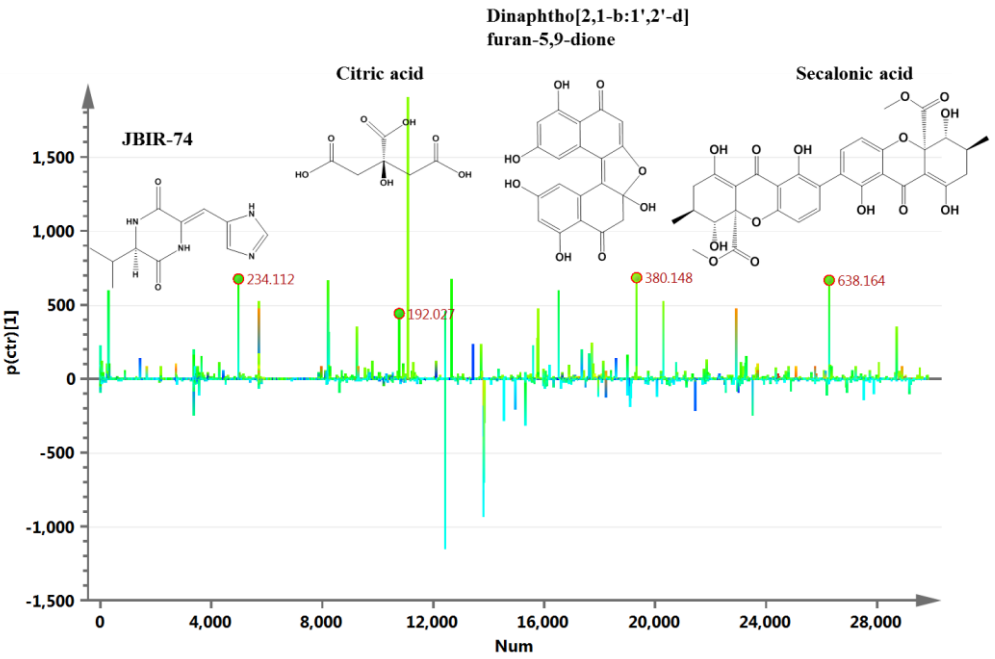

Fig.30 S-line of the active vs inactive fractions of 7-day RC extract of *A. aculeatus*

3.2.4. Biological activity

3.2.4.1. Anticancer activity

The viability assays, for all fungal extracts against prostate cancer cell line (PC3) and chronic myelogenous leukaemia cancer cell line (K562) (Fig.31, 32), showed a significant anticancer activity against both cancer cell lines for samples number 7 and 23 which were represented by codes (Ter-YL-F1b) and (Markh-ST-F2a) equivalent for *A. aculeatus* and *A. flocculus*, respectively (Table 4). The percentage of cell viability was recorded as 5 % and 7 % for *A. aculeatus* and *A. flocculus* respectively against K562 cancer cell line. While they achieved 7% and 18% cell viability respectively against PC3 cancer cell lines. The viability assays were accomplished for *A. aculeatus* extracts (Fig.33, 34) and a remarkable activity against both cancer cell lines has been observed for the 7-days RC extract over other fungal extracts of *A. aculeatus* with cell viability 10 % and 6 % against PC3 and K562 respectively. Moreover, 15-days RC extract showed good bioactivity toward K562 with 10% cell viability and a moderate activity against PC3 cancer cell lines with viability 50%. (Fig.35, 36) exhibited the active pooled fractions were resulted from the MPLC fractionation of 7-days RC extract. These

active fractions have been further fractionated and purified to give 11 pure compounds. The cytotoxicity of the purified compounds was tested against the cancer cell lines PC3 and K562 as well as the normal epithelial cells (PNT2a) (Fig.37). The results showed that compounds AA6, 7, 8, 9, 10 and AA11 (homogenistic acid, secalonic acid D, C, B, uridine and JBIR-75, respectively) exhibited strong cytotoxicity against K562 cancer cell line affording % cell viabilities of 40, 15, 15, 10, 7 and 20, respectively. However, compounds AA7, AA8, and AA9 were found to be cytotoxic on normal cells causing percentage viabilities 50, 70 and 60 %, respectively. On the other hand, compound AA5 (secalonic acid F) showed no cytotoxicity against either normal or lymphoma cells which indicated that a little modification of the structure stereochemistry could change and/or decrease the activity. The non-selective bioactivity of the secalonic acids, which upon slight modification can produce improved therapeutic analogues, will potentially lead them to be in the list of the pro-drugs or drug lead compounds. Compounds AA6 (homogenistic acid), AA10 (uridine) and AA11 (JBIR75) exhibited a strong cytotoxic effect on K562 cell line while they were less toxic to the normal cells exhibiting % cell viability 70, 80 and 90, respectively. None of these metabolites has been previously reported in the literature as anticancer. Furthermore, secalonic acid derivatives (AA7, 8, 9) and JBIR 75 (AA11) have been earlier dereplicated in this study through metabolomics tools as being among the putative metabolites in 7-days rice culture extract which were predicted to be responsible for crude extract's anticancer activity. This confirmed how effective the metabolomics tools in early identification of the active components.

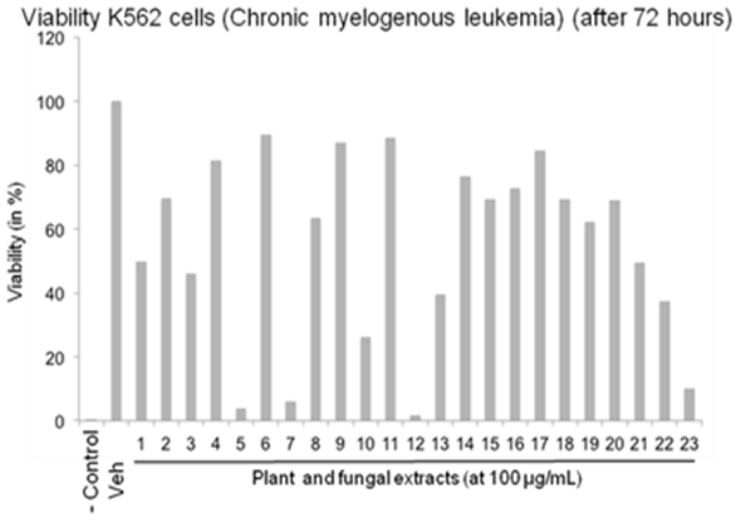

K562 cells were treated with plant and fungal extracts (at 100 µg/mL) for 72 hours.

	BuOH extract	13	*Syzygium* stem-f2
2	Water extract	14	*Terminalia* leaves-f1b
3	EtOAc extract	15	*Markhamia* stem-f3b
4	*Dracaena*-Mid	16	*Markhamia* stem-f3a
5	*Terminalia* AL-f2b	17	*Tabebuia* Leaves-f1a
6	*Dracaena* froz-f1	18	*Tabebuia* Leaves-f1b
7	*Terminalia* YL-f1b	19	*Terminalia* stem-f1
8	*Markhamia* leaves	20	*Terminalia* stem-f2
9	*Terminalia* AL-f2	21	Syzygium stem-f1
10	*Markhamia* Flowers	22	*Markhamia* stem-f1
11	*Terminalia* AL-f2a	23	*Markhamia* stem-f2a
12	*Terminalia* AL-f1		

Fig.31 Anticancer activity of all fungal extracts from MA plates against K562 cancer cell line

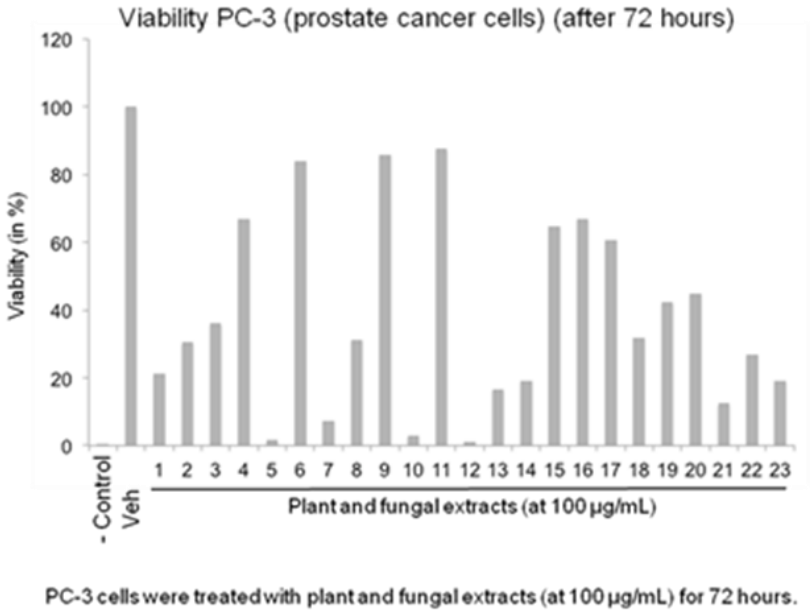

Fig.32 Anticancer activity of all fungal extract from MA plates against PC3 cancer cell line

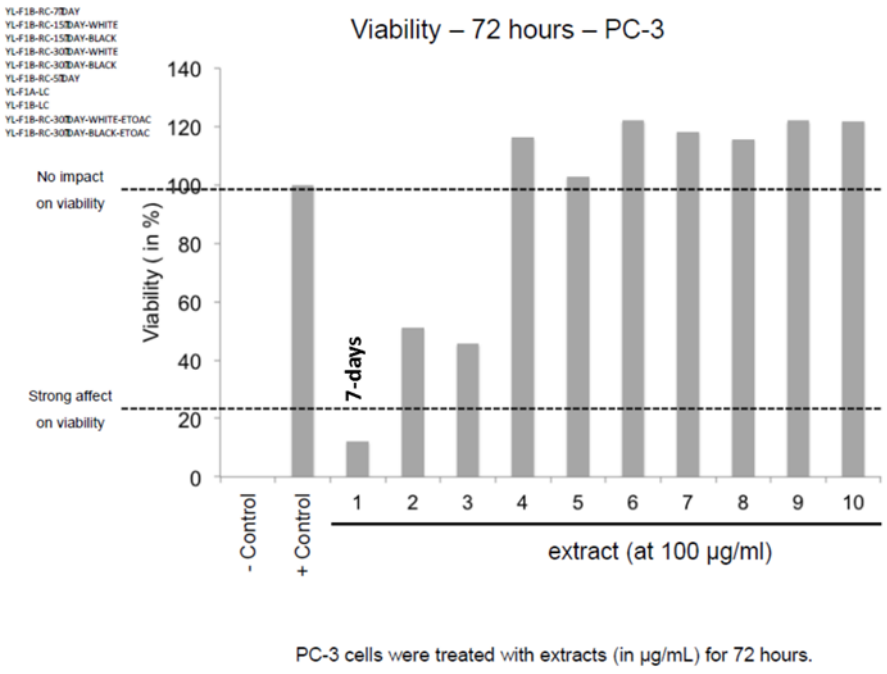

Fig.33 Viability assay of different culture extracts of *A. aculeatus* against PC3 cell line

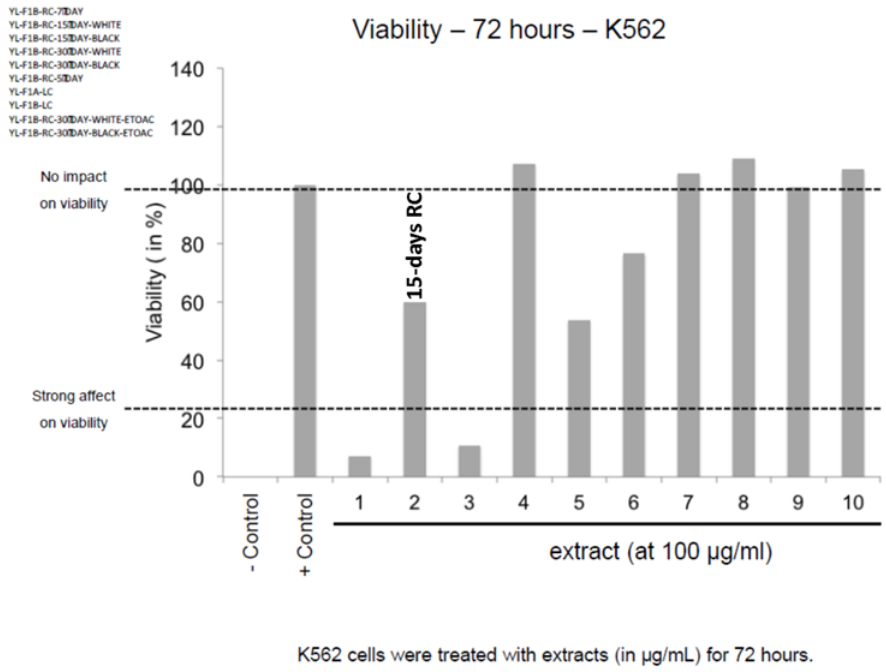

Fig.34 Viability assay of different culture extracts of *A. aculeatus* against K562 cell line

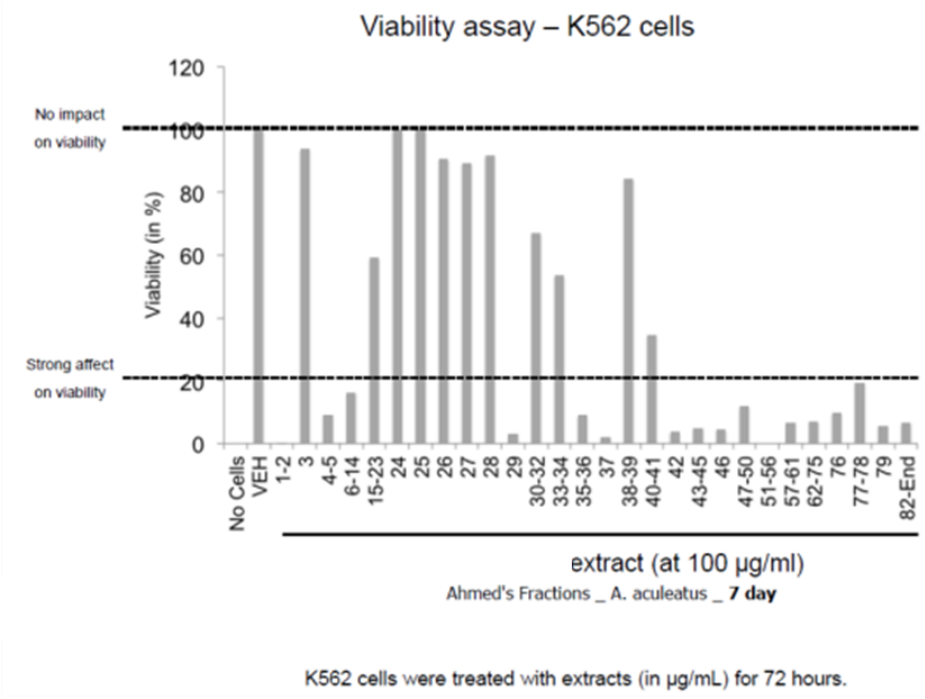

Fig.35 Anticancer activity of MPLC fractions from 7-day rice culture extract of *A. aculeatus* against K562 cancer cell line

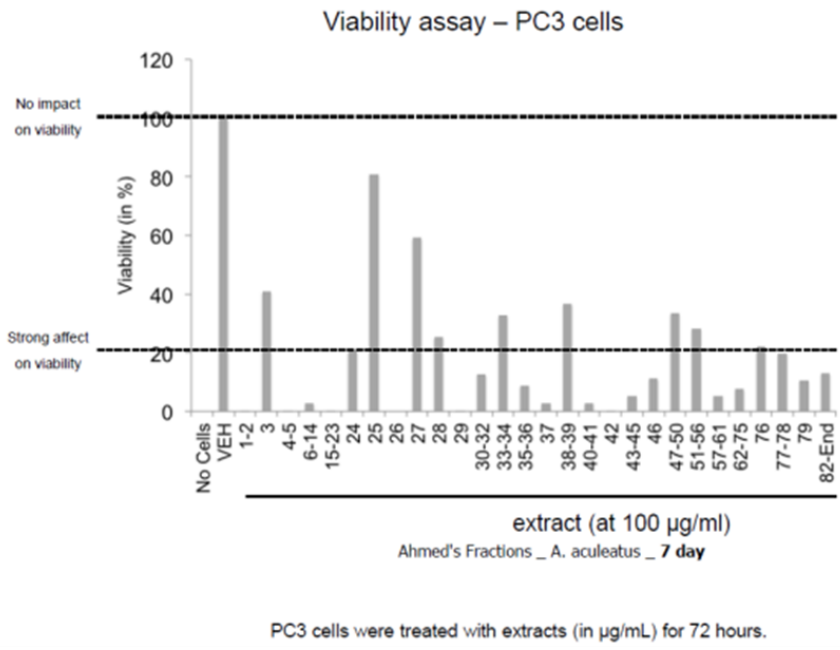

Fig.36 Anticancer activity of MPLC fractions from 7-day rice culture extract of *A. aculeatus* against PC3 cancer cell line

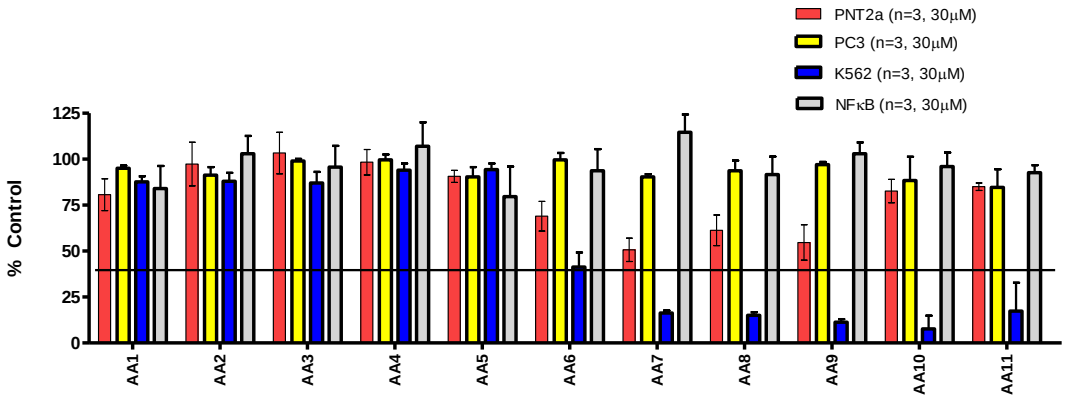

Fig.37 Activity of the purified compounds against both cancer cell lines and normal cells (●) normal cells, (●) PC3, (●) K562 and (●) NF-κB

3.2.4.2. Antimicrobial and antitrypanosome activity

Testing *A. aculeatus* extract (code: Ter-YL-F1B) against *T. brucei brucei* did not show any significant activity with an approximately 90 % cell viability for the tested cells (Fig.38). However, some of the MPLC fractions showed a remarkable activity as shown in (Fig.39). Most of the fractions achieved more than 90 % growth inhibition with MICs between 0.19-20.0 µg/mL. Furthermore, testing the purified compounds showed that compounds AA1, 2, 5, 6, 7, 8, 9 and AA10 showed a significant activity against *T. brucei brucei* with MIC values of 29.2,

121.4, 19.6, 18.6, 0.6, 0.6, 4.9, and 204.9 µM, respectively (Fig.40). Compounds AA7, AA8 and AA9 have been identified as secalonic acids D, C and B respectively. These compounds are generally cytotoxic as mentioned in the previous section and as reported in the literature (Hong, 2011, Ishida, 2000, Ishida et al., 1974, Li et al., 2008, Ren et al., 2005, Tang et al., 2012, Yuan et al., 2010, Zhang et al., 2009a). So their activity against *T. b. brucei* was expected to occur. However, compound AA5 (secalonic acid F) showed a selective cytotoxicity against *T. b. brucei* while it was not cytotoxic to any of the cancer cell lines as well as the normal cells. Secalonis acid F is a hybrid dimer of tetrahydroxanthone moieties in which the stereogenic centers are like (5R, 5'S, 6S, 6'S, 10aR, 10'aR). Compounds AA1, 2, 6 and 10 were described as ergosterol peroxide, nymphasterol, homogenistic acid and uridine, respectively (section 3.2.5). None of these compounds has been reported in the literature as antimicrobial or antitrypanosome, which indicated that the antitrypanosomal activity of these compounds is being reported for the first time. Although compounds AA1 and AA2 are both steroidal compounds, only compound AA1 showed a selective antimicrobial activity against *M. marinum* with MIC value of 233.64 µM (Fig.41). All other compounds isolated from 7-days RC extract exhibited no activity against *M. marinum*.

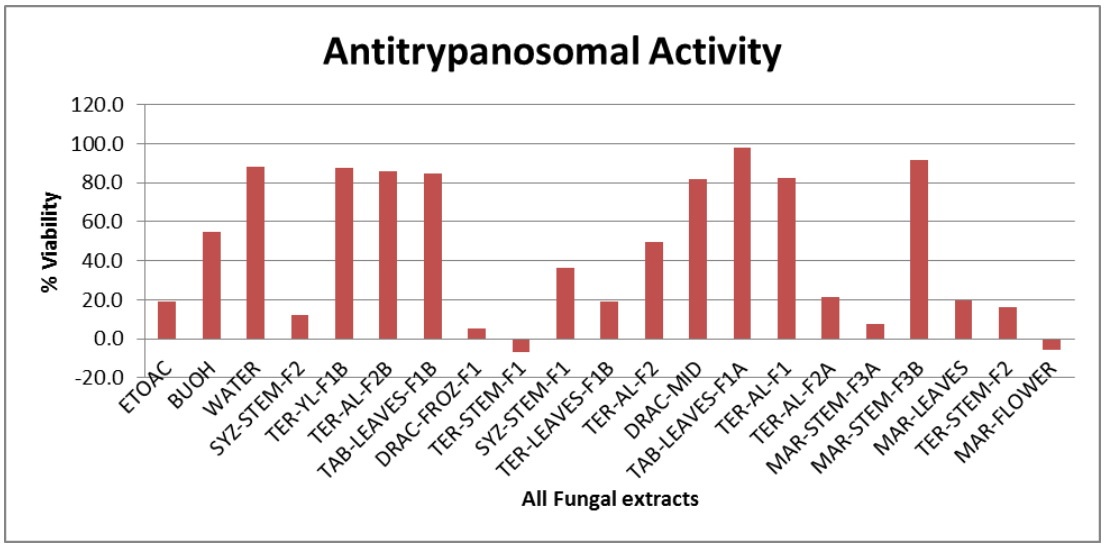

Fig.38 Antitrypanosomal activity of fungal extracts

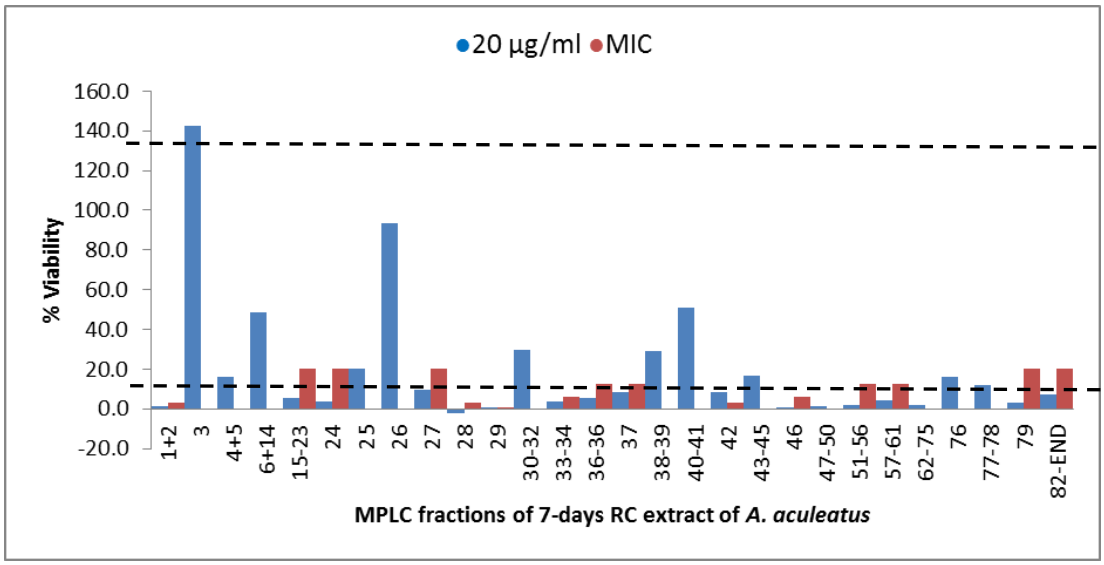

Fig.39 Antitrypanosomal activity of MPLC fraction of 7-day rice culture extract of *A. aculeatus*

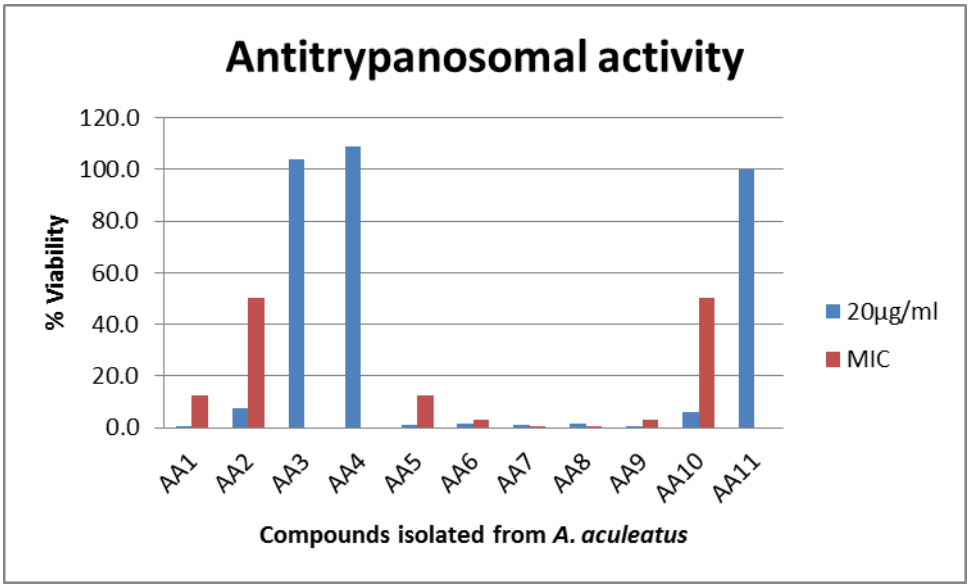

Fig.40 Antitrypanosomal activity of pure compounds isolated from *A. aculeatus*

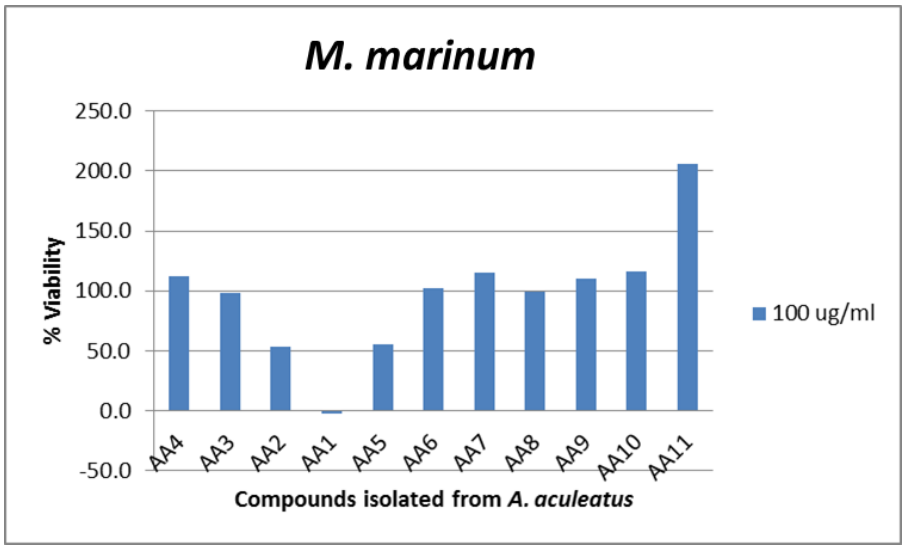

Fig.41 Activity of *A. aculeatus* compounds against *Mycobacterium marinum*

3.2.5. Isolated compounds

3.2.5.1. Compound AA1 (ergosterol peroxide)

3β-hydroxy-5,8-epidioxyergosta-6,22-diene	
Synonyms	Ergosterol peroxide
Sample codes	AA1
Sample Amount	13 mg
Physical Description	colourless needles
Molecular Formula	$C_{28}H_{44}O_3$
Molecular Weight	428 g/mol
Retention time (LC-MS)	30 min

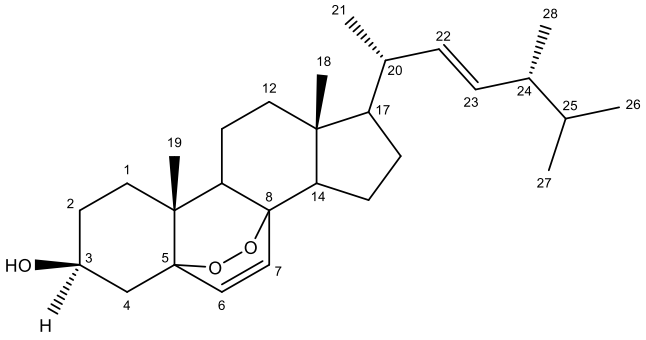

LC-HRFTMS spectrum $[M+H]^+$ 429.3368

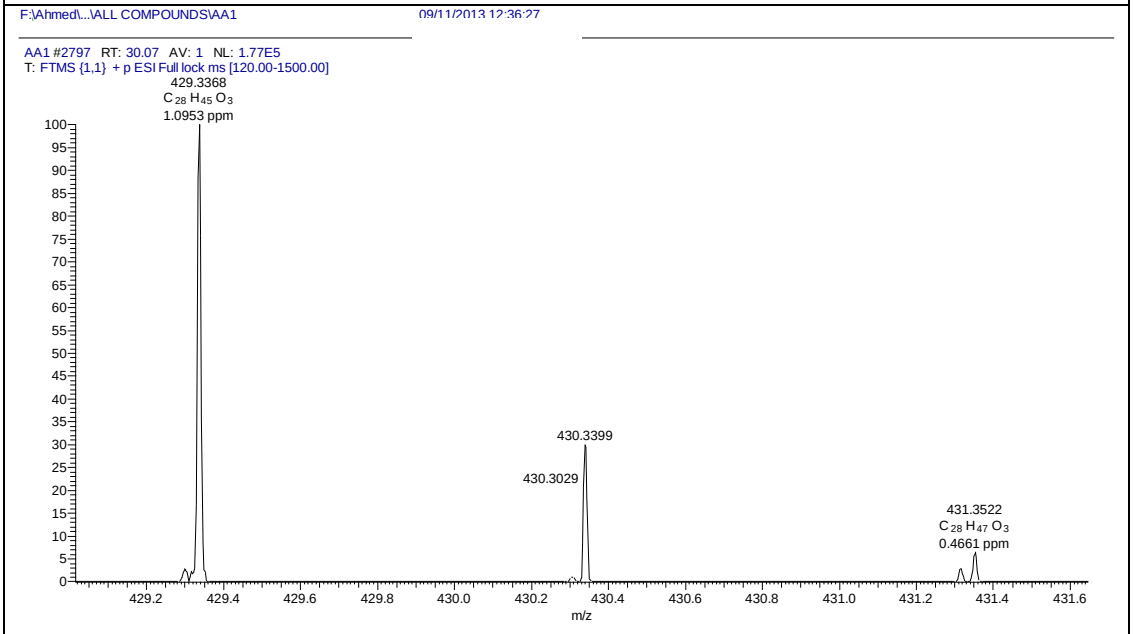

Compound AA1 (13 mg) was isolated as colourless needles, recrystallized from

MeOH, exhibited molecular formula $C_{28}H_{44}O_3$ estalished on the basis of ESI-HRMS at *m/z* 429.3368 $[M+H]^+$. The ^{13}C NMR and DEPT spectra (DMSO, 400 MHz) (Fig.42) of AA1 showed 28 carbon signals, which consists of six methyls, seven methylenes, six methines, two quaternary, four olefinics and three oxygen-bound carbons indicating the molecular formula $C_{28}H_{44}O_3$ in total. The carbinolic proton on ring A appeared in its **^{1}H NMR** spectrum (Fig.43) at δ_H 3.56 (*m*) attributable to position 3 which in the **^{1}H-^{1}H COSY** (Fig.44), coupled with two methylene groups at δ_H 1.80/ 1.83 assigned to position 4 and to 1.62/ 1.23 for position 2. The spin system was further exhibited in the 2D-TOCSY spectrum (Fig.45) which also showed a correlation of H-3 with the OH-group (δ_H = 4.6) on C-3. The C*H*$_2$-2 in turn correlated with another methylene at δ_H 1.70/ 1.57 for position 1. These positions were further confirmed by long-range coupling observed in **HMBC** (Fig.46), wherein the singlet methyl Me-19 (δ_H = 0.79) correlated with C-1 (δ_C 35.1), C-4 (δ_C 37.5) and C-5 (δ_C 82.0). Ring B structure was confirmed by the **COSY** correlations between the two olefinic protons at δ_H 6.2 (d, *J = 8.5 Hz*) for H-6 and δ_H 6.4 (d, *J = 8.5* Hz) for H-7. The ring was sustained by long range **HMBC** coupling wherein, H-6 correlated with C-4, C-5 and C-8 (δ_C 78.0) while H-7 correlated to C-5, C-8 and C-9 (δ_C 51.4). Rings C and D were confirmed by the HMBC correlation of the Me-18 singlet (δ_H 0.76) to C-12 (δ_C 39.4), C-13 (44.5), C-14 (δ_C 51.8) and C-17 (δ_C 56.3). The attachment of the side chain (5,6-dimethylhept-3-ene) to C-17 was confirmed from the HMBC correlation of Me-21 (δ_H 0.96, d) with C-17. The structure of the side chain was obtained from the correlation of Me-21 to C-20 (δ_C 39.9) and the olefinic C-22 (δ_C 135.7). In turn, the proton H-22 δ_H 5.21 correlated with C-20. Furthermore, the olefinic proton H-23 (δ_H 5.18, δ_C 132.1) correlated with C-24 (δ_C 42.6) which was seen by Me-28 (δ_H 0.88, d). Me-28 correlated with C-23, C-24 and C-25 (δ_C 33.1). The two methyl doublets Me-26 (δ_H 0.78, δ_C 20.1) and Me-27 (δ_H 0.81, δ_C 20.3) were found to correlate with each other and C-25. The NMR data (Table 8) showed signals typical of an ergostane sterol, which led to its identification as ergosterol peroxide, a well-known sterol in fungi (Fig.47). This was confirmed by high resolution MS, and comparison of its ^{1}H and ^{13}C NMR data with those reported in the literature (Lee et al., 2009) and (Kim et al., 1997).

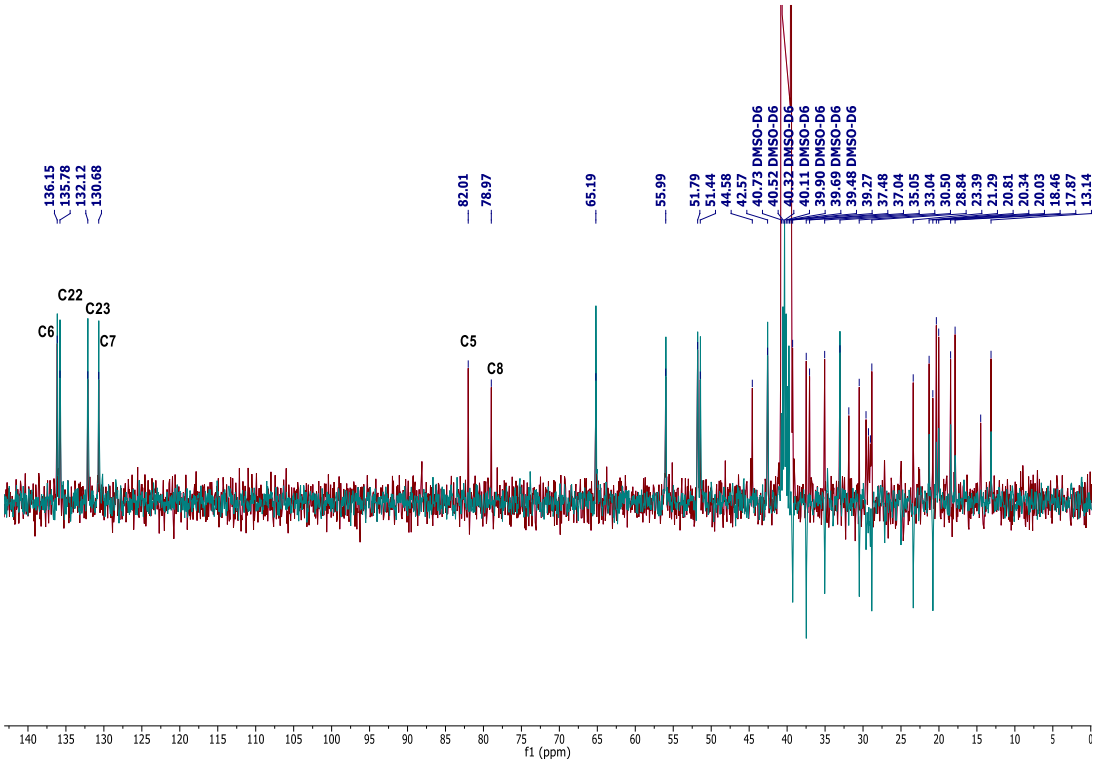

Fig.42 ^{13}C NMR and Dept spectra of compound AA1

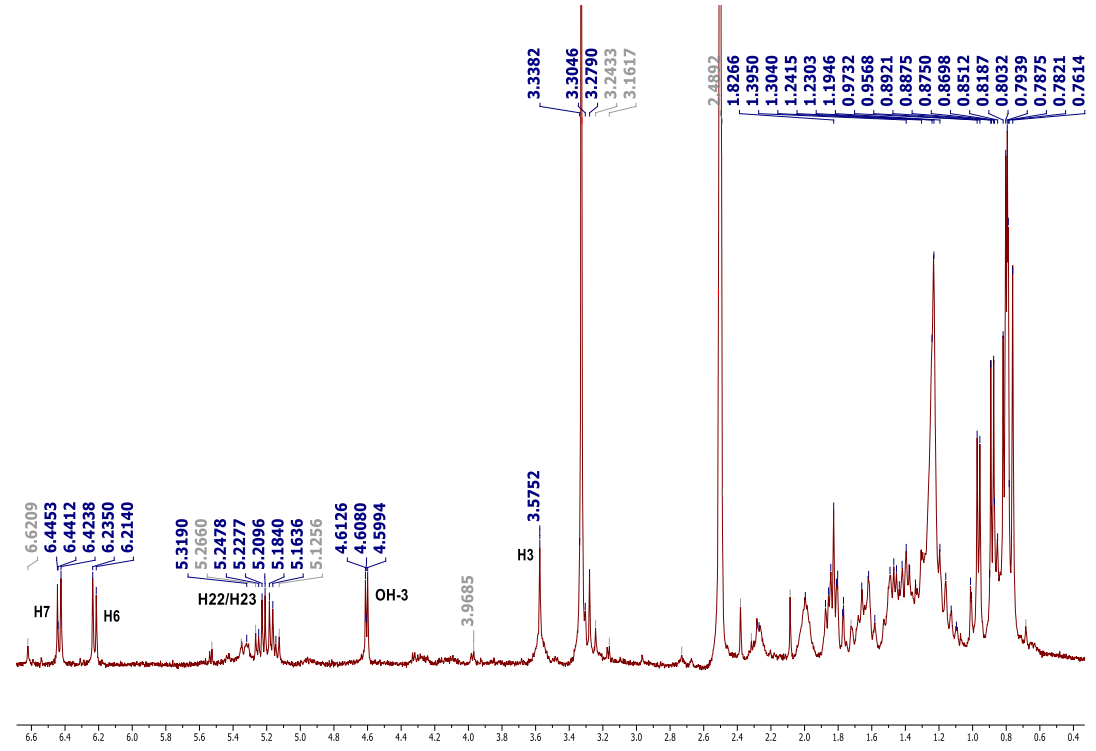

Fig.43 ^{1}HNMR spectrum of compound AA1

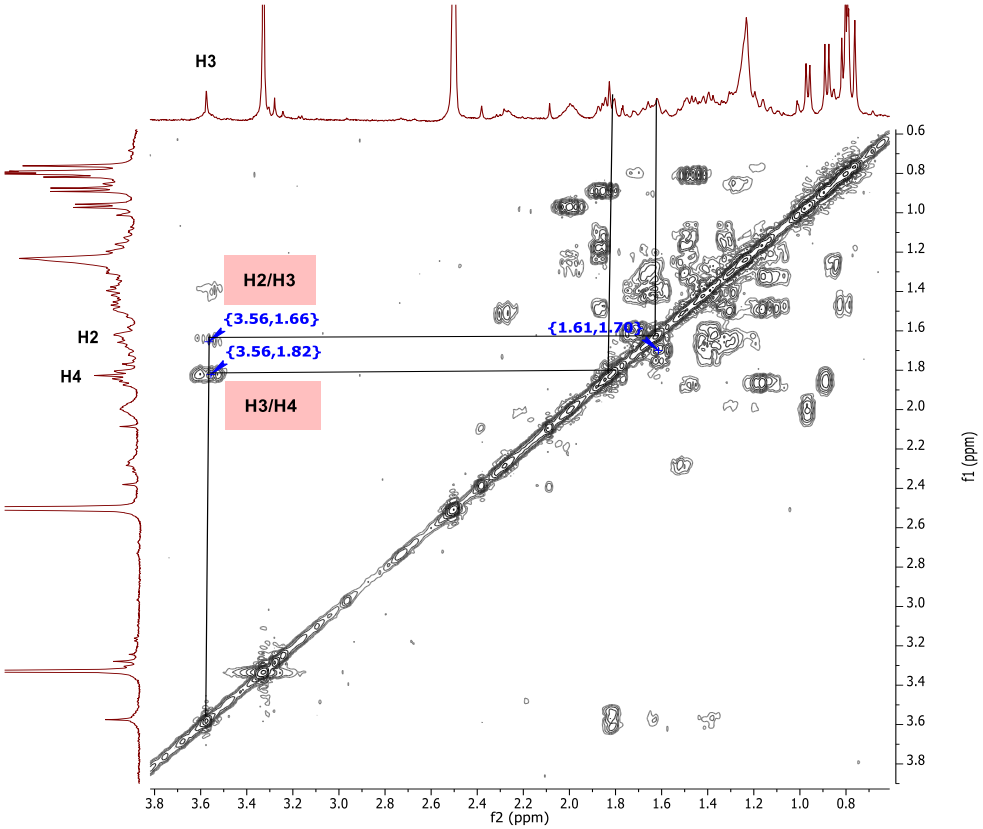

Fig.44 ^{1}H-^{1}H COSY spectrum of compound AA1 showing the spin system

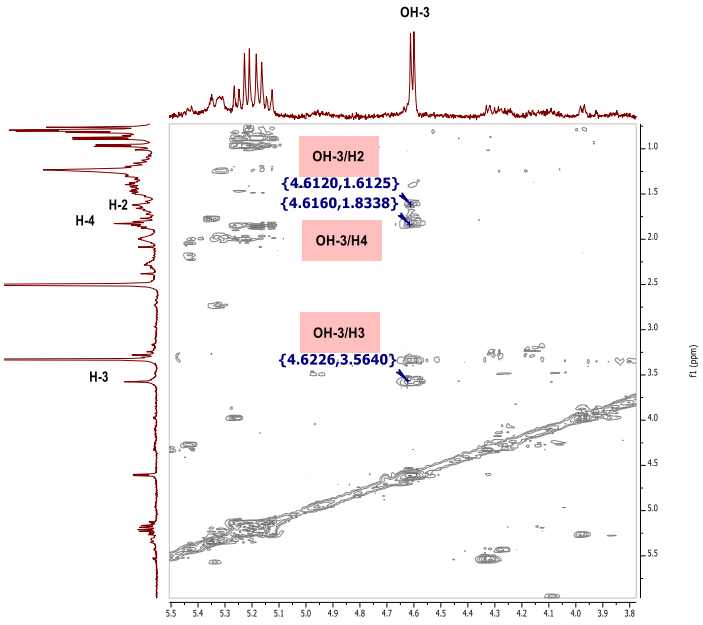

Fig.45 Expansion of 2D-TOCSY spectrum of compound AA1 showing correlation of OH-3 with H-3, H-2 and H-4

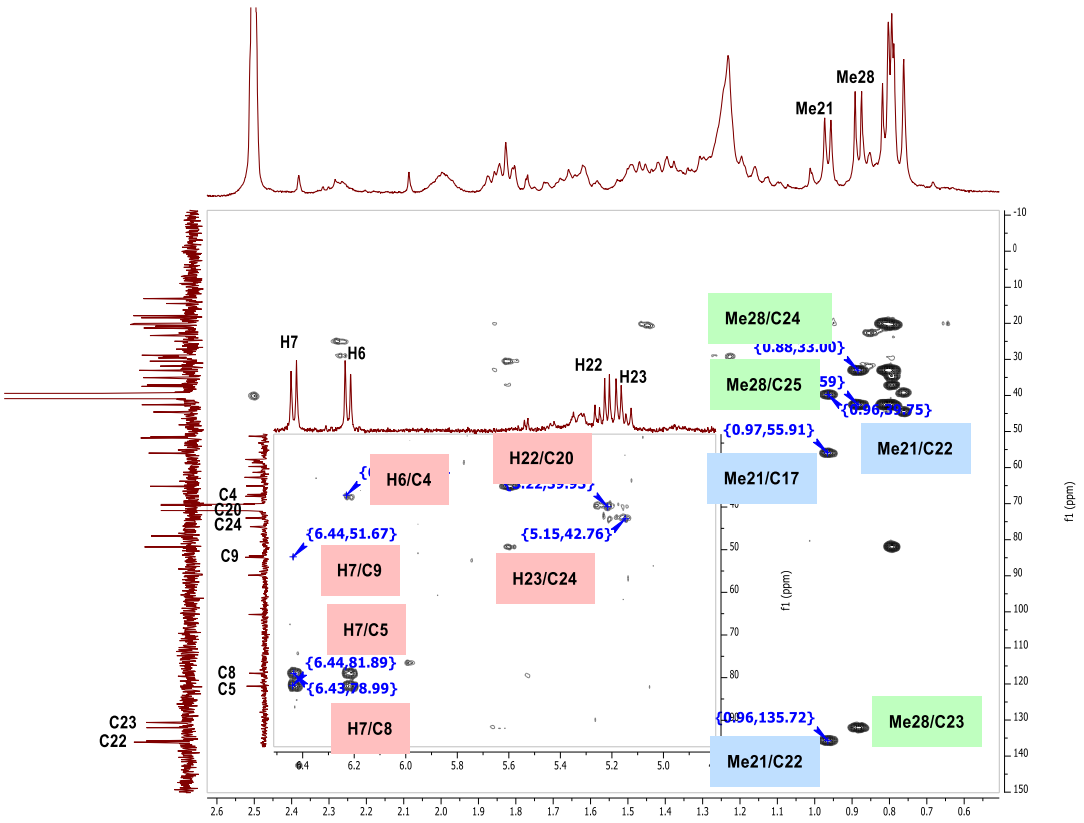

Fig.46 HMBC spectrum of compound AA1

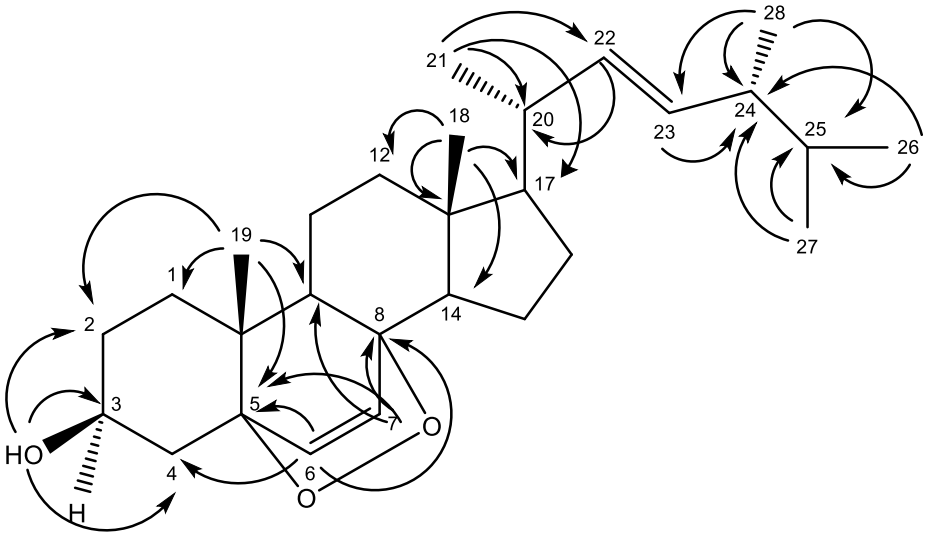

Fig.47 HMBC correlations of compound AA1

Table 8: ^{13}C NMR and ^{1}H NMR data of compound AA1

Atom No.	Lee 2009 $CDCl_3$ δc	Kim 1997 $CDCl_3$ δc	AA1 DMSO δc (m)	-AA1 DMSO δ_H (m, *J* in Hz)	-Lee 2009 $CDCl_3$ δ_H (m, *J* in Hz)	-Kim 1997 $CDCl_3$ δ_H (m, *J* in Hz)
1	37.0	35.1	37.1 (CH_2)	1.57, 1.72 (m)		
2	30.2	30.5	30.5 (CH_2)	1.62, 1.23 (m)		
3	66.4	66.8	65.2 (CH)	3.57 (m)	3.95 m	3.98 m
4	34.7	37.3	37.5 (CH_2)	1.83, 1.80 (m)		
5	79.4	83.1	82.0 (C)			
6	135.3	135.8	136.1 (CH)	6.22 (d, 8.5 Hz)	6.22 (d, 8.8 Hz)	6.51 (d, 8.6 Hz)
7	130.6	131.1	130.7 (CH)	6.44 (d, 8.5 Hz)	6.48 (d, 8.8 Hz)	6.25 (d, 8.6 Hz)
8	82.1	79.8	78.9 (C)			
9	51.1	51.4	51.4 (CH)	1.41 (m)		
10	37.0	37.3	36.9 (C)			
11	20.7	23.8	23.4 (CH_2)	1.5, 2.3 (m)		
12	39.4	39.7	39.4 (CH_2)	1.16, 1.84 (m)		
13	44.6	44.9	44.6 (C)			
14	51.7	52.1	51.8 (CH)	1.34 (m)		
15	28.7	21.0	20.8 (CH_2)	1.28, 1.30 (m)		
16	23.5	29.1	28.8 (CH_2)	1.66, 1.69 (m)		
17	56.2	56.1	56.3 (CH)	1.19 (m)		
18	12.9	13.3	13.1 (CH_3)	0.76 (s)	0.79 s	0.83 s
19	18.2	18.6	18.5 (CH_3)	0.79 (s)	0.87 s	0.89 s
20	39.8	40.1	39.9 (CH)	2.0 m		
21	20.9	21.1	21.3 (CH_3)	0.96 (d, 6.55 Hz)	0.98 (d, 6.8 Hz)	1.00 (d, 6.6 Hz)
22	132.2	135.6	135.8 (CH)	5.20 (dd, 7.2, 15.2 Hz)	5.2 (dd, 8.0, 15.6 Hz)	5.15 (dd, 7.7, 15.2 Hz)
23	135.1	132.4	132.1 (CH)	5.18 (dd, 8.03, 15.29 Hz)	5.11 (dd, 7.6, 15.6 Hz)	5.22 (dd, 8.2, 15.2 Hz)
24	42.8	43.1	42.6 (CH)	1.84 (m)		
25	33.1	33.4	33.1 (CH)	1.46 (m)		
26	20.0	20.0	20.0 (CH_3)	0.78 (d, 6.28 Hz)	0.81 (d, 6.8 Hz)	0.82 (d, 6.7 Hz)
27	19.7	20.3	20.3 (CH_3)	0.81 (d, 6.2 Hz)	0.79 (d, 6.4 Hz)	0.84 (d, 6.7 Hz)
28	17.6	17.9	17.9 (CH_3)	0.88 (d, 6.86 Hz)	0.88 (d, 6.8 Hz)	0.91(d, 6.7 Hz)

3.2.5.2. Compound AA2 (nymphasterol)

24-methyl-cholesta-5-ene-3-ol-(23,24,29)-cyclopropane	
Synonyms	Nymphasterol
Sample codes	AA2
Sample Amount	9 mg
Physical Description	white needles
Molecular Formula	$C_{29}H_{48}O$
Molecular Weight	412 g/mol
Optical Rotation $[\alpha]_D^{20}$	-11 (*c* 0.1 in $CHCl_3$)
Retention time (LC-MS)	25.60 min

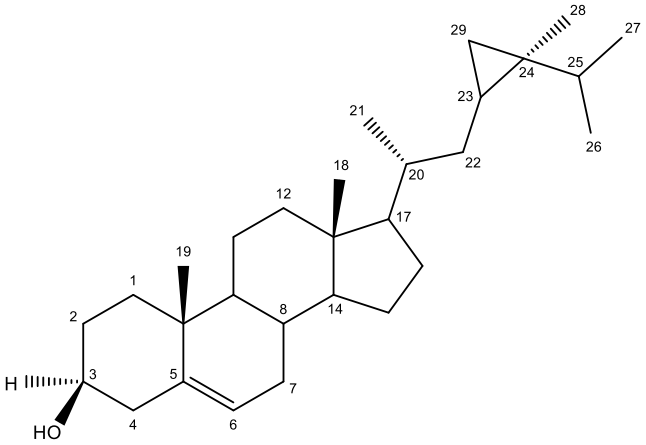

LC-HRFTMS spectrum $[M+H]^+$ 413.3775

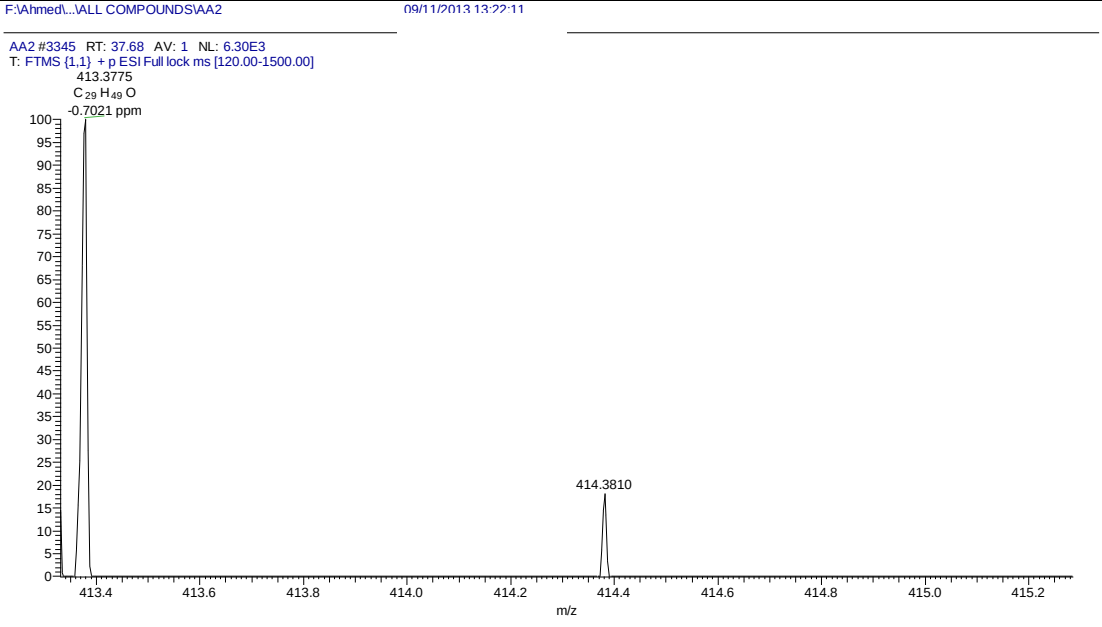

Compound AA2 (9 mg) was isolated as white needles, recrystallized from MeOH,

exhibited molecular formula $C_{29}H_{48}O$ established by ESI-HRMS at *m/z* = 413.3775 [M+H]+. The optical rotation $[\alpha]^{20}_{D}$ = -11 (*c* 0.1 in $CHCl_3$). The **^{1}H NMR** spectrum of AA2 ($CDCl_3$, 400 MHz) (Fig.48) showed three methyl singlet signals at δ_H 0.67, 1.00 and 0.83 equivalent for Me-18, Me-19 and (Me-28); three methyl doublet signals at δ_H 0.91 (d, *J* = 6.5 Hz) for Me-21, δ_H 0.83 (d, *J* = 7.2 Hz) for Me-26 and Me-27 at δ_H 0.82 (d, *J* = 7.2 Hz). Furthermore, the olefinic proton H-6 at δ_H 5.35 indicated the presence of stigma-6-ene sterol type. One carbinolic proton H-3 was observed at δ_H 3.51 (m, *J* = 6 Hz), the coupling constant indicated the α-orientation of the carbinolic proton. The **^{13}C NMR** and **DEPT** spectra ($CDCl_3$, 400 MHz) (Fig.49) showed 29 carbon signals that included six methyls, ten methylenes, seven methines, four quaternary, one olefinic and one carbinolic. Ring A was confirmed to be similar to that of compound AA1 through the **^{1}H-^{1}H COSY** correlations (Fig.51) of the carbinolic proton H-3 (δ_H 3.5) to the other methylene groups at δ_H 1.48, 1.85 for C*H*$_2$-2 and at δ_H 2.22, 2.26 for C*H*$_2$-4. Moreover, the **HMBC** spectrum (Fig.50) showed the correlations of the methylene groups C*H*$_2$-1 at δ_H 1.83, 1.07 with the oxygenated carbon C-3 (δ_C 71.9), other methylene group C*H*$_2$-2 (δ_C 31.7) and C-10 (δ_C 36.6); C*H*$_2$-4 at δ_H 2.28, 2.22 correlated with C-2 and C-10 (δ_C 36.6). Ring B was sustained by the HMBC correlations of the olefinic proton H-6 (δ_H 5.35) to C-10 and C-8 (δ_C 31.9). Moreover, the correlations of Me-19 with C-10, C-9 (δ_C 50.2) and C-5 (δ_C 140.8) gave further confirmation. Rings C and D were similar to compound AA1, evidenced by the correlations of Me-18 to C-12 (δ_C 39.8), C-13 (δ_C 42.4), C-14 (δ_C 56.8) and C-17 (δ_C 56.1). The attachment of the side chain on C-17 was indicated by the correlation between C-17 and Me-21. Me-21 correlated with C-20 (δ_C 36.2) and C-22 (δ_C 34.0). The upfield chemical shift for C-22 confirmed the absence of the double bond between C-22 and C-23 (δ_C 29.23) compared to compound AA1 (ergosterol peroxide). The cyclopropane structure was sustained from the HMBC correlations of Me-28 to the methylene group C*H*$_2$-29 (δ_C 23.22) and C-23. Further confirmation was indicated by the ROESY correlation (Fig.52) between Me-28 (δ_H 0.83) and the methine proton of C-23 (δ_H 1.61). The rest of 5,6-dimethyl-heptyl-4,5,8-cyclo-propane side chain was confirmed through the HMBC correlation of Me-28 to C-25 (δ_C 45.9) which was

further correlated with the two methyl doublets Me-26 and Me-27. Therefore, compound AA2 was identified as 24-methyl-cholesta-5-ene-3-ol-(23,24,29)-cyclopropane (Fig.53) and this was confirmed by comparison to the spectroscopic data of nymphasterol in the literature (Table 9). Nymphasterol was previously isolated from *Nymphaea stellate* (Verma et al., 2012) and isolated for the first time from *Aspergillus aculeatus* endophyte. This was indicative to the ability of the endophytes to produce the plant metabolites with the advantage of the upscaling so larger quantity of the bioactive metabolites can be produced. Moreover, the method of cultivation is sustainable so it can be used at any time in the fermentation laboratory.

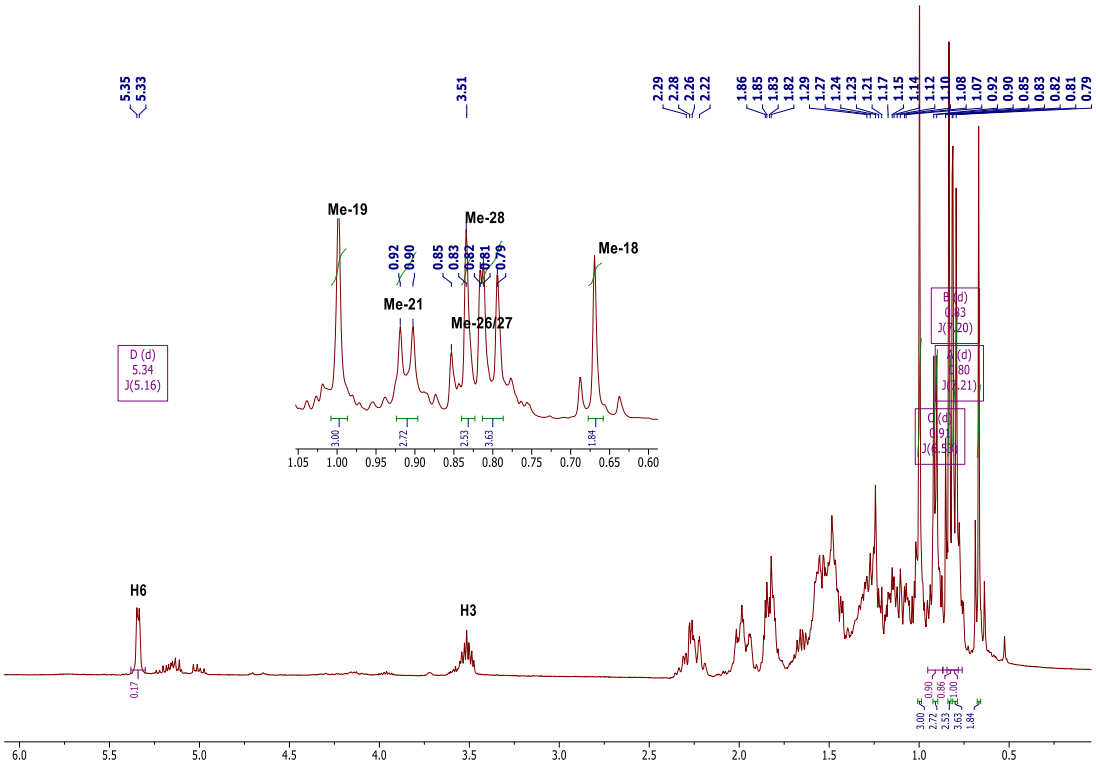

Fig.48 ^{1}H NMR spectrum of compound AA2

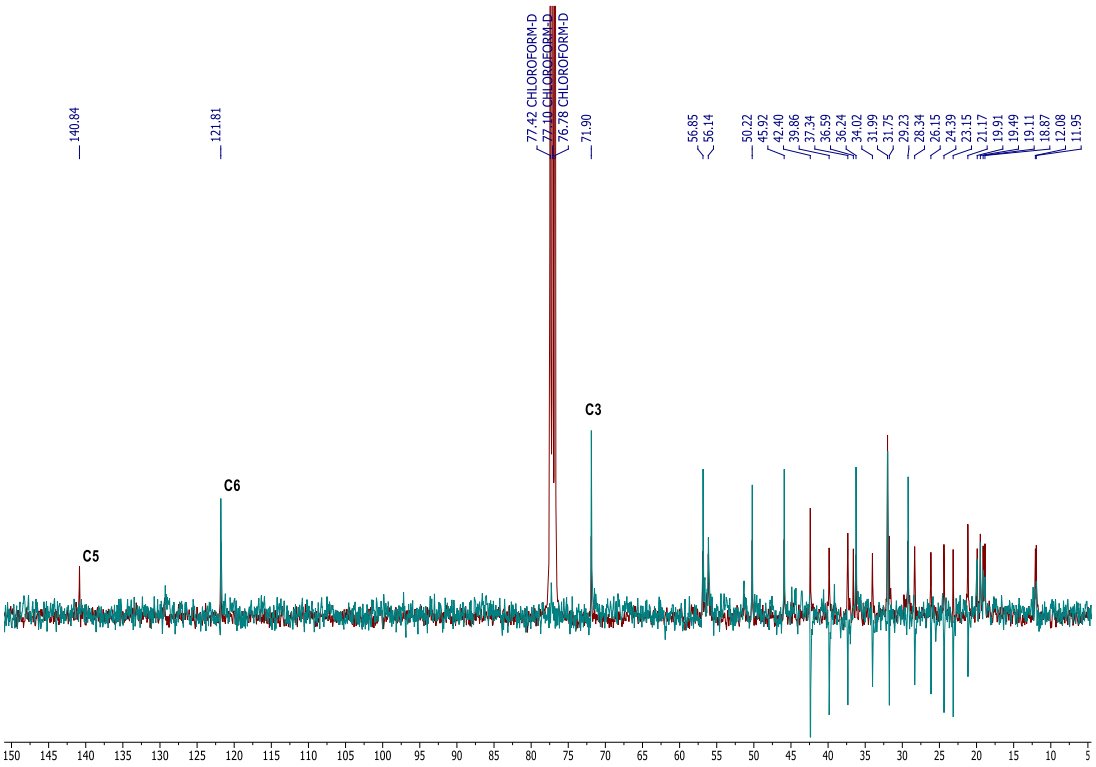

Fig.49 ^{13}C NMR and DEPT spectra of compound AA2

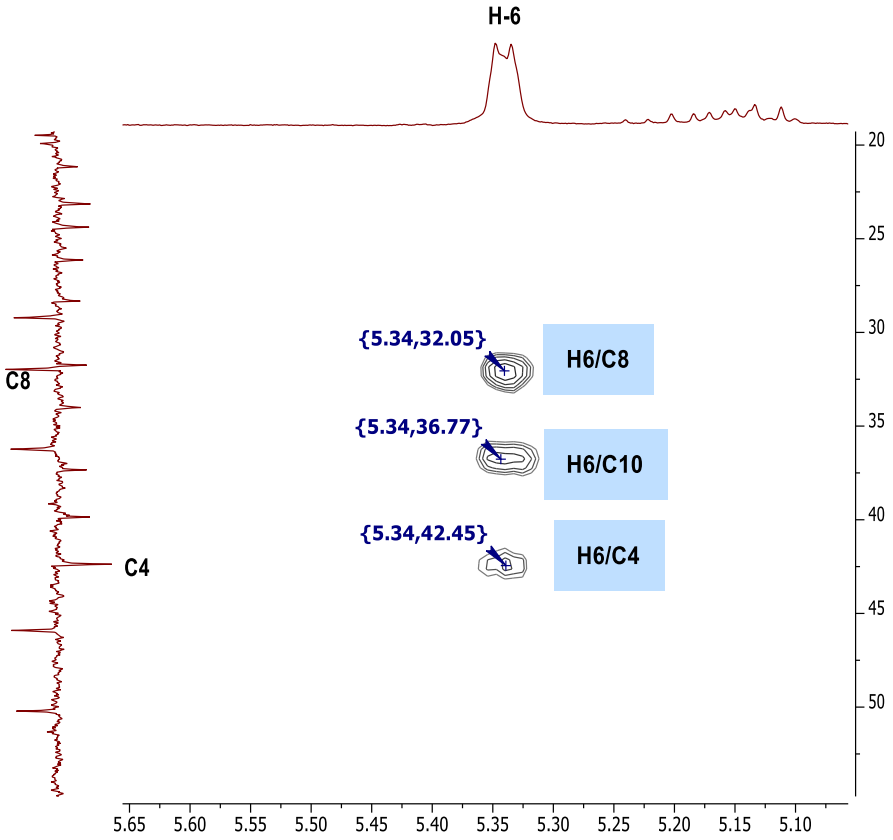

Fig.50 Expansion of HMBC spectrum of compound AA2 showing correlation of H6 with C8, C10 and C4

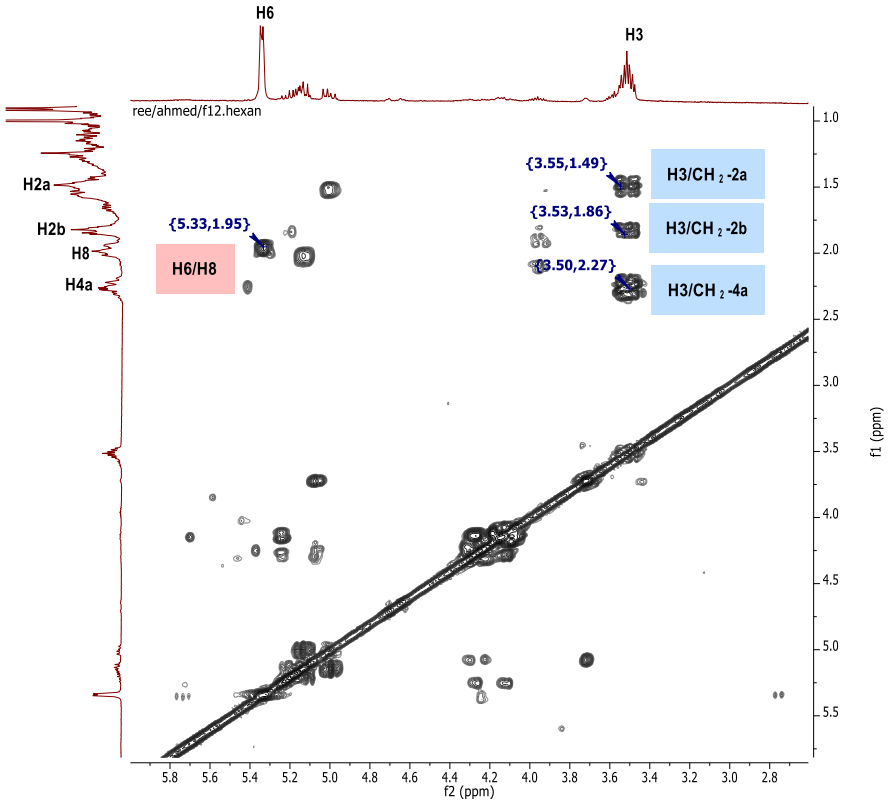

Fig.51 Expansion of ^{1}H-^{1}H COSY spectrum of compound AA2 showing correlation of H-3 to C*H*$_2$-2 and C*H*$_2$-4

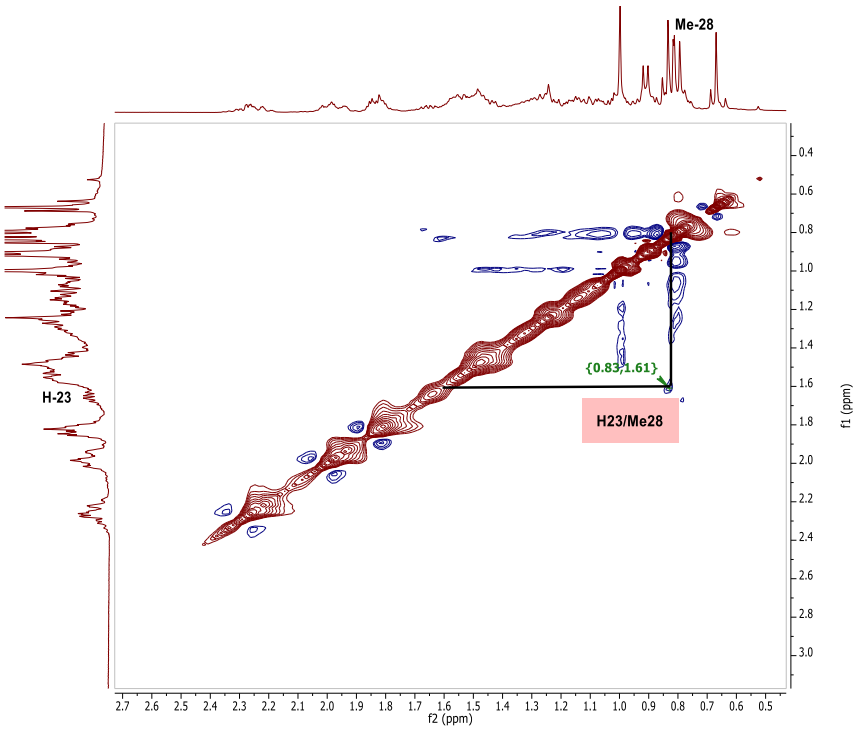

Fig.52 Expansion of ROESY spectrum of compound AA2 showing the correlation of Me-28 with C*H*$_2$-23

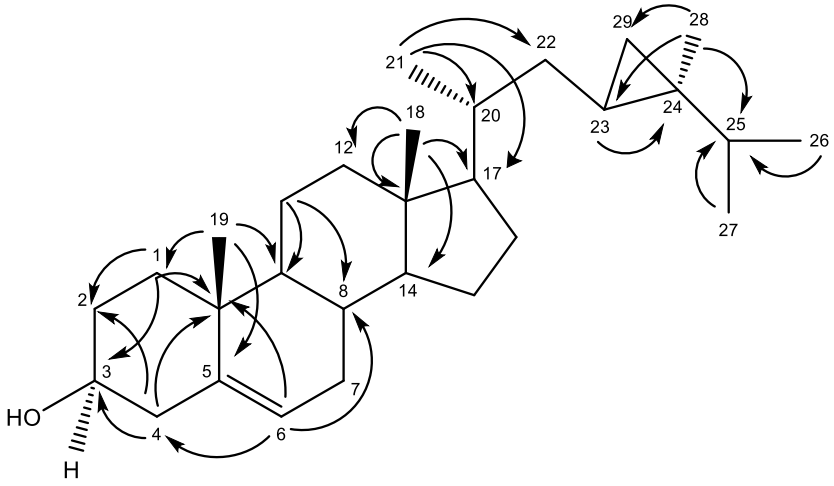

Fig.53 HMBC correlations of compound AA2

Table 9: ^{13}C NMR and ^{1}H NMR-$CDCl_3$ data of compound AA2

Carbon No.	Verma 2012 δ_C (m)	AA-2 δ_C (m)	Verma 2012 δ_H (m, *J* in Hz)	AA-2 δ_H (m, *J* in Hz)
1	36.2	37.3 (CH_2)		1.07, 1.83 (m)
2	31.6	31.7 (CH_2)		1.48, 1.85 (m)
3	71.8	71.9 (CH)	3.52 (m)	3.50 (m)
4	42.3	42.4 (CH_2)		2.22, 2.26 (m)
5	140	140.8 (C)		
6	121	121.8 (CH)	5.35 (t, 5.5 Hz)	5.35 (t, 5.16 Hz)
7	33.9	34.0 (CH_2)		1.03, 2.31 (m)
8	29.1	32.0 (CH)		1.94 (m)
9	50.1	50.2 (CH)		0.91 (m)
10	36.1	36.6 (C)		
11	21	21.2 (CH_2)		1.45, 1.50 (m)
12	39.7	39.9 (CH_2)		2.02, 1.97 (m)
13	42.2	42.5 (C)		
14	56.7	56.8 (CH)		0.96 (m)
15	24.3	24.4 (CH_2)		1.55, 1.59 (m)
16	28.2	28.3 (CH_2)		1.80, 1.84 (m)
17	56	56.1 (CH)		1.07 (m)
18	11.9	11.9 (CH_3)	0.68 (s)	0.67 (s)
19	19.4	19.5 (CH_3)	1.0 (s)	1.0 (s)
20	36.1	36.2 (CH)		1.33
21	18.7	18.9 (CH_3)	0.92 (d, 5.5 Hz)	0.92 (d, 6.5 Hz)
22	26	34.0 (CH_2)		1.01
23	39.9	29.2 (CH)	1.15 (m)	1.61 (m)
24	37.2	39.1 (C)		
25	29.1	45.9 (CH)		0.91 (m)
26	19.8	19.9 (CH_3)	0.82 (d, 5.4 Hz)	0.83 (d, 7.2 Hz)
27	19	19.1 (CH_3)	0.80 (d, 5.5 Hz)	0.80 (d, 7.2 Hz)
28	11.8	12.1 (CH_3)		0.83 (s)
29	23	23.1 (CH_2)	1.59 (m)	1.25 (m)

3.2.5.3. Compound AA3 (pentahydroxy-dihydro-dinaphthofuran-dione)

2,4,6a,10,12-pentahydroxy-6,6a-dihydrodinaphtho[2,1-b:1',2'-d]furan-5,9-dione	
Synonyms	-
Sample codes	AA3
Sample Amount	3 mg
Physical Description	brown amorphous powder
Molecular Formula	$C_{20}H_{12}O_8$
Molecular Weight	380 g/mol
Optical Rotation $[\alpha]_D^{20}$	-38 (*c* 0.05 in MeOH)
Retention time (LC-MS)	12.43 min

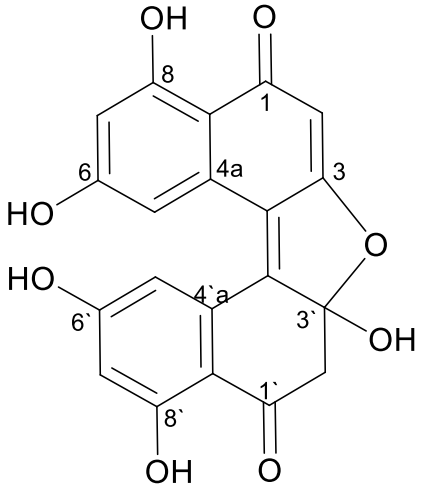

LC-HRFTMS spectrum $[M-H]^-$ 379.0460

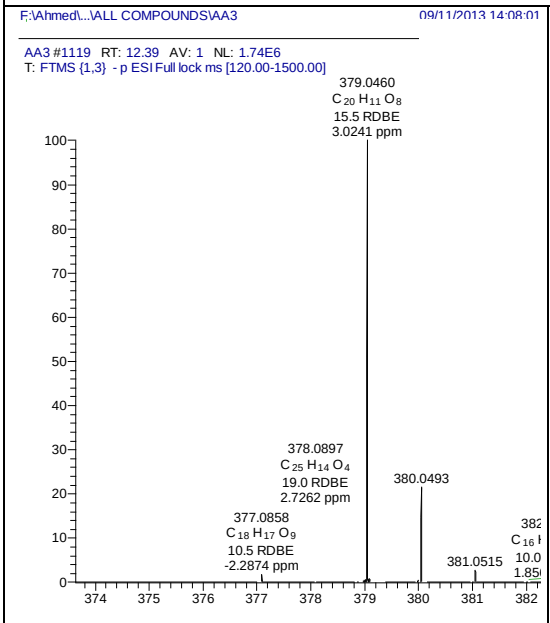

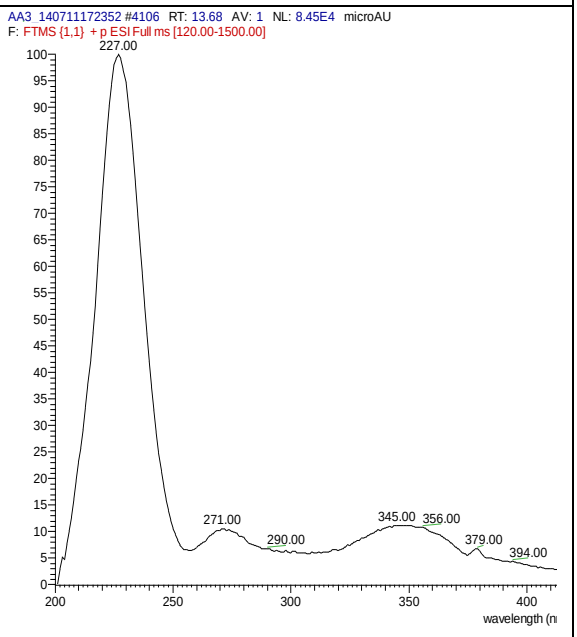

Compound AA3 (3 mg) was obtained as brown amorphous powder, exhibited a molecular formula $C_{20}H_{12}O_8$ from ESI-HRMS at *m/z* = 379.0460 [M-H^+] with DBE = 15. The optical rotation $[\alpha]^{20}_D$ = -38 (*c* 0.05 in MeOH). The **^{1}H NMR** and **HMQC** spectra of AA3 (DMSO, 400 MHz) (Fig.54, 55) indicated the presence of four doublet signals in the aromatic region at δ_H 7.5 (d, *J* = 2.3 Hz), 7.12 (d, *J* = 2.25 Hz), 6.47 (d, *J* = 2.18 Hz) and 6.36 (d, *J* = 2.12 Hz). These chemical shifts were assigned for protons H-5, H-5`, H-7` and H-7, respectively which corresponded to carbon shifts at δ_C 106, 109.5, 105.74 and 105.61 while the singlet signals at δ_H 5.89 was assigned to H-2 whose carbon was found at δ_C 99.76. The **^{1}H-^{1}H COSY** spectrum (Fig.56) showed the correlation between *meta* coupled protons H-5 and H-7 and between H-5` and H-7`. The upfield carbon shift of C-5, C-7, C-5` and C-7` signified the presence of electronegative atoms (OH) attached to the positions C-6 (δ_C 163.0), C-8 (δ_C 165.1), C-6` ($\delta_C$ 163.0) and C-8` (δ_C 165.2) which was further indicated by the downfield shift of these carbons. The **HMBC** spectrum (DMSO, 600 mHz) (Fig.57) confirmed the presence of two naphthalene units; the first one was indicated by the correlation of H-5 with C-6, C-8a (δ_C 108.2) and C-4 (δ_C 122.2) together with the correlation of H-2 with C-4 and the carbonyl carbon C-1 (δ_C 191.6). The second unit was confirmed through cross peaks between H-5` and C-7`, C-8`A ($\delta_C$ 109.8) and C-4` (δ_C 146.7) together with the correlations of the two methylene protons of C*H*$_2$-2`at $\delta_H$ 3.4, 3.2 to the carbonyl C-1` (δ_C 199.3) and C-3` ($\delta_C$ 112.8). The downfield shift of C-3` indicated the presence of a strong electronegative effect of the two oxygens attached to C-3`. Moreover, the downfield shift of C-4` (δ_C 146.7) gave further evidence for the structure. Therefore, compound AA3 was elucidated to be (2,4,6a,10,12-pentahydroxy-6,6a-dihydrodinaphtho[2,1-b:1',2'-d]furan-5,9-dione) (Fig.58), by comparison to a structurally related compound isolated from the fungus *Sphaeropsidales* sp. and previously described by Bode and Zeeck (2000) (Table 10). It was reported only once in the literature as a patented aldose reductase inhibitor (Yoshida et al., 1993).

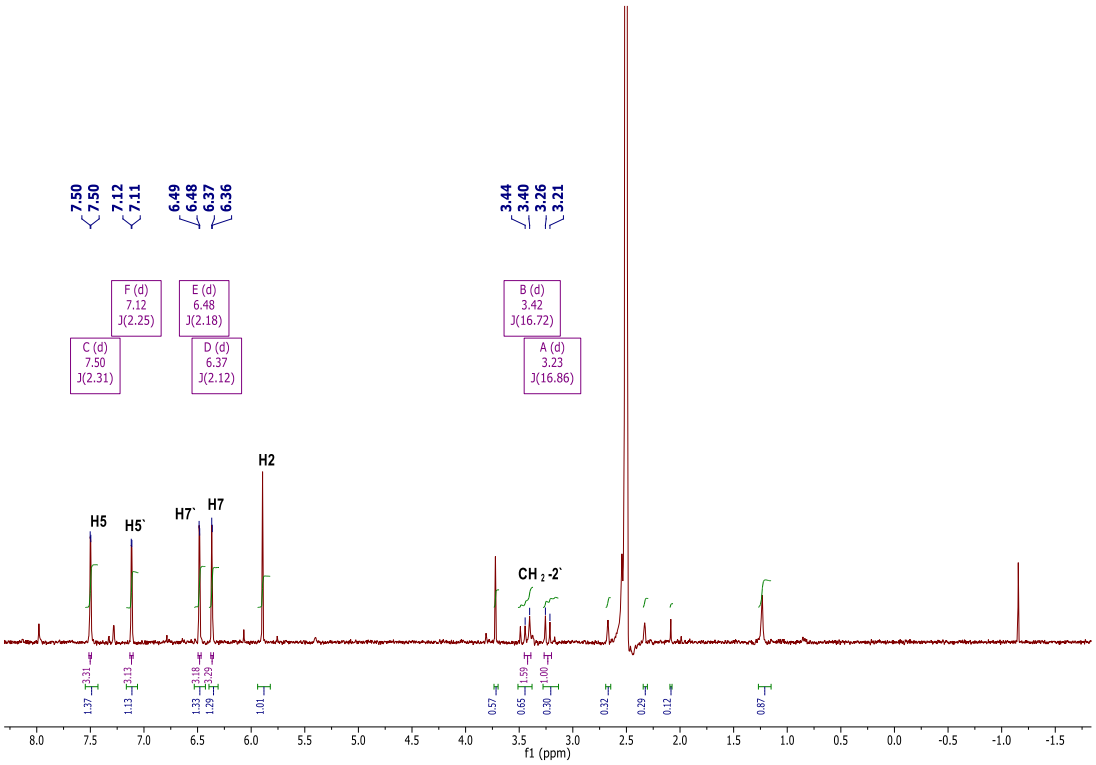

Fig.54 ^{1}HNMR spectrum of compound AA3

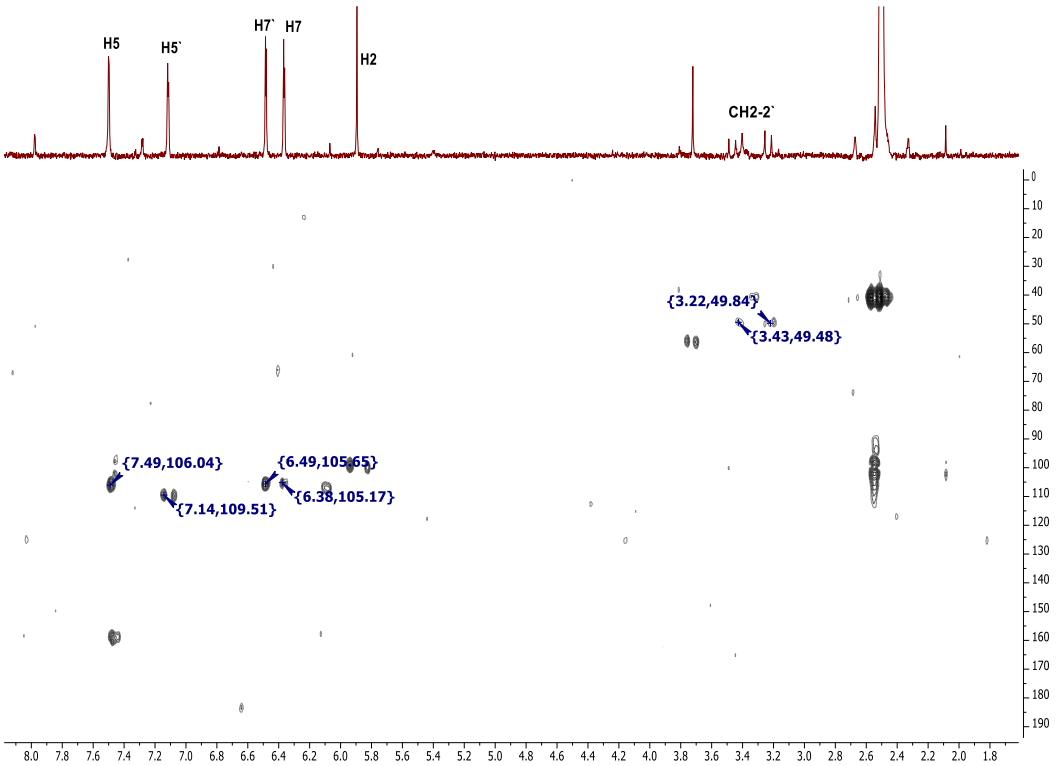

Fig.55 HMQC spectrum of compound AA3

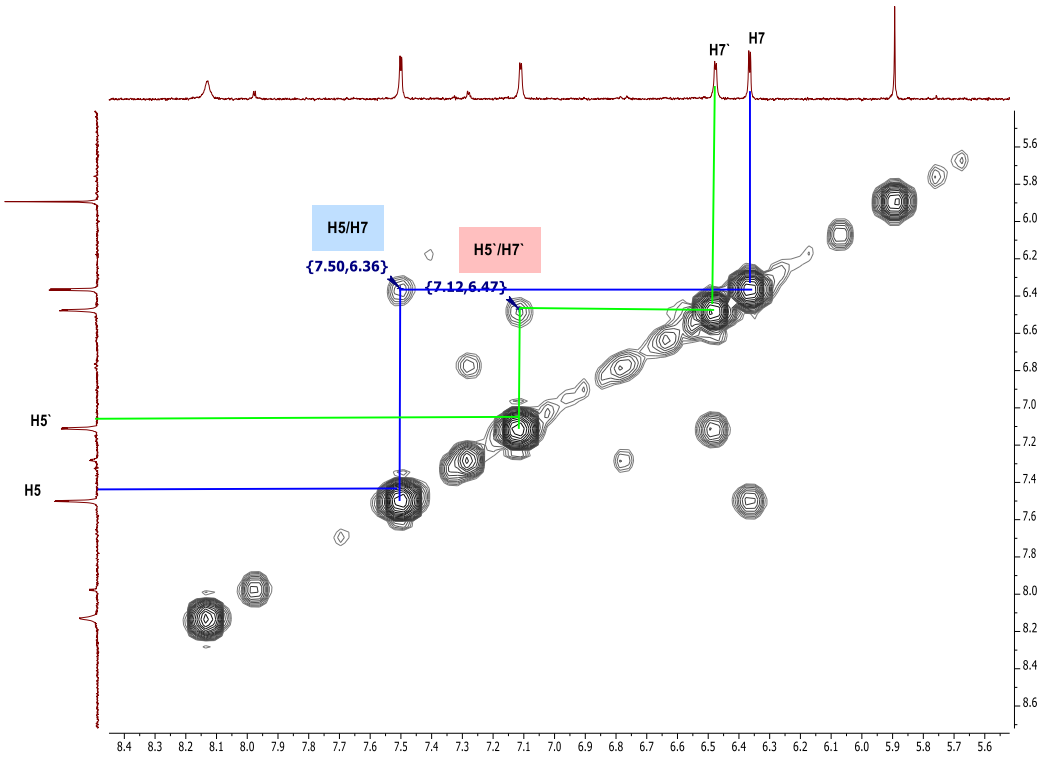

Fig.56 Expansion of ^{1}H-^{1}H COSY spectrum of compound AA3 showing two different spin systems

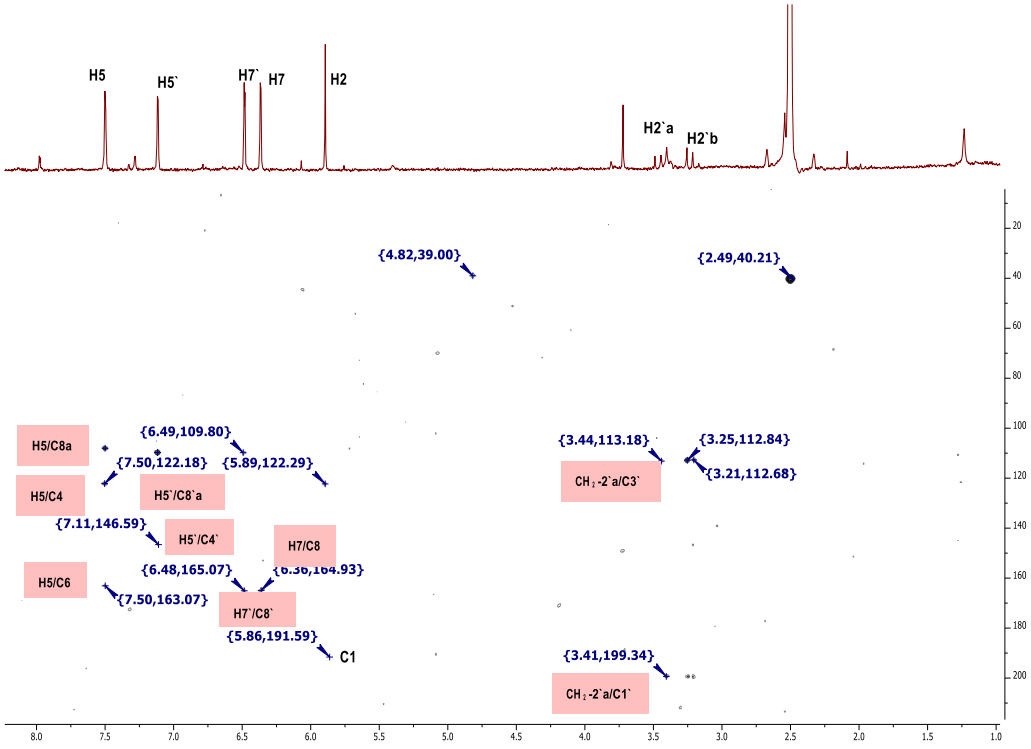

Fig.57 HMBC spectrum of compound AA3

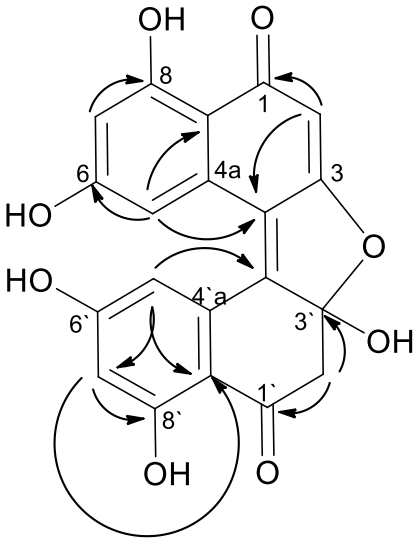

Fig.58 HMBC correlations of compound AA3

Table 10: ^{1}H NMR and ^{13}C NMR data of Compound AA3 (DMSO-600MHz)

	Bode and Zeck 2000		Yoshida 1993		AA-3	
No	δ_C (m)	δ_H (m, *J* in Hz)	δ_C (m)	δ_H (m, *J* in Hz)	δ_C (m)	δ_H (m, *J* in Hz)
1`	200.8		199.1		199.3 (C)	
1	190.8		190.3		191.5 (C)	
3	172.5		172.0			
8	161.8		165.2		165.1 (C)	
8`	161.7		164.4		165.1 (C)	
4`	146.6		146.6		146.7 (C)	
6`	136.9	7.81 (t, 8.0 Hz)	162.3			
6	134.2	7.52 (t, 8.0 Hz)			163.0 (C)	
4`a	133.0		135.1			
4a	128.8		130.8			
4	121.4		122.0		122.2 (C)	
7`	120.9	7.23 (d, 8.0 Hz)	109.5	6.36 (d, 2.2 Hz)	105.9 (CH)	6.47 (d, 2.2 Hz)
5`	120.1	7.74 (d, 8.0 Hz)	109.4	6.45 (d, 2.2 Hz)	109.5 (CH)	7.12 (d, 2.2 Hz)
7	119.6	7.05 (d, 8.0 Hz)	107.9	7.09 (d, 2.0 Hz)	105.6 (CH)	6.36 (d, 2.2 Hz)
5	115.9	7.99 (d, 8.0 Hz)	105.4	7.5 (d, 2.0 Hz)	106.0 (CH)	7.50 (d, 2.2 Hz)
8`a	115.5		105.1		109.8 (C)	
8a	114				108.2 (C)	
3`	112.3		112.6		112.8 (C)	
2	99.6	6.05	99.3	5.83 (s)	99.8 (CH)	5.89 (s)
2`	49.5	3.52 (dd, 16.5,1.0 Hz) 3.38 (d, 16.5 Hz)	49.6	3.23 (d, 16.8 Hz), 3.40 (d, 16.8 Hz)	49.5 (CH_2)	3.23 (d, 16.8 Hz) 3.42 (d, 16.72 Hz)
8-OH		13.66		13.85		13.85
3`-OH		8.27 (d, 1.0 Hz)				8.12 (brs)
8`-OH		12.18		12.56		12.56
6-OH				11.33		11.34
6`-OH				10.71		10.71

3.2.5.4. Compounds AA7 (secalonic acid D)

(5R,5'R,6S,6'S,10aR,10'aR)-dimethyl 1,1',5,5',8,8'-hexahydroxy-6,6'-dimethyl-9,9'-dioxo-6,6',7,7',9,9',10a,10'a-octahydro-5H,5'H-[2,2'-bixanthene]-10a,10'a-dicarboxylate	
Synonyms	Secalonic acid D
Sample codes	AA7
Sample Amount	16 mg
Physical Description	yellow amorphous powder
Molecular Formula	$C_{32}H_{30}O_{14}$
Molecular Weight	638 g/mol
Optical Rotation $[\alpha]_D^{20}$	+51 (*c* 0.1 in $CHCl_3$)
Retention time (LC-MS)	17.87 min

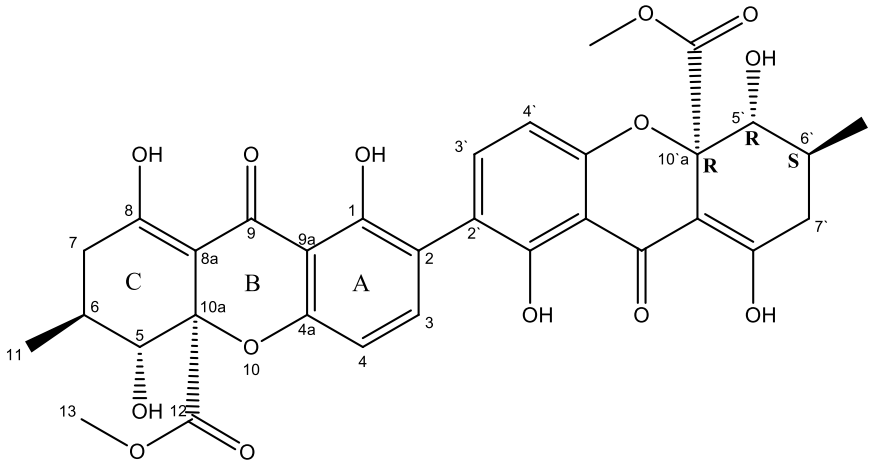

LC-HRFTMS spectrum $[M+H]^+$ 639.1711

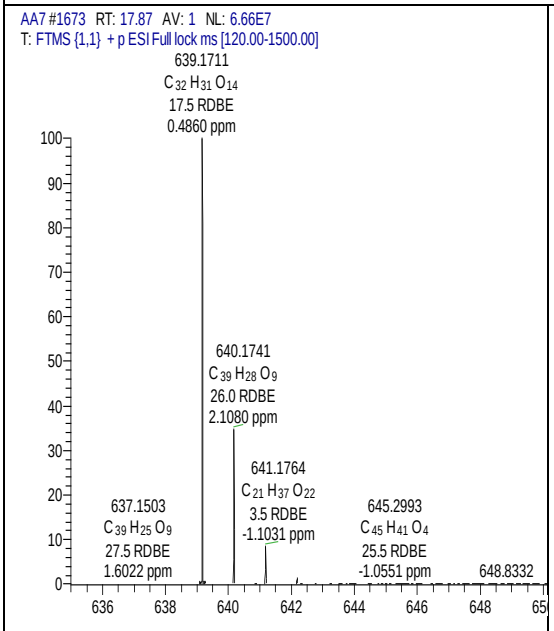

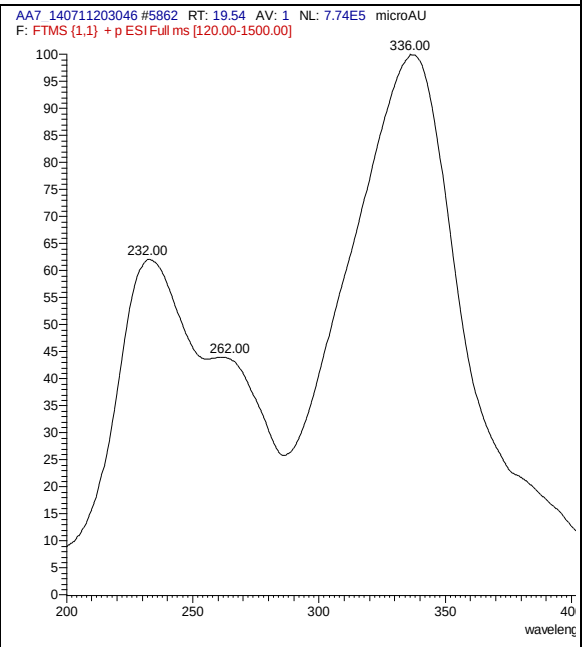

Compound AA7 (16 mg) was obtained as a yellow amorphous powder, exhibited a molecular formula $C_{32}H_{30}O_{14}$ established by ESI-HRMS at *m/z* = 639.1711 $[M+H]^+$. The optical rotation $[\alpha]^{20}_D$ = +51 (*c* 0.1 in $CHCl_3$). The **^{1}H NMR** spectrum ($CDCl_3$, 600 MHz) (Fig.59) for compound AA7 indicated the presence of two symmetrical xanthene moieties attached to each other by a 2,2` linkage. Each xanthene moiety was characterized by the occurrence of two ortho-coupled aromatic protons in ring A at $\delta_H$ 7.39 (brd) and 6.56 (brd) for H-3/H-3` and H-4/H-4` respectively (Table 12). Ring C in compound AA7 was characterized by the presence of a proton signals at $\delta_H$ 3.87 (d, *J* = 11.2 Hz) for H-5/H-5`, the methine protons (H-6/H-6`) at $\delta_H$ 2.35 and two methylene protons at $\delta_H$ 2.67 and 2.25 for (H-7/H-7`α,β). Moreover, the methyl doublet Me-11/Me-11` at $\delta_H$ 1.11 (6H, *J* = 6 Hz) and the methoxy groups Me-13/Me-13` at δ_H 3.66 (s, 6H). The **^{1}H NMR** data (DMSO, 400 MHz) of compound AA7 (Table 12) was found to be similar to that of secalonic acid D as reported in the literature (Ren et al., 2005). The xanthene moiety of compound AA7 was indicated by characteristic signals shown, on its **^{13}C NMR** and **Dept** spectra ($(CD_3)_2CO$, 400 MHz) (Table 12) (Fig.60), as 16 carbon signals which included seven quaternary, two carbonyl, one methoxy, one methyl, four methines (two aromatics, one alcoholic and one aliphatic) and one methylene. **^{1}H-^{1}H-COSY** ($(CD_3)_2CO$, 400 MHz) (Fig.61) showed coupling of H-3 (δ_H 7.49) and H-4 (δ_H 6.56) which confirmed the structure of ring A. Moreover, ring C was confirmed through two spin systems, the first one started from H-5 (δ_H 3.95) to H-6 (δ_H 2.48) which coupled with the methyl doublet Me-11 (δ_H 1.15, J = 5.9 Hz). The second spin system is H-6 to H-7α (δ_H 2.72) which coupled with H-7β (δ_H 2.44). The structure of ring A was further confirmed through the **HMBC** correlations (Fig.62, 63) of H-3 with C-2 (δ_C 117.8) and C-1 (δ_C 159.4). In addition, H-4 showed cross peaks with C-2, C-4a (δ_C 159.3), carbonyl C-9 (δ_C 187.7) and C-9a (δ_C 106.7). Moreover, O*H*-1 (δ_H 11.64) correlated with C-1, C-2, and C-9a. While, ring C was confirmed through the correlations of H-5 with C-6 (δ_C 29.9) and C-10a (δ_C 85.4); H-6 with C-8 (δ_C 178.6) and Me-11 (δ_C 17.5); the methylene proton H-7α (δ_H 2.72) with C-6, C-8, C-5 (δ_C 76.3) and C-8a (δ_C 102.1). The positions of OH-5, Me-11 and Me-13 were indicated through the correlation of O*H*-5 (δ_H 5.17) with C-5 and C-6; Me-11

with C-6, C-5 and C-7 (36.0) and finally Me-13 with the carbonyl C-12 (δ_C 170.0). So from the above compound AA7 was assigned in accordance to the reported data as secalonic acid D (Ren et al. 2005). The absolute configurations of 2,2`-secalonic acids such as secalonic acid D had been determined by their n-$\pi^*$ CD bands around 330 nm which were correlated with the configuration of C-10a and C-10a` stereogenic centers (Andersen et al., 1977a). A positive n-π^* CD band around 330 nm (Fig.64) indicated C-10a*R*, C-10a`*R* configuration (Zhang et al., 2008b). Thus the absolute configuration of compound AA7 was assigned as (+)-(5*R*,5'*R*,6*S*,6'*S*,10a*R*,10'a*R*)-secalonic acid D.

3.2.5.5. Compound AA9 (secalonic acid B)

(5S,5'S,6S,6'S,10aR,10'aR)-dimethyl 1,1',5,5',8,8'-hexahydroxy-6,6'-dimethyl-9,9'-dioxo-6,6',7,7',9,9',10a,10'a-octahydro-5H,5'H-[2,2'-bixanthene]-10a,10'a-dicarboxylate	
Synonyms	Secalonic acid B
Sample codes	AA9
Sample Amount	5 mg
Physical Description	yellow amorphous powder
Molecular Formula	$C_{32}H_{30}O_{14}$
Molecular Weight	638 g/mol
Optical Rotation $[\alpha]_D^{20}$	-5 (*c* 0.1 in $CHCl_3$)
Retention time (LC-MS)	19.68 min

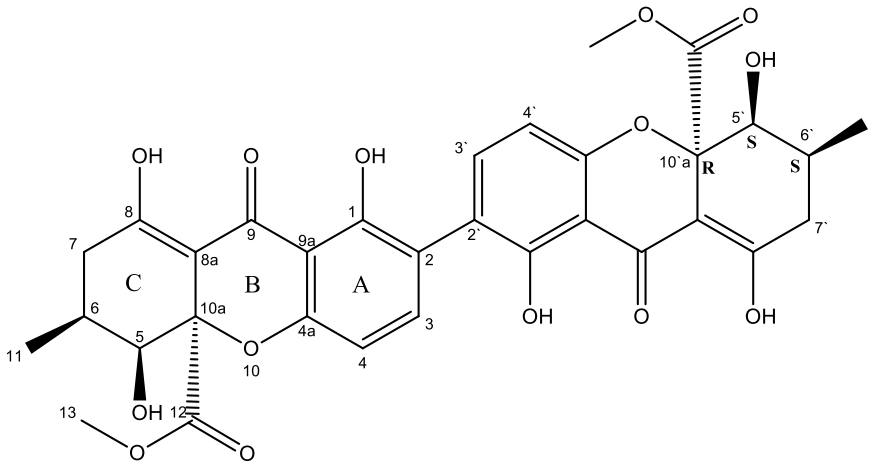

LC-HRFTMS spectrum $[M+H]^+$ 639.1716

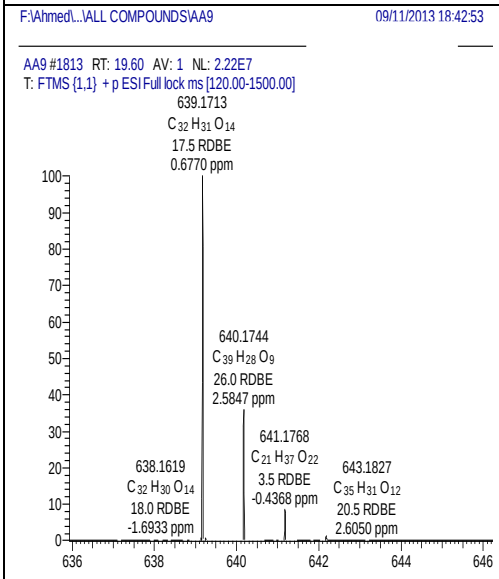

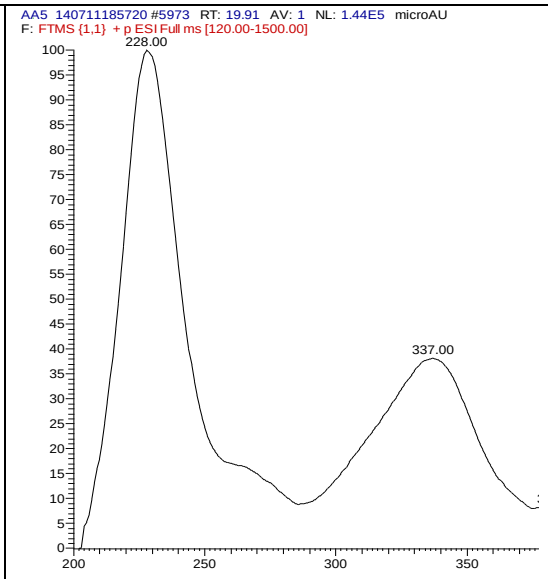

Compound AA9 (5 mg), secalonic acid diastereomer, was obtained as a yellow amorphous powder, exhibited a molecular formula $C_{32}H_{30}O_{14}$ established by ESI-HRMS at *m/z* = 639.1716 $[M+H]^+$. The optical rotation $[\alpha]^{20}_D$ = -5 (*c* 0.1 in $CHCl_3$). The **^{1}H NMR** spectrum ($CDCl_3$, 600 MHz) (Fig.59) of compound AA9 showed the following resonances at δ_H 8.02, 6.6, 3.74, 2.35, 2.64, 2.2, 1.05 and 3.77 for H-3/H-3`, H-4/H-4`, H-5/H-5`, H-6/H-6`, H-7α/H-7`α, H-7β/H-7`β, Me-11/Me-11` and Me-13/Me-13` respectively. Like compound AA7, The ^{1}H NMR data of compound AA9 exhibited one set of signals equivalent for the two symmetric xanthene units. The replacement of H-5 at δ_H 3.87 (d, 4.6 Hz) in AA7 by a broad peak at δ_H 3.74 in AA9 could be indication to the change in the orientation of H-5 in AA9 in comparsion to AA7. So in accordance to the biosynthetic pathway of the secalonic acid (discussion section 4.2), compound AA9 is a one of the homologous dimer which are secalonic A, B, D or E. As shown in (Fig.59 and Table 11) the ^{1}H NMR of both compounds AA7 and AA9 were not completely superimposable. So the possibility to be secalonic D or its enantiomer seclaonic A was excluded (Kurobane et al., 1978). Thus compound AA9 supposed to be secalonic acid B or E or racemic mixture of both. The CD spectrum of compound AA9 (Fig.64) showed in addition to the positive n-π^* CD band around 330 nm, a more intense negative one was detected at 220 nm. The positive band between 260-400 nm was due to the six stereogenic centers which can be assigned as 5*S*, 5*S*`, 6*S*, 6*S*`, 10a*R* and 10a`*R* which referred to seclonic acid B (C-5 epimer of secalonic acid D). This was also corroborated with the reported data (Zhang et al. 2008) and the positive n-π^* CD band around 330 nm.

3.2.5.6. Compound AA5 (secalonics acid F)

(5R,5'S,6S,6'S,10aR,10'aR)-dimethyl 1,1',5,5',8,8'-hexahydroxy-6,6'-dimethyl-9,9'-dioxo-6,6',7,7',9,9',10a,10'a-octahydro-5H,5'H-[2,2'-bixanthene]-10a,10'a-dicarboxylate	
Synonyms	Secalonic acid F
Sample codes	AA5
Sample Amount	9 mg
Physical Description	yellow amorphous powder
Molecular Formula	$C_{32}H_{30}O_{14}$
Molecular Weight	638 g/mol
Optical Rotation $[\alpha]_D^{20}$	+18 (*c* 0.1 in $CHCl_3$)
Retention time (LC-MS)	18.18 min

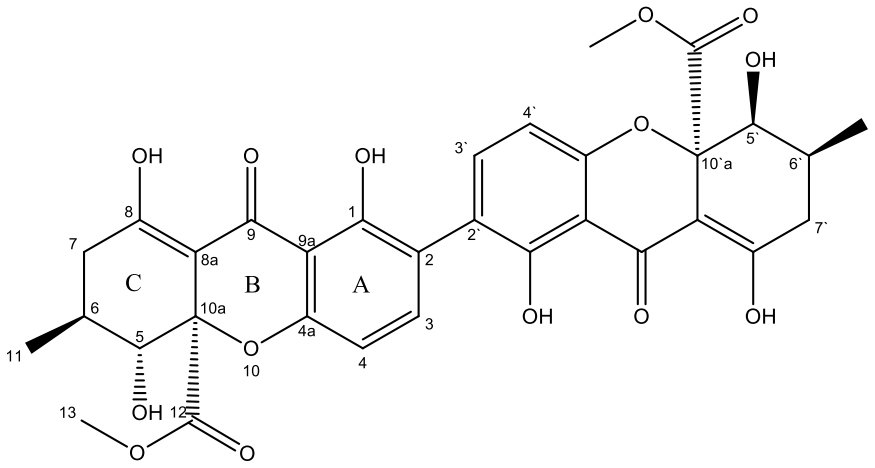

LC-HRFTMS spectrum $[M+H]^+$ 639.1716

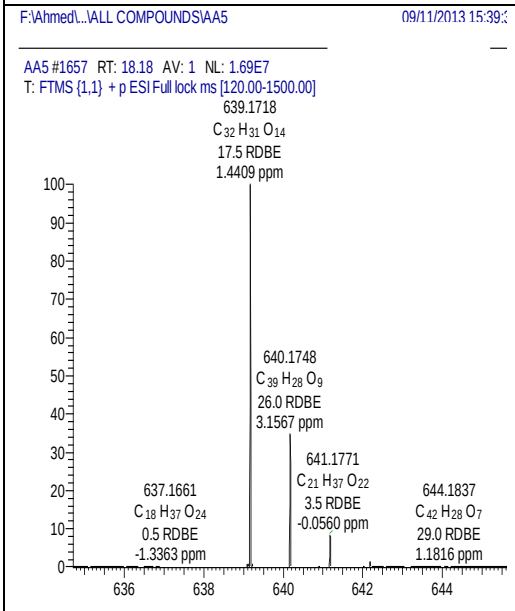

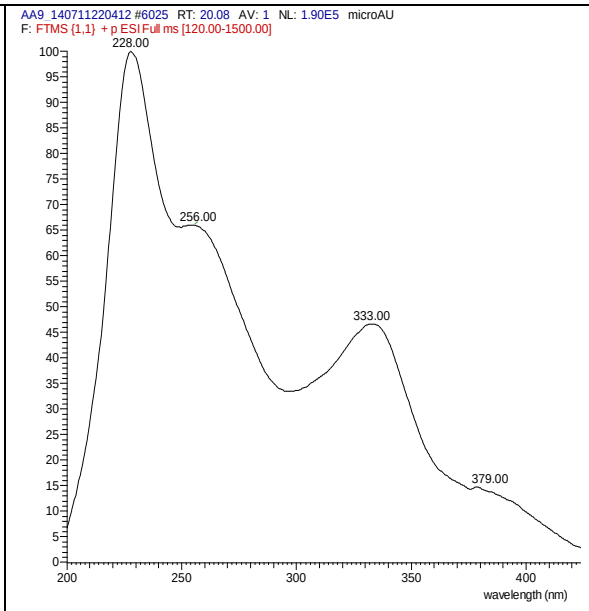

Compound AA5 (9 mg) was obtained as a yellow amorphous powder, exhibited a molecular formula $C_{32}H_{30}O_{14}$ established by ESI-HRMS at *m/z* = 639.1716 $[M+H]^+$. The optical rotation $[\alpha]^{20}_D$ = +18 (*c* 0.1 in $CHCl_3$. The **^{1}H NMR** data ($CDCl_3$, 400 MHz) (Table 12) of Compound AA5 showed two sets of signals which represented two asymmetric xanthine moieties at δ_H 13.90, 13.71, 11.79, 11.66, 7.39, 7.36, 6.56, 6.51, 4.06, 3.87, 3.65, 3.66, 1.11, 1.09. These were equivalent for OH-8, OH-8`, OH-1, OH-1`, H-3, H-3`, H-4, H-4`, H-5, H-5`, Me-13, Me-13`, Me-11, Me-11` respectively and a multiplet peak at $\delta_H$ 2.0-3.0 ppm equivalent for H-6, H-6`, H-7(α,β) and H-7` (α,β). The asymmetry in compound AA5 was due to the variance of the stereochemistry of O*H*-5 between xanthine units. The ^{1}H NMR data was found to be similar to that of secalonic acid F (hybrid dimer of D and B xanthine units) (Andersen et al., 1977b). The **CD spectrum** (Fig.64) exhibited a negative CD band around 220 in addition to the positive CD transition between 260-400 nm. Thus in accordance to the biosynthetic pathway (see discussion section 4.2) and the reported data (Table 12), compound AA5 was assigned as (+)-(5R,5'S,6S,6'S,10aR,10'aR)-secalonic acid F.

3.2.5.7. Compound AA8 (secalonic acid C)

(5S,5'S,6R,6'S,10aS,10'aR)-dimethyl 1,1',5,5',8,8'-hexahydroxy-6,6'-dimethyl-9,9'-dioxo-6,6',7,7',9,9',10a,10'a-octahydro-5H,5'H-[2,2'-bixanthene]-10a,10'a-dicarboxylate	
Synonyms	Secalonic acid C
Sample codes	AA8
Sample Amount	6 mg
Physical Description	yellow amorphous powder
Molecular Formula	$C_{32}H_{30}O_{14}$
Molecular Weight	638 g/mol
Optical Rotation $[\alpha]_D^{20}$	+19 (*c* 0.1 in $CHCl_3$)
Retention time (LC-MS)	18.24 min

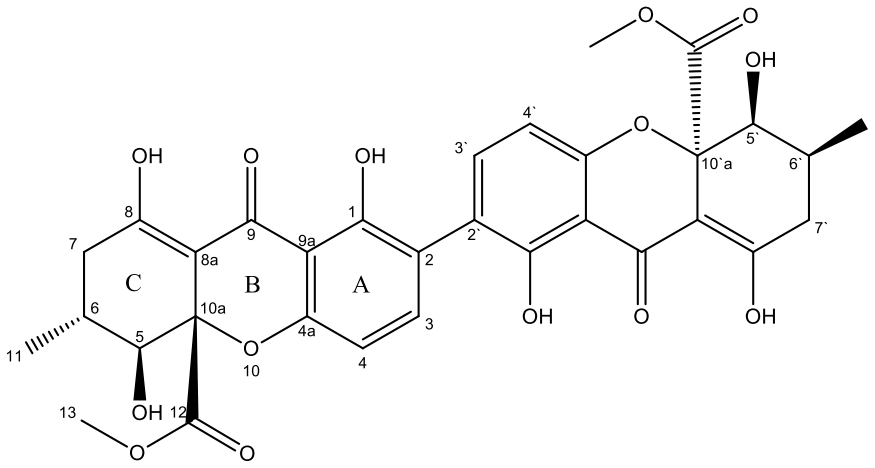

LC-HRFTMS spectrum $[M+H]^+$ 639.1709

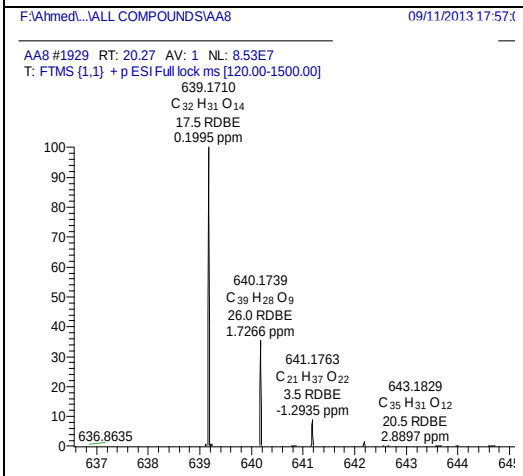

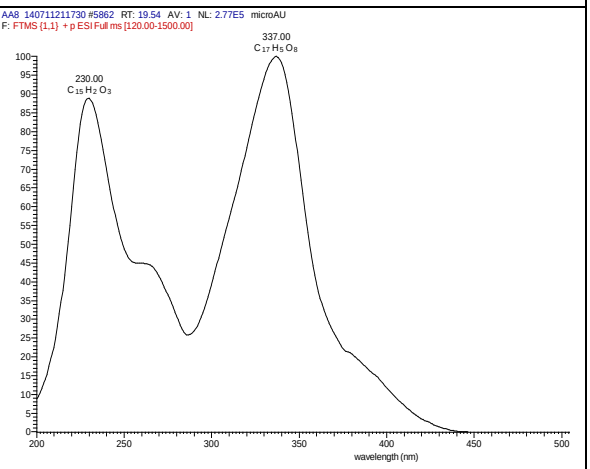

Compound AA8 (6 mg), secalonic acid diastereomer, was obtained as a yellow

amorphous powder, exhibited a molecular formula $C_{32}H_{30}O_{14}$ established by ESI-HRMS at *m/z* = 639.1709 $[M+H]^+$. The optical rotation $[\alpha]^{20}_D$ = +19 (*c* 0.1 in $CHCl_3$. Like Compound AA5, the **^{1}H NMR** data of compound AA8 (Table 11) showed two sets of signals at δ_H 7.72, 7.42, 6.56, 6.54, 3.87, 3.77, 3.66, 3.61, 1.1, 1.05 and 2.0-3.0 (m, 6H) for H-3, H-3`, H-4, H-4`, H-5, H-5`, Me-13, Me-13`, Me-11, Me-11`, H-6, H-6`, H-7(α,β) and H-7` (α,β), respectively. Compound AA8 is also a hybrid dimer however its ^{1}H NMR spectrum (Fig.21) was not superimposed with compound AA5 which exclude the possibility to be secalonic acid F or its enantiomer secalonic acid G. Thus in accordance to the biosynthetic pathway of the secalonic acid, compound AA8 is supposed to be secalonic acid C. The CD spectrum of compound AA8 (Fig.60) showed in addition to the positive band at 260-400 nm due to the three stereo centers 5`S, 6`S and 10`aR which was similar to xanthine unit (type B) involved in the secalonic acid F, a positive CD band at 220 nm opposite to that of compound AA5 (secalonic acid F). The other xanthine unit of compound AA8 can be indicated as (type A), according to the biosynthetic pathway (Kurobane et al., 1979), could be responsible for the positive CD band at 220 nm. So from the above compound AA8 was assigned as (+)-(5*S*,5'*S*,6*R*,6'*S*,10a*S*,10'a*R*)-secalonic acid C.

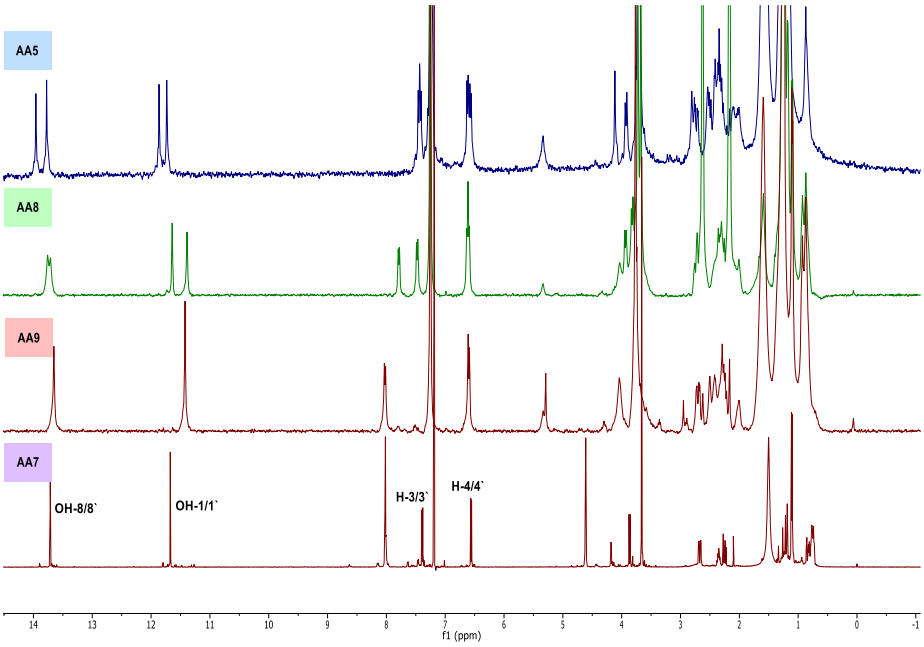

Fig.59 ^{1}HNMR spectra of compounds AA5, AA7, AA8 and AA9

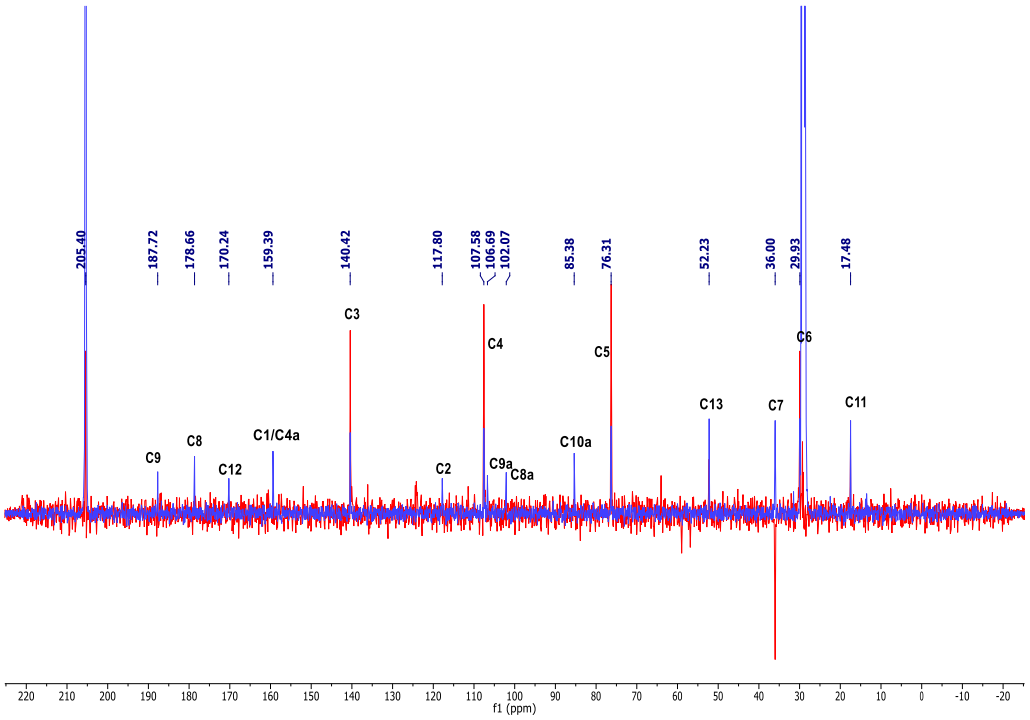

Fig.60 ^{13}C NMR and Dept spectra of Compound AA7-Acetone-d$_6$

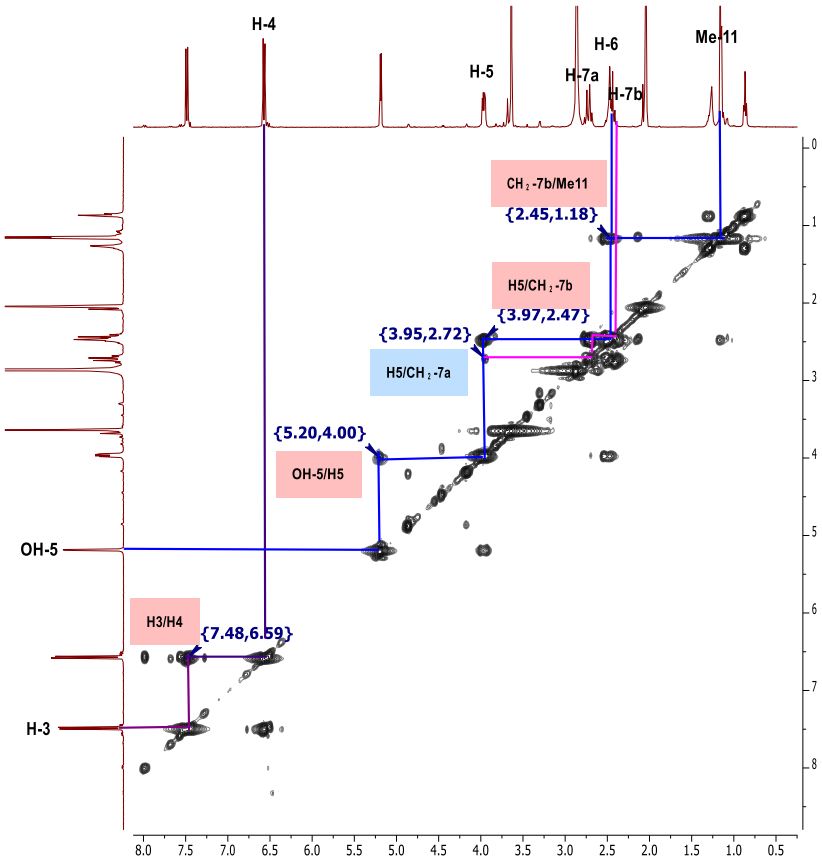

Fig.61 ^{1}H-^{1}H COSY spectrum (400 MHz, aceton-d6) of compound AA7-acetone-d$_6$

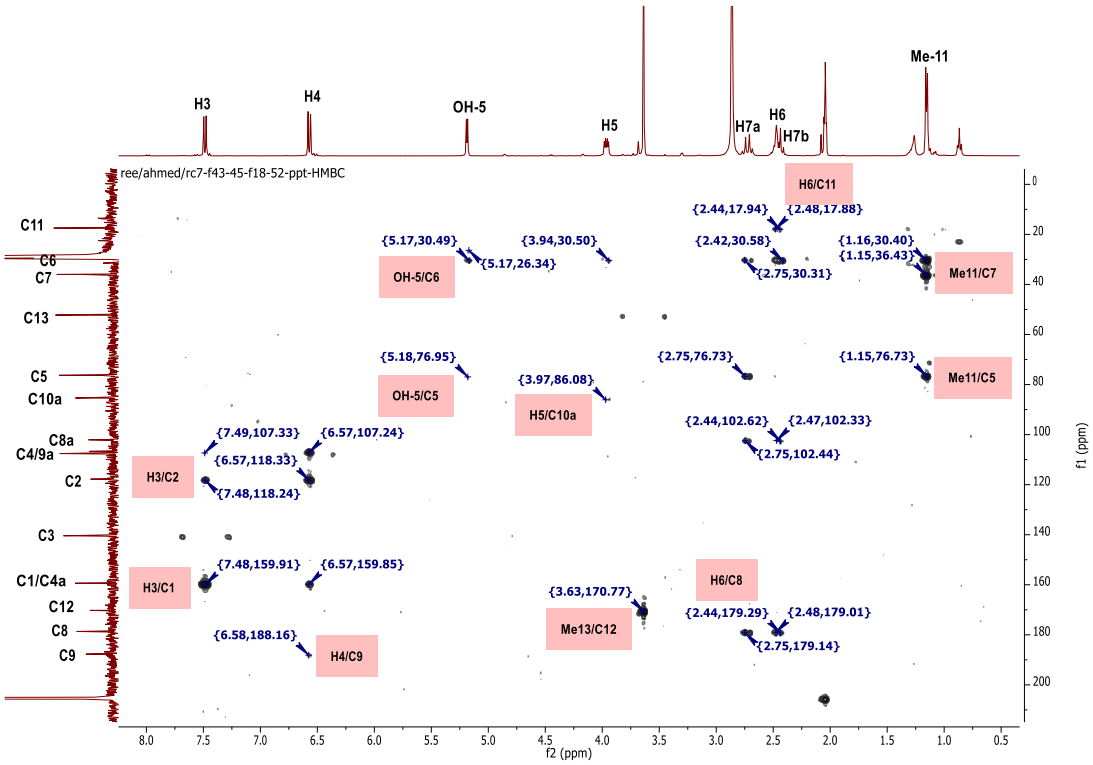

Fig.62 HMBC spectrum (400 MHz, acetone-d_6) of compound AA7

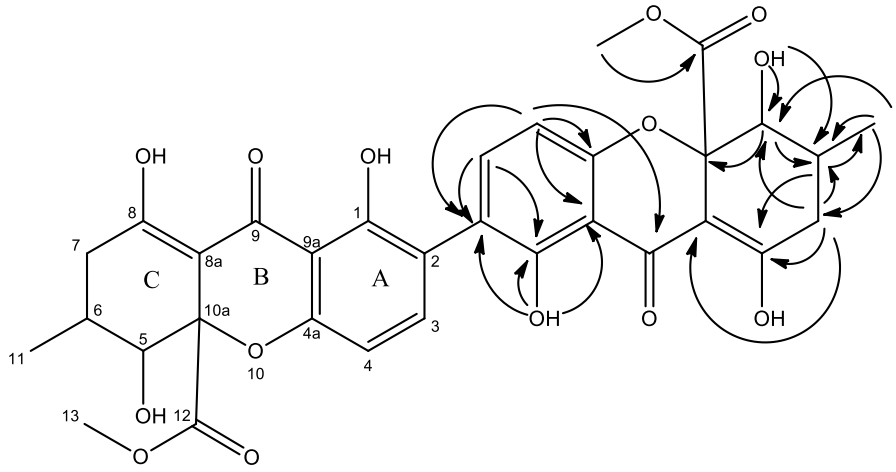

Fig.63 HMBC correlations of compound AA7

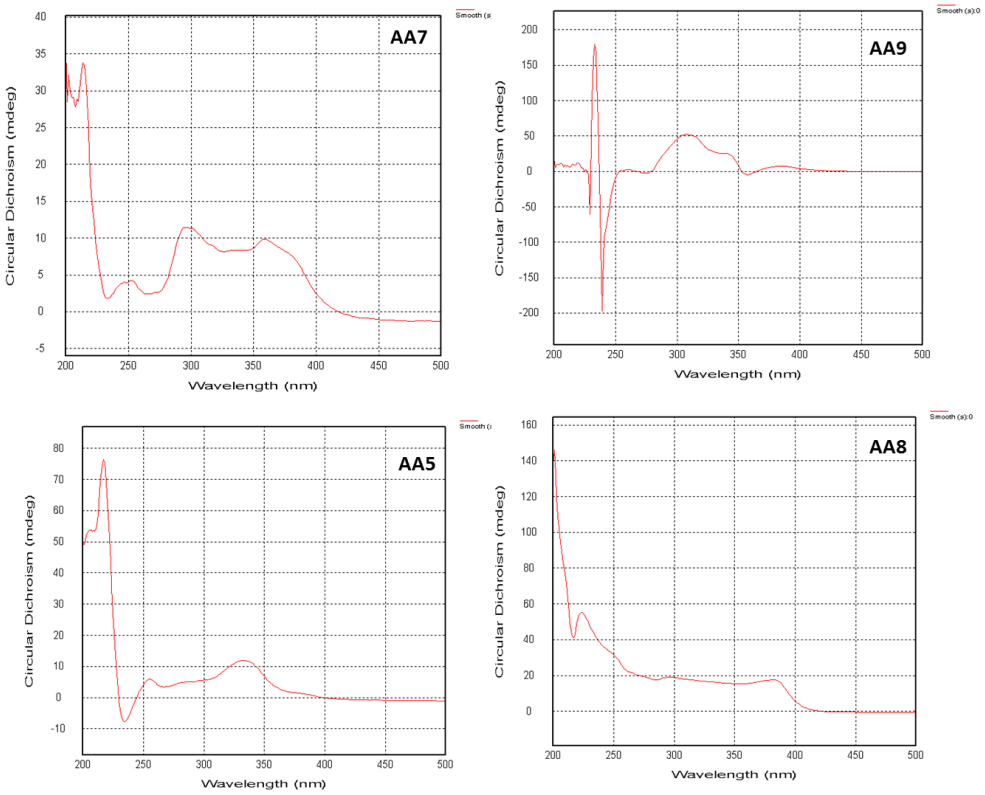

Fig.64 CD spectra for compounds AA7, AA5, AA8 and AA9

Table 11: ^{1}H NMR data of compound AA5, AA7, AA8 and AA9 (600 MHz, $CDCl_3$)

	AA7 δ_H (m, *J* in Hz)	**AA5** δ_H (m, *J* in Hz)	**AA9** δ_H (m, *J* in Hz)	**AA8** δ_H (m, *J* in Hz)
OH-8/8`	13.71 (s)	13.9, 13.71	13.65	13.70,13.65
OH-1/1`	11.67 (s)	11.79, 11.66	11.42	11.57, 11.32
H-3/3`	7.39 (d, 8.5 Hz)	7.39, 7.36	8.02	7.72, 7.42
H-4/4`	6.56 (d, 8.5 Hz)	6.56, 6.51	6.6	6.56, 6.54
OH-5/5`	4.61 (d, 4.6 Hz)			5.34
H-5	3.87 (d, 4.6 Hz, H-5/5`)	4.06 br	3.74 (brd, H-5/5`)	3.87
H-5`		3.87 (d, 11.25 Hz)		3.77
Me-13,13`	3.66 (s, 6H)	3.65, 3.66	3.77	3.66, 3.61
H-6/6`	2.35 (m)	2.0-3.0 (m, 6H)	2.36	2.37
H-7β, 7`β	2.25 (dd, 10.6, 19.2 Hz)		2.2	2.25
H-7α/7`α	2.67 (dd, 6.3, 19.2 Hz)		2.64	2.66
Me-11/11`	1.11 (d, 6.0 Hz)	1.11, 1.09	1.05	1.1, 1.05

Table 12: Comparison of ^{1}H NMR data of compound AA7 (DMSO) and AA5 ($CDCl_3$) to the literature (400 MHz)

	AA7-DMSO δ_H (m, *J* in Hz)	**secalonic D-DMSO Ren 2005**	**AA5-$CDCl_3$** δ_H (m, *J* in Hz)	**seclonic F- $CDCl_3$ Andresen 1977**
OH-8,8`	13.6 (s)	13.6	13.96, 13.78	13.70, 13.88
OH-1,1`	11.66 (s)	11.62	11.86, 11.73	11.65, 11.80
H-3,3`	7.46 (d, 8.5 Hz)	7.45	7.45, 7.42	7.35 , 7.39
H-4,4`	6.63 (d, 8.5 Hz)	6.63	6.62, 6.57	6.52 , 6.58
OH-5,5`	6.04 (d, 4.6 Hz)			
H-5	3.82 (d, 4.6 Hz)	3.81	4.12	4.09
H-5`	3.80 (d, 4.6 Hz)		3.92	3.87
Me-13,13`	3.61 (s)	3.61	3.72	3.67
H-6/6`	2.65 (dd, 6.0, 19.0 Hz)	2.65	2.0-3.0 (m,6H)	2.0-3.0 (m,6H)
H-7β/7`β	2.47 (brd)	2.49		
H-7α/7`α	2.3 (m)	2.31		
Me-11/11`	1.04 (d, 6.0 Hz)	1.03	1.17	1.14

Table 13: ^{13}C NMR and ^{1}H NMR of compound AA7 (400 MHz, $(CD_3)_2CO$) and literature

Carbon No.	**AA7-$(CD_3)_2CO$** δ_C (m)	**AA7-$(CD_3)_2CO$** δ_H (m, *J* in Hz)	**Secalonic D-DMSO Ren 2005** δ_C (m)	**Secalonic B-$CDCl_3$ Zhang 2008** δ_C (m)
C9,9`	187.72 (C)		186.6	187.7
8,8`	178.66 (C)	13.76 (s)	178.2	179.8
12,12`	170.07 (C)		170	171.2
1,1`	159.39 (C)	11.64 (s)	158.9	159.4
4A,4A`	159.34 (C)		158.5	157.2
3,3`	140.64 (CH)	7.49 (d, 8.5 Hz)	140.2	139.7
2,2`	117.88 (C)		117.3	118.7
4,4`	107.45 (CH)	6.57 (d, 8.5 Hz)	107.5	107.5
9A,9`A	106.69 (C)		106.3	
8A,8A`	102.07 (C)		101.7	99.9
10A,10A`	85.46 (C)		85.2	84.8
5,5`	76.31 (CH)	3.95, 3.92 (d, 4.6 Hz)	75.2	71.4
13,13`	52.23 (CH_3)	3.64 (s)	52.6	53.4
7,7`	36 (CH_2)	2.45 (m, H-7,7`β); 2.73 (m, H-7,7`α)	35.8	32.6
6,6`	29.93 (CH)	2.47 (m)	29.9	28.5
11,11`	17.5 (CH_3)	1.15 (s)	17.8	17.5

3.2.5.8. Compound AA4a and AA4b (citric acid and citric acid methyl ester)

2-hydroxypropane-1,2,3-tricarboxylic acid and its 5-methyl ester	
Synonyms	Citric acid and citric acid methyl ester
Sample codes	AA4a and AA4b
Sample Amount	11 mg
Physical Description	brown amorphous powder
Molecular Formula	$C_6H_8O_7$ and $C_7H_{10}O_7$
Molecular Weight	192, 206 g/mol
Optical Rotation $[\alpha]_D^{20}$	-5 (*c* 0.1 in MeOH)
Retention time (LC-MS)	2 min

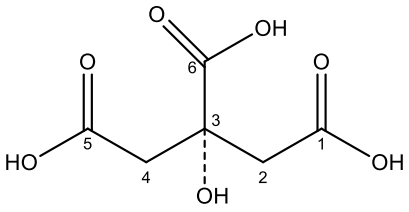

AA4a

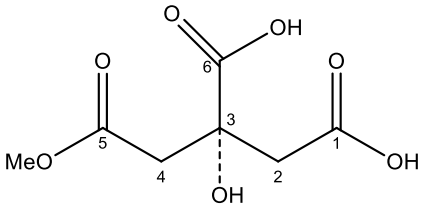

AA4b

LC-HRFTMS spectrum $[M-H]^+$ 191.0197, 205.0352

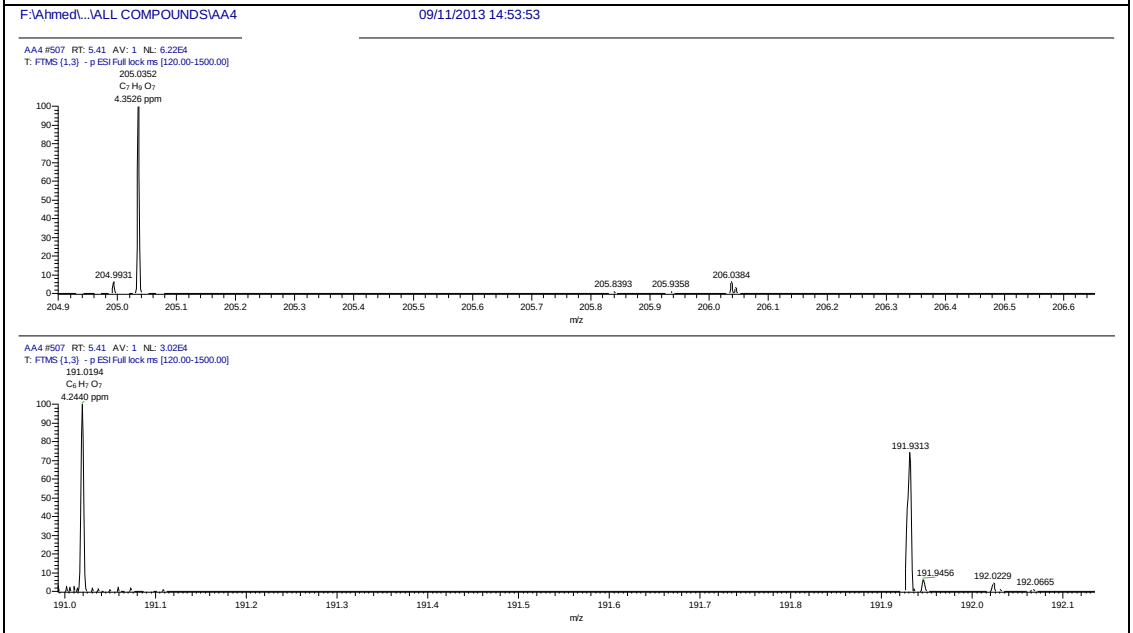

Compounds AA4a (citric acid) and AA4b (citric acid methyl ester) isolated as a mixture (11 mg), brown amorphous powder, exhibited a molecular formula $C_6H_8O_7$ and $C_7H_{10}O_7$ established by ESI-MS at *m/z* = 191.0197 and 205.0352 [M-H^+] for AA4a and AA4b respectively. The optical rotation $[\alpha]^{20}_D$ = -5 (*c* 0.1 in

MeOH). The **^{1}H NMR** spectrum of compounds AA4a and AA4b was found as a mixture with a ratio of 1:2 (Fig.65, DMSO-400 MHz) showed four doublets with large *J*-values at δ_H 2.82, 2.73 (d, *J* = 14.5 Hz) and 2.76, 2.65 (d, *J*= 15.5 Hz). These were equivalent for four methylene protons of compound AA4b (citric acid methyl ester) together with one methyl singlet at δ_H 3.56. The presence of an extra proton peak at δ_H 2.64 (d, *J* = 15.5 Hz) at smaller integral in comparison to AA4b peaks indicated the presence of compound AA4a (citric acid) at lower ratio whose other peaks seemed to be underneath the peaks of compound AA4b. The **^{13}C NMR** and **DEPT** spectra (Fig.68) showed seven carbons including four quaternary (three carbonyls and one carbinolic) and one methyl and two methylenes. The structure was confirmed through the **HMBC** correlations (Fig.66, 67) which showed the correlation of the four methylene protons with the carbinolic carbon C-3 at δ_C 73.0. Moreover, confirmation was shown by correlation of the methylene protons C*H*$_2$-2 (δ_H 2.65, 2.76) with the carbonyl at C-1 (δ_C 174.9) and the carbonyl C-6 (δ_C 171.7) together with the correlation of methylene protons C*H*$_2$-4 with the carbonyl at C-5 (δ_C 170.5). The position of the methyl group was confirmed by the correlation of the methyl singlet δ_H 3.56 to the carbonyl C-5. Searching the database using the accurate masses indicated that compound AA4a is citric acid and compound AA4b is citric acid methyl ester.

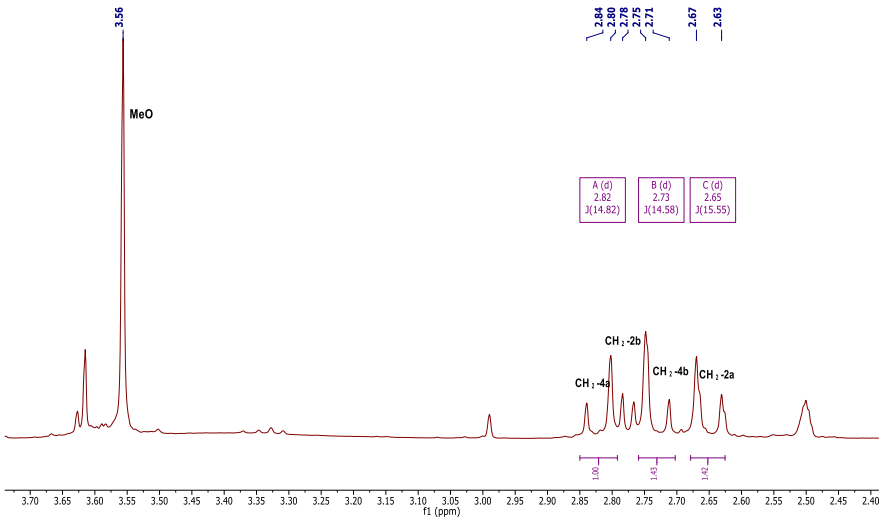

Fig.65 ^{1}H NMR spectrum of compound AA4b

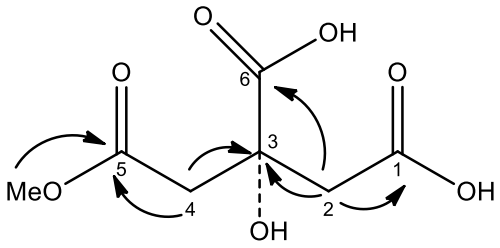

Fig.66 HMBC correlations of compound AA4b

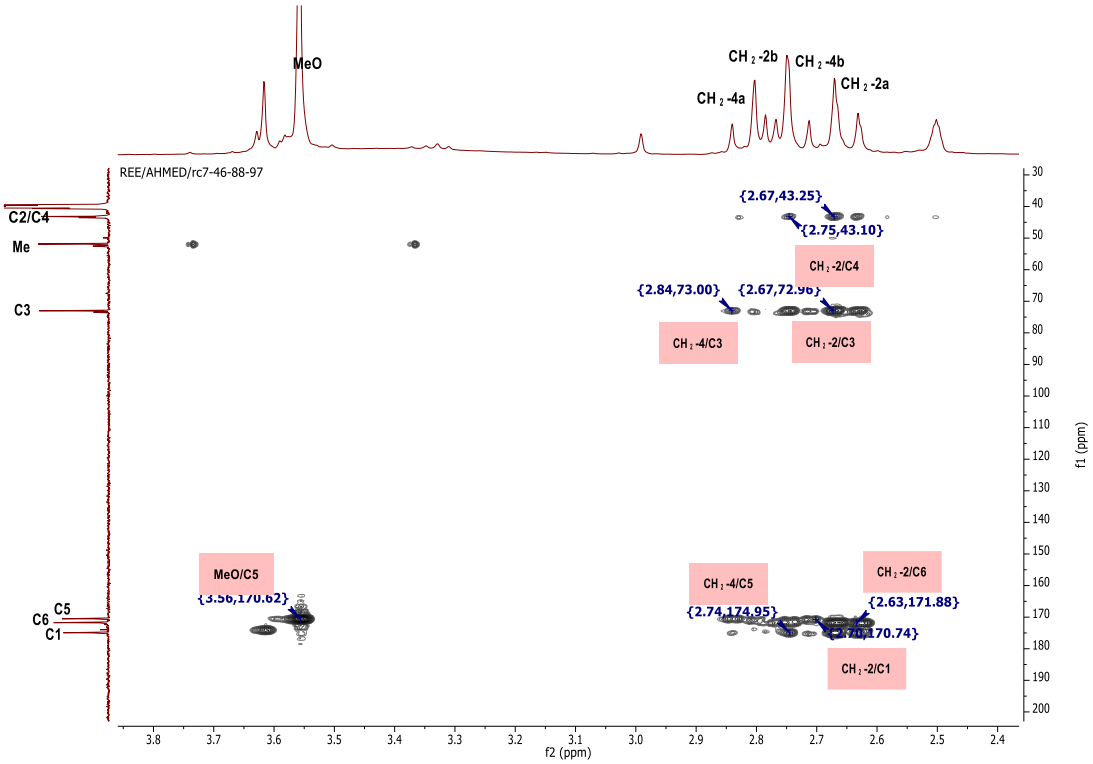

Fig.67 Expansion of HMBC spectrum of compound AA4b

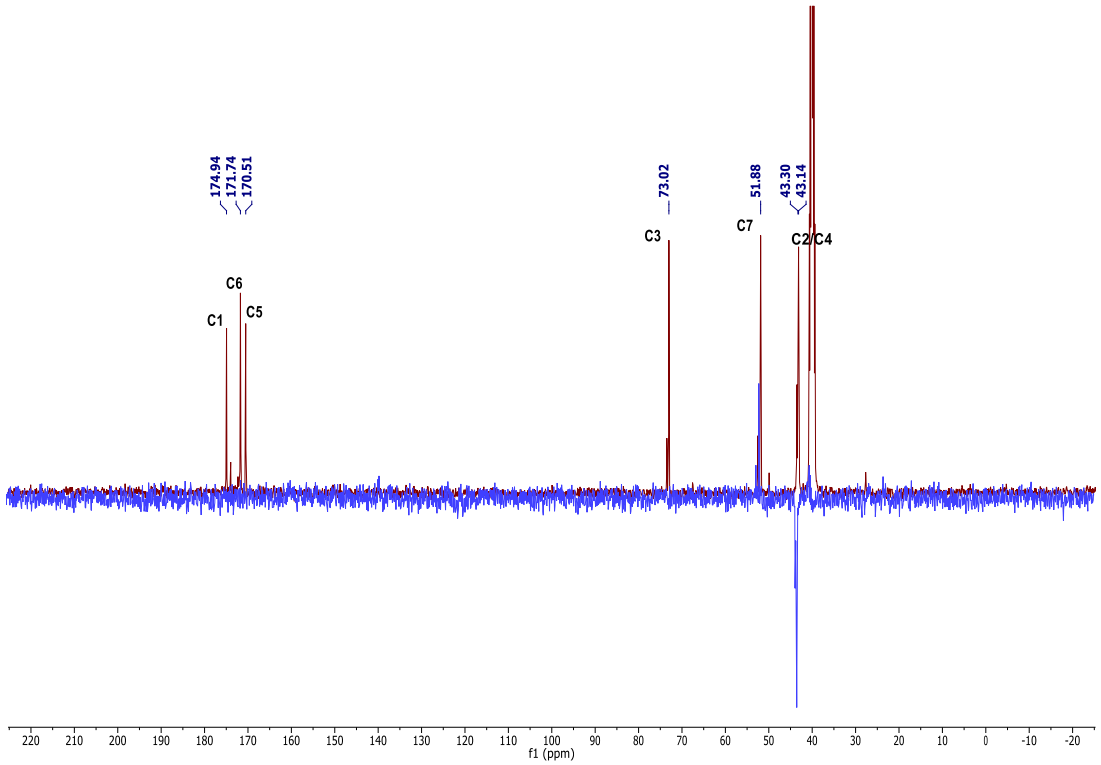

Fig.68 ^{13}C NMR and DEPT spectra of compound AA4b

3.2.5.9. Compound AA6 (homogenistic acid)

2-(2,5-dihydroxyphenyl)acetic acid	
Synonyms	Homogenistic acid
Sample codes	AA6
Sample Amount	14 mg
Physical Description	brown amorphous powder
Molecular Formula	$C_8H_8O_4$
Molecular Weight	168 g/mol
Retention time (LC-MS)	2.48 min

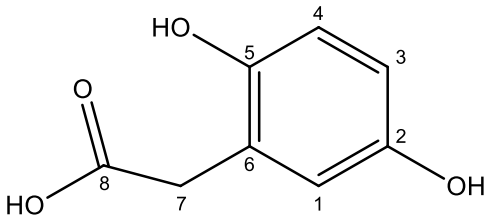

LC-HRFTMS spectrum $[M-H]^-$ 167.0347

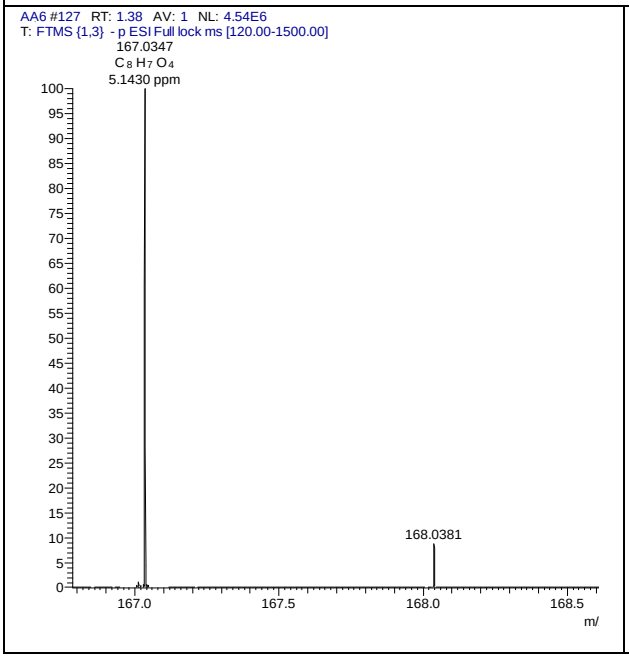

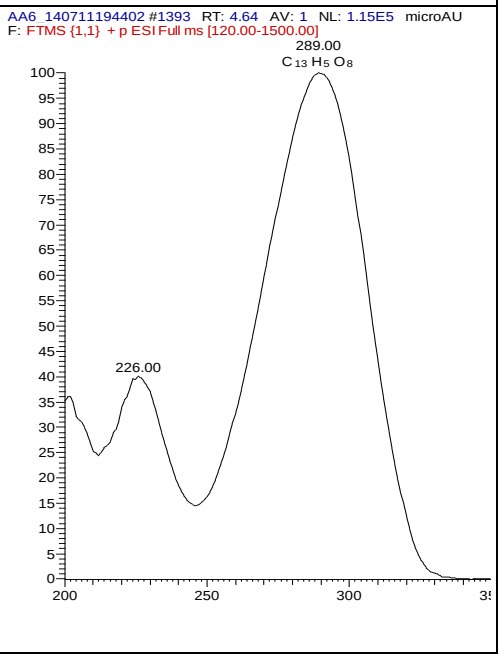

Compound AA6 (14 mg) was isolated as brown amorphous powder, exhibited a molecular formula $C_8H_8O_4$ established by ESI-HRMS at *m/z* = 167.0347 $[M-H]^-$. The **^{1}H NMR** spectrum of compound AA6 (DMSO, 400 MHz) (Fig.69) showed three aromatic protons at δ_H 6.56 (d, *J* = 8.5 Hz), 6.51 (d, *J* = *2.7* Hz) and 6.45

(dd, *J* = 2.9, 8.6 Hz) which are the protons of an ABX spin system on the aromatic ring and one singlet signals equivalent for two protons at δ_H 3.36. The **^{13}C NMR** and **DEPT** spectra (DMSO, 400 MHz) (Fig.70) showed eight carbon signals including four quaternaries (one carbonyl, two phenolic and one aromatic), three aromatic methine and one methylene. The cosy spectrum (Fig.71) gave further evidence for an ABX spin system through the correlation of the aromatic protons H-1 (δ_H 6.51), H-3 (δ_H 6.45) and H-4 (δ_H 6.56). The structure was confirmed through the HMBC correlations (Fig.72, 73) of the aromatic protons H-1 with C-2 (δ_C 148.5) and the methylene C-7 (δ_C 36.9) and the correlation of H-4 with C-5 (δ_C 150.0) and C-6 (δ_C 123.1). The position of the acetic acid substitution was confirmed through the correlation of methylene protons C*H*$_2$-7 (δ_H 3.36) with C-6, C-2, C-4 (δ_C 118.0) and the carbonyl C-8 (δ_C 173.6). So from the above, compound AA6 was identified as 2-(2,5-dihydroxyphenyl) acetic acid.

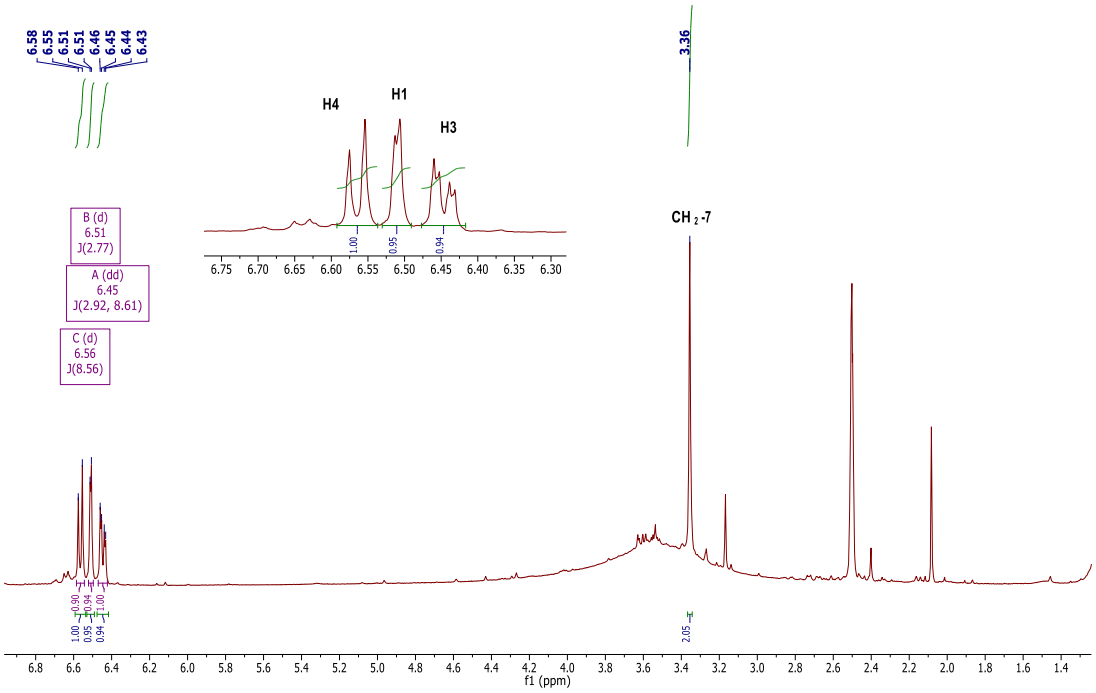

Fig.69 ^{1}H NMR spectrum of compound AA6 DMSO-400 MHz

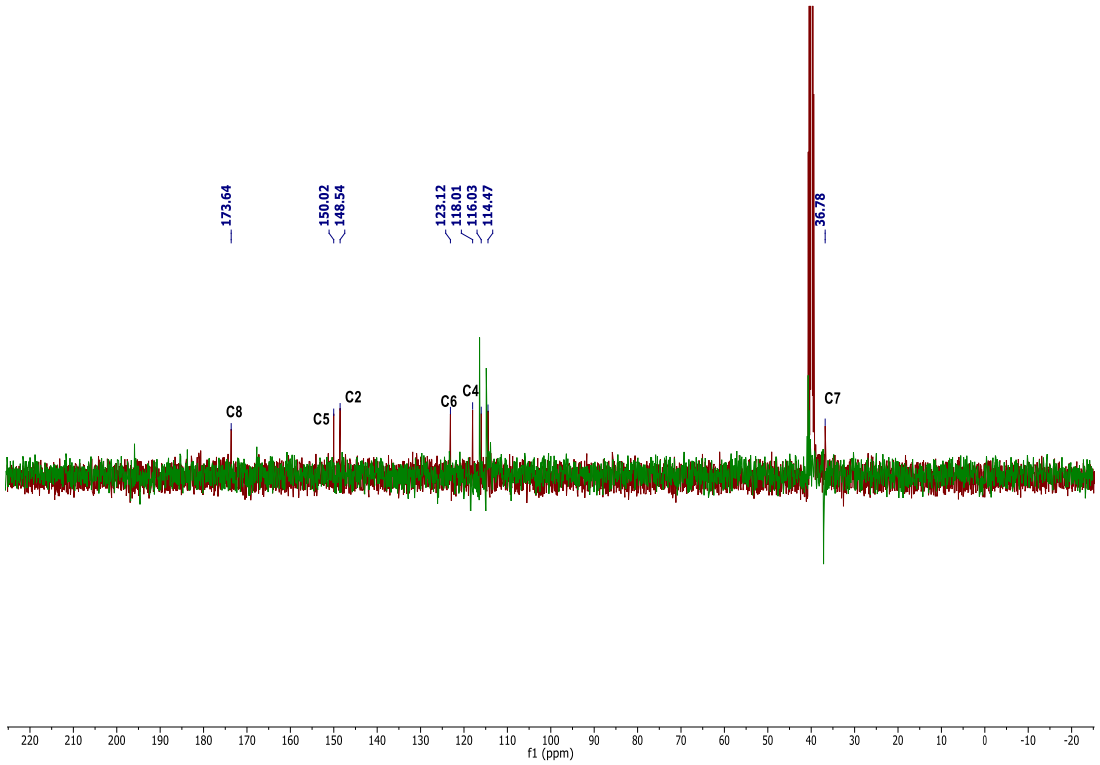

Fig.70 ^{13}C NMR and DEPT spectra of compound AA6

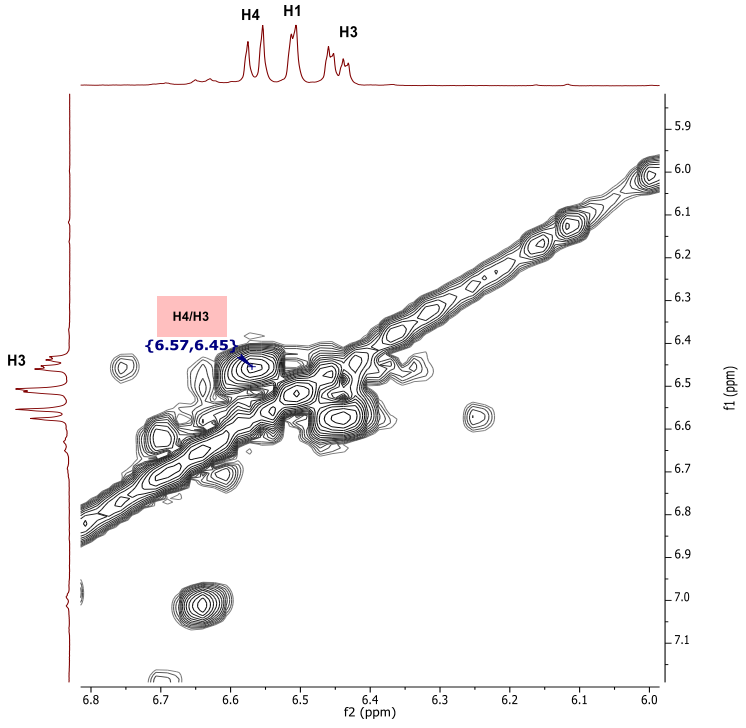

Fig.71 Expansion of ^{1}H-^{1}H cosy spectrum of compound AA6 showing ABX spin system

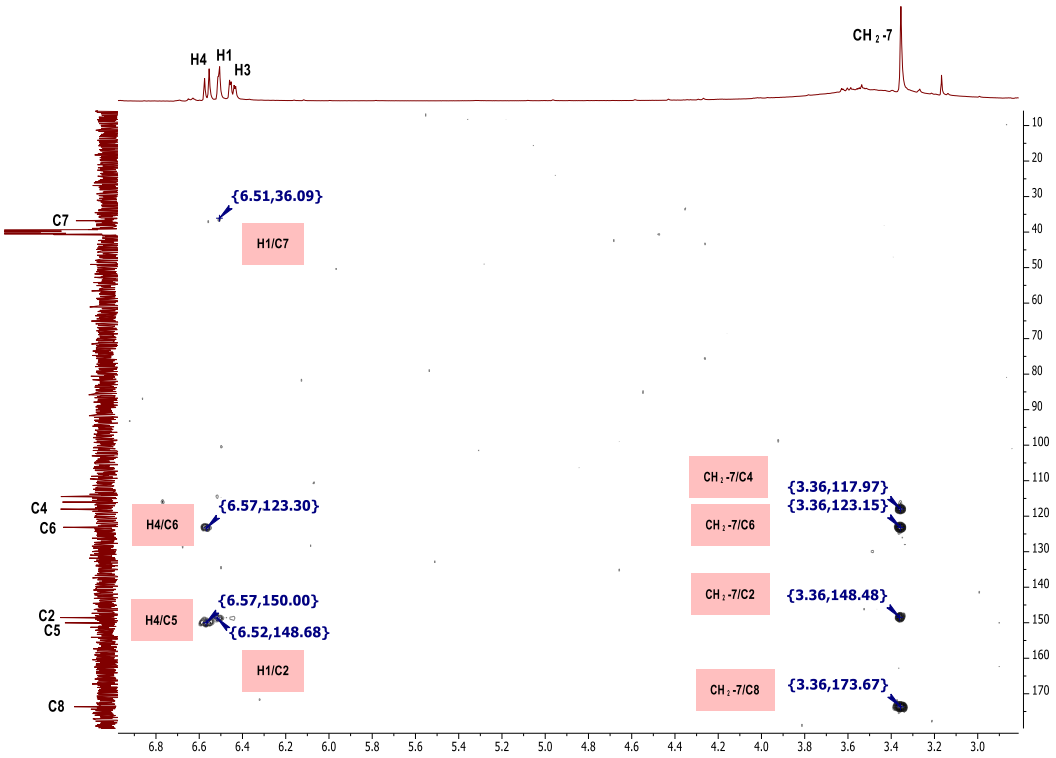

Fig.72 Expansion of HMBC spectrum of compound AA6

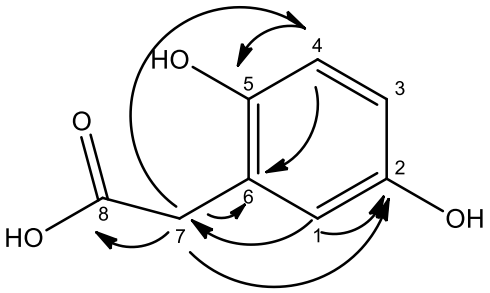

Fig.73 HMBC correlation of compound AA6

3.2.5.10. Compound AA10 (uridine)

1-(3,4-dihydroxy-5-(hydroxymethyl)tetrahydrofuran-2-yl)pyrimidine-2,4(1H,3H)-dione	
Synonyms	Uridine
Sample codes	AA10
Sample Amount	11 mg
Physical Description	brown amorphous powder
Molecular Formula	$C_9H_{12}N_2O_6$
Molecular Weight	244 g/mol
Retention time (LC-MS)	1.55 min

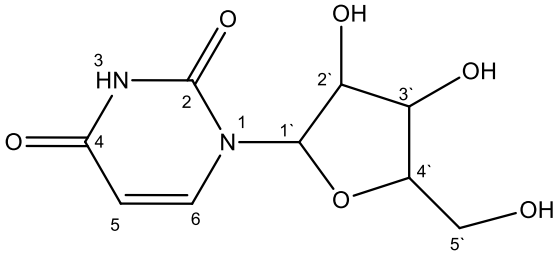

LC-HRFTMS spectrum $[M+H]^+$ 245.0771

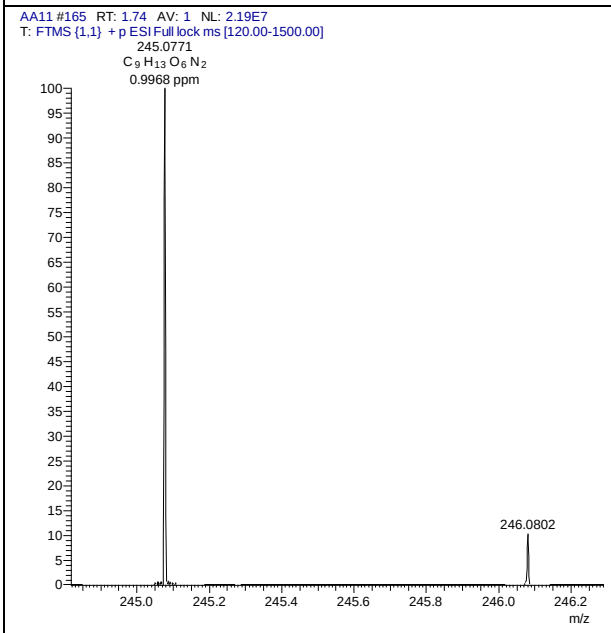

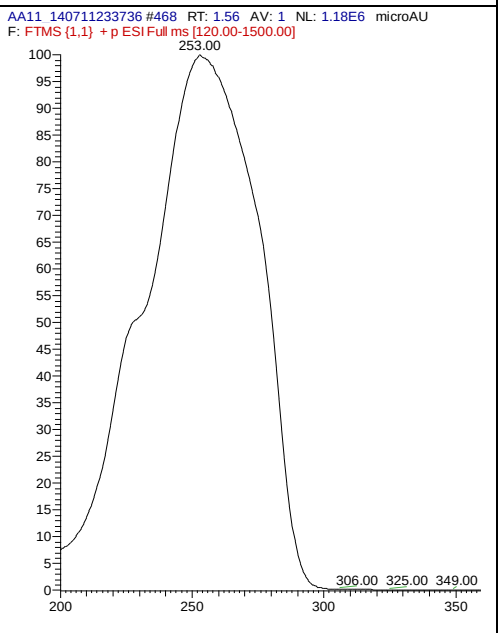

Compound AA10 (11 mg) was isolated as brown amorphous powder, exhibited a molecular formula $C_9H_{12}N_2O_6$ established by ESI-HRMS at *m/z* = **245.0771** $[M+H]^+$. The **^{1}H NMR** spectrum of compound AA10 (Fig.74, DMSO-400 MHz) showed two olefinic protons at δ_H = 7.89 (d, *J* = 8.1 Hz, H-6) and 5.64 (d, *J* = 8.0

Hz, H-5) which are equivalent for the protons of the pyrimidine-2,4-dione moiety. Moreover, the protons of the tetrahydrofuran moiety appeared at δ_H 5.78 (d, *J* = 5.3 Hz, H-1`), 4.00 (q, *J* = 5.2 Hz, H-2`), 3.96 (q, *J* = 4.3, H-3`), 3.84 (q, *J* = 3.4 Hz, H-4`), 3.62 (m, H-5`a) and 3.54 (m, H-5`b). The **^{13}C NMR** and **DEPT** spectra (DMSO, 400 MHz) (Fig.75) indicated nine carbons including two carbonyls, two olefinics, four methines and one methylene. The **^{1}H-^{1}H COSY** spectrum (Fig.77) exhibited two spin systems, the first between the two olefinic protons on the pyrimidine ring and the second connecting the tetrahydrofuran protons starting from the anomeric proton H-1`( $\delta_H$ 5.78) to H-2`, H-3`, H-4` and the C*H*$_2$-5`. The pyrimidine-2,4-dione ring was confirmed through the **HMBC** correlations (Fig.76, 78) of the olefinic proton H-6 (δ_H 7.89) with the carbonyls C-2 (δ_C 151.2), C-4 (δ_C 163.6) and the olefinic carbon C-5 at δ_C 102.4 while H-5 (δ_H 5.64) correlated with C-4. The position of the tetrahydro furan ring on the nitrogen N-1 of the pyrimidine ring was confirmed by the correlation of H-6 with C-1` ($\delta_C$ 88.4) and the correlation of H-1` (δ_H 5.78) with C-2, C-6 (δ_C 141.3) and C-2` ($\delta_C$ 74.1). Furthermore, the tetrahydrofuran ring was confirmed through cross peaks between H-2` (δ_H 4.00) and C-1` ($\delta_C$ 88.4) as well as C-4` (δ_C 85.3); H-3` ($\delta_H$ 3.96) to C-1` and C-5` ($\delta_C$ 61.4); H-4` (δ_H 3.84) to C-2` and C-3` (δ_C 70.5) and H-5`b ($\delta_H$ 3.54) to C-3`. So from the above and comparison to the literature, compound AA10 was identified as uridine (Sato et al., 2006) (Table 14).

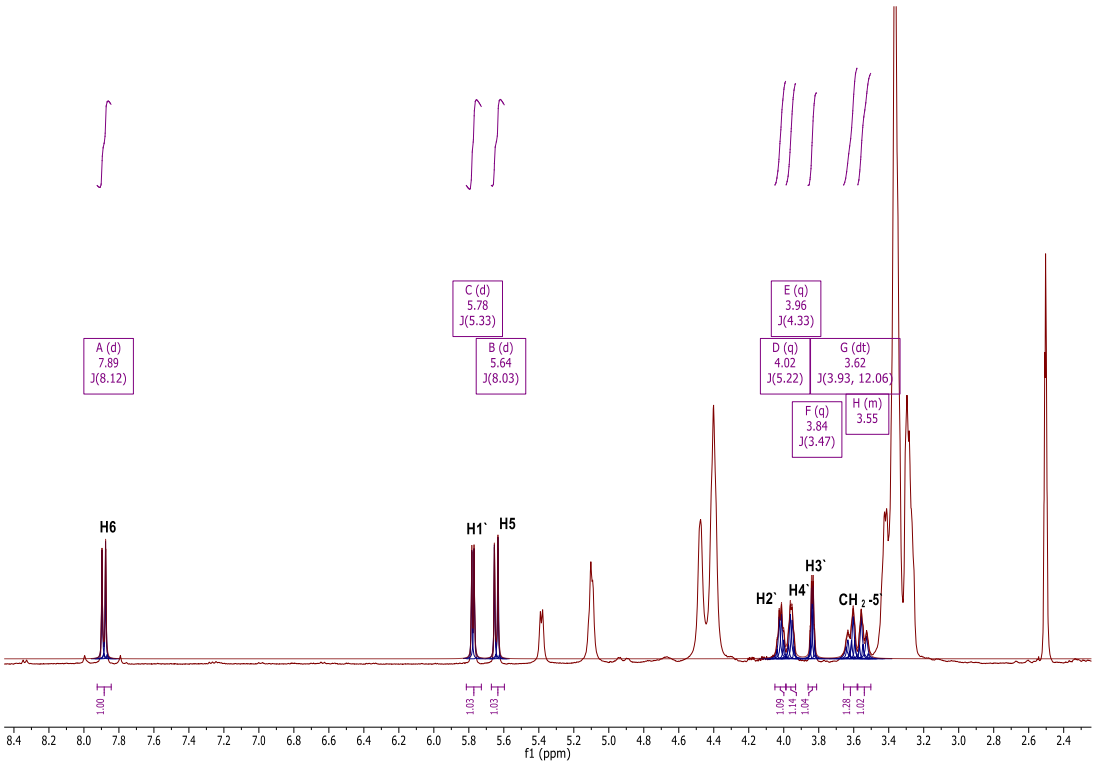

Fig.74 ^{1}H NMR spectrum of compound AA10

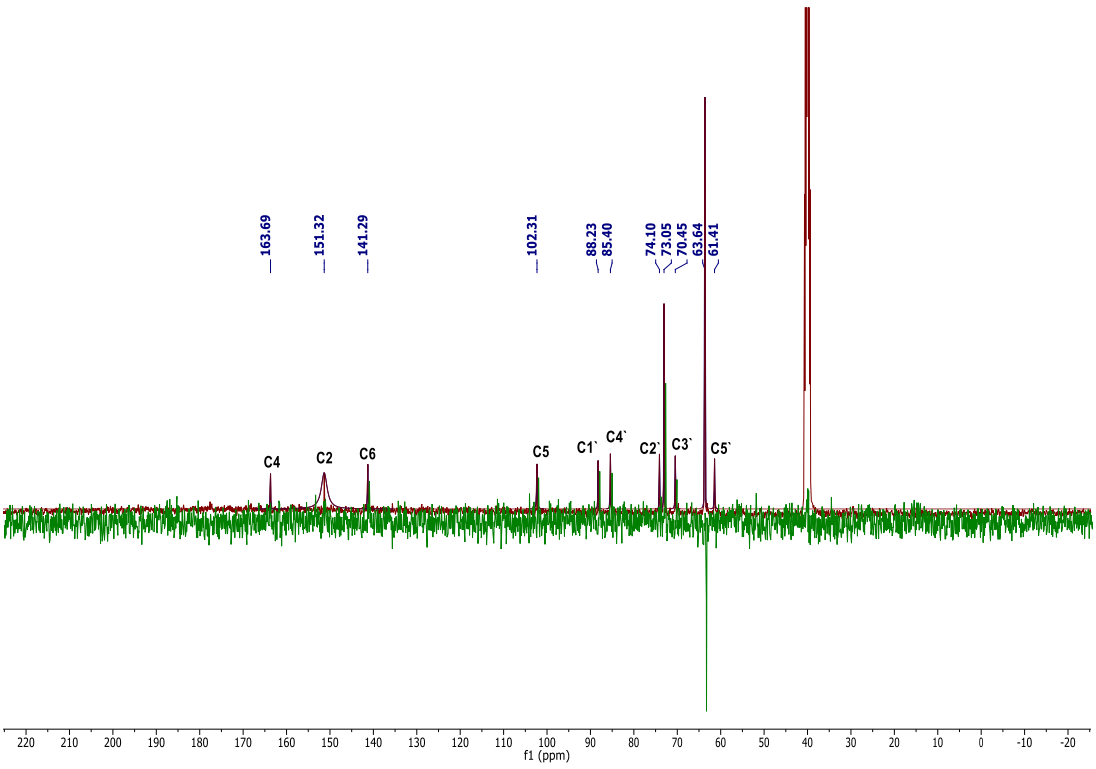

Fig.75 ^{13}C NMR and DEPT spectra of compound AA10

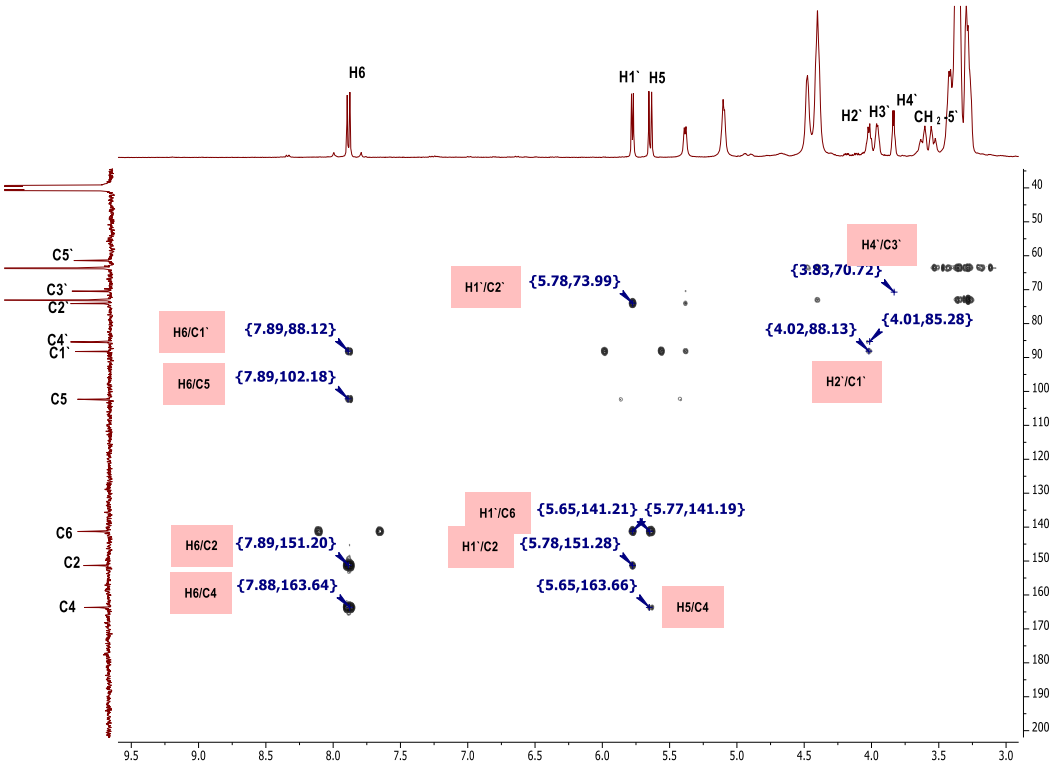

Fig.76 HMBC spectrum of compound AA10

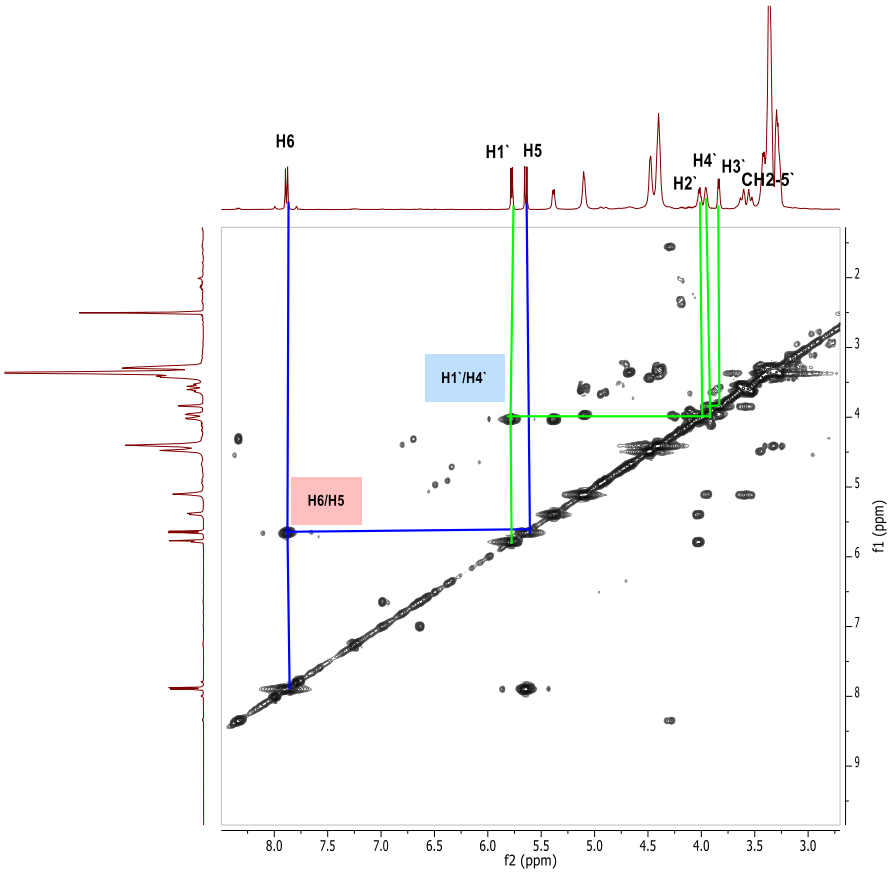

Fig. 77 ^{1}H-^{1}H COSY spectrum of compound AA10 showing two different spin systems

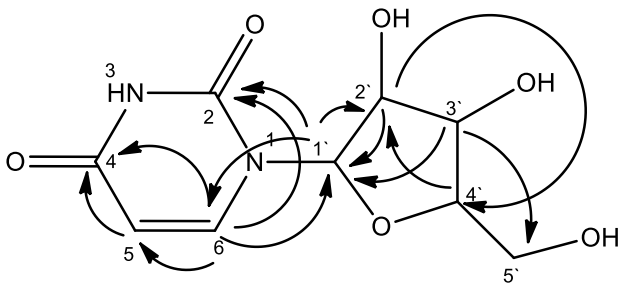

Fig.78 HMBC correlations of compound AA10

Table 14: ^{1}HNMR and ^{13}C NMR of compound AA10 and literature

Position	AA10		Sato 2006-uridine	AJP117510
	δ_H (m, *J* in Hz)	δ_C (m)	δ_H (m, *J* in Hz)	δ_C (m)
2		151.2 (C)		153.7
4		163.5 (C)		168.4
5	5.66 (d, 8.0 Hz)	102.4 (CH)	5.9 (d, 8.4 Hz)	104.6
6	7.9 (d, 8.1 Hz)	141.3 (CH)	7.8 (d, 8.4 Hz)	144.3
1`	5.8 (d, 5.3 Hz)	88.4 (CH)	5.9 (d, 4.8 Hz)	92.5
2`	4.0 (q, 5.2 Hz)	74.1 (CH)	4.3 (dd, 4.8, 5.2 Hz)	75.1
3`	3.96 (q, 4.3 Hz)	70.5 (CH)	4.2 (dd, 5.2, 5.6 Hz)	74.5
4`	3.84 (q, 3.4 Hz)	85.3 (CH)	4.1 (ddd, 2.8, 4.4, 5.6 Hz)	82
5`a	3.62 brd	61.4 (CH_2)	3.9 (dd, 2.8, 12.8 Hz)	39.7
5`b	3.54 brd		3.8 (dd, 4.4, 12.8 Hz)	
6`				176.9 (C)

3.2.5.11. Compound AA11 (JBIR-75)

(Z)-3-((1H-imidazol-5-yl)methylene)-6-isopropylpiperazine-2,5-dione	
Synonyms	JBIR-75
Sample codes	AA11
Sample Amount	16 mg
Physical Description	white amorphous powder
Molecular Formula	$C_{11}H_{14}N_4O_2$
Molecular Weight	234 g/mol
Optical Rotation $[\alpha]_D^{20}$	-5 (*c* 0.1 in MeOH)
Retention time (LC-MS)	3.20 min

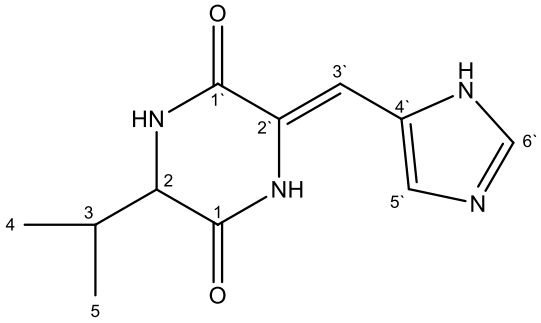

LC-HRFTMS spectrum $[M+H]^+$ 235.1189

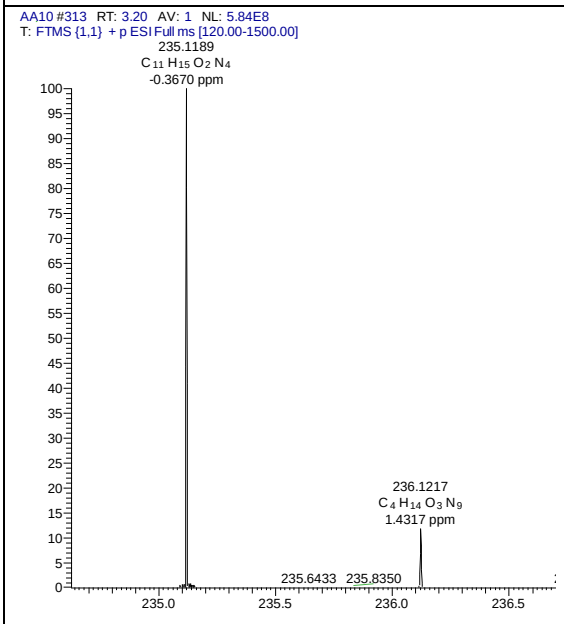

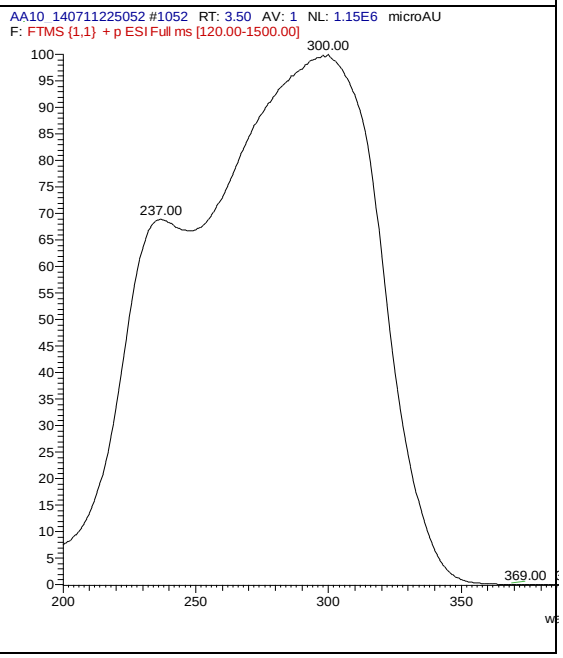

Compound AA11 (16 mg) was isolated as a white amorphous powder, exhibited a molecular formula $C_{11}H_{14}N_4O_2$ established by ESI-HRMS at *m/z* = 235.1189

$[M+H]^+$. The optical rotation $[\alpha]^{20}_D$ = -5 (*c* 0.1 in MeOH). The **^{1}H NMR** spectrum (DMSO, 400 MHz) (Fig.79) showed three singlet signals at δ_H 7.9, 7.47 and 6.52 equivalent for H-6` and H-5` of the imidazole ring and H-3` of the olefinic bridge, respectively. The aliphatic region was characterized by the presence of two methyl doublets at δ_H = 0.84 (d, 6.8 Hz, Me-5) and 0.94 (d, 7.0 Hz, Me-4); multiplet signal of H-3 of the isopropyl substitution at δ_H = 2.16 (m) and triplet signal for H-2 of the piperzine ring at δ_H = 3.94 (brd). The **^{13}C NMR** spectrum (DMSO, 400 MHz) (Fig.80) showed 11 carbon signals including two carbonyls, five olefinics, two methines and two methyls. The piperazine dione ring was confirmed through the **HMBC** correlation (Fig.82, 83) of H-2 (δ_H 3.94) with the two carbonyls at C-1 (δ_C 165.3) and C-1` (δ_C 159.8) while the position of the isopropyl substitution was confirmed through the correlation of H-2 with C-3 (δ_C 33.9) and the correlation of the two methyls Me-4, Me-5 with C-2 (δ_C 60.7). The presence of isopropyl unit was indicated through the correlation of the two geminal methyl units with each other and C-3 as well as through coupling of their protons in the **^{1}H-^{1}H COSY** spectrum (Fig.81). H-3 (δ_H 2.16) in return correlated with the two methyls Me-4 (δ_C 18.7) and Me-5 (δ_C 17.2). Moreover, the imidazole ring was confirmed through the correlation of H-6` with C-4` (δ_C 137.0), C-5` ($\delta_C$ 119.1) and H-5` with C-6` ($\delta_C$ 136.9). Furthermore, the connectivity of the two rings through the olefinic bridge was evident through the correlation of H-5` with the olefinic carbon C-3` ($\delta_C$ 103.9) and the correlation of the olefinic proton H-3` (δ_H 6.52) with C-4`, C-5` of the imidazole ring, C-1 and C-1` of the diketopiperazine ring. Compound A11 was identified as JBIR-75 by comparison with the literature (Takagi et al., 2010) (Table 15).

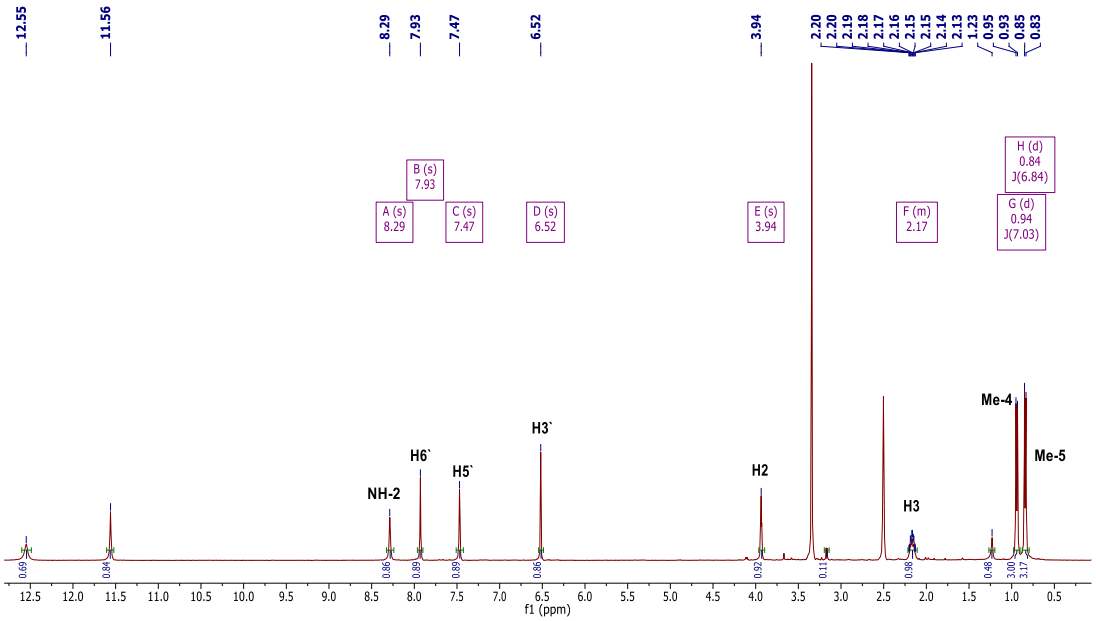

Fig.79 ^{1}H NMR of compound A11

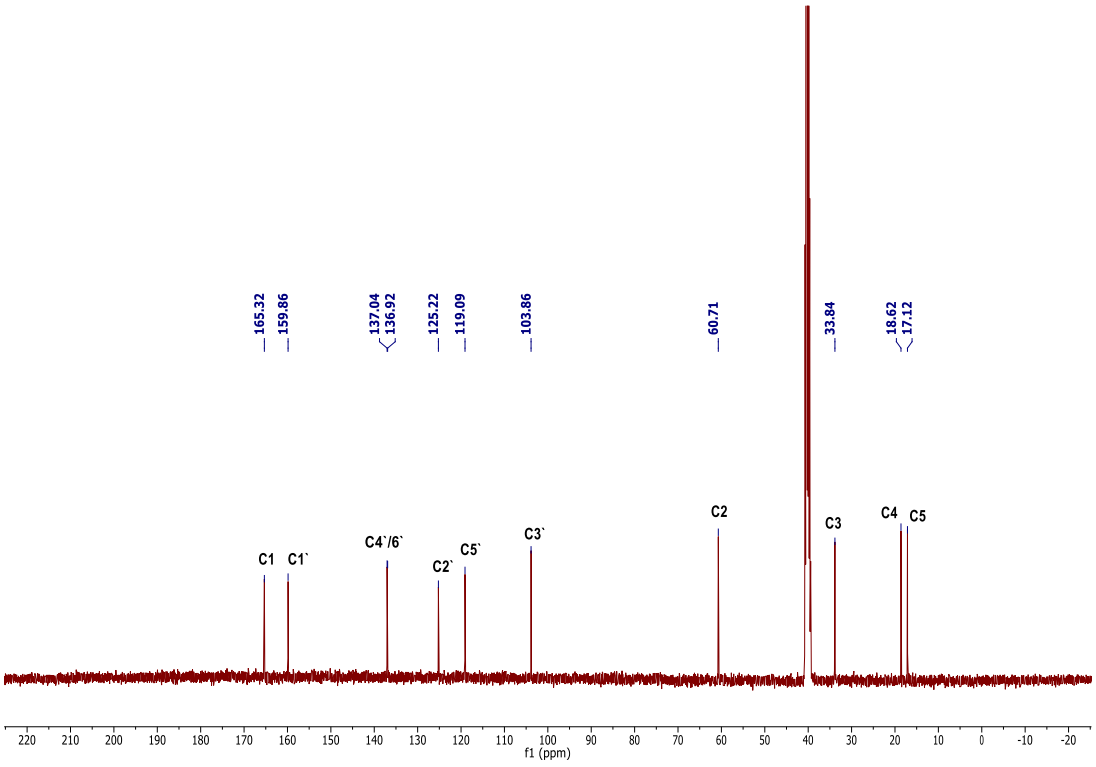

Fig.80 ^{13}C NMR of compound A11

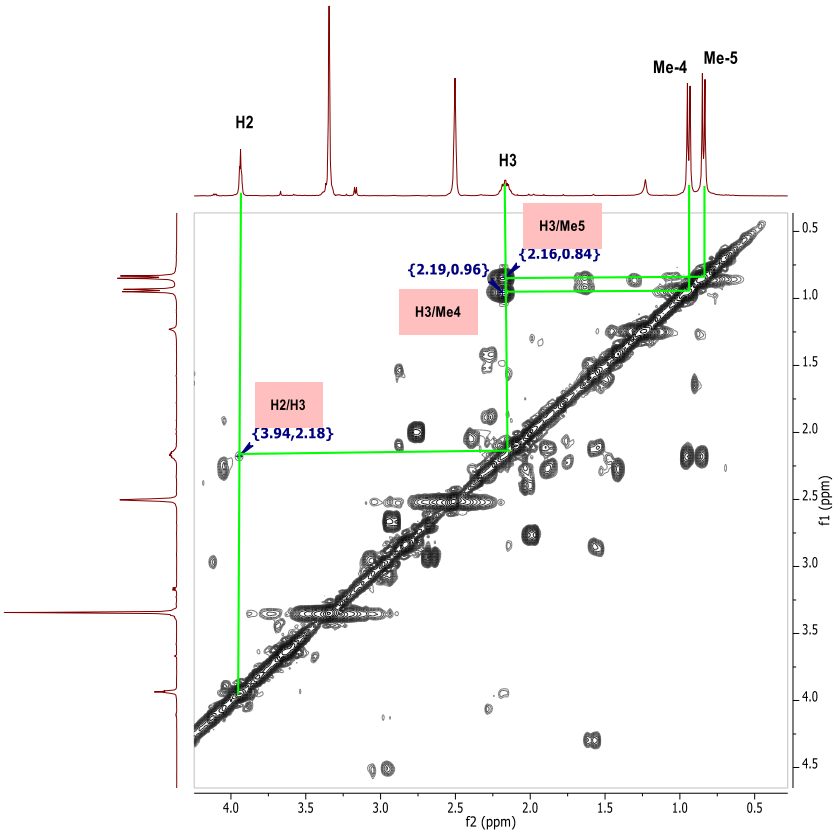

Fig.81 Expansion of ^{1}H-^{1}H COSY spectrum of compound AA11 showing the spin system connecting H-2, H-3, Me-4 and Me-5

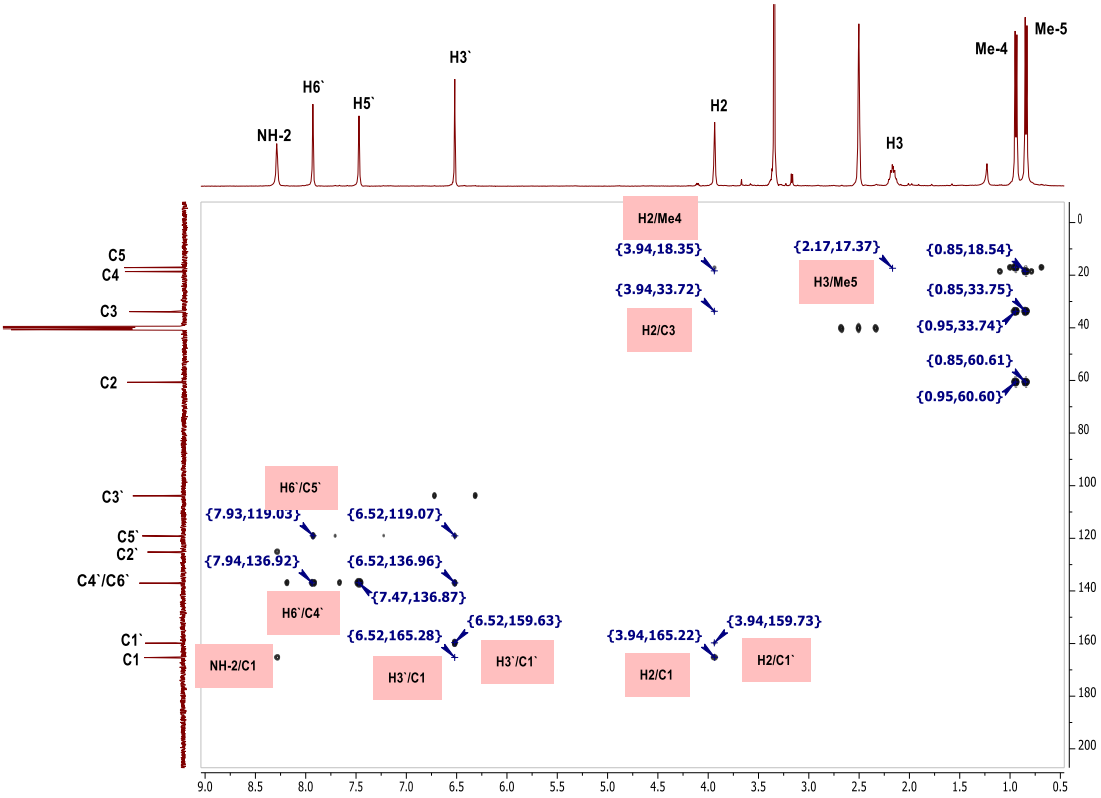

Fig.82 HMBC spectrum of compound AA11

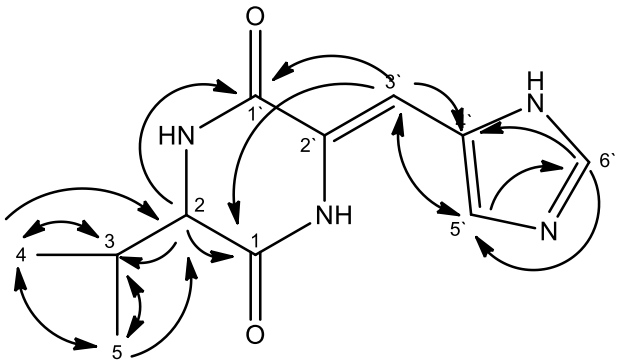

Fig.83 HMBC correlations of compound AA11

Table 15: ^{1}H NMR and ^{13}C NMR data of compound A11 compared to literature

Position	AA11		Takagi 2010	
	δ_H (m, *J* in Hz)	δ_C (m)	δ_H (m, *J* in Hz)	δ_C (m)
1		165.3 (C)		165.5
2	3.94 (t)	60.7 (CH)	3.94 (m)	60.9
3	2.16 (m)	33.9 (CH)	2.18 (m)	34.0
4	0.94 (d, 7.0 Hz)	18.7 (CH_3)	0.94 (d, 7.0 Hz)	18.8
5	0.84, (d, 6.8 Hz)	17.2 (CH_3)	0.85 (d, 7.0 Hz)	17.3
1`		159.8 (C)		160.0
2`		125.2 (C)		125.3
3`	6.52 (s)	103.9 (CH)	6.51 (s)	104.1
4`		137.0 (C)		137.0
5`	7.47 (s)	119.1 (CH)	7.48 (s)	119.2
6`	7.9 (s)	136.9 (CH)	7.93 (s)	137.0
2-NH	8.29 (s)		8.28 (brs)	
2`-NH	11.56 (s)		11.53 (s)	
4`-NH	12.55 (brs)		12.75 (brs)	

3.3. Aspergillus flocculus

3.3.1. Dereplication studies using NMR spectroscopy

From the dereplication and the biological study of *A. aculeatus*, it was observable that the huge difference in the metabolites produced as well as the biological activity was between 7-days and 30-days culture extracts while 15-days culture was just an intermediate stage. Therefore, this motivated to initially compare 7-days and 30-days of both rice and liquid culture extracts of *A. flocculus*. Comparison of the ^{1}H NMR spectra between different extracts of *A. flocculus* showed no significant difference between the 30-days rice and liquid culture extracts (Fig.84). However, the 7-days rice culture extract indicated the presence of more signals in the aromatic region than the 7-days liquid culture extract of *A. flocculus*, which signified an ABC aromatic spin system, (Fig.85). The difference in terms of the abundance of the peaks in the aromatic region, between 7-days and 30-days extracts from both rice and liquid culture was remarkable indicating that the 30-days culture condition should be chosen for upscaling.

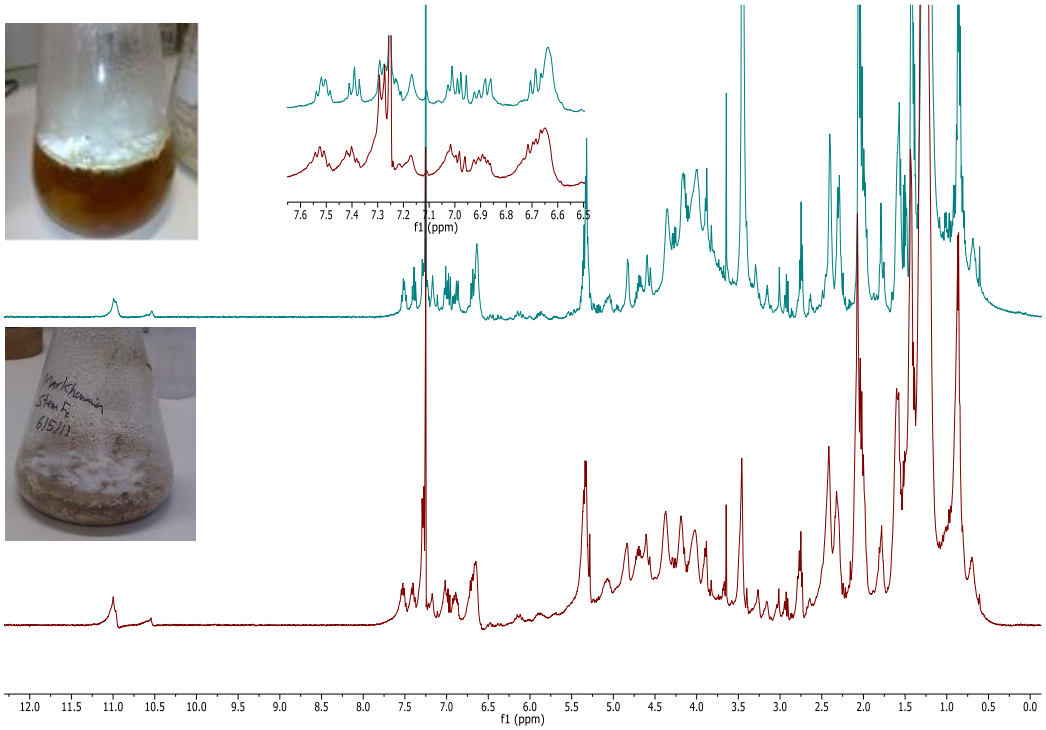

Fig.84 ^{1}H NMR spectra of *A. flocculus* 30-days liquid culture extract (●) vs 30-day rice culture extract (●)

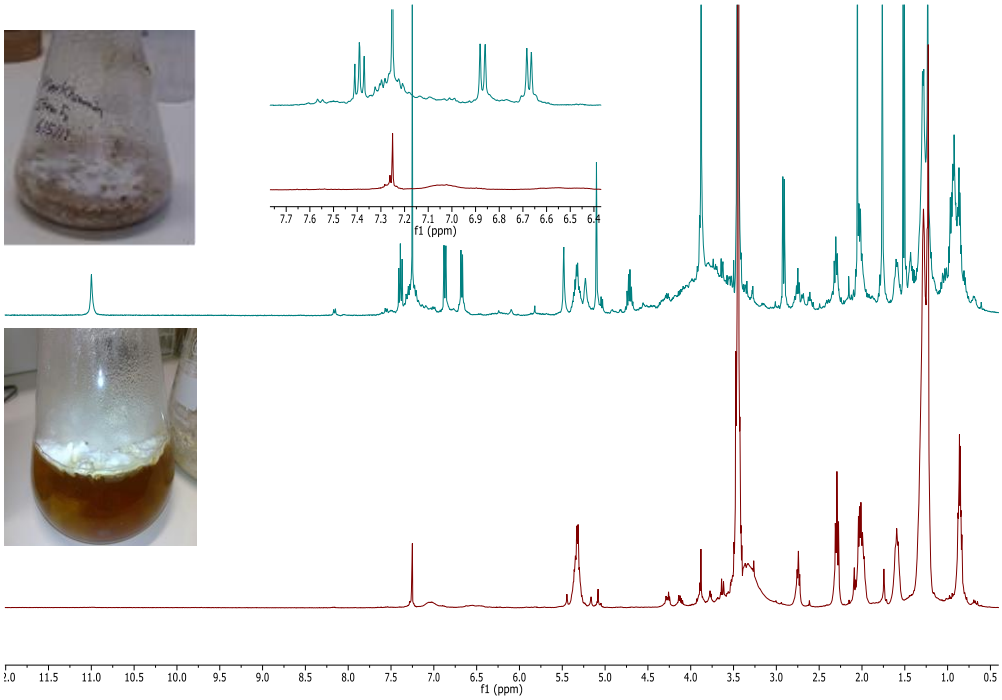

Fig.85 ^{1}H NMR spectra of *A. flocculus* 7-days liquid culture extract (●) vs 7-days rice culture extract (●)

3.3.2. Dereplication studies using MZmine

The MS raw files of both rice and liquid culture extracts of *A.flocculus* have been imported into the MZmine 2.10 software for data processing. Comparison of the total ion chromatogram of both rice and liquid culture extracts (Fig.86) exhibited no remarkable differences in the abundance of the predominant metabolites. The scatter plot (Fig.87) also showed no obvious variation between rice and liquid culture extracts in terms of number of the produced metabolites represented by the blue dots. This was an indication of the expected similarity in chemical profile between both extracts. The processed data was subjected to in-house macro-database file (Macintyre et al., 2014) for further clean up as well as database searching using DNP databases. The dereplication table (Table 16), was accomplished for fungal extracts, the ethyl acetate and water extracts of the *Markhamia* plant from which *A. flocculus* was isolated. Table (16) exhibited that some of the fungal metabolites produced in both rice and liquid culture extracts were found at smaller peak area in either EtOAc or H_2O extracts of *Markhamia* stem (MS). This indicated lower concentration of these metabolites in the plant

extract in comparison to the fungal extract. These metabolites corresponded to ion peaks at *m/z* (retention time in minutes) 194.058 (9.45), 210.053 (6.50), 208.069 (2.47), 184.073 (5.24) and 186.090 (2.71) which have been described in table (16) as 5-hydroxymellein, 4,5-dihydroxymellein, 3-Methyl-3,8-dihydroxy-3,4-dihydroisocoumarin, 7-O-acetylkojic acid and dihydroaspyrone, respectively. This was an indication that *A. flocculus* was able to produce the same plant metabolites in larger quantities. Moreover, presence of the fungal metabolites in the plant extracts proved the source of the endophyte. Furthermore, metabolites with corresponding ion peaks at *m/z* 339.253, 678.497, 418.198, 802.544 eluted at 8.28, 8.13, 13.34 and 32.8 min were found to be undescribed before in the literature, which showed that *A.flocculus* extracts could be a source for new chemical entities. In addition, no significant difference was observed between the concentrations of the produced metabolites between 30-days rice and liquid culture extracts of *A.flocculus* that also afforded similar chemical constituents as shown by the dereplication results using NMR experiments.

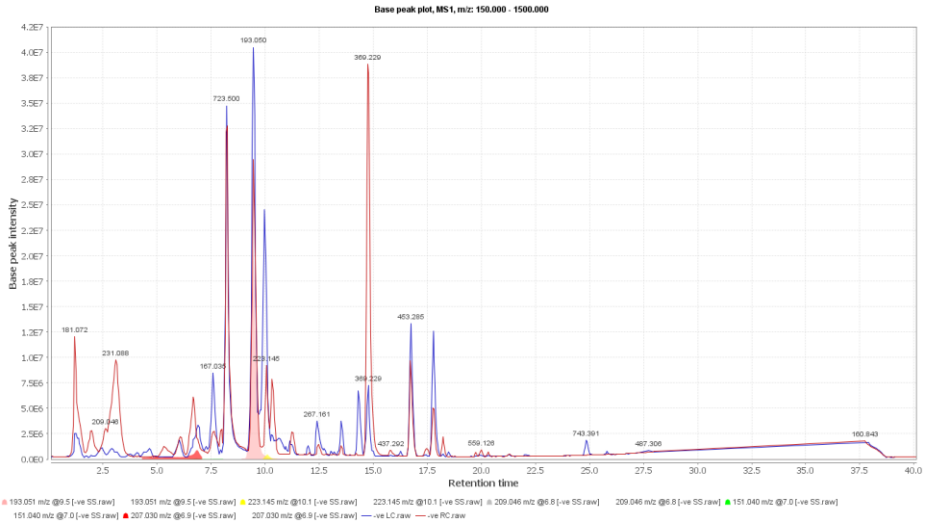

Fig.86 TIC of both rice culture (●) and liquid culture (●)

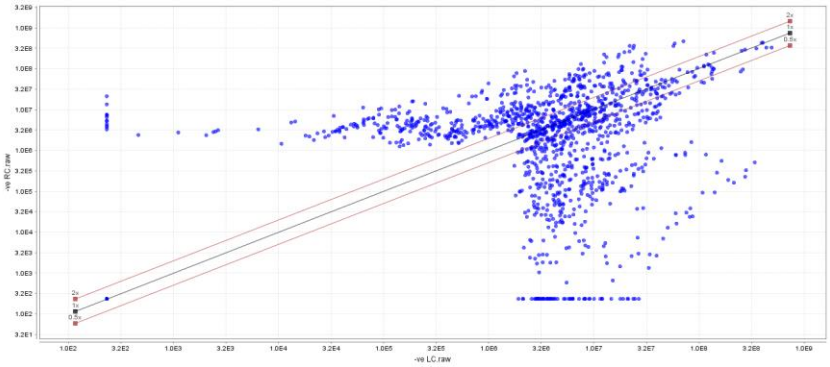

Fig.87 Scatter plot of rice culture (Y-axis) and liquid culture (X-axis)

Table 16: Dereplication table of fungal extracts of *A.flocculus* including mass to charge ratio (*m/z*), retention time (RT), molecular formula, name and source of the detected metabolites in 30 days liquid culture (LC) and 30 days rice culture (RC) fungal extracts, water extract (MS-H_2O) and ethyl acetate extract (MS-EtOAc) of the plant stem. The comparison based on the peak area of the produced metabolites. Highlighted rows represented the metabolites were isolated from the fungal extract and present at lower quantities in either water or ethyl acetate plant extracts

m/z	RT	Name/Source	MS-H_2O	MS-EtOAc	30-days LC	30-days RC
317.274	16.99	**caldaphnidine** ($C_{21}H_{35}NO$) *Daphniphyllum calycinum*	0	1.18E+03	1.20E+09	1.90E+07
339.253	8.28	**Unknown**	1.15E+04	0	1.00E+09	1.80E+09
224.152	10.07	**aspergillic acid** $C_{12}H_{20}N_2O_2$ *Aspergillus flavus*	0	0	3.40E+08	1.20E+08
186.090	2.71	**dihydroaspyrone** $C_9H_{14}O_4$ *A.ochraceus*	1.19E+04	0	1.40E+09	1.50E+08
678.497	8.13	**Unknown**	1.20E+03	0	4.10E+08	1.30E+09
432.278	13.49	**aspochracin** $C_{23}H_{36}N_4O_4$ *A.ochraceus*	0	0	6.40E+08	1.80E+09
194.058	9.45	**5-hydroxymellein** $C_{10}H_{10}O_4$ *Botryosphaeria obtusa*	9.55E+04	8.02E+05	3.10E+08	3.50E+08
418.198	13.34	**Unknown**	5.67E+02	4.20E+03	2.00E+07	1.20E+07
412.263	32.73	**alisolide** ($C_{26}H_{36}O_4$) *Alisma orientale*	0	0	7.80E+06	5.60E+06
474.311	36.66	**Etzionin** $C_{26}H_{42}N_4O_4$ *Didemnum rodriguesi*	3.03E+02	0	6.60E+08	7.20E+08
802.544	32.8	**Unknown**	0	5.19E+04	1.04E+07	1.08E+07
210.053	6.5	**4,5-dihydroxymellein** $C_{10}H_{10}O_5$ *Phomopsis* sp. ZH-111	3.20E+04	2.43E+04	6.50E+07	1.00E+06
208.069	2.47	**3-Methyl-3,8-dihydroxy-3,4-dihydroisocoumarin** $C_{11}H_{12}O_4$ *Botryosphaeria* sp.	3.82E+05	6.31E+03	1.30E+08	1.00E+07
184.073	5.24	**7-O-acetylkojic acid** $C_8H_8O_5$ *Aspergillus* spp.	1.77E+05	1.04E+04	7.70E+07	1.90E+07

.

3.3.3. Metabolomic study using SIMCA-P^{+}

3.3.3.1. *A. flocculus* different extracts vs *Markhamia* stem and leaves extracts

Principal component analysis (PCA) of *A. flocculus* extracts over SIMCA-P^{+} software showed that all fungal extracts were clustered together (Fig.88) which was an indication that all extracts of *A. flocculus* produced nearly the same set of metabolites. All rice and liquid culture extracts of *A. flocculus* exhibited nearly an equal significant inhibition activity on NF-κB pathway, which indicated the similarity in the putative metabolites as shown by the PCA plot. The PCA and OPLS-DA loading plots (Fig.89, 91) showed nearly the same outlier metabolites. Some of these outlying metabolites were described in the dereplication table (Table 16) for example those ion peaks at *m/z* (retention time in minutes) 186.090 (2.71), 194.058 (9.45) for dihydroaspyrone and 5-hydroxymellein, respectively. Dihydrospyrone and 5-hydroxymellein were earlier characterized from the culture extracts of *Aspergillus ochraceus* and *Botryosphaeria obtusa*, respectively (Fuchser and Zeeck, 1997, Venkatasubbaiah and Chilton, 1990). The S-line (Fig.92) showed the structures of the metabolites that have been isolated from the 30-days rice culture extract of *A. flocculus* and predicted by the metabolomics study to be responsible for the inhibition activity on NF-κB pathway. These metabolites at *m/z* 186.090, 194.058 and 152.047 eluted at 2.71, 9.45 and 6.08 minutes, were identified and elucidated as dihydroaspyrone, 5-hydroxymellein and 2- or 4-hydroxyphenyl acetic acid (Zhou et al., 2005, Milne et al., 2011). Furthermore, 5-hydroxymellien was reported in the literature as antibacterial, antialgal, and antifungal (Hussain et al., 2009). Metabolomics tools and the dereplication study were effectively employed in the early identification of the bioactive metabolites in the biologically active fungal extracts.

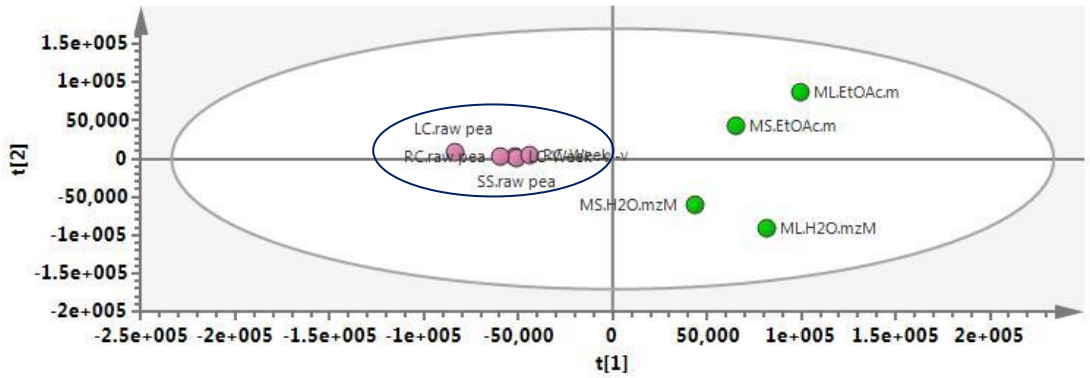

Fig.88 PCA score plot of *A. flocculus* extracts (●) against *Markhamia* plant extracts (●)

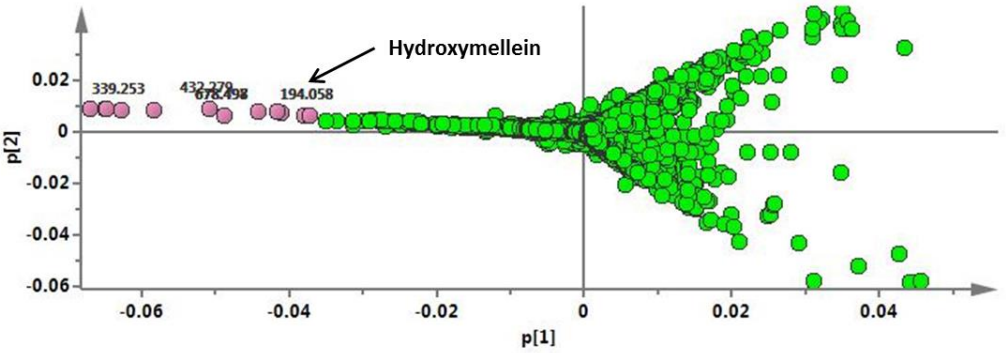

Fig.89 PCA loading plot of *A. flocculus* and *Markhamia* plant extracts showed the discriminated metabolites (●) belonged to the fungal extracts

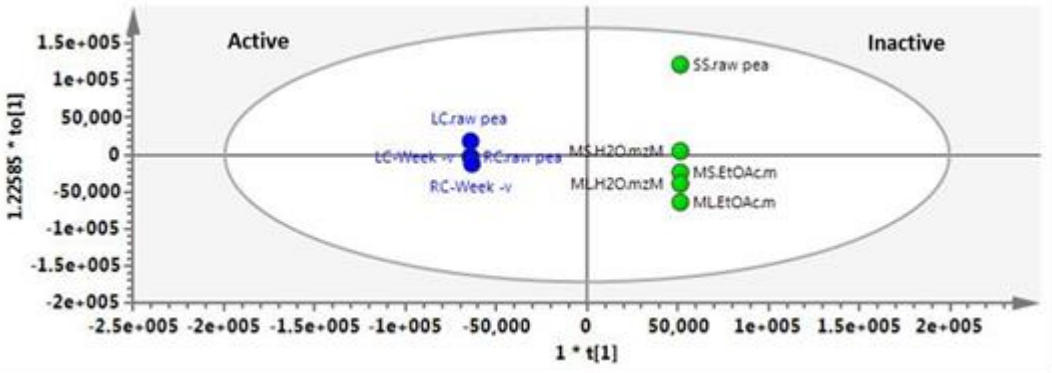

Fig.90 OPLS-DA score plot of *A. flocculus* extracts (●) against *Markhamia* plant extracts (●)

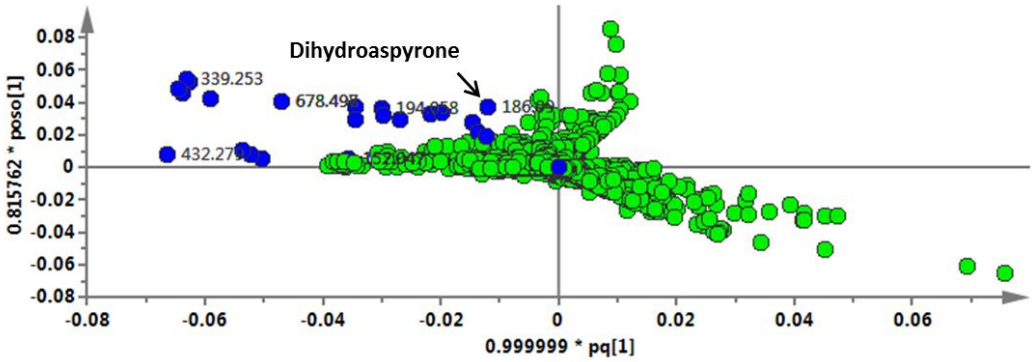

Fig.91 OPLS-DA loading plot of *A. flocculus* extracts against *Markhamia* plant extracts showing the putative metabolites (●) were predicted to be responsible for the biological activity

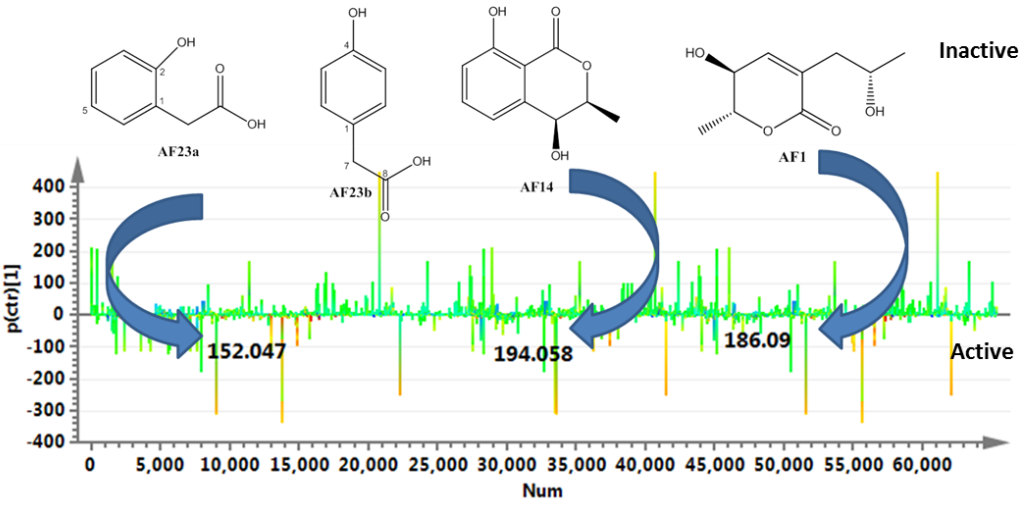

Fig.92 S-line of *A. flocculus* extracts active vs inactive showing the isolated metabolites with their structure

3.3.3.2. Dereplication of the MPLC fractions of 30 day rice culture extract

The thirty days rice culture extract of *A. flocculus* was subjected to fractionation using flash chromatography. The resulted fractions were subjected to the chemometric analysis using SIMCA-P^{+}. The PCA score plot (Fig.93) showed mainly two groups while fractions 136-240, 395-399 and 400 were outliers. The PCA loading plot (Fig.94) showed the discriminated metabolites belonged to each group. These metabolites were at *m/z* (retention time in minutes) 317.272 (15.90), 238.132 (12.4), 194.058 (9.6), 186.089 (2.71), 230.094 (14.9), 262.084 (10.98) and 276.092 (15.5) which have been described in the literature as caldaphnidine isolated from *Daphniphyllum calycinum*, flutimide from *Delitshia confertaspora*, 5-hydroxymellien, dihydroaspyrone, diorcinol from *Aspergillus versicolor*, N-

asparaginyl-N-hydroxyasparagine from *Mycobacterium avium* and casegravol from *Casearia graveolens* (Table 16). The bioassay guided MPLC fractionation of the 30-days rice culture extract led to sorting the active from the inactive fractions. The fractions were tested against both cancer cell lines PC3 and K562 as well as *T. brucei brucei*. The active fractions were compared to the inactive ones in order to help in prediction which metabolites exactly could be responsible for the remarked activity. OPLS-DA analysis was accomplished twice one for anticancer active vs inactive fractions and another for antitrypanosomal active against inactive ones. The first module included the OPLS-DA score plot (Fig.95) which showed two main groups of fractions one for the antitrypanosome active fractions which included fractions 18-29, 30-32, 33-42, 43-48, 51-52, 53-55, 56-64, 65-71, 72-89 and the other group included the inactive fractions. The OPLS-DA loading plot (Fig.96) exhibited the putative unique metabolites belonged to these fractions and were predicted to be responsible for the antitrypanosomal activity like metabolites at *m/z* 238.132, 194.058, 186.089, 230.094 and 280.240 eluted at 12.4, 9.6, 2.71, 14.9 and 27.5 minutes for flutimide, 5-hydroxymellien, dihydroaspyrone, diorcinol and an unknown compound, respectively. Flutimide was reported in the literature as an endonuclease inhibitor of influenza virus (Tomassini et al., 1996) while 5-hydroxymellein and diorcinol were reported as antimicrobials (Hussain et al., 2009, Yurchenko et al., 2010). This led to the conclusion that the exhibited activity could be due to one or more of the identified compounds or due to a previously undescribed compound at *m/z* 280.240. The second module consisted of the anticancer active vs inactive fractions, as shown on an OPLS-DA score plot (Fig.97) which distinguished the active fractions 51-52 and 53-55 from the rest of the fractions. The OPLS-DA loading plot (Fig.98) discriminated the metabolites belonging to the aforementioned active fractions and predicted to be responsible for the anticancer activity. These metabolites were observed at *m/z* (retention time in minutes) 238.132 (12.4), 152.047 (10.53), 168.115 (15.6) and 228.147 (16.3). Metabolites at *m/z* 238.132 and 152.047 were described as flutimide and 2- or 4-hydroxyphenylacetic acid which have never been reported to exhibit anticancer activity while metabolites at *m/z* 168.115 and 228.17 have never been described

in the literature. This indicated that the observed anticancer activity could be due to new chemical entities as well as identified ones. The third module included in the OPLS-DA score and loading plot (Fig.99, 100), collected both anticancer and antitrypanosomal active vs inactive fractions in order to test the ability of the module to differentiate between the unique metabolites of each group at the same time. The OPLS-DA score plot (Fig.99) showed three main groups; first was for the anticancer active fractions 51-52 and 53-55 which also showed antitrypanosomal activityies, second for the antitrypanosome active fractions 18-29, 30-32, 33-42, 43-48, 56-64, 65-71, 72-89 and the third group consisted of the inactive fractions. The OPLS-DA loading plot (Fig.100) discriminated the metabolites belonging to each group which were identical to the metabolites detected by the OPLS-DA loading plots from the first two modules (Fig.96, 98) which confirmed the ability of the module to distinguish the putative unique metabolites for variable active fractions at the same time.

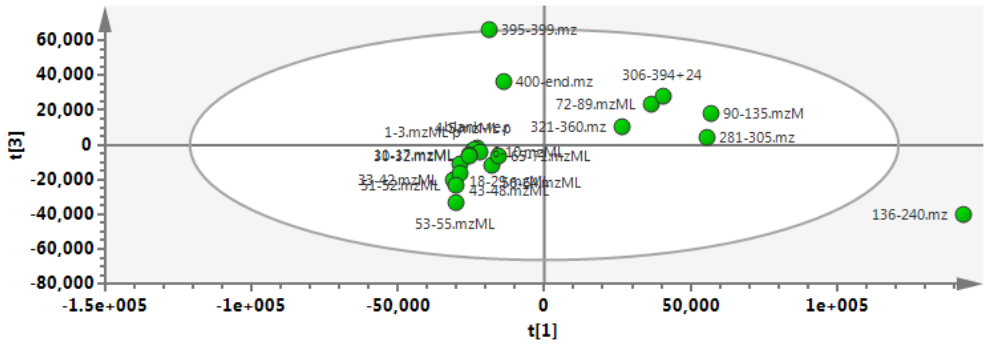

Fig.93 PCA score plot of MPLC fractions of 30-day rice culture extract of *A. flocculus* showed two groups of fractions

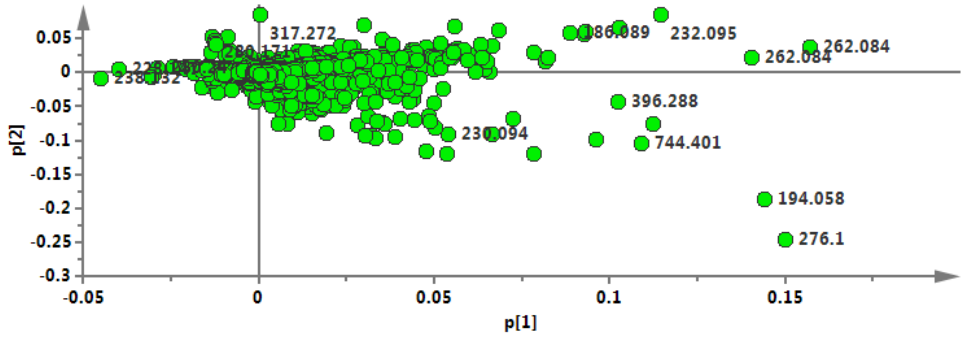

Fig.94 PCA loading plot of MPLC fractions of 30-day rice culture extract of *A. flocculus* showed the discriminated metabolites in each group

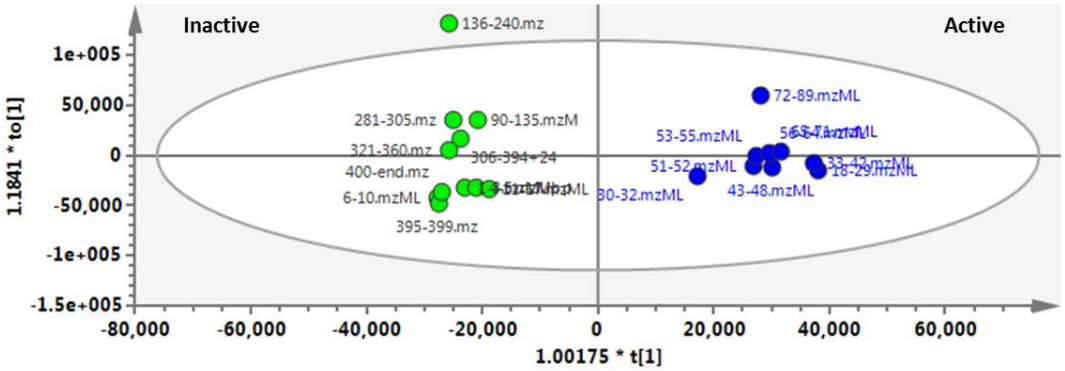

Fig.95 OPLS-DA score plot showing antitrypanosome active (●) vs inactive fractions (●)

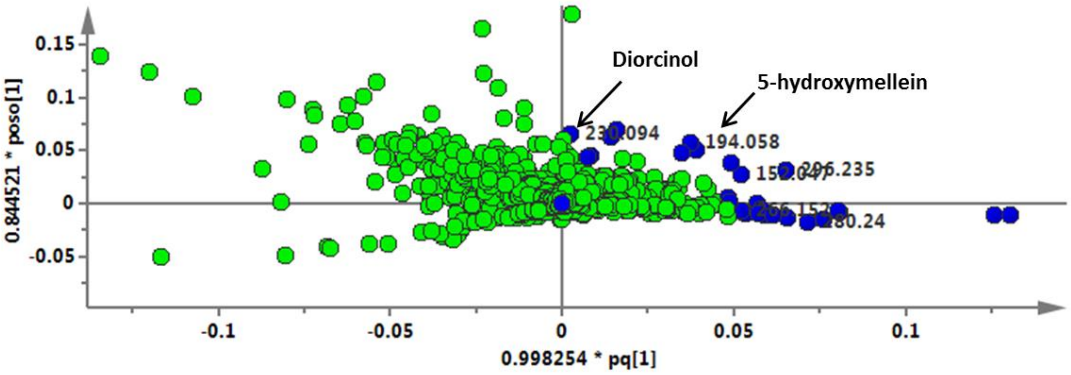

Fig.96 OPLS-DA loading plot showed the putative metabolites (●) were predicted to be responsible for the antitrypanosomal activity

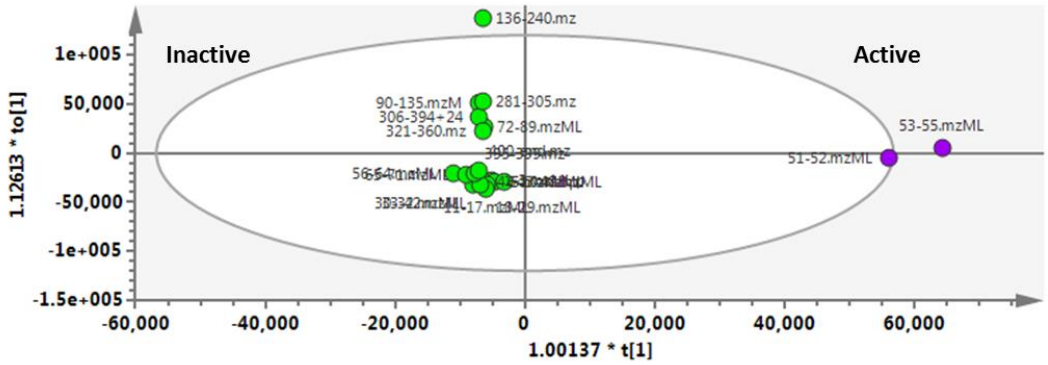

Fig.97 OPLS-DA score plot showing anticancer active (●) vs inactive fractions (●)

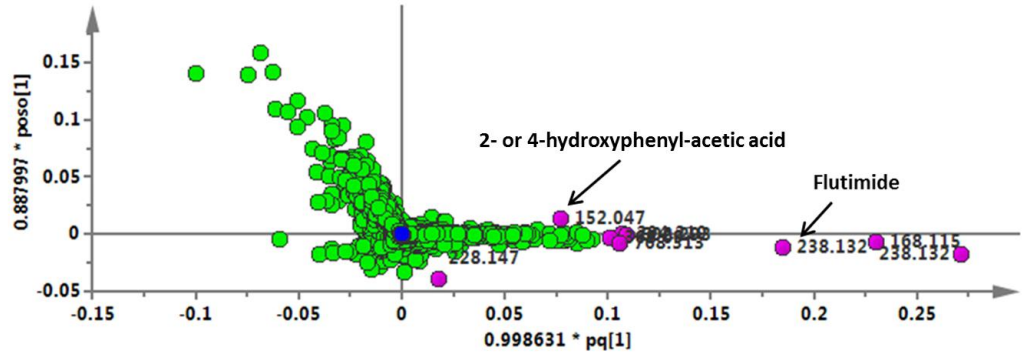

Fig.98 OPLS-DA loading plot showed the putative metabolites (●) were predicted to be responsible for the anticancer activity

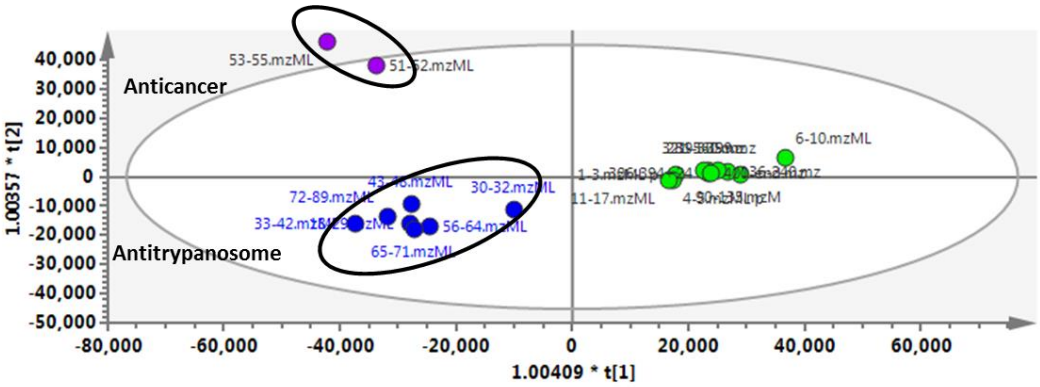

Fig.99 OPLS-DA score plot of the active vs inactive fractions of 30-day rice culture extract of *A. flocculus* (●) Anticancer & antitrypanosome (●) antitrypanosome (●) inactive

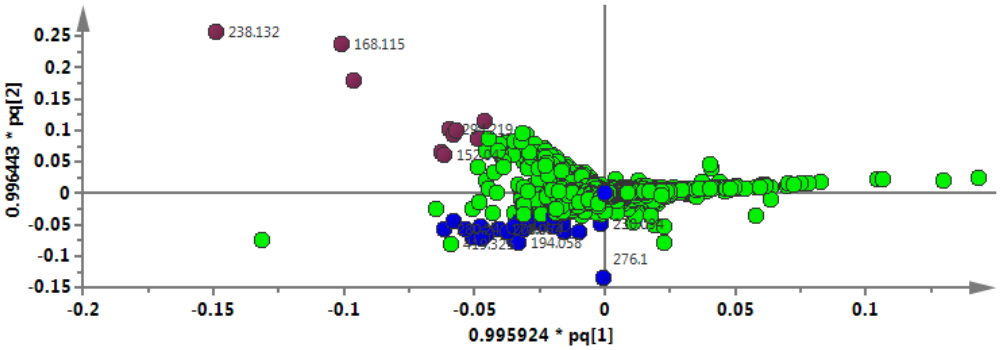

Fig.100 OPLS-DA loading plot of the active vs inactive fractions of 30-day rice culture extract of *A. flocculus* (●) Anticancer & antitrypanosome (●) antitrypanosome (●) inactive

3.3.4. Biological activity

3.3.4.1. Anticancer activity

As mentioned in the previous section (3.2.4.1), *A. flocculus* extracts (Code:

Markh-st-F2a) exhibited a significant anticancer activity against both cancer cell lines K562 and PC3. All fractions along with their parent extracts were tested for its NF-κB inhibition activity on K562 cancer cell line. All fungal extracts of *A. flocculus*, fraction (Seph-5) resulted from fractionation using sephadex and MPLC fractions (3-10) showed a significant inhibition of NF-κB (Fig.101, 102). Testing the cytotoxicity for the MPLC fractions from the medium scaled up batch of 30-days rice culture extract against both cell lines showed that fraction F10 (pooled from F50-52) exhibited a remarkable activity against K562 cell lines (Fig.103) while F11 (pooled from F53-55) was active against both K562 and PC3 cell lines (Fig.104). The active fractions have been further fractionated and purified to give 25 pure compounds. Testing the cytotoxicity of the purified compounds from the 30-days rice culture extract of *A. flocculus* showed a significant activity of compounds AF14, AF15, AF16 and AF17 against K562 cell lines (Fig.105). The results detected that none of the active compounds showed a cytotoxic effect on the normal cells. The three compounds AF14, AF15 and AF16 are structurally related compounds and were identified as *cis*-4-hydroxymellein, 5-hydroxymellein and mellein while AF17 was identified as diorcinol. Although compound AF14 (*cis*-4-hydroxy mellein) was active, the *trans*-4-hydroxy mellein (compound AF13) was found to be inactive which indication for the stereo-specificity of the active compound. Moreover, presence of an extra hydroxyl group (4-OH) or (3-OH) in compounds AF18 and AF11 respectively over AF15 (5-hydroxymellein) caused a complete loss in the activity. Compound AF16 was a mixture of botryoisocoumarin A (3-methoxymellein) and mellein, so the observed activity could be due to either one of them or both. None of these compounds was reported in the literature as anticancer compound however mellein was reported as antiinflamatory (Pongprayoon et al., 1991). Furthermore, (Fig.105) showed that compound AF17 (diorcinol) exhibited a significant inhibition of the NF-κB pathway which could be an indication of the mechanism of the anticancer action of this compound.

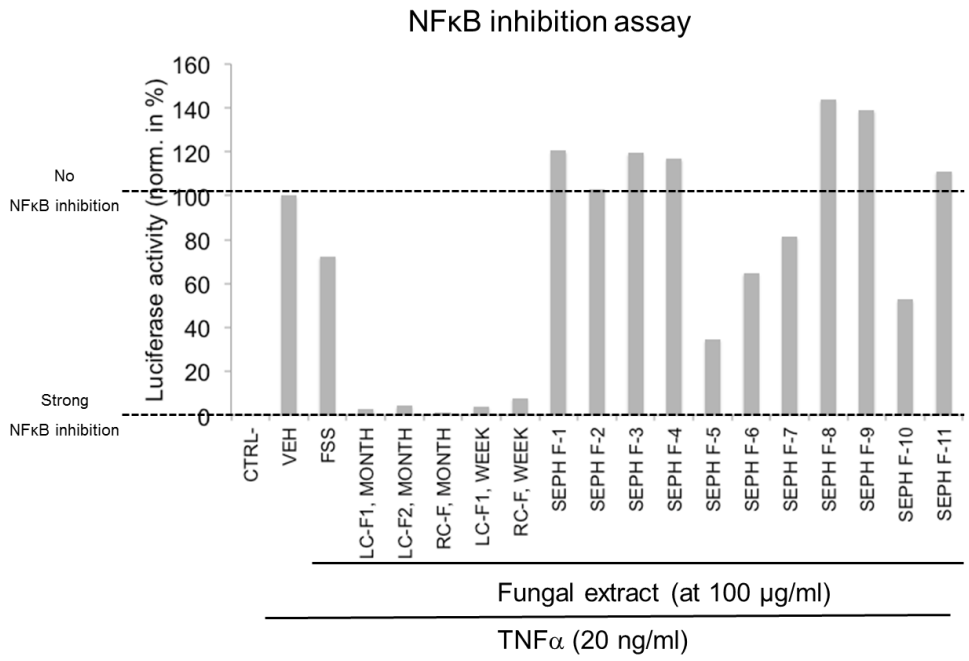

Fig.101 NF-κB inhibition activity for different extracts (small scale) of *A. flocculus* and its sephadex fractions

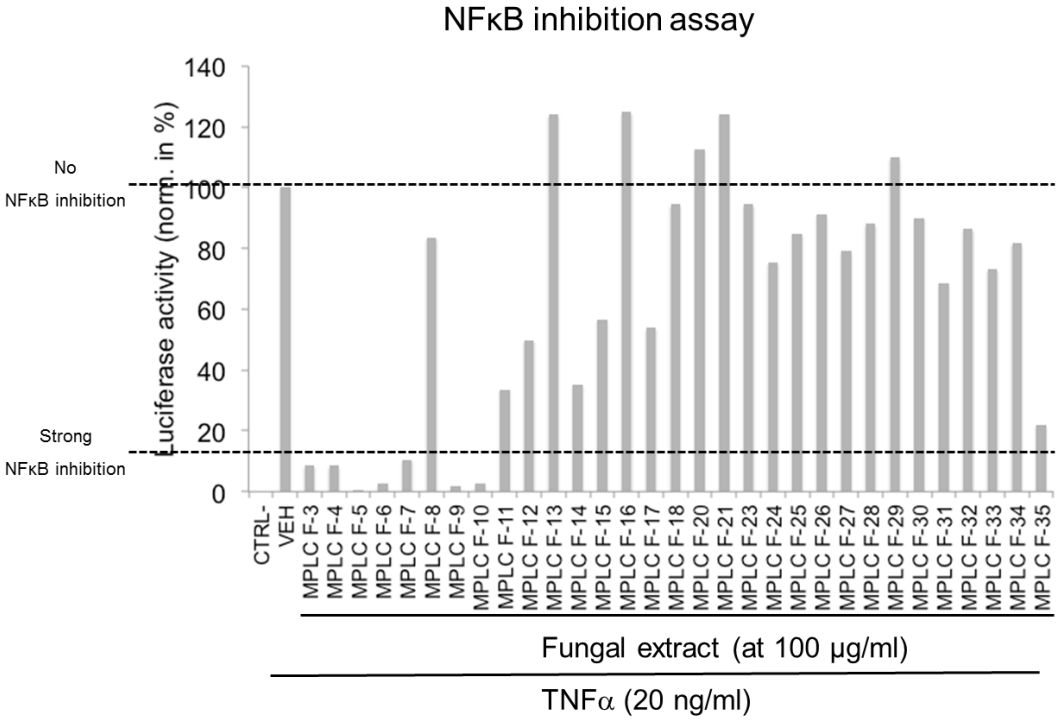

Fig.102 NF-κB inhibitios activity of MPLC fractions of small scaled 30-days rice culture of *A.flocculus*

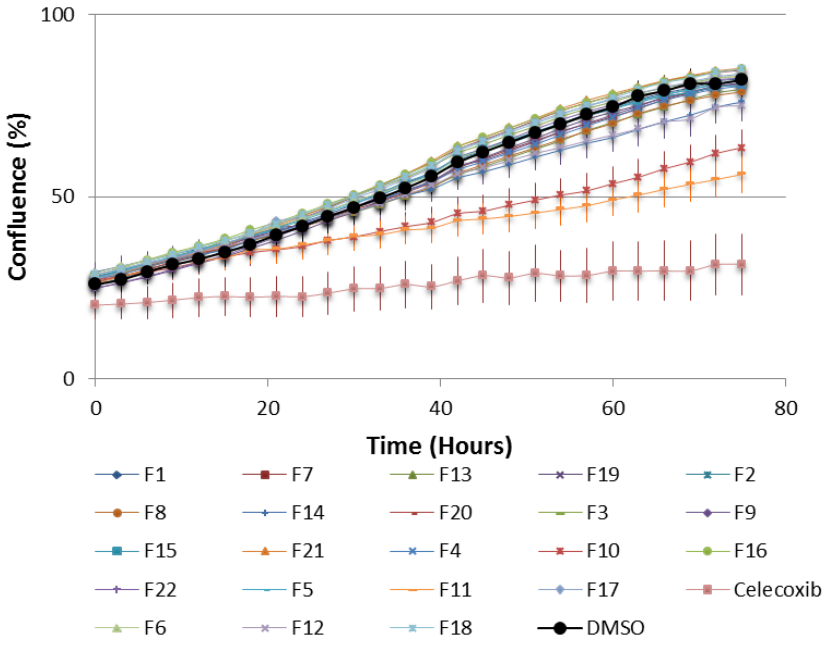

Fig.103 Bioactivity chart showing the anticancer effect of fractions F10 and F11 of MPLC fractions from medium scaled batch of 30-days rice culture extract of *A.flocculus* on K562 cells at 10µg/mL

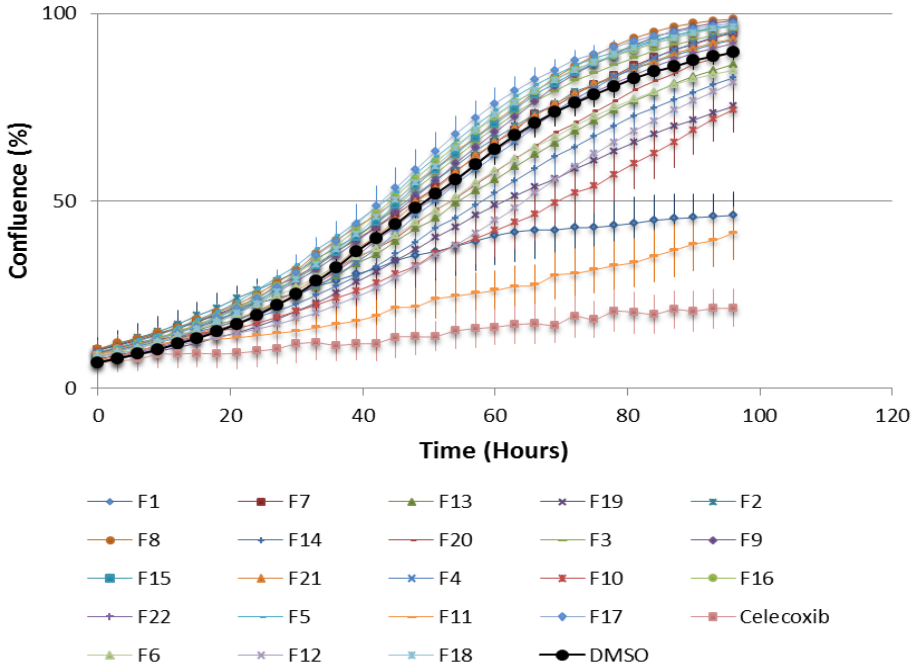

Fig.104 Bioactivity chart showing the anticancer activity of F11 of MPLC fractions from medium scaled batch of 30-days rice culture extract of *A.flocculus* on PC3 cells at 10µg/mL

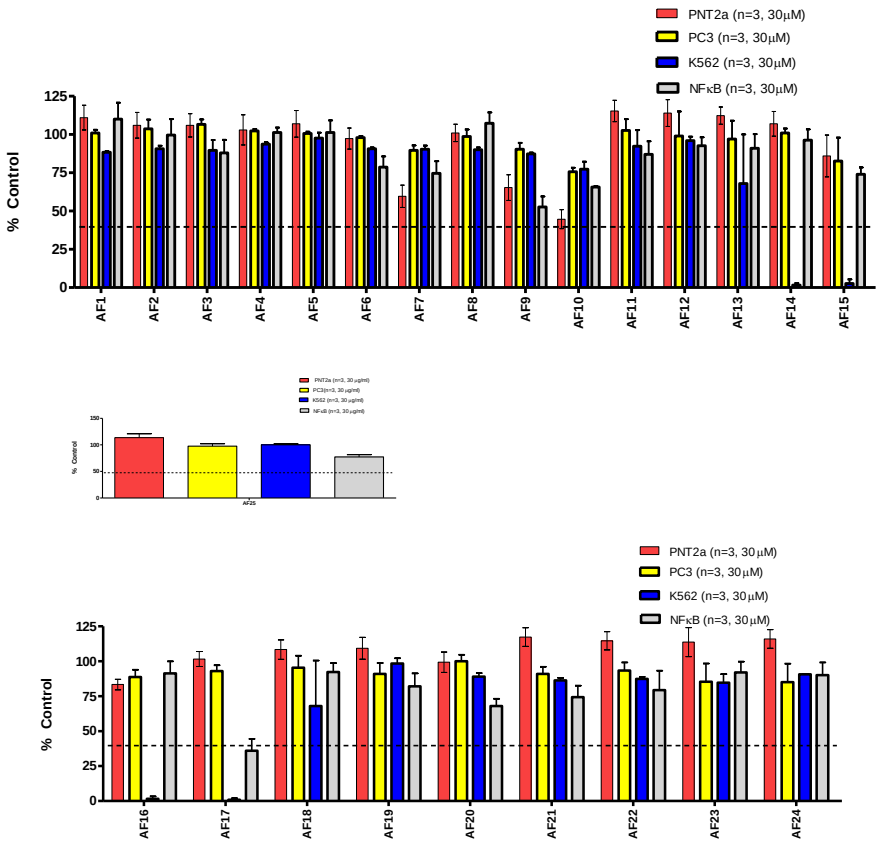

Fig.105 The anticancer activity for the pure compounds against K562 (●) and PC3 (●) cancer cell lines and the normal cells (●) while (●) represented NF-κB pathway

3.3.4.2. Antimicrobial and Antitrypanosomal activity

Testing the extracts of *A. flocculus* against *Trypanosome brucei brucei* showed a significant growth inhibitory activity for 7-day rice culture extract over other extracts of *A. flocculus* (Fig.106). However, the metabolomics study proved that all extracts produced nearly the same set of active metabolites. So due to the high yield of 30-days rice culture extract, it was subjected to MPLC fractionation. Investigating the antitrypansomal activity of the MPLC fractions of 30-day rice culture extract showed a remarkable activity with more than 90% inhibition for A6, A7, A8, A9, A10, A11, B2, B3 and B4 equivalent for fractions 18-29, 30-32, 33-42, 43-48, 50-52, 53-55, 56-64, 65-71 and 72-89, respectively (Fig.107). The active fractions were subjected to further fractionation and the antitrypanosomal activity of the pure compounds was tested. The results showed that compounds AF3, 6, 7, 8, 9, 10, 17, 20, 21 and AF22 exhibited a significant antitrypanosomal activity (more than 90% inhibition) with MIC 145.35, 31.57, 7.29, 62.81, 15.78,

108.70, 88.03, 409.84 and 301.20 µM, respectively (Fig.108). Compounds AF6, AF7, AF8 and AF9 were structurally related steroidal compounds and identified as ergosterol, ergosterol peroxide, campesterol and unknown steroidal compound, respectively. None of these metabolites has been reported in the literature before as antimicrobial compound. Compound AF3 was described as dihydropenicillic acid and reported in the literature as a NF-κB inhibitor (Tachibana et al., 2008) which could be an indication for the mechanism of its cytotoxicity. Moreover, compound AF17 (diorcinol) was reported in the literature as a strong antimicrobial to which the antimicrobial activity of the total extract from *A. versicolor* can be attributed (Yurchenko et al., 2010). Although compound AF20, identified as phomaligol-2-epimer, exhibited a remarkable antitrypanosomal activity, its congener AF19 (phomaligol) exhibited no activity which suggested the required stereospecificity of the active compound. Compound AF22, is the methylated derivative of AF23 that was identified as 4-hydroxyphenyl acetic acid, exhibited a significant antitrypanosomal activity however its congener AF23 was inactive. Furthermore, compounds AF7 (ergosterol peroxide), AF17 (diorcinol), AF21 (p-hydroxybenzaldehyde) and AF22 showed a selective antimicrobial activity against *Mycobacterium marinum* with MIC 233.64, 108.89, 409.83 and 602.40 µM respectively (Fig.109).

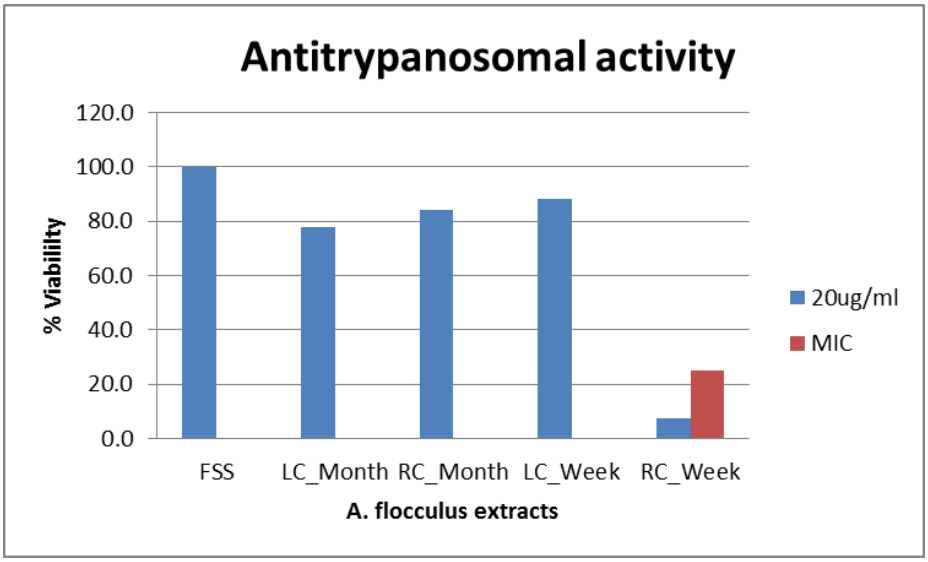

Fig.106 Antitrypanosomal activity of fungal extracts of *A. flocculus*

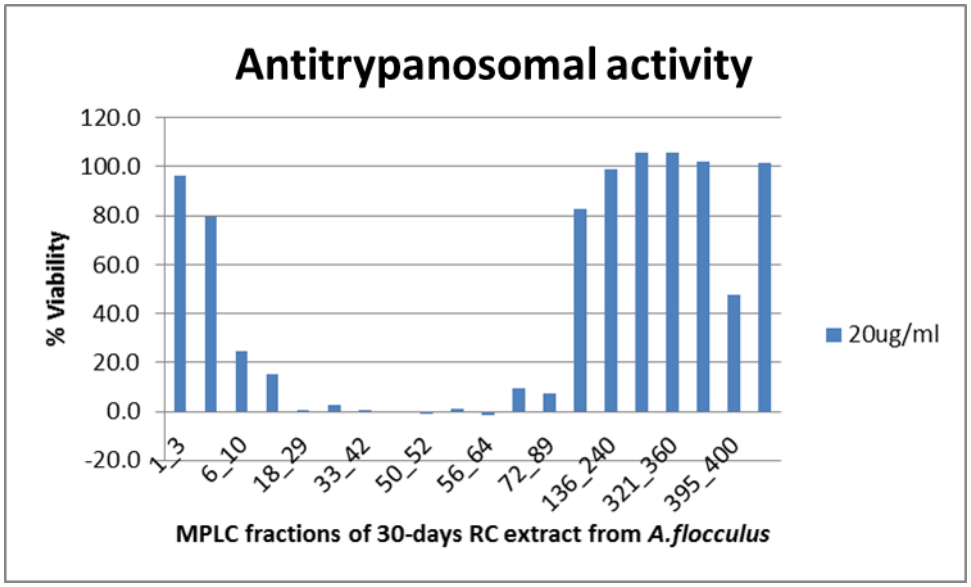

Fig.107 Antitrypanosomal activity of MPLC fractions of 30 day rice culture extract of *A. flocculus*

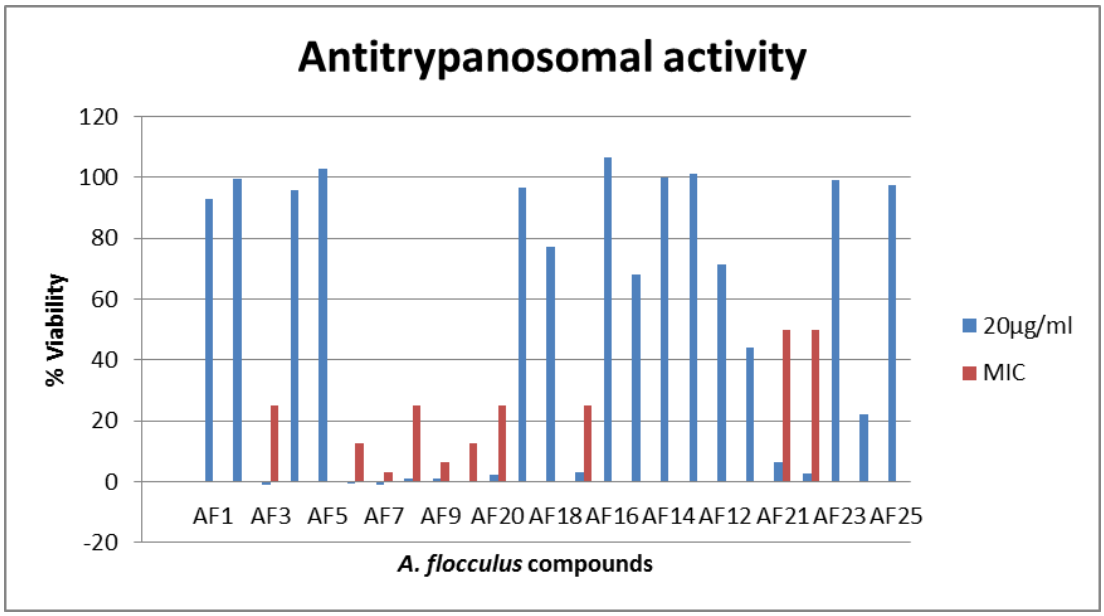

Fig.108 Antitrypanosome activity of the pure compounds of *A. flocculus* 30-days rice culture extract

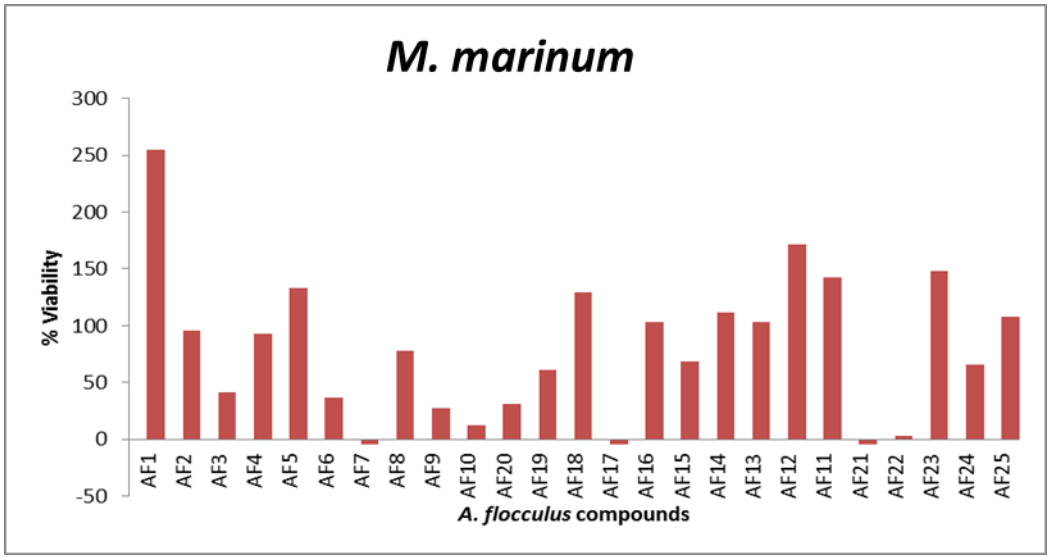

Fig.109 Antimicrobial activity of the pure compounds *of A.flocculus* from 30-days rice culture extract

3.3.5. Isolated compounds

3.3.5.1. Compound AF1 (dihydroaspyrone)

5-hydroxy-3-(2-hydroxypropyl)-6-methyl-5,6-dihydro-2H-pyran-2-one	
Synonyms	Dihydroaspyrone
Sample codes	AF1
Sample Amount	16 mg
Physical Description	brown amorphous powder
Molecular Formula	$C_9H_{14}O_4$
Molecular Weight	186 g/mol
Optical Rotation $[\alpha]_D^{20}$	+18 (*c* 0.05 in MeOH)
Retention time (LC-MS)	12.09 min

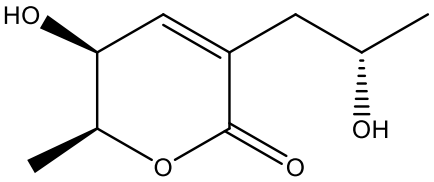

LC-HRFTMS spectrum $[M+H]^+$ 187.0965

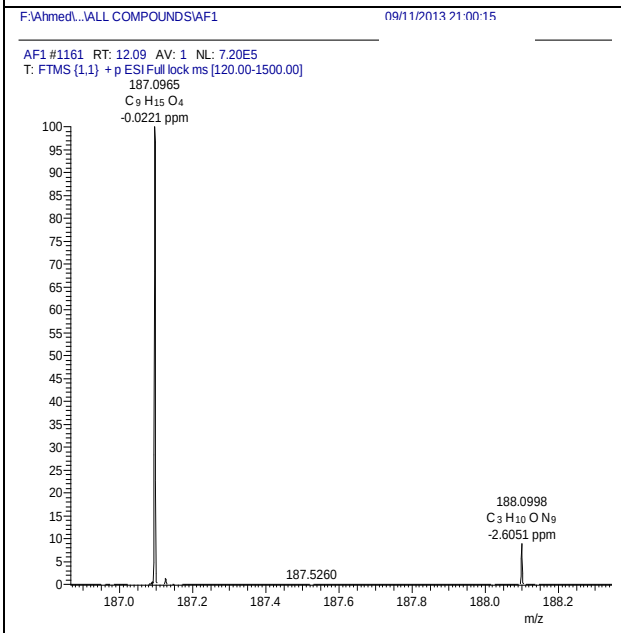

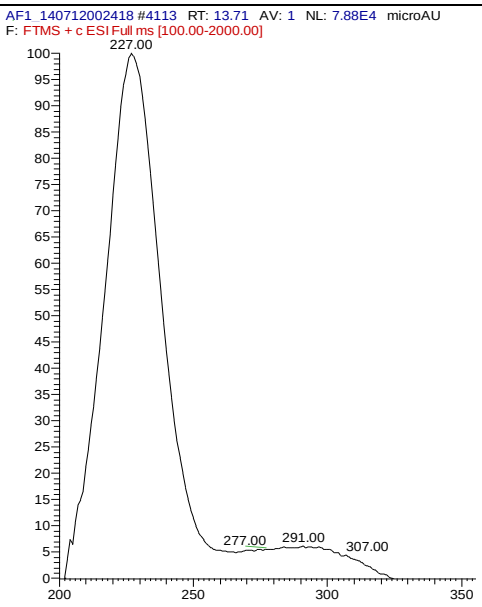

Compound AF1 (16 mg) was isolated as a brown amorphous powder, exhibited the molecular formula of $C_9H_{15}O_4$ established by ESI-HRMS at *m/z* = 187.0965 $[M+H]^+$. The optical rotation $[\alpha]^{20}_D$ = +18 (c 0.05 in MeOH). The **^{1}H NMR**

spectrum (DMSO, 400 MHz) (Fig.110) showed two methyl doublets at δ_H 1.03 (d, *J* = 6.2 Hz) and 1.30 (d, *J* = 6.3 Hz); three alcoholic protons at δ_H 3.72 (m), 4.03 (brd) and 4.16 (m); one olefinic proton at δ_H 6.58 (d, *J* = 2.08*)* and two methylene protons (C*H*$_2$) at δ_H 2.20 (m*)*. The **^{13}C NMR** and **DEPT** spectra (DMSO, 400 MHz) (Fig.111) showed nine carbon signals including two quaternary (carbonyl at δ_C 164.7 and olefinic at δ_C 128.0), four methines (three oxygenated carbons at δ_C 79.2, 67.1, 65.2 and olefinic carbon at δ_C 147.1), two methyls (δ_C 18.4 and 23.8) and one methylene at δ_C 40.4. The **^{1}H-^{1}H COSY** spectrum (Fig.112) showed two spin systems, the first one connected the olefinic proton H-4 (δ_H 6.58), H-5 (δ_H 4.03), H-6 (δ_H 4.16) and methyl protons Me-7 (δ_H 1.30) and the second spin system connected the C*H*$_2$-8 protons (δ_H 2.20), H-9 (δ_H 3.72) and Me-10 (δ_H 1.03). The **HMBC** spectrum (Fig.113) confirmed the presence of the hydroxyl propyl moiety through the correlations of C*H*$_2$-8 (δ_H 2.20) with C-3 (δ_C 128.0), C-4 (δ_C 147.0), C-2 (δ_C 164.7), C-9 (δ_C 65.2) and Me-10 (δ_C 23.8) while the correlations of H-9 (δ_H 3.72) with C-3 (δ_C 128.0), C-8 (δ_C 40.4) and Me-10 confirmed the attachment at position C-3. Furthermore, the dihydropyranone ring was confirmed from the correlations of H-4 (δ_H 6.58) with C-2, C-6 and C-8 while H-5 (δ_H 4.03) correlated with C-2, C-3, C-4, C-6 and Me-7 (δ_C 18.5) and H-6 (δ_H 4.16) correlated with C-2, C-4, C-5 (δ_C 67.2) and Me-7. The configuration of both protons H-5 and H-6 was axial from calculating the *J*-value from ^{1}H NMR data ($CDCl_3$, 400 MHz) which was 8.0 Hz for both protons (Table 17). So compound AF1 was identified as dihydroaspyrone (Fig.114)from comparison of the proton and carbon NMR data with the literature (Fuchser and Zeeck, 1997) (Table 17).

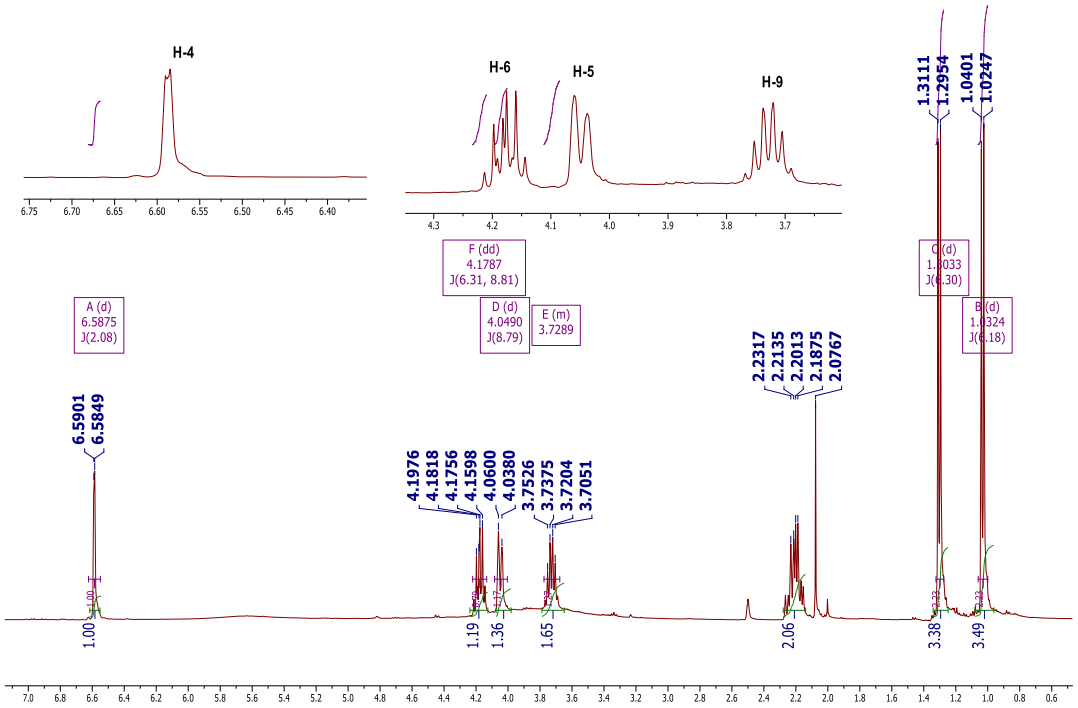

Fig.110 ^{1}H NMR spectrum of compound AF1

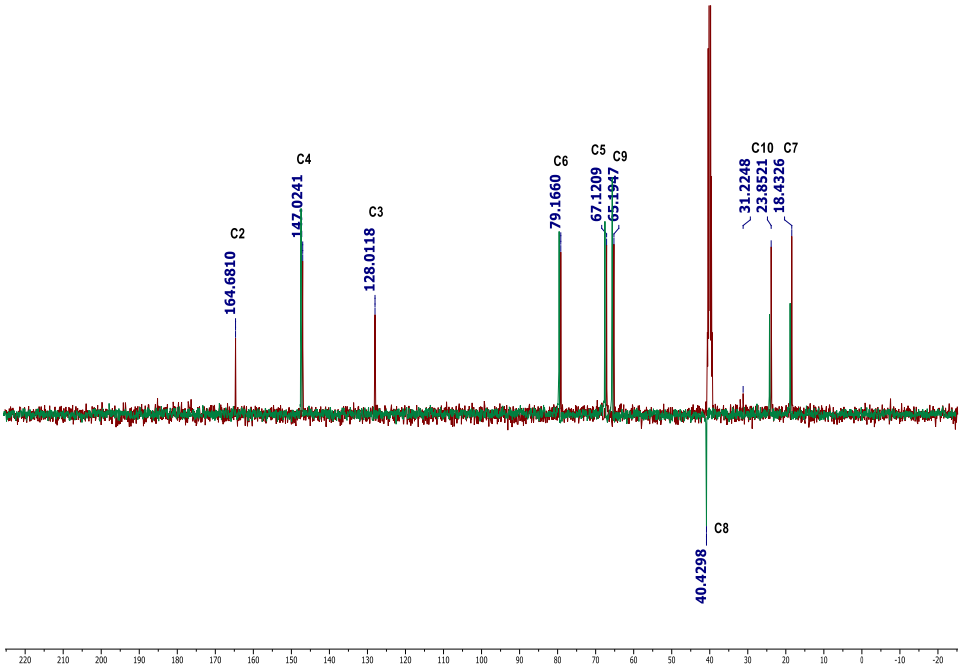

Fig.111 ^{13}C NMR and DEPT spectra of compound AF1

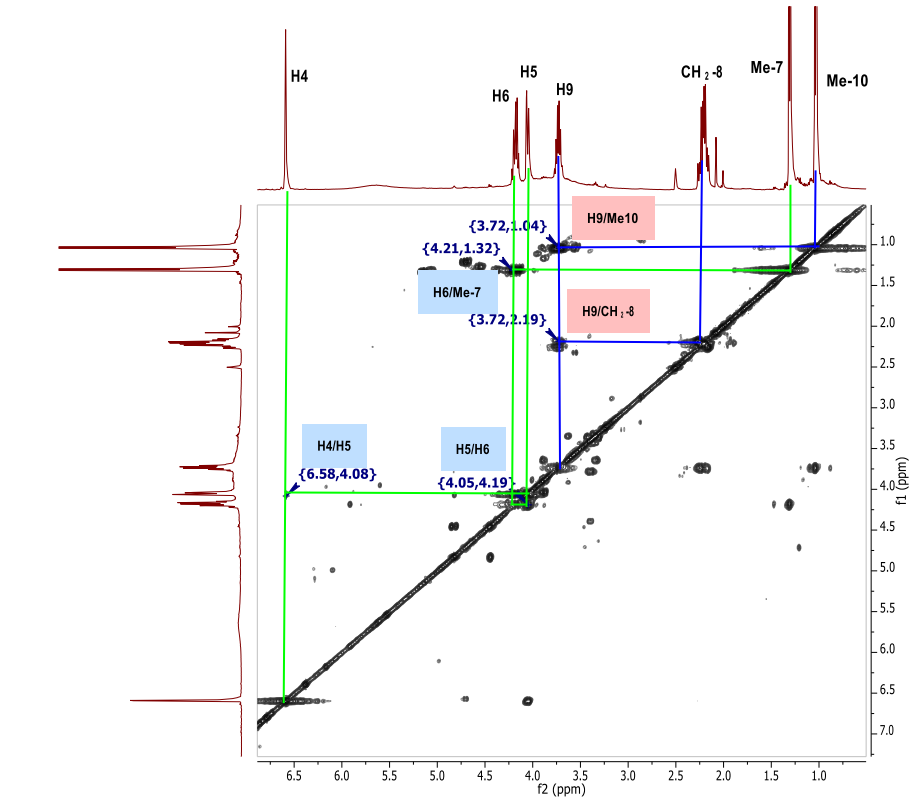

Fig.112 ^{1}H-^{1}H COSY spectrum of compound AF1 showing two different spin systems

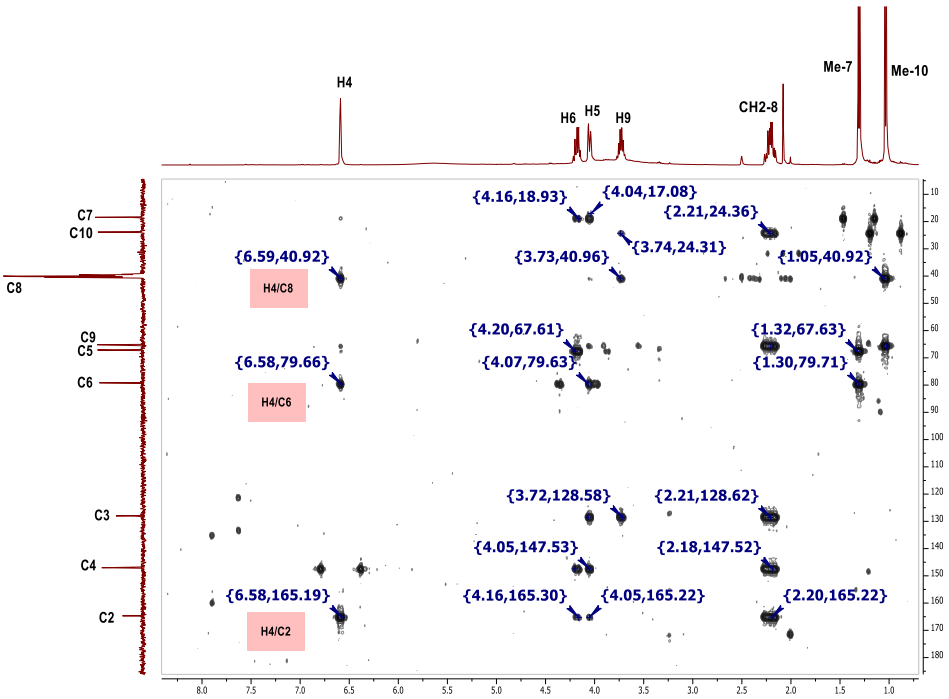

Fig.113 HMBC spectrum of compound AF1

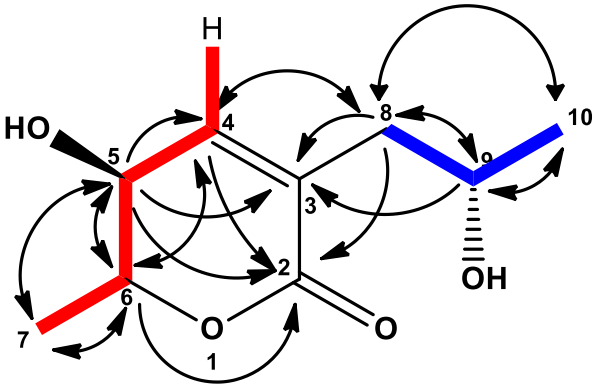

Fig.114 AF1 structure showing HMBC correlations and the two different spin systems of compound AF1

Table 17: ^{13}C NMR and ^{1}H NMR data of compound AF1 and literature

		Fuchser and Zeeck 1997-$CDCl_3$		AF1	
Carbon No.	δ_C	δ_H (m, *J* in Hz)	δ_H (m, *J* in Hz)-$CDCl_3$	δ_H (m, *J* in Hz)-DMSO	δ_C (m)-DMSO
2	165.3				164.7 (C)
3	129.0				128.0 (C)
4	144.6	6.68 (d, 3.0 Hz)	6.63 (d, 2.7 Hz)	6.58 (d, 2.1 Hz)	147.0 (CH)
5	64.5	4.17 (dd, 3.0,8.0 Hz)	4.14 (dd, 2.7, 8.0 Hz)	4.04 (d, 8.8 Hz)	67.1 (CH)
6	79.4	4.38 (dq, 8.0, 6.5 Hz)	4.35 (m)	4.17 (dq, 6.3, 8.8 Hz)	79.2 (CH)
7	18.1	1.52 (d, 6.5 Hz)	1.41 (d, 6.4 Hz)	1.3 (d, 6.3 Hz)	18.4 (CH_3)
8	35.5	2.43 (d, 6.0 Hz, 2H)	2.38 (d, 5.9 Hz, 2H)	2.2 (m)	40.4 (CH_2)
9	66.8	3.99 (tq, 6.0, 6.0 Hz)	3.96 (h, 6.2 Hz)	3.72 (m)	65.2 (CH)
10	23.3	1.29 (d, 6.0 Hz)	1.18 (d, 6.2 Hz)	1.03 (d, 6.2 Hz)	23.8 (CH_3)
		3.1 (brs, 2 OH)	3.59 (brs, 2 OH)		

3.3.5.2. Compound AF2 (new)

(2E,6E,10E)-5,9-dihydroxy-2,4,6,8,10-pentamethyldodeca-2,6,10-trienal	
Synonyms	New
Sample codes	AF2
Sample Amount	12 mg
Physical Description	white amorphous powder
Molecular Formula	$C_{17}H_{28}O_3$
Molecular Weight	280 g/mol
Optical Rotation $[\alpha]_D^{20}$	- 10 (*c* 0.05 in MeOH)
Retention time (LC-MS)	16.59 min

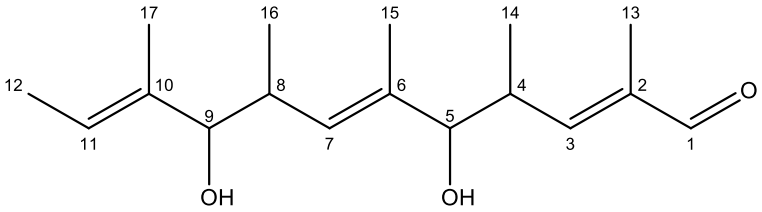

LC-HRFTMS spectrum $[M+H]^+$ 281.2110

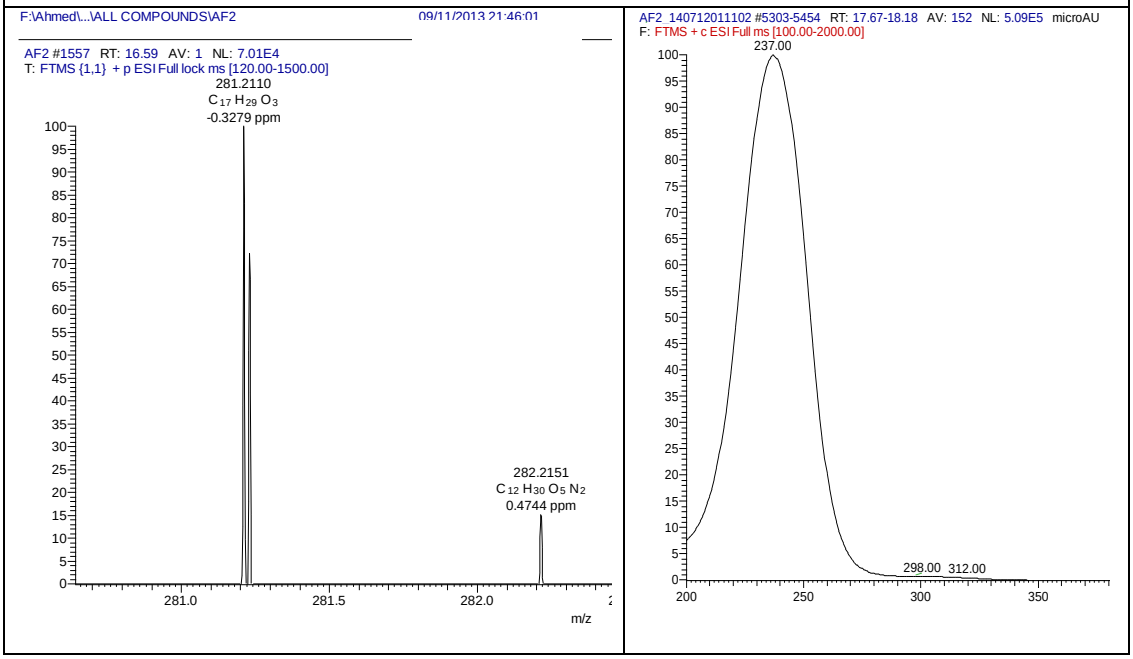

Compound AF2 (12 mg) was obtained as white powder, exhibited a molecular formula of $C_{17}H_{29}O_3$ established at *m/z* = 281.2110 $[M+H]^+$. The optical rotation $[\alpha]^{20}_D$ = - 10 (*c* 0.05 in MeOH). The **^{1}H NMR** spectrum (DMSO, 400 MHz) (Fig.115) showed resonances at δ_H 9.37 which indicated the presences of an

aldehyde proton for H-1; three protons in the olefinic region at δ_H 6.56 (d, *J* = 9.5 Hz), 5.33 (q, *J* = 6.6 Hz) and 5.25 (d, *J* = 5.2 Hz) for H-3, H-11 and H-7, respectively. Furthermore, two protons in the oxygenated region at δ_H 3.74 (d, *J* = 7.3 Hz) and 3.58 (d, *J* = 7.2 Hz) equivalent for H-5 and H-9, respectively; two protons at δ_H 2.77 (q, *J* = 7.4 Hz) and 2.46 (*m*) for H-4 and H-8, respectively. In addition, three methyl doublets equivalent for Me-14 at δ_H = 0.85 (3H, d, *J* = 6.6 Hz), Me-16 at δ_H 0.73 (3H, d, *J* = 6.8 Hz) and Me-12 at δ_H 1.53 (3H, brs) and three methyl sharp singlets for Me-13 at δ_H 1.65 (3H, s), Me-15 at δ_H 1.55 (3H, s) and Me-17 at δ_H 1.51 (3H, s). Moreover, the presence of two broad exchangeable protons at δ_H 4.78 and 4.26 confirmed the presence of OH-5 and OH-9, respectively. The **^{13}C NMR** spectrum (400 MHz-DMSO, Fig.116) showed 17 carbon signals including six methyls at δ_C 11.8, 9.7, 17.4, 12.2, 18.6 and 13.4. These were equivalent for Me-12, Me-13, Me-14, Me-15, Me-16 and Me-17, respectively. Moreover, three olefinic quaternaries at δ_C 138.4, 136.2 and 138.1 for C-2, C-6, and C-10, respectively, three olefinic methines at δ_C 160.0, 131.4 and 120.0 for C-3, C-7, and C-11, respectively. In addition, two methines at δ_C 37.9 and 36.5 for C-4 and C-8, respectively, two hydroxylated methine carbons at δ_C 81.0 and 81.5 for C-5 and C-9, respectively and the carbonyl of the aldehyde group for C-1 at δ_C 196.0. The **^{1}H-^{1}H COSY** spectrum (Fig.117) showed three spin systems, the first connected H-3 with H-4 and Me-14; H-4 further connected to H-5 and OH-5; along with the allylic coupling between H-3 and Me-13. The second spin system connected H-7 with H-8 and Me-16; H-8 with H-9 and OH-9; H-7 allylic with Me-15. The third one correlated H-11 with Me-12. The structure was further confirmed from the **HMBC** spectrum (Fig.118) through the correlations of the allylic protons H-3 at δ_H 6.57 with carbons (δ_C) C-13 (9.7), C-14 (17.4), C-4 (37.9), C5 (81.0) and C1 (196.0). Furthermore, H-7 at δ_H 5.25 with carbons (δ_C) C-15 (12.2), C-16 (18.6), C-8 (36.5) and C-5 (81.0); H-11 (δ_H 5.33) with carbons at δ_C 13.4 and 81.5 equivalent for C-17 and C-9 respectively. Moreover, the position of OH-5 and OH-9 was confirmed from the correlations of H-5 (δ_H 3.74) with C-15, C-14, C-4, C-7 (δ_C 131.4) and C-3 (δ_C 160.0); H-9 (δ_H 3.58) with C-12 (δ_C 11.8), C-16, C-8, C-11 (δ_C 120.0), C-7 and C-10 (δ_C 138.1) (Table.2). Searching the databases for compound AF2 confirmed it was not

described before. The closest structure in the literature described by (Kohno et al., 1999) (Fig.120) was a bigger polyketide molecule with an extra substitution at C-1 forming an ester linkage which was found upfield at δ_C 167.2 when compared to the aldehydic C-1 (δ_C 196.0) of compound AF2. Therefore compound AF2 (Fig.119) is a new compound isolated for the first time in nature. The structure was further confirmed by comparison of compound AF2 to the closely related structure in the literature (Fig.120) (Kohno et al., 1999) (Table 18).

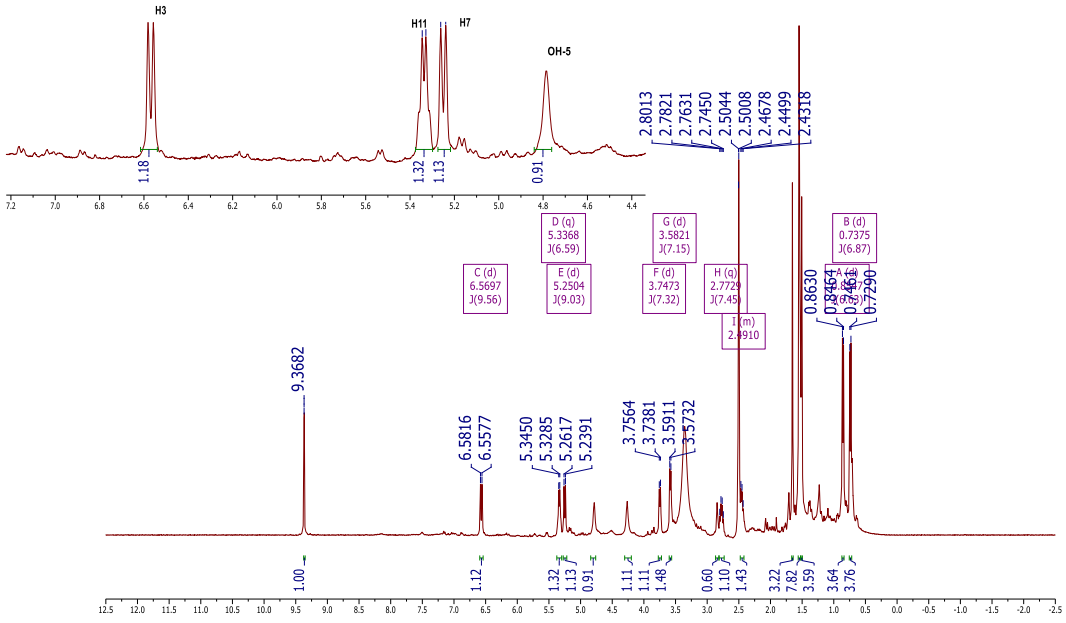

Fig.115 ^{1}H NMR spectrum of compound AF2

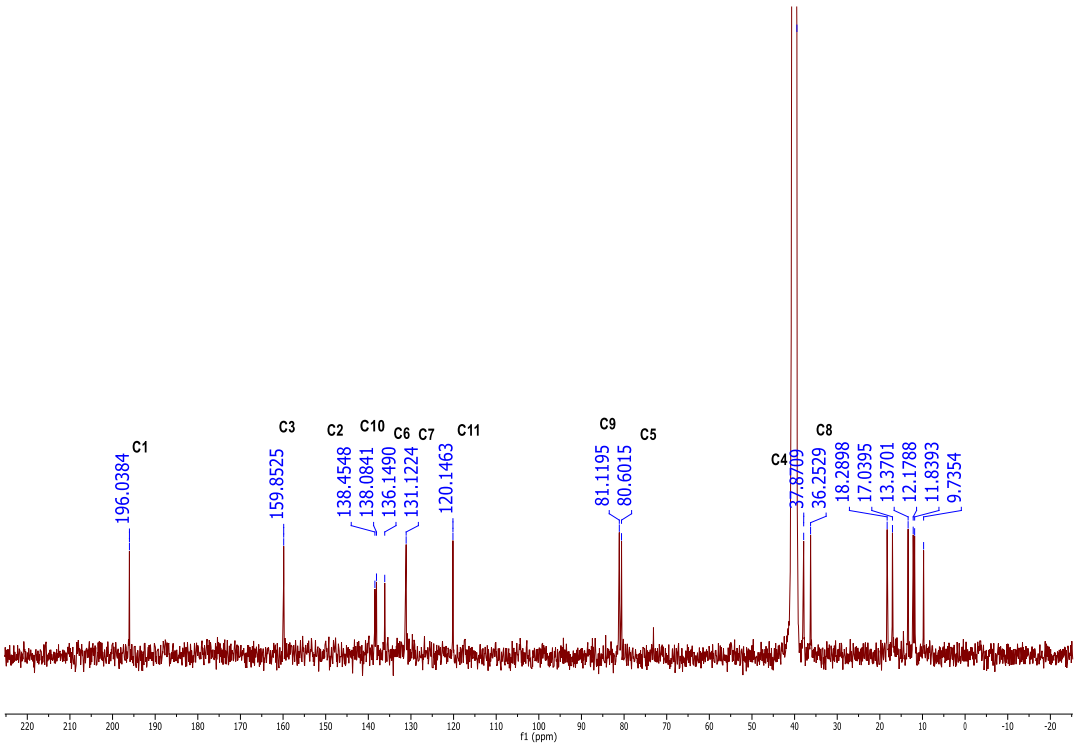

Fig.116 ^{13}C NMR spectrum of compound AF2

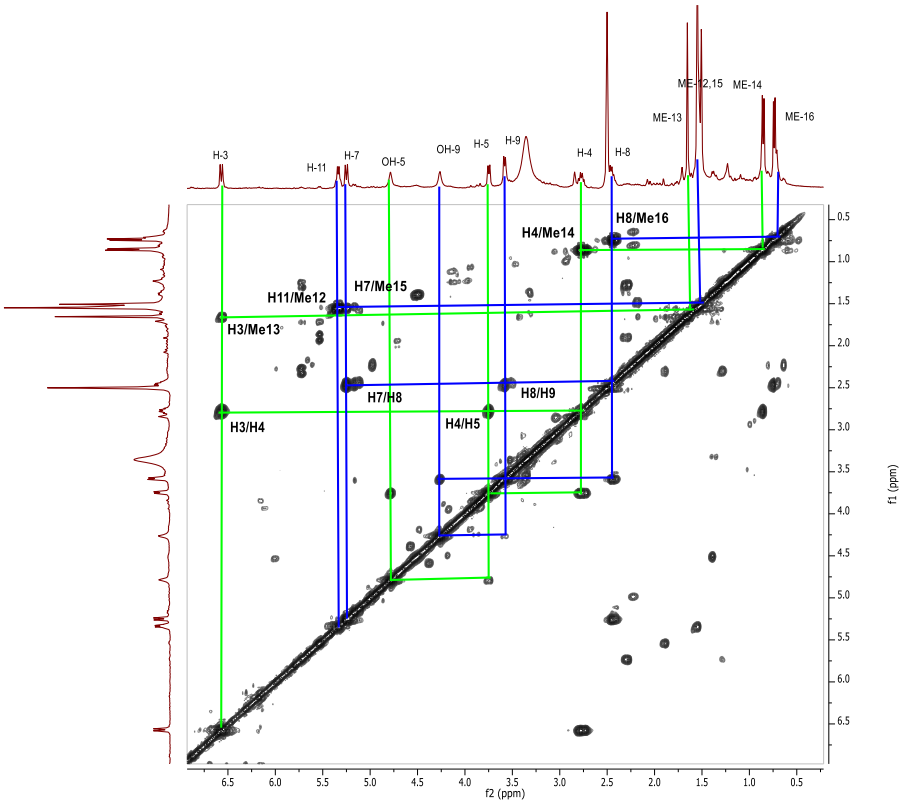

Fig.117 ^{1}H-^{1}H COSY spectrum of compound AF2 showing two different spin systems

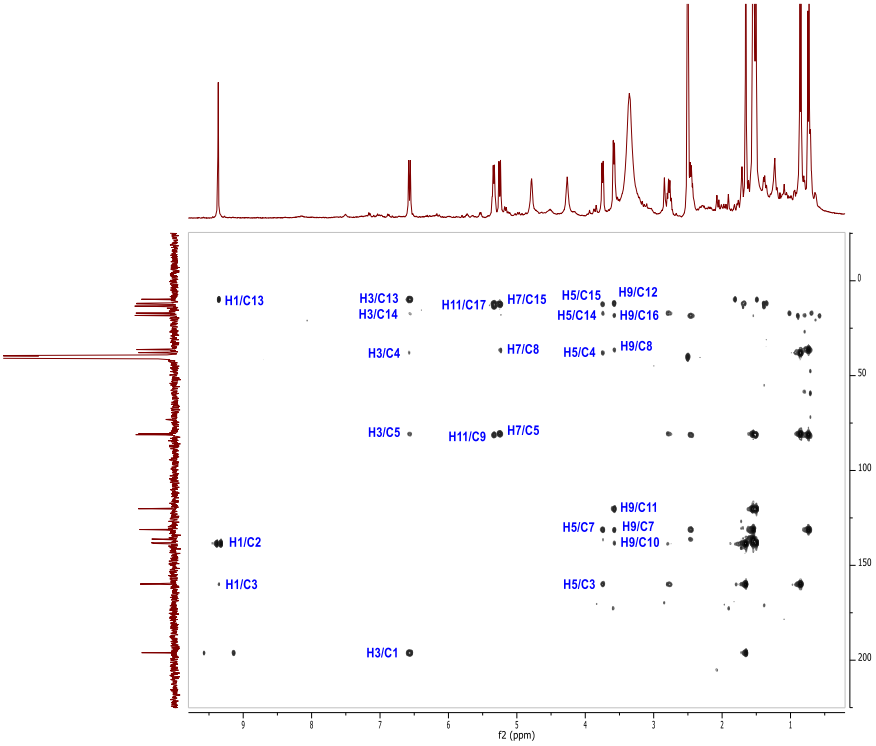

Fig.118 HMBC spectrum of AF2

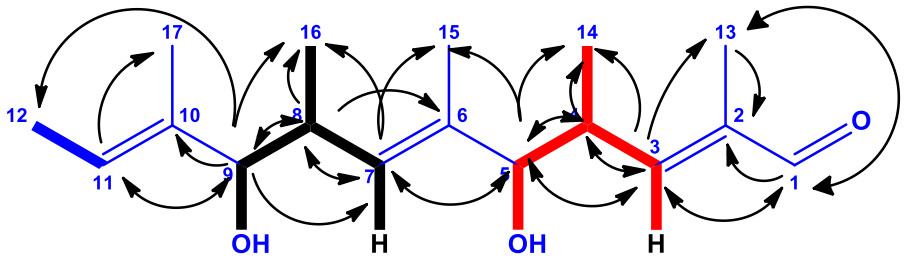

Fig.119 The structure showing the HMBC correlations and the three spin systems of compound AF2

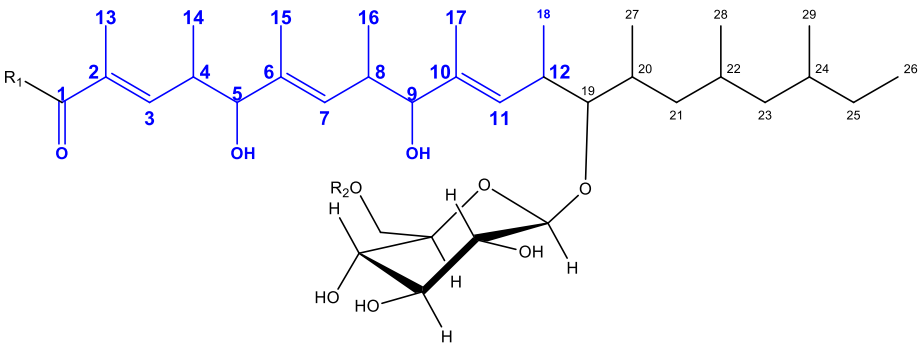

Fig.120 The comparable structure found in the literature

Table 18: ^{1}H NMR, ^{13}C NMR data and HMBC correlations of AF2 and closely related literature

Atom No.	AF2-DMSO			Kohno 1999-DMSO	
	δ_H (m, *J* in Hz)	δ_C (m)	HMBC correlations	δ_H (m, *J* in Hz)	δ_C (m)
1	9.37 (s)	196.0 (CH)	C-13, C-2, C-3		167.2 (C)
2		138.4 (C)			126.5 (C)
3	6.57 (d, 9.5 Hz)	160.0 (CH)	C-13, C-14, C-4, C-5, C-1	6.70 (dd, 10.1 Hz)	146.8 (CH)
4	2.77 (q, 7.4 Hz)	37.9 (CH)	C-14, C-5, C-3, C-2	2.56 (m)	36.9 (CH)
5	3.74 (d, 7.3 Hz)	81.0 (CH)	C-15, C-14, C-4, C-7, C-3	3.67 (m)	80.9 (CH)
6		136.1 (C)			136.0 (C)
7	5.25 (d, 9.0 Hz)	131.4 (CH)	C-15, C-16, C-8, C-5	5.19 (brd, 9.0 Hz)	131.6 (CH)
8	2.46 (m)	36.5 (CH)	C-16, C-9, C-7, C-6	2.45 (m)	36.1 (CH)
9	3.58 (d, 7.1 Hz)	81.5 (CH)	C-12, C-16, C-8, C-11, C-7, C-10	3.55 (dd, 8.5, 3.4 Hz)	81.2 (CH)
10		138.1 (C)			134.5 (C)
11	5.33 (q, 6.6 Hz)	120.0 (CH)	C-17, C-9	5.39 (brd, 9.0 Hz)	130.1 (CH)
12	1.53 (brs)	11.8 (CH_3)			
13	1.65 (s)	9.7 (CH_3)	C-2, C-3, C-1	1.80 (d, 1.0 Hz)	12.6 (CH3)
14	0.85 (d, 6.6 Hz)	17.4 (CH_3)	C-4, C-5, C-3	0.76 (d, 6.8 Hz)	16.4 (CH3)
15	1.55 (s)	12.2 (CH_3)	C-5, C-7	1.56 (brs)	11.0 (CH3)
16	0.73 (d, 6.8 Hz)	18.6 (CH_3)	C-8, C-9, C-7	0.70 (d, 6.8 Hz)	17.4 (CH3)
17	1.51 (s)	13.4 (CH_3)	C-10, C-11, C-9	1.55 (brs)	11.3 (CH3)

3.3.5.3. Compound AF3 (dihydropenicillic acid)

5-hydroxy-5-isopropyl-4-methoxyfuran-2(5H)-one	
Synonyms	Dihydropenicillic acid
Sample codes	AF3
Sample Amount	11 mg
Physical Description	brown amorphous powder
Molecular Formula	$C_8H_{12}O_4$
Molecular Weight	172 g/mol
Optical Rotation $[\alpha]_D^{20}$	-14 (c, 0.05 in MeOH)
Retention time (LC-MS)	6.96 min

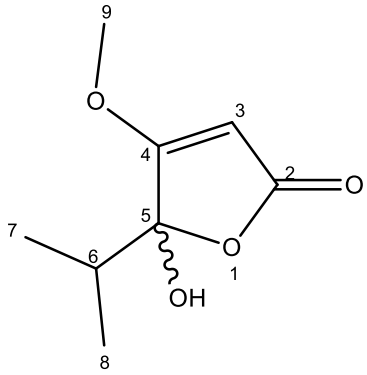

LC-HRFTMS spectrum $[M+H]^+$ 173.0809

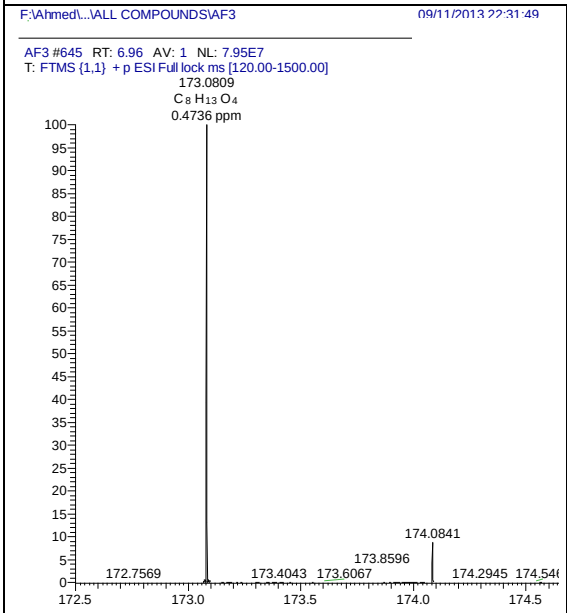

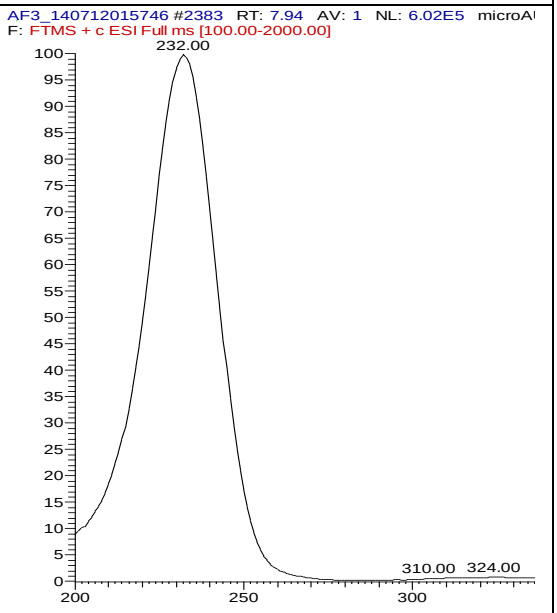

Compound AF3 (11 mg) was obtained as a brown amorphous powder, exhibited a

molecular formula of $C_8H_{13}O_4$ established by ESI-HRMS at *m/z* = 173.0809 [M+H]+. The optical rotation $[\alpha]^{20}_D$ = -14 (*c* 0.05 in MeOH). The **^{1}H NMR** spectrum (DMSO, 400MHz) (Fig.121) showed two methyl doublets at δ_H 0.94 (3H, d, *J* = 6.8 Hz) and 0.78 (3H, d, *J* = 6.9 Hz) equivalent for Me-7 and Me-8, respectively. Moreover, one singlet peak at δ_H 3.85 equivalent for methoxy group Me-9, one singlet peak equivalent for olefinic methine H-3 at δ_H 5.33, one methine proton H-6 at δ_H 1.99 (dq, *J* = 6.8, 13.5 Hz) and an exchangeable proton at δ_H 7.42 for OH-5. The **^{13}C NMR** spectrum (DMSO, 400MHz) (Fig.122) showed eight carbon signals including one carbonyl at δ_C 170.0 (C-2), two quaternary carbons at δ_C 105.4 (C-5) and δ_C 180.4 (C-4), two olefinic methine carbons for C-3 at δ_C 90.0 and C-6 at δ_C 33.6 and three methyls at δ_C 16.2, 16.9 and 60.2 for Me-7, Me-8, and Me-9, respectively. The **^{1}H-^{1}H COSY** spectrum (Fig.123) confirmed the presence of isopropyl unit through the spin system connecting H-6, Me-7 and Me-8. The **HMBC** spectrum (Fig.124) confirmed the furanone ring through the correlation of H-3 with C-2 and C-5 while the position of the methoxy Me-9 was confirmed through the correlation of Me-9 with C-4. Moreover, the position of OH-5 was confirmed from the correlation of OH-5 with C-5, C-4 and C-6 while H-6 exhibited correlations with C-5, C-4, Me-7, Me-8 and a long-range coupling (4J) with C-2, which confirmed the position of the isopropyl unit on C-5 of the furanone ring. Furthermore, Me-7 and Me-8 in return correlated with C-6, C-5 and with each other that confirmed the isopropyl unit. So from the above and comparison to the literature (Sassa et al., 1971) (Table 19) compound AF3 (Fig.125) was identified as 5,6-dihydropenicillic acid.

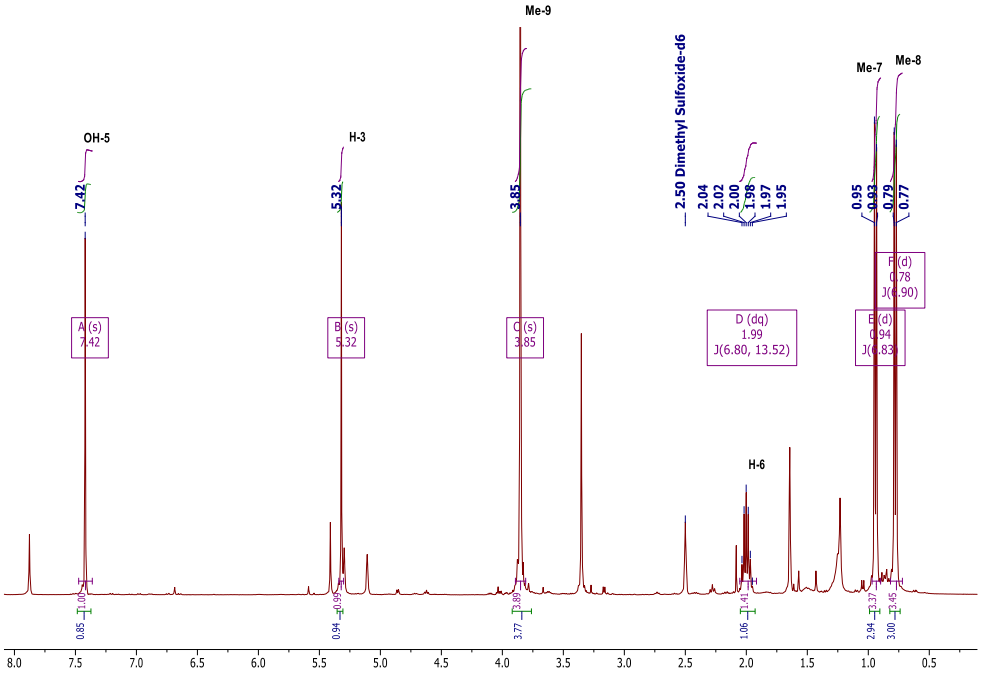

Fig.121 ^{1}H NMR spectrum of compound AF3

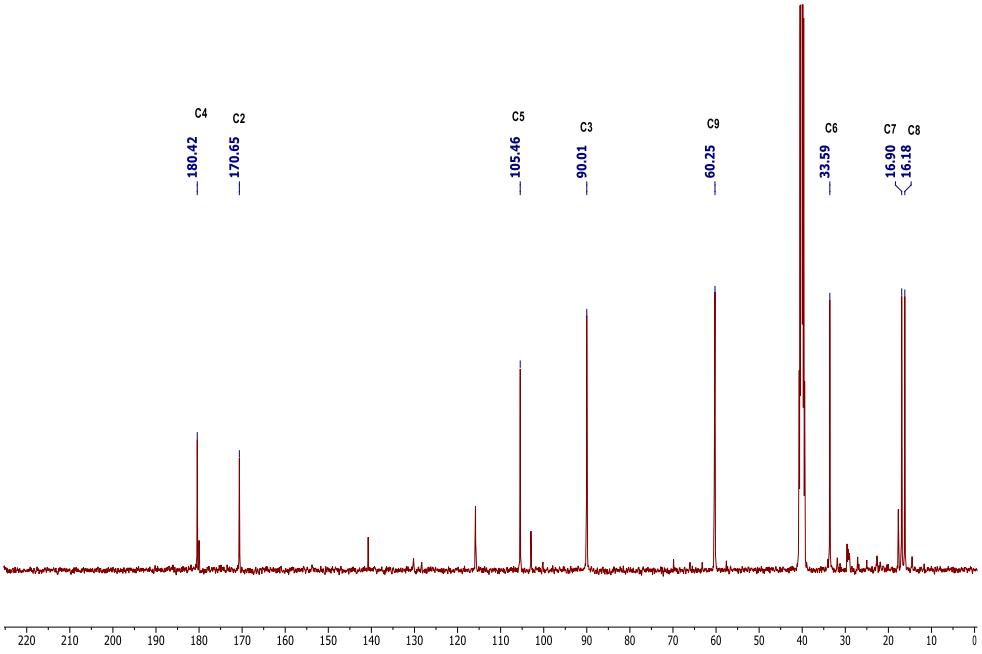

Fig.122 ^{13}C NMR spectrum of compound AF3

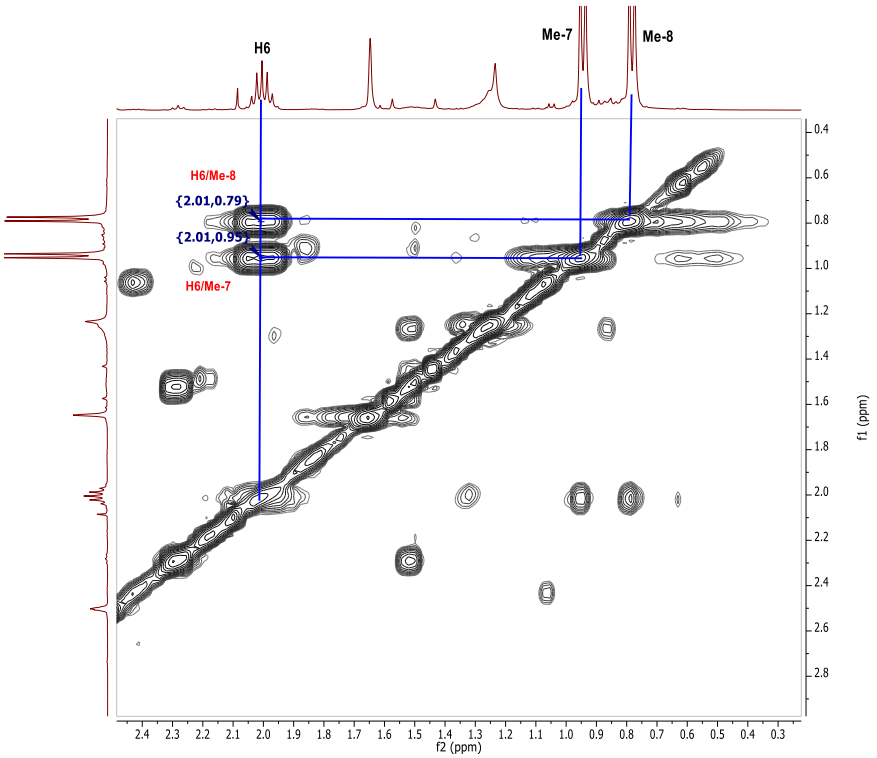

Fig.123 Expansion of ^{1}H-^{1}H COSY spectrum of compound AF3 showing spin system connecting the protons of the isopropyl unit

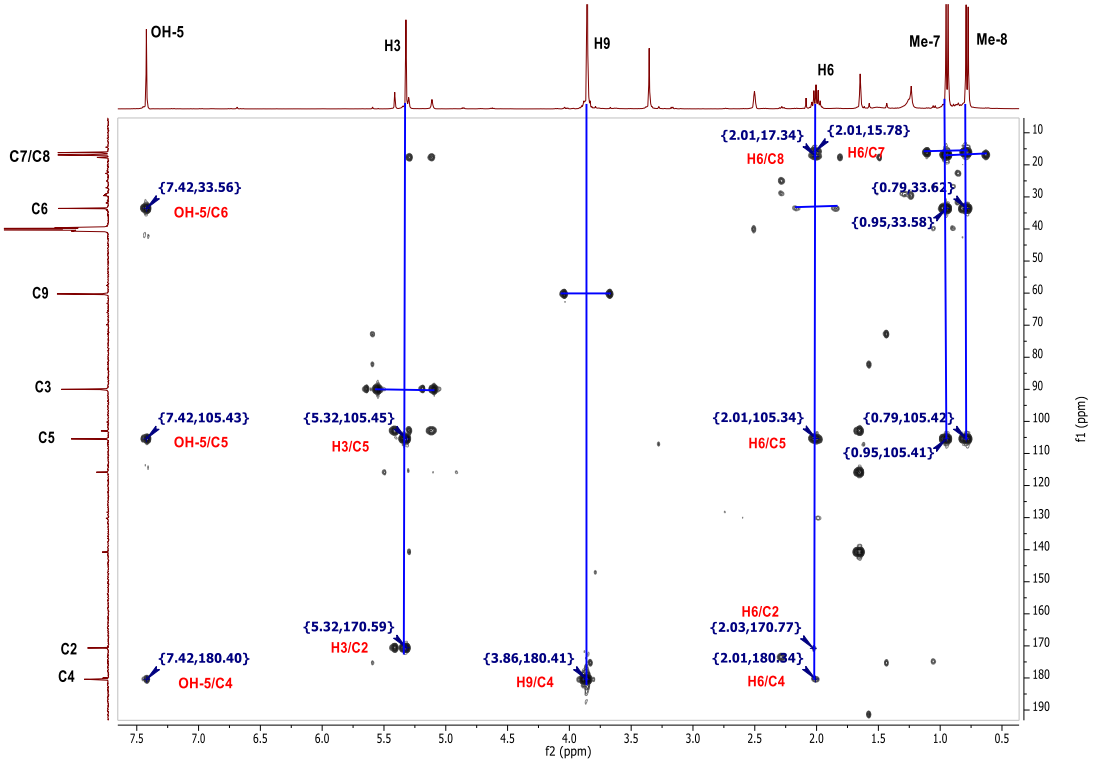

Fig.124 HMBC spectrum of compound AF3

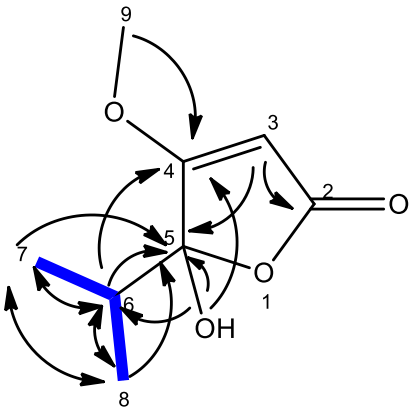

Fig.125 The structure showing HMBC correlations and spin systems of compound AF3

Table 19: ^{1}H and ^{13}C NMR data of compound AF3 and literature

Atom No.	AF3-DMSO		Sassa 1971
	δ_H (m, *J* in Hz)	δ_C (m)	δ_H (m, *J* in Hz)
1			
2		170.0 (C)	
3	5.32 (s)	90.0 (CH)	5.02
4		180.4 (C)	
5		105.4 (C)	
6	1.99 (dq, 6.8, 13.5 Hz)	33.6 (CH)	2.18
7	0.94 (3H, d, 6.8 Hz)	16.2 (CH_3)	1.06
8	0.78 (3H, d, 6.9 Hz)	16.9 (CH_3)	0.88
9	3.85 (3H, s)	60.2 (CH_3)	3.9
OH-5	7.42		

3.3.5.4. Compound AF4 (kojic acid)

5-hydroxy-2-(hydroxymethyl)-4H-pyran-4-one	
Synonyms	Kojic acid
Sample codes	AF4
Sample Amount	4.8 g
Physical Description	brown crystals
Molecular Formula	$C_6H_6O_4$
Molecular Weight	142 g/mol
Retention time (LC-MS)	1.84 min

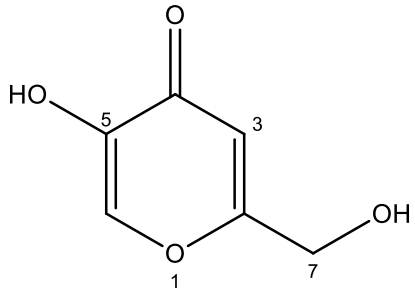

LC-HRFTMS spectrum $[M+H]^+$ 143.0339

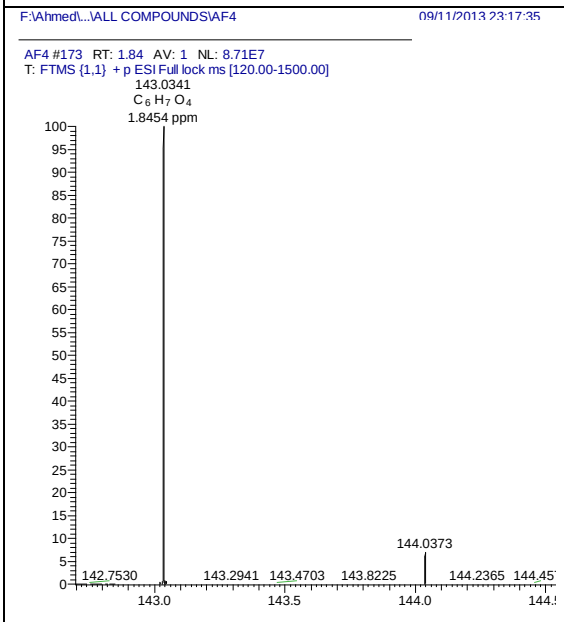

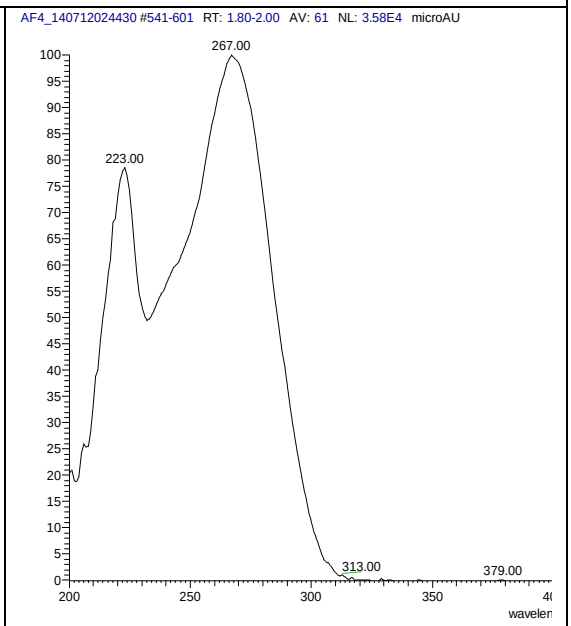

Compounds AF4 (4.8 g) was obtained as a brown crystals, exhibited a molecular formula $C_6H_7O_4$ established by ESI-HRMS at *m/z* = 143.0339 $[M+H]^+$. The **^{1}H NMR** spectrum (DMSO, 400 MHz) (Fig.126) of compound AF4 showed five singlet proton signals at δ_H 9.08, 8.03, 6.33, 5.68 and 4.29 equivalent for OH-5,

H-6, H-3, OH-7 and C*H*$_2$-7, respectively. The **^{13}C NMR** spectrum (DMSO, 400 MHz) (Fig.128) of compound AF4 showed six carbon signals including one carbonyl at δ_C 174.4 equivalent for C-4, two quaternaries at δ_C 168.6 and 146.2 equivalent for C-2 and C-5 respectively, two olefinic methines at δ_C 110.3 and 139.8 equivalent for C-3 and C-6 respectively and one methylene at δ_C 60 (C-7). The **^{1}H-^{1}H COSY** spectrum of compound AF4 (Fig.130) showed a correlation between CH_2-7 and both OH-7 and H-3. The structure of compound AF4 was confirmed through the **HMBC** spectrum (Fig.131) which showed the correlations of H-6 with C-2, C-4 and C-5; H-3 with C-2, C-4 and C-7; C*H*$_2$-7 with C-3 and C-2; OH-7 with C-7 and OH-5 with C-5. So from the above and in accordance to the ^{1}H NMR and ^{13}C NMR data reported in literature (Li et al. 2003), compound AF4 was identified as kojic acid (Fig.133).

3.3.5.5. Compound AF5 (7-O-acetyl kojic acid)

5-hydroxy-4-oxo-4H-pyran-2-yl) methyl acetate	
Synonyms	7-O-acetyl kojic acid
Sample codes	AF5
Sample Amount	189 mg
Physical Description	brown crystals
Molecular Formula	$C_8H_8O_5$
Molecular Weight	184 g/mol
Retention time (LC-MS)	6.92 min

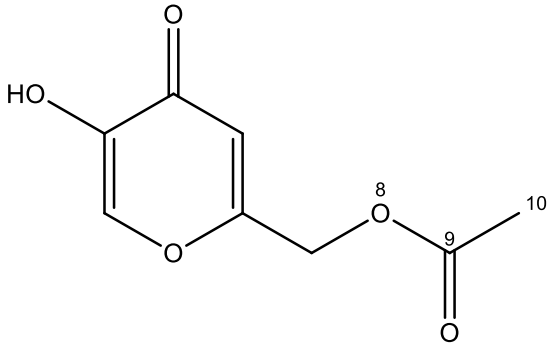

LC-HRFTMS spectrum $[M+H]^+$ 185.0444

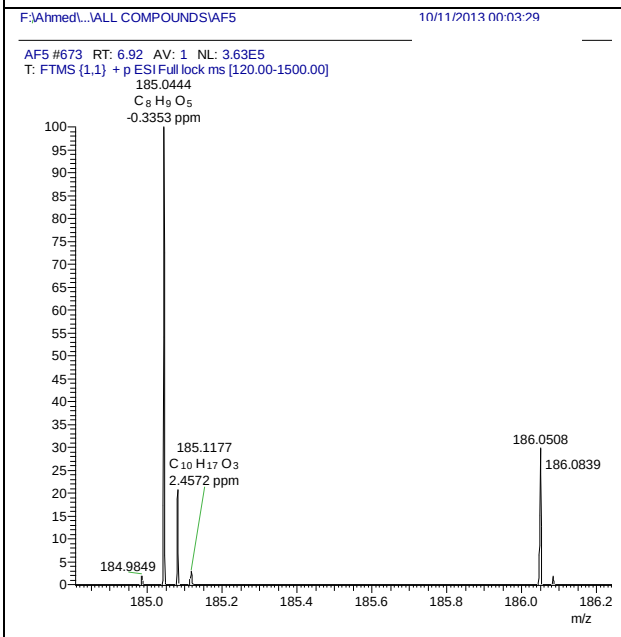

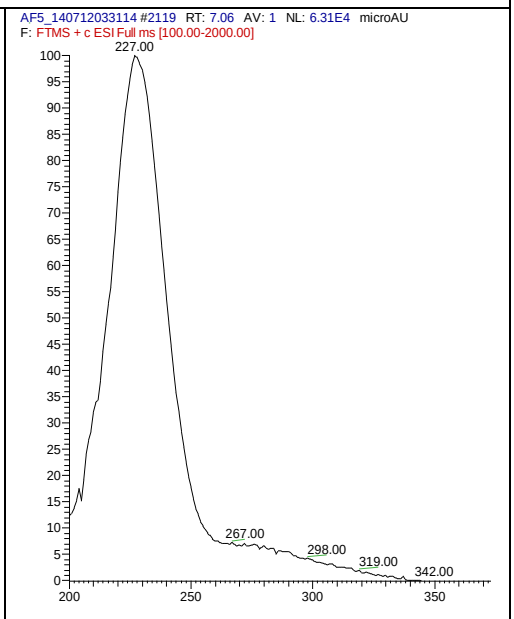

Compounds AF5 (189 mg) was obtained as a brown crystals, exhibited a molecular formula $C_8H_9O_5$ established by ESI-HRMS at *m/z* = 185.0444 [M+H]+.

The **^{1}H NMR** spectrum of compound AF5 (Fig.127) resembled AF4 suggesting the same 5-hydroxy-4-oxo-4H-pyran-2-yl skeleton. However difference observed in the chemical shift of C*H*$_2$-7 which was found at more downfield shift δ_H 4.93 due to the withdrawing effect of the carbonyl C-9. Moreover an extra peak was detected at δ_H 2.11 (s) equivalent for the methyl group (C-10). The **^{13}C NMR** spectrum of compound AF5 (Fig.129) resembled that of AF4 (Table.4) but with extra two carbon signals equivalent for the carbonyl C-9 (δ_C 170.3) and the methyl C-10 (δ_C 20.98). The presence of acetyl group in compound AF5 was confirmed in the **HMBC** spectrum (Fig.132) through the correlations of C*H*$_2$-7 (4.93) and Me-10 (2.11) with the carbonyl group C-9 (δ_C 170). So from the above and comparison of the ^{1}H NMR and ^{13}C NMR data with literature (Li et al., 2003, Kremnicky et al., 2004) (Table 20) compound AF5 was identified as 7-O-acetyl congener of kojic acid (Fig.133).

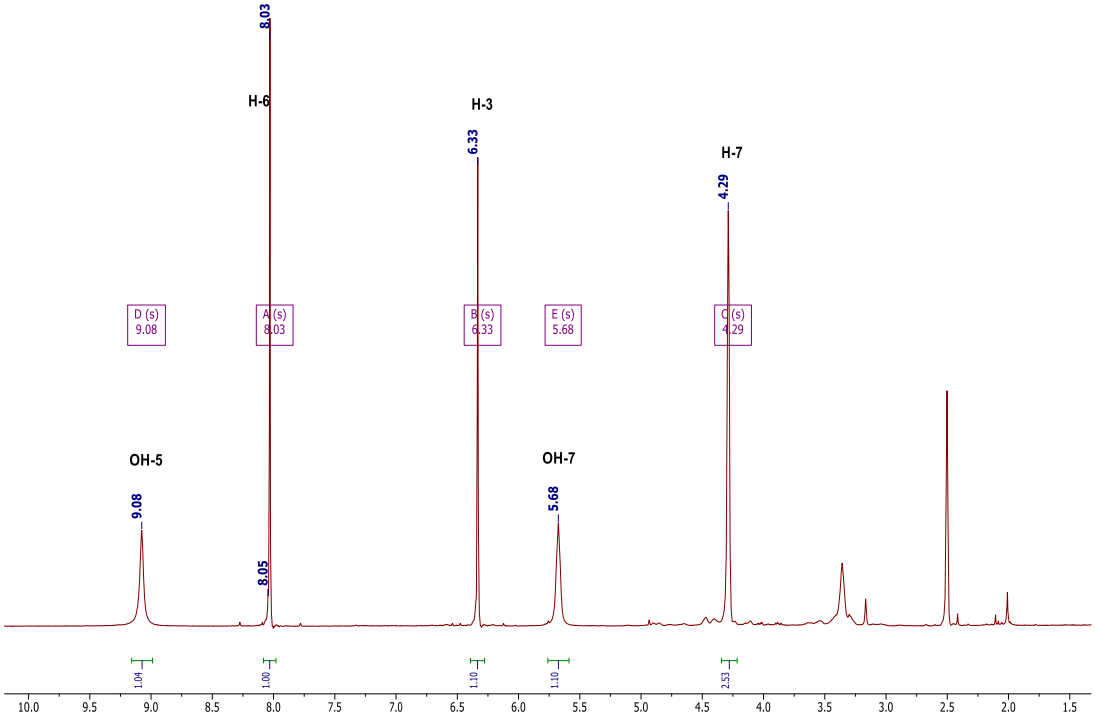

Fig.126 ^{1}H NMR spectrum of compound AF4

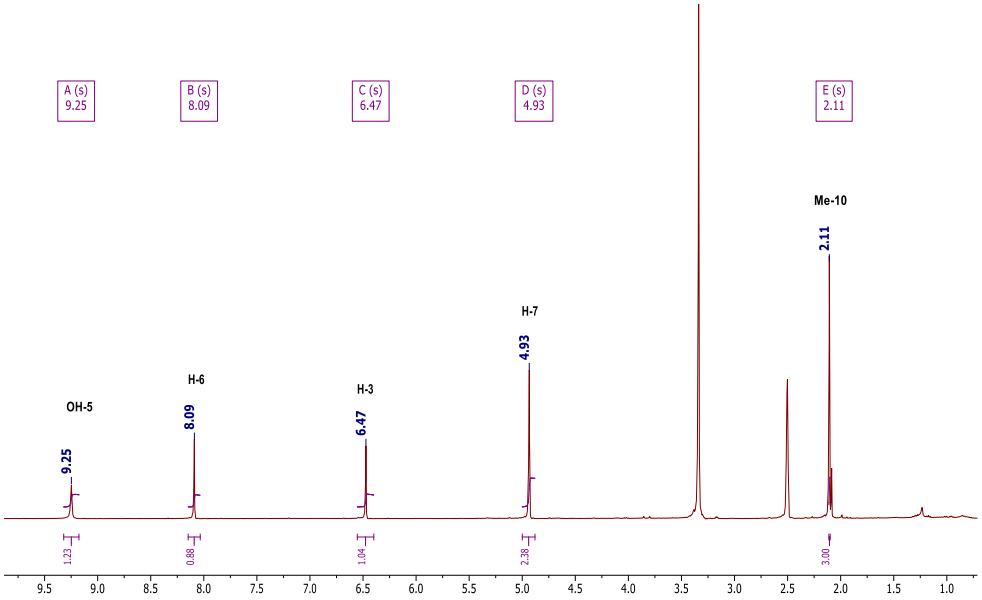

Fig.127 ^{1}H NMR spectrum of compound AF5

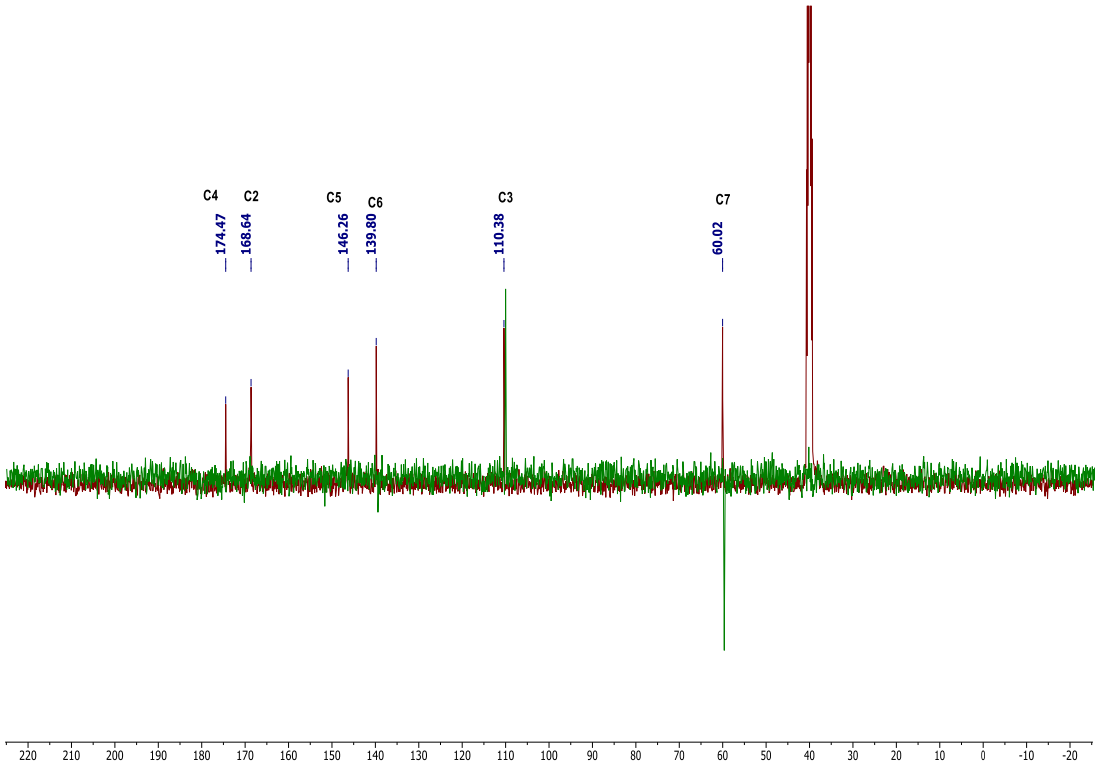

Fig.128 ^{13}C NMR and DEPT spectra of compound AF4

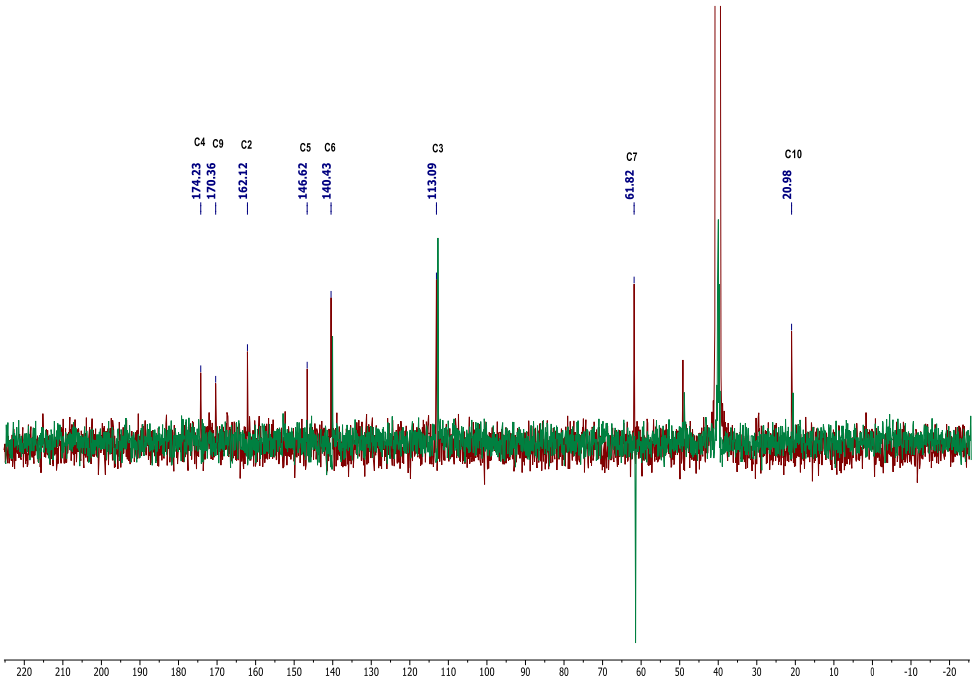

Fig.129 ^{13}C NMR and DEPT spectra of compound AF5

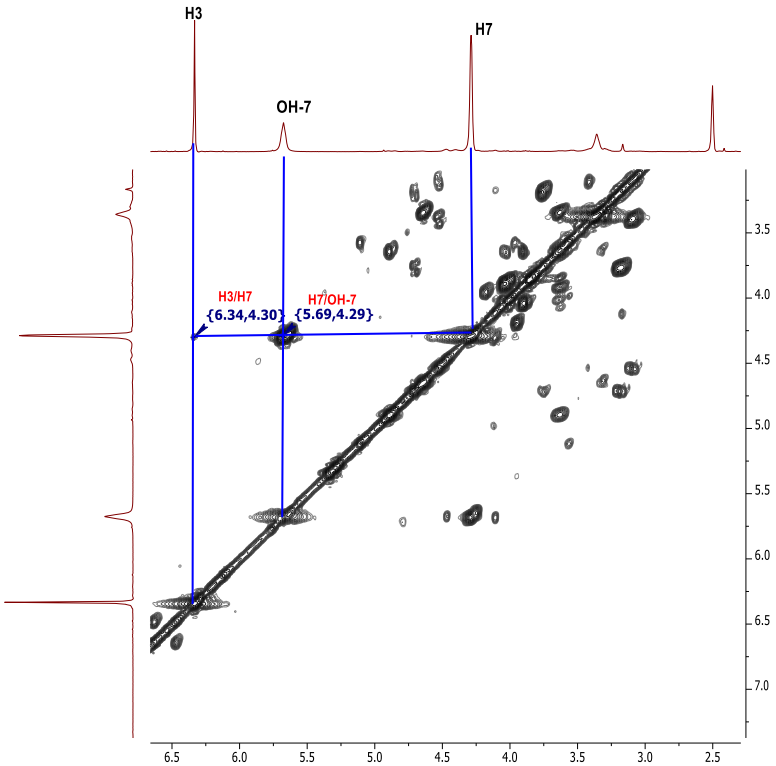

Fig.130 ^{1}H-^{1}H COSY spectrum of compound AF4 showing the spin system

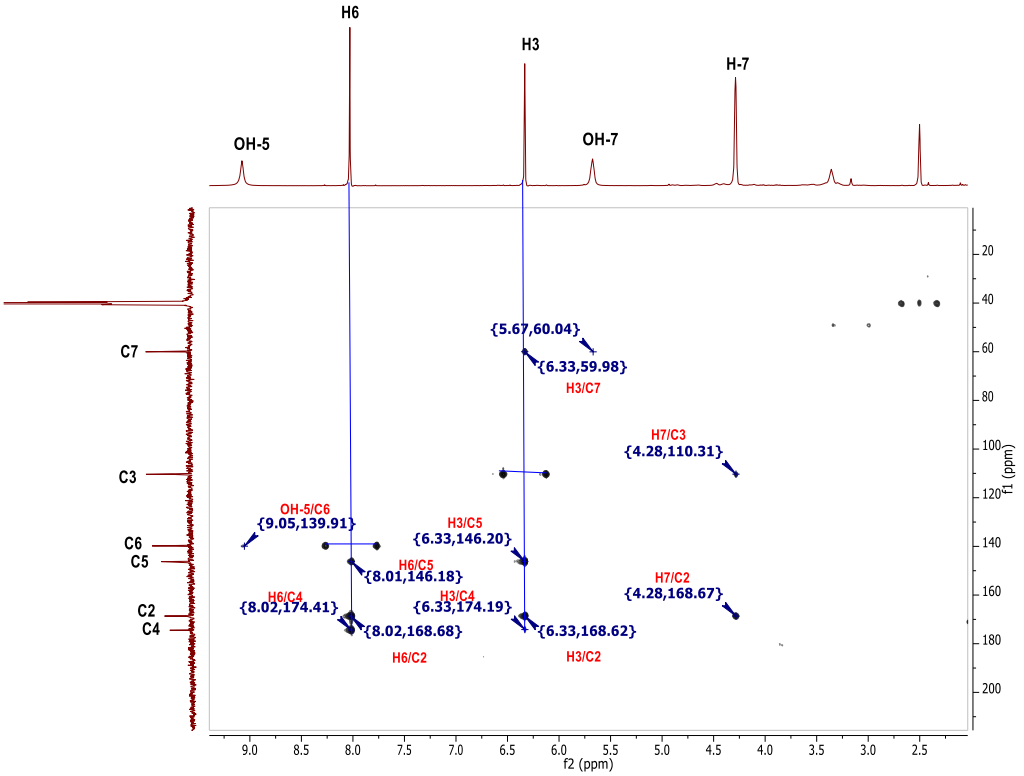

Fig.131 HMBC spectrum of compound AF4

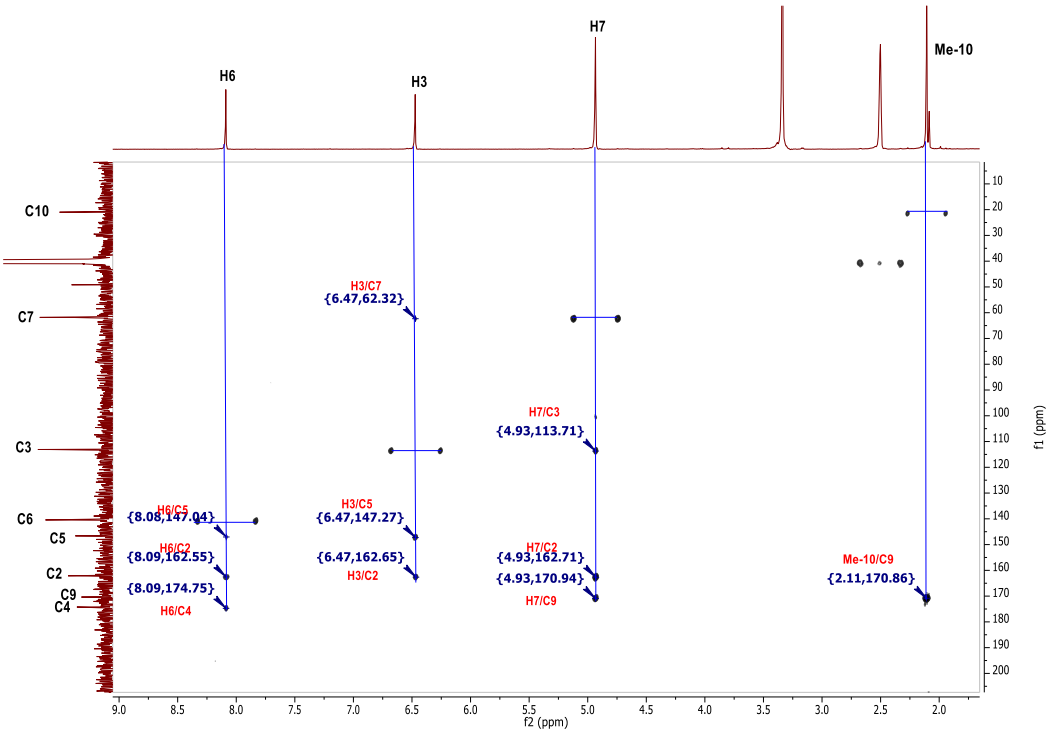

Fig.132 HMBC spectrum of compound AF5

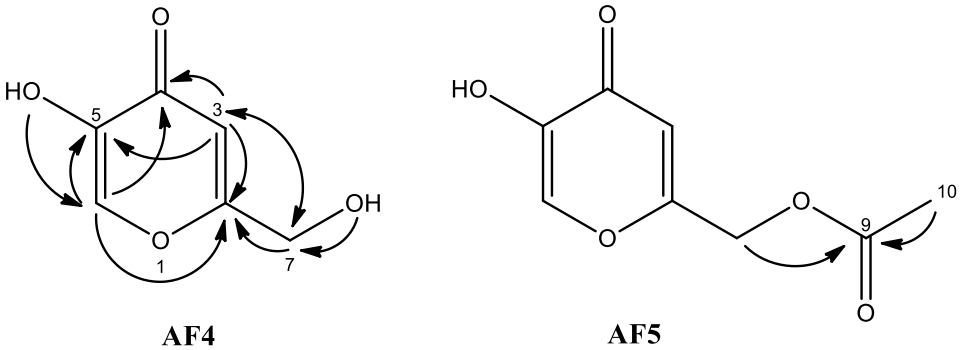

AF4 **AF5**

Fig.133 Structure and HMBC correlations of compounds AF4 and AF5

Table 20: ^{1}H NMR and ^{13}C NMR data of compounds AF4, AF5 and literature

Atom No.	AF4-DMSO		Li 2003-DMSO		AF5-DMSO	Kremnicky 2004-$CDCl_3$	
	δ_H (m, *J* in Hz)	δ_C	δ_H (m, *J* in Hz)	δ_C	δ_H (m, *J* in Hz)	δ_C (m)	δ_H (m, *J* in Hz)
2		168.6		168.0		162.1 (C)	
3	6.33(s)	110.3	6.33 (s)	109.8	6.47 (s)	113.1 (CH)	6.49 (s)
4		174.4		173.9		174.2 (C)	
5		146.2		145.7		146.6 (C)	
OH-5	9.08 (brs)		9.06 (s)		9.25 (brs)		
6	8.03 (s)	139.8	8.02 (s)	139.2	8.09 (s)	140.4 (CH)	7.84 (s)
7	4.29 (s)	60.0	4.28 (s)	59.4	4.93 (s)	61.8 (CH_2)	4.93 (s)
OH-7	5.68 (brs)		5.67 (s)				
9						170.4 (C)	
10					2.11 (3H, s)	20.9 (CH_3)	2.16 (COCH3)

3.3.5.6. Compounds AF6 (ergosterol)

(22E,24R)-Ergosta-5,7,22-trien-3β-ol	
Synonyms	Ergosterol
Sample codes	AF6
Sample Amount	8 mg
Physical Description	White needles
Molecular Formula	$C_{28}H_{44}O$
Molecular Weight	396 g/mol
Retention time (LC-MS)	31.5 min

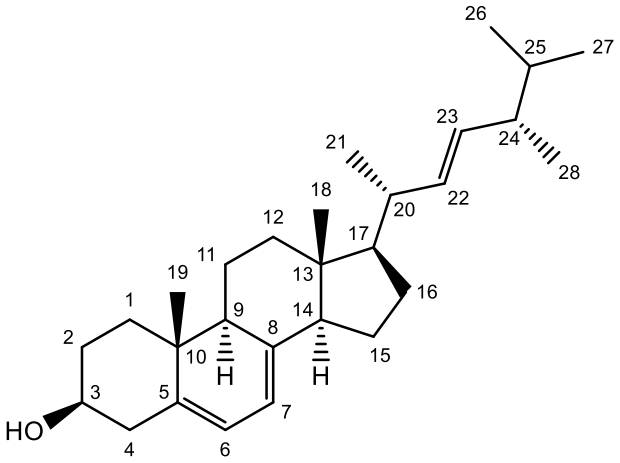

LC-HRFTMS spectrum $[M-H]^-$ 395.3309

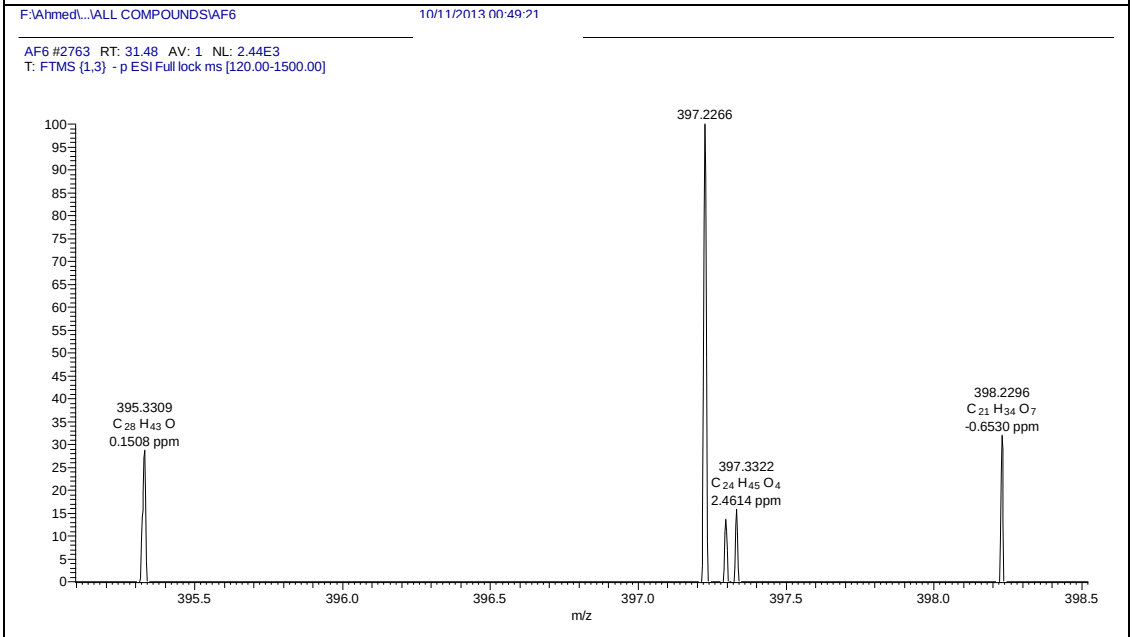

3.3.5.7. Compound AF7 (ergosterol peroxide)

5,8-Epidioxy-5α,8α-ergosta-6,22-dien-3β-ol	
Synonyms	Ergosterol peroxide
Sample codes	AF7
Sample Amount	7 mg
Physical Description	White needles
Molecular Formula	$C_{28}H_{44}O_3$
Molecular Weight	428 g/mol
Retention time (LC-MS)	29.2 min

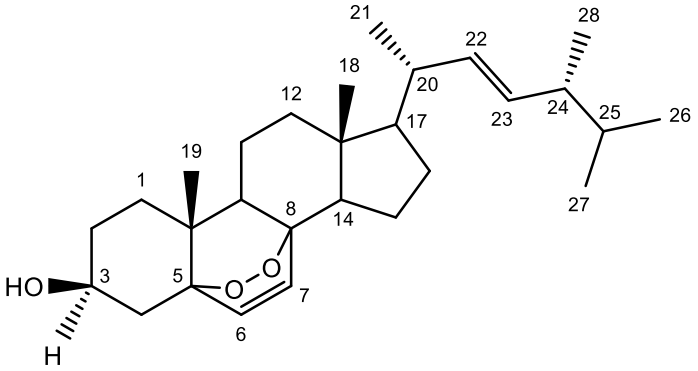

LC-HRFTMS spectrum $[M+H]^+$ 429.3372

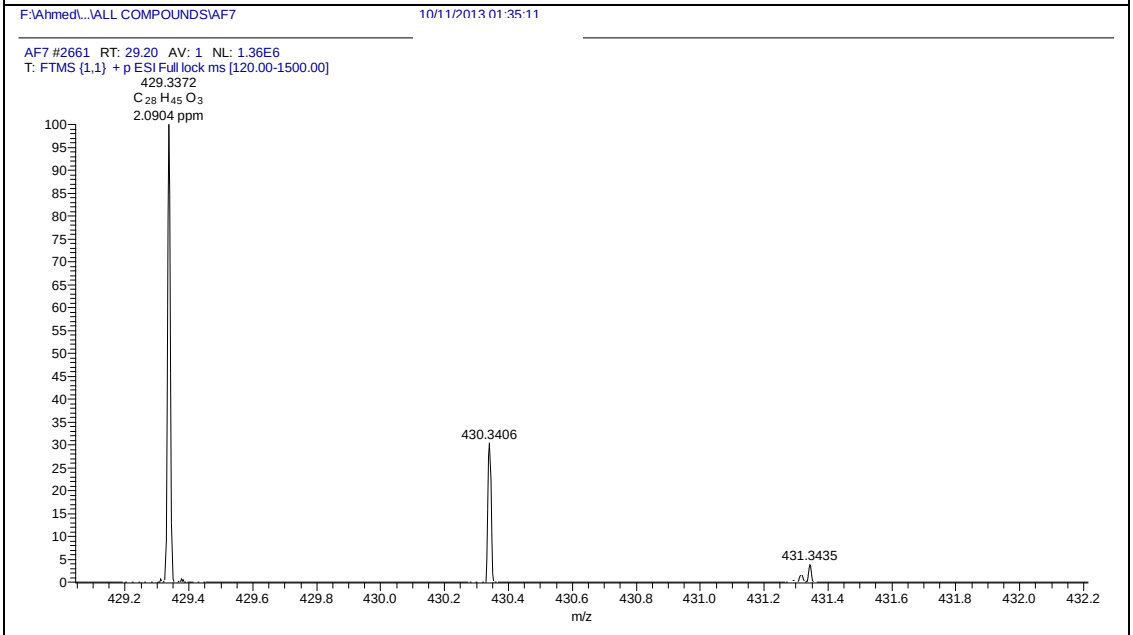

Compounds AF6 (8 mg) and AF7 (7 mg) were obtained as white needles, exhibited a molecular formula $C_{28}H_{44}O$ established by ESI-HRMS at *m/z* = 395.3309 $[M-H]^-$, $C_{28}H_{44}O_3$ at *m/z* = 429.3372 $[M+H]^+$ respectively. Compound

AF7 was found to be similar to compound AA1 (Ergosterol peroxide) isolated from *A. aculeatus* endophyte and described in details in section [3.1.5.1]. The **^{1}H NMR** spectrum of compound AF6 ($CDCl_3$, 400 MHz) (Fig.134) resembled that of compound AF7 (Fig.136) except for an upfield chemical shift of the two olefinic protons H-6 at δ_H 5.34 (brd) and H-7 at δ_H 5.52 (brd) in comparison to the chemical shifts of the same protons in compound AF7 (Table.5). This was due to the absence of the deshielding effect resulted from the absence of the peroxide bridge between C-5 and C-8. The **^{13}C NMR** spectrum of compound AF6 ($CDCl_3$, 400 MHz) (Fig.135) showed the same resonances as compound AF7 except for the downfield shift of carbons C-5 (δ_C 141.3) and C-8 (δ_C 140.1) due to the conjugated double bond at C5-C6 and C7-C8. So from above and comparison of The ^{1}H NMR and ^{13}C NMR data of compounds AF6 and AF7 to the literature (Table 21), it was indicated that compound AF6 is ergosterol (Chobot et al., 1997) and AF7 is ergosterol peroxide (Lee et al., 2009).

3.3.5.8. Compound AF8

(24R)-5-Ergosten-3β-ol	
Synonyms	Campesterol
Sample codes	AF8
Sample Amount	9 mg
Physical Description	White needles
Molecular Formula	$C_{28}H_{46}O$
Molecular Weight	398 g/mol
Retention time (LC-MS)	37.8 min

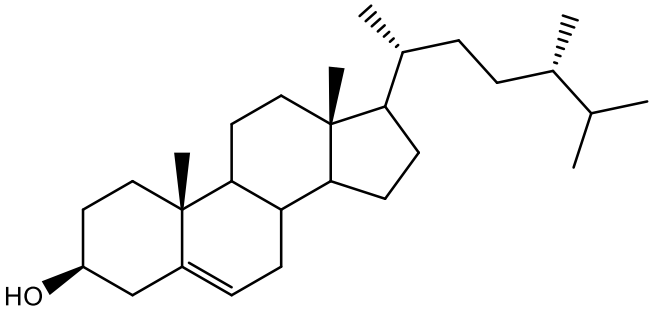

LC-HRFTMS spectrum $[M+H]^+$ 399.3623

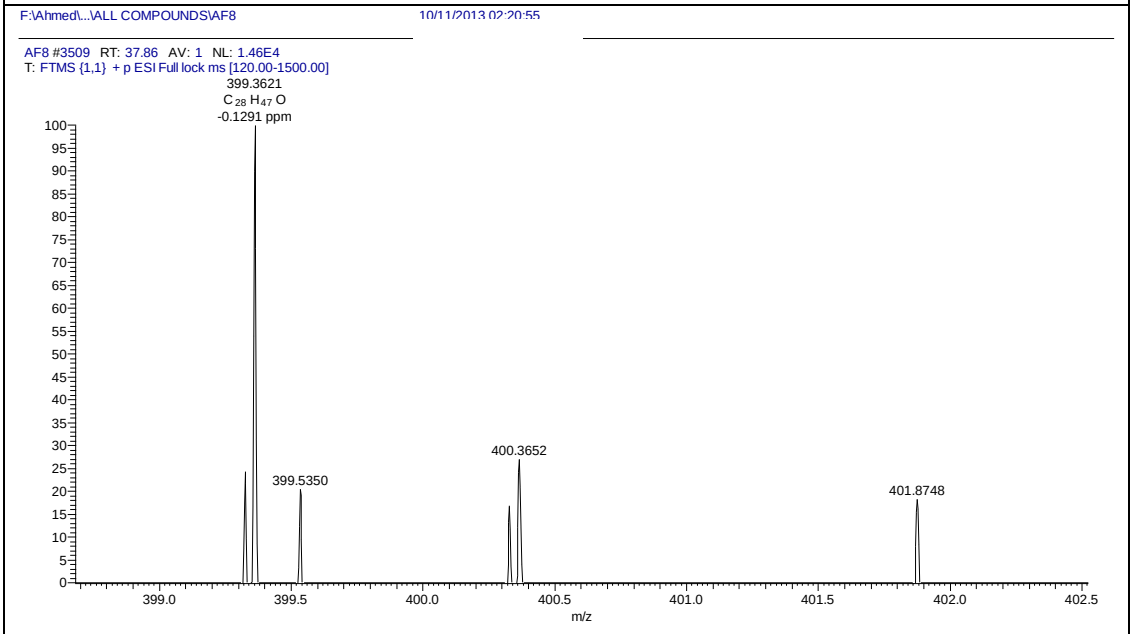

Compounds AF8 (9 mg) was obtained as white needles, exhibited a molecular formula $C_{28}H_{46}O$ established by ESI-HRMS at *m/z* = 399.3621 $[M+H]^+$. The **^{1}H NMR** spectrum of compound AF8 ($CDCl_3$, 400 MHz) (Fig.137) showed only one

proton in the olefinic region equivalent for H-6 at δ_H 5.34 (d, 4.7 Hz). Together with the rest of resonances at δ_H 3.51(m), 0.66 (s), 0.99 (s), 0.90 (d, 6.4 Hz), 0.85 (d, 6.6 Hz), 0.83 (d, 6.6 Hz) and 0.79 (d, 7.1 Hz) equivalent for H-3, Me-18, Me-19, Me-21, Me-26, Me-27 and Me-28. The **^{13}C NMR** spectrum (Fig.138) showed only two olefinic carbons at δ_C 140.8 and 121.8 equivalent for C-5 and C-6. However, the rest of carbons were similar to that of compound AF6 except for C-22 and C-23, which were found at δ_C 34.1 and 33.9 due to absence of the double bond C22-C23. So from the above and comparison of the proton and carbon data to the literature (Table 22), compound AF8 was identified as campesterol (Zhang et al., 2006).

Table 21: ^{1}HNMR and ^{13}CNMR data of compounds AF6, AF7 and literature

Atom No.	Chobot 1997- $CDCl_3$		AF6-$CDCl_3$		AF7-$CDCl_3$	Lee 2009-$CDCl_3$
	δ_C (m)	δ_H (m, *J* in Hz)	δ_C	δ_H (m, *J* in Hz)	δ_H (m, *J* in Hz)	δ_H (m, *J* in Hz)
1	31.4 (CH_2)		29.7			
2	32.0 (CH_2)		32.0			
3	70.4 (CH)	3.64 (m)	70.2	3.57 (m)	3.96 (m)	3.95 (m)
4	40.8 (CH_2)		40.8			
5	141.4 (C)		141.3			
6	119.6 (CH)	5.38 (d, 2.8 Hz)	119.6	5.34 (brd)	6.23 (d, 8.4 Hz)	6.22 (d, 8.8 Hz)
7	116.3 (CH)	5.57 (d, 2.8 Hz)	116.3	5.52 (brd)	6.49 (d, 8.5 Hz)	6.48 (d, 8.8 Hz)
8	139.8 (C)		140.1			
9	46.3 (CH)		46.3			
10	37.0 (C)		37.1			
11	21.1 (CH_2)		21.2			
12	39.1 (CH_2)		39.1			
13	42.8 (C)		42.9			
14	54.5 (CH)		54.6			
15	23.0 (CH_2)		23.0			
16	28.3(CH_2)		28.3			
17	55.7 (CH)		55.8			
18	12.1 (CH_3)		12.1	0.58 (s)	0.80 (s)	0.79 (s)
19	16.3 (CH_3)		16.4	0.89 (s)	0.87 (s)	0.87 (s)
20	40.4 (CH)		40.3			
21	19.7 (CH_3)		19.7	0.99 (d, 6.5 Hz)	0.98 (d, 6.5 Hz)	0.98 (d, 6.8 Hz)
22	135.6 (CH)	5.2 (2H, m)	135.6	5.16 (2H, m)	5.20 (dd, 7.8, 15.2 Hz)	5.22 (dd, 8.0, 15.6 Hz)
23	132.0 (CH)		132.0		5.13 (dd, 7.0, 15.2 Hz)	5.11 (dd, 7.6, 15.6 Hz)
24	42.8 (CH)		40.5			
25	33.1 (CH)		33.1			
26	21.1 (CH_3)		21.2	0.79 (d, 6.3 Hz)	0.81 (d, 6.6 Hz)	0.81 (d, 6.8 Hz)
27	20.0 (CH_3)		20.0	0.77 (d, 6.3 Hz)	0.79 (d, 6.5 Hz)	0.79 (d, 6.4 Hz)
28	17.6 (CH_3)		17.7	0.87 (d, 6.8 Hz)	0.89 (d, 6.8 Hz)	0.88 (d, 6.8 Hz)

Table 22: ^{1}H NMR and ^{13}C NMR data of compounds AF8 and literature

Atom No.	AF8-$CDCl_3$		Zhang 2006-$CDCl_3$	
	δ_H (m, *J* in Hz)	δ_C (m)	δ_H (m, *J* in Hz)	δ_C
1		37.3 (CH_2)		37.2
2		29.8 (CH_2)		31.7
3	3.51 (m)	71.9 (CH)	3.51 (m)	71.8
4		42.3 (CH_2)		
5		140.8 (C)		140.8
6	5.34 (d, 4.7 Hz)	121.8 (CH)	5.34 (brd)	121.7
7		31.6 (CH_2)		31.9
8		24.4 (CH)		24.3
9		50.2 (CH)		50.1
10		36.6 (C)		
11		21.1 (CH_2)		21.1
12		39.8 (CH_2)		39.8
13		42.4 (C)		42.3
14		56.8 (CH)		56.7
15		28.3 (CH_2)		30.3
16		26.1 (CH_2)		28.2
17		56.1 (CH)		56.1
18	0.66 (s)	11.9 (CH_3)	0.68 (s)	11.9
19	0.99 (s)	18.8 (CH_3)	1.01 (s)	18.2
20		33.1 (CH)		36.5
21	0.90 (d, 6.4 Hz)	19.1 (CH_3)	0.91 (d, 6.5 Hz)	18.7
22		34.1 (CH_2)		35.9
23		33.9 (CH_2)		33.7
24		36.2 (CH)		38.8
25		31.9 (CH)		32.4
26	0.85 (d, 6.6 Hz)	19.9 (CH_3)	0.85 (d, 6.5 Hz)	20.2
27	0.83 (d, 6.6 Hz)	19.4 (CH_3)	0.80 (d, 6.5 Hz)	19.4
28	0.79 (d, 7.1 Hz)	14.2 (CH_3)	0.77 (d, 6.5 Hz)	15.4

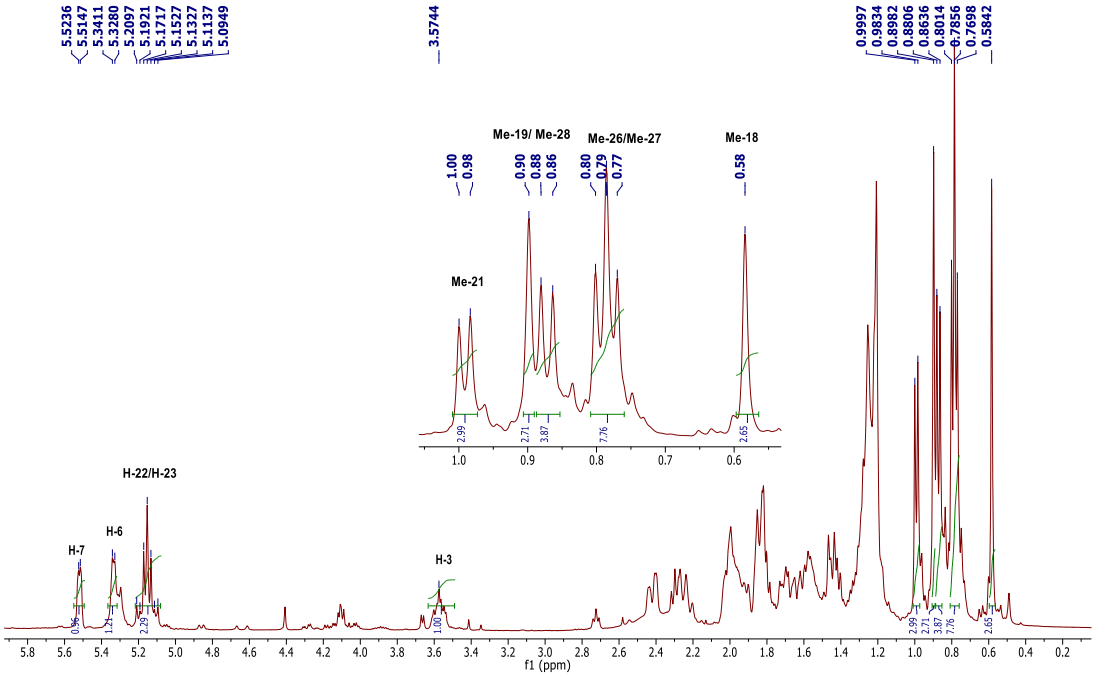

Fig.134 ^{1}HNMR spectrum of compound AF6

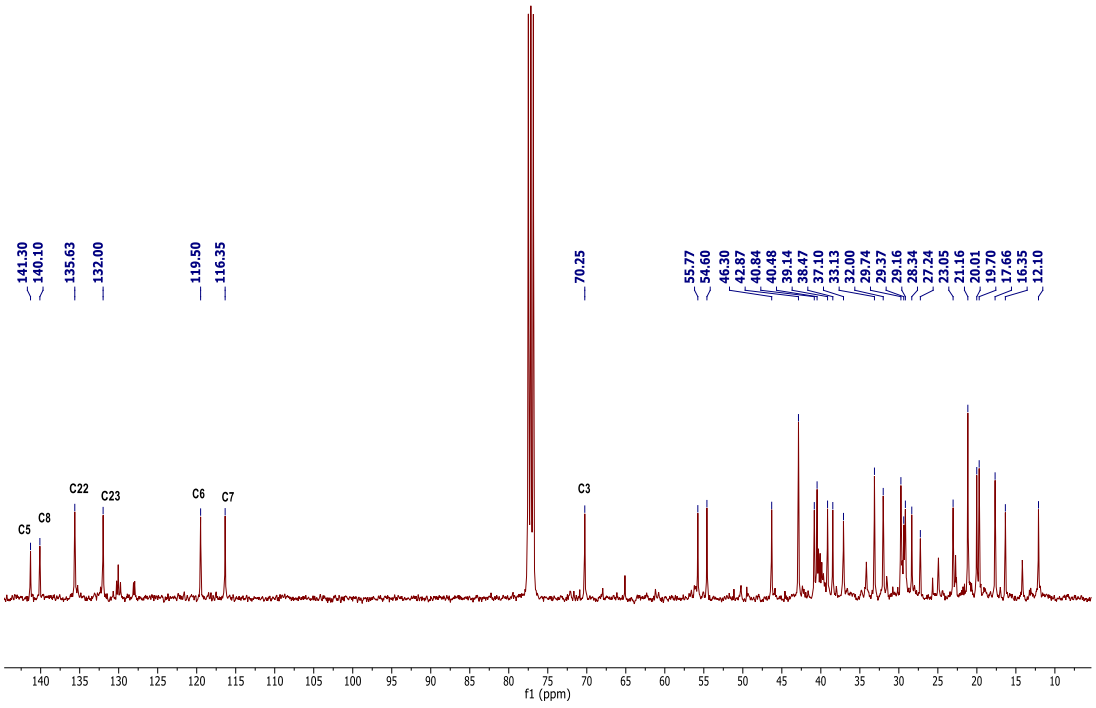

Fig.135 ^{13}CNMR spectrum of compound AF6

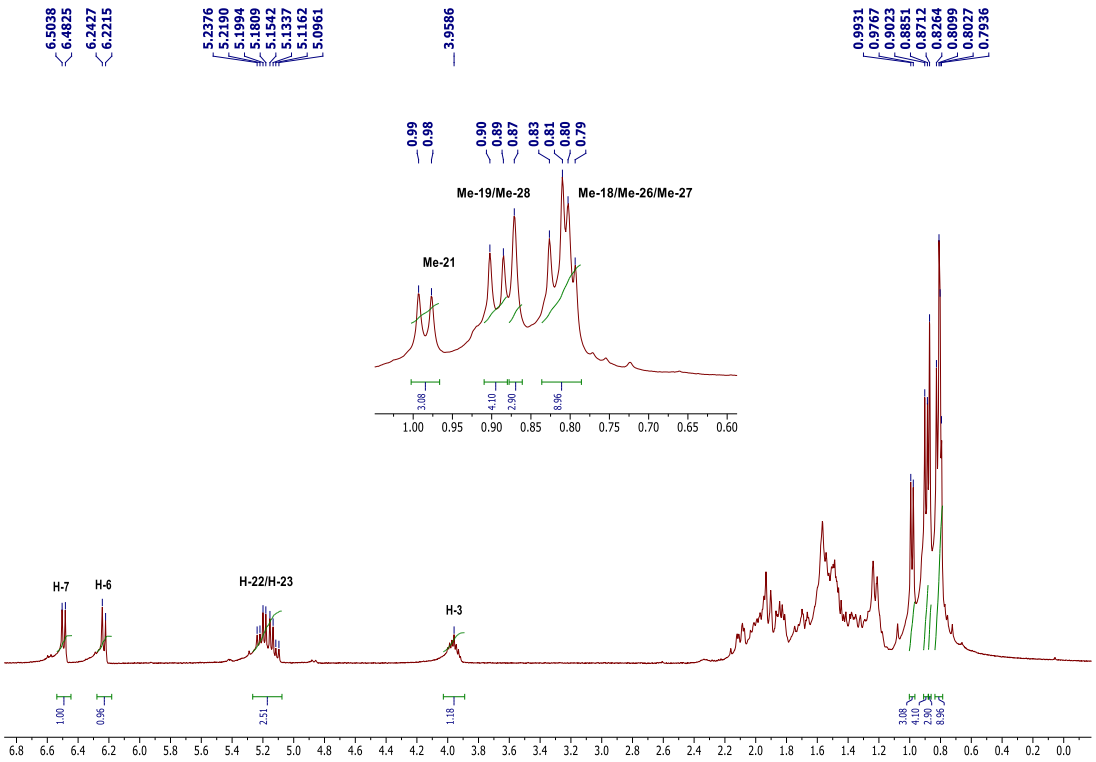

Fig.136 [1]HNMR spectrum of compound AF7

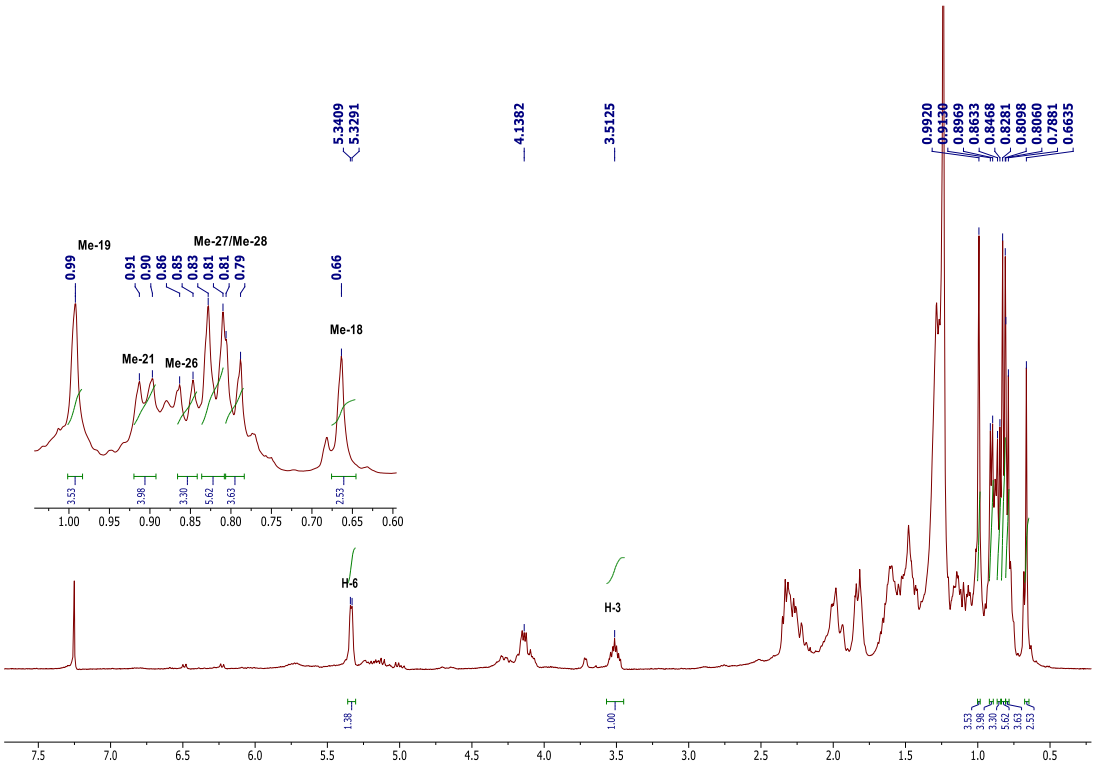

Fig.137 [1]HNMR spectrum of compound AF8

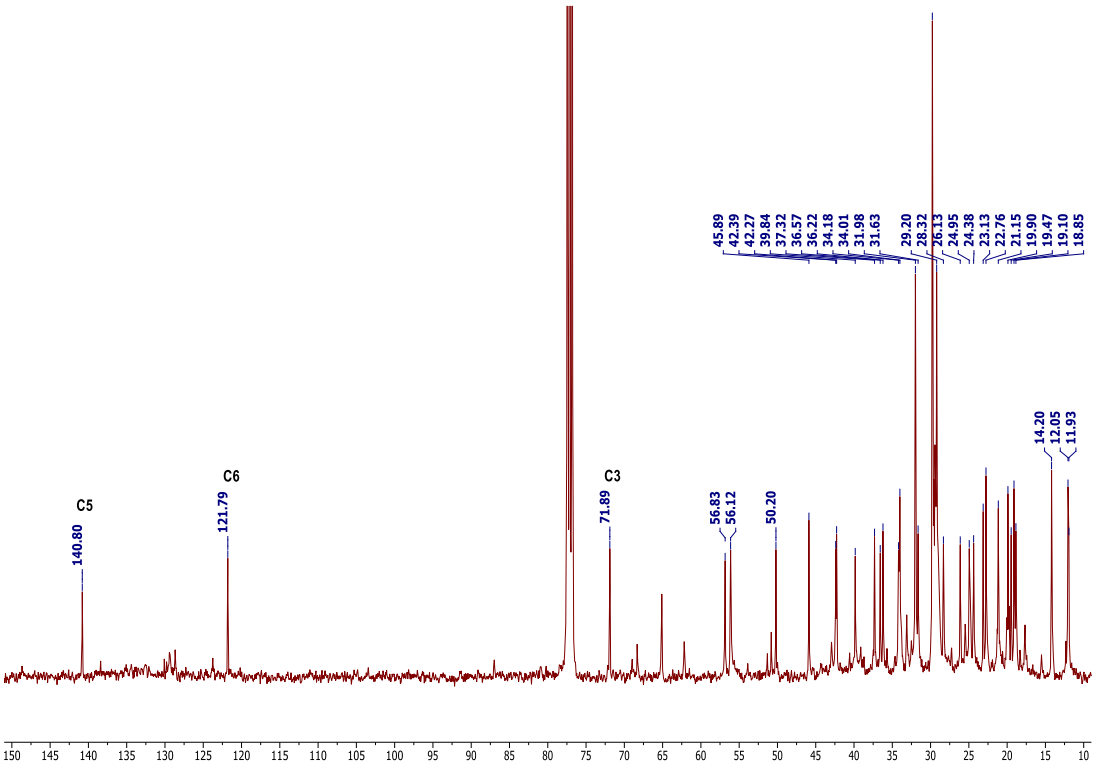

Fig.138 ^{13}CNMR spectrum of compound AF8

3.3.5.9. Compound AF9 (new)

Ergosta-4,22-dien-3-one	
Synonyms	-
Sample codes	AF9
Sample Amount	4 mg
Physical Description	White amorphous powder
Molecular Formula	$C_{28}H_{44}O$
Molecular Weight	396 g/mol
Optical Rotation $[\alpha]_D^{20}$	- 10 (*c* 0.05 in MeOH)
Retention time (LC-MS)	30.4 min

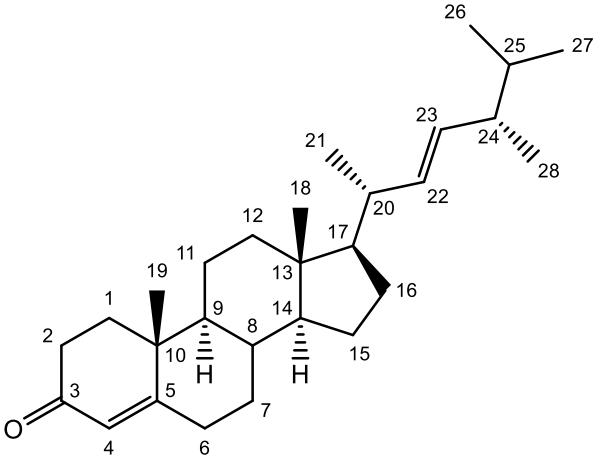

LC-HRFTMS spectrum $[M+H]^+$ 397.3466

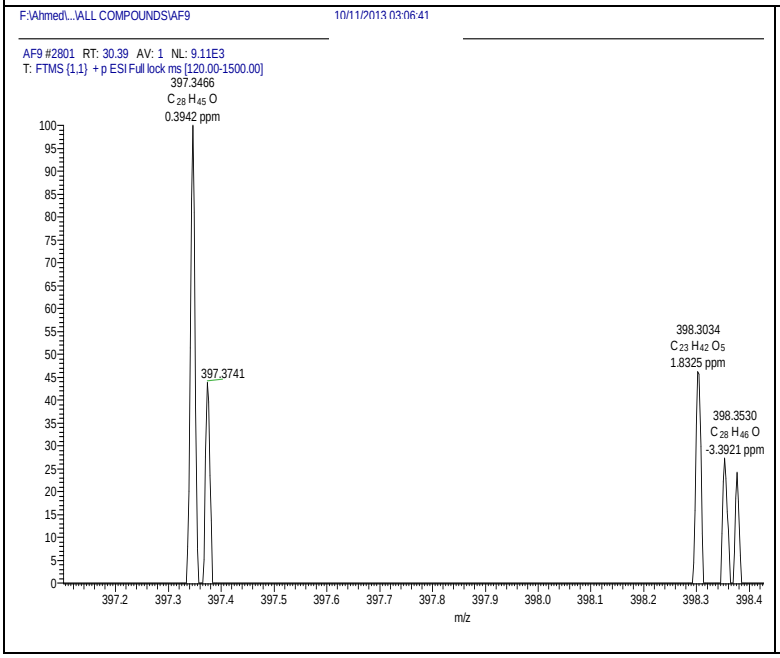

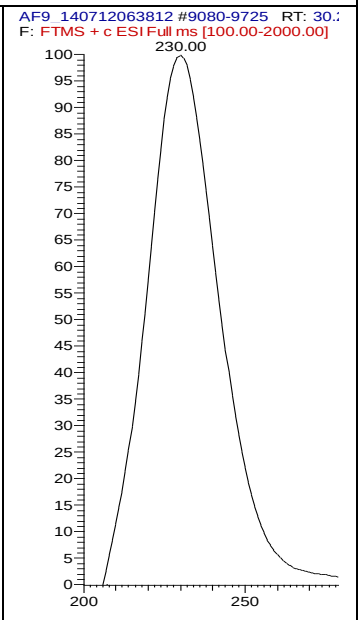

Compound AF9 (4 mg) was obtained as a white powder, exhibited a molecular formula $C_{28}H_{45}O$ established by ESI-HRMS at *m/z* = 397.3466 $[M+H]^+$. The optical rotation $[\alpha]^{20}_D$ = - 10 (*c* 0.05 in MeOH). The **^{1}H NMR** spectrum ($CDCl_3$, 600MHz) (Fig.139) showed two methyl singlets equivalent for Me-18 at δ_H 0.98 and Me-19 at δ_H 1.26; four methyl doublet at δ_H 1.09 (d, *J* = 6.9 Hz), 0.81 (d, 6.8), 0.83 (d, 6.7) and 0.91 (d, 6.8) equivalent for Me-21, Me-26, Me-27 and Me-28 respectively. Moreover, three olefinic protons at δ_H 6.36 (*brd*) equivalent for H-4 and 5.27 (2H, *m*) for H-22, H-23 and the region from 1.5-3.0 ppm (23H, *m*) which was typically similar to steroidal methylene protons. The **^{13}C NMR** spectrum ($CDCl_3$, 400 MHz) (Fig.140) showed 28 carbons including six methyls, eight methylenes, seven methines, four quaternaries and three olefinic methines (Table 23). The **HMBC** spectrum ($CDCl_3$, 600MHz) (Fig.141) showed correlation of H-4 with the carbonyl C-3 (δ_C 199.3) and C-2 (δ_C 34.4) and another correlation of Me-19 with C-5 (δ_C 156.3) which confirmed the structure of ring A. While the correlations of Me-21 with C-22 (δ_C 132.4), Me-28 with C-23 (δ_C 135.1); the two methyl Me-26 and Me-27 with each other and with C-25 (δ_C 37.3) and C-24 (δ_C 43.4) confirmed the presence of the side chain (5,6-dimethylhept-3-one). So from the above data and comparison to the most related structure in the literature (Duh et al., 2004, Kawahara et al., 1995), compound AF9 (Fig.142) was identified as Ergosta-4,22-dien-3-one which was isolated for the first time from a natural source. (Note: the NMR data in first reference in table.7 (Duh et al. 2004) was for dendronesterone (Ergosta-1,22-dien-3-one) and the second reference (Kawahara et al. 1995) for 14-hydroxyergosta-4,7,9,22-tetraene-3,6-dione (Fig.143). The structure elucidation seems to be not completely matched with the reported data however it is very close.

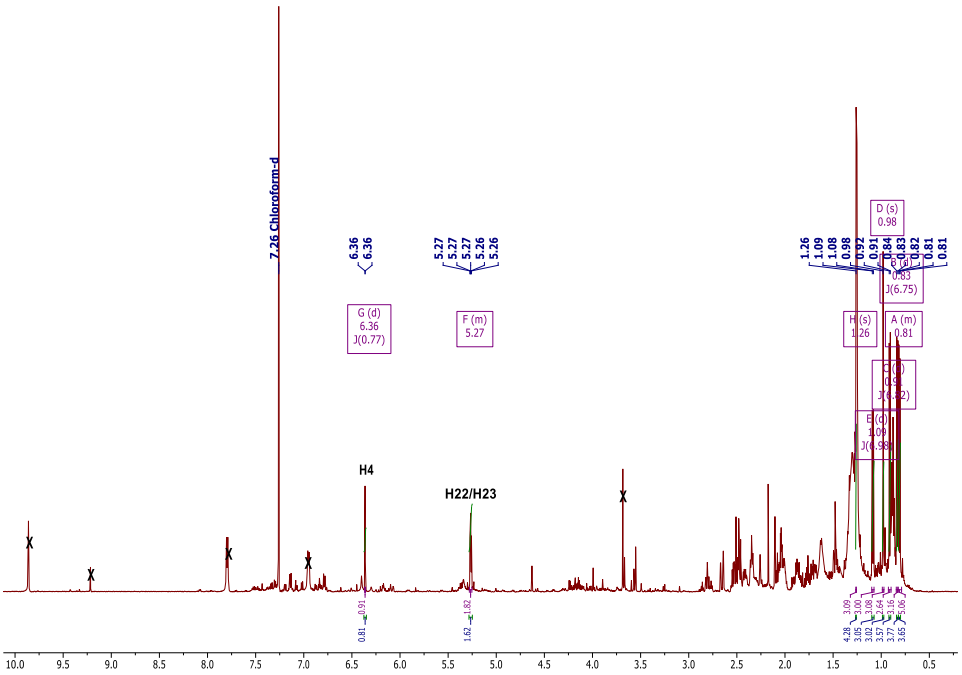

Fig.139 ^{1}HNMR spectrum of compound AF9 the crossed peaks (X) are belonging to impurities

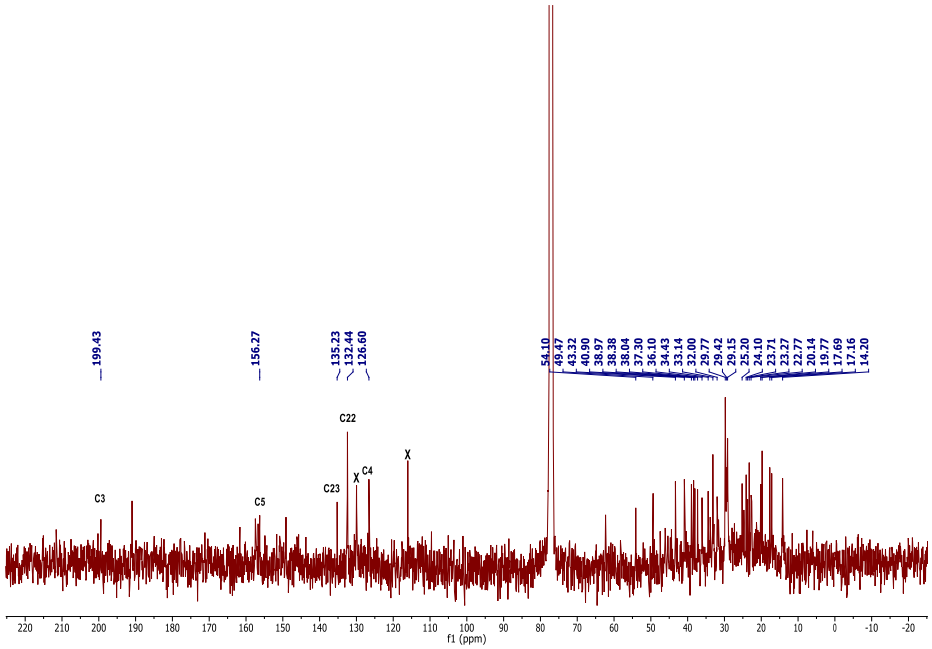

Fig.140 ^{13}CNMR spectrum of compound AF9-the crossed peaks (X) are belonging to impurities

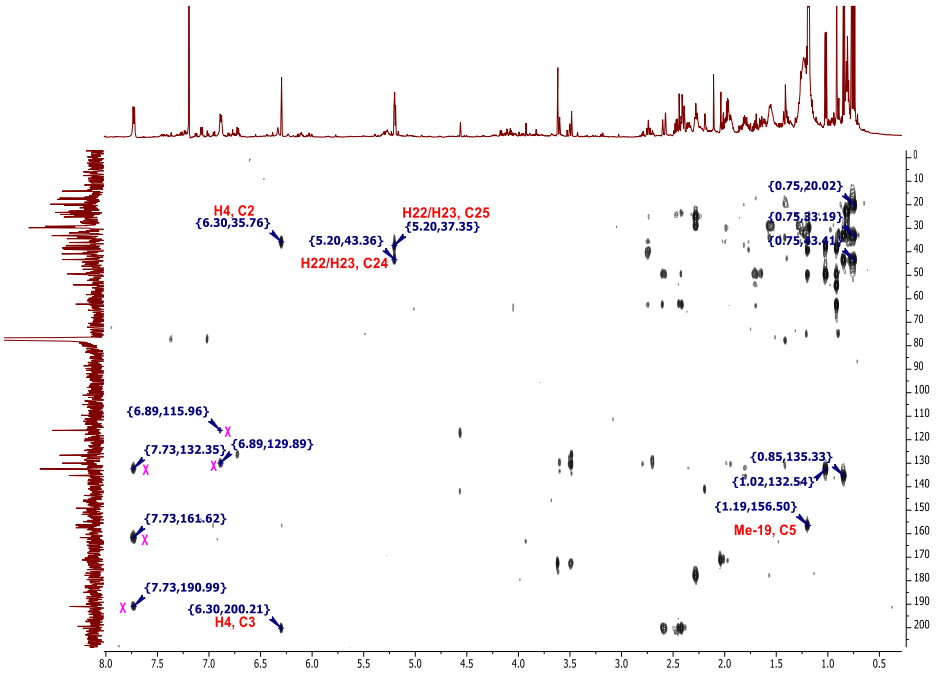

Fig.141 HMBC spectrum of AF9- the crossed peaks (X) are belonging to impurities

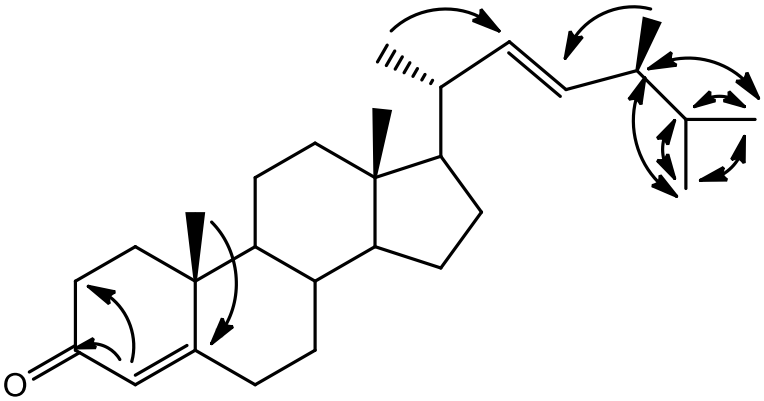

Fig.142 structure and HMBC correlations of AF9

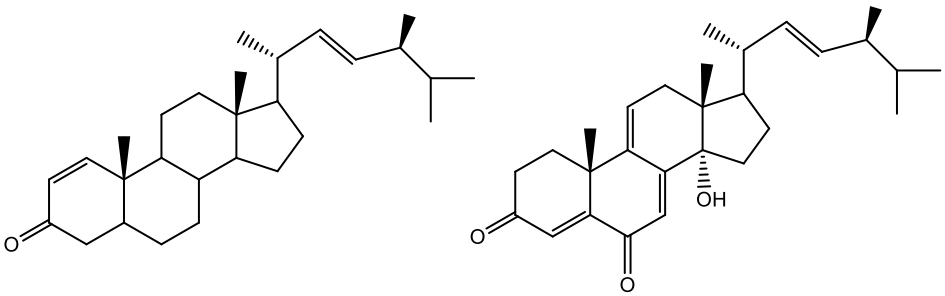

dendronesterone

14-hydroxyergosta-4,7,9,22-tetraene-3,6-dione

Fig.143 the comparable structures from the literature

Table 23: ^{1}H NMR and ^{13}C NMR data of compound AF9 and literature, the highlighted rows represented the carbon values variant from compound AF9

Atom No.	Duh 2004-$CDCl_3$	AF9-CDCl3		Kawahara 1995-CDCl3	
	δ_C (m)	δ_C (m)	δ_H (m, *J* in Hz)	δ_C (m)	δ_H (m, *J* in Hz)
1	158.7 (CH)	36.1 (CH_2)		34.5	
2	127.4 (CH)	34.4 (CH_2)		34.3	
3	200.4 (C)	199.3 (C)		199.7	
4	41.1 (CH_2)	126.4 (CH)	6.36 (brd)	127.0	6.45 (s)
5	44.4 (CH)	156.3 (C)		156.3	
6	28.7	32.0 (CH_2)		188.7 (C)	
7	31.4	29.7 (CH_2)		121.8 (CH)	
8	35.7	33.1 (CH)		156.0 (C)	
9	50.1	49.4 (CH)		138.5 (C)	
10	39.1	38.0 (C)		38.8	
11	21.3	25.2 (CH_2)		132.9 (CH)	
12	39.7	38.4 (CH_2)		37.4	
13	42.7	40.9 (C)		46.3	
14	56.7	54.1 (CH)		84.7 (CH)	
15	24.2	29.1 (CH_2)		31.2	
16	27.7	29.4 (CH_2)		27.2	
17	56	49.5 (CH)		50.4	
18	12.4	17.1 (CH_3)	0.98 (s)	16.2	0.76 (s)
19	13	19.7 (CH_3)	1.26 (s)	29.5	1.49 (s)
20	40.2	39.9 (CH)		40.1	
21	20.9	20.1 (CH_3)	1.09 (d, 6.9 Hz)	20.9	1.04 (d, 5.9 Hz)
22	138	132.4 (CH)	5.27 (m)	135.4	5.22 (dd, 7.7, 15.4 Hz)
23	126.5	135.1 (CH)		133.3	5.30 (dd, 7.7, 15.4 Hz)
24	42	43.4 (CH)		42.9	
25	28.6	37.3 (CH)		33.2	
26	22.4	24.1 (CH_3)	0.81 (d, 6.8 Hz)	20.0	0.84 (d, 6.9 Hz)
27	22.3	23.7 (CH_3)	0.83 (d, 6.7 Hz)	19.7	0.85 (d, 6.9 Hz)
28		17.6 (CH_3)	0.91 (d, 6.8 Hz)	17.6	0.93 (d, 6.6 Hz)

3.3.5.10. Compounds AF11 (3,8-dihydroxy-3-methylisochroman-1-one)

3,8-dihydroxy-3-methylisochroman-1-one	
Synonyms	-
Sample codes	AF11
Sample Amount	10 mg
Physical Description	yellow powder
Molecular Formula	$C_{10}H_{10}O_4$
Molecular Weight	194 g/mol
Optical Rotation $[\alpha]_D^{20}$	- 2 (*c* 0.05 in MeOH)
Retention time (LC-MS)	8.6 min

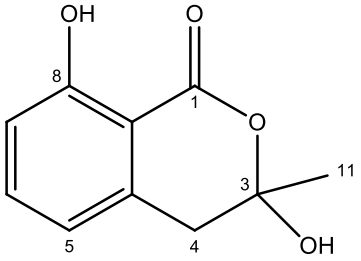

LC-HRFTMS spectrum $[M+H]^+$ 195.0653

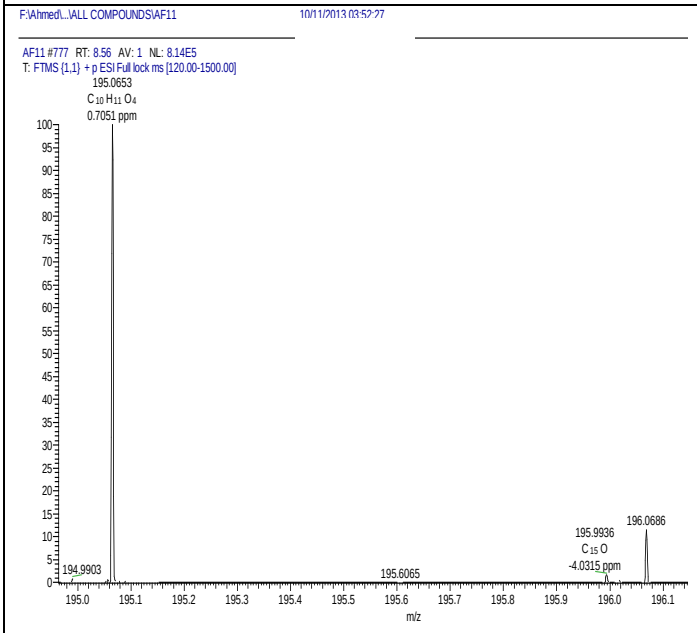

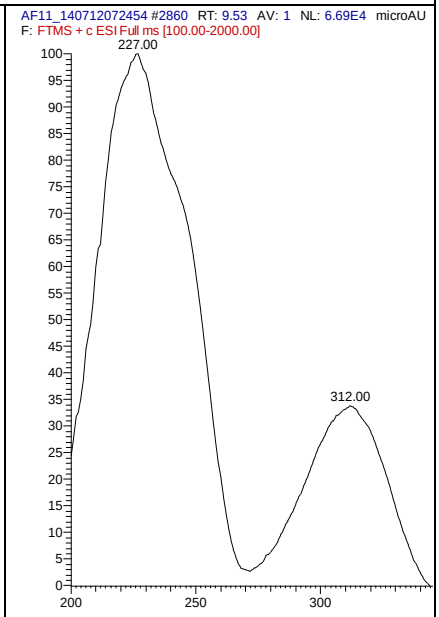

Compounds AF11 (10 mg) was obtained as yellow powder, exhibited molecular formula $C_{10}H_{10}O_4$ established by ESI-HRMS at *m/z* = 195.0653 $[M+H]^+$. The optical rotation $[\alpha]^{20}_D$ = -2 (*c* 0.05 in MeOH). The **^{1}H NMR** spectrum ($CDCl_3$, 400 MHz) (Fig.144) of compound AF11 showed three proton signals in the

aromatic region at δ_H 7.43 (t, 7.9 Hz), 6.89 (d, 8.4 Hz) and 6.73 (d, 7.4 Hz) equivalent for H-6, H-7 and H-5 of the benzene ring and the phenolic OH-8 at δ_H 10.94. The aliphatic region was characterized by presence of the methylene protons CH_2-4 at δ_H 3.19 (q, 16.17, 16.8 Hz) and the methyl Me-11 at δ_H 1.77 (s). The **^{13}C NMR** spectrum ($CDCl_3$, 400 MHz) (Fig.146) of compound AF11 showed ten carbons five aromatic, one phenolic, one carbonyl, one methylene, one quaternary and one methyl. The **^{1}H-^{1}H COSY** spectrum (Fig.147) of compound AF11 showed the ABC spin system connecting the three aromatic protons H-5, H-6 and H-7. The structure of compound AF11 was confirmed from **HMBC** spectrum (Fig.148) through the correlations of H-5 with C-4 (δ_C 38.5), C-9 (δ_C 107.7) and C-7 (δ_C 116.5). In addition, H-6 correlated with C-10 (δ_C 137.4) and C-8 (δ_C 162.2); H-7 with C-8, C-9 and C-5 (δ_C 119.0) and OH-8 with C-8, C-9 and C-7. Moreover, the position of Me-11 was indicated from the correlations of Me-11 with C-3 (δ_C 103.4) and C-4. So from the above and in accordance to the reported data (Xu et al., 2012, Dimitriadis et al., 1997) (Table 24), Compound AF11 (Fig.150) was identified as 3-hydroxymellein (3,8-dihydroxy-3-methylisochroman-1-one).

3.3.5.11. Compounds AF16a and AF16b (botryoisocoumarin A and mellein)

8-hydroxy-3-methoxy-3-methylisochroman-1-one and (S)-8-hydroxy-3-methylisochroman-1-one	
Synonyms	Botryoisocoumarin A and Mellein
Sample codes	AF16a and AF16b
Sample Amount	11 mg
Physical Description	yellow powder
Molecular Formula	$C_{11}H_{12}O_4$ and $C_{10}H_{10}O_3$
Molecular Weight	208 and 178 g/mol
Optical Rotation $[\alpha]_D^{20}$	- 8 (c 0.05 in MeOH)
Retention time (LC-MS)	14 min

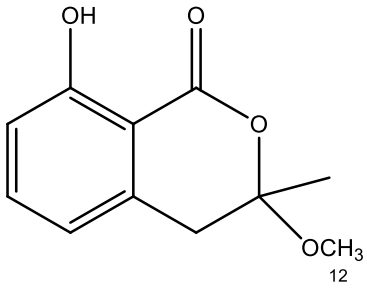

AF16a

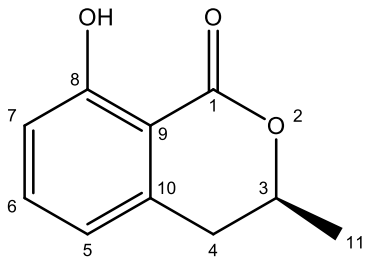

AF16b

LC-HRFTMS spectrum $[M+H]^+$ 209.0808 and 179.0703

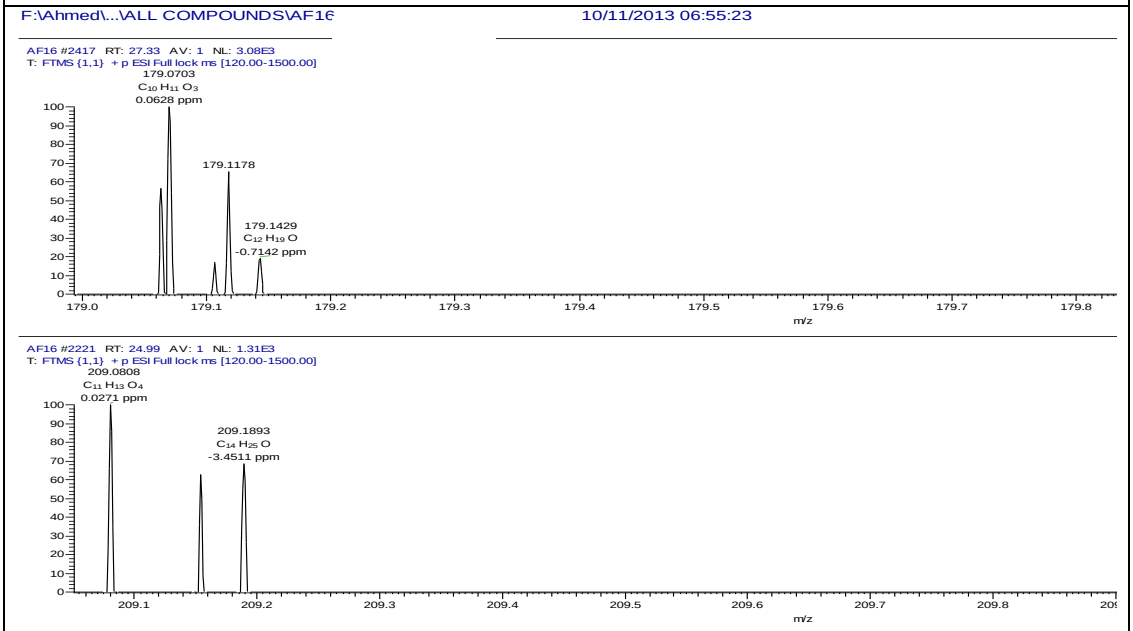

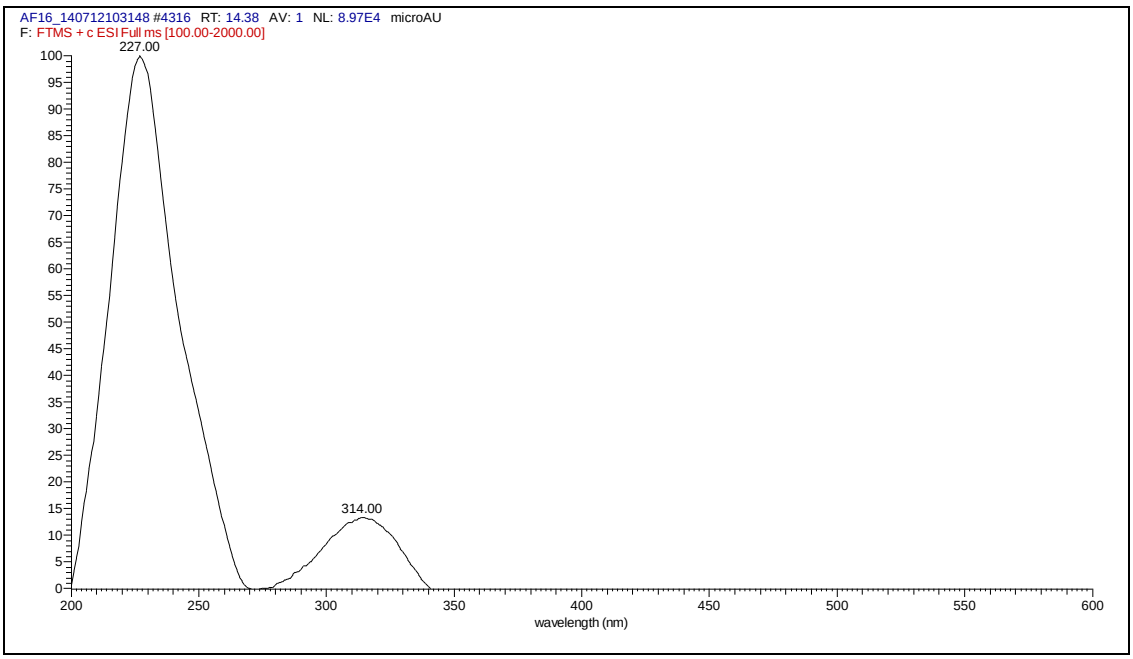

Compounds AF16a and AF16b (11 mg), were obtained in a mixture as yellow powder, exhibited molecular formula $C_{11}H_{12}O_4$ and $C_{10}H_{10}O_3$ established by ESI-HRMS at *m/z* = 209.0808 and 179.0703 [M+H]+ respectively. The optical rotation $[\alpha]^{20}_D$ = -8 (*c* 0.05 in MeOH). Compounds AF16a and AF16b were isolated as a mixture with ratio (1:1). The **^{1}H NMR** spectrum (Fig.145) ($CDCl_3$, 400 MHz) resembled that of AF11 in the aromatic region however each peak was equivalent for two protons and also characterized by the presence of two phenolic OHs (one for each compound). The aliphatic region of compound AF16a was also similar to AF11 except for an extra methoxy group OC*H*$_3$-12 at δ_H 3.39 (s). Furthermore, The **HMBC** spectrum (Fig.149) showed a correlation of OMe-12 with C-3 (δ_C 105.8) which confirmed the presence of OMe replacing the OH gp of compound AF11. The **^{1}H NMR** spectrum (Fig.145) of AF16b was different in the aliphatic region from the other two compounds due to the absence of the oxygen at C-3 therefore a multiplet signal equivalent to H-3 appeared at δ_H 4.73 while the methylene protons C*H*$_2$-4 was represented by doublet at δ_H 2.92. Moreover, absence of OH gp on C-2 in compound AF16b was confirmed from the HMBC correlation of H-3 with C-10 (δ_C 139.3); the correlations of Me-11 with C-3 (δ_C 76.1), C-4 (δ_C 34.6) and C-1 (δ_C 170.0) and also the correlations of C*H*$_2$-4 with Me-11, C-3, C-10, C-9 (δ_C 108.2) and C-5 (δ_C 117.9). So from the above and

comparison to the literature (Xu et al., 2012, Dimitriadis et al., 1997) (Tables 24, 25) compound AF16a was identified as botryoisocoumarin A (8-hydroxy-3-methoxy-3-methylisochroman-1-one) and AF16b was Mellein (Fig.150).

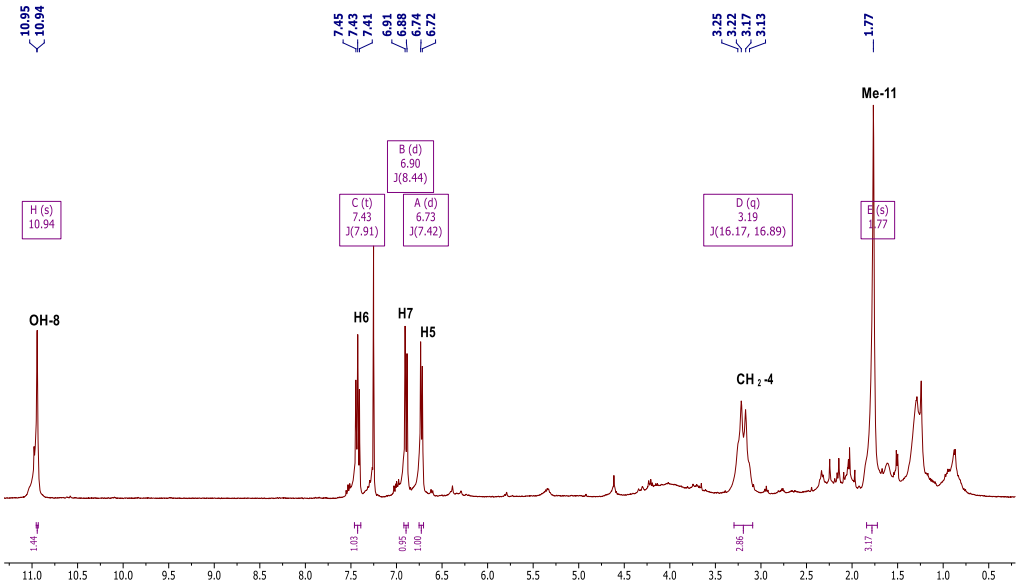

Fig.144 [1]HNMR spectrum of compound AF11

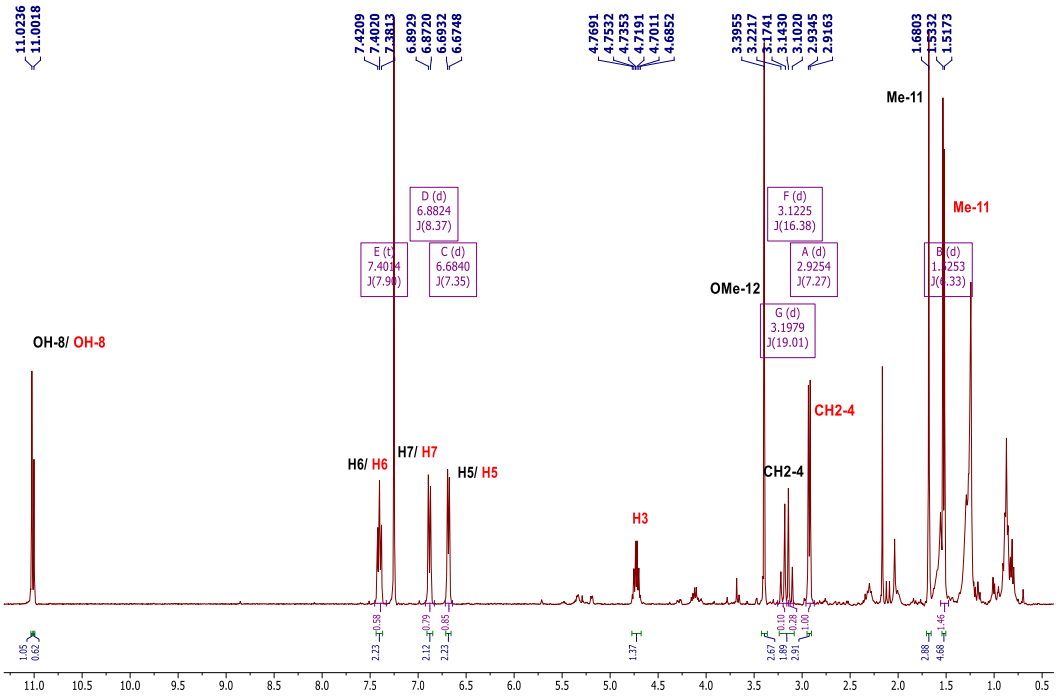

Fig.145 [1]HNMR spectra of compounds AF16a (●) and AF16b (●)

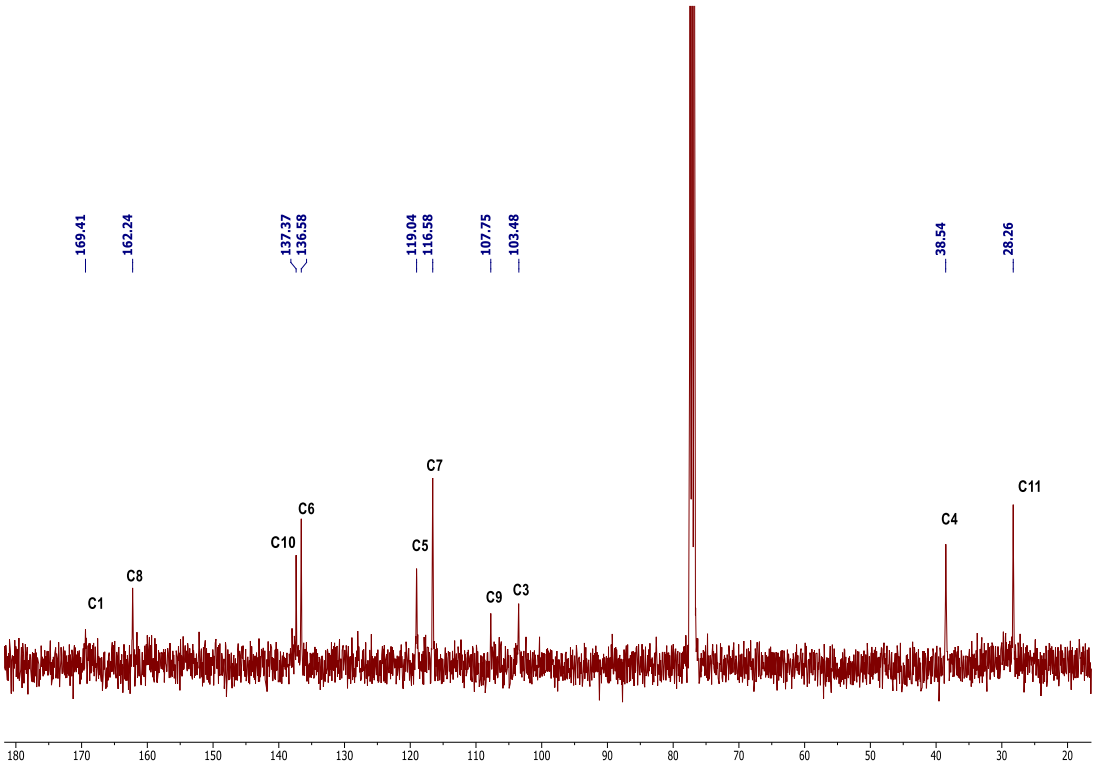

Fig.146 ^{13}CNMR spectrum of compound AF11

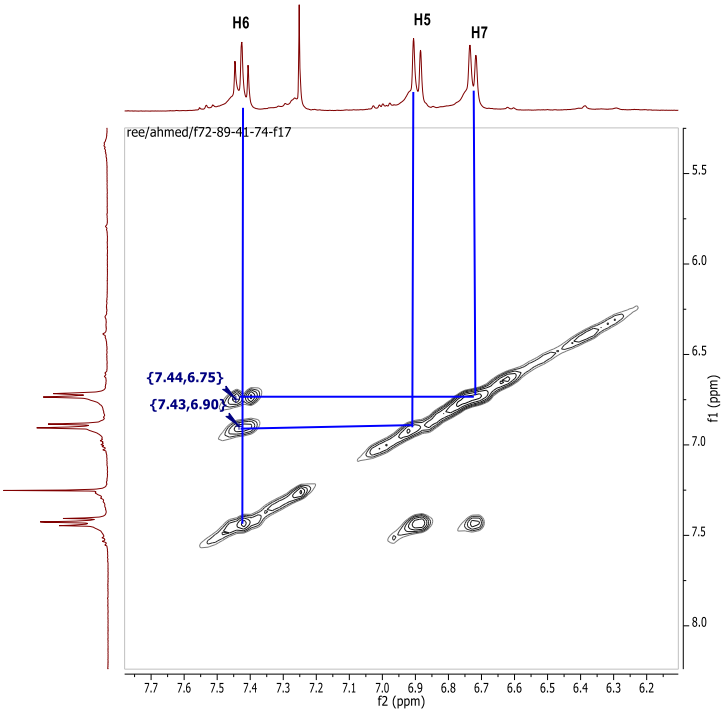

Fig.147 Expansion of ^{1}H-^{1}H COSY spectrum of compound AF11 showing the ABC spin system

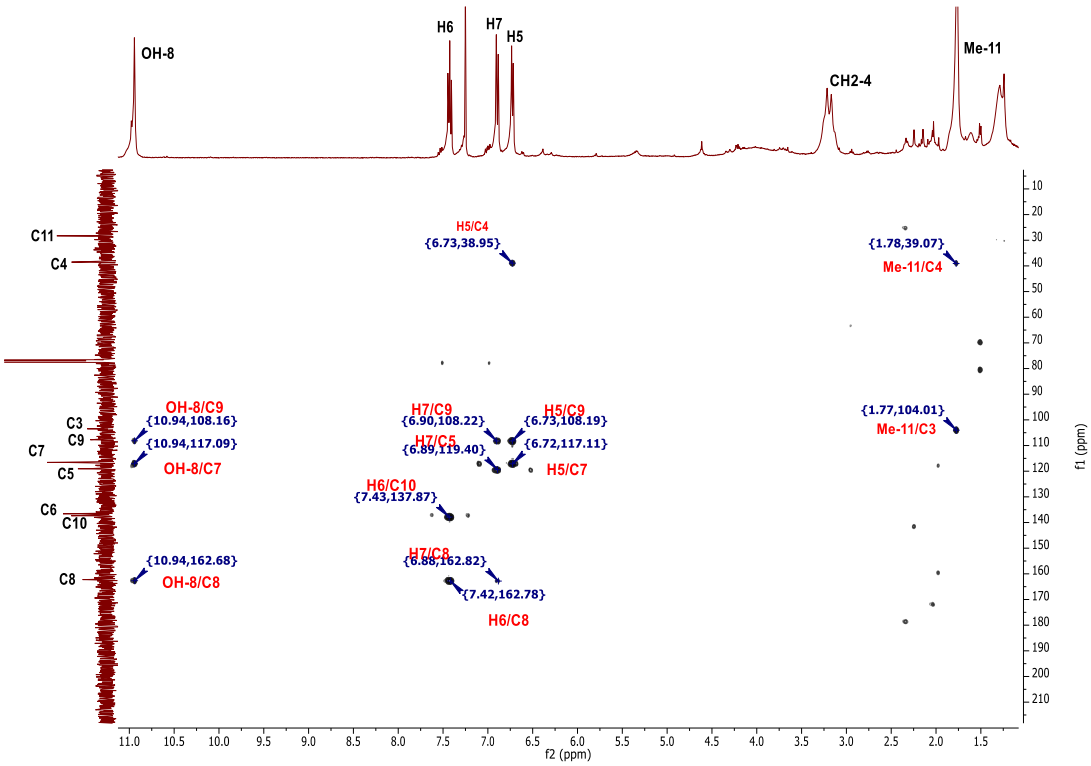

Fig.148 HMBC spectrum of compound AF11

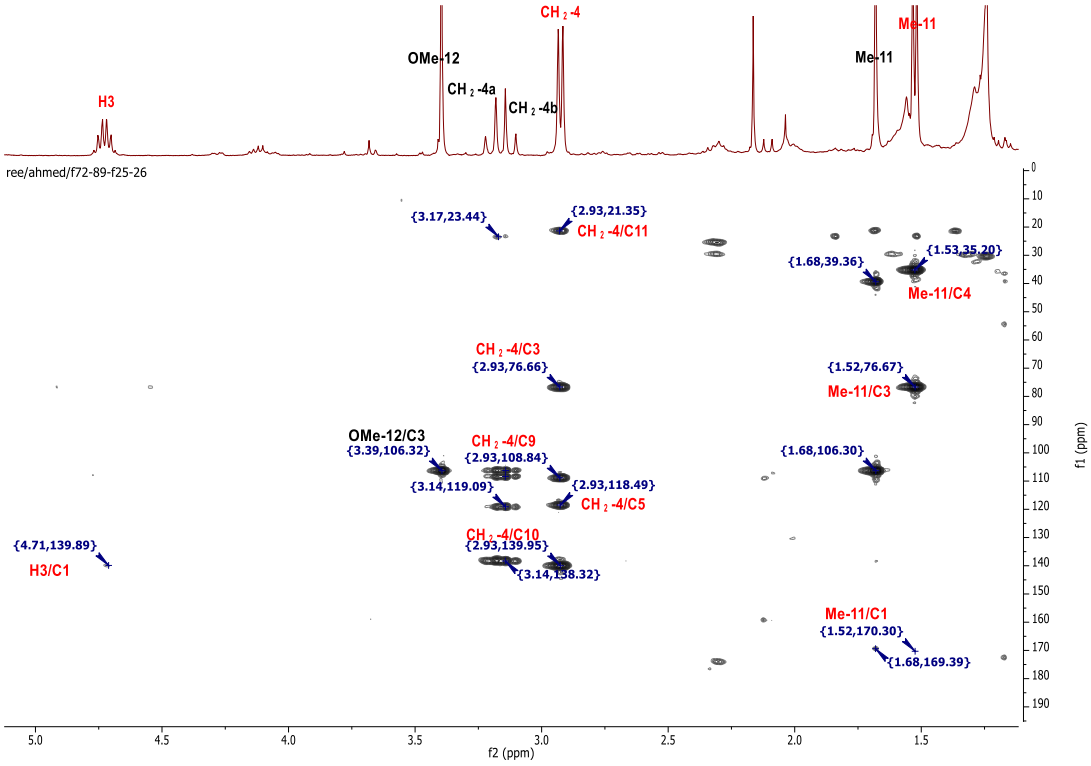

Fig.149 Expansion of HMBC spectra of compounds AF16a and AF16b (underlined)

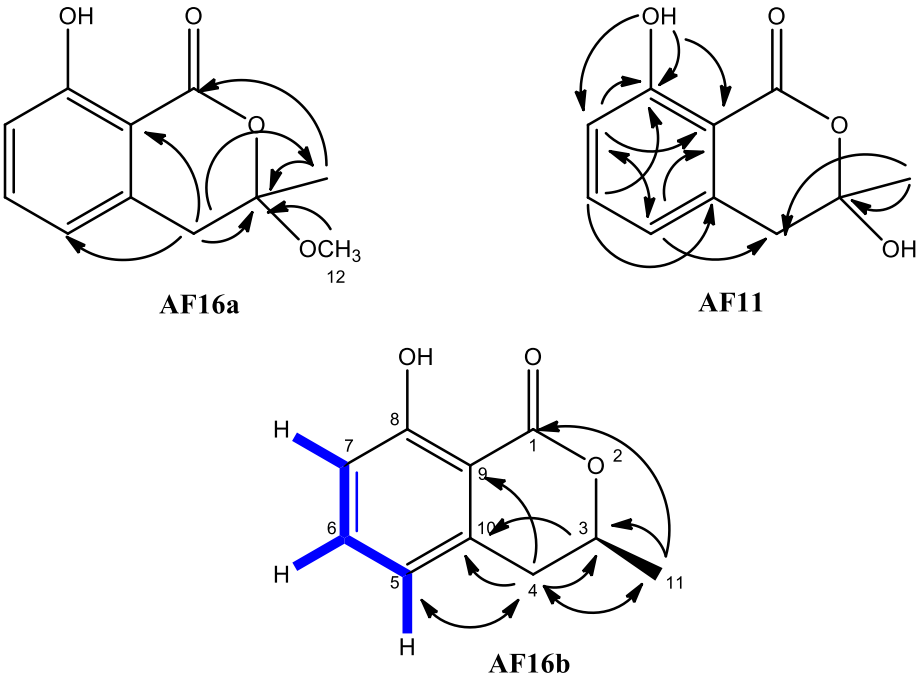

Fig.150 HMBC correlations of compounds AF11, AF16a and AF16b

Table 24: ^{1}H NMR and ^{13}C NMR data of compounds AF11, AF16 and literature

Atom No.	AF11-$CDCl_3$		AF16a-$CDCl_3$		Botryoisocoumarin A-$CDCl_3$ Xu 2012	
	δ_C	δ_H (m, *J* in Hz)	δ_C (m)	δ_H (m, *J* in Hz)	δ_C	δ_H (m, *J* in Hz)
1	169.4		169.0 (C)		168.9	
3	103.4		105.8 (C)		105.5	
4	38.5	3.19 (q, 16.1, 16.8 Hz)	38.8 (CH_2)	3.12 (d, 16.4 Hz), 3.19 (d, 19.0 Hz)	38.7	3.22 (d, 16.3 Hz), 3.15 (d, 16.3 Hz)
5	119.0	6.73 (d, 7.4 Hz)	118.6 (CH)	6.60 (d, 7.3 Hz)	118.5	6.70 (dd, 0.5, 7.3 hz)
6	136.5	7.43 (t, 7.9 Hz)	136.4 (CH)	7.40 (t, 7.9 Hz)	136.3	7.40 (dd, 7.3, 8.8 Hz)
7	116.5	6.89 (d, 8.4 Hz)	116.3 (CH)	6.80 (d, 8.3 Hz)	116.2	6.9 (d, 8.4 Hz)
8	162.2	10.94 (OH-8, s)	162.2 (C)	11.0 (OH-8, s)	162.1	
9	107.7		107.8 (C)		107.8	
10	137.3		137.8 (C)		137.7	
11	28.2	1.77 (3H, s)	22.9 (CH_3)	1.68 (3H, s)	22.8	1.69 (s)
12			50.4 (CH_3)	3.40 (3H, s)	50.4	3.41 (s)

Table 25: ^{1}H NMR and ^{13}C NMR data of compounds of AF16b and literature

Atom No.	AF16b-$CDCl_3$		Mellein-$CDCl_3$ Dimitriadis 1997	
	δ_C (m)	δ_H (m, *J* in Hz)	δ_C	δ_H (m, *J* in Hz)
1	170.0 (C)		169.9	
3	76.1 (CH)	4.70 (m)	76.1	4.73 (m)
4	34.6 (CH_2)	2.92 (d, 7.2)	34.6	2.93 (d, 7.3)
5	117.9 (CH)	6.60 (d, 7.3)	117.9	6.89 (d, 8.3)
6	136.2 (CH)	7.40 (t, 7.9)	136.1	7.41 (m)
7	116.2 (CH)	6.80 (d, 8.3)	116.2	6.69 (d, 7.3)
8	162.1 (C)	11.0 (OH-8, s)	162.1	11.03 (OH-8, s)
9	108.3 (C)		108.2	
10	139.4 (C)		139.3	
11	20.8 (CH_3)	1.50 (3H, d, 6.3)	20.8	1.53 (d, 6.3)
12				

3.3.5.12. Compound AF14 (cis-4-hydroxymellein)

(3R,4S)-4,8-dihydroxy-3-methylisochroman-1-one	
Synonyms	*cis*-4-hydroxymellein
Sample codes	AF14
Sample Amount	15 mg
Physical Description	yellow amorphous powder
Molecular Formula	$C_{10}H_{10}O_4$
Molecular Weight	194 g/mol
Optical Rotation $[\alpha]_D^{20}$	- 42 (*c* 0.05 in MeOH)
Retention time (LC-MS)	7.05 min

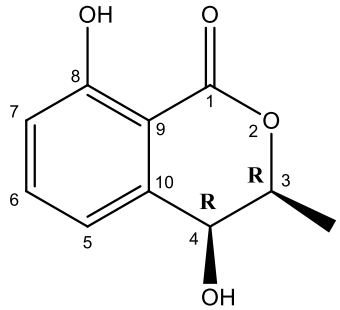

LC-HRFTMS spectrum $[M+H]^+$ 195.0649

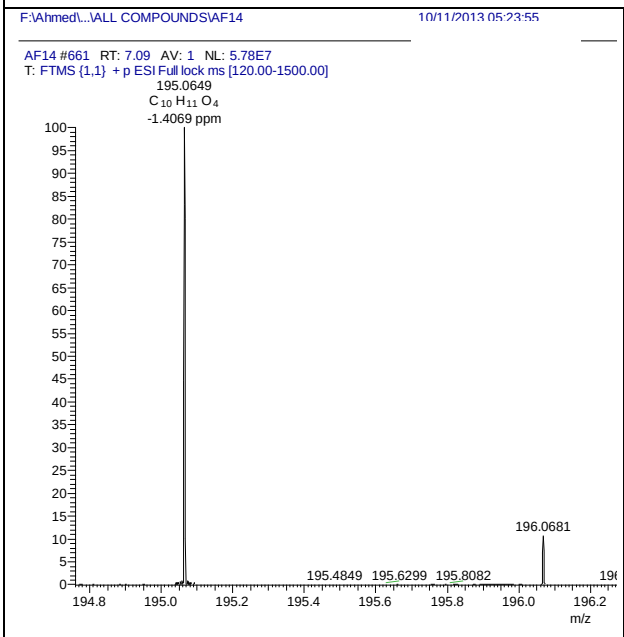

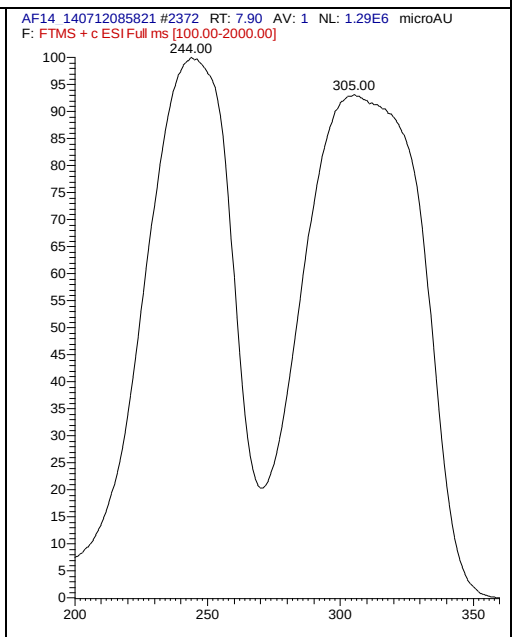

Compound AF14 (15 mg), was obtained as a yellow powder, exhibited a molecular formula $C_{10}H_{10}O_4$ established by ESI-HRMS at *m/z* = 195.0649

$[M+H]^{+\cdot}$ The optical rotation $[\alpha]^{20}_{D}$ = -42 (*c* 0.05 in MeOH). The **^{1}H NMR** spectrum ($CDCl_3$, 400 MHz) (Fig.151) of compound AF14 showed the three ABC aromatic protons of the benzene ring at δ_H 7.5 (m, H-6), 7.01 (d, 8.4 Hz, H-7) and 6.91 (d, 7.3 Hz, H-5) while OH-8 was at δ_H 10.98 (s). The oxygenated region showed two protons at δ_H 4.69 (qd, 1.85, 6.56 Hz, H-3) and 4.56 (d, 1.72 Hz, H-4) while the aliphatic region was characterized by presence of the methyl protons Me-11 at δ_H 1.58 (d, 6.61 Hz). The **^{13}C NMR** spectrum ($CDCl_3$, 400 MHz) (Fig.153) of compound AF14 showed ten carbons including five aromatic, one phenolic, one carbonyl, two oxygenated methines and one methyl. The **^{1}H-^{1}H COSY** spectrum (Fig.154) of compound AF14 showed the ABC spin system connecting the three aromatic protons and another spin system connected H-3 to the methyl gp Me-11. The structure was confirmed from the **HMBC** spectrum (Fig.155) through the correlations of H-5 with C-4 (δ_C 67.3), C-9 (δ_C 106.9) and C-7 (δ_C 118.6). In addition, H-6 correlated with C-8 (δ_C 162.1) and C-10 (δ_C 140.5); H-7 with C-5 (δ_C 118.3), C-8 and C-9; OH-8 with C-7, C-8 and C-9; H-4 with C-3 (δ_C 78.28), C-5, C-9 and C-10. Finally Me-11 with C-4 and C-3. So from the above and comparison to the literature (Asha et al., 2004) (Table 26), Compound AF14 (Fig.156) was identified as *cis*-4-hydroxymellein ((3R,4R)-4,8-dihydroxy-3-methylisochroman-1-one).

3.3.5.13. Compounds AF13 (trans-4-hydroxymellein)

(3R,4R)-4,8-dihydroxy-3-methylisochroman-1-one	
Synonyms	*trans*-4-hydroxymellein
Sample codes	AF13
Sample Amount	13 mg
Physical Description	yellow amorphous powder
Molecular Formula	$C_{10}H_{10}O_4$
Molecular Weight	194 g/mol
Optical Rotation $[\alpha]_D^{20}$	- 16 (*c* 0.05 in MeOH)
Retention time (LC-MS)	8.12 min

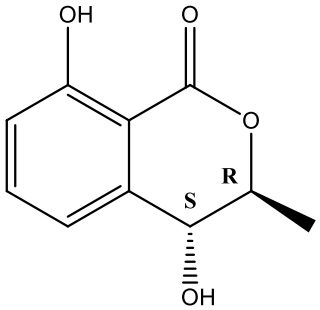

LC-HRFTMS spectrum $[M+H]^+$ 195.0652

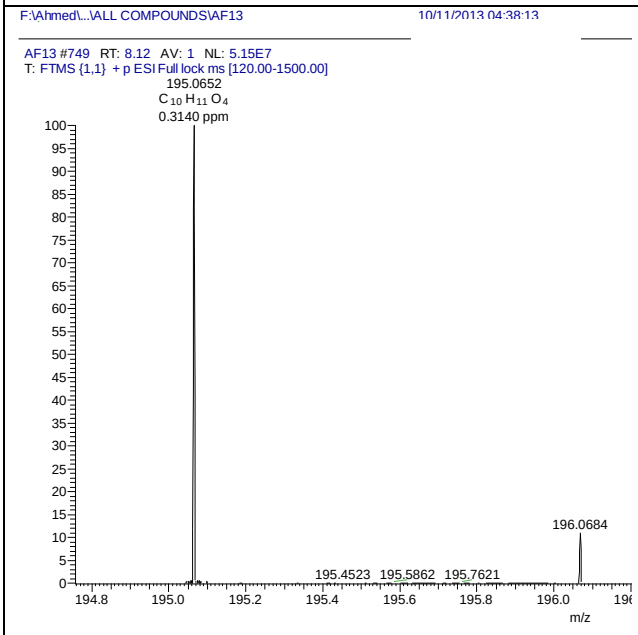

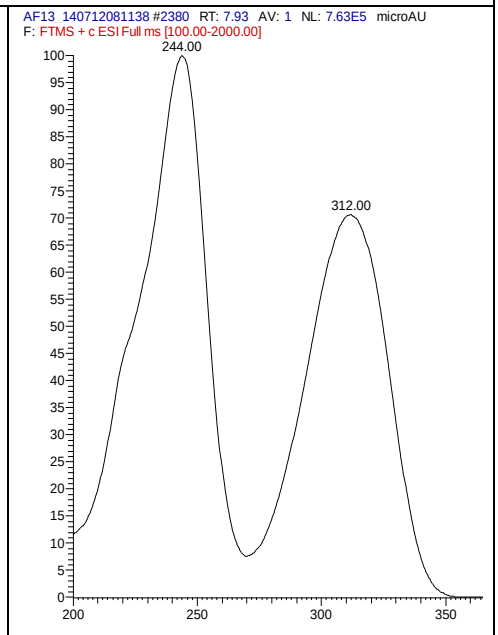

Compound AF13 (13 mg) was obtained as a yellow powder, exhibited a

molecular formula $C_{10}H_{10}O_4$ established by ESI-HRMS at *m/z* = 195.0652 $[M+H]^+$. The optical rotation $[\alpha]^{20}_D$ = -16 (*c* 0.05 in MeOH). Compounds AF13 and AF14 are diastereomers of 4-hydroxymellein so the ^1H NMR data included the same proton peaks with some variance in the chemical shift of some protons which were affected by the change in configuration of OH-4 (Table 26). The **^{1}H NMR** spectrum (Fig.152) of compound AF13 was characterized by the downfield shift of H-5 at δ_H 6.97 (d, 8.4 Hz) and H-4 at δ_H 4.60 (brs) and upfield shift of H-3 at δ_H 4.56 (dd, 1.55, 5.3 Hz) and Me-11 at δ_H 1.49 (d, 6.14 Hz). So from the above and in accordance to the reported data (Asha et al., 2004) (Table 26), compound AF13 (Fig.156) was identified as *trans*-4-hydroxymellien (3R,4S)-4,8-dihydroxy-3-methylisochroman-1-one.

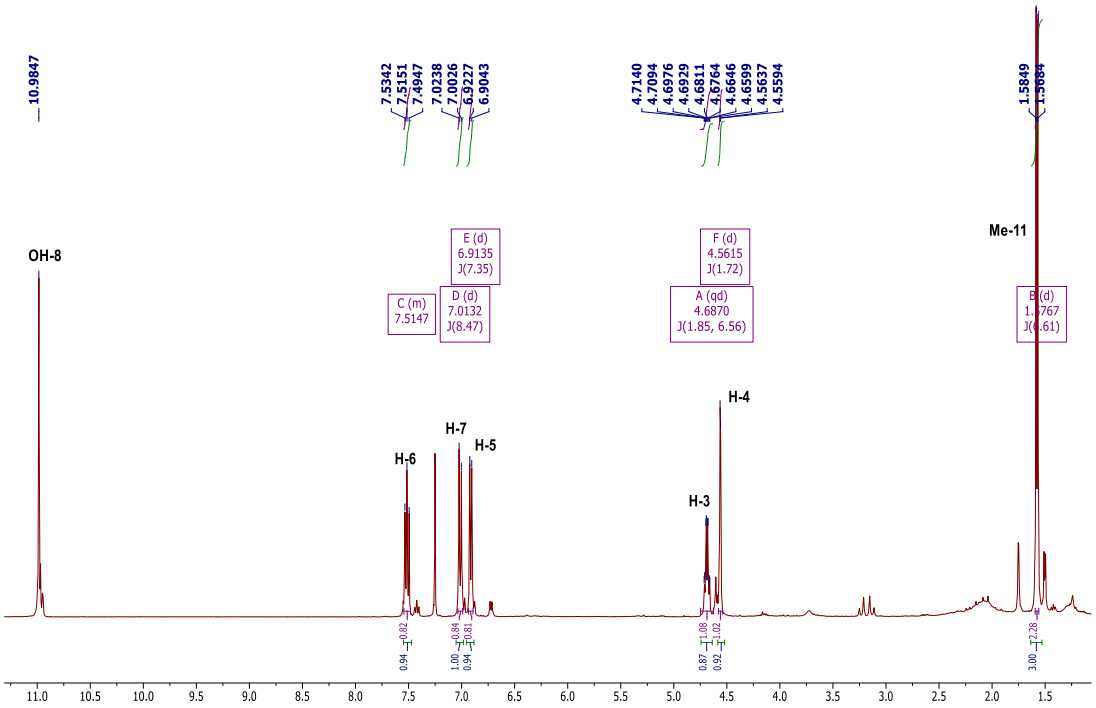

Fig.151 ^{1}HNMR spectrum of compound AF14

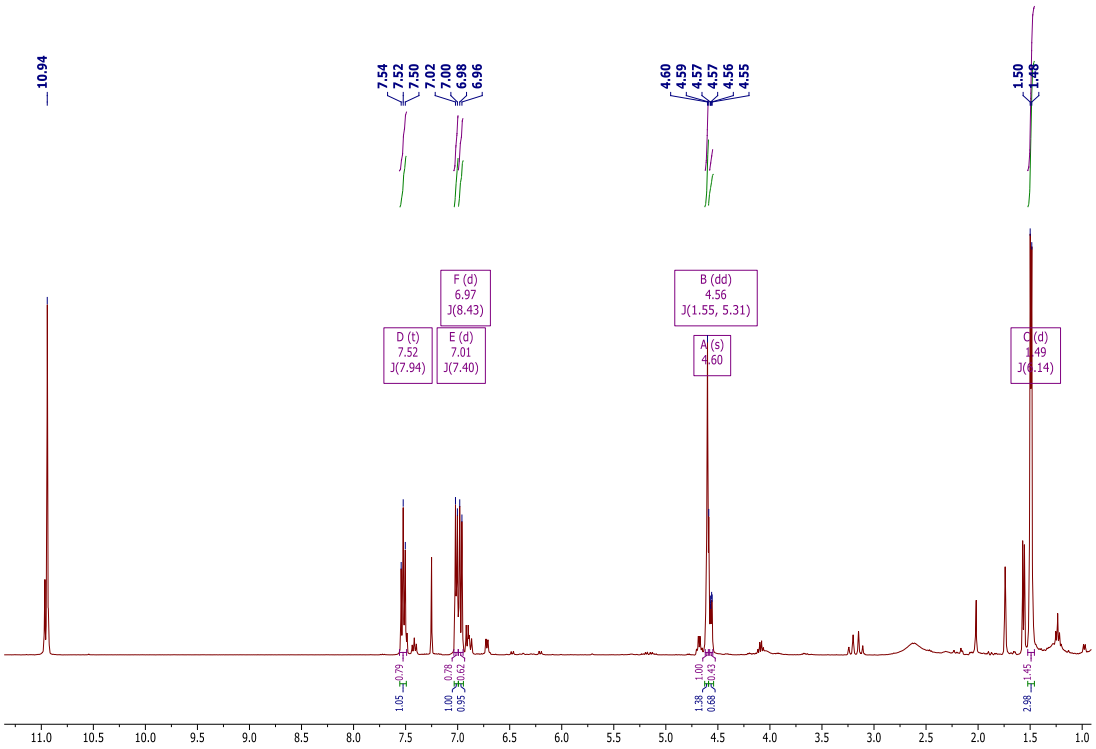

Fig.152 ^{1}H NMR spectrum of compound AF13

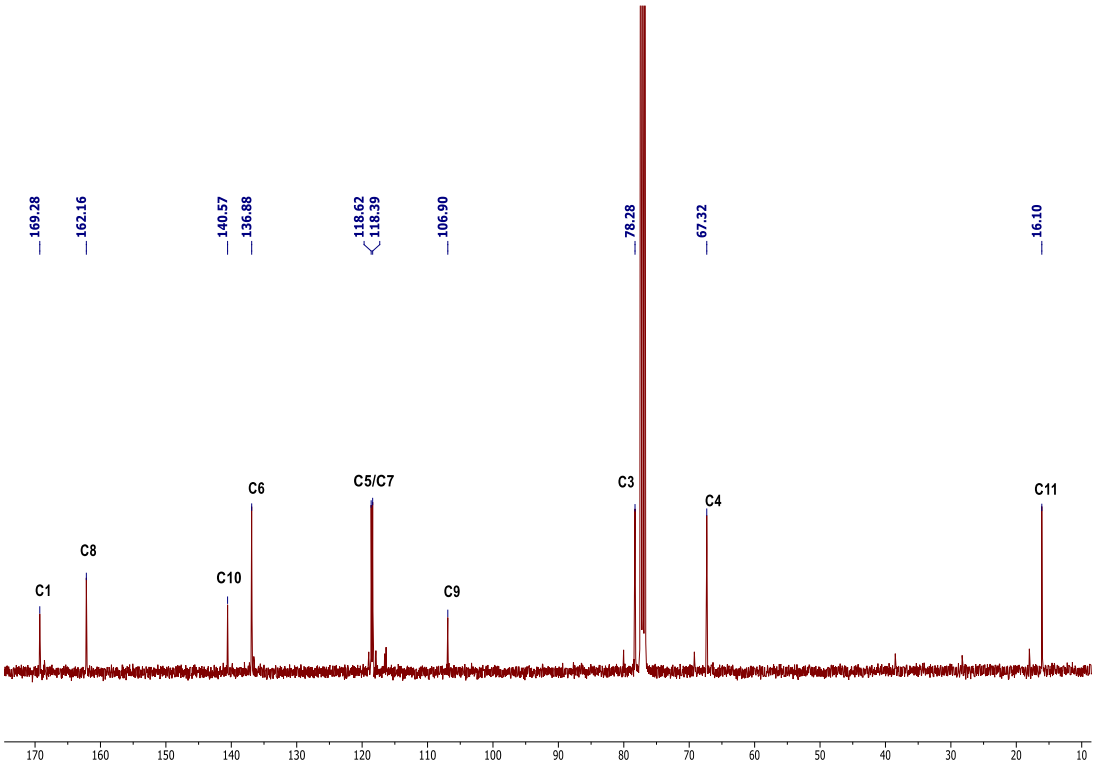

Fig.153 ^{13}CNMR spectrum of compound AF14

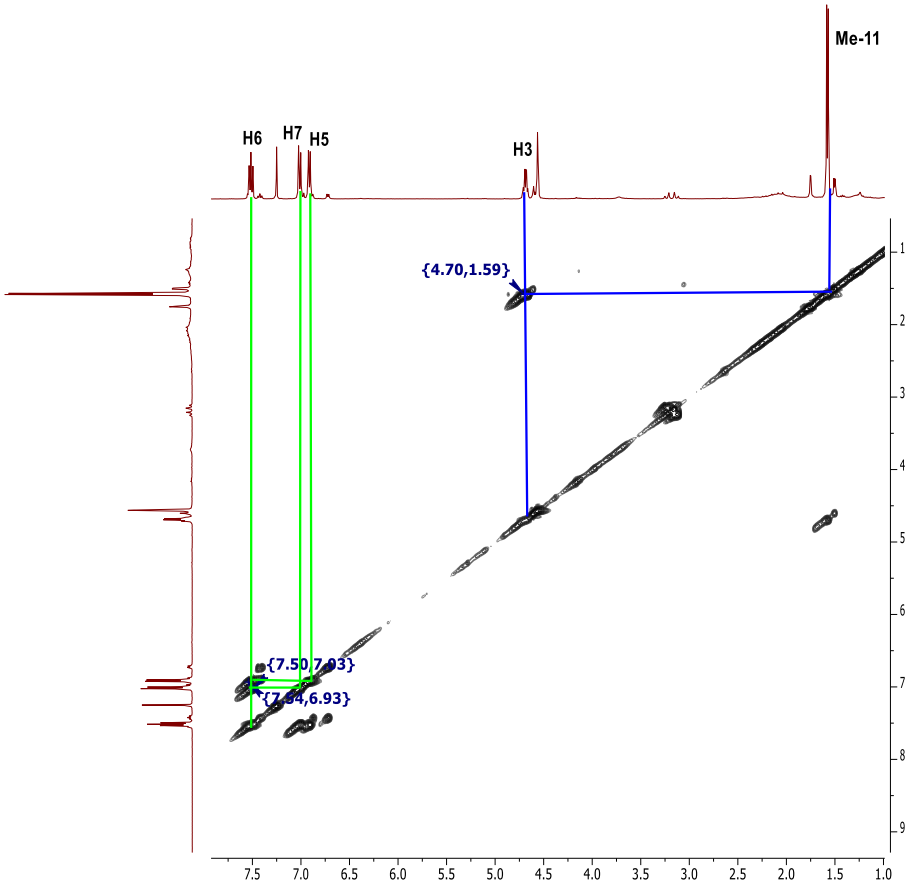

Fig.154 ^{1}H-^{1}H COSY spectrum of compound AF14 showing two spin systems

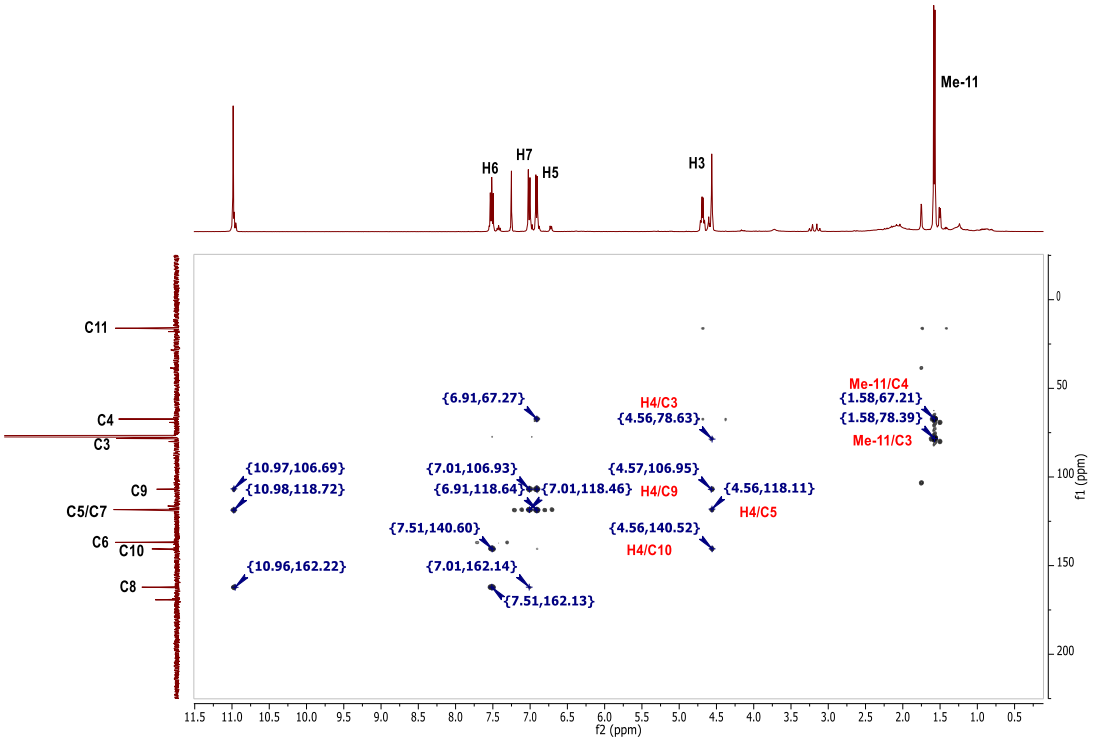

Fig.155 HMBC spectrum of compound AF14

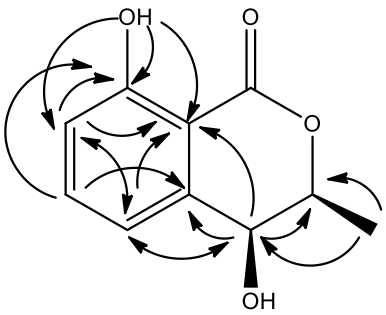

AF14

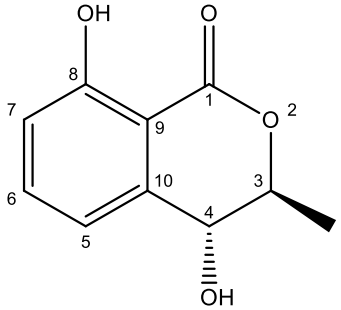

AF13

Fig.156 HMBC correlations of AF13 and AF14

Table 26: ^{1}H NMR and ^{13}C NMR data of compounds AF13, AF14 and literature

No.	AF14-$CDCl_3$		AF13-$CDCl_3$	*cis*-4-hydroxymellein-$CDCl_3$, Asha 2004		*trans*-4-hydroxymellein-$CDCl_3$	
	δ_C (m)	δ_H (m, *J* in Hz)	δ_H (m, *J* in Hz)	δ_H (m, *J* in Hz)	δ_C	δ_H (m, *J* in Hz)	δ_C
1	169.3 (C)				162.0		161.9
3	78.3 (CH)	4.69 (qd, 1.85, 6.56 Hz)	4.56 (dd, 1.55, 5.3 Hz)	4.67 (dq, 1.5, 6.5 Hz)	77.9	4.58 (dq, 4.5, 7.0)	79.8
4	67.3 (CH)	4.56 (d, 1.72 Hz)	4.60 (brs)	4.55 (brs)	67.1	4.60 (brs)	69.1
5	118.3 (CH)	6.91 (d, 7.3 Hz)	6.97 (d, 8.4 Hz)	6.90 (d, 7.0 Hz)	140.8	7.0 (d, 8.5 Hz)	141.0
6	136.8 (CH)	7.50 (t, 8.1 Hz)	7.50 (t, 7.9 Hz)	7.47 (t, 7.0 Hz)	118.1	7.52 (t, 8.5 Hz)	116.1
7	118.6 (CH)	7.01 (d, 8.4 Hz)	7.01 (d, 7.4 Hz)	7.01 (d, 7.0 Hz)	137.0	6.97 (d, 8.5 Hz)	136.7
8	162.1 (C)	10.98 (s, OH-8)	10.94 (s, OH-8)	11.01 (s)	118.4	10.97 (s)	117.8
9	106.9 (C)				162.0		161.9
10	140.5 (C)				106.9		106.7
11	16.1 (CH_3)	1.58 (d, 6.61 Hz)	1.49 (d, 6.14 Hz)	1.56 (d, 6.5 Hz)	15.9	1.49 (d, 6.5 Hz)	17.8

3.3.5.14. Compounds AF15 (5-hydroxy mullein)

(S)-5,8-dihydroxy-3-methylisochroman-1-one	
Synonyms	5-hydroxy mellein
Sample codes	AF15
Sample Amount	10 mg
Physical Description	white amorphous powder
Molecular Formula	$C_{10}H_{10}O_4$
Molecular Weight	194 g/mol
Optical Rotation $[\alpha]_D^{20}$	- 52 (*c* 0.05 in MeOH)
Retention time (LC-MS)	9.53 min

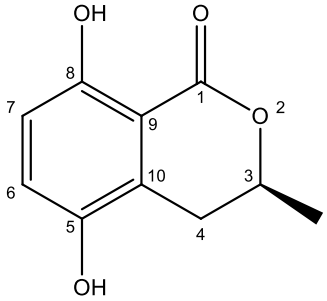

LC-HRFTMS spectrum $[M+H]^+$ 195.0653

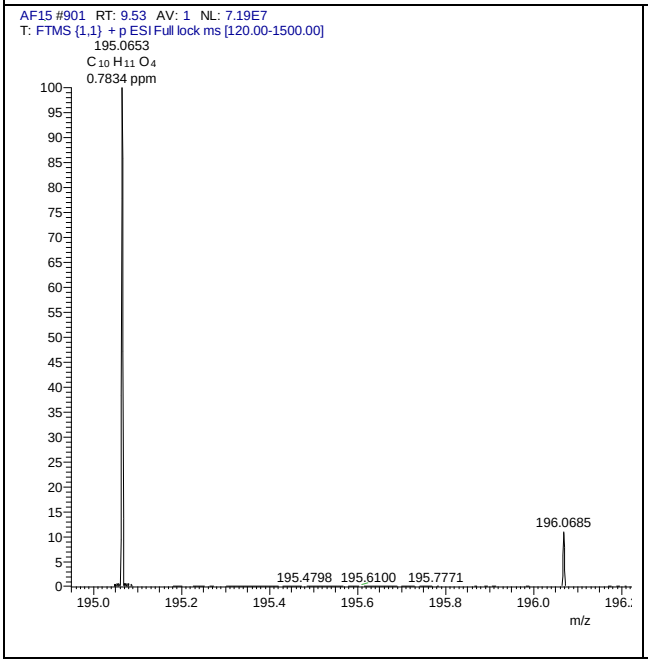

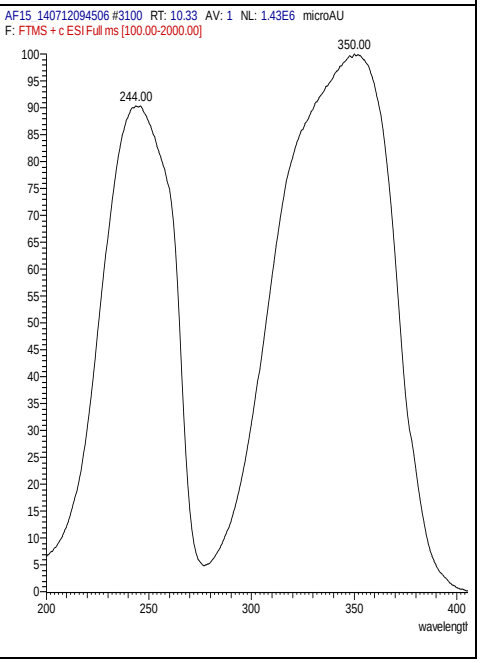

Compound AF15 (10 mg) was obtained as a white powder, exhibited a molecular formula $C_{10}H_{10}O_4$ established at *m/z* = 195.0653 $[M+H]^+$. The optical rotation

$[\alpha]^{20}_{D}$ = -52 (*c* 0.05 in MeOH). The **^{1}H NMR** spectra of compound AF15 ($(CD_3)_2CO$, 400 MHz) (Fig.157) showed the aromatic protons including two ortho-coupled protons of the benzene ring at δ_H 7.11 (d, 8.9 Hz, H-6) and 6.71 (d, 8.7 Hz, H-7). The aliphatic region showed the same protons as mellein at δ_H 3.18 (dd, 3.4, 16.9 Hz, H-4a); 2.64 (dd, 11.6, 16.8 Hz, H-4b); 4.74 (m, H-3) and 1.49 (d, 6.24 Hz, Me-11). The **^{1}H-^{1}H COSY** spectrum of compound AF15 (Fig.159) showed the AB spin system connected the ortho-coupled protons H-6 and H-7 of the aromatic ring and the other spin system connected H-3, H-4a, H-4b and Me-11. The **^{13}C NMR** spectrum of compound AF15 ($(CD_3)_2CO$, 400 MHz) (Fig.160) showed ten carbons including six aromatic (two of them phenolic), one carbonyl, one oxygenated methine, one methylene and one methyl. The **HMBC** spectrum of compound AF15 (Fig.161) confirmed the structure through the correlations of OH-8 (δ_H 10.57) with C-8 (δ_C 155.4), C-7 (δ_C 115.3) and C-9 (δ_C 108.3); OH-5 (δ_H 8.28) with C-5 (δ_C 145.4) and C-10 (δ_C 124.8). In addition, H-6 correlated with C-5, C-10 and C-8; H-7 with C-8 and C-9; H-4a with C-5, C-10 and C-9; H-4b with C-3 (δ_C 76.1) and Me-11 (δ_C 20.2) which further correlated with C-3 and C-4 (δ_C 28.2). So from the above and in accordance to the reported data (Araujo et al. 2012) (Table 27), compound AF15 was identified as 5-hydroxymellein (Fig.162).

3.3.5.15. Compound AF18 (4,5-dihydroxy mullein)

(3S,4R)-4,5,8-trihydroxy-3-methylisochroman-1-one	
Synonyms	4,5-dihydroxy mellein
Sample codes	AF18
Sample Amount	17 mg
Physical Description	white amorphous powder
Molecular Formula	$C_{10}H_{10}O_5$
Molecular Weight	210 g/mol
Optical Rotation $[\alpha]_D^{20}$	+ 8 (*c* 0.05 in MeOH)
Retention time (LC-MS)	6.02 min

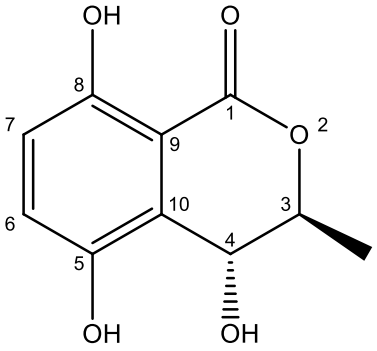

LC-HRFTMS spectrum $[M+H]^+$ 211.0599

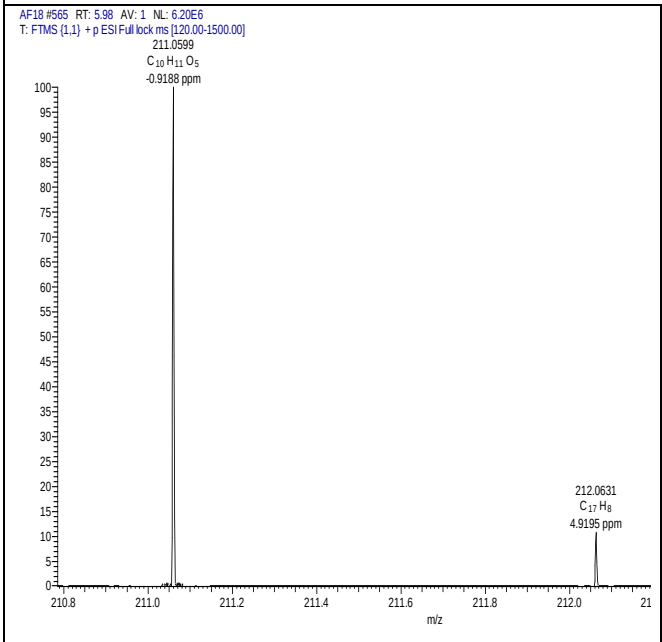

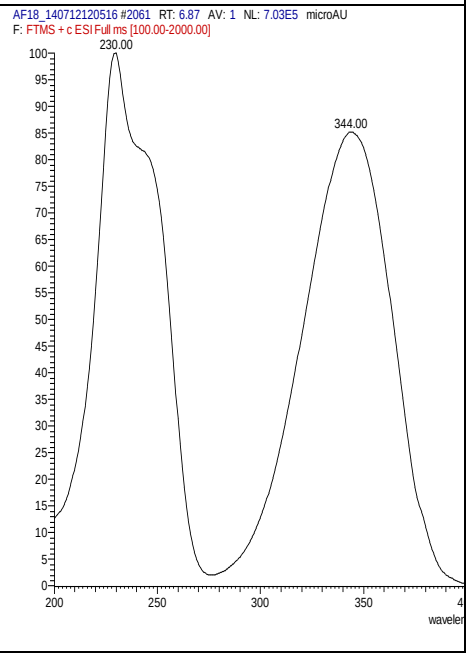

Compound AF18 (17 mg) was obtained as a white powder, exhibited a molecular

formula $C_{10}H_{10}O_5$ established at *m/z* = 211.0599 $[M+H]^+$. The optical rotation $[\alpha]^{20}_D$ = +8 (*c* 0.05 in MeOH). The **^{1}H NMR** spectrum of compound AF18 ($CDCl_3$, 400 MHz) (Fig.158) was a mixture of 4,5-dihydroxymellein (major) and 4-hydroxymellein (minor) with a ratio (2:1). So by exclusion of the proton signals belonged to the minor compound, the aromatic region resembled that of AF15. It was characterized by the ortho-coupled aromatic protons at δ_H 7.07 (d, 9.06 Hz, H-6) and 6.89 (d, 9.07 Hz, H-7) while the aliphatic region was distinguished by the replacement of C*H*$_2$-4 in AF15 by carbinolic H-4 at δ_H 4.99 (d, 8.2 Hz, H-4). Moreover, H-3 and Me-11 was assigned at 4.6 (m) and 1.53 (d, 6.4 Hz) respectively. The **^{13}C NMR** data (Table 28) of compound AF18 was similar to that of AF15. However, the methylene group C*H*$_2$-4 was replaced by one oxygenated methine C-4 (δ_C 66.3). The presence of the methine proton (H-4), instead of the methylene in AF15, was confirmed through the **HMBC** correlation of H-4 with C-5 (δ_C 146.6), C-10 (δ_C 121.9), C-9 (δ_C 106.17), C-3 (δ_C 78.9) and Me-11 (δ_C 17.75). So from the above and comparison to the literature (Jian et al. 2011) (Table 28) compounds AF18 was 4-hydroxy congener of compound AF15 (5-hydroxymellein) (Fig.162).

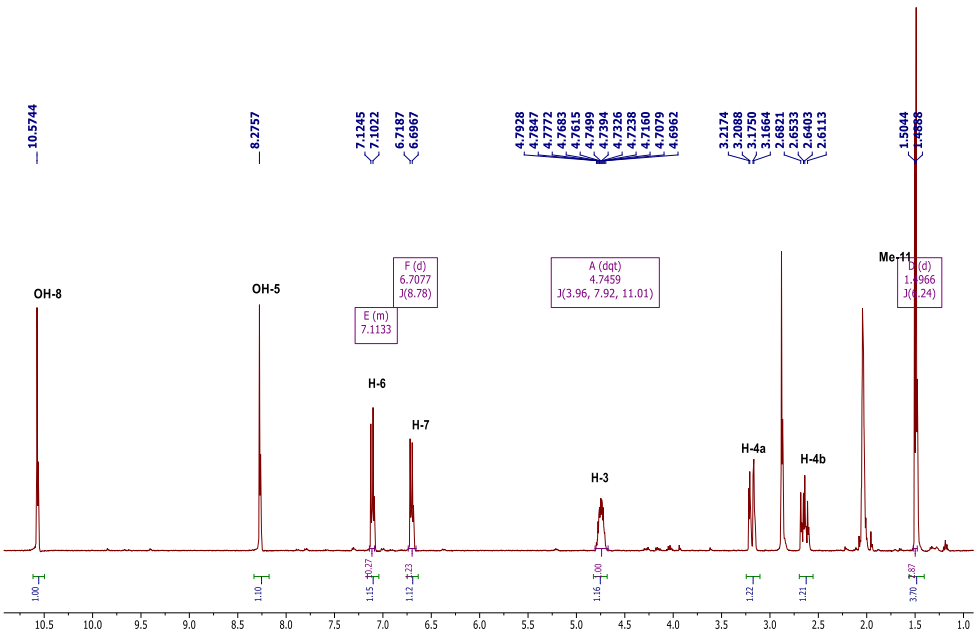

Fig.157 ^{1}H NMR spectrum of compounds AF15

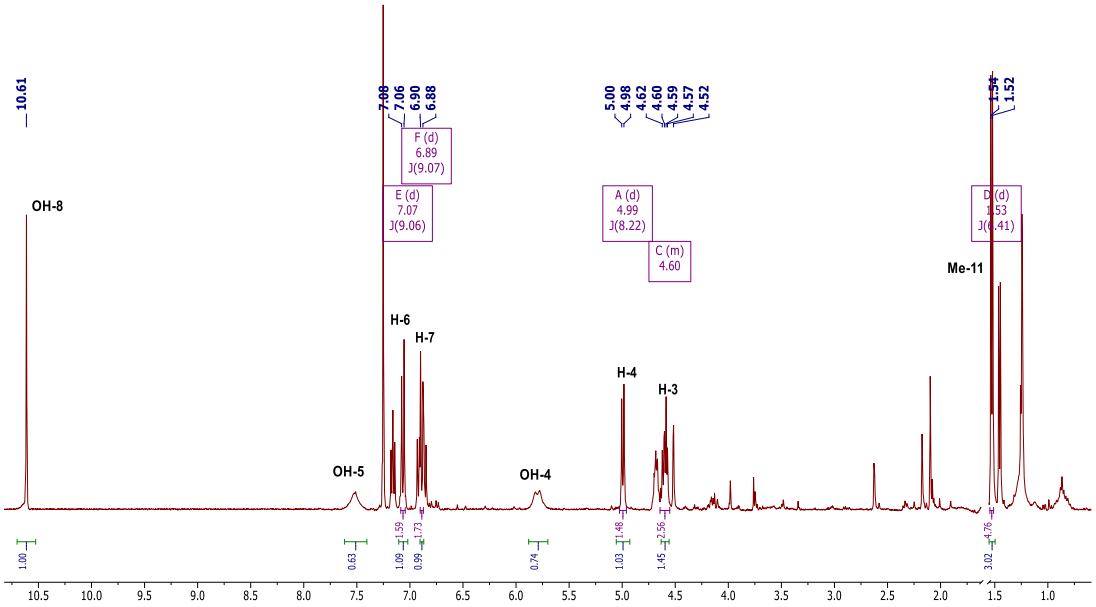

Fig.158 ^{1}H NMR spectrum of compound AF18

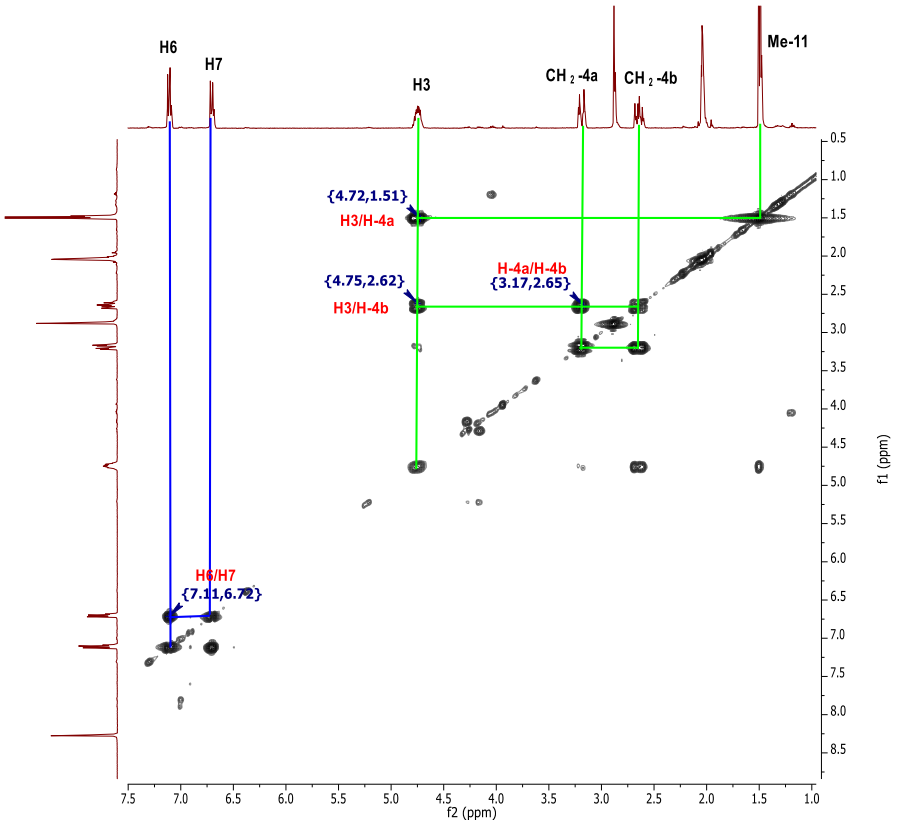

Fig.159 Expansion of ^{1}H-^{1}H COSY spectrum of compound AF15 showing two different spin systems

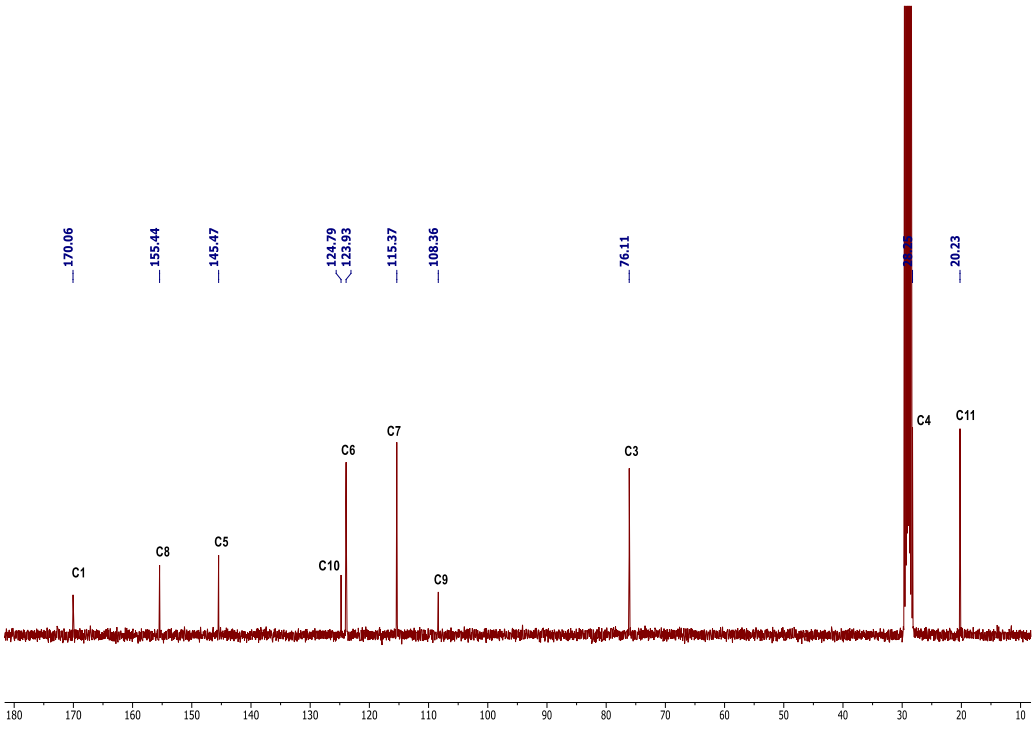

Fig.160 ^{13}C NMR spectrum of compound AF15

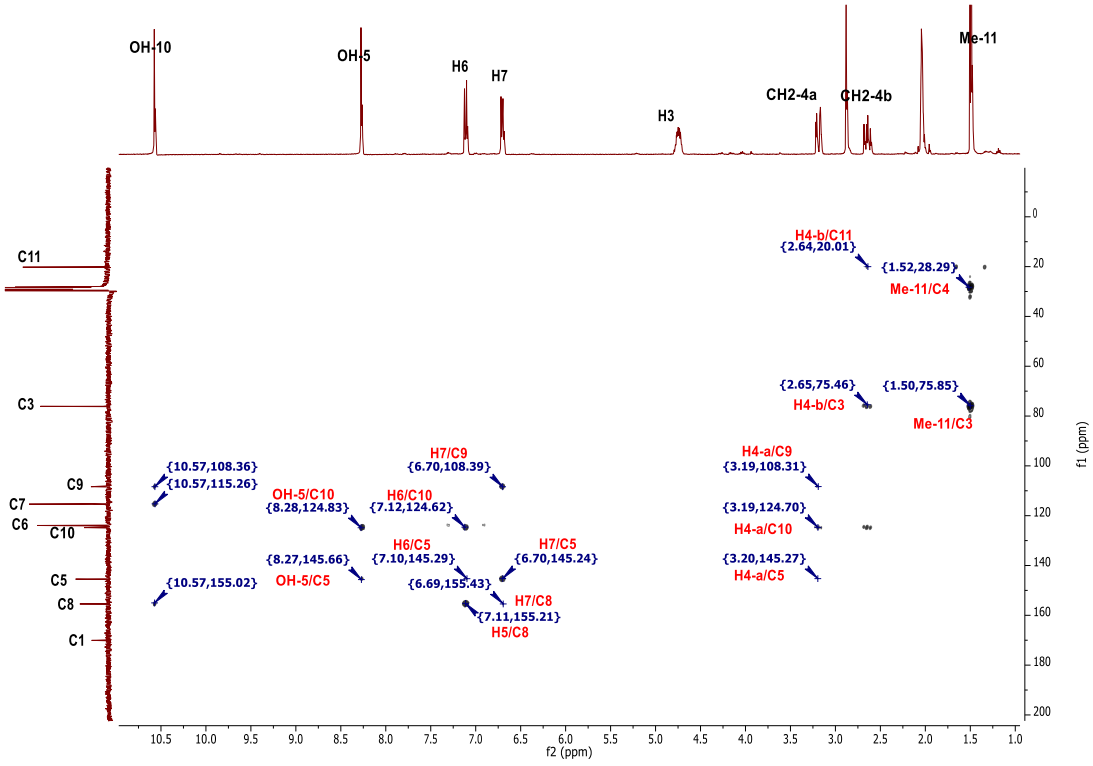

Fig.161 HMBC spectrum of compound AF15

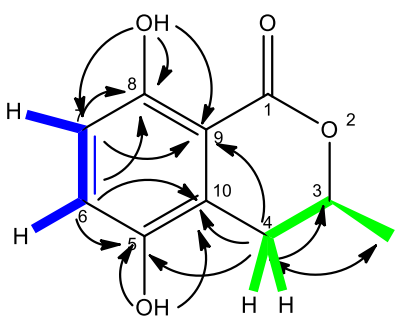

AF15

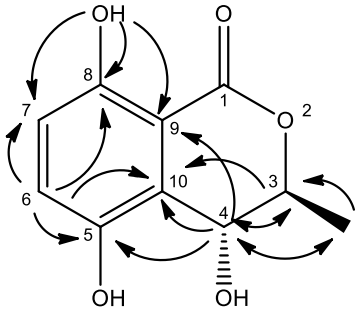

AF18

Fig.162 HMBC correlations of compounds AF15 and AF18

Table 27: ^{1}H NMR and ^{13}C NMR data of AF15 and literature

Atom No.	AF15-$(CD_3)2CO$		Araujo 2012-$CDCl_3$	
	δ_C (m)	δ_H (m, *J* in Hz)	δ_C	δ_H (m, *J* in Hz)
1	170.1 (C)		170.9	
3	76.1 (CH)	4.74 (m)	77.0	4.75 (m)
4	28.2 (CH_2)	3.18 (dd, 3.4, 16.9 Hz, H-4a), 2.64 (dd, 11.6, 16.8 Hz, H-4b)	21.1	3.19 (dd, 11.5, 16.9 Hz, H-4a), 2.65 (dd, 3.4, 16.9 Hz, H-4b)
5	145.4 (C)	8.28 (s, OH-5)	146.4	8.38 (s, OH)
6	123.9 (CH)	7.11 (d, 8.9 Hz)	124.8	7.41 (d, 8.9 Hz)
7	115.3 (CH)	6.71 (d, 8.7 Hz)	116.2	6.71 (d, 8.9 Hz)
8	155.4 (C)	10.57 (s, OH-8)	156.3	10.57 (s, OH)
9	108.3 (C)		109.2	
10	124.8 (C)		125.7	
11	20.2 (CH_3)	1.49 (3H, d, 6.24 Hz)	20.3	1.50 (3H, d, 6.3 Hz)

Table 28: ^{1}H NMR and ^{13}C NMR data of AF18 and literature

Atom No.	AF18-$CDCl_3$			Jian 2011-$(CD_3)2CO$	
	δ_C (m)	δ_H (m, *J* in Hz)	HMBC	δ_C	δ_H (m, *J* in Hz)
1	168.7 (C)			170.3	
3	78.9 (CH)	4.6 (m)	C4, C10	82.5	4.81 (dq, 4.4, 6.8 Hz)
4	69.0 (CH)	4.99 (d, 8.2 Hz)	C3, 5, 9, 10, Me-11	66.3	4.99 (brd, 4.4 Hz)
5	146.6 (C)	7.51 (s, OH)		149.2	4.58 (brs, OH)
6	126.5 (CH)	7.07 (d, 9.06 Hz)	C5, 7, 8, 10	127.2	7.16 (d, 8.8 Hz)
7	118.9 (CH)	6.89 (d, 9.07 Hz)	C5, 9	119.4	6.81 (d, 8.8 Hz)
8	156.3 (C)	10.61 (s, OH)	C7, 8, 9	157.0	10.66 (s, OH)
9	106.2 (C)			108.9	
10	121.9 (C)			125.7	
11	17.7 (CH_3)	1.53 (3H, d, 6.4 hz)	C3, 4	19.1	
		5.78 (brd, OH-4)			4.52 (brs)

3.3.5.16. Compound AF17 (diorcinol)

5,5'-oxybis(3-methylphenol)	
Synonyms	Diorcinol
Sample codes	AF17
Sample Amount	12 mg
Physical Description	brown amorphous powder
Molecular Formula	$C_{14}H_{14}O_3$
Molecular Weight	230 g/mol
Retention time (LC-MS)	14.60 min

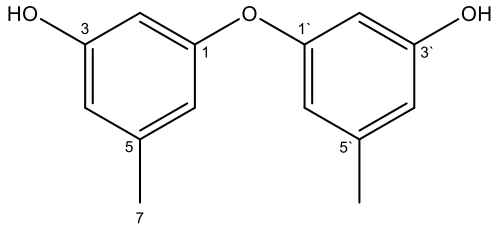

LC-HRFTMS spectrum $[M+H]^+$ 231.1015

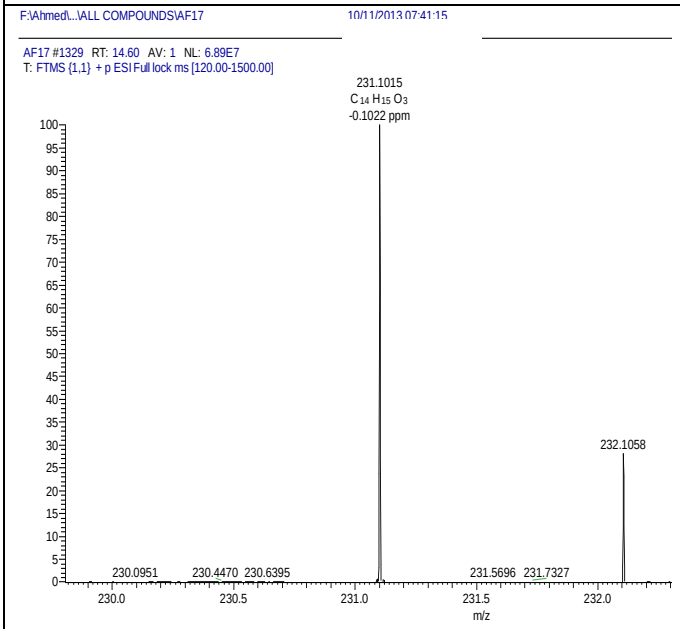

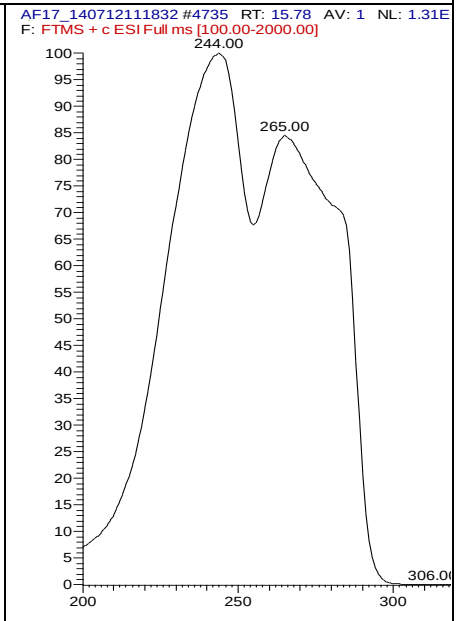

Compound AF17 (12 mg) was obtained as a brown powder, exhibited a molecular formula $C_{14}H_{14}O_3$ established by ESI-HRMS at *m/z* = 231.1015 $[M+H]^+$. The **^{1}H NMR** spectrum (DMSO, 400 MHz) (Fig.163) showed three broad singlets in the aromatic region at δ_H 6.16 (2H, br.t, H-2,2`), 6.34 (2H, brs, H-4,4`) and 6.24 (2H,

brs, H-6,6`) while the aliphatic region was only containing one singlet signal equivalent for Me-7,7` at δ_H 2.18 (6H, *s*). The **^{13}C NMR** spectrum (DMSO, 400 MHz) (Fig.164) showed seven carbon signals including six aromatic (two of them oxygenated) and one methyl. The structure was confirmed from the **HMBC** spectrum (Fig.165) through the correlations of OH-3/OH-3` ($\delta_H$ 9.43) with C-3/C-3` (δ_C 158.8), C-2/C-2` ($\delta_C$ 103.4) and C-4/C-4` (δ_C 111.6); H-2/H-2` with C-1/C-1` (δ_C 158.1), C-3/C-3` and C-4/C-4`. In addition, H-4/H-4` correlated with C-2/C-2`, C-6/C-6` ($\delta_C$ 110.6) and Me-7/Me-7` (δ_C 21.6); H-6/H-6` with C-1/C-1`, C-2/C-2`, C-4/C-4` (δ_C 111.6) and Me-7/Me-7` which further correlated with C-5/C-5` (δ_C 140.6) and C-4/C-4`. So from the above and comparison to the literature (Fremlin et al., 2009) (Table 29), compound AF17 (Fig. 166) was identified as diorcinol.

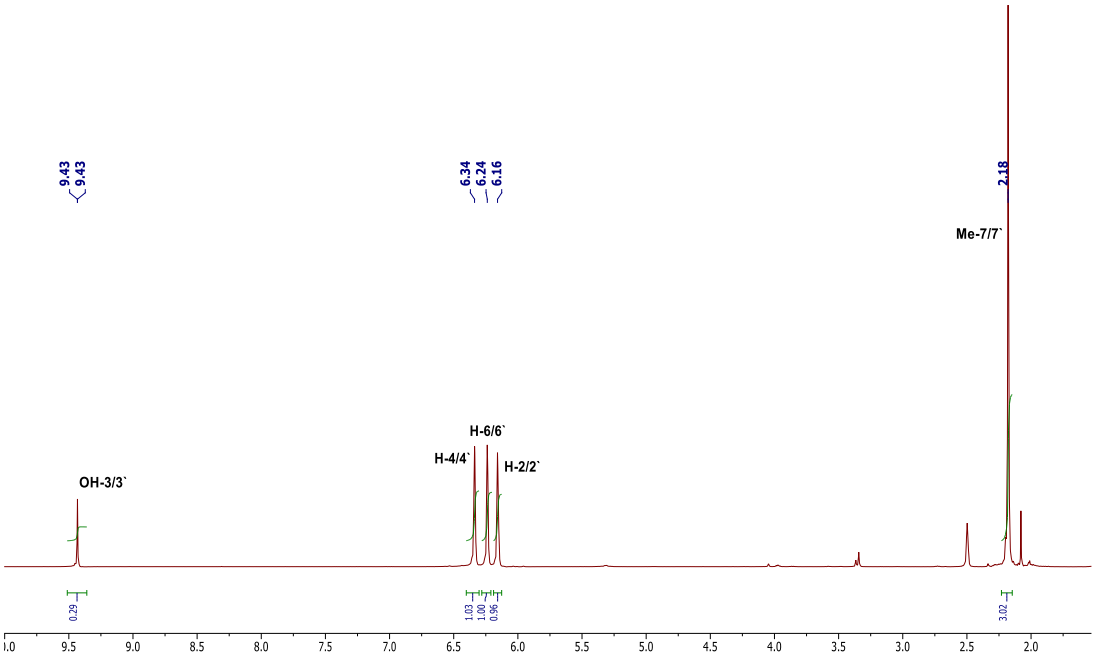

Fig.163 ^{1}H NMR spectrum of compound AF17

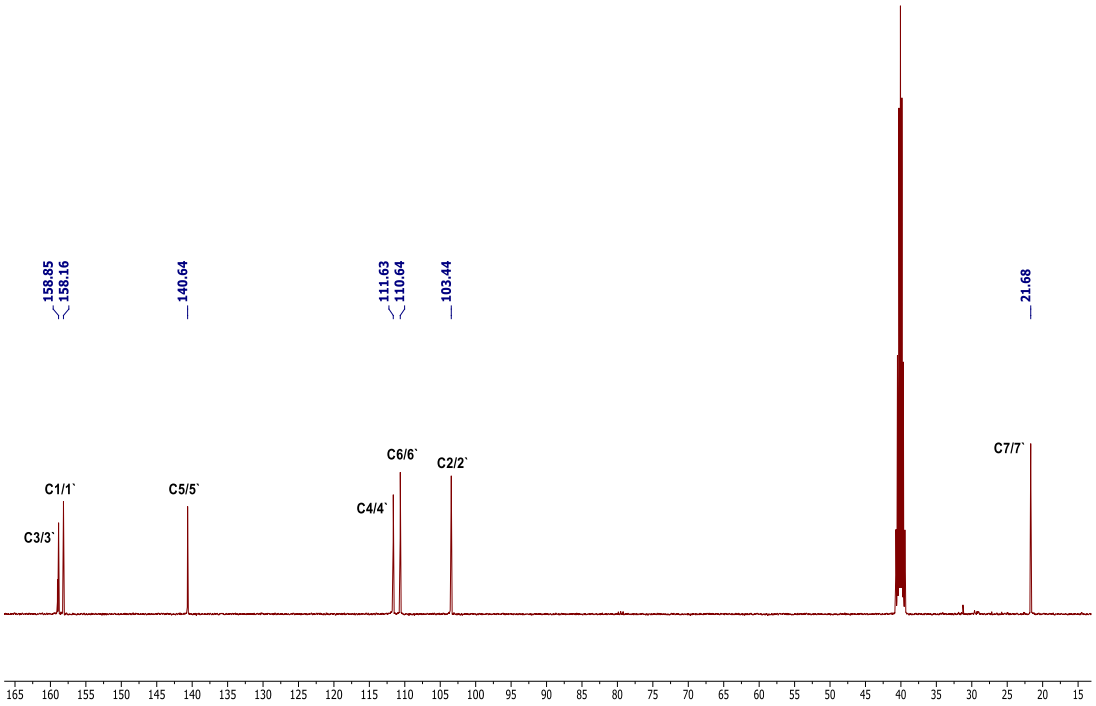

Fig.164 ^{13}C NMR spectrum of compound AF17

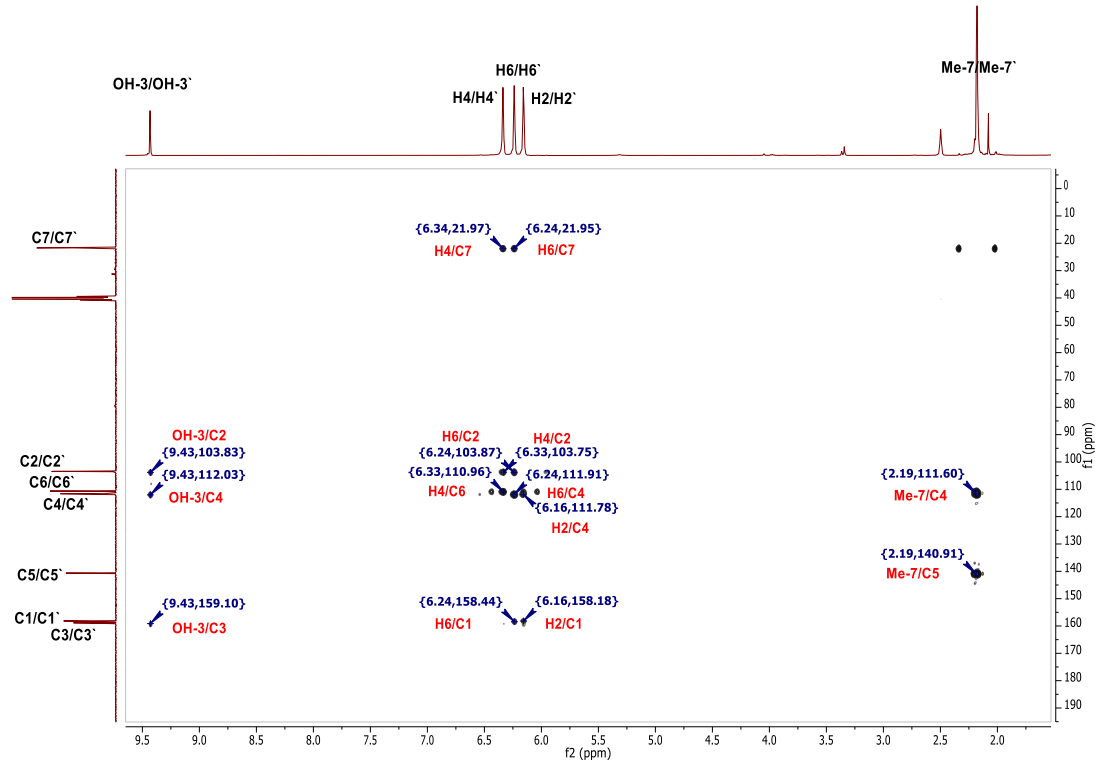

Fig.165 HMBC spectrum of compound AF17

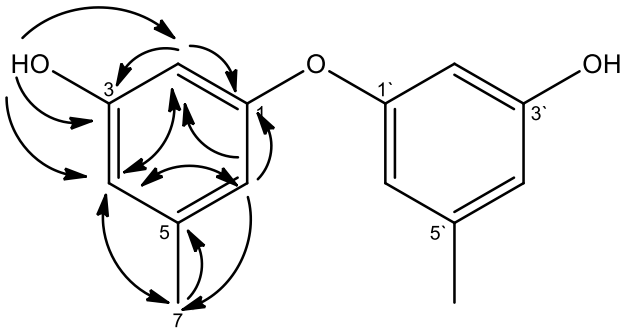

Fig.166 HMBC correlations of compound AF17

Table 29: ^{1}H NMR and ^{13}C NMR data of compound AF17 and literature

Atom No.	AF17-DMSO (400 MHz)		FremLin 2009-DMSO (600 MHz)	
	δ_C (m)	δ_H (m, *J* in Hz)	δ_C	δ_H (m, *J* in Hz)
1/1`	158.2 (C)		157.6	
2/2`	103.4 (CH)	6.16 (br.t)	102.9	6.45 (t, 2.0)
3/3`	158.8 (C)	9.43 (brs, OH)	158.4	9.45 (s, OH)
4/4`	111.6 (CH)	6.34 (brs)	111.1	6.33 (m)
5/5`	140.6 (C)		140.0	
6/6`	110.6 (CH)	6.24 (brs)	110.0	6.24 (m)
Me-7/Me-7`	21.6 (CH_3)	2.18 (s)	21.1	2.18 (s)

3.3.5.17. Compounds AF19 (phomaligol A)

(2S)-2-hydroxy-3-methoxy-2,6-dimethyl-1,5-dioxocyclohex-3-en-6-yl 2-methylbutanoate	
Synonyms	Phomaligol A
Sample codes	AF19
Sample Amount	7 mg
Physical Description	yellow oily
Molecular Formula	$C_{14}H_{20}O_6$
Molecular Weight	284 g/mol
Optical Rotation $[\alpha]_D^{20}$	-49 (*c* 0.1, $CHCl_3$)
Retention time (LC-MS)	12 min

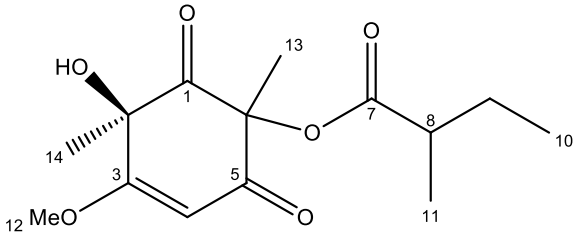

LC-HRFTMS spectrum $[M+H]^+$ 285.1329

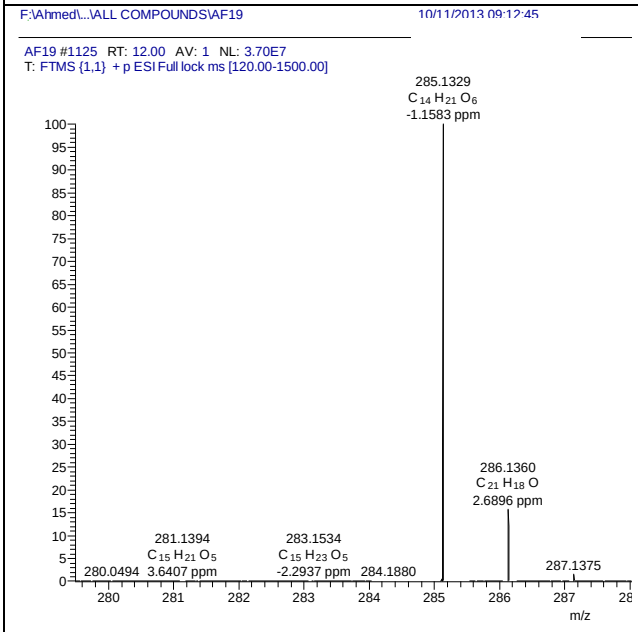

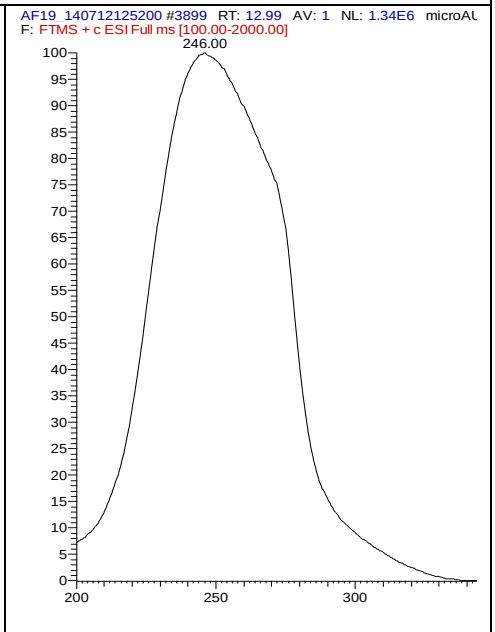

Compounds AF19 (7 mg) was obtained as yellow oil, exhibited a molecular formula $C_{14}H_{20}O_6$ established by ESI-HRMS at *m/z* = 285.1329 $[M+H]^+$. The optical rotation of compound AF19 $[\alpha]^{20}_D$ = -49 (*c* 0.1, $CHCl_3$). The **^{1}H NMR**

spectrum of compound AF19 (DMSO, 400 MHz) (Fig.167) showed ten signals at δ_H 6.69 (1H, s, OH-2), 5.59 (1H, s, H-4), 3.83 (3H, s, Me-12), 2.42 (1H, m, H-8), 1.57 (3H, s, Me-13), 1.56 (1H, m, H-9a), 1.43 (3H, s, Me-14), 1.42 (1H, s, H-9b), 1.05 (3H, d, 6.9 Hz, Me-11) and 0.89 (3H, t, 6.6 Hz, Me-10). The **^{13}C NMR** spectrum of compound AF19 (DMSO, 400 MHz) (Fig.168) showed 14 carbon signals including three carbonyls, three quaternaries, one olefinic methine, one methine, one methylene and five methyls. The structure was confirmed from the **HMBC** spectrum (Fig.169) through the correlations of OH-2 with C-1 (δ_C 201.8), C-2 (δ_C 72.8), C-3 (δ_C 175.3) and Me-14 (δ_C 21.9); H-4 with C-2, C-3, C-5 (δ_C 191.4) and C-6 (δ_C 82.8); Me-12 with C-3; Me-13 with C-5, C-6 and C-1; Me-14 with C-1, C-2 and C-3. While the butanoate substitution was confirmed through the correlations of H-8 with C-7 (δ_C 174.9), C-9 (δ_C 26.8) and Me-11 (δ_C 16.8) which in turn correlated to C-7, C-8 (δ_C 39.86) and C-9 (δ_C 26.8); H-9a with C-7 and C-8; H-9b to Me-10 which in turn correlated to C-9 and C-8. The **^{1}H-^{1}H COSY** spectrum (Fig.170) showed two spin systems one connected H-8 and Me-11 and the other connected H-9a, H-9b and Me-10. So from the above and in comparison to the literature (Elbandy et al., 2009) (Table 30), compound AF19 (Fig.171) was identified as phomaligol A.

3.3.5.18. Compound AF20 (phomaligol A1)

(2R)-2-hydroxy-3-methoxy-2,6-dimethyl-1,5-dioxocyclohex-3-en-6-yl 2-methylbutanoate	
Synonyms	Phomaligol A1
Sample codes	AF20
Sample Amount	5 mg
Physical Description	yellow oily
Molecular Formula	$C_{14}H_{20}O_6$
Molecular Weight	284 g/mol
Optical Rotation $[\alpha]_D^{20}$	+ 6 (*c* 0.05, $CHCl_3$)
Retention time (LC-MS)	10.64 min

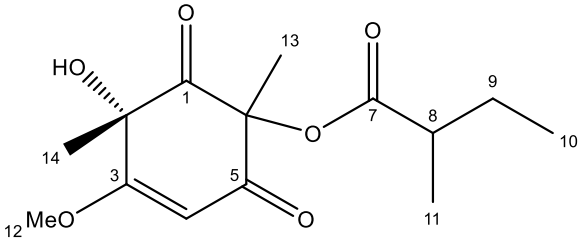

LC-HRFTMS spectrum $[M+H]^+$ 285.1331

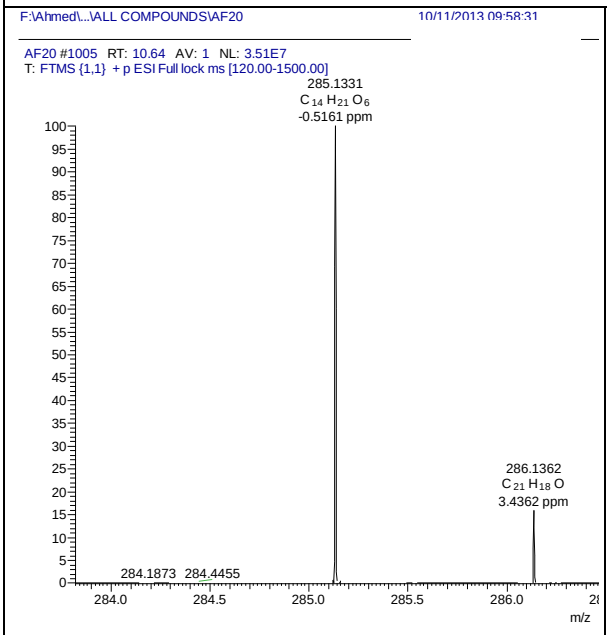

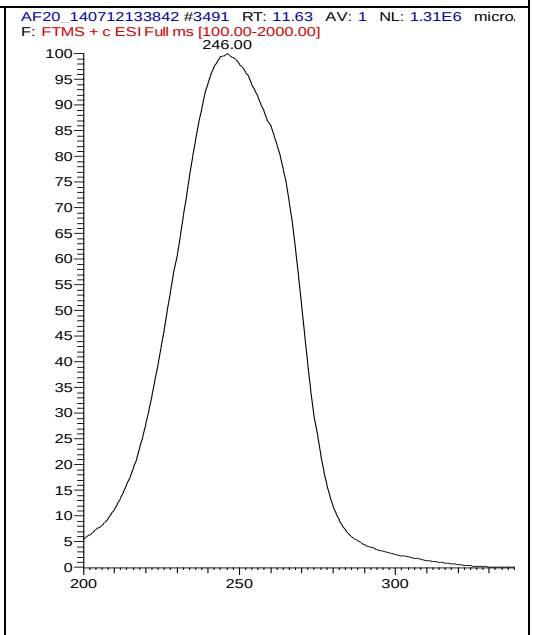

Compounds AF20 (5 mg) were obtained as yellow oil, exhibited a molecular formula $C_{14}H_{20}O_6$ established by ESI-HRMS at *m/z* = 285.1331 $[M+H]^+$. The optical rotation of compound AF20 $[\alpha]^{20}_D$= +6 (*c* 0.05, $CHCl_3$). The **^{1}H NMR**

data of compound AF20 (Table 31) resembled that of AF19 except for OH-2 was found upfield at δ_H 6.25 and Me-14 was downfield at δ_H 1.52. The **^{13}C NMR** data of compound AF20 (Table 31) showed the same carbon signals as AF19 except for Me-14 was found downfield at δ_C 26.7. Reversing of the optical rotation and changing of chemical shifts particularly OH-2 and Me-14 indicated that AF20 was a 2-epimer congener of AF19 and was identified as phomaligol A1 (Fig.171) in accordance to the reported data (Elbandy et al., 2009) (Table 31).

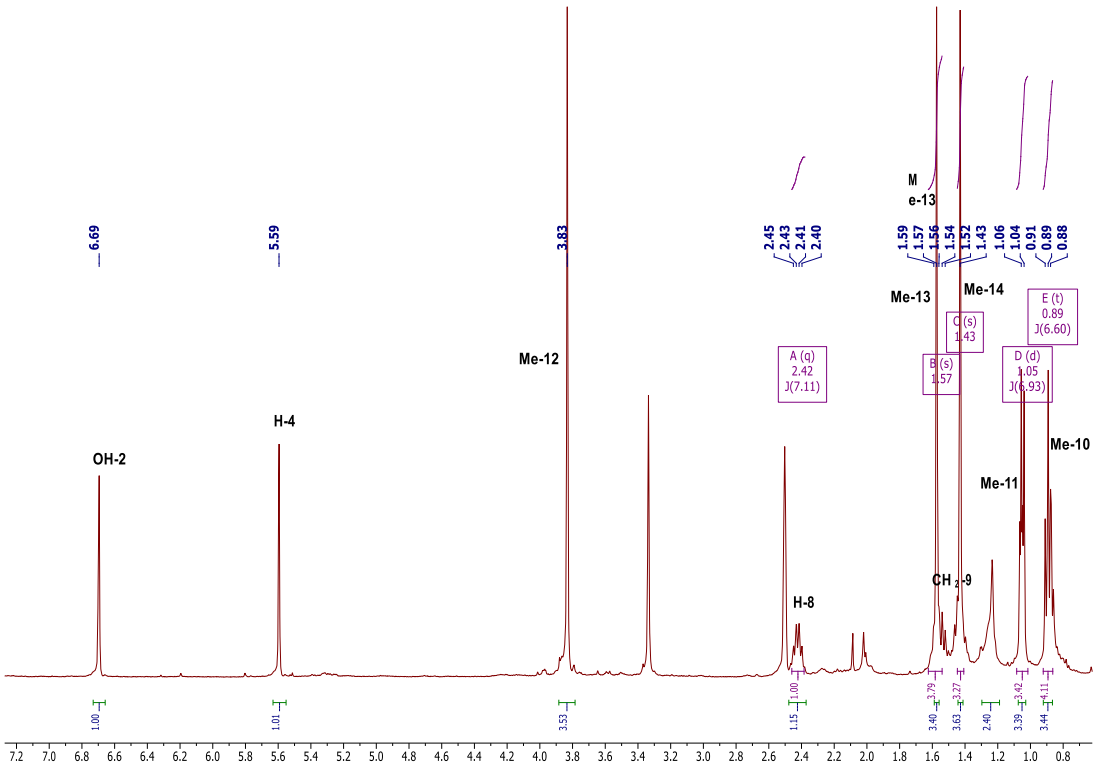

Fig.167 ^{1}H NMR spectrum of compound AF19

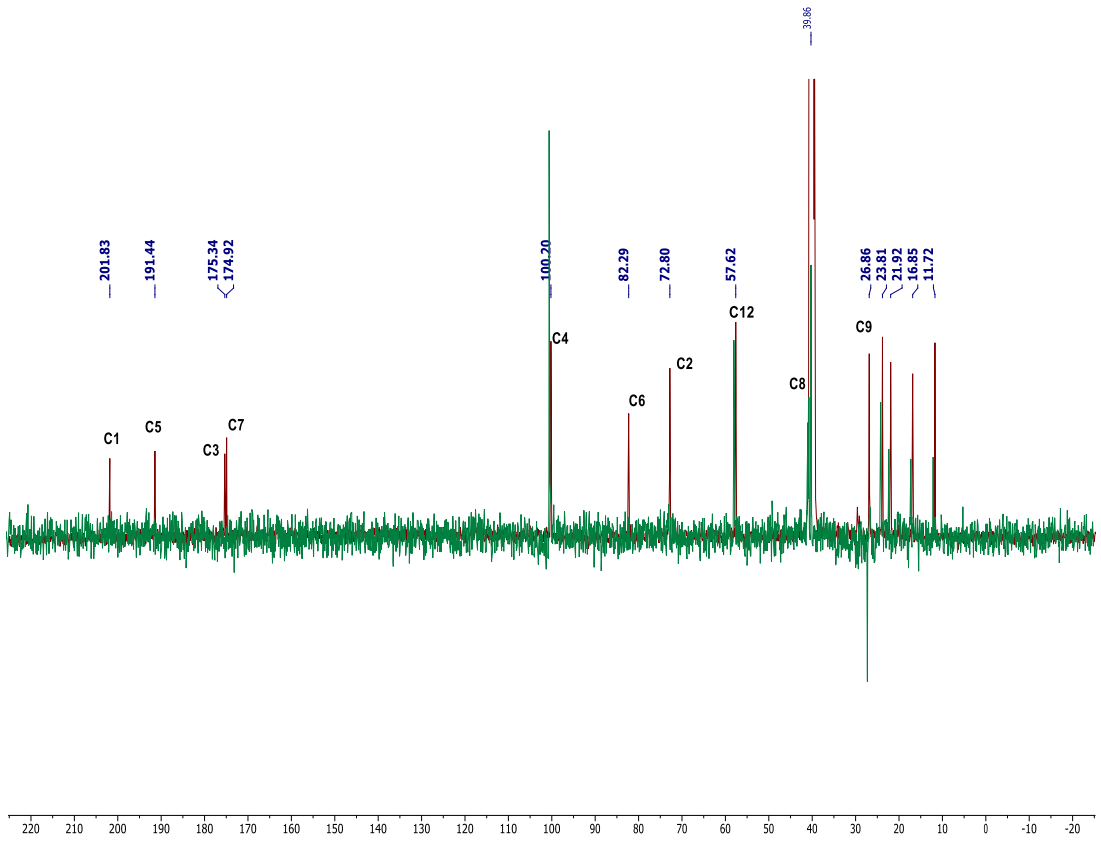

Fig.168 ^{13}C NMR and DEPT spectra of compound AF19

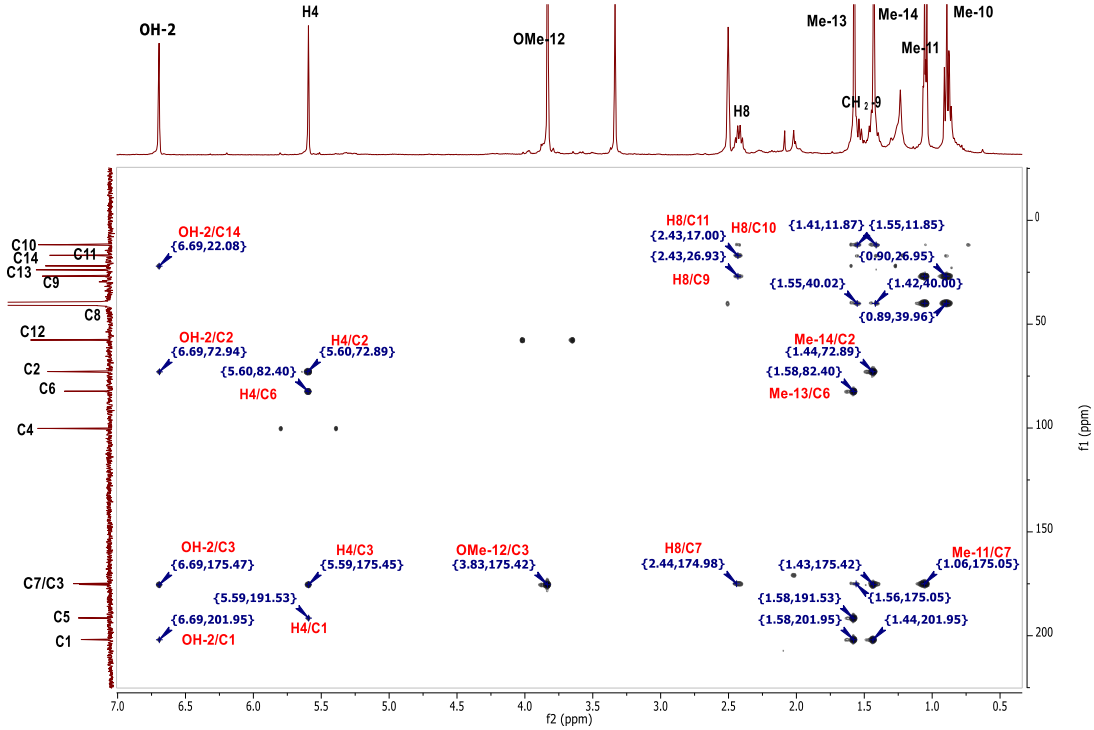

Fig.169 HMBC spectrum of compound AF19

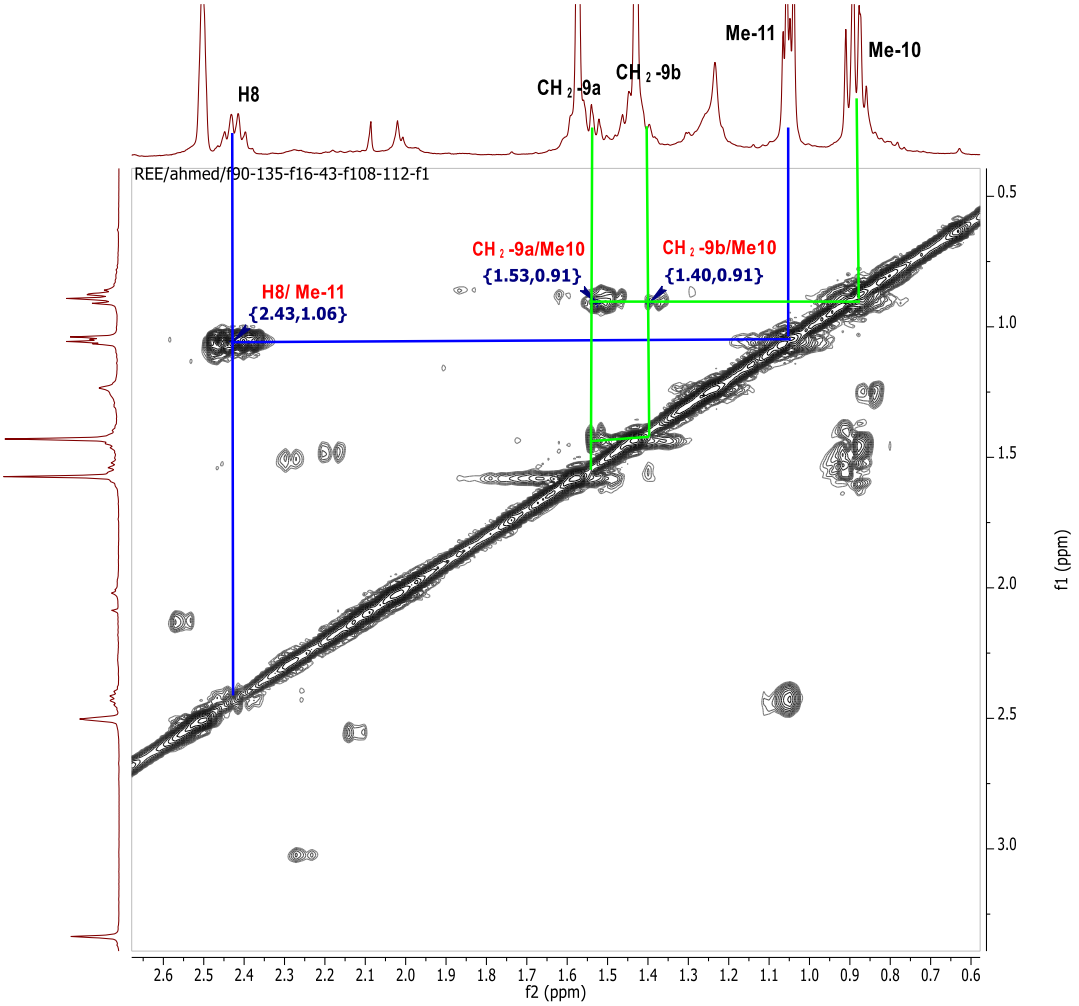

Fig.170 Expansion of ^{1}H-^{1}H COSY spectrum of compound AF19 showing two spin systems

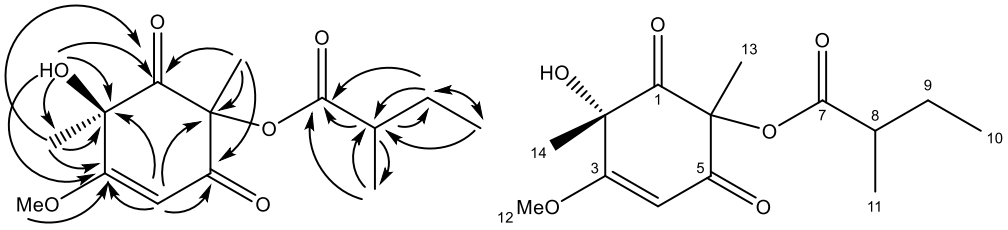

AF19 **AF20**

Fig.171 HMBC correlations of AF19 and AF20

Table 30: ^{1}H NMR and ^{13}C NMR data of compound AF19 and literature

Atom No.	AF19-DMSO			Elbandy 2009-CD_3OD	
	δ_C (m)	δ_H (m, *J* in Hz)	δ_H (m, *J* in Hz)-CDCl3	δ_C	δ_H (m, *J* in Hz)-CDCl3
1	201.8 (C)			202.5	
2	72.8 (C)	6.69 (s, OH)	2.77 (brs, OH)	73.5	2.8 (brs, OH)
3	175.3 (C)			173.0	
4	100.2 (CH)	5.59 (s)	5.55 (s)	99.9	5.56 (s)
5	191.4 (C)			191.7	
6	82.8 (C)			81.1	
7	174.9 (C)			175.8	
8	39.9 (CH)	2.42 (m)	2.48 (m)	39.8	2.5 (m)
9	26.8 (CH_2)	1.56 (m, H-9a), 1.42 (m, H-9b)	1.72 (m, H-9a), 1.49 (m, H-9b)	26.6	1.73 (m, H-9a), 1.51 (m, H-9b)
10	11.7 (CH_3)	0.89 (3H, t, 6.6 Hz)	0.94 (3H, t, 7.5 Hz)	11.3	0.96 (3H, t, 7.5 Hz)
11	16.8 (CH_3)	1.05 (3H, d, 6.9 Hz)	1.16 (3H, d, 6.5 Hz)	16.1	1.17 (3H,d, 7.0 Hz)
12	57.6 (CH_3)	3.83 (3H, s)	3.86 (3H,s)	56.8	3.87 (3H, s)
13	23.8 (CH_3)	1.57 (3H, s)	1.64 (3H, s)	24.1	1.65 (3H, s)
14	21.9 (CH_3)	1.43 (3H, s)	1.69 (3H, s)	23.3	1.7 (3H, s)

Table 31: ^{1}H NMR and ^{13}C NMR data of compound AF20 and literature

Atom No.	AF20-DMSO		Elbandy 2009-CD_3OD
	δ_C (m)	δ_H (m, *J* in Hz)	δ_H (m, *J* in Hz)
1	204.8 (C)		
2	74.4 (C)	6.25 (s, OH)	3.58 (brs, OH)
3	175.6 (C)		
4	99.5 (CH)	5.57 (s)	5.61 (s)
5	191.5 (C)		
6	83.2 (C)		
7	174.3 (C)		
8	39.7 (CH)	2.41 (m)	2.44 (m)
9	26.9 (CH_2)	1.57 (m, H-9a), 1.44 (m, H-9b)	1.73 (m, H-9a), 1.51 (m, H-9b)
10	11.7 (CH_3)	0.91 (3H, t, 8.0 Hz)	0.97 (3H, s, 7.5 Hz)
11	16.9 (CH_3)	1.05 (3H, d, 6.8 Hz)	1.13 (3H, s, 7.0 Hz)
12	57.5 (CH_3)	3.82 (3H, s)	3.89 (3H, s)
13	23.5 (CH_3)	1.53 (3H, s)	1.60 (3H, s)
14	26.7 (CH_3)	1.52 (3H, s)	1.63 (3H, s)

3.3.5.19. Compounds AF23a and AF23b (2- and 4-hydroxy phenyl acetic acid)

2-hydroxyphenyl acetic acid and 4-hydroxy phenyl acetic acid	
Synonyms	-
Sample codes	AF23a and AF23b
Sample Amount	15 mg
Physical Description	brown oily
Molecular Formula	$C_8H_8O_3$
Molecular Weight	152 g/mol
Retention time (LC-MS)	6.08 min

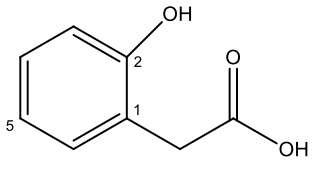

AF23a

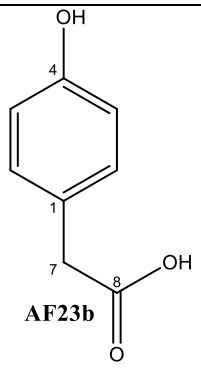

AF23b

LC-HRFTMS spectrum [M-H]$^-$ 151.0400

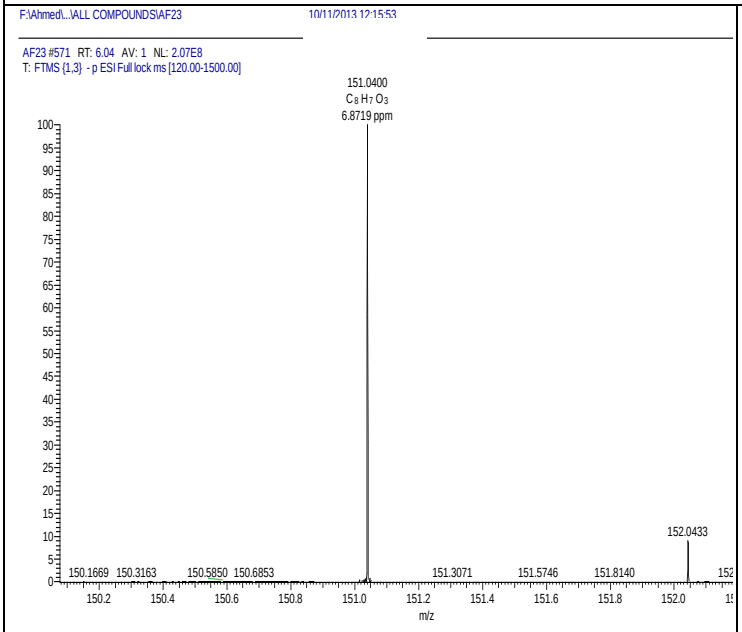

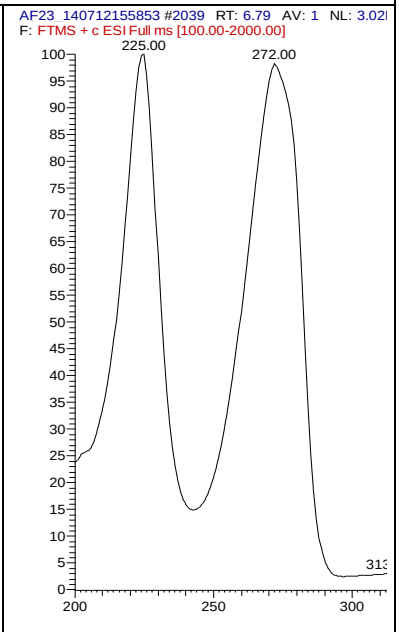

Compounds AF23a and AF23b (15 mg) were obtained in mixture as a brown oil, exhibited a molecular formula $C_8H_8O_3$ established by ESI-MS at *m/z* = 151.0400 [M-H]$^-$. The **^{1}H NMR** spectrum (DMSO, 400MHz) (Fig.172) showed a mixture of both compounds with ratio (1:1). The aromatic region included two sharp

doublets equivalent for the ortho-coupled protons of the benzene ring of AF23b at δ_H 6.68 (2H, d, 8.4 Hz) and 7.03 (2H, d, 8.4 Hz) and a sharp signal in the aliphatic region at δ_H 3.41 (2H, s) equivalent for the (C*H*$_2$-7) gp of AF23b. The **^{13}C NMR** spectrum (Fig.173) showed 12 aromatic carbons (six for each compound), two methylenes (one for each) and two carbonyls (one for each). The structure of compound AF23b structure was confirmed from the **HMBC** spectrum (Fig.174) through the correlations of H-2/H-6 (δ_H 7.03) with C-7 (δ_C 40.4), C-2/C-6 (δ_C 130.8) and C-4 (δ_C 156.6); H-3/H-5 (δ_H 6.68) to C-4 and C-3/C-5 (δ_C 115.3); C*H*$_2$-7 (δ_H 3.41) to C-1, C-2/C-6 and C-8 (δ_C 173.7). Although the structure has a plane of symmetry however carbons like C-2 and C-6 seemed to be chemically equivalent but not magnetically therefore cross peaks were seen between H-6 and C-2; H-2 and C-6. This was also observed between H-5 and C-3; H-3 and C-5. So from the above and in accordance to reported data (Zhou et al. 2005) (Table 33), compound AF23b (Fig.175) was identified as 4-hydroxy phenyl acetic acid.

Compound AF23a proton resonances were shown in the **^{1}H NMR** spectrum (Fig.172) as four (ABCD) proton signals of the benzene ring at δ_H 6.72 (1H, t, 7.3 Hz, H-5), 6.77 (1H, d, 7.9 Hz, H-3), 7.04 (1H, t, 7.3 Hz, H-4) and 7.07 (1H, d, 7.2 Hz, H-6). In addition, a sharp singlet signals at δ_H 3.45 (2H, s) equivalent for (C*H*$_2$-7) group of AF23a. The structure of compound AF23a was sustained from the **HMBC** correlation of H-3 (δ_H 6.77) with C-1 (δ_C 122.4) and C-5 (δ_C 119.2); H-5 (δ_H 6.72) with C-1; H-6 (δ_H 7.07) with C-2 (δ_C 155.9), C-4 (δ_C 128.3) and C-7 (δ_C 35.9); C*H*$_2$-7 (δ_H 3.45) to C-2, C-1, C-6 (δ_C 131.6) and C-8 (δ_C 173.3). So from the above and comparison to the literature (Milne et al. 2011) (Table 32), compounds AF23a (Fig.175) was identified as 2-hydroxyphenyl acetic acid (congener of AF23b).

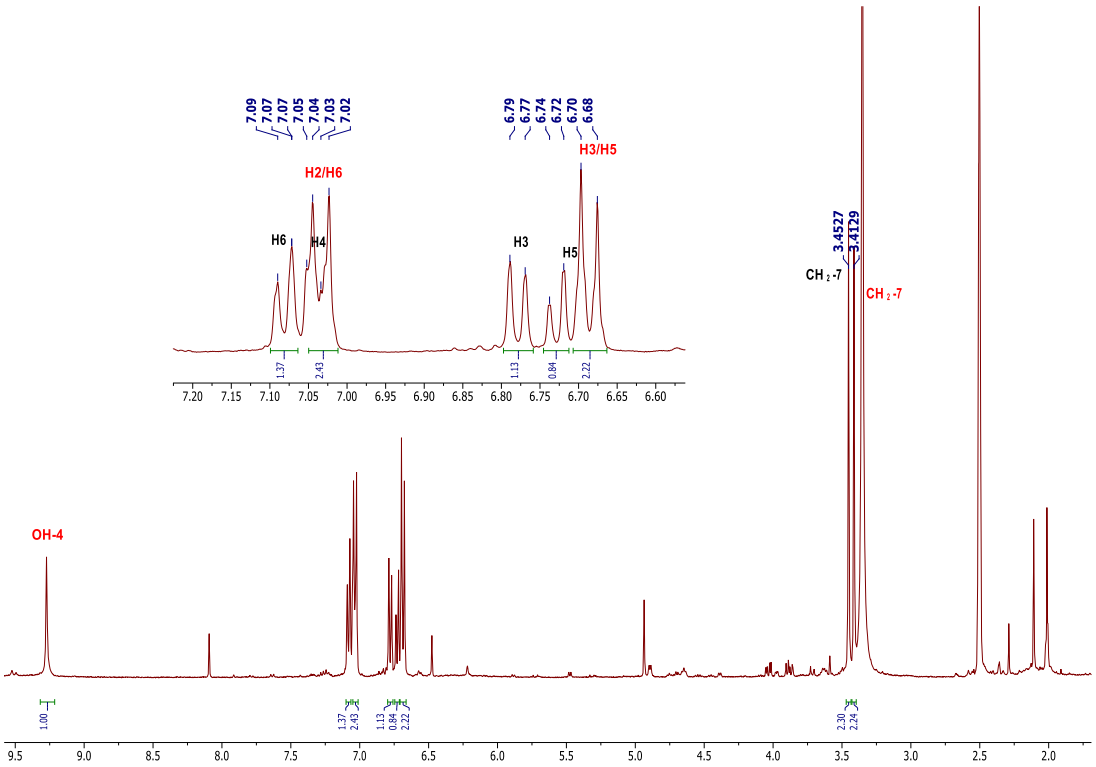

Fig.172 ^{1}H NMR spectrum of compounds AF23a (●) and AF23b (●)

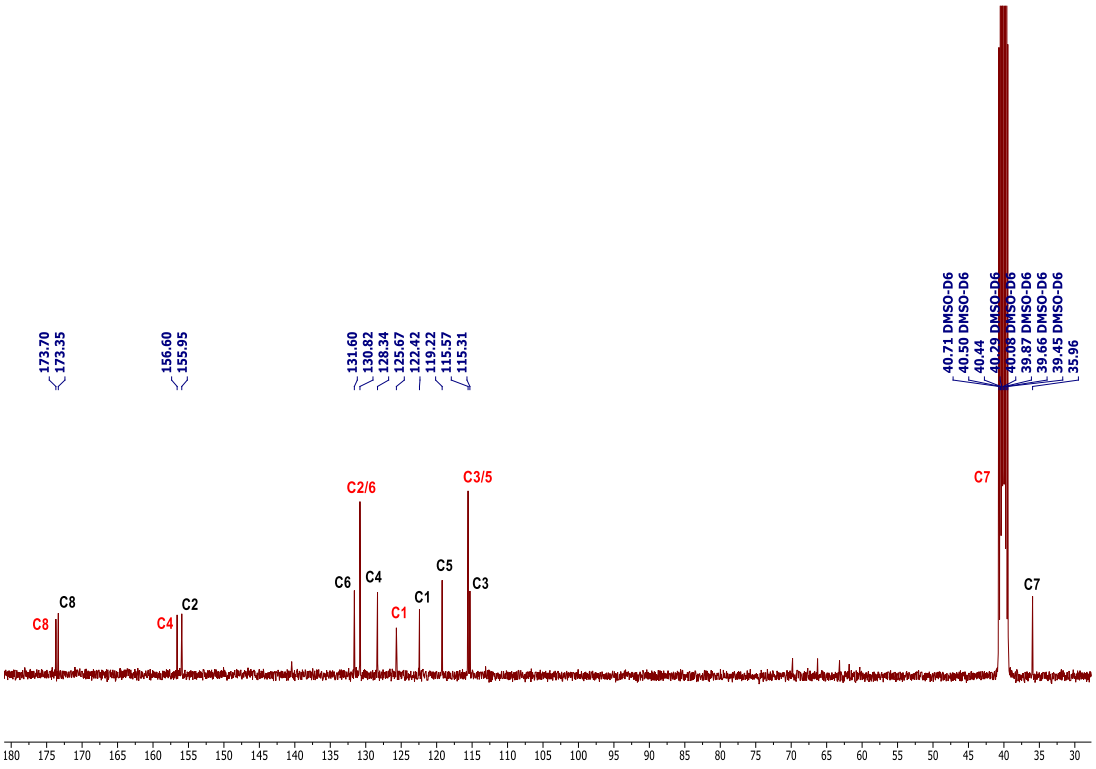

Fig.173 ^{13}C NMR spectrum of compounds AF23a (●) and AF23b (●)

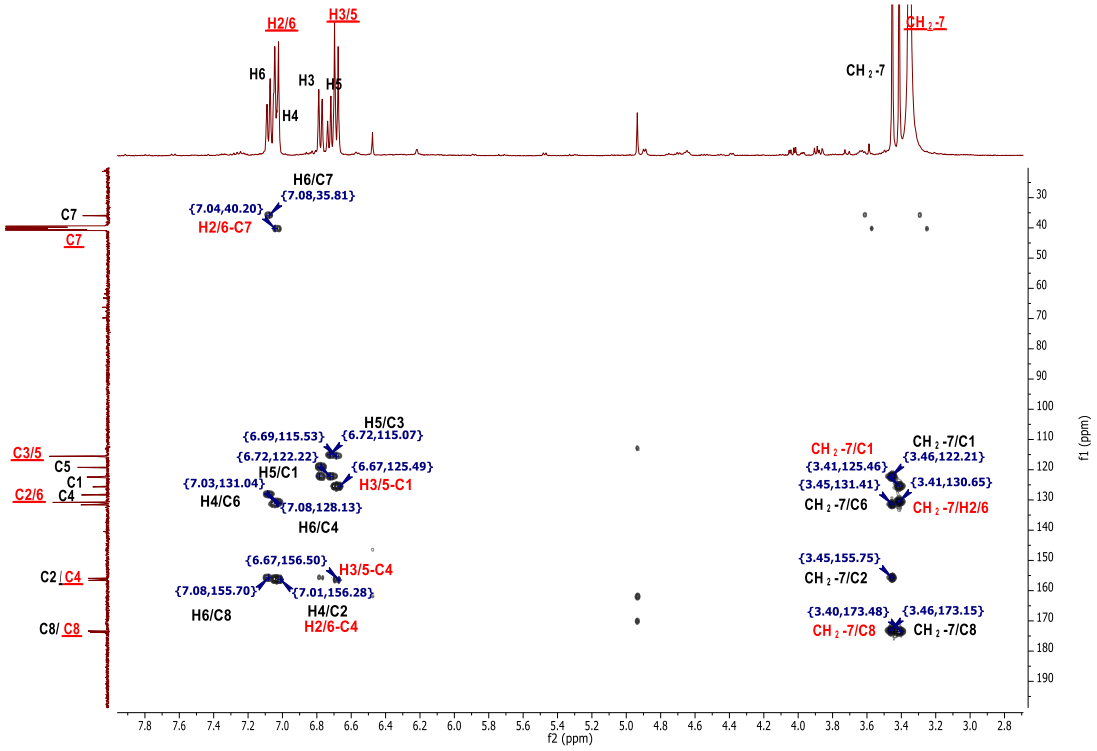

Fig.174 HMBC spectrum of compounds AF23a (●) and AF23b (●)

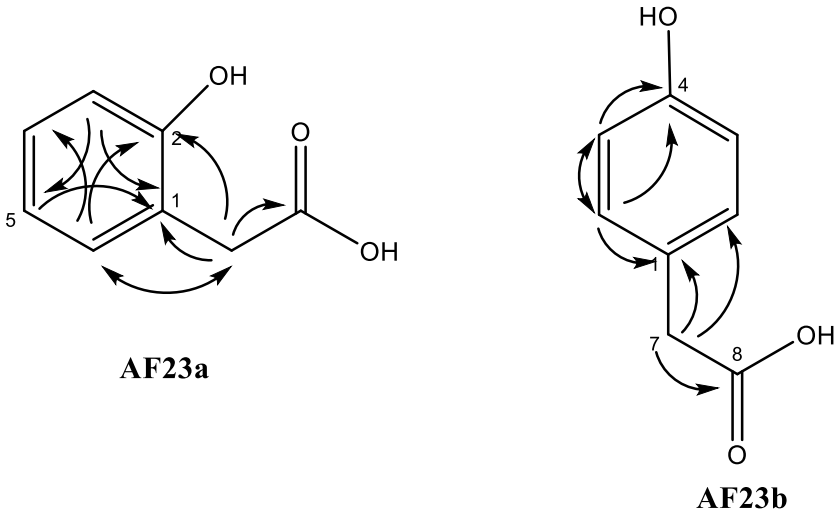

Fig.175 HMBC correlations of compounds AF23a and AF23b

Table 32: ^{1}H NMR and ^{13}C NMR data of compound AF23a and literature

Atom No.	AF23a-DMSO		Zhou 2005-D_2O	
	δ_C (m)	δ_H (m, *J* in Hz)	δ_C	δ_H (m, *J* in Hz)
1	122.4 (C)		119.2	
2	155.9 (C)		161.0	
3	115.5 (CH)	6.77 (d, 7.9 Hz)	117.5	6.95 (d, 7.7 Hz)
4	128.3 (CH)	7.04 (t, 7.3 Hz)	132.7	7.36 (t, 8.0 Hz)
5	119.2 (CH)	6.72 (t, 7.3 Hz)	118.4	6.89 (t, 7.0 Hz)
6	131.6 (CH)	7.07 (d, 7.2 Hz)	133.6	7.29 (d, 7.8 Hz)
7	35.9 (CH_2)	3.45 (s)	45.6	4.6 (s)
8	173.3 (C)		191.2	

Table 33: ^{1}H NMR and ^{13}C NMR data of compound AF23b and literature

Atom No.	AF23b-DMSO		Milne 2011-DMSO	
	δ_C (m)	δ_H (m, *J* in Hz)	δ_C	δ_H (m, *J* in Hz)
1	125.6 (C)		125.1	
2/6	130.8 (CH)	7.03 (2H, d, 8.4 Hz)	130.2	7.03 (2H, d)
3/5	115.3 (CH)	6.68 (2H, d, 8.4 Hz)	114.9	6.68 (2H, d)
4	156.6 (C)	9.27 (s, OH)	155.9	9.24 (brs, OH)
7	40.4 (CH_2)	3.41 (2H, s)	39.8	3.41 (2H, s)
8	173.7 (C)		173.1	

3.3.5.20. Compound AF22 (methyl 2-(4-hydroxyphenyl)acetate

methyl 2-(4-hydroxyphenyl)acetate	
Synonyms	-
Sample codes	AF22
Sample Amount	12 mg
Physical Description	brown sugary
Molecular Formula	$C_9H_{10}O_3$
Molecular Weight	166 g/mol
Retention time (LC-MS)	6.02-8.82 min

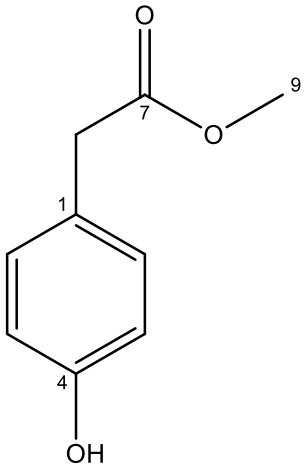

LC-HRFTMS spectrum $[M-H]^-$ 165.0557

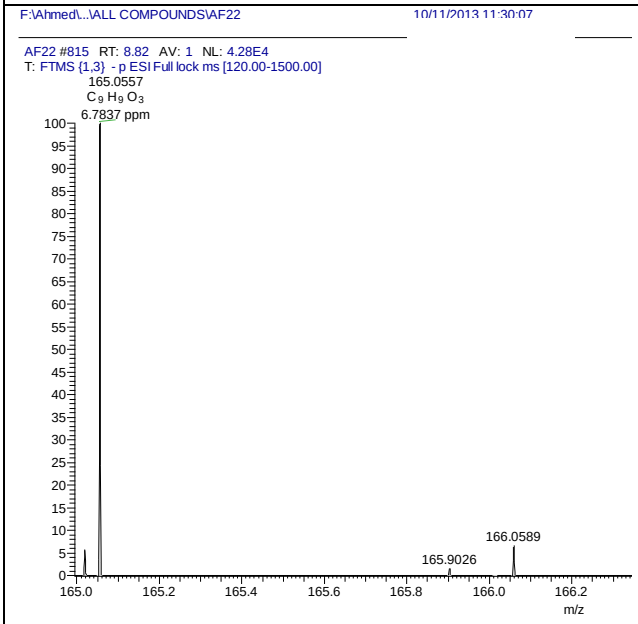

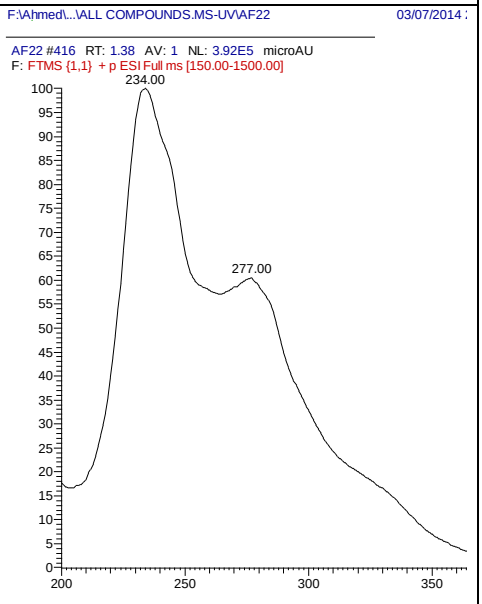

Compounds AF22 (12 mg) was obtained as brown sugary substance, exhibited a molecular formula $C_9H_{10}O_3$ established by ESI-MS at *m/z* = 165.0557 $[M-H]^-$. The **^{1}H NMR** spectrum of compound AF22 ($CDCl_3$, 400 MHz) (Fig.176) showed the same proton resonances as compound AF23b with extra singlet peak at δ_H 3.69 equivalent for Me-9. The structure was confirmed from the **HMBC** spectrum (Fig.177), which demonstrated a correlation of H-2/H-6 (δ_H 7.13) with C-7 (40.9), C-2/C-6 (δ_C 131.1) and C-4 (δ_C 155.4); H-3/H-5 (δ_H 6.76) with C-4, C-3/C-5 (δ_C 116.1) and C-1 (δ_C 126.6). Moreover, C*H*$_2$-7 (δ_H 3.55) correlated with C-1, C-2/C-6 and C-8 (δ_C 173.2) and finally the correlation of Me-9 (δ_H 3.68) to C-8 which indicated the position of the extra methyl group. So from the above compound AF22 was identified as the methyl congener of AF23b (methyl 2-(4-hydroxyphenyl) acetate).

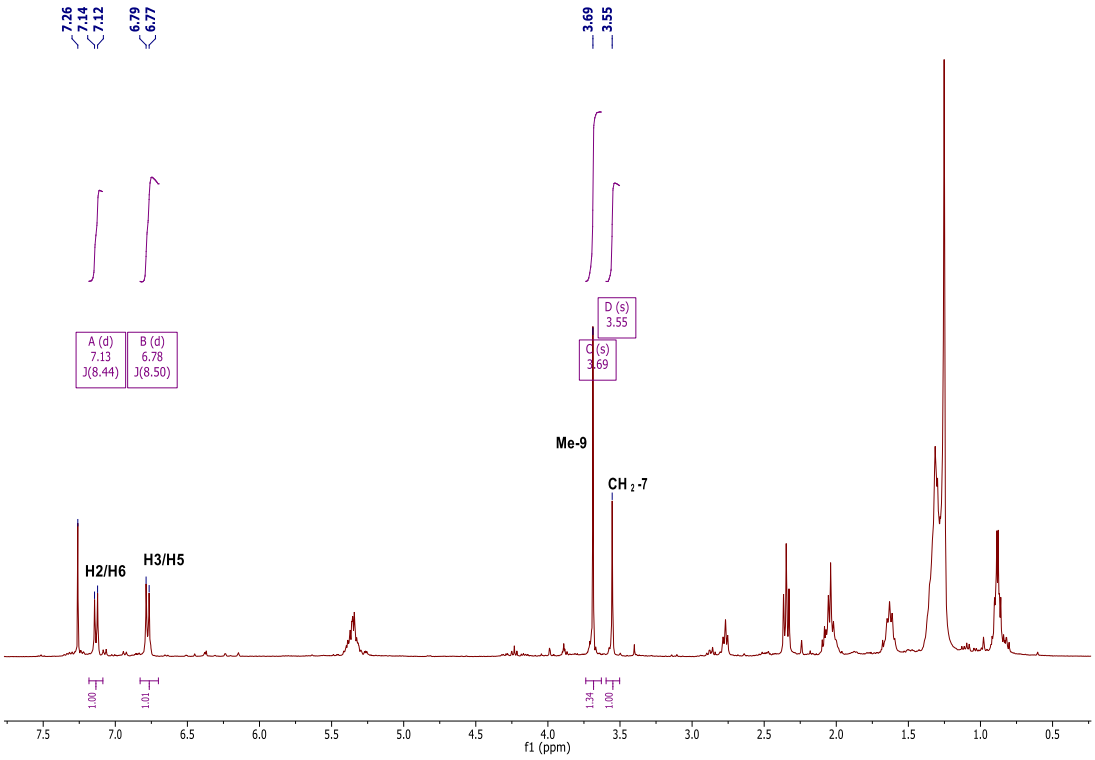

Fig.176 ^{1}HNMR of compound AF22

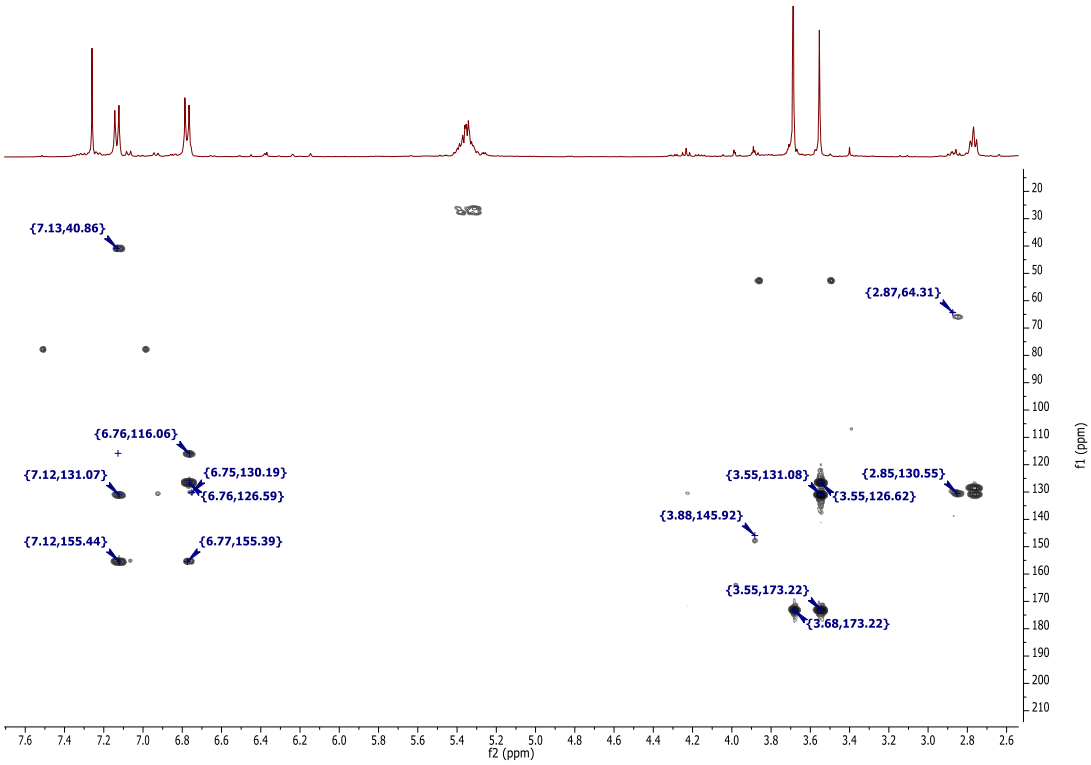

Fig.177 HMBC spectrum of compound AF22

3.3.5.21. Compound AF21 (p-hydroxybenzaldehyde)

p-hydroxybenzaldehyde	
Synonyms	-
Sample codes	AF21
Sample Amount	8 mg
Physical Description	brown sugary
Molecular Formula	$C_7H_6O_2$
Molecular Weight	120 g/mol
Retention time (LC-MS)	5.57 min

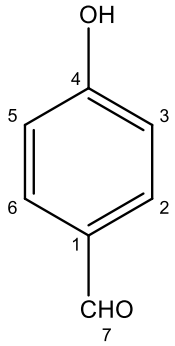

LC-HRFTMS spectrum $[M+H]^+$ 121.0296

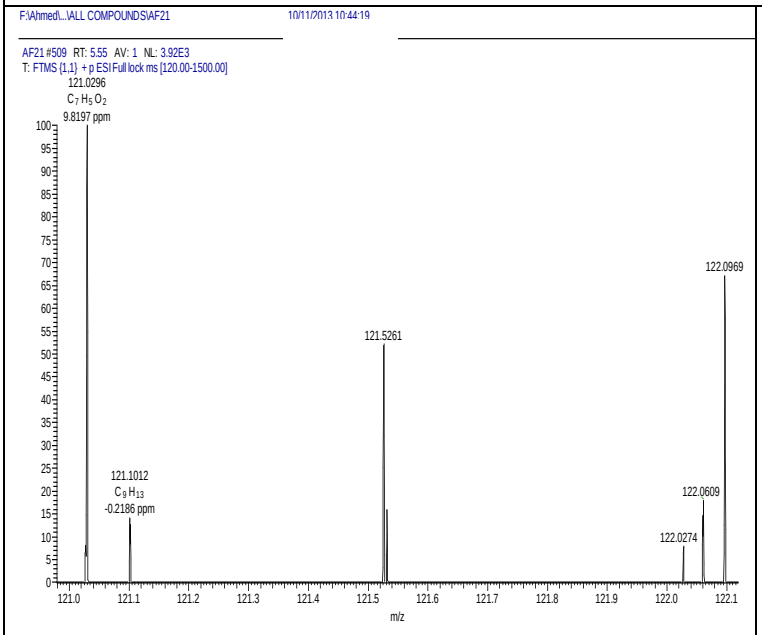

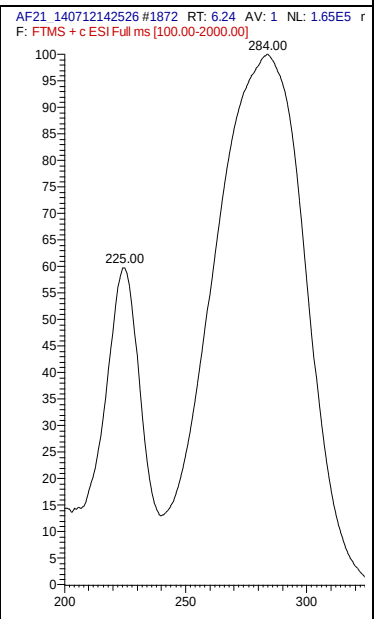

Compounds AF21 (8 mg) was obtained as brown sugary substance, exhibited a molecular formula $C_7H_6O_2$ established by ESI-MS at *m/z* = 121.0296 $[M+H]^+$.

The **^{1}H NMR** spectrum of compound AF21 ($CDCl_3$, 400 MHz) (Fig.178) showed two doublet signals in the aromatic region at δ_H 7.80 (2H, d, 8.4 Hz) equivalent for H-2/H-6 and 6.95 (2H, d, 8.4 Hz) for H-3/H-5. Moreover, a singlet signal equivalent for CHO group was found at δ_H 9.85 (1H, s). The **^{13}C NMR** spectrum (Fig.179) showed seven carbons including six aromatic and one aldehyde. So from the above and comparison of the ^{1}H NMR and ^{13}C NMR data to the literature (Kim et al., 2003) (Table 34), compound AF21 was identified as p-hydroxybenzaldehyde.

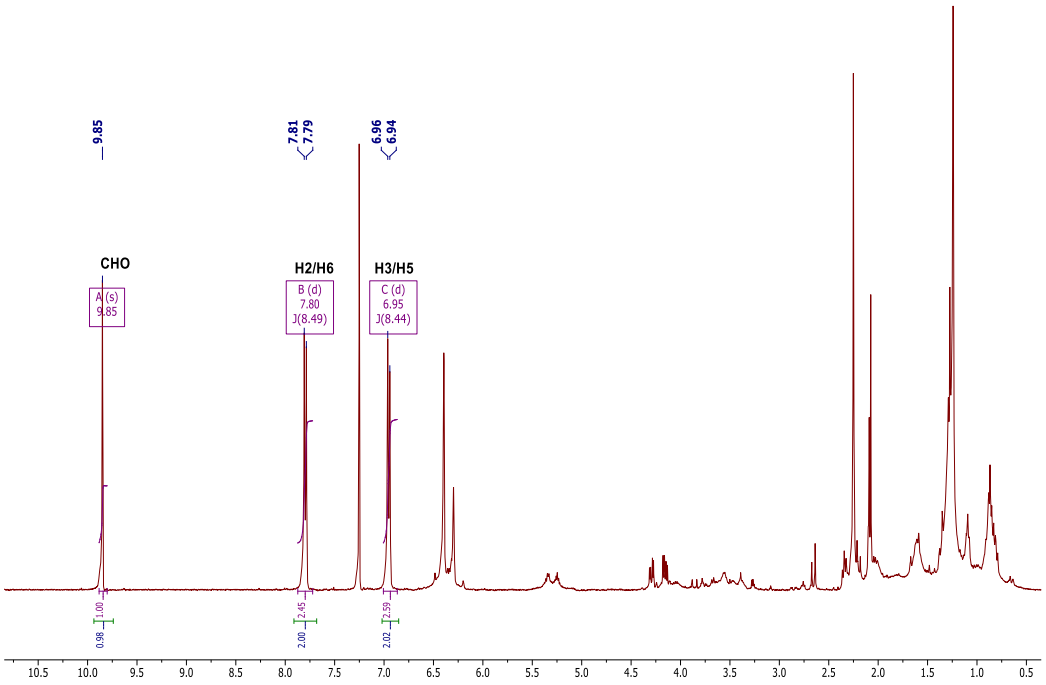

Fig.178 ^{1}H NMR spectrum of compound AF21

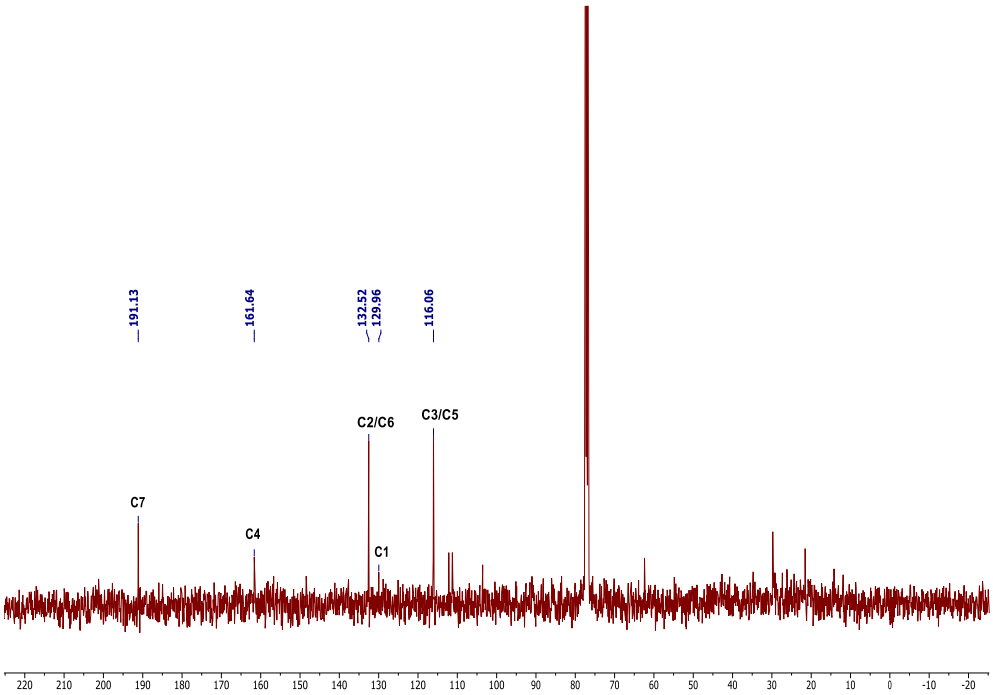

Fig.179 ^{13}C NMR spectrum of AF21

Table 34: ^{1}H NMR and ^{13}C NMR data of compound AF21 and literature

Atom No.	AF21-$CDCl_3$		Kim 2003-$(CD_3)2CO$	
	δ_C (m)	δ_H (m, *J* in Hz)	δ_C	δ_H (m, *J* in Hz)
1	129.96 (C)		130.3	
2/6	132.52 (CH)	7.80 (d, 8.4 Hz)	132.8	7.79 (d, 8.7 Hz)
3/5	116.05 (CH)	6.95 (d, 8.4 Hz)	116.6	7.0 (d, 8.7 Hz)
4	161.64 (C)		163.8	
7	191.13 (CH)	9.85 (s)	191	9.84 (s)

3.3.5.22. Compound AF12 (4-methyl-5,6-dihydro-2H-pyran-2-one)

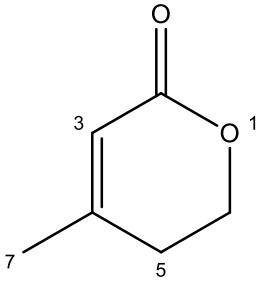

Compound AF12 was obtained in a mixture with mellein, **^{1}H NMR** spectrum ($CDCl_3$, 400 MHz) (Fig.180) showed four proton signals at δ_H 5.81 (1H, s, H-3),

4.37 (2H, t, 6.3 Hz, C*H*$_2$-6), 2.37 (2H, t, 6.2 Hz, C*H*$_2$-5) and 1.99 (3H, s, Me-7). The **^{1}H-^{1}H COSY** spectrums (Fig.181) showed a spin system connecting H-3, C*H*$_2$-5, C*H*$_2$-6 and Me-7. The structure was confirmed from **HMBC** spectrum (Fig.182) through the correlations of H-3 with C-5 (δ_C 29.6) and Me-7 (δ_C 23.26); C*H*$_2$-6 with C-5, C-4 (δ_C 158.3) and C-2 (δ_C 165.3); C*H*$_2$-5 with C-4, C-6 (δ_C 66.4) and C-3 (δ_C 117.4); Me-7 with C-3, C-4 and C-5. So form the above compound AF12 was identified as 4-methyl-5,6-dihydro-2H-pyran-2-one (Fig.183).

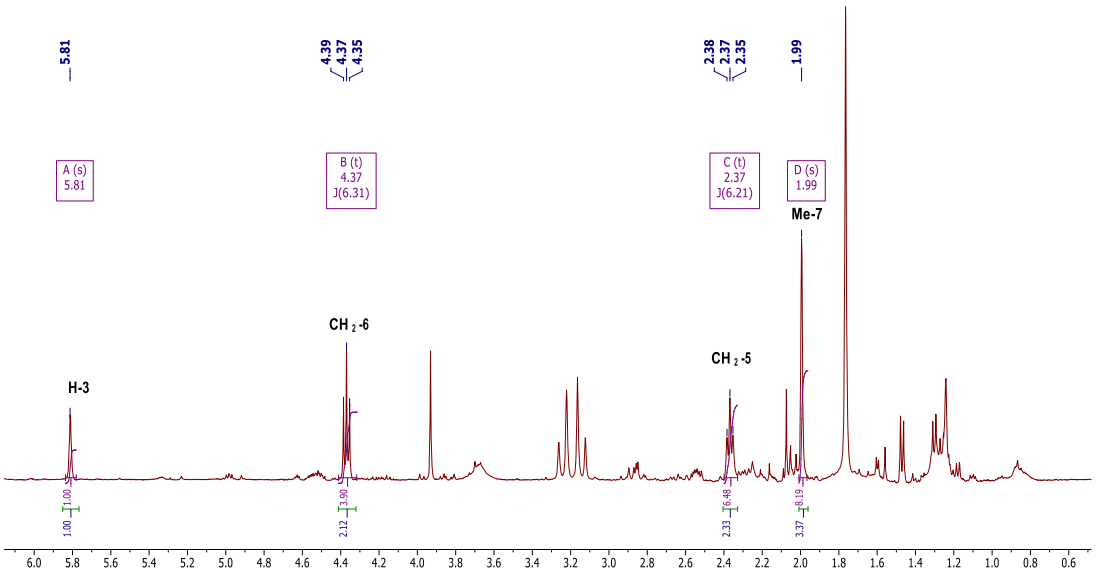

Fig.180 ^{1}HNMR spectrum of compound AF12

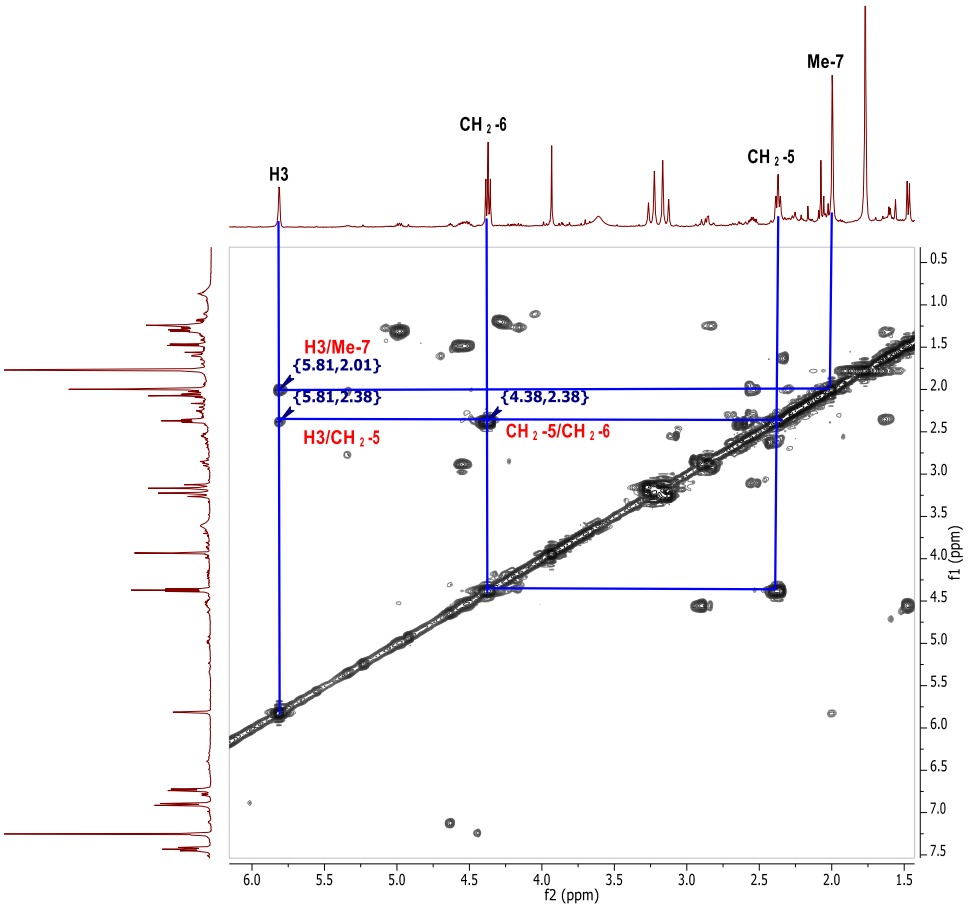

Fig.181 ^{1}H-^{1}H COSY spectrum of compound AF12

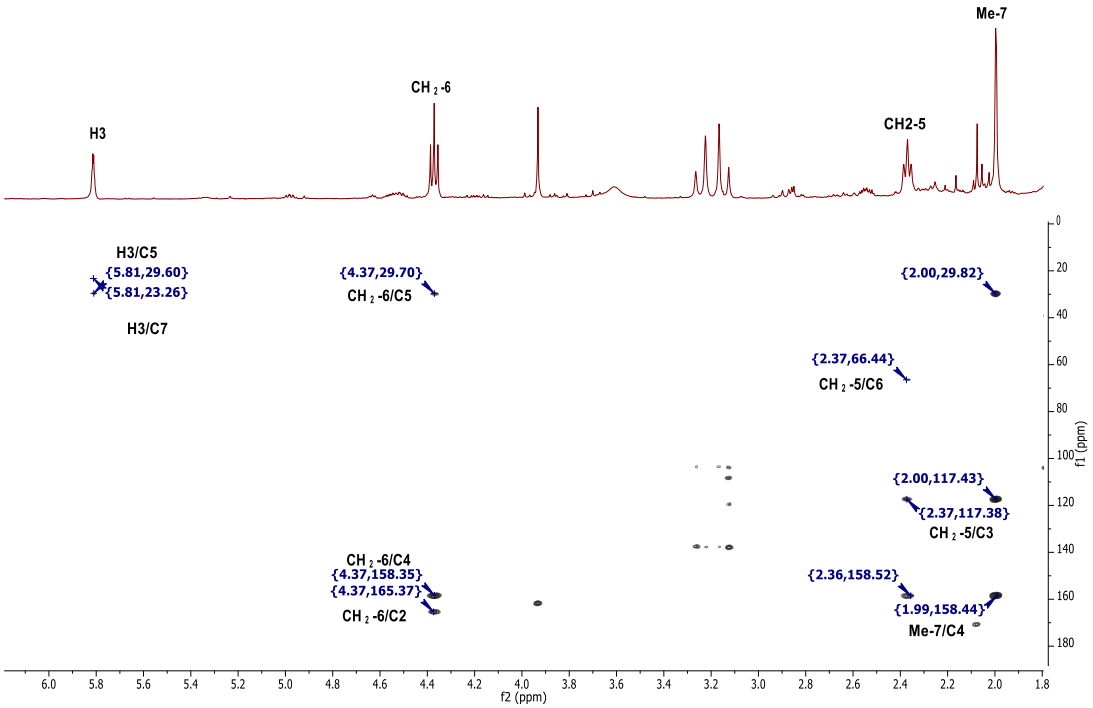

Fig.182 HMBC spectrum of compound AF12

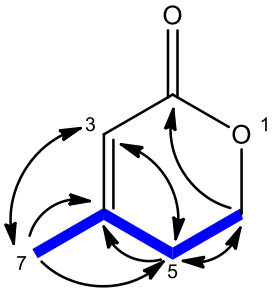

Fig.183 The structure showing the HMBC correlations and spin system of compound AF12

3.4. Curvularia sp.

3.4.1. Dereplication studies using NMR spectroscopy

Comparison of the ^{1}H NMR spectra of the rice and liquid culture extracts of *Curvularia sp.* showing no significant difference between 7 and 30-days rice culture extracts however the 15-days liquid culture extract showed more peaks in the aromatic region (Fig.184).

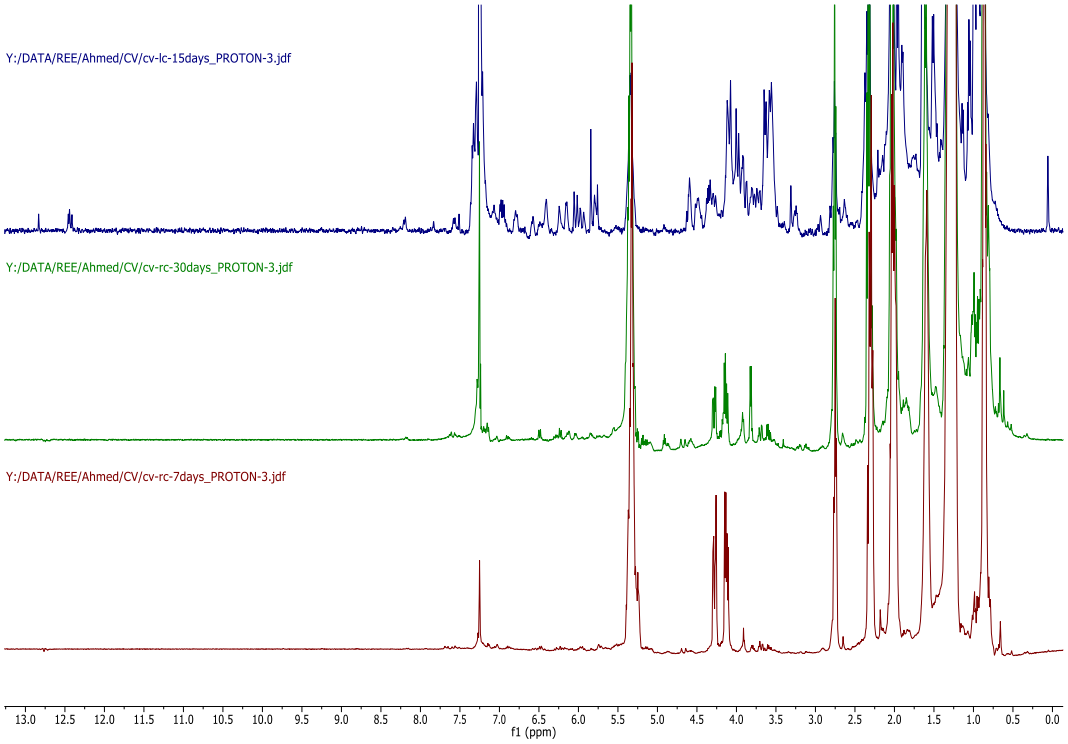

Fig.184 ^{1}H NMR spectra of *Curvularia sp.* 7 days rice culture (●), 30 days rice culture (●) and 15 days liquid culture extracts (●)

3.4.2. Dereplication studies using MZmine

Comparison of the total ion chromatogram of 7, 30-days rice culture and 15-days liquid culture extracts of *Curvularia* sp. (Fig.185) indicated that 7 and 30-days rice culture extracts showed nearly the same TIC except for few variant ion peaks. This was shown also in the MZmine's scatter plot (Fig.186) and both exhibited more peaks than 15-days liquid culture extract. The MS raw files of the fungal extracts as well as the plant extracts were processed in MZmine 2.10 to make multiple data file comparable (Methods section 2.4.5.1). The score scatter

plot (Fig.187) showed a comparison between 7-days rice culture and 15-days liquid culture extracts in terms of the abundance of the produced metabolites which confirmed that 7-days rice culture extract produced more metabolites which represented by the increase in density of the blue dots below the diagonal. Moreover, the histogram (Fig.188) exhibited more abundant metabolites in the 30-days rice culture extract than 15-days liquid culture extract which represented by the blue bars. While the scatter plot showed nearly similar abundance of the produced metabolites for 7-days and 30-days rice culture extracts. Furthermore, the heatmap was accomplished using R software (Fig.189) exhibited a comparison between 7, 15 and 30 days extracts of *Curvularia* sp. which established that 7-days and 30-days fungal extracts produced more metabolites than 15-days extract. This indicated that 15-days fungal culture is an intermediate stage in which the metabolites were produced in 7-days culture, consumed by the fungi in 15-days to produce other secondary metabolites by 30-days culture as a survival process. Molecular formula prediction and/or customized database search tools, using Antibase and Dictionary of Natural products (DNP) databases, were enabled for dereplicating the afforded metabolites in the rice culture and liquid culture extracts of *Curvularia sp.* as well as the ethyl acetate and butanol extracts of the *Terminalia laxiflora* leaves from which *Curvularia* sp. has been isolated. A CSV file exported from the MZmine and imported simultaneously into a macro written in excel which allowed further clean up and database searching (MacIntyre et al, 2014). The majority of the metabolites found to be produced by all fungal and plant extracts. Moreover, most of these metabolites were previously described as shown in the dereplication table (Table 35) with observation of some unknown hits. Some of the fungal metabolites produced in either rice or liquid culture extracts were found in very small intensities in either EtOAc or BuOH extracts of *Terminalia* leaves. Moreover, some of these metabolites with corresponding ion peaks at *m/z* 207.097, 354.165 and 467.249 eluted at retention time 6.54, 8.89 and 11.55 minutes respectively, were isolated later from the upscaled batch of 30-days fungal extract. These metabolites were described in dereplication table (Table 35) as rhexifoline from *Castilleja rhexifolia*, picroroccellin from *Roccella fuciformis* and cyclopiamine B from

Aspergillus caespitosus, respectively. While (Table 36) exhibited that these metabolites were also found at smaller peak area in the plant extracts than the fungal ones, which indicated that the endophyte could produce the same plant metabolites in larger quantities that made it extractable with advantage of method sustainability.

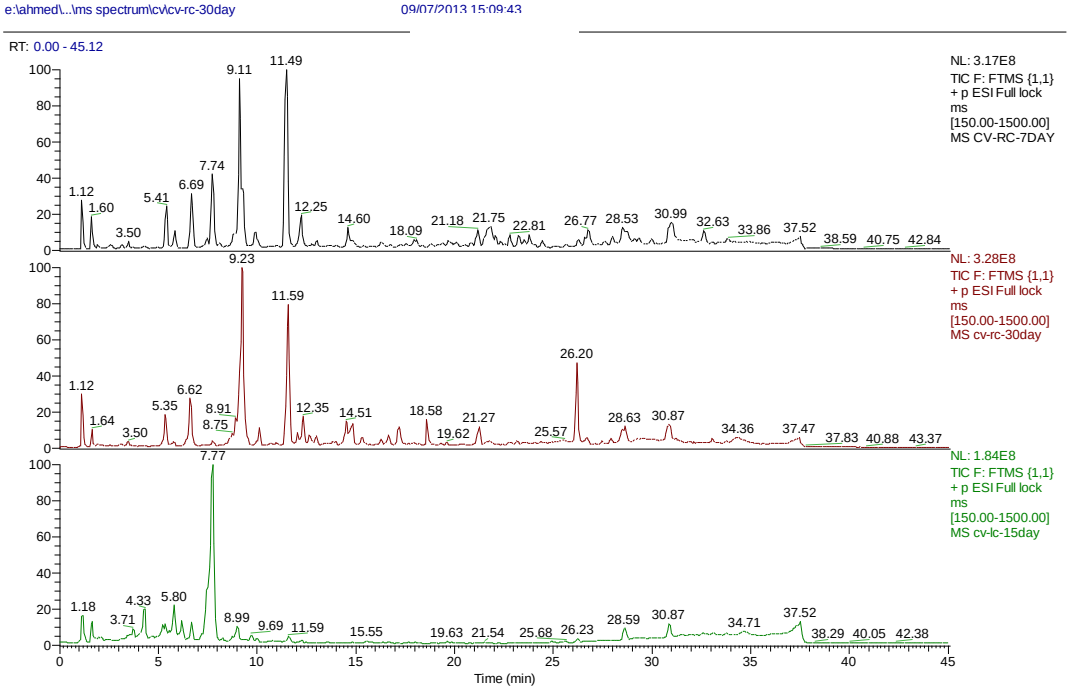

Fig.185 TIC of 7 days (●), 30 days rice culture (●) and 15 days LC (●) of Curvularia sp.

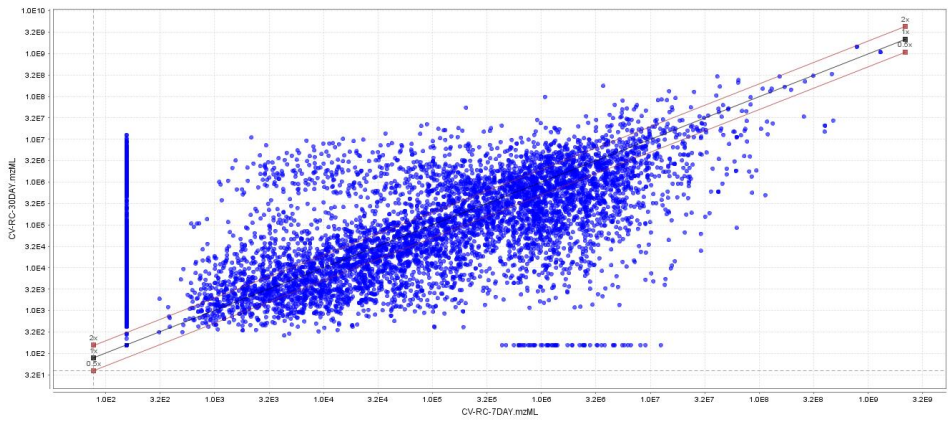

Fig.186 Scatter plot of 7 days rice culture (X-axis) and 30 days rice culture (Y-axis)

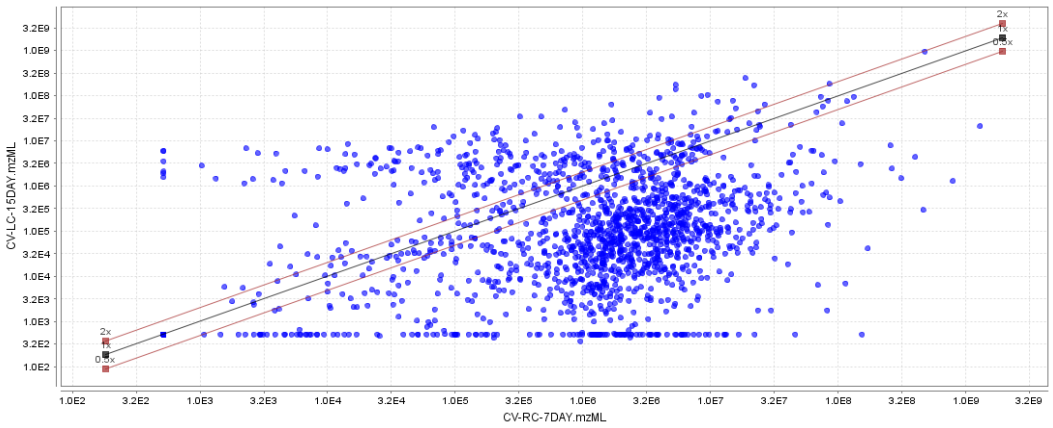

Fig.187 Scatter plot of 7 days rice culture (X-axis) and 15 days LC (Y-axis)

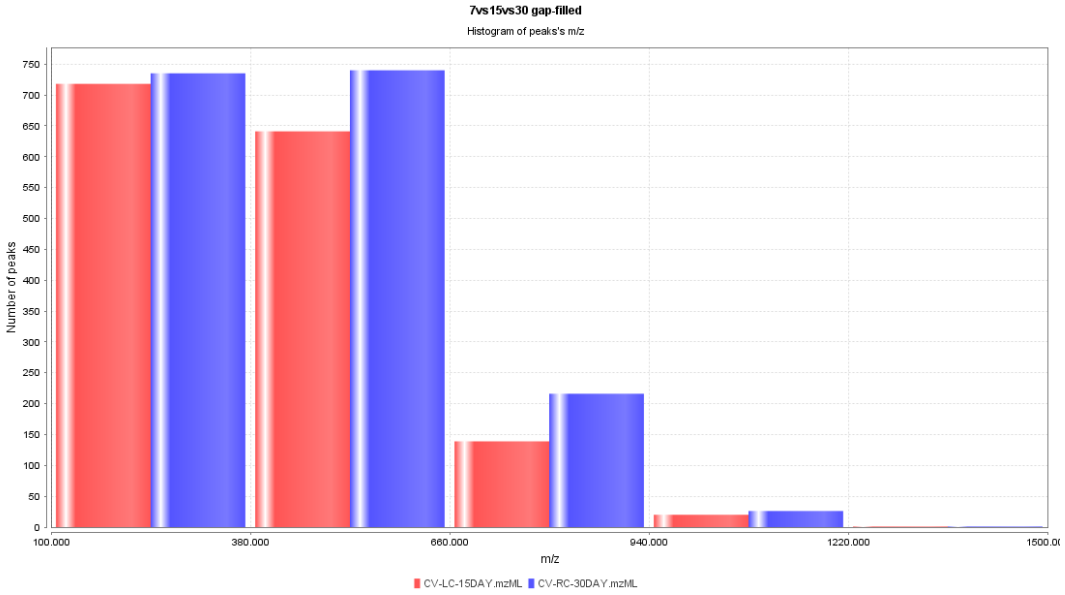

Fig.188 Histogram of 15 days LC (●) vs 30 days rice culture (●)

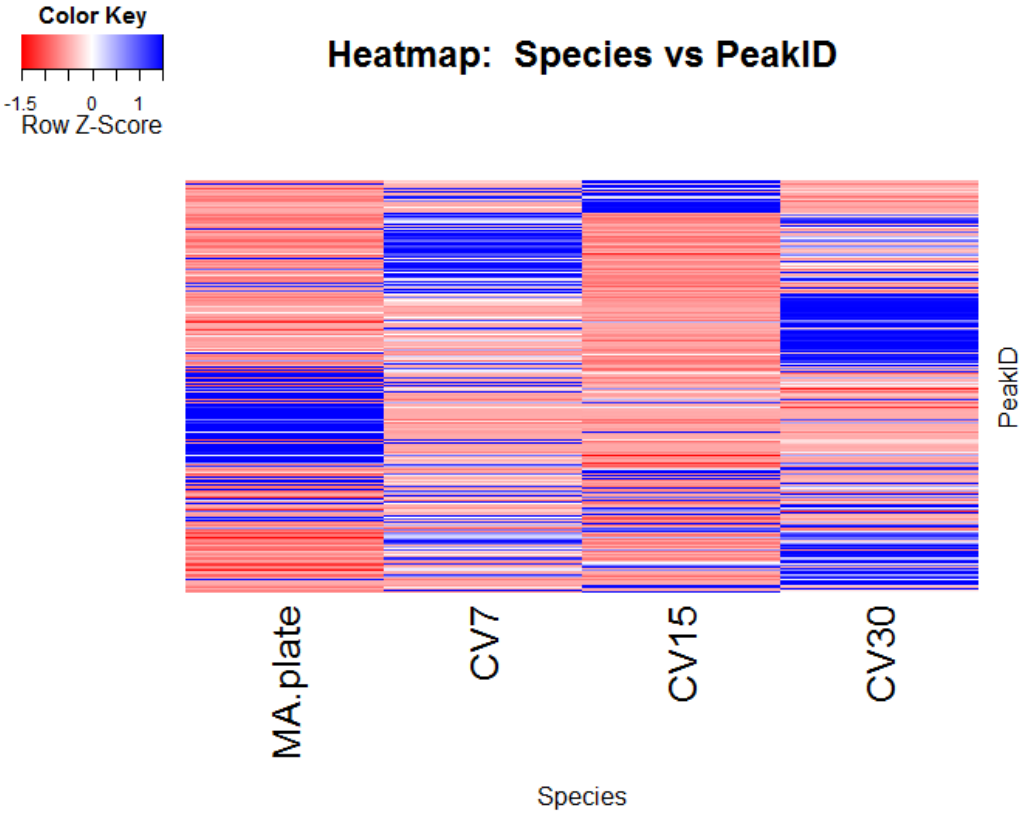

Fig.189 Heatmap of 7, 15 and 30 days culture extracts of *Curvularia* sp.

Table 35: Dereplication table for *Curvularia sp*. extracts which includes mass to charge ratio (*m/z*), retention time (RT), formula, name and source of the detected metabolites in liquid culture fungal extract (LC), 7 days, 30 days rice culture (RC) fungal extracts, butanol extract (BuOH ext.) and ethyl acetate extract (EtOAc ext.) of plant leaves. The highlighted rows represented the purified metabolites, which were found at lower intensities in the extracts of the source plant. The extracts were compared according to the peak height of the produced metabolites.

Rt	M.wt	Name /formula	7-days RC	30-days RC	15-days LC	BuOH ext.	EtOAc ext.
11.55	934.482	**complex of 467.24**	1.17E+08	9.83E+07	2.42E+05	2.21E+03	0
9.19	708.324	**taxinine J** $C_{38}H_{48}O_{12}$ ***Taxus cuspidata***	1.14E+08	1.50E+08	0	0	0
6.71	414.171	**Complex of 207.08**	1.12E+08	0	0	0	0
6.54	207.096	**rhexifoline** $C_{11}H_{13}NO_3$ ***Castilleja rhexifolia***	1.10E+08	8.00E+07	5.45E+05	1.77E+04	6.32E+04
11.55	467.249	**cyclopiamine B** $C_{26}H_{33}N_3O_5$ ***Aspergillus caespitosus***	9.69E+07	9.20E+07	5.48E+06	0	0
8.89	354.165	**picroroccellin** $C_{20}H_{22}N_2O_4$ ***Roccella fuciformis***	9.64E+07	1.10E+08	1.44E+03	2.03E+03	1.80E+02
29.27	298.251	**E-11-hydroxy-octadeca-12-enoic acid** $C_{18}H_{34}O_3$	5.99E+07	2.27E+07	5.83E+05	2.88E+02	2.05E+03
23.14	536.290	**sengosterone** $C_{29}H_{44}O_9$ ***Cyathula capitata***	5.14E+07	2.25E+07	4.49E+05	0	0
29.09	596.502	**unknown**	4.47E+07	1.53E+07	1.67E+04	1.77E+02	0
9.34	425.234	**dihydroxyisoechinulin A** $C_{24}H_{31}N_3O_4$ ***Aspergillus*** **strain MFA 212 KACC**	3.93E+07	2.94E+06	0	0	0
7.99	236.064	**herbarin A** $C_{12}H_{12}O_5$ ***Cladosporium herbarum***	3.71E+07	1.98E+06	5.53E+07	5.37E+02	1.02E+03

Table 36: Peak area of the metabolites produced by *Curvularia sp.* extracts including liquid culture fungal extract (LC), 7 days, 30 days rice culture (RC) fungal extracts, butanol extract (BuOH ext.) and ethyl acetate extract (EtOAc ext.) of plant leaves. The highlighted rows represented the purified metabolites produced at lower concentration in the plant extracts. All metabolites represented by $[M+H]^+$

row *m/z*	row RT	7-days RC	30-days RC	15-days LC	BuOH ext.	EtOAc ext.
468.2495	11.56	1.30E+09	1.09E+09	2.13E+07	0	0
355.1651	9.04	7.90E+08	1.46E+09	1.30E+06	1.66E+04	7.79E+02
237.0757	7.61	4.77E+08	2.74E+07	9.46E+08	1.57E+03	5.85E+03
935.4923	11.49	4.65E+08	3.31E+08	2.95E+05	7.58E+02	0
426.2389	9.37	4.02E+08	2.08E+07	4.40E+06	0	0
208.0969	6.65	3.13E+08	3.01E+08	1.48E+06	7.58E+03	2.96E+04
174.1126	5.51	2.63E+08	2.22E+08	2.43E+06	2.73E+04	4.56E+04
295.2267	21.88	2.57E+08	3.39E+07	7.96E+06	5.55E+04	4.64E+06
394.2223	12.32	1.71E+08	1.67E+08	4.15E+04	0	4.30E+02
709.324	9.17	1.54E+08	2.90E+08	0	0	0.00E+00
174.1125	5.51	1.50E+08	1.91E+08	3.05E+06	2.73E+04	4.56E+04
221.081	7.67	1.33E+08	2.35E+07	9.43E+07	2.73E+03	9.61E+03
221.0809	9.10	1.18E+08	2.58E+07	7.50E+07	4.95E+03	1.22E+04

3.4.3. Metabolomic study using SIMCA-P+

3.4.3.1. *Curvularia* sp. different extracts vs *Terminalia* leaves extracts

Chemometric analysis of the *Curvularia* extracts against *Terminalia* leaves extracts were done using SIMCA-P^+ software employing PCA as an unsupervised method and OPLS-DA, a supervised method. The PCA analysis (Fig.190) showed that all fungal liquid culture extracts as well as *Terminalia* extracts were clustered together in the left hand side. While 7- and 30-days rice culture extracts were the outliers and separated from each other in the right hand side, which indicated that 7- and 30-days rice cultures produced some unique metabolites. Although they showed nearly the same TIC chromatogram and NMR spectra, however 7- and 30-days extracts showed a variance in the minor metabolites. 30-days rice culture of *Curvularia* sp. produced a higher yield, which prioritized it for further fractionation and biological studies. The OPLS-DA score plot (Fig.192) showed three different groups, based on its classification according to the cultivation

media, which were 7 and 30-days rice culture extracts together and liquid culture extracts (MeOH and water extracts) were grouped together while the EtOAc and BuOH extracts of *Terminalia* leaves were clustered together. The loading plot (Fig.193) showed that metabolites at ion peaks *m/z* (retention time in minutes) 207.089 (6.56), 354.158 (9.16), 467.242 (11.55) and 708.315 (9.19). These metabolites, were derepliacted before in (Table 35), are the most predominant, unique, and discriminated features detected in the rice culture extracts of *Curvularia* sp. and were predicted to be responsible for the outlying of the rice culture extracts in the PCA score plot (Fig.190). Principle component analysis of the fractions from 30-days rice culture extracts (Fig.194) showed a discrimination of fractions 60-86 and 116-130, which was indicative to the unique set of metabolites in each fraction. PCA loading plot (Fig.195) exhibited that metabolites with corresponding ion peaks at *m/z* (retention time in minutes) 173.106 (5.40), 346.212 (5.37), 354.158 (9.45), 708.316 (9.43), 380.197 (6.02) and 207.090 (5.74) equivalent for N-acetyl-leucine, unknown, picrorocelline, taxinine J, unknown and N-acetyl-phenylalanine respectively, were mostly predominant in fraction 60-86. While metabolites at *m/z* 708.329, 354.165 and 590.192 eluted at 9.41, 9.47 and 9.00 minutes, equivalent for taxinine J, picrorocelline and unknown compound respectively, were the outlier belonged to fraction 116-130. OPLS-DA score plot of active vs inactive fractions (Fig.196) showed the outlying of the active fraction 60-86 while the other two active fractions 4-32 and 96-103 were clustered together. The OPLS-DA loading plot (Fig.197) exhibited the putative unique metabolites belonging to fraction 60-86 that were identical to that shown in PCA loading plot (Fig.195) and predicted to be responsible of its anticancer activity. Moreover, metabolites at *m/z* (retention time in minutes) 207.090 (6.81) and 312.114 (1.77) equivalent for N-acetyl-phenylalanine and unknown compound respectively, were the outliers belonged to fractions 4-32 and 96-113 and predicted to be responsible for its anticancer activity. Therefore, from above, it was indicated that compound at *m/z* 207.090 eluted at 5.71 and 6.81 minutes, equivalent for N-acetyl-phenylalanine, was detected in all active fractions and strongly predicted to be responsible for the anticancer activity of the active fractions. Otherwise, it could be one of the other

putative metabolites.

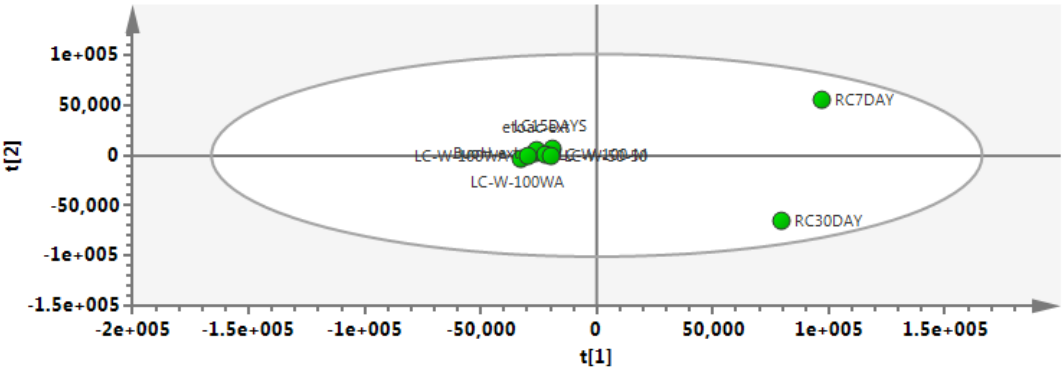

Fig.190 PCA score plot ofrice culture and LC *Curvularia* extracts vs *Terminalia* extracts

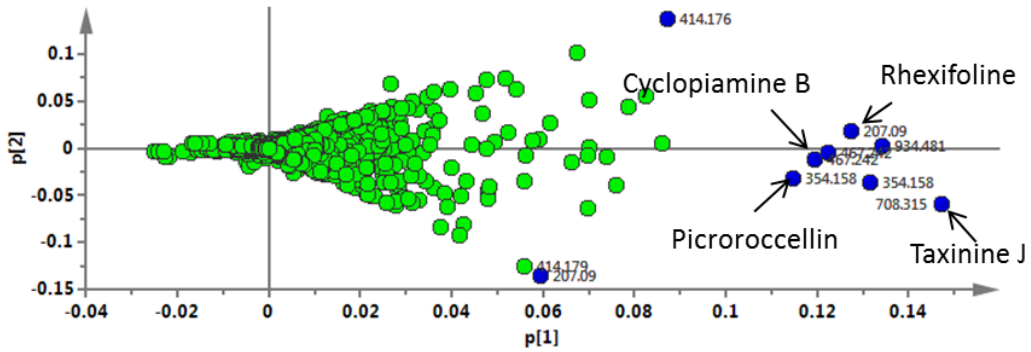

Fig.191 PCA loaading plot ofrice culture and LC extracts of *Curvularia* sp. vs *Terminalia* extracts. (●) the outlier metabolites belonged to 30-days rice culture ectract

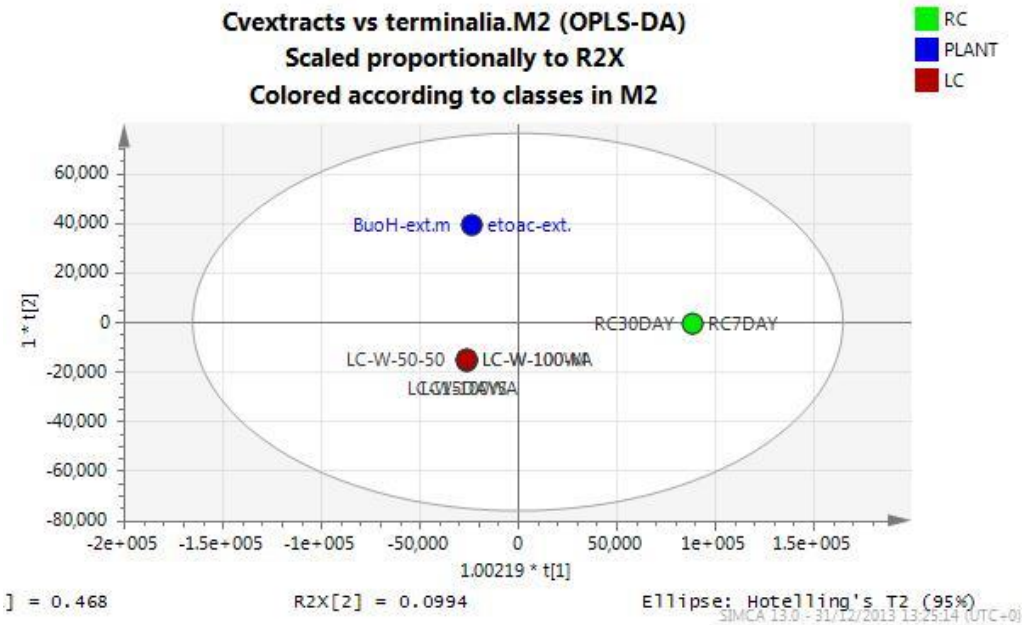

Fig.192 OPLS-DA score plot of *Curvularia* extracts against *Terminalia* plant extracts. (●) Rice culture extracts (●) LC extracts (●) Plant extracts

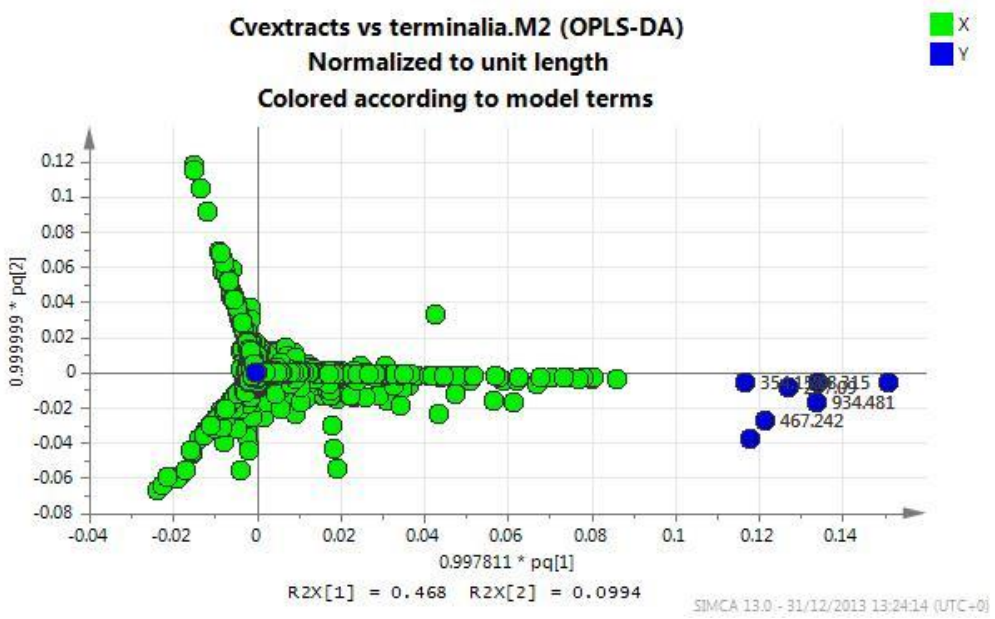

Fig.193 OPLS-DA loading plot of *Curvularia* extracts against *Terminalia* plant extracts. (•) the putative unique metabolites belonged torice culture extracts of *Curvularia* sp.

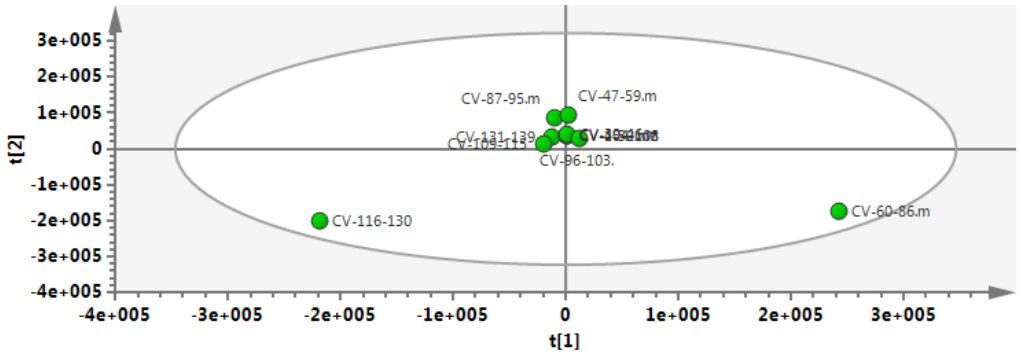

Fig.194 PCA score plot of fractions from 30-days rice culture extract of *Curvularia* sp.

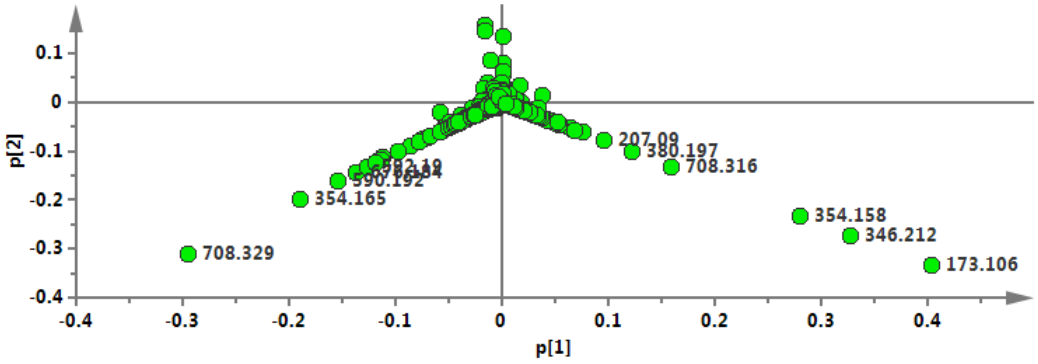

Fig.195 PCA loading plot of fractions from 30-days rice culture extract of *Curvularia* sp.

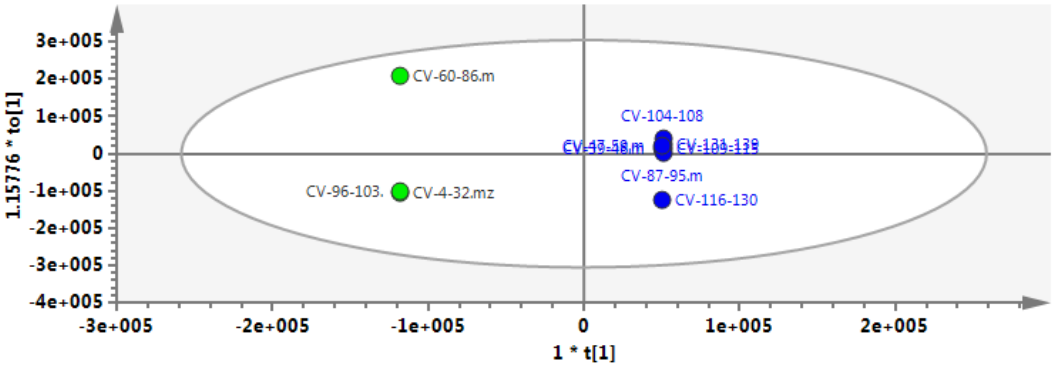

Fig.196 OPLS-DA score plot of fractions from 30-days rice culture extract of *Curvularia* sp. (●) active fractions (●) inactive fractions

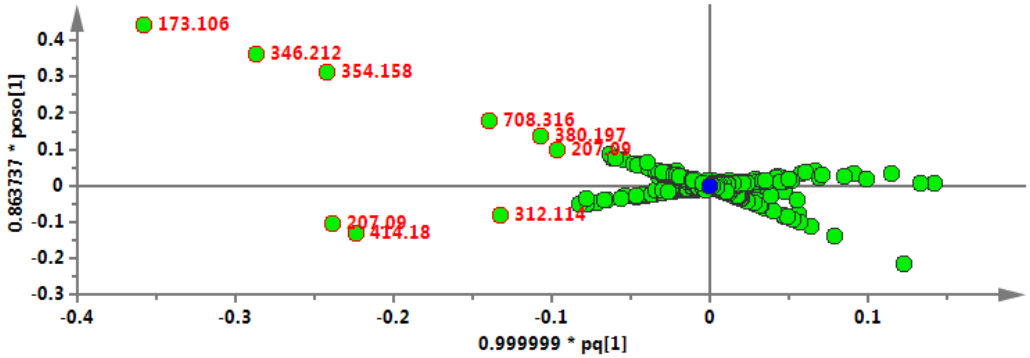

Fig.197 OPLS-DA loading plot of fractions from 30-days rice culture extract of *Curvularia* sp. showed the putative unique metabolites belonging to the active fractions

3.4.4. Biological activity

Although, MA plate extract of *Curvularia* sp. (codes *Terminalia* AL-F2, AL-F2a) showed no significant anticancer activity against both cancer cell lines (Fig.31, 32), the variance in the produced metabolites between the MA plate extract and the small upscaled culture extracts of *Curvularia* sp. shown in the heat map (Fig.189) was motivating to continue the metabolomics study and isolate the major outlying metabolites in the active extracts. Testing the *Curvularia* extracts and/or fractions against both PC3 and K562 cell lines (Fig.198) demonstrated that CV7, equivalent for 30-days rice culture extract, exhibited NF-κB inhibition activity. However, the purified fractions and/or compounds from 30-days rice culture extracts showed that fractions only CV9, CV10 and CV11, equivalent to fractions 4-32, 96-103 and 60-86, respectively, were active against K562 cancer cell line with no NF-κB inhibition activity observed. CV10 was a mixture of CV6 (N-acetylphenylalanine) and ferulic acid

as shown from the NMR spectra. This indicated that ferulic acid might be the compound responsible for the activity of this fraction because CV6 was not active. Although the amount of CV9 and CV11 was not enough for further fractionation, however the metabolomics study predicted that metabolites at *m/z* 346.212 eluting at 5.37 min that was an undescribed compound and/or at *m/z* 708.316 eluted at 9.43 min, identified as taxinine J, could be responsible for the remarked anticancer activity. The other predicted metabolites like those at *m/z* 207.090 and 354.158 equivalent for CV6 and CV5, respectively, were not active. Moreover, testing all fractions against *T. b. brucei* showed no significant activity. However, compound CV5 (N-acetylphenylalanine-L-phenylalanine) showed a significant activity against *Mycobacterium marinum* with more than 90% growth inhibition and MIC 282.48 µM (Fig.199).

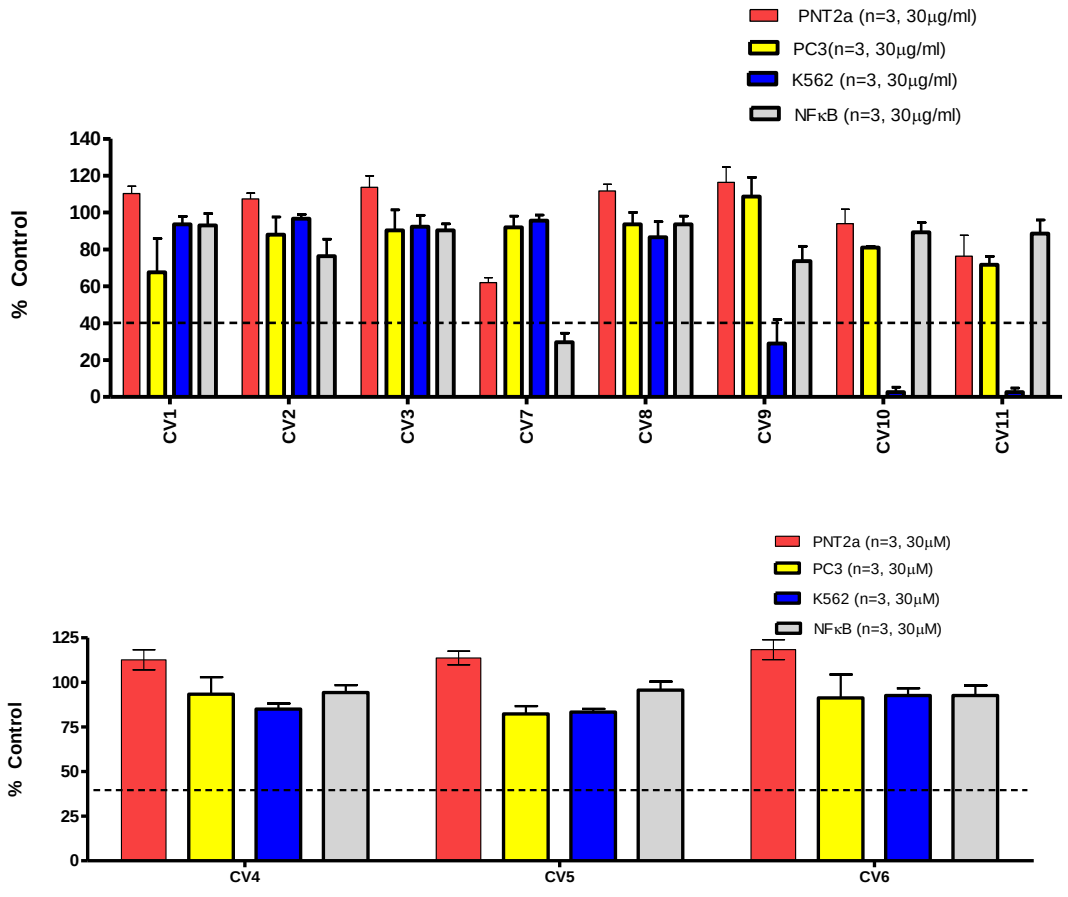

Fig.198 Cytotoxicity of fractions and/or compounds from 30-days rice culture extract of *Curvularia* sp.

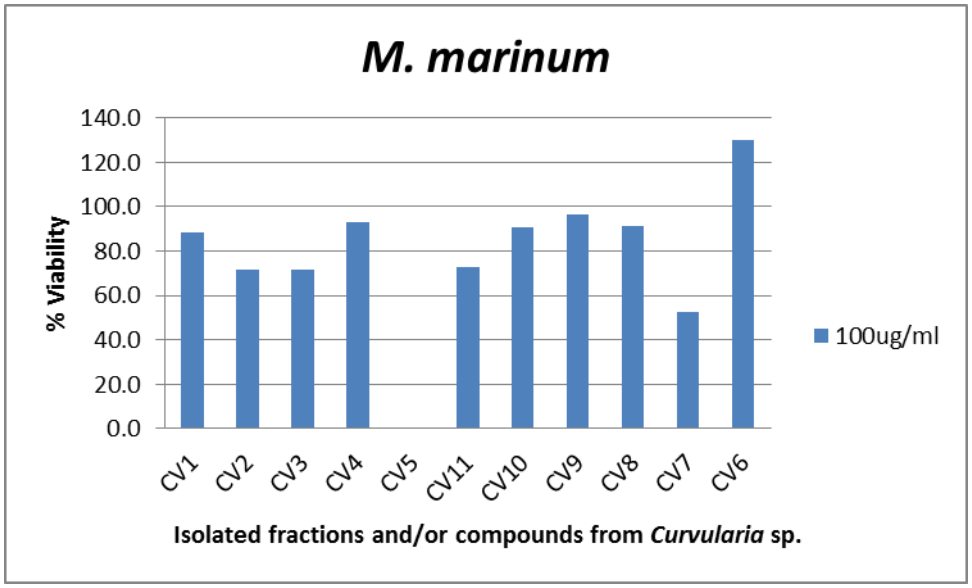

Fig.199 Antimicrobial activity of fractions and/or compounds from 30-days rice culture extract of *Curvularia* sp.

3.4.5. Isolated compounds

3.4.5.1. Compound CV5 (new)

(2-(2-acetamido-3-phenylpropanamido)-3-phenylpropanoic acid)	
Synonyms	N-acetyl-phenylalanine-L-phenylalanine
Sample codes	CV5
Sample Amount	15 mg
Physical Description	Yellow amorphous powder
Molecular Formula	$C_{20}H_{22}N_2O_4$
Molecular Weight	354 g/mol
Retention time (LC-MS)	10.56 min

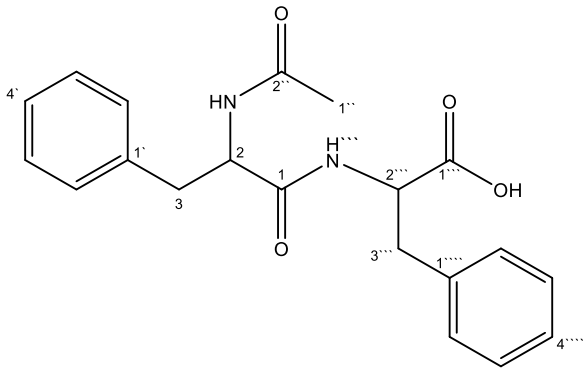

LC-HRFTMS spectrum $[M+H]^+$ 355.1645

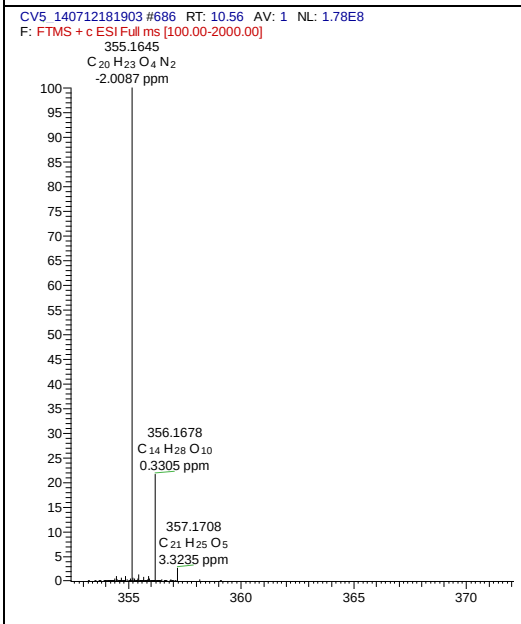

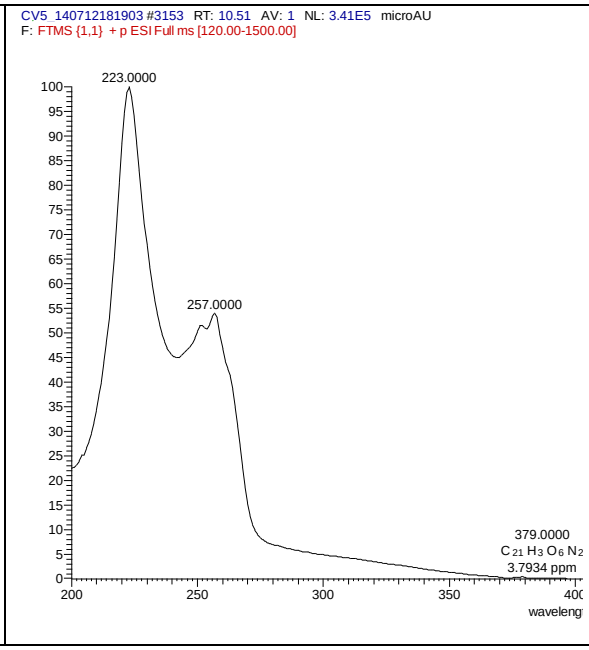

Compound CV5 (15 mg) was obtained as a yellow powder, exhibited a molecular formula $C_{20}H_{22}N_2O_4$ established by ESI-HRMS at *m/z* = 355.1645 $[M+H]^{+\cdot}$ While the tandem **MS/MS** spectrum (Fig.200) showed fragments at *m/z* = 190.0946 equivalent for $C_{11}H_{12}NO_2$ and 164.0712 for $C_9H_{10}NO_2$. The **^{1}HNMR** spectrum (DMSO, 400 MHz) (Fig.201, Table 37) showed proton resonances at δ_H 8.39 (d, *J* = 8.12 Hz, 1H), 8.35 (d, *J* = 8.53 Hz, 1H), 7.05-7.27 (m, 10H), 5.18 (m, 1H), 5.12 (m, 1H), 2.43-2.70 (m, 4H) and 1.80 (s, 3H). The **^{13}C NMR** spectrum (DMSO, 400 MHz) (Fig.202) showed 20 carbon signals including five quaternaries, ten aromatic methines, two methylene, two carbinolic methines and one methyl. The **TOCSY** spectrum (Fig.203) showed a correlation between N*H* at δ_H 8.39 and α-C*H*NH-2``` (δ_H 5.12) and C*H*$_2$-3``` gp (δ_H 2.43-2.70) of L-phenylalanine moiety, while the N*H* at δ_H 8.35 correlated with α-C*H*NH-2 (δ_H 5.18) and C*H*$_2$-3 gp (δ_H 2.43-2.70) of the N-acetyl-phenylalanine moiety. The structure of the N-acetyl-phenylalanine was confirmed from the **HMBC** spectrum (Fig.204) through the correlations of α-C*H*NH-2 (δ_H 5.18) with C-3 (δ_C 43.0), C-2`` ($\delta_C$ 168.8), C-1` ($\delta_C$ 143.3) and C-2`/6` ($\delta_C$ 127.2). In addition, NH ($\delta_H$ 8.35) with C-2``, C-2 (δ_C 50.5), while the structure of L-phenylalanine moiety was confirmed through the correlations of α-C*H*NH-2``` (δ_H 5.12) with C-1``` (δ_C 172.3), C-3``` (δ_C 41.3), C-1 (δ_C 168.9), C-1'''' (δ_C 142.8), C-2''''/6'''' (δ_C 126.9); NH (δ_H 8.39) with C-2``` (δ_C 49.83) and C-1. The correlation of α-C*H*NH and NH of L-phenylalanine moiety with the carbonyl C-1 (δ_C 168.9) of the N-acetyl-phenylalanine moiety confirmed the attachment of the two moieties through the amide linkage including N*H* of the second (δ_H 8.39) and C-1 (δ_C 168.9) of the first. Furthermore, the configuration of the L-phenylalanine was assigned through Marfey's reagent experiment (Ibrahim et al., 2010) and HPLC-MS of the reaction products (Fig.206) showed CV5 reaction product equivalent for $C_{19}H_{19}O_6N_4F$ at *m/z* 419.1393 $[M+H]^+$ eluted at 13.77 min which was approximately superimposable with the standard L-phenylalanine reaction product (Rt 13.70 min). So from the above, compound CV5 (Fig.205) was identified as N-acetyl-phenylalanyl-L-phenylalanine (2-(2-acetamido-3-phenylpropanamido)-3-phenylpropanoic acid) and it is a new dipeptide isolated for the first time in nature.

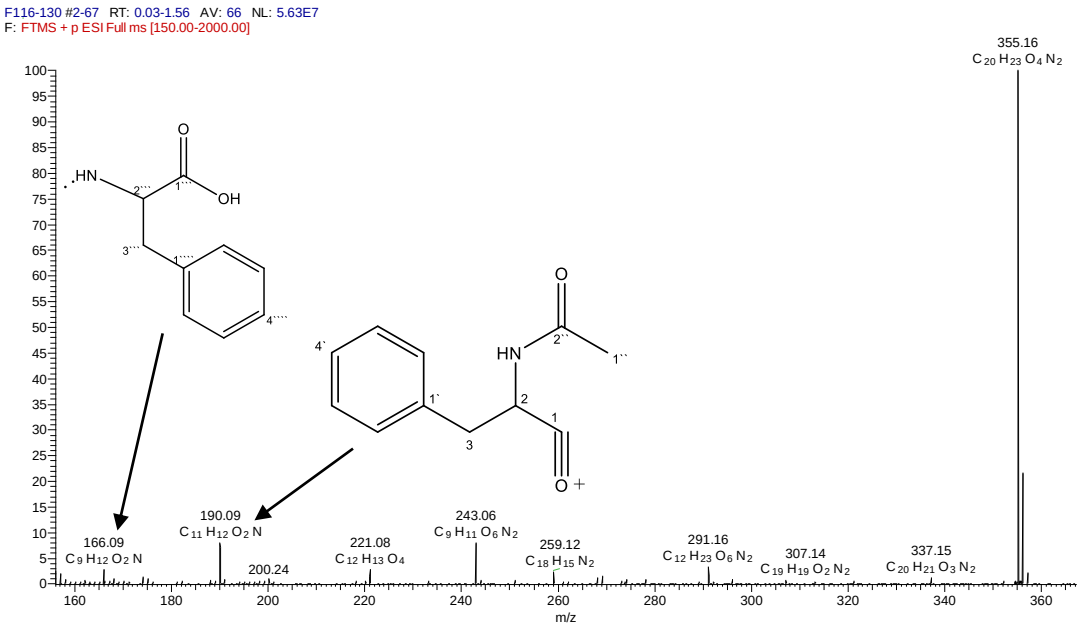

Fig.200 MS-MS spectrum of compound CV5

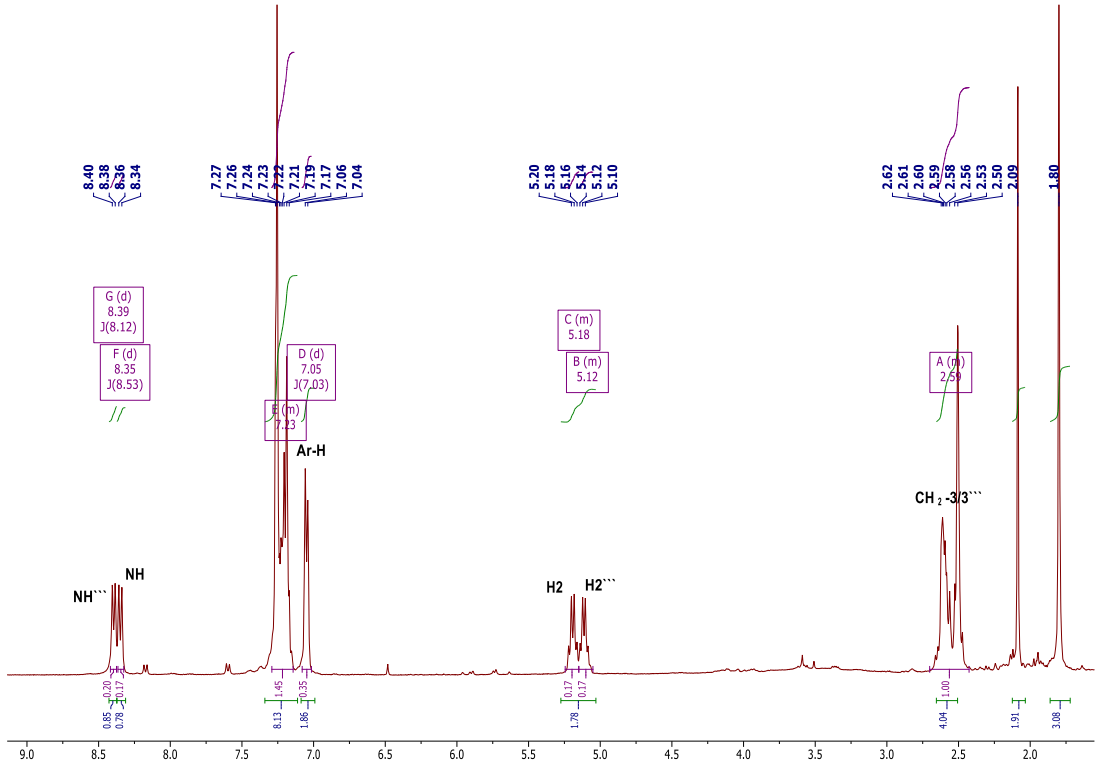

Fig.201 ^{1}H NMR spectrum of compound CV5

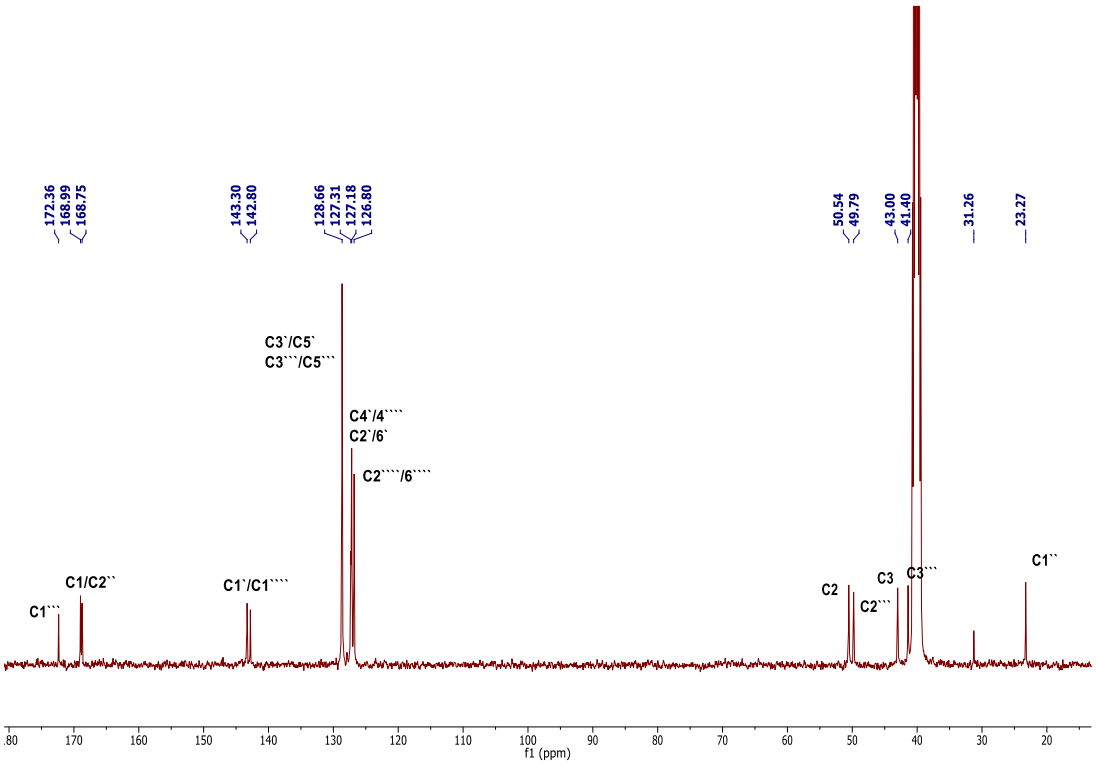

Fig.202 ^{13}C NMR spectrum of compound CV5

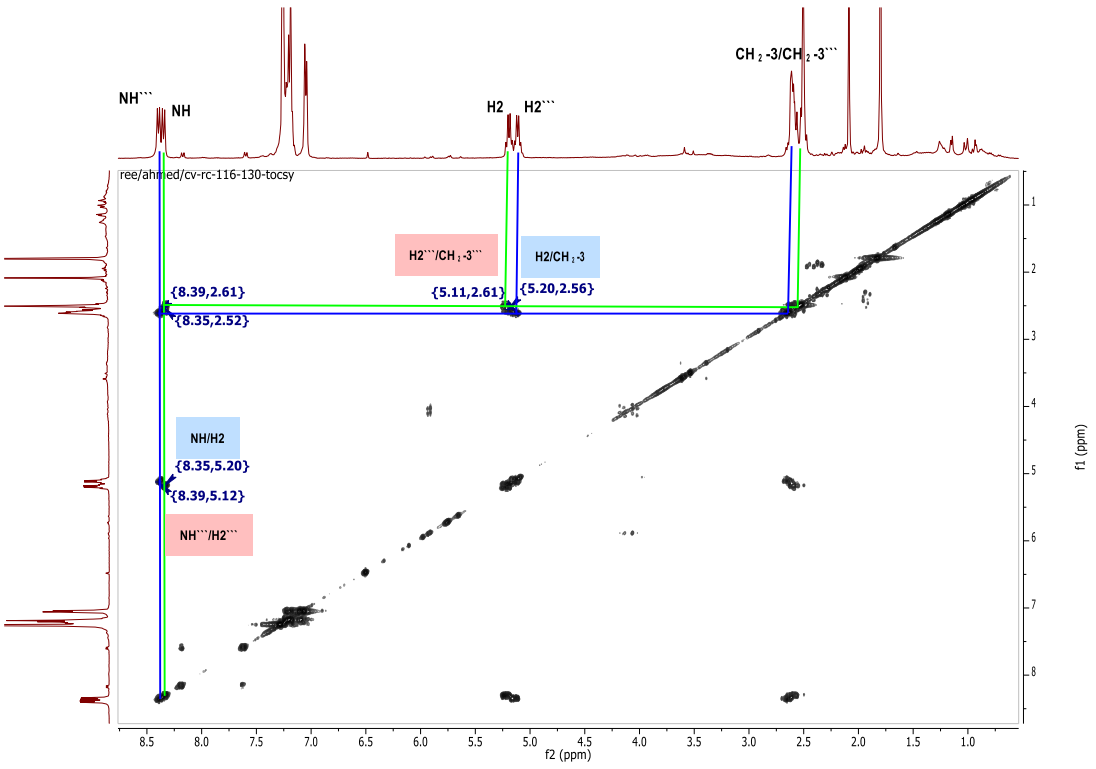

Fig.203 Expansion of TOCSY spectrum of compound CV5 showing two spin system (●) L-phenylalanine and (●) N-acetyl-D-phenylalanine

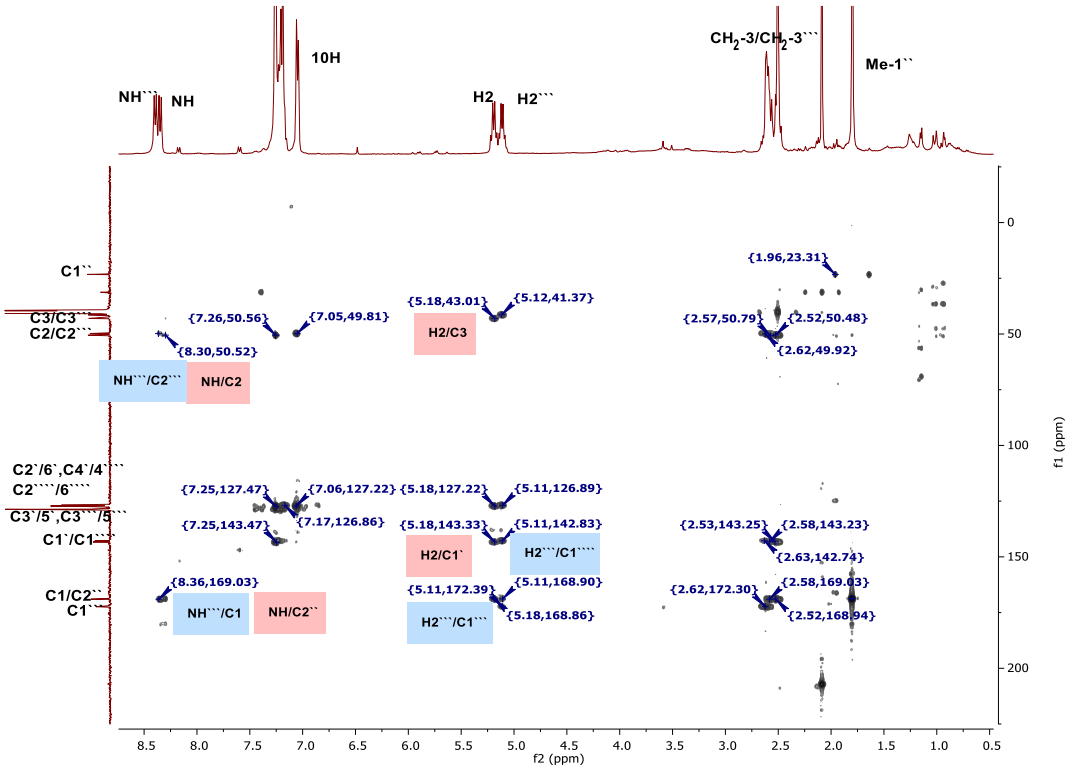

Fig.204 HMBC spectrum of compound CV5

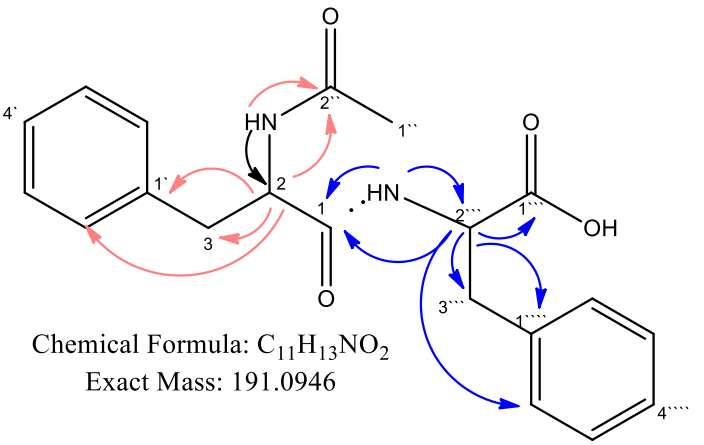

Fig.205 HMBC correlations and MS-MS fragments of compound CV5. (●) represents N-acetylphenylalanine moiety and (●) for L-phenylalanine

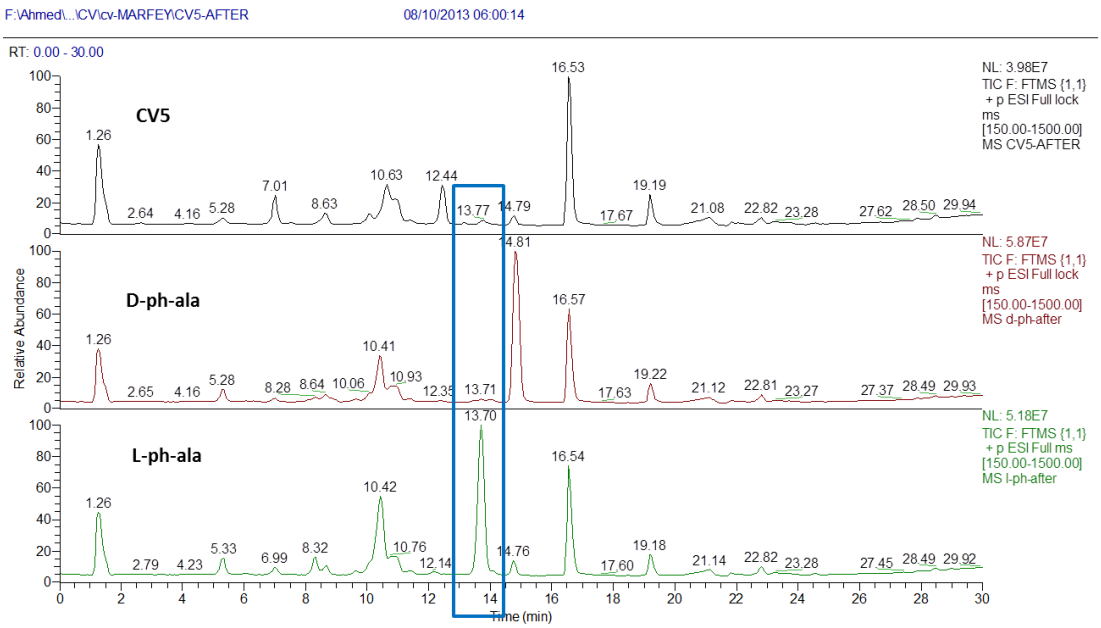

Fig.206 TIC of marfey's products for compound CV5, standard L-phenylalanine and standard D-phenylalanine

Table 37: ^{1}H NMR and ^{13}C NMR data of compound CV5

Atom No.	CV5-DMSO		
	δ_C (m)	δ_H (m, *J* in Hz)	HMBC
1	168.9 (C)		
2	50.5 (CH)	5.18 (m, 1H)	C3, C2``,C1`, C2`/6`
3	43.0 (CH_2)	2.52-2.61 (m)	C1, C1`, C2
1`	143.3 (C)		
2`/6`	127.2 (CH)	7.05-7.27 (m, 10H)	
3`/5`,3````/5````	128.6 (CH)		
4`/4````	127.3 (CH)		
1``	23.3 (CH_3)	1.8 (s,)	
2``	168.8 (C)		
1```	172.3 (C)		
2```	49.8 (CH)	5.12 (m)	C1```, C3```, C1, C1````, C2````/6````
3```	41.3 (CH_2)	2.52-2.61 (m)	C1```, C1````,C2```
1````	142.8 (C)		
2````/6````	126.9 (CH)	7.05-7.27 (m, 10H)	
NH		8.35 (d, 8.12 Hz)	C2``, C2
NH```		8.39 (d, 8.53 Hz)	C2```, C1

3.4.5.2. Compound CV4 (new)

(2-(2-(2-acetamido-3-phenylpropanamido)-3-phenylpropanamido)-4-methylpentanoic acid)	
Synonyms	N-acetyl-phenylalanine-L-phenylalanine-L-leucine
Sample codes	CV4
Sample Amount	16 mg
Physical Description	Brownish white amorphous powder
Molecular Formula	$C_{26}H_{33}N_3O_5$
Molecular Weight	467 g/mol
Retention time (LC-MS)	13.0 min

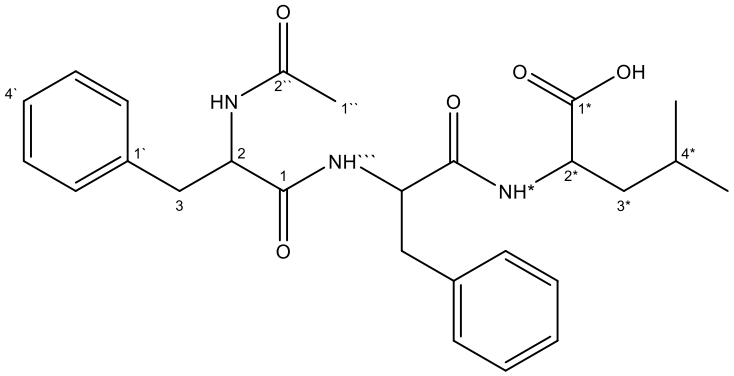

LC-HRFTMS spectrum $[M+H]^+$ 468.2490

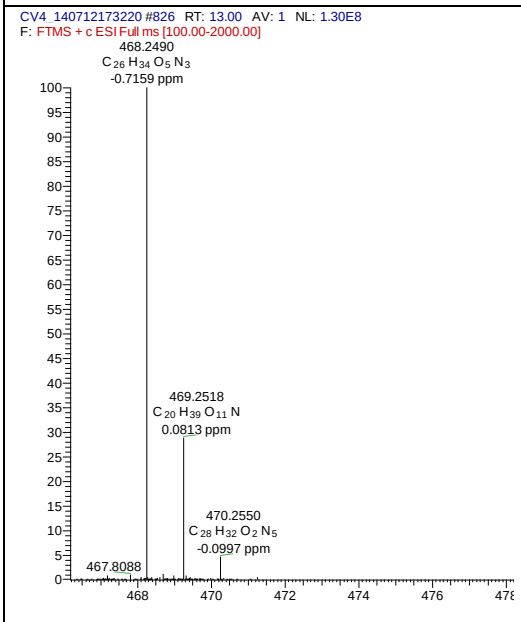

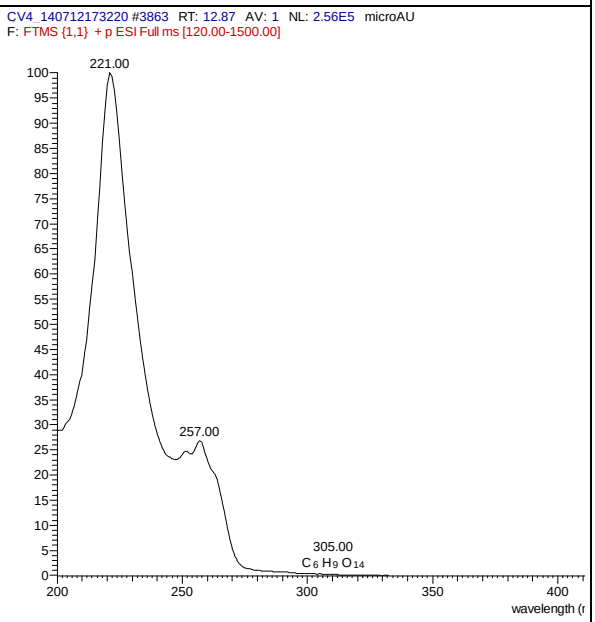

Compound CV4 (16 mg) was obtained as a brownish white, exhibited a molecular

formula **$C_{26}H_{33}N_3O_5$** established by **ESI-HRMS** at *m/z* = 468.2490 $[M+H]^+$. Moreover, the MS-MS (Fig.207) showed three main fragments which were 337.1545 ($C_{20}H_{21}O_3N_2$), 279.1702 ($C_{15}H_{23}O_3N_2$) and 190.0864 ($C_{11}H_{12}ON_2$). The **^{1}H NMR** spectrum (DMSO, 400 MHz) (Fig.208, Table 38) showed proton signals at δ_H 8.38 (d, *J* = 8.5 Hz, 1H), 8.29 (d, *J* =7.9 Hz, 1H), 8.08 (d, *J* = 8.2 Hz, 1H), 7.05-7.25 (m, 10H), 5.19 (m, 1H), 5.09 (m, 1H), 4.11 (m, 1H), 2.40-2.61 (m, 4H), 1.37 (*m*, 2H), 1.27 (*m*, 1H), 0.78 (*d*, 5.9, 3H) and 0.68 (*d*, 5.8, 3H). The **^{13}C NMR** spectrum (DMSO, 400 MHz) (Fig.209) showed 26 carbon signals including six quaternaries, ten aromatic methines, three methylene, three methyles and four methines (Three α-C*H*NH and one aliphatic). The **TOCSY** spectrum (Fig.210) showed a correlation of N*H* (8.38) with α-C*H*NH-2 (5.19) which connected to CH_2-3 (2.40-2.61) of the N-acetyl-phenylalanine moiety while N*H*``` (8.29) correlated with α-C*H*NH-2``` (5.09) and CH_2-3``` (2.40-2.61) of the L-phenylalanine moiety. Moreover, the L-leucine moiety was confirmed through the correlation of the NH^* group (8.09) with α-C*H*NH-2* (4.11), CH_2-3* (1.37) and the two methyl doublets Me-5* (δ_H 0.78) and Me-6* (δ_H 0.68). The connectivity of the three amino acids moieties were confirmed from the **HMBC** spectrum (Fig.211) through the correlation of α-C*H*NH-2 (δ_H 5.19) of the N-acetyl-phenylalanine with C-3 (δ_C 43.0), C-2`` ($\delta_C$ 168.8),C-1` ($\delta_C$ 143.4) and C-2`/6` ($\delta_C$ 127.1). Moreover, N*H* ($\delta_H$ 8.38) with C-2``, C-2 (δ_C 50.5), while the structure of L-phenylalanine moiety was confirmed through the correlations of α-C*H*NH-2``` (δ_H 5.1) with C-1``` (δ_C 169.7), C-3``` (δ_C 42.6), C-1 (δ_C 168.7), C-1'''' (δ_C 142.8), C-2''''/6'''' (δ_C 126.9); NH``` (δ_H 8.29) with C-2``` (δ_C 50.5) and C-1. Moreover, the structure of L-leucine and its position on C-1``` was confirmed through the correlation of α-C*H*NH-2* (δ_H 4.11) with C-1```, C-1* (δ_C 174.8) and C-3* (δ_C 40.63); CH_2-3* (δ_H 1.37) with C-2* (δ_C 50.6) and the two methyl doublets Me-5* (δ_C 21.6) and Me-6* (δ_C 23.6) which in return correlated with C-3*, C-4* (δ_C 24.4). The configuration of the L-phenylalanine and L-leucine were assigned through Marfey's reagent experiment (Ibrahim et al., 2010) and the HPLC-MS of the products (Fig.212) showed CV4 reaction products equivalent for $C_{16}H_{21}FN_4O_6$ at *m/z* 385.1548 $[M+H]^+$ were eluted at 13.80 min which was approximately similar to the standard L-leucine eluted at 13.76 min. The mass

spectrum also showed a corresponding ion peak equivalent for $C_{19}H_{19}O_6N_4F$ at *m/z* 419.1393 $[M+H]^+$ eluted at 13.80 min which was approximately synonymous to the standard L-phenylalanine reaction product eluted at 13.70 min. So from the above, compound CV4 (Fig.213) was identified as N-acetyl-phenylalanine-L-phenylalanine-L-leucine ((2-(2-(2-acetamido-3-phenylpro panamido)-3-phenylpropanamido)-4-methylpentanoic acid) and it is a new compound isolated for the first time in nature from *Curvularia* sp.

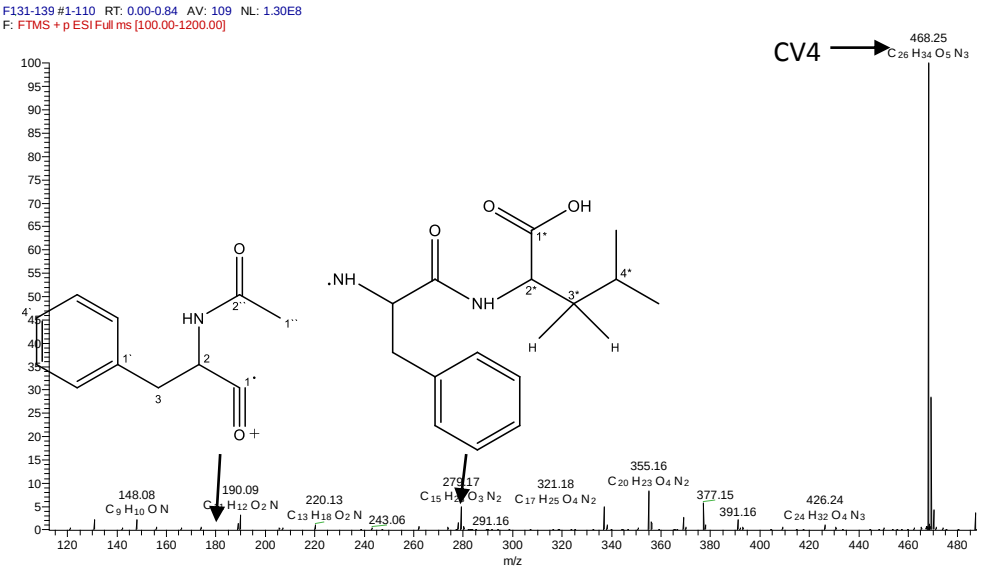

Fig.207 HRESI-MS-MS spectrum of compound CV4

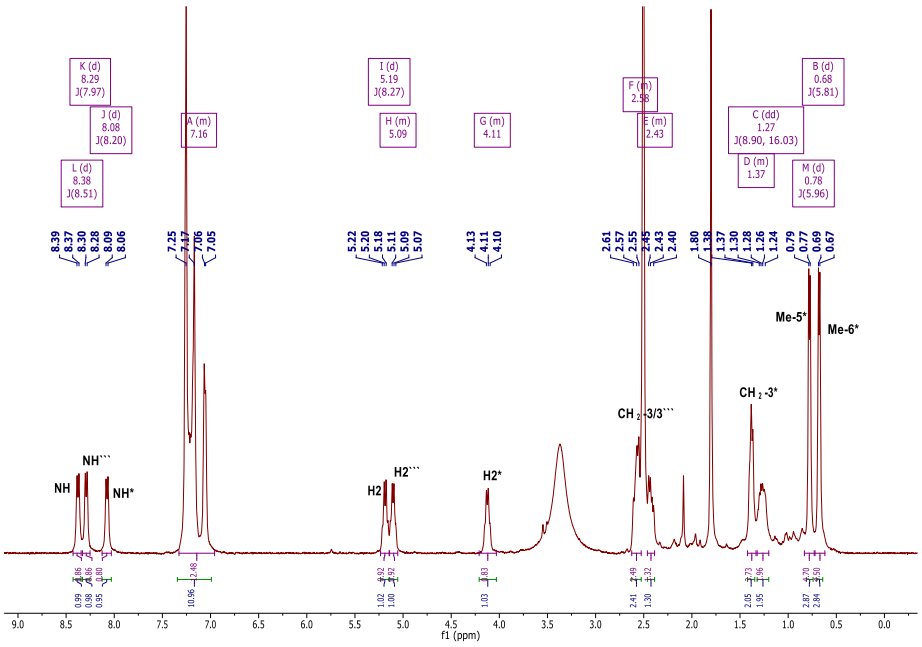

Fig.208 ^{1}H NMR spectrum of compound CV4

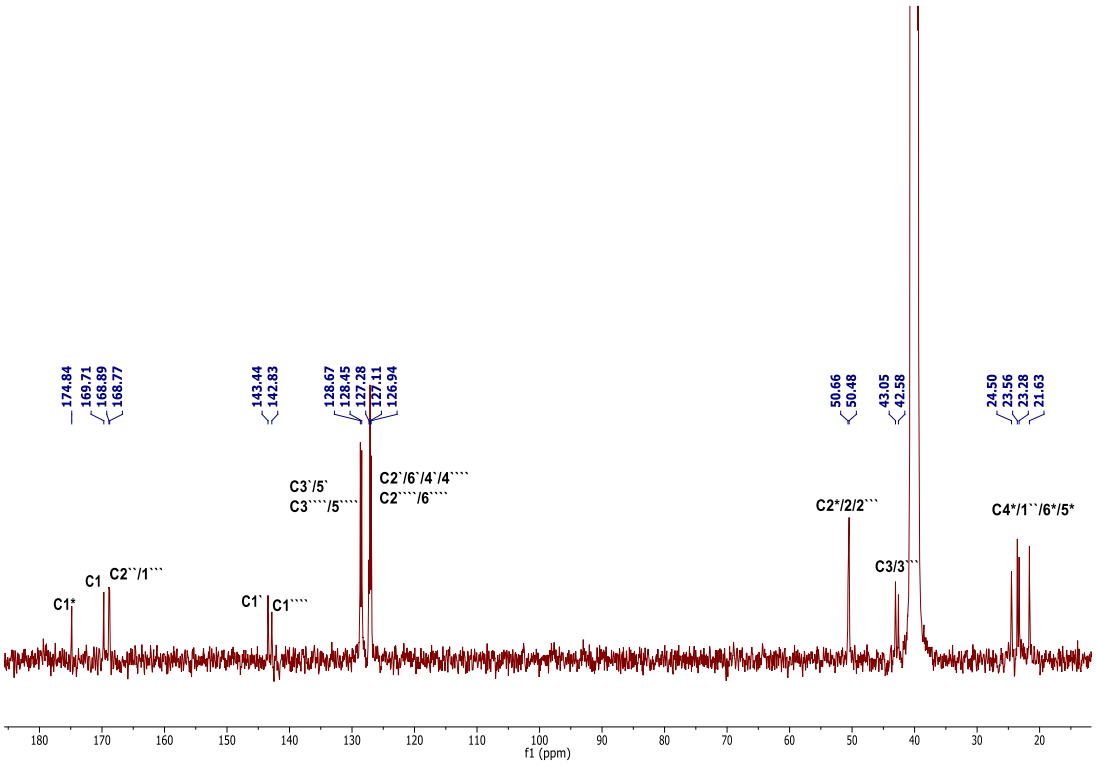

Fig.209 ^{13}C NMR spectrum of compound CV4

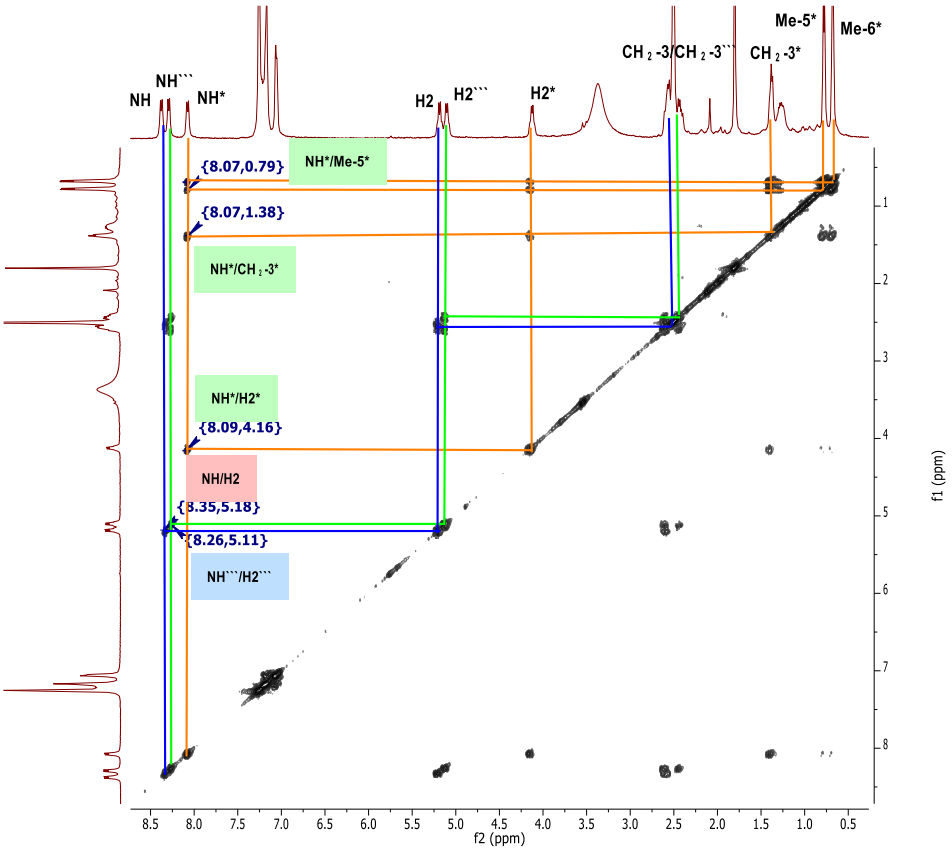

Fig.210 TOCSY spectrum of compound CV4 showing three spin systems

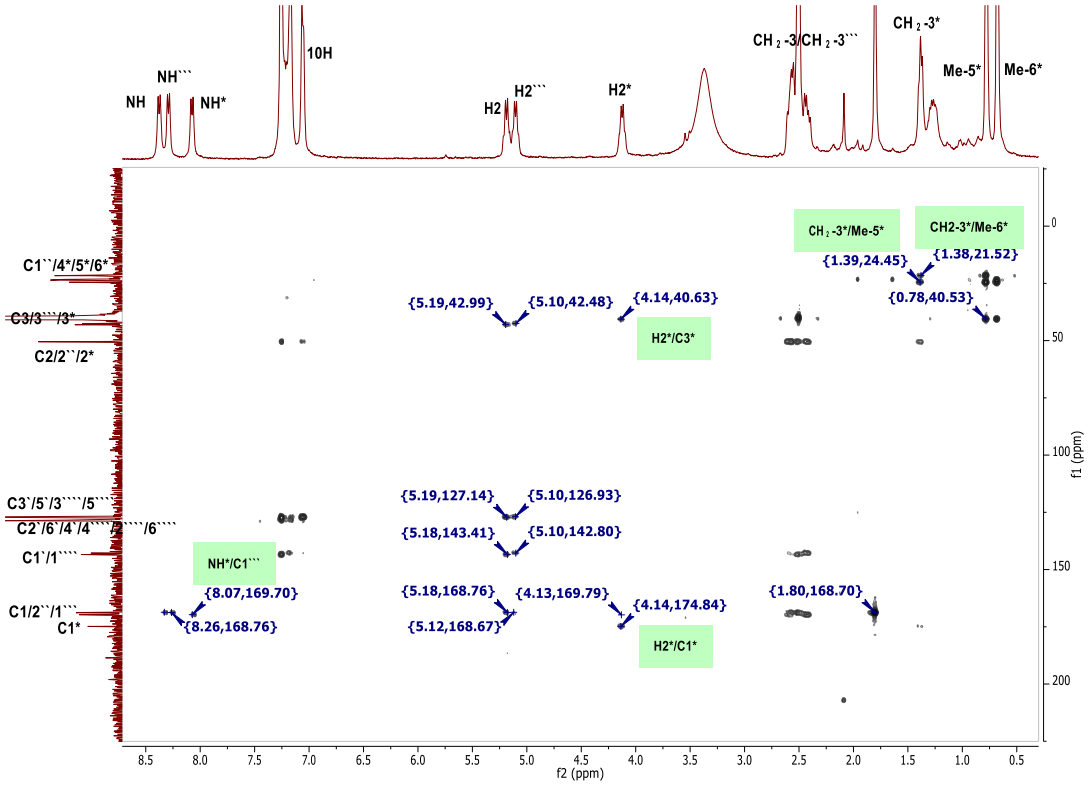

Fig.211 HMBC spectrum of compound CV4

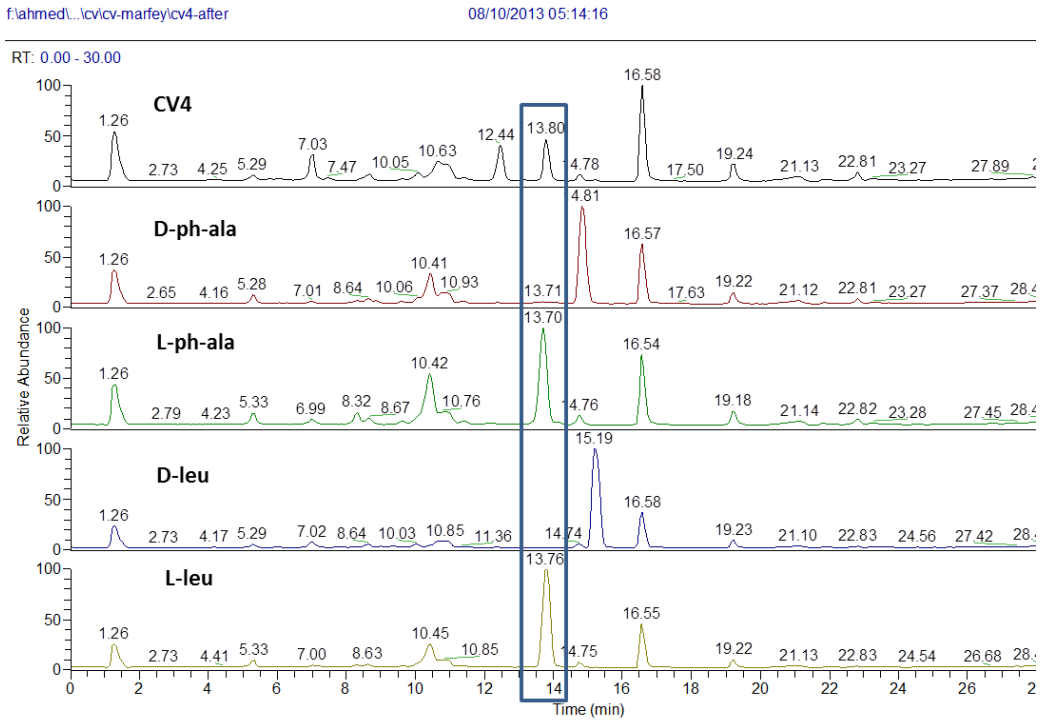

Fig.212 TIC of CV4 Marfey's products and the standard amino acids

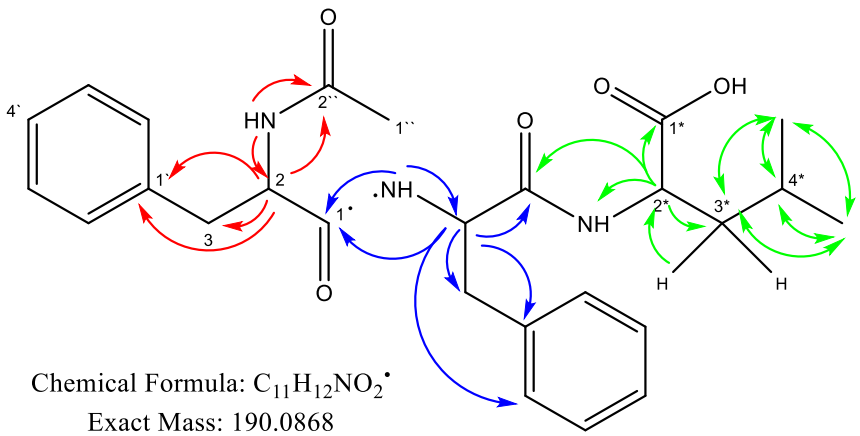

Chemical Formula: $C_{11}H_{12}NO_2^{\bullet}$
Exact Mass: 190.0868

Chemical Formula: $C_{15}H_{21}N_2O_3$
Exact Mass: 277.1552

Fig.213 HMBC correlations and fragmentation hypothesis of compound CV4. (●) N-acetylphenylalanine, (●) L-phenylalanine and (●) L-leucine

Table 38: ^{1}H NMR, ^{13}C NMR, TOCSY and HMBC correlations of compound CV4

Atom No.	CV4-DMSO			
	δ_C (m)	δ_H (m, *J* in Hz)	TOCSY	HMBC
1	168.7 (C)			
2	50.5 (CH)	5.19 (m)	3	C3, C2``,C1`, C2`/6`
3	43.0 (CH_2)	2.40-2.61 (m`)		C1, C1`, C2
1`	143.4 (C)			
2`,6`	127.1 (CH)	7.05-7.25 (m, 10H)		
3`,5`	128.6 (CH)			
4`,4````	127.2 (CH)			
1``	23.3 (CH_3)	1.8 (s)		
2``	168.8 (C)			
1```	169.7 (C)			
2```	50.5 (CH)	5.09 (m)	3```	C1```, C3```, C1, C1````, C2````/6````
3```	42.6 (CH_2)	2.40-2.61 (m)		C1```, C1````,C2```
1````	142.8 (C)			
2````,6````	126.9 (CH)	7.05-7.25 (m, 10H)		
3````,5````	128.4 (CH)			
1*	174.8 (C)			
2*	50.6 (CH)	4.11 (m)	3*, 5*, 6*	C1*, C3*, C1```
3*	40.6 (CH_2)	1.37 (m)		C2*, C5*, C6*
4*	24.4 (CH)	1.27 (m)		
5*	23.6 (CH_3)	0.68 (d, 5.8 Hz)		C3*, C4*, C6*
6*	21.6 (CH_3)	0.78 (d, 5.9 Hz)		C3*, C4*, C5*
NH		8.38 (d, 8.5 Hz)	3, 2	C2``, C2
NH```		8.29 (d, 7.9 Hz)	3```, 2```	C2```, C1
NH*		8.08 (d, 8.2 Hz)	2*, 3*, 5*, 6*	C1```

3.4.5.3. Compound CV6 (N-acetylphenylalanine)

2-acetamido-3-phenylpropanoic acid	
Synonyms	N-acetylphenylalanine
Sample codes	CV6
Sample Amount	8 mg
Physical Description	yellowish brown amorphous powder
Molecular Formula	$C_{11}H_{13}O_3N$
Molecular Weight	207 g/mol
Optical Rotation $[\alpha]_D^{20}$	+12 (*c* 0.05 in MeOH)
Retention time (LC-MS)	6.76 min

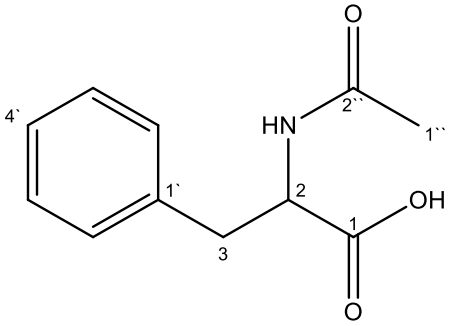

LC-HRFTMS spectrum $[M+H]^+$ 208.0964

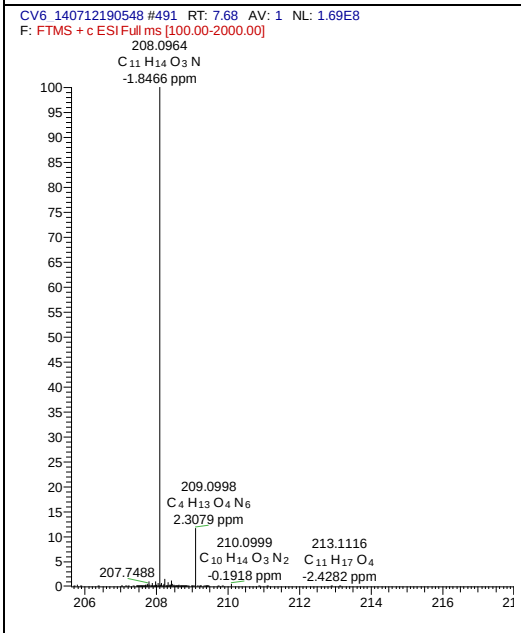

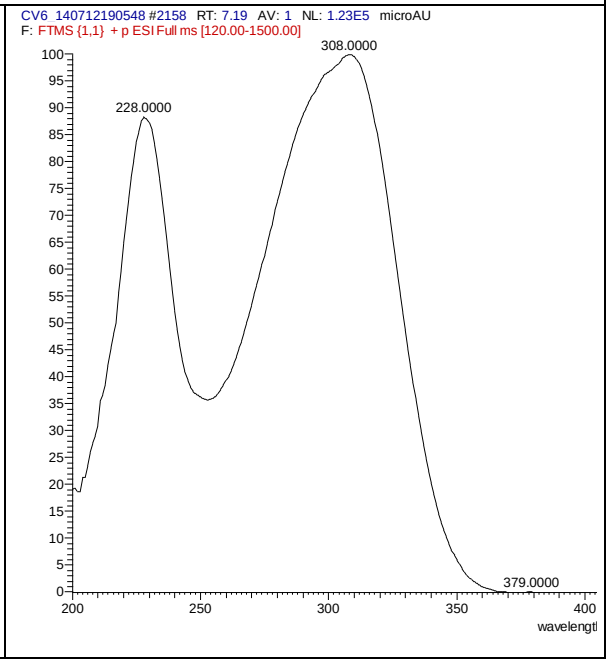

Compound CV6 (8 mg) was isolated as yellowish brown amorphous powder, exhibited molecular formula $C_{11}H_{12}O_3N$ established on the basis of **ESI-HRMS**

at *m/z* **208.0964** [M+H]+. The **^{1}H NMR** spectrum (DMSO, 400 MHz) (Fig.214) showed six proton signals at δ_H 8.15 (d, 1H, *J* = 7.84 Hz), 7.24 (m, 5H), 4.37 (m, 1H), 3.04 (dd, 1H, *J* = 13.8, 4.6 Hz), 2.82 (dd, 1H, *J* = 13.6, 9.5 Hz) and 1.77 (s, 3H). The structure of the amino acid spin system was detected from ^{1}H-^{1}H **TOCSY** spectrum (Fig.215) which showed the correlation between N*H* group at δ_H 8.15 and CH_{2A} (δ_H 3.04), CH_{2B} (δ_H 2.82) and α-C*H*NH at δ_H 4.37. HMBC experiment was not accomplished because of the low yield and also because CV6 is already a component of CV5 and CV4. So from the TOCSY spectrum and comparison of ^{1}HNMR data to the literature and to compounds CV5 and CV4 (Dressen et al., 2009, Naturale et al., 2012, Koshti et al., 2005) (Table 39), compound CV6 was identified as N-acetyl-phenylalanine.

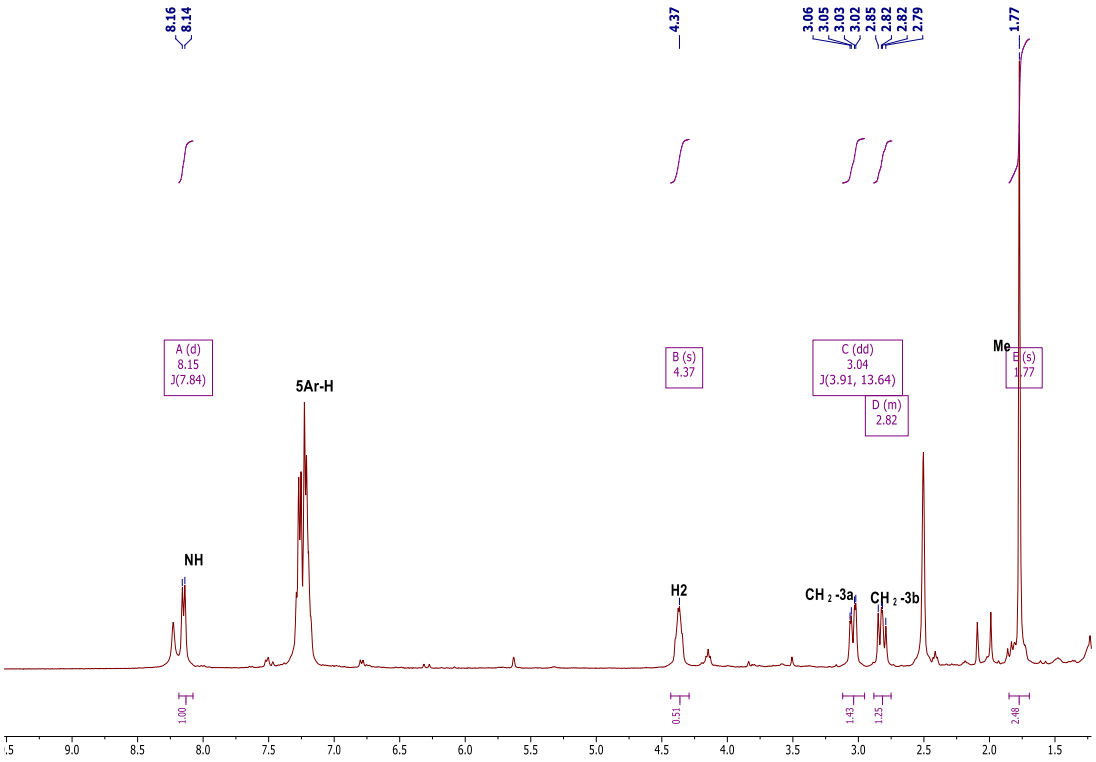

Fig.214 ^{1}HNMR spectrum of compound CV6

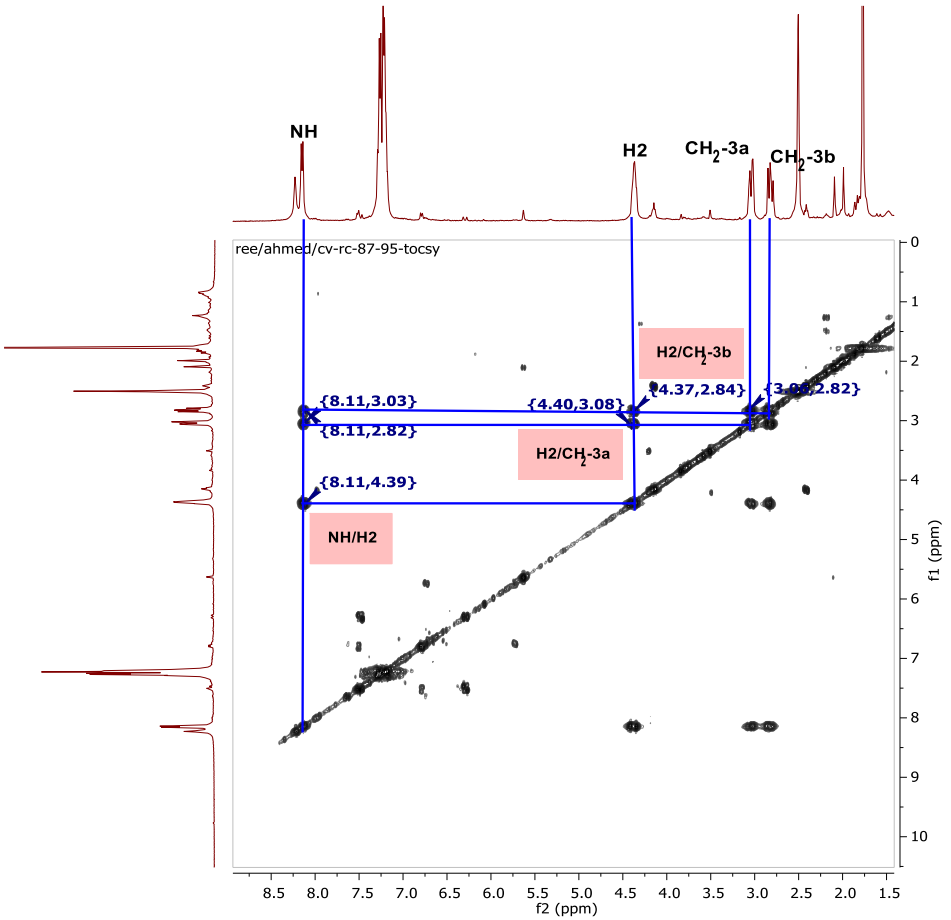

Fig.215 ^{1}H-^{1}H TOCSY spectrum of CV6 showing the spin system

Table 39: ^{1}H NMR and ^{13}C NMR data of CV6 and literature

Atom No.	N-acetyl-L-phenylalanine-CD_3OD Dressen 2009		N-acetyl-D,L-phenylalanine-CD_3OD-Koshti 2005	CV6-DMSO	
	δ_C (m)	δ_H (m, *J* in Hz)	δ_H (m, *J* in Hz)	δ_H (m, *J* in Hz)	δ_C (m)
1	174.8 (C)				173.9
2	55.2 (CH)	4.92 (m)	4.60-4.72 (m, 1H)	4.37 (m)	54.4
3	38.4 (CH_2)	3.45 (dd, CH_2a), 3.20 (dd, CH_2b)	3.21 (dd, 1H), 2.95 (dd, 1H)	3.04 (dd, 3.9, 13.6 Hz, CH_2-a), 2.82 (m, CH_2-b)	37.5
1`	138.5 (C)				138.6
2`,6`	129.4 (CH)	7.51 (m, 5H)	7.13-7.38 (m, 5H)	7.24 (m, 5H)	128.7
3`,5`	130.2 (CH)				129.7
4`	127.8 (CH)				126.9
1``	22.3 (CH_3)	2.15 (s)	1.91 (s)	1.77 (s)	23.0
2``	173.1 (C)				169.6
NH				8.15 (d, 7.8 Hz)	

Chapter 4: Discussion

4. Discussion

4.1. Introduction

Plants contain countless numbers of endophytes. Endophytes associated with plants can be considered as an infinite undisclosed reservoir of metabolic diversity and an important area for discovery of novel bioactive secondary metabolites (Strobel et al., 2004). In many cases endophytic fungi might be involved in the biosynthesis of plant products or the producers of several groups of new pharmacologically active and structurally diverse secondary metabolites (Arnold, 2007). Endophytes from Egyptian medicinal plants of various diverse habitats were explored and screened for anti-cancer and antimicrobial activity. Five endophytic fungi, *Aspergillus aculeatus*, *A. orayza* and *Curvularia sp*. isolated from *Terminalia laxiflora* leaves; *A. flocculus* and *Syncephalastrum racemosum* isolated from *Markhamia platyclayx* stem showed a significant anticancer activity against prostate cancer cell line (PC3), chronic myolgenous leukemia cell line (K562) and a remarkable activity against *T. b. brucei* (Table 4). Efficient cultivation and production processes at a small volume scale fermenter were developed through real time metabolomic-assisted optimization. Metabolomics was applied to identify and track active compounds highlighted by the bioscreening assays during culture optimization. Metabolomics is applied particularly in bioactive screening to improve dereplication and identification procedures, where fast dereplication of known compounds and identification of lead bioactive metabolites is important. Dereplication studies have been accomplished by sending HRFTMS data to differential analysis utilizing an MZmine software, in order to compare different extracts in terms of chemical profile and highlighting the most abundant and significant metabolites which can be later correlated to the observed bioactivity using a multivariate analysis software like SIMCA-P^+.

4.2. Metabolomic studies, isolation and biosynthetic pathways of bioactive metabolites from *Aspergillus aculeatus*

The metabolomics study of *A. aculeatus* fungal extracts showed that 7-days rice culture extract produced relatively more abundant metabolites than other fungal

extracts. Comparison of *A. aculeatus* extracts has been accomplished using MZmine 2.10 software and heatmaps generated by the program R (version 2.15.2) in order to visualise and choose the optimum cultivation conditions, which produce the largest quantity of the bioactive metabolites. A heatmap for 7, 15 and 30-days rice culture exhibited that the 15-days extract produced the lowest quantity of metabolites (Results section: 3.2.2). This indicated that 15-days extract was an intermediate stage when nutrients are being depleted while metabolites are starting to be produced in the form of secondary metabolites as a survival mechanism. Moreover, the ^{1}HNMR spectrum of 7-days culture extract exhibited more resolved peaks in the aromatic region with the presence of broad peak around 12 ppm equivalent for a hydrogen bound phenolic OH like those found in flavonoids and/or anthraquinone. Searching the databases like DNP and AntiBase® for the most prominent metabolites in the extract led to the dereplication of both known and undescribed top metabolites produced in the 7-day rice culture (Table 5). PCA analysis for plant and fungal extracts (Fig.22) using SIMCA-P^{+} displayed that 7-days and 30-days rice culture extracts were discriminated which was indicative to the unique secondary metabolites produced in these extracts. The bioactivity results showed that 7-days RC extract was the most active against PC3 and K562 cancer cell lines. The OPLS-DA analysis (Fig.25) showed the unique putative metabolites belonging to the 7-days RC extract, which were synonymous to those exhibited in the PCA loading plot (Fig.23). These metabolites corresponded to ion peaks at *m/z* (retention time) 203.118 (9.38 min), 639.171 (18.55 min), 379.141 (10.18), 191.020 (1.94 min) and 235.119 (3.20 min), which were described in the dereplication table (Table 5). In addition, some of these metabolites were found in smaller quantities in either EtOAc or BuOH extracts of *Terminalia laxiflora* leaves. This was an evidence for the biological source of *A. aculeatus* as an endophyte (Table 6). So in accordance to chemical, biological metabolomics profiling and dereplication studies (Results section: 3.2.3), 7-days rice culture extract was chosen for further fractionation work. Thus, *A. aculeatus* was cultivated in a rice culture for 7 days in large-scale batch employing 20 oneL Erlenmeyer flasks. The fungal mycelia was then extracted using EtOAc. The fungal extract was dried, dissolved in 10%

aqueous MeOH and defatted by shaking with n-hexane. MeOH extract was then subjected to bioassay guided-fractionation using MPLC which yielded 74 fractions. The fractions were evaporated and pooled after they qualitatively analysed using TLC. Fractions 47-50, 51-56 and 76 were active against K562, while fractions 15-25, 26, 30-32 and 40-41 exhibited activity against PC3 cancer cell line. Chemometric and principal component analysis using SIMCA-P^+ of active vs. inactive fractions as shown in the results section (3.2.3.2) provided useful predictions of metabolites plausibly responsible for the respective bioactivities. In addition, metabolomics tools have been accomplished to aid in further fractionation. So this led to a targeted isolation work for the putative bioactive metabolites corresponding to ion peaks at *m/z* (retention time) 639.171 $[M+H]^+$ (18.1 min), 191.020 $[M-H]^-$ (1.94 min), 235.119 $[M+H]^+$ (3.2 min), as predicted by multivarialte analysis to be responsible for the anticancer activity against K562 cell lines. From the dereplication study (Table 7), these metabolites were identified as secalonic acid, citric acid and JBIR 75, respectively. While the ion peak at *m/z* 379.046 $[M-H]^-$ (Rt = 10.1 min) corresponded to dinaphtho[2,1-b:1',2'-d]furan-5,9-dione, was predicted to be responsible for the anticancer activity against PC3 cell line. Further fractionation and purification of the active fractions using flash systems either Reveleris® or Biotage® led to the isolation of the bioactive compounds (Methods section: 2.4.7). Testing the biological activity of the isolated compounds against PC3 and K562 cancer cell lines showed that compounds AA6 (homogenistic acid), AA10 (uridine) and AA11 (JBIR-75) exhibited a strong cytotoxicity against K562 cancer lines while they were less cytotoxic to the normal epithelial cells (PNT2a) (Results section: 3.2.4). Furthermore, compounds AA7 (secalonic acid D), AA8 (secalonic acid C) and AA9 (secalonic acid B) exhibited a strong cytotoxicity toward both K562 cancer cell lines and the normal cells. This was indicative that these compounds are generally cytotoxic. Although compound AA5 (secalonic acid F) was one of the isolated secalonic acids, it exhibited no cytotoxic effect on the cancer cell lines as well as the normal cells which indicated that the biological activity depends on the stereo-specificity of the structure. Therefore, it was deduced that structural modification of the isolated secalonic acids would lead to analogues that are more

therapeutic.

In spite of the fungal extracts of *A. aculeatus* showed no significant activity toward *T. b brucei,* most of the MPLC fractions achieved more than 90 % inhibition with MICs between 0.19 to 20.0 µg/mL. Moreover, the purified compounds ergosterol peroxide, nymphasterol, secalonic acid F, homogenistic acid, secalonic acid D, seclaonic acid C, secalonic acid B and uridine showed a significant activity against *T. b. brucei* with MIC values of 29.2, 121.4, 19.6, 18.6, 0.6, 0.6, 4.9, and 204.9 µM, respectively. Secalonic acids (D, C and B) are generally cytotoxic so their activity toward *T. b. brucei* was expected. Although compound AA5 (secalonic acid F) was not cytotoxic to any of the cancer cell lines as well as the normal cells, it exhibited a selective cytotoxicity against *T. b. brucei*. Furthermore, compounds AA1 (ergosterol peroxide), AA2 (nymphasterol), AA6 (homogenistic acid) and AA10 (uridine) were not reported in the literature as antimicrobial or antitrypanosome which indicated that the antitrypanosomal activity of these compounds is being reported for the first time. Even though compounds ergosterol peroxide and nymphasterol are both steroidal compounds, only ergosterol peroxide showed a selective antimicrobial activity against *M. marinum* with MIC value of 233.64 µM. All compounds were elucidated by means of 1D, 2D-NMR and LC-HRFTMS with aid of DNP databases in results section (3.2.5).

Secalonic acids are generally cytotoxic compounds as shown in the bioactivity results and as reported in the literature (Hong 2011; Ishida 2000; Ishida et al. 1974; Li et al. 2008; Ren et al. 2005; Tang et al. 2012; Yuan et al. 2010; Zhang et al. 2009). Engineering of the biosynthetic pathway of secalonic acid may lead to more therapeutic analogues. The biosynthetic pathway of secalonic acids (Kurobane et al., 1979) led to a reasonable explanation of the presence of citric acid among the bioactive predicted compounds as shown in the OPLS-DA. Citric acid is not a bioactive metabolite but a precursor in the biosynthesis of secalonic acid congeners. However, as shown in Fig.216, the biosynthetic pathway started with successive addition of acetic acid and citric acid units as precursors on PKSs to form polyketone open chain, which can be reduced by ketoreductase and

cyclized by cyclase/aromatase to form emodin the precursor of the tetrahydroxanthone unit. Four isomeric tetrahydroxanthones can be synthesized by reduction then cyclization of the benzophenone carboxylic acid ester intermediate (Fig.216). The pairs differ in configuration either at a single location, C-5, or at the *trans*-substituted positions, C-6 and C-10a. Cyclization can produce two products, differing in configuration at C-10a. Taking into account trans orientation of the C-6 and C-10a substituents, it is likely that the C-10a configuration was already pre-determined during the cyclization step and directed the stereochemistry at positions 5 and 6 (Kurobane et al. 1979). Tetrahydroxanthones A, B, D and E are the precursors of the most common known secalonic acids.

Homologous dimers are represented by secalonic acid analogues A, B, D and E. Secalonic acid C is a "hybrid dimer" containing one monomeric unit each of tetrahydroxanthones A and B (Franck et al., 1966); secalonic acid G similarly contains monomeric units from each of tetrahydroxanthones A and E (Kurobane et al., 1978), while secalonic acid F is a hybrid of tetrahydrxanthones B and D (Andersen et al., 1977b). According to Kurobane et al. 1978 secalonic acids E and G have the same 2,2` linkage as secalonic acid A. Secalonic acid D is an enantiomer having the same linkage as secalonic acid A while secalonic acid F is an enantiomer having the same linkage as secalonic acid G. Thus all seven isolated secalonic acids (A, B, C, D, E, F, G) have the 2,2` linkage. In this study, four secalonic acids were isolated from *A. aculeatus*; three of them were comparable to secalonic acids B, D and F as reported in the literature while the other was deduced to be secalonic acid C. However, previous studies (Andersen et al., 1977b, Franck et al., 1966, Kurobane et al., 1978) on secalonic acid productions in *A. aculeatus* indicated that the fungus either failed to yield secalonic acid B or its concentration in the extract must be very low to be detected or isolated. The tetrahydroxanthone B monomer is mainly demonstrated in the hybrid secalonic acid (F). Kurobane et al. 1979 reported that each organism can only produce two seclaonic acids for example secalonic acid D and F from *A. aculeatus*. Where linking of two tetrahydroxanthone B units was not preferred, reaction between one such unit and tetrahydroxanthone D unit competed strongly

with their dimerization. One probable explanation, according to Kurobane and co-workers, that enzyme responsible for coupling the precursors in these organisms has marked the specificity for the initial monomer substrate, but is relatively non-specific in binding to the second monomer, recognizing primarily the benzenoid ring.

An indication based on the biosynthetic pathway of secalonic acid given by Kurobane and co-workers as well as comparison of the NMR data to the literature showed that compound AA7 was identified as the homologous dimer secalonic acid D and AA5 was secalonic acid F which is a hybrid dimer of tetrahydrxanthones B and D (Ren et al., 2005), (Andersen et al., 1977b). The NMR data of compound AA9 (homologous dimer) was not wholly superimposable with seclanonic acid D therefore the possibility to be elucidated as secalonic acid D or A (enantiomer of secalonic acid D) was excluded. So compound AA9 was deduced to be secalonic acid B or E however it is more likely to be secalonic acid B because the monomeric unit tetrahydroxanthone B moiety is already biosynthesized by *A. aculeatus* and a component of secalonic acid F (compound AA5). This was confirmed by comparison of the CD scan and NMR data of compound AA9 to those reported in the literature (Zhang et al., 2008b). The NMR data of compound AA8 (a hybrid dimer) was also not superimposable with secalonic acid F and so the possibility to be secalonic acid F or G (enantiomer of secalonic acid F) was excluded. Thus, compound AA8 was elucidated as secalonic acid C that carried monomers of A and B. In addition, the NMR data of secalonic acid C was comparable to that reported for tetrahydrxanthones A and B. Furthermore, presence of the citric acid (compound AA4) among the isolated metabolites as observed in the active side of the S-line by OPLS-DA (Fig.30) indicated its importance as a precursor, to which acetic acid units can be added and cyclized to form emodin and then tetrahydroxanthone. Emodin and tetrahydroxanthone were detected in the dereplication study among the metabolites of the 7-days rice culture extract of *A. aculeatus* corresponding to ion peak at *m/z* 271.060 $[M+H]^+$ (Rt = 12.3 min) and 319.083 $[M-H]^-$ (Rt = 9.9 min) for emodin and tetrahydroxanthone, respectively. So citric acid, emodin and tetrahydroxanthone can be used as precursor and/or biomarkers for the occurrence of secalonic acid biosynthesis during fermentation.

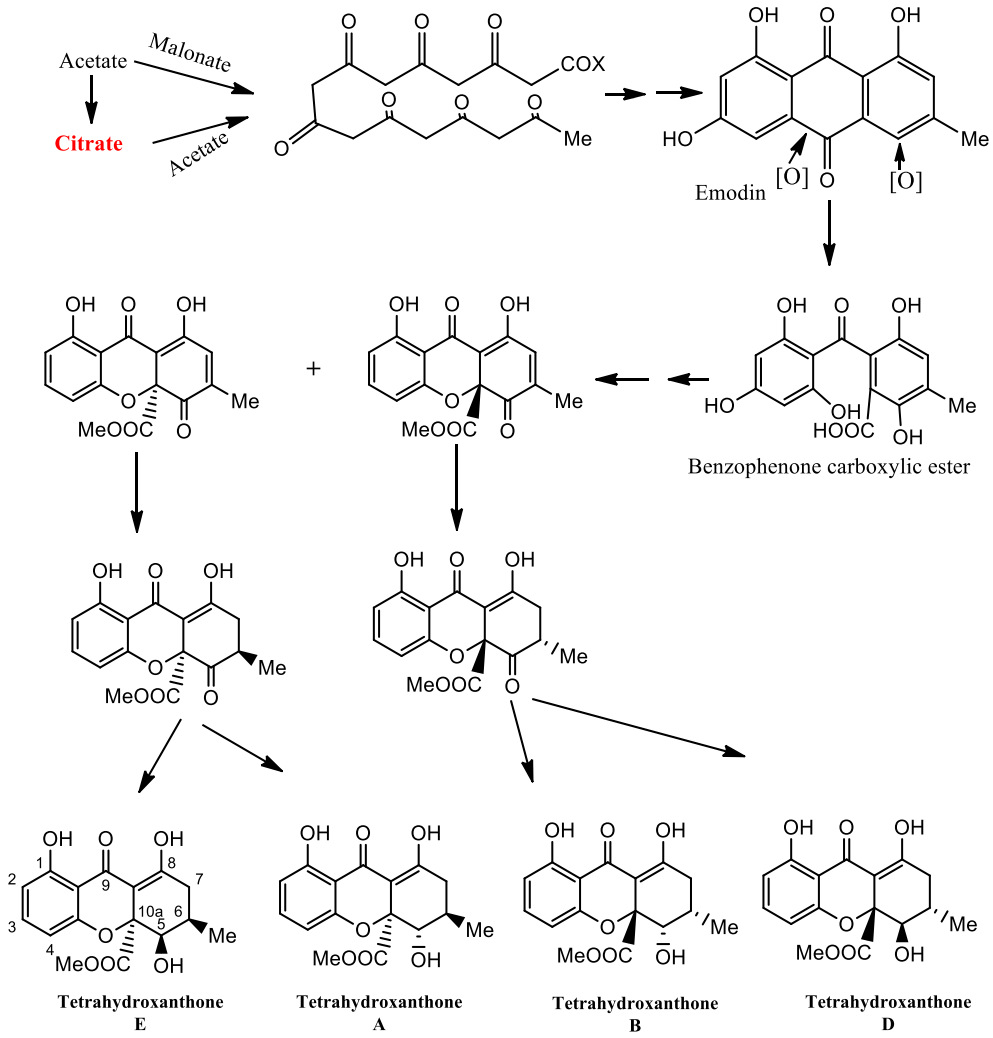

Fig.216 A possible route for the formation of stereo isomeric tetrahydroxanthone precursors of secalonic acids

4.3. Metabolomic studies, isolation and biosynthetic pathways of bioactive metabolites from *Aspergillus flocculus*

Metabolites finger printing using NMR for *A. flocculus* extracts indicated no difference between the 30-days rice and liquid culture extracts. However the ^{1}H NMR spectrum of 7-days rice culture extract exhibited three aromatic signals equivalent for an ABC spin system of a benzene ring which was missing in the ^{1}H NMR spectrum of the 7-days liquid culture extract (Results section: 3.3.1). It was observed from the NMR spectra that 30-days fungal extract exhibited more peaks

in the aromatic region than 7-days culture extract, which indicated that 30-days extract, produced more metabolites. Dereplication studies (section: 3.3.2) using the LCHR-MS data of fungal extracts showed no significant variation between the rice culture and liquid extracts in terms of presence and abundance of the produced metabolites. Furthermore, some of the metabolites were produced in the fungal extracts were detected at smaller concentration in either water or EtOAc extracts of *Markhamia platycalyx* stem which again confirmed the endophytic nature of the fungus with the respective plant. These metabolites corresponded to ion peaks at *m/z* (retention time in minutes) 194.058 (9.45), 210.053 (6.50), 208.069 (2.47), 184.073 (5.24) and 186.090 (2.71) which were described in the dereplication study (Table 16) as 5-hydroxymellein, 4,5-dihydroxymellein, 3-Methyl-3,8-dihydroxy-3,4-dihydroisocoumarin, 7-O-acetylkojic acid and dihydroaspyrone, respectively. Bioactivity results displayed significant activity against PC3 and K562 cancer cell lines for all fungal extracts. In addition, principle component analysis showed that all extracts of *A. flocculus* were clustered together that indicated similarity of produced metabolites between extracts. This further explained the similarity in their biological activity. The extract of small-scale batch of the 30-days rice culture was divided into two portions to be fractionated using two different chromatographic techniques in order to optimize the suitable method for separation of bioactive compounds. The first chromatographic method employed normal phase MPLC fractionation. This afforded 253 fractions that were pooled to yield 32 fractions from which fraction MPLC-24 yielded compound AF1 (dihydroaspyrone). The second method used size exclusion chromatography over Sephadex LH-20, which gave 11 fractions and submitted to be tested for NF-κB assay. Fraction Seph-5 was the most active fraction and selected for further MPLC fractionation work. Sub-fraction M6 eluted with 70% MeOH corresponded to compound AF2, a new polyketide. It was deduced that chromatographic method employing MPLC gave better purification and decreased the isolation steps (Methods section: 2.4.8).

In accordance to the extract yield, 30-days rice culture was chosen for further upscaling and isolation work. Therefore *A. flocculus* was cultivated in rice culture

employing ten 1L Erlenmeyer flasks for 30 days. EtOAc extract of the fungal culture was then dried, reconstituted in MeOH and slowly evaporated precipitating crystals of kojic acid (compound AF4). The hexanee soluble portion was fractionated over a silica gel open column to yield compounds AF6 (ergosterol), AF7 (ergosterol peroxide) and AF8 (campesterol). While the MeOH soluble portion was subjected to chromatographic separation using the Reveleris® flash system by normal phase using n- hexanee and EtOAc as mobile phase on gradient elution followed by EtOAc and MeOH system up to 30% MeOH eluted highly polar compounds. 400 fractions were collected which were pooled to 20 fractions. The fractions were subjected to further purifications step using either Reveleris® or Biotage® flash systems to afford 22 pure compounds. The fractions were subjected to supervised multivariate analysis to sort and predict metabolites that may be responsible for the anticancer activity of the extracts (Results section: 3.3.3). The OPLS-DA (Fig.100) discriminated the metabolites belonging to the anticancer active fractions 51-52 and 53-55. These metabolites were detected at *m/z* (retention time in minutes) 238.132 (12.4), 152.047 (10.53), 168.115 (15.6) and 228.147 (16.3). Metabolites at *m/z* 238.132 and 152.047, were described as flutimide and 2- or 4-hydroxyphenylacetic acid (compounds AF23a or AF23b) respectively, have never been reported for any anticancer activity but flutimide was reported as an endonuclease inhibitor of influenza virus (Tomassini et al., 1996). Moreover, metabolites at *m/z* 168.115 and 228.17 were not found in the database. This was an indication that the observed anticancer activity could be due to either novel or new natural products. Another multivariate module showed two main groups of fractions one for the antitrypanosomal active fractions which included fractions 18-29, 30-32, 33-42, 43-48, 51-52, 53-55, 56-64, 65-71, 72-89 vs inactive fractions. The OPLS-DA (Fig.96) exhibited the putative unique metabolites belonging to these respective fractions and were predicted to be responsible for the antitrypanosomal activity like metabolites at *m/z* 238.132, 194.058, 186.089, 230.094 and 280.240 eluted at 12.4, 9.6, 2.71, 14.9 and 27.5 min equivalent for flutimide, 5-hydroxymellien (AF15), dihydroaspyrone (AF1), diorcinol (AF17) and a new natural product (AF2), respectively. Compounds AF15 (5-hydroxymellien) and AF17 (diorcinol)

were previously reported as an antimicrobials (Hussain et al. 2009; Yurchenko et al. 2010). This led to the conclusion that the exhibited activity could be due to these identified compounds or due to a new natural compound AF2. Testing the cytotoxicity of the isolated compounds against PC3 and K562 cancer cell lines indicated that compounds AF14 (*cis*-4-hydroxymellein), AF15 (5-hydroxymellein), AF16 (mixture of botryoisocoumarin A and mellein) and AF17 (diorcinol) exhibited a significant cytotoxic effect on K562 cancer line (Results section: 3.3.4). Compound AF13 (*trans*-4-hydroxymellein) showed no activity even though compound AF14 (*cis*-4-hydroxy mellein) was active which indicated that trans orientation of OH group at position four led to a more active compound. Furthermore, compounds AF18 (4,5-dihydroxymellein) and AF11 (3-hydroxymellien) were inactive. However, compound AF15 (5-hydroxymellien) showed a strong activity which indicated that a change in the OH position or the addition of another OH will lead to loss of the activity. Compound AF17 (diorcinol) exhibited a significant inhibition of the NF-κB pathway which could indicate the mechanism of the anticancer activity for this compound. None of these purified compounds was reported in the literature as anticancer compound. Mellein (AF16b) was reported as antiinflamatory (Pongprayoon et al., 1991). Moreover, compounds AF3, 6, 7, 8, 9, 17, 20, 21 and AF22 exhibited a remarkable antitrypanosomal activity achieving more than 90% inhibition with MIC values 145.35, 31.57, 7.29, 62.81, 15.78, 108.70, 88.03, 409.84 and 301.20 µM, respectively. Compounds AF6 (ergosterol), AF7 (ergosterol peroxide), AF8 (campesterol) and AF9 (an undescribed steroidal compound) were structurally related steroidal compounds and none of them has been reported before in the literature either as antimicrobial or antitrypanosomal compound. Compound AF3 (dihydropenicillic acid) was reported in the literature as a NF-κB inhibitor (Tachibana et al. 2008). Moreover, compound AF17 (diorcinol) was reported in the literature as a strong antimicrobial (Yurchenko et al. 2010). Again, the stereo-specificity was an essential parameter in the detected antitrypanosomal activity of compound AF20 (phomaligol-2-epimer) when compared with its congener AF19 (phomaligol). Compound AF22, the methylated derivative of AF23 (4-hydroxyphenyl acetic acid), exhibited a significant antitrypanosomal activity

however its congener AF23 was inactive which indicated that methylation led to a more active analogue of AF23. Furthermore, compounds AF7 (ergosterol peroxide), AF17 (diorcinol), AF21 (p-hydroxybenzaldehyde) and AF22 showed a selective antimicrobial activity against *Mycobacterium marinum* with MIC 233.64, 108.89, 409.83 and 602.40 µM. All compounds were elucidated by means of 1D, 2D-NMR and LC-HRFTMS with aid of DNP databases in results section (3.3.5).

Metabolomics studies of *A. flocculus* extracts and/or fractions using PCA and OPLS-DA allocated the mellein derivatives compounds AF14, AF15 and AF16 among the unique putative metabolites predicted to be responsible for the antitrypanosomal activity. However, bioassays of these purified compounds only exhibited their anticancer activities. This indicated that compound AF17 (diorcinol, *m/z* 230.094) is, the only predicted metabolite, actually responsible for the antitrypanosomal activity of the highlighted extracts and/or fractions of *A. flocculus*. Only fractions 51-52 and 53-55 exhibited anticancer activity however, they also possessed antitrypanosomal activity. The metabolomics studies did not highlight both mellein derivatives and diorcinol among the unique features for these fractions because they were also present in other fractions. This was an indication that the anticancer activity of fractions 51-52 and 53-55 could be due to synergism of all or some of these active metabolites together with their respective unique metabolites which were not possible to be isolated.

Mellein derivatives and steroids were found to share the same biosynthetic pathway as those for the polyketides. One new polyketide (AF2), mellein derivatives (AF13-AF18) as well as ergosterol (AF6), ergosterol peroxide (AF7) and campesterol (AF8) were identified from the rice culture of *A. flocculus.* Presence of compounds AF12 (4-methyl-5,6-dihydro-2H-pyran-2-one), AF21 (p-hydroxybenzaldehyde), AF23a (4-hydroxy phenyl acetic acid) and AF23b (2-hydroxy phenyl acetic acid) were among the isolated compounds which were highlighted in the dereplication studies confirmed their importance as precursors and/or biomarkers. These compounds can be biosynthesized after aromatisation step particularly in the biosynthesis of mellein

derivatives compounds. One of the central routes to aromatic compounds in nature includes chain extension of a starter acid residue such as acetate or acetyl CoA on a polyketide synthase by successive additions of three or more C-2 units from malonate to generate an enzyme bound polyketone chain. The polyketone then subjected to reduction via ketoreductase to form compound AF2 (new polyketide). Subsequent cyclization via aldol or Claisen reactions followed by aromatisation provides a versatile approach to aromatic systems (Abell et al., 1982). Starting from the polyketides backbone intermediate like farnesyl, a wide range of phytosterols can be synthesized (Fig.217).

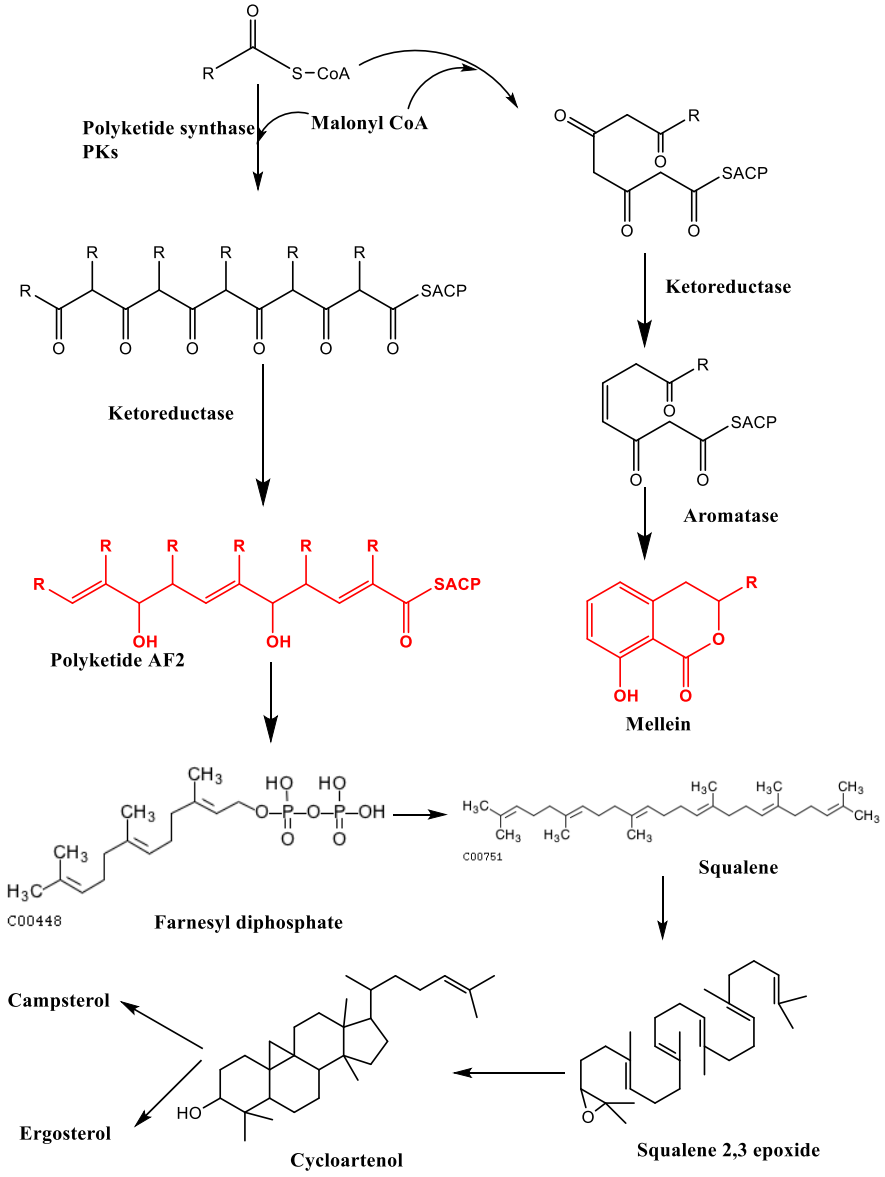

Fig.217 A possible route for the formation of polyketides, mellein and steroids

4.4. Metabolomic studies, isolation and biosynthetic pathways of bioactive metabolites from *Curvularia sp.*

The dereplication studies of fungal extracts from *Curvularia sp*. using ^{1}H NMR exhibited that liquid culture extracts showed more peaks in the aromatic region. However LCHR-MS data was processed on software MZmine 2.10, revealed the production of more metabolites in the rice culture than liquid culture as shown in the result section (3.4.2). Multivariate analysis of fungal extracts from *Curvularia sp*. displayed the outlying metabolites which corresponded to ion peaks at *m/z* (retention time in min) 207.09 (6.5), 354.158 (9.16), 467.242 (11.55) and 708.315 (9.19) were dereplicated as rhexifoline previously encountered in *Castilleja rhexifolia*, picroroccellin from *Roccella fuciformis*, cyclopiamine B from *Aspergillus caespitosus* and taxinine J from *Taxus cuspidate*, respectively (Table 35). Biological investigation of fungal extracts exhibited no significant activity in either anticancer or antitrypanosomal activities. However, the 30-days rice culture extract showed NF-κB inhibition activity (Results section 3.4.4). Moreover, the interesting change in the chemical profile of the small scaled batch of fungal extracts from MA plate extracts showed by the heat map (Fig.189) was encouraging for further metabolomics and isolation work (Methods section 2.4.9). Thus, based on the yield and biological activity, the small-scale batch of 30-days RC extract was chosen for further isolation work. This led to seven pooled fractions included F87-95 which gave compound CV6 (N-acetyl-phenylalanine), F116-130 which afforded compound CV5 (a new dipeptide) and F131-139 equivalent for compound CV4 (a new tripeptide,). Furthermore, CV9 (F4-32), CV10 (F96-103) and CV11 (F60-86) showed a significant anticancer activity against K562 cancer cell line. The ^{1}H NMR spectrum of fraction CV10 exhibited proton resonances indicating a mixture of compound CV6 (N-acetyl-phenylalanine) and ferulic acid. Ferulic acid was hypothesized to be responsible for the bioactivity because CV6 was found to be inactive. CV9 and CV10 are semi-purified fractions whose amounts were not sufficient for further purification however metabolomics studies using PCA and OPLS-DA proposed that metabolites at *m/z* 346.212 eluting at 5.37 min which was an undescribed

compound and/or at 708.316 at 9.43 min identified as taxinine J, could be responsible for the observed anticancer activity. None of the isolated fractions and/or compounds exhibited antitrypanosomal activity however compound CV5 (N-acetyl-phenylalanine-L-phenylalanine) showed a significant activity against *Mycobacterium marinum* with MIC value of 282.48 µM.

Two new peptides were isolated from the rice culture of *Curvularia* sp. The dipeptide compound consisted of of L-phenylalanine and N-acetyl-phenyl alanine, while the tripeptide had L-phenylalanine, L-leucine and N-acetyl-phenylalanine. KEGG biosynthesis databases, demonstrated the biosynthesis of previously mentioned amino acid Figures (218, 219 and 220) which could be connected via a peptide bond by a peptide synthase enzyme to form the di- and tri-peptides. The dereplication studies (Results section 3.4.3) showed among the metabolites a corresponding ion peak at *m/z* 166.086 (Rt = 9.5 min) for L-phenylalanine amino acid which as shown from the biosynthetic pathway is a precursor for the N-acetyl-phenylalanine (compound CV6). Compound CV6 can be used as a precursor for the di and tri-peptides compounds CV5 and CV4.

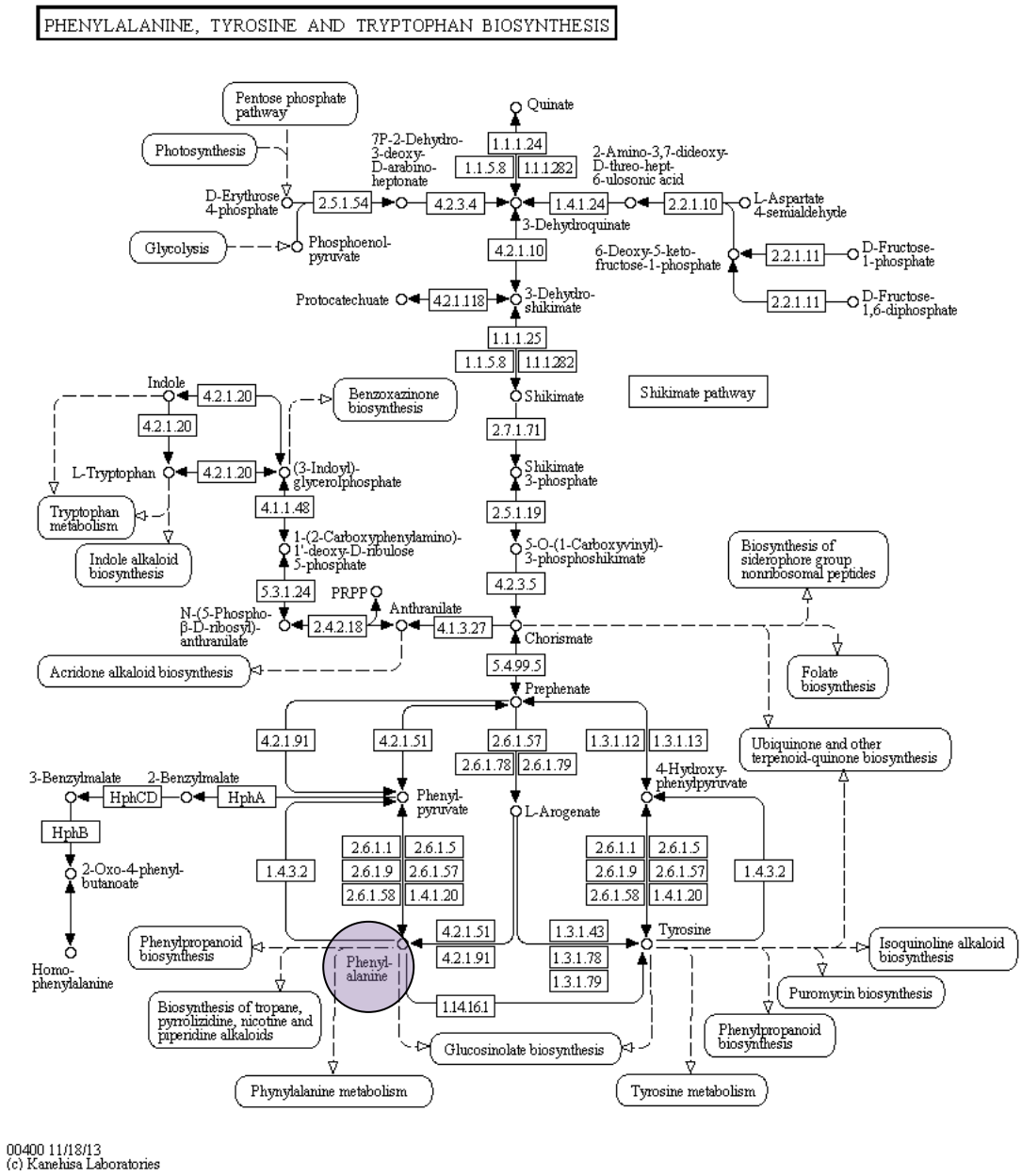

Fig.218 Biosynthetic pathway of Phenylalanine

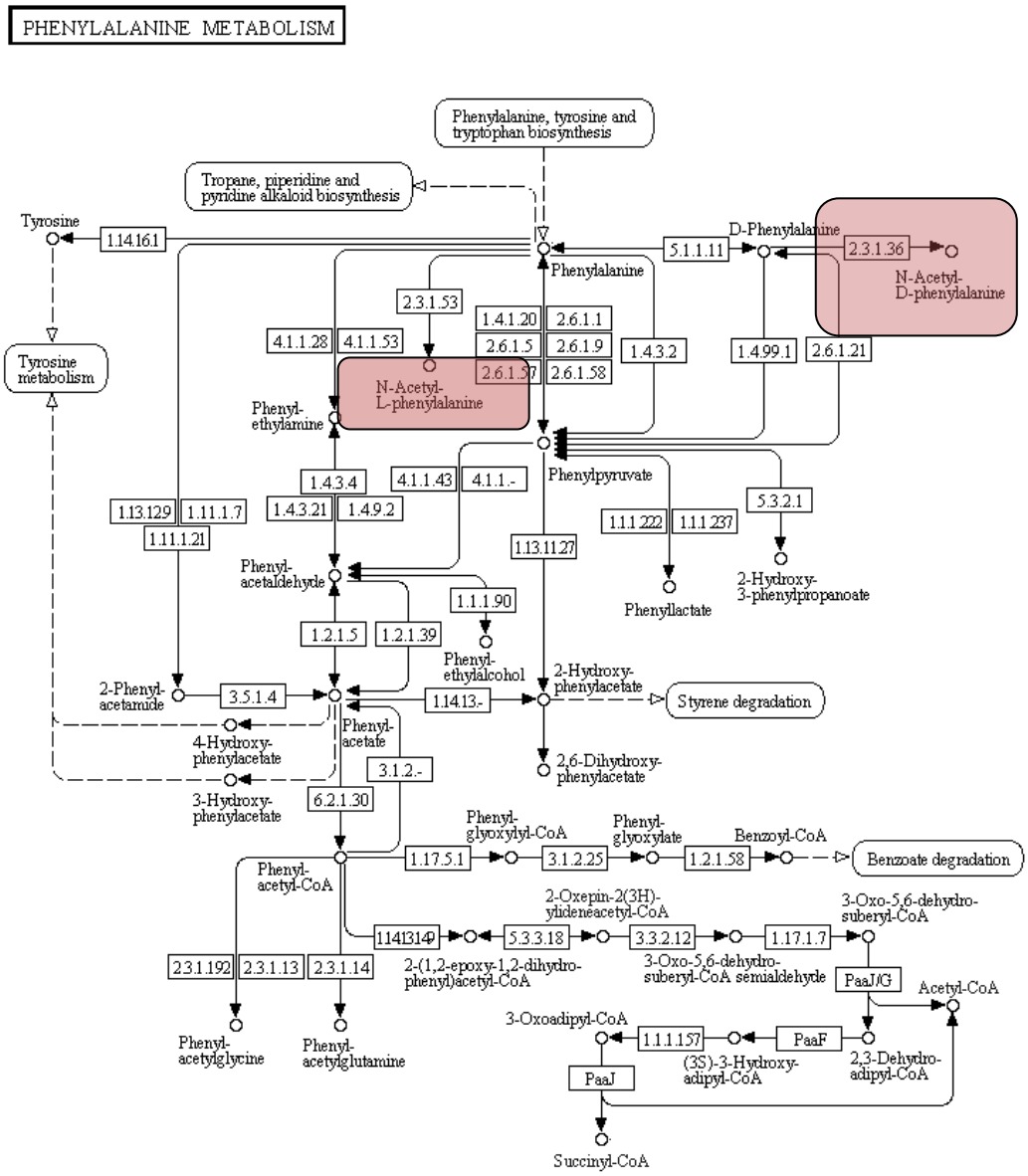

Fig.219 Biosynthetic pathway of N-acetyl-phenylalanine

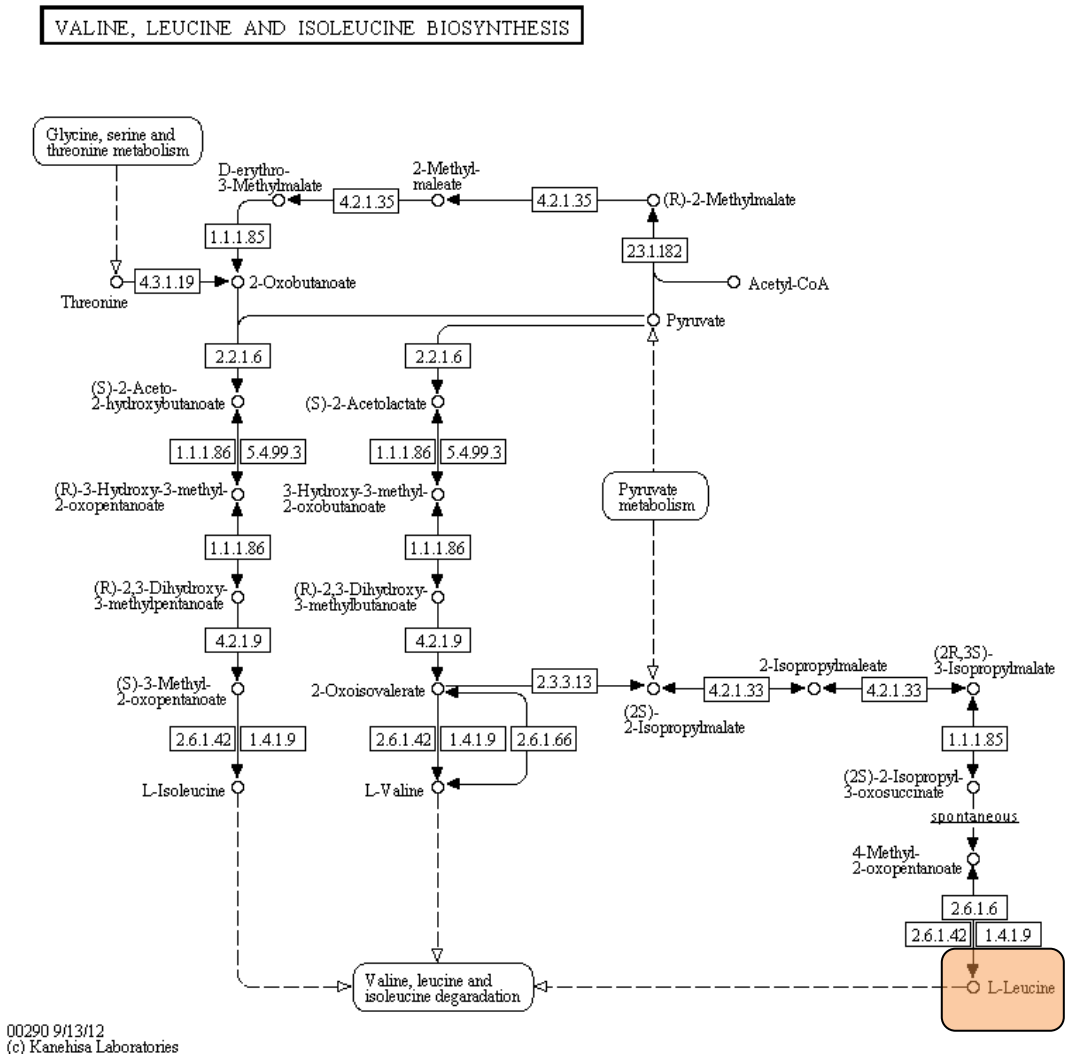

Fig.220 Biosynthetic pathway of L-leucine

Chapter 5: Conclusion and Future work

5. Conclusion and future work

5.1. Introduction

The main aim of this study was to find novel potential anti-cancer and/or antimicrobial compounds isolated from endophytic fungi of some important Egyptian medicinal plants, which can be later cultivated and fermented to produce the active secondary metabolites on a larger scale. Molecular biological procedures, including DNA extraction, PCR, gel electrophoresis, purification and sequencing, have been successfully accomplished to identify the endophytic fungi. Metabolomics and dereplication studies, employing NMR, HRFT-MS, MZmine 2.10 software, SIMCA-P^+ 13.0.2 and databases like DNP and AntiBase, were efficiently used in early prediction of the bioactive secondary metabolites. In addition, it can be used for optimization of culture conditions, improvement of the productivity of downstream fermentation methods, comparison of the active vs inactive extracts and/or fractions in order to associate metabolic profile to bioactivity directly on line. Furthermore, prioritising the fractions that will go further for purification work and highlighting the precursor metabolites used in the biosynthesis of the active metabolites. High-throughput chromatography utilizing Reveleris® and/or Biotage® flash systems enhanced the purification process of the bioactive metabolites and minimized the number of isolation steps.

5.2. Metabolomics and dereplication studies of *A. aculeatus*

Metabolomics tools have been employed to optimize the cultivation media in which the endophyte produces the largest quantity of the bioactive metabolites. The LCHR-MS data processed on MZmine 2.10 software exhibited that rice culture of *A. aculeatus* produced more abundant metabolites than the liquid culture. Moreover, comparison of 7-days and 30-days rice culture extracts using the heat map on program R showed two different chemical profiles while 15-days rice culture extract was an intermediate stage that produced the least amount of the metabolites. Multivariate analysis, using PCA over SIMCA-P^+ software, revealed that 7-days rice culture extract was the most unique extract in terms of the produced metabolites. This was confirmed from the biological investigation,

which demonstrated that 7-days rice culture extract was the most active extract against K562 and PC3 cancer cell lines. Multivariate analysis using SIMCA-P+ software employed OPLS-DA to predict that metabolites like secalonic acids (compounds AA7, AA8 and AA9), JBIR-75 (compound AA11), citric acid (compound AA4) and Dinaphthofurandione (compound AA3) are the the unique putative metabolites expected to be responsible for the anticancer activity of 7-days rice culture extract of *A. aculeatus*. These metabolites were dereplicated using in-house macro Excel files with built in DNP database. This was verified from the bioassay results of the purified compounds which showed that compounds AA7 (secalonic acid D), AA8 (secalonic acid C) and AA9 (secalonic acid B), AA11 (JBIR-75) and AA6 (homogenistic acid) exhibited a strong anticancer activity toward the K562 cancer line. Moreover, compounds AA1 (ergosterol peroxide), AA2 (nymphasterol), AA5 (secalonic acid F), AA6 (homogenistic acid), AA7 (secalonic acid D), AA8 (secalonic acid C), AA9 (secalonic acid B) and AA10 (uridine) showed a significant activity against *T. b. brucei* with MIC values of 29.2, 121.4, 19.6, 18.6, 0.6, 0.6, 4.9, and 204.9 µM respectively. In addition, compound AA1 demonstrated a good antimicrobial activity toward *Mycobacterium marinum* with MIC 233.64 µM.

5.3. Isolation of the bioactive metabolites from 7-days RC extract of *A. aculeatus*

Flash chromatography using BUCHI® MPLC system was employed for a bioassay-guided fractionation of 7-days rice culture extract. Bioactive fractions were subjected to further fractionation using Biotage® flash system and conventional column employing a normal silica gel column with variable mobile phases led to isolation of 11 pure compounds. These compounds were subjected to 1D, 2D NMR and LCHR-MS analysis to be elucidated in accordance to the data reported in the literature. CD scans for the secalonic acids were much valuable in confirmation of the structure stereochemistry particularly in compound AA9 (secalonic acid B). Moreover, understanding the biosynthetic pathway of secalonic acid was much helpful in deducing that compound AA8 could be secalonic acid C. Unfortunately, secalonic acids B, C and D were

generally cytotoxic compounds affecting the normal cells as well as the cancer cells, while secalonic acid F exhibited no cytotoxicity against either normal or cancer cells. Furthermore, it was demonstrated that a significant change in antitrypanosomal activity observed with a slight modification in the stereochemistry of the compounds that may lead to more selective therapeutic analogues. Detection of citric acid, emodine and tetrahydroxanthone in the dereplication study emphasized their importance as precursors or biomarkers in the biosynthesis of secalonic acids.

5.4. Metabolomics and dereplication studies of *A. flocculus*

Metabolomics tools indicated that there was no significant difference in terms of the abundance of the produced metabolites between rice culture and liquid culture extracts of *A. flocculus*. This was verified from the biological investigation of the fungal extracts, which demonstrated a strong NF-κB inhibition activity expressed by both fungal extracts. Multivariate analysis using PCA indicated that metabolites like dihydroaspyrone (compound AF1), 5-hydroxymellein (AF15) and 2- or 4-hydroxyacetic acid (AF23a or AF23b) were the unique putative metabolites that belonged to the active extracts and predicted to be responsible for NF-κB inhibition activity. The multivariate analysis employing anticancer bioactivity for the MPLC fractions of 30-days rice culture of *A. flocculus* exhibited that the putative unique metabolites were compound AF23a or AF23b and a metabolite at *m/z* 238.132. The latest was dereplicated as flutimide together with another two undescribed metabolites at *m/z* 168.115 and 228.147 eluted at 15.6 and 16.3 minute, respectively. However, compounds AF1, AF15, AF17 (diorcinol) and AF2 (a new polyketide) were the distinguishing metabolites for the antitrypanosomal active fractions. The biological investigation revealed that compounds AF14 (*cis*-4-hydroxymellein), AF15, AF16 (mellien) and AF17 exhibited a strong anticancer activity against K562 cell lines. Moreover, compounds AF3 (dihydropenicillic acid), AF6 (ergosterol), AF7 (ergosterol peroxide), AF8 (Campesterol), AF9 (unknown steroid), AF17, AF20 (phomaligol A), AF21 (p-hydroxy benzaldehyde) and AF22 (4-hydroxyphenyl-methoxy-acetic acid) exhibited significant antitrypanosome activities (with MIC values of 145.35,

31.57, 7.29, 62.81, 15.78, 108.70, 88.03, 409.84 and 301.20 µM, respectively. Furthermore, compounds AF7, AF17, AF21 and AF22 showed a selective antimicrobial activity against *Mycobacterium marinum* with MIC values of 233.64, 108.89, 409.83 and 602.40 µM, respectively.

5.5. Isolation of the bioactive metabolites from 7-days RC extract of *A. flocculus*

Flash chromatography was more efficient when compared to the conventional column in the separation of small-scale batch of 30-days rice culture extract of *A. flocculus*, which led to isolation of compounds AF1 and AF2. Reveleris® flash system was employed for bioassay-guided fractionation of medium-scaled batch of 30-days rice culture extract. The active fraction were subjected to further fractionation on either Buchi®, Reveleris® or Biotage® flash systems which led to the isolation of 22 compounds. Compound AF4 (kojic acid crystals) was obtained by decantation after slowly evaporating MeOH from the fungal extract. Mainly mellein derivatives compounds AF14, AF15, AF16 and diorcinol (AF17) exhibited strong anticancer activity which as predicted by the results of the metabolomics studies while, only AF17 was found responsible for NF-κB inhibition activity of the 30-days rice culture extract. Moreover, it exhibited a strong activity toward *T. b. brucei* and *M. marinum*. Compound AF2 is a new polyketide, could be used as a precursor for the biosynthesis of other steroidal compounds like AF6 (ergosterol), AF7 (ergosterol peroxide), AF8 (campesterol) and AF9 (undescribed steroidal compound) which exhibited a strong antitrypanosomal activity. Mellein derivatives were found to be biosynthesized using the same polyketide pathway as compound AF2.

5.6. Metabolomics and dereplecation studies of *Curvularia sp.*

Metabolomics studies using heatmaps with the program R were very helpful to visualise the variation in the chemical profile between MA plate extract and other upscaled extracts of *Curvularia* sp. The bioassays of the fungal extracts demonstrated that the 30-days rice culture exhibited a significant NF-κB inhibition activity. Multivariate analysis using PCA highlighted the unique

metabolites that belonged to the 30-days rice culture. These metabolites like N-acetyl-phenylalanine (compound CV6), N-acetyl-phenylalanine-L-phenylalanine (compound CV5), N-acetyl-phenylalanine-L-phenylalanine-L-leucine (compound CV4) and taxinine J (corresponding ion peak at *m/z* 708.316). OPLS-DA of the active vs inactive fractions from the 30-days rice culture extract showed that the undescribed metabolite at *m/z* 346.212 eluting at 5.37 min and/or taxinine J could be responsible for the anticancer activity of the active fractions.

5.7. Isolation of bioactive metabolites from 30-days RC extract of *Curvularia* sp.

The 30-days rice culture extract was fractionated using Biotage® flash system coupled to a PDA detector. The resulted fractions were pooled according to TLC which led to isolation of three compounds CV6 (F87-95), CV5 (F116-130) and CV4 (F131-139). Compounds CV4 (N-acetyl-phenylalanine-L-phenylalanine-L-leucine) and CV5 (N-acetyl-phenylalanine-L-phenylalanine) are new peptides. Bioassays demonstrated that fractions CV9, CV10 and CV11 were active against K562 cancer cell lines. None of the isolated fractions exhibited a significant activity toward *T. b. brucei* and/or *M. marinum* except CV5 that was active against *M. marinum* with an MIC value of 282.48 µM.

5.8. Future work

Secalonic acids from 7-days rice culture extract of *A. aculeatus* and mellein derivatives from 30-days rice culture extract of *A. flocculus* were mainly the active metabolites responsible for the anticancer activity of both endophytes. Engineering of the biosynthetic pathway of these metabolites might lead to more effective and selective anticancer analogues. Many of the isolated compounds, showed a remarkable activity against *T. b. brucei* and/or *M. marinum*, can be tested later on other microorganisms to measure their selectivity. Compound AF2 isolated from *A. flocculus* in addition to compounds CV4 and CV5 from *Curvularia* sp. were undescribed before in the literature so they are new and isolated for the first time in nature. Compound CV5 showed significant activity against *M. marinum* and can be used as a drug lead for a more therapeutic antimicrobial agent. Upscaling for 30-days

rice culture of *Curvularia sp.* is recommended to isolate the anticancer metabolites responsible for the activity.

References

6. References

ARNOLD, E. A., 2007. Understanding the diversity of foliar endophytic fungi: progress, challenges, and frontiers. *Fun. Bio. Rev.,* 21**,** 51-66.

ABDELMOHSEN, U. R., CHENG, C., VIEGELMANN, C., ZHANG, T., GRKOVIC, T., AHMED, S., QUINN, R. J., HENTSCHEL, U. & EDRADA-EBEL, R. 2014. Dereplication strategies for targeted isolation of new antitrypanosomal actinosporins A and B from a marine sponge associated-*Actinokineospora* sp. EG49. *Mar. Drugs,* 12**,** 1220-1244, 25.

ABELL, C., GARSON, M. J., LEEPER, F. J. & STAUNTON, J. 1982. Biosynthesis of the fungal metabolites alternariol, mellein, rubrofusarin, and 6-methylsalicylic acid from acetic acid-2,2,2-d3. *J. Chem. Soc., Chem. Commun.***,** 1011-13.

ADELIN, E., SERVY, C., CORTIAL, S., LEVAIQUE, H., GALLARD, J. F., MARTIN, M.-T., RETAILLEAU, P., BUSSABAN, B., LUMYONG, S. & OUAZZANI, J. 2011. Biotransformation of natural compounds. Oxido-reduction of Sch-642305 by *Aspergillus ochraceus* ATCC 1009. *Bioorg. Med. Chem. Lett.,* 21**,** 2456-2459.

ADIKO, V. A., ATTIOUA, B. K., TONZIBO, F. Z., ASSI, K. M., SIOMENAN, C. & DJAKOURE, L. A. 2013. Separation and characterization of phenolic compounds from *Terminalia ivoiriensis* using liquid chromatography-positive electro-spray ionization tandem mass spectroscopy. *Afr. J. Biotechnol.,* 12**,** 4393-4398.

AGGARWAL, B. B., DANDA, D., GUPTA, S. & GEHLOT, P. 2009. Models for prevention and treatment of cancer: Problems vs. promises. *Biochem. Pharmacol.,* 78**,** 1083-1094.

AN, C.-Y., LI, X.-M., LI, C.-S., WANG, M.-H., XU, G.-M. & WANG, B.-G. 2013. Aniquinazolines A-D, four new quinazolinone alkaloids from marine-derived endophytic fungus *Aspergillus nidulans*. *Mar. Drugs,* 11**,** 2682-2694, 13 pp.

ANDERSEN, R., BUCHI, G., KOBBE, B. & DEMAIN, A. L. 1977a. Secalonic acids D and F are toxic metabolites of *Aspergillus aculeatus*. *J Org Chem,* 42**,** 352-3.

ANDERSEN, R., BUECHI, G., KOBBE, B. & DEMAIN, A. L. 1977b. Secalonic acids D and F are toxic metabolites of *Aspergillus aculeatus*. *J. Org. Chem.,* 42**,** 352-3.

ARNOLD, A. 2007. Understanding the diversity of foliar endophytic fungi: Progress, challenges, and frontiers. *Fun. Bio. Rev.,* 21**,** 51–66.

ASATI, R. K., SINGHAL, M. & SAXENA, M. 2008. Antimicrobial study of luteolin 7-O-α-L-rhamnopyranoside from heartwood of *Terminalia bellerica* (Roxb.). *J. Pure Appl. Microbiol.,* 2**,** 599-602.

ASHA, K. N., CHOWDHURY, R., HASAN, C. M. & RASHID, M. A. 2004. Steroids and polyketides from *Uvaria hamiltonii* stem bark. *Acta Pharm. (Zagreb, Croatia),* 54**,** 57-63.

ATTA UR, R., ZAREEN, S., CHOUDHARY, M. I., AKHTAR, M. N., SHUJAAT, S. & NGOUNOU, F. N. 2005. Some chemical constituents of *Terminalia glaucescens* and their enzymes inhibition activity. *Z. Naturforsch., B: Chem. Sci.,* 60**,** 347-350.

BAG, A., BHATTACHARYYA, S. K. & CHATTOPADHYAY, R. R. 2013. Isolation and identification of a gallotannin 1,2,6-tri-O-galloyl-β-D-glucopyranose from hydroalcoholic extract of *Terminalia chebula* fruits effective against multidrug-resistant uropathogens. *J. Appl. Microbiol.,* 115**,** 390-397.

BARRETT, M. P. 1999. The fall and rise of sleeping sickness. *Lancet,* 353**,** 1113-4.

BAYES, M., RABASSEDA, X. AND PROUS, J. R. 2007a. Gate ways to clinical trials. *Methods & Findings in Experimental & Clinical Pharmacology* 29.

BAYES, M., RABASSEDA, X. AND PROUS, J. R. 2007b. Gate ways to clinical trials. *Methods & Findings in Experimental & Clinical Pharmacology,* 29**,** 303–311.

BISWAS, M., GHOSH, A. K. & HALDAR, P. K. 2010. Anti-leishmanial and anti-cancer activities of a pentacyclic triterpenoid isolated from the leaves of *Terminalia arjuna* Combretaceae. *Trop. J. Pharm. Res.,* 9**,** 135-140.

BLUNT, J. W., COPP, B.R., MUNRO, M.H.G. 2006. Marine natural product. *Natural Product Reports,* 23**,** 26-78.

BRUN, R., SCHUMACHER, R., SCHMID, C., KUNZ, C. & BURRI, C. 2001. The phenomenon of treatment failures in Human African Trypanosomiasis. *Trop Med Int Health,* 6**,** 906-14.

BUDHIRAJA, A., NEPALI, K., SAPRA, S., GUPTA, S., KUMAR, S. & DHAR, K. L. 2013. Bioactive metabolites from an endophytic fungus of *Aspergillus* species isolated from seeds of *Gloriosa superba* Linn. *Med. Chem. Res.,* 22**,** 323-329.

BUGUET, A., BOUTEILLE, B., CESPUGLIO, R., BISSER, S., CHAPOTOT, F., BOURDON, L., VINCENDEAU, P., RADOMSKI, M. W. & DUMAS, M. 2003. Sleeping sickness: forgotten research? *Med Trop (Mars),* 63**,** 223-7.

BUSI, S., PEDDIKOTLA, P., UPADYAYULA, S. M. & YENAMANDRA, V. 2009. Secondary metabolites of *Curvularia oryzae* MTCC 2605. *Rec. Nat. Prod.,* 3**,** 204-208.

CAO, S., BRODIE, P. J., CALLMANDER, M., RANDRIANAIVO, R., RAKOTOBE, E., RASAMISON, V. E. & KINGSTON, D. G. I. 2009. Saponins and a lignan derivative of *Terminalia tropophylla* from the Madagascar Dry Forest. *Phytochemistry (Elsevier),* 71**,** 95-99.

CAO, S., BRODIE, P. J., MILLER, J. S., RANDRIANAIVO, R., RATOVOSON, F., BIRKINSHAW, C., ANDRIANTSIFERANA, R., RASAMISON, V. E. & KINGSTON, D. G. I. 2007. Antiproliferative Xanthones of *Terminalia calcicola* from the Madagascar Rain Forest. *J. Nat. Prod.,* 70**,** 679-681.

CARROLL, G. C. 1988. Fungal endophytes in stems and leaves: From latent pathogen to mutualistic symbiont. *Ecology,* 69**,** 2-9.

CHEN, C. C. & LEE, M. H. 1986. Constituents of *Markhamia hildebrandtii* (Baker) Sprague and their antitumor activity. *Hua Hsueh*, 44**,** 61-4.

CHEN, L.-G., HUANG, W.-T., LEE, L.-T. & WANG, C.-C. 2009. Ellagitannins from *Terminalia calamansanai* induced apoptosis in HL-60 cells. *Toxicol. in Vitro,* 23**,** 603-609.

CHEN, P.-S. & LI, J.-H. 2006. Chemopreventive effect of punicalagin, a novel tannin component isolated from *Terminalia catappa*, on H-ras-transformed NIH3T3 cells. *Toxicol. Lett.,* 163**,** 44-53.

CHOBOT, V., OPLETAL, L., JÁHODÁŘ, L., PATEL, A. V., DACKE, C. G. & BLUNDEN, G. 1997. Ergosta-4,6,8,22-tetraen-3-one from the edible fungus, *Pleurotus ostreatus* (oyster fungus). *Phytochemistry,* 45**,** 1669-1671.

CHOUKSEY, B. K. & SRIVASTAVA, S. K. 2001. New constituent from the roots of *Terminalia arjuna*: antifungal agent. *Indian J. Chem., Sect. B: Org. Chem. Incl. Med. Chem.,* 40B**,** 354-356.

CICHEWITZ, R. H., KOUZI, S.A. 2004. Chemistry, biological activity, and chemotherapeutic potential of betulinic acid for the prevention and treatment of cancer and HIV infection. *Medical Research Reviews*, 24**,** 90–114.

CLAY, K. 1988. Fungal endophytes of grasses: A defensive mutualism between plants and fungi. *Ecology*, 69**,** 10-16.

COLLINS, L. A. & FRANZBLAU, S. G. 1997. Microplate Alamar blue assay versus BACTEC 460 system for high-throughput screening of compounds against *Mycobacterium tuberculosis* and *Mycobacterium avium*. *Antimicrob. Agents Chemother.,* 41**,** 1004-1009.

CONRAD, J., VOGLER, B., REEB, S., KLAIBER, I., PAPAJEWSKI, S., ROOS, G., VASQUEZ, E., SETZER, M. C. & KRAUS, W. 2001. Isoterchebulin and 4,6-O-isoterchebuloyl-D-glucose, novel hydrolyzable tannins from *Terminalia macroptera*. *J. Nat. Prod.,* 64**,** 294-299.

CRAGG, G. M., KINGSTON, D.G.I., NEWMAN, D.J. 2005. *Anticancer Agents from Natural Products*, Brunner-Routledge Psychology Press, Taylor & Francis Group, Boca Raton, FL.

CUI, J.-L., GUO, S.-X., DONG, H. & XIAO, P. 2011. Endophytic Fungi from Dragon's Blood Specimens: Isolation, Identification, Phylogenetic Diversity and Bioactivity. *Phytotherapy Research,* 25**,** 1189-1195.

DAI, J., KROHN, K., FLOERKE, U., PESCITELLI, G., KERTI, G., PAPP, T., KOEVER, K. E., BENYEI, A. C., DRAEGER, S., SCHULZ, B. & KURTAN, T. 2010. Curvularin-type metabolites from the fungus *Curvularia* sp. isolated from a marine alga. *Eur. J. Org. Chem.***,** 6928-6937, S6928/1-S6928/5.

DENG, C.-M., LIU, S.-X., HUANG, C.-H., PANG, J.-Y. & LIN, Y.-C. 2013. Secondary metabolites of a mangrove endophytic fungus *Aspergillus terreus* (No. GX7-3B) from the South China Sea. *Mar. Drugs,* 11**,** 2616-2624, 9 pp.

DHANKHAR, S., DHANKHAR, S. & YADAV, J. P. 2013. Investigating antimicrobial properties of endophytic fungi associated with *Salvadora oleoides* Decne. *Anti-Infect. Agents,* 11**,** 48-58.

DIMITRIADIS, C., GILL, M. & HARTE, M. F. 1997. The first stereospecific approach to both enantiomers of mellein. *Tetrahedron: Asymmetry,* 8**,** 2153-2158.

DIXIT, D., DIXIT, A. K., LAD, H., GUPTA, D. & BHATNAGAR, D. 2013. Radioprotective effect of *Terminalia chebula* Retzius extract against γ-irradiation-induced oxidative stress. *Biomed. Aging Pathol.,* 3**,** 83-88.

DON, R. H., COX, P. T., WAINWRIGHT, B. J., BAKER, K. & MATTICK, J. S. 1991. 'Touchdown' PCR to circumvent spurious priming during gene amplification. *Nucleic Acids Res,* 19**,** 4008.

DRESSEN, M. H. C. L., VAN DE KRUIJS, B. H. P., MEULDIJK, J., VEKEMANS, J. A. J. M. & HULSHOF, L. A. 2009. From Batch to Flow Processing: Racemization of N-Acetylamino Acids under Microwave Heating. *Organic Process Research & Development,* 13**,** 888-895.

DUH, C.-Y., EL-GAMAL, A. A. H., SONG, P.-Y., WANG, S.-K. & DAI, C.-F. 2004. Steroids and sesquiterpenoids from the soft corals *Dendronephthya gigantea* and *Lemnalia cervicorni*. *J. Nat. Prod.,* 67**,** 1650-1653.

DUVOIX, A., DELHALLE, S., BLASIUS, R., SCHNEKENBURGER, M., MORCEAU, F., FOUGÈRE, M., HENRY, E., GALTEAU, M. M., DICATO, M. & DIEDERICH, M. 2004. Effect of chemopreventive agents on glutathione S-transferase P1-1 gene expression mechanisms via activating protein 1 and nuclear factor kappaB inhibition. *Biochemical Pharmacology,* 68**,** 1101-1111.

EBADA, S. S., EDRADA, R. A., LIN, W. & PROKSCH, P. 2008. Methods for isolation, purification and structural elucidation of bioactive secondary metabolites from marine invertebrates. *Nat. Protoc.,* 3**,** 1820-1831.

ELBANDY, M., SHINDE, P. B., HONG, J., BAE, K. S., KIM, M. A., LEE, S. M. & JUNG, J. H. 2009. α-pyrones and yellow pigments from the sponge-derived fungus *Paecilomyces lilacinus*. *Bull. Korean Chem. Soc.,* 30**,** 188-192.

ELDEEN, I. M. S., ELGORASHI, E. E., MULHOLLAND, D. A. & VAN, S. J. 2006. Anolignan B: A bioactive compound from the roots of *Terminalia sericea*. *J. Ethnopharmacol.,* 103**,** 135-138.

ELDEEN, I. M. S., VAN, H. F. R. & VAN, S. J. 2008. Isolation and biological activities of termilignan B and arjunic acid from *Terminalia sericea* roots. *Planta Med.,* 74**,** 411-413.

ENANGA, B., BURCHMORE, R. J. S., STEWART, M. L. & BARRETT, M. P. 2002. Sleeping sickness and the brain. *Cell. Mol. Life Sci.,* 59**,** 845-858.

FAETH, S. H., AND FAGAN, W. F. 2002. Fungal endophytes: Common host plant symbionts but uncommon mutualists. *Integr. Comp. Biol.,* 42**,** 360-368.

FRANCK, B., GOTTSCHALK, E.-M., OHNSORGE, U. & HÜPER, F. 1966. Mutterkorn-Farbstoffe, XII. Trennung, Struktur und absolute Konfiguration

der diastereomeren Secalonsäuren A, B und C. *Chemische Berichte,* 99**,** 3842-3862.

FRANZBLAU, S. G., WITZIG, R. S., MCLAUGHLIN, J. C., TORRES, P., MADICO, G., HERNANDEZ, A., DEGNAN, M. T., COOK, M. B., QUENZER, V. K., FERGUSON, R. M. & GILMAN, R. H. 1998. Rapid, low-technology MIC determination with clinical *Mycobacterium tuberculosis* isolates by using the microplate Alamar Blue assay. *J. Clin. Microbiol.,* 36**,** 362-366.

FREMLIN, L. J., PIGGOTT, A. M., LACEY, E. & CAPON, R. J. 2009. Cottoquinazoline A and cotteslosins A and B, metabolites from an Australian marine-derived strain of *Aspergillus versicolor*. *J. Nat. Prod.,* 72**,** 666-670.

FUCHSER, J. & ZEECK, A. 1997. Secondary metabolites by chemical screening. Part 34. Aspinolides and aspinonene/aspyrone co-metabolites, new pentaketides produced by *Aspergillus ochraceus*. *Liebigs Ann./Recl.***,** 87-95.

GARCEZ, F. R., GARCEZ, W. S., SANTANA, A. L. B. D., ALVES, M. M., DE, F. M., MATOS, C. & SCALIANTE, A. D. M. 2006. Bioactive flavonoids and triterpenes from *Terminalia fagifolia* (combretaceae). *J. Braz. Chem. Soc.,* 17**,** 1223-1228.

GASTELLU-ETCHEGORRY, M. & LEGROS, D. 1999. Sleeping sickness: danger in indifference! *Med Trop (Mars),* 59**,** 347-8.

GE, H. M., YU, Z. G., ZHANG, J., WU, J. H. & TAN, R. X. 2009. Bioactive alkaloids from endophytic *Aspergillus fumigatus*. *J. Nat. Prod.,* 72**,** 753-755.

GLASER, K. B. 2007. HDAC inhibitors: Clinical update and mechanism-based potenial *Biochenical Pharmacology,* 74**,** 659-671.

GOURDEAU, H., JAMES, B. M., RANGER, M., SIMARD, B., BERGER, F., BEAUDRY, F., AND FALARDEAU, P. 2007. Identification, characterization and potent antitumor activity of ECO-4601, a novel peripheral benzodiazepine receptor ligand. *Cancer chemotherapy and pharmacology,* 61**,** 911-921.

GREVE, H., SCHUPP, P. J., EGUEREVA, E., KEHRAUS, S., KELTER, G., MAIER, A., FIEBIG, H.-H. & KONIG, G. M. 2008. Apralactone A and a new stereochemical class of curvularins from the marine fungus *Curvularia* sp. *Eur. J. Org. Chem.***,** 5085-5092, S5085/1-S5085/40.

GU, W. & QIAO, C. 2012. Furandiones from an endophytic *Aspergillus terreus* residing in *Malus halliana*. *Chem. Pharm. Bull.,* 60**,** 1474-1477.

GUERITTE, F., FAHY, J. 2005. The vinca alkaloids *In:* CRAGG, G. M., KINGSTON, D.G.I., NEWMAN, D.J. (ed.) *Anticancer Agents from Natural Products.* Brunner-Routledge Psychology Press, Taylor & Francis Group, Boca Raton, FL.

HALL, R. D. 2006. Plant metabolomics: from holistic hope, to hype, to hot topic. *New Phytol.,* 169**,** 453-468.

HOET, S., OPPERDOES, F., BRUN, R. & QUETIN-LECLERCQ, J. 2004. Natural products active against african trypanosomes: A step towards new drugs. *Nat. Prod. Rep.,* 21**,** 353-364.

HONDA, Y., UEKI, M., OKADA, G., ONOSE, R., USAMI, R., HORIKOSHI, K. & OSADA, H. 2001. Isolation, and biological properties of a new cell cycle inhibitor, curvularol, isolated from *Curvularia* sp. RK97-F166. *J. Antibiot.,* 54**,** 10-16.

HONG, R. 2011. Secalonic acid D as a novel DNA topoisomerase I inhibitor from marine lichen-derived fungus *Gliocladium* sp. T31. *Pharm. Biol. (London, U. K.),* 49**,** 796-799.

HUANG, D.-H., YAN, X.-F., HUANG, Y.-J. & ZHANG, L.-R. 2008. Study on bioactivity of endophytic fungi from *Ephedra*. *Xiamen Daxue Xuebao, Ziran Kexueban,* 47**,** 248-252.

HUANG, H.-B., XIAO, Z.-E., FENG, X.-J., HUANG, C.-H., ZHU, X., JU, J.-H., LI, M.-F., LIN, Y.-C., LIU, L. & SHE, Z.-G. 2011. Cytotoxic Naphtho-γ-pyrones from the Mangrove Endophytic Fungus *Aspergillus tubingensis* (GX1-5E). *Helv. Chim. Acta,* 94**,** 1732-1740.

HUANG, X., HUANG, H., LI, H., SUN, X., HUANG, H., LU, Y., LIN, Y., LONG, Y. & SHE, Z. 2013. Asperterpenoid A, a New Sesterterpenoid as an Inhibitor of *Mycobacterium tuberculosis* Protein Tyrosine Phosphatase B from the Culture of *Aspergillus* sp. 16-5c. *Org. Lett.,* 15**,** 721-723.

HUSSAIN, H., KROHN, K., DRAEGER, S., MEIER, K. & SCHULZ, B. 2009. Bioactive chemical constituents of a sterile endophytic fungus from *Meliotus dentatus*. *Rec. Nat. Prod.,* 3**,** 114-117.

IBRAHIM, S. R. M., MIN, C. C., TEUSCHER, F., EBEL, R., KAKOSCHKE, C., LIN, W., WRAY, V., EDRADA-EBEL, R. & PROKSCH, P. 2010. Callyaerins A-F and H, new cytotoxic cyclic peptides from the Indonesian marine sponge *Callyspongia aerizusa*. *Bioorg. Med. Chem.,* 18**,** 4947-4956.

ISHIDA, T. 2000. Anti-microbial, anti-tumor and immunostimulation properties of secalonic acid D derivatives. *Suzuka Iryo Kagaku Gijutsu Daigaku Kiyo,* 7**,** 61-68.

ISHIDA, T., OHOISHI, J., YOSHIDA, K., AKASHI, K. & TAKEDA, I. 1974. *Antitumorous secalonic acid D derivatives*.

ITOKAWA, H., WANG, X., LEE, K.-H. 2005. Homoharringtonine and related compounds. *In:* CRAGG, G. M., KINGSTON, D.G.I., NEWMAN, D.J. (ed.) *Anticancer Agents from Natural Products.* Brunner-Routledge Psychology Press, Taylor & Francis Group, Boca Raton, FL.

JACOBSON, K. R., TIERNEY, D. B., JEON, C. Y., MITNICK, C. D. & MURRAY, M. B. 2010. Treatment outcomes among patients with extensively drug-resistant tuberculosis: systematic review and meta-analysis. *Clin Infect Dis,* 51**,** 6-14.

JI, Y., BI, J.-N., YAN, B. & ZHU, X.-D. 2006. Taxol-producing fungi: a new approach to industrial production of taxol. *Sheng Wu Gong Cheng Xue Bao,* 22**,** 1-6.

KANDIL, F. E. & NASSAR, M. I. 1998. A tannin anti-cancer promoter from *Terminalia arjuna*. *Phytochemistry,* 47**,** 1567-1568.

KAWAHARA, N., SEKITA, S. & SATAKE, M. 1995. Two steroids from *Calvatia cyathiformis*. *Phytochemistry,* 38**,** 947-50.

KAWAZU, K., KOBAYASHI, A. & OE, K. 1991. *Cell division-inhibiting harveynones from Curvularia harveyi*.

KEAN, G., SMITH, J., OGDEN, M., ABADI, G., BARBAS, J. & MANNING, T. J. The Florida Yew Tree and Taxol. 2007. American Chemical Society, GEN-838.

KERNAN, M. R., AMARQUAYE, A., CHEN, J. L., CHAN, J., SESIN, D. F., PARKINSON, N., YE, Z.-J., BARRETT, M., BALES, C., STODDART, C. A., SLOAN, B., BLANC, P., LIMBACH, C., MRISHO, S. & ROZHON, E. J. 1998. Antiviral Phenylpropanoid Glycosides from the Medicinal Plant *Markhamia lutea*. *J. Nat. Prod.,* 61**,** 564-570.

KHAN, M. R. & MLUNGWANA, S. M. 1999. γ-Sitosterol, a cytotoxic sterol from *Markhamia zanzibarica* and *Kigelia africana*. *Fitoterapia,* 70**,** 96-97.

KIM, D. S., BAEK, N.-I., OH, S. R., JUNG, K. Y., LEE, I. S., KIM, J. H. & LEE, H.-K. 1997. Anticomplementary activity of ergosterol peroxide from *Naematoloma fasciculare* and reassignment of NMR data. *Arch. Pharmacal Res.,* 20**,** 201-205.

KIM, H., RALPH, J., LU, F., RALPH, S. A., BOUDET, A.-M., MACKAY, J. J., SEDEROFF, R. R., ITO, T., KAWAI, S., OHASHI, H. & HIGUCHI, T. 2003. NMR analysis of lignins in CAD-deficient plants. Part 1. Incorporation of hydroxycinnamaldehydes and hydroxybenzaldehydes into lignins. *Org. Biomol. Chem.,* 1**,** 268-281.

KOHNO, J., NISHIO, M., SAKURAI, M., KAWANO, K., HIRAMATSU, H., KAMEDA, N., KISHI, N., YAMASHITA, T., OKUDA, T. & KOMATSUBARA, S. 1999. Isolation and structure determination of TMC-151s: Novel polyketide antibiotics from *Gliocladium catenulatum* Gilman & Abbott TC 1280. *Tetrahedron,* 55**,** 7771-7786.

KOSHTI, N., NAIK, S. & PARAB, B. 2005. Polymer-bound cationic Rh(I) phosphine catalyst for homogeneous asymmetric hydrogenation. *Indian J. Chem., Sect. B: Org. Chem. Incl. Med. Chem.,* 44B**,** 2555-2559.

KREMNICKY, L., MASTIHUBA, V. & COTE, G. L. 2004. *Trichoderma reesei* acetyl esterase catalyzes transesterification in water. *J. Mol. Catal. B: Enzym.,* 30**,** 229-239.

KUO, P.-L., HSU, Y.-L., LIN, T.-C., LIN, L.-T., CHANG, J.-K. & LIN, C.-C. 2005. Casuarinin from the bark of *Terminalia arjuna* induces apoptosis and cell cycle arrest in human breast adenocarcinoma MCF-7 cells. *Planta Med.,* 71**,** 237-243.

KUROBANE, I., VINING, L. C. & MCINNES, A. G. 1978. A new secalonic acid. Linkage between tetrahydroxanthone units determined from deuterium isotope carbon-13 chemical shifts. *Tetrahedron Lett.***,** 4633-6.

KUROBANE, I., VINING, L. C. & MCINNES, A. G. 1979. Biosynthetic relationships among the secalonic acids. Isolation of emodin, endocrocin and

secalonic acids from *Pyrenochaeta terrestris* and *Aspergillus aculeatus*. *J. Antibiot.,* 32**,** 1256-66.

KUSARI, S., LAMSHOEFT, M. & SPITELLER, M. 2009. *Aspergillus fumigatus* Fresenius, an endophytic fungus from *Juniperus communis* L. Horstmann as a novel source of the anticancer pro-drug deoxypodophyllotoxin. *J. Appl. Microbiol.,* 107**,** 1019-1030.

LACROIX, D., PRADO, S., DEVILLE, A., KRIEF, S., DUMONTET, V., KASENENE, J., MOURAY, E., BORIES, C. & BODO, B. 2009. Hydroperoxy-cycloartane triterpenoids from the leaves of *Markhamia lutea*, a plant ingested by wild chimpanzees. *Phytochemistry (Elsevier),* 70**,** 1239-1245.

LEE, D.-Y., LEE, S.-J., KWAK, H.-Y., LAKOON, J., HEO, J., HONG, S., KIM, G.-W. & BAEK, N.-I. 2009. Sterols isolated from Nuruk (*Rhizopus oryzae* KSD-815) inhibit the migration of cancer cells. *J. Microbiol. Biotechnol.,* 19**,** 1328-1332.

LEE, F. Y., BORZILLERI, R., FAIRCHILD, C.R., KAMATH, A., SMYKLA, R., KRAMER, R., VITE, G. 2008. Preclinical discovery of ixabepilone, a highly active antineoplastic agent. *Cancer Chemotherapy and Pharmacology,* 63**,** 157-166.

LEE, K.-H., XIAO, Z. 2005. Podophyllotoxins and analogs. *In:* CRAGG, G. M., KINGSTON, D.G.I., NEWMAN, D.J. (ed.) *Anticancer Agents from Natural Products.* Brunner-Routledge Psychology Press, Taylor & Francis Group, Boca Raton, FL.

LEE, S.-H., RYU, S. Y., CHOI, S. U., LEE, C. O., NO, Z., KIM, S.-K. & AHN, J.-W. 1995. Hydrolyzable tannins and related compound having cytotoxic activity from the fruits of *Terminalia chebula*. *Arch. Pharmacal Res.,* 18**,** 118-20.

LEGROS, D., FOURNIER, C., GASTELLU, E. M., MAISO, F. & SZUMILIN, E. 1999. Therapeutic failure of melarsoprol among patients treated for late stage *T.b. gambiense* human African trypanosomiasis in Uganda. *Bull Soc Pathol Exot,* 92**,** 171-2.

LI, Q., SHAM, H.L. 2002. Discovery and development of antimitotic agents that inhibit tubulin polymerisation for the treatment of cancer. *Expert Opinion on Therapeutic Patents,* 12**,** 417–425.

LI, Q., XIA, X., ZHANG, Y., LIU, F., YANG, L., SHE, Z. & LIN, Y. 2008. Research on fungal metabolite Secalonic acid D and its pharmacological activity. *Zhongyaocai,* 31**,** 1274-1278.

LI, S., WEI, M., CHEN, G. & LIN, Y. 2012a. Two new dihydroisocoumarins from the endophytic fungus *Aspergillus* sp. collected from the South China Sea. *Chem. Nat. Compd.,* 48**,** 371-373.

LI, X.-B., XIE, F., LIU, S.-S., LI, Y., ZHOU, J.-C., LIU, Y.-Q., YUAN, H.-Q. & LOU, H.-X. 2013. Naphtho-γ-pyrones from endophyte *Aspergillus niger*

occurring in the liverwort Heteroscyphus tener (Steph.) Schiffn. *Chem. Biodiversity,* 10**,** 1193-1201.

LI, X.-J., ZHANG, Q., ZHANG, A.-L. & GAO, J.-M. 2012b. Metabolites from *Aspergillus fumigatus*, an Endophytic Fungus Associated with *Melia azedarach*, and Their Antifungal, Antifeedant, and Toxic Activities. *J. Agric. Food Chem.***,** Ahead of Print.

LI, X., JEONG, J. H., LEE, K. T., RHO, J. R., CHOI, H. D., KANG, J. S. & SON, B. W. 2003. γ-pyrone derivatives, kojic acid methyl ethers from a marine-derived fungus *Altenaria* sp. *Arch. Pharmacal Res.,* 26**,** 532-534.

LI, Y., SONG, Y. C., LIU, J. Y., MA, Y. M. & TAN, R. X. 2005. Anti-*Helicobacter pylori* substances from endophytic fungal cultures. *World J. Microbiol. Biotechnol.,* 21**,** 553-558.

LIN, Z.-J., ZHANG, G.-J., ZHU, T.-J., LIU, R., WEI, H.-J. & GU, Q.-Q. 2009. Bioactive Cytochalasins from *Aspergillus flavipes*, an Endophytic Fungus Associated with the Mangrove Plant *Acanthus ilicifolius*. *Helv. Chim. Acta,* 92**,** 1538-1544.

LIN, Z., ZHU, T., FANG, Y. & GU, Q. 2008. 1H and 13C NMR assignments of two new indolic enamide diastereomers from a mangrove endophytic fungus *Aspergillus* sp. *Magn. Reson. Chem.,* 46**,** 1212-1216.

LIU, D., LI, X.-M., MENG, L., LI, C.-S., GAO, S.-S., SHANG, Z., PROKSCH, P., HUANG, C.-G. & WANG, B.-G. 2011. Nigerapyrones A-H, Î±-pyrone derivatives from the marine mangrove-derived endophytic fungus *Aspergillus niger* MA-132. *J Nat Prod,* 74**,** 1787.

LIU, J., LU, X., LIU, X., CHEN, B., JIAO, B., LI, H., FENG, Z. & ZHANG, J. 2013. *Cytochalasin Z24, cytochalasin Z25 and cytochalasin Z26 with anti-tumor activity, their preparation method application in prepn. of antineoplastic*.

LIU, J. Y., SONG, Y. C., ZHANG, Z., WANG, L., GUO, Z. J., ZOU, W. X. & TAN, R. X. 2004. *Aspergillus fumigatus* CY018, an endophytic fungus in *Cynodon dactylon* as a versatile producer of new and bioactive metabolites. *J. Biotechnol.,* 114**,** 279-287.

LU, X., LIU, J., LIU, X., CHEN, B., JIAO, B., LI, H., FENG, Z. & ZHANG, J. 2013. *Diterpenoids of libertellenone G and libertellenone H with anti-tumor activity, their preparation method and application in prepn. of antineoplastic*.

MACINTYRE, L., ZHANG, T., VIEGELMANN, C., MARTINEZ, I. J., CHENG, C., DOWDELLS, C., EDRADA-EBEL, R., ABDELMOHSEN, U. R., GERNERT, C. & HENTSCHEL, U. 2014. Metabolomic tools for secondary metabolite discovery from marine microbial symbionts. *Mar Drugs,* 12**,** 3416-48.

MANOSROI, A., JANTRAWUT, P., OGIHARA, E., YAMAMOTO, A., FUKATSU, M., YASUKAWA, K., TOKUDA, H., SUZUKI, N., MANOSROI, J. & AKIHISA, T. 2013. Biological Activities of Phenolic

Compounds and Triterpenoids from the Galls of *Terminalia chebula*. *Chem. Biodiversity,* 10**,** 1448-1463.

MARTINEZ-LUIS, S., CHERIGO, L., ARNOLD, E., SPADAFORA, C., GERWICK, W. H. & CUBILLA-RIOS, L. 2012. Antiparasitic and anticancer constituents of the endophytic fungus *Aspergillus* sp. strain F1544. *Nat. Prod. Commun.,* 7**,** 165-168.

MARTINEZ-LUIS, S., CHERIGO, L., HIGGINBOTHAM, S., ARNOLD, E., SPADAFORA, C., IBANEZ, A., GERWICK, W. H. & CUBILLA-RIOS, L. 2011. Screening and evaluation of antiparasitic and in vitro anticancer activities of Panamanian endophytic fungi. *Int Microbiol,* 14**,** 95-102.

MARZOUK, M. S. A., EL-TOUMY, S. A. A., MOHARRAM, F. A., SHALABY, N. M. M. & AHMED, A. A. E. 2002. Pharmacologically active ellagitannins from *Terminalia myriocarpa*. *Planta Med.,* 68**,** 523-527.

METZ, A. M., HADDAD, A., WORAPONG, J., LONG, D. M., FORD, E. J., HESS, W. M. AND STROBEL, G. A. 2000. *Induction of the sexual stage of Pestalotiopsis microspora, a taxol producing fungus*, Reading, United Kingdom.

MILNE, J. E., STORZ, T., COLYER, J. T., THIEL, O. R., DILMEGHANI, S. M., LARSEN, R. D. & MURRY, J. A. 2011. Iodide-Catalyzed Reductions: Development of a Synthesis of Phenylacetic Acids. *J. Org. Chem.,* 76**,** 9519-9524.

MOSLEY, C. A., LIOTTA, D. C., SNYDER J. P. 2007. Highly active anticancer curcumin analogues. *Advances in Experimental Medicine and Biology* 595**,** 77-103.

MUDDATHIR, A. M., YAMAUCHI, K. & MITSUNAGA, T. 2013. Anti-acne activity of tannin-related compounds isolated from *Terminalia laxiflora*. *J. Wood Sci.,* 59**,** 426-431.

NATURALE, G., LAMBLIN, M., COMMANDEUR, C., FELPIN, F.-X. & DESSOLIN, J. 2012. Direct C–H Alkylation of Naphthoquinones with Amino Acids Through a Revisited Kochi–Anderson Radical Decarboxylation: Trends in Reactivity and Applications. *European Journal of Organic Chemistry,* 2012**,** 5774-5788.

NCHU, F., ADEROGBA, M. A., MDEE, L. K. & ELOFF, J. N. 2010. Isolation of anti-*Candida albicans* compounds from *Markhamia obtusifolia* (Baker) Sprague (Bignoniaceae). *S. Afr. J. Bot.,* 76**,** 54-57.

NEWMAN, D. J., CRAGG, G.M., HOLBECK, S., SAUSVILLE, E.A. 2002. Natural products as leads to cell cycle pathway targets in cancer chemotherapy. *Current Cancer Drug Targets,* 2**,** 279–308.

NEWMAN, D. J., CRAGG, G.M., SNADER, K.M 2003. Natural products as sources of new drugs over the period 1981–2002. *Journal of Natural Products,* 66**,** 1022–1037.

NGUYEN, D.-M.-C., SEO, D.-J., NGUYEN, V.-N., KIM, K.-Y., PARK, R.-D. & JUNG, W.-J. 2013. Nematicidal activity of gallic acid purified from

Terminalia nigrovenulosa bark against the root-knot nematode Meloidogyne incognita. *Nematology,* 15**,** 507-518.

OPIYO, S. A., MANGURO, L. O. A., OWUOR, P. O., OCHIENG, C. O., ATEKA, E. M. & LEMMEN, P. 2011. Antimicrobial compounds from *Terminalia brownii* against sweet potato pathogens. *Nat. Prod. J.,* 1**,** 116-120.

PANG, Y.-W., ZHANG, L.-J., FANG, J.-S., LIU, Q.-F., ZHANG, H., XIANG, W.-S., WANG, J.-D. & WANG, X.-J. 2013. Two new antitumor constituents from a soil fungus *Curvularia inaequalis* (strain HS-FG-257). *J. Antibiot.,* 66**,** 287-289.

PELLATI, F., BRUNI, R., RIGHI, D., GRANDINI, A., TOGNOLINI, M., PIO, P. F., POLI, F., BENVENUTI, S., DEL, R. D. & ROSSI, D. 2013. Metabolite profiling of polyphenols in a *Terminalia chebula* Retzius ayurvedic decoction and evaluation of its chemopreventive activity. *J. Ethnopharmacol.,* 147**,** 277-285.

PETTIT, G. R., HOARD, M. S., DOUBEK, D. L., SCHMIDT, J. M., PETTIT, R. K., TACKETT, L. P. & CHAPUIS, J.-C. 1996. Antineoplastic agents 338. The cancer cell growth inhibitory. Constituents of *Terminalia arjuna* (Combretaceae). *Journal of Ethnopharmacology,* 53**,** 57-63.

PHONGPAICHIT, S., NIKOM, J., RUNGJINDAMAI, N., SAKAYAROJ, J., HUTADILOK-TOWATANA, N., RUKACHAISIRIKUL, V. & KIRTIKARA, K. 2007. Biological activities of extracts from endophytic fungi isolated from *Garcinia* plants. *FEMS Immunol. Med. Microbiol.,* 51**,** 517-525.

PINHEIRO, E. A. A., CARVALHO, J. M., DOS, S. D. C. P., FEITOSA, A. D. O., MARINHO, P. S. B., GUILHON, G. M. S. P., DE, S. A. D. L., DA, S. F. M. A. & MARINHO, A. M. D. R. 2013. Antibacterial activity of alkaloids produced by endophytic fungus *Aspergillus* sp. EJC08 isolated from medical plant *Bauhinia guianensis*. *Nat. Prod. Res.,* 27**,** 1633-1638.

PINNEY, K. G., JELINEK, C., EDVARDSEN, K., CHAPLIN, D.J., PETTIT, G.R. 2005. The discovery and development of the combretastatins. *In:* CRAGG, G. M., KINGSTON, D.G.I., NEWMAN, D.J. (ed.) *Anticancer Agents from Natural Products.* Brunner-Routledge Psychology Press, Taylor & Francis Group, Boca Raton, FL.

PONGPRAYOON, U., BACKSTROEM, P., JACOBSSON, U., LINDSTROEM, M. & BOHLIN, L. 1991. Compounds inhibiting prostaglandin synthesis isolated from *Ipomoea pescaprae*. *Planta Med.,* 57**,** 515-18.

PONOU, B. K., TEPONNO, R. B., RICCIUTELLI, M., NGUELEFACK, T. B., QUASSINTI, L., BRAMUCCI, M., LUPIDI, G., BARBONI, L. & TAPONDJOU, L. A. 2011. Novel 3-Oxo- and 3,24-Dinor-2,4-secooleanane-Type Triterpenes from *Terminalia ivorensis* A. Chev. *Chem. Biodiversity,* 8**,** 1301-1309.

PONOU, B. K., TEPONNO, R. B., RICCIUTELLI, M., QUASSINTI, L., BRAMUCCI, M., LUPIDI, G., BARBONI, L. & TAPONDJOU, L. A. 2010.

Dimeric antioxidant and cytotoxic triterpenoid saponins from *Terminalia ivorensis* A. Chev. *Phytochemistry (Elsevier),* 71**,** 2108-2115.

PONOU, B. K., TEPONNO, R. B., RICCIUTELLI, M., QUASSINTI, L., BRAMUCCI, M., LUPIDI, G., BARBONI, L., TAPONDJOU, L. A., 2010. Dimeric antioxidant and cytotoxic triterpenoid saponins from *Terminalia ivorensis* A. Chev. *Phytochemistry,* 71**,** 2108-2115.

PRABAVATHY, D. & NACHIYAR, C. V. 2011. Screening and characterization of antimicrobial compound from endophytic *Aspergillus* sp. isolated from *Ficus carica*. *J. Pharm. Res.,* 4**,** 1935-1936.

RAGHUNATH, R., RADHAKRISHNA, A., ANGAYARKANNI, J. & PALANISWAMY, M. 2012. Production and cytotoxicity studies of lovastatin from *Aspergillus niger* PN2 an endophytic fungi isolated from *Taxus baccata*. *Int. J. Appl. Biol. Pharm. Technol.,* 3**,** 342-351.

RAHIER, N. J., THOMAS, C.J., HECHT, S.M. 2005. Camptothecin and its analogs *In:* CRAGG, G. M., KINGSTON, D.G.I., NEWMAN, D.J. (ed.) *Anticancer Agents from Natural Products.* Brunner-Routledge Psychology Press, Taylor & Francis Group, Boca Raton, FL.

RAMESH, A. S., CHRISTOPHER, J. G., RADHIKA, R., SETTY, C. R. & THANKAMANI, V. 2012. Isolation, characterisation and cytotoxicity study of arjunolic acid from *Terminalia arjuna*. *Nat. Prod. Res.,* 26**,** 1549-1552.

RAVELO, A. G., ESTEVEZ-BRAUN, A., CHAVENZ-ORELLANA, H., PEREZ-SACAU, E. AND MESA-SIVERIO, D. 2004. Recent studies on natural products as anticancer agents. *Current topics in medicinal chemistry,* 4**,** 241-265.

RAVINDRAN, C., NAVEENAN, T., VARATHARAJAN, G. R., RAJASABAPATHY, R. & MEENA, R. M. 2012. Antioxidants in mangrove plants and endophytic fungal associations. *Bot. Mar.,* 55**,** 269-279.

RÄZ, B., ITEN, M., GRETHER-BÜHLER, Y., KAMINSKY, R. & BRUN, R. 1997. The Alamar Blue® assay to determine drug sensitivity of African trypanosomes (*T.b. rhodesiense* and *T.b. gambiense*) in vitro. *Acta Tropica,* 68**,** 139-147.

REN, H., TIAN, L., GU, Q. & ZHU, W. 2005. Secalonic acid D; a cytotoxic constituent from marine lichen-derived fungus *Gliocladium* sp. T31. *Arch. Pharmacal Res.,* 29**,** 59-63.

ROCHFORT, S. 2005. Metabolomics Reviewed: A New "Omics" Platform Technology for Systems Biology and Implications for Natural Products Research. *J. Nat. Prod.,* 68**,** 1813-1820.

ROGE, A. B., FIRKE, S. N., KAWADE, R. M., SARJE, S. K. & VADVALKAR, S. M. 2011. Brief review on: Flash chromatography. *Int. J. Pharm. Sci. Res.,* 2**,** 1930-1937.

ROSS, S. A., EL-FISHAWY, A. M., SAID, A., HAWAS, U. W., TEKWANI, B. L., RADWAN, M. M. & ABOELMAGD, M. 2013. A new fatty alcohol from

Terminalia arjuna leaves with antileishmanial activity. *Med. Chem. Res.,* 22**,** 5844-5847.

RUDGERS, J. A., KOSLOW, J. M., AND CLAY, K. 2004. Endophytic fungi alter relationships between diversity and ecosystem properties. *Ecology letters,* 7**,** 42-51.

RYCHLIK, W., SPENCER, W. J. & RHOADS, R. E. 1990. Optimization of the annealing temperature for DNA amplification in vitro. *Nucleic Acids Res,* 18**,** 6409-12.

SADANANDA, T. S., NIRUPAMA, R., CHAITHRA, K., GOVINDAPPA, M., CHANDRAPPA, C. P. & VINAY, R. B. 2011. Antimicrobial and antioxidant activities of endophytes from *Tabebuia argentea* and identification of anticancer agent (lapachol). *J. Med. Plants Res.,* 5**,** 3643-3652.

SAIKKONEN, K., FAETH, S. H., HELANDER, M., AND SULLIVAN, T. J. 1998. Fungal endophytes: A continuum of interactions with host plants. *The Annual Review of Ecology, Evolution, and Systematics,* 29**,** 319-343.

SASSA, T., HAYAKARI, S., IKEDA, M. & MIURA, Y. 1971. Plant growth inhibitors produced by fungi. I. Isolation and identification of penicillic acid and dihydropenicillic acid. *Agr. Biol. Chem.,* 35**,** 2130-1.

SATO, S., FUTAKI, F., FUKUCHI, N., KAIDA, K., HIRAGA, M., KOBARU, S. & TSUJI, T. 2006. A new nucleoside derivative, AJP117510, as an inhibitor of integrin α2β1-collagen binding. *J. Antibiot.,* 59**,** 251-253.

SCHARDL, C. L., LIU, J.-S., WHITE, J. F., FINKEL, R. A., AN, Z., AND SIEGEL, M. R. 1991. Molecular phylogenetic relationships of nonpathogenic grass mycosymbionts and clavicipitaceous plant pathogens. *Plant Systematic and Evolution,* 178**,** 27-41.

SCHIFF, P. B., AND HOROWITZ, S. B. 1980. Taxol stabilizes microtubules in mouse fibroblast cells. *Proceedings of the National Academy of Science,* 77**,** 1561-1565.

SCHULZ, B., RÖMMERT, A.-K., DAMMANN, U., AUST, H.-J., AND STRACK, D. 1999. The endophyte-host interaction: a balanced antagonism? *Mycol. Res.,* 103**,** 1275-1283.

SCHUMACHER, M., CERELLA, C., EIFES, S., CHATEAUVIEUX, S., MORCEAU, F., JASPARS, M., DICATO, M. & DIEDERICH, M. 2010. Heteronemin, a spongean sesterterpene, inhibits TNFα-induced NF-κB activation through proteasome inhibition and induces apoptotic cell death. *Biochemical Pharmacology,* 79**,** 610-622.

SETTE, L. D., PASSARINI, M. R. Z., DELARMELINA, C., SALATI, F. & DUARTE, M. C. T. 2006. Molecular characterization and antimicrobial activity of endophytic fungi from coffee plants. *World J. Microbiol. Biotechnol.,* 22**,** 1185-1195.

SHAABAN, M., NASR, H., HASSAN, A. Z. & ASKER, M. S. 2013. Bioactive secondary metabolites from endophytic *Aspergillus fumigatus*: structural elucidation and bioactivity studies. *Rev. Latinoam. Quim.,* 41**,** 50-60.

SHEN, L., YE, Y.-H., WANG, X.-T., ZHU, H.-L., XU, C., SONG, Y.-C., LI, H. & TAN, R.-X. 2006. Structure and total synthesis of aspernigerin: a novel cytotoxic endophyte metabolite. *Chem.--Eur. J.,* 12**,** 4393-4396.

SONG, Y. C., LI, H., YE, Y. H., SHAN, C. Y., YANG, Y. M. & TAN, R. X. 2004. Endophytic naphthopyrone metabolites are co-inhibitors of xanthine oxidase, SW1116 cell and some microbial growths. *FEMS Microbiol. Lett.,* 241**,** 67-72.

SRIVASTAVA, S. K. & SRIVASTAVA, S. D. 2004. New biologically active constituents from *Terminalia chebula* stem bark. *Indian J. Chem., Sect. B: Org. Chem. Incl. Med. Chem.,* 43B**,** 2731-2733.

SRIVASTAVA, S. K., SRIVASTAVA, S. D. & CHOUKSEY, B. K. 2000. A triterpenoidal saponin and other new constituents from *Terminalia alata*. *Proc. Phytochem. Soc. Eur.,* 45**,** 107-111.

STEVENS, P. J. Thin layer chromatography. 1969. McGraw-Hill, 46-73.

STIERLE, A., STROBEL, G. & STIERLE, D. 1993. Taxol and taxane production by *Taxomyces andreanae,* an endophytic fungus of Pacific yew. *Science,* 260**,** 214-6.

STROBEL, G., DAISY, B., CASTILLO, U. & HARPER, J. 2004. Natural products from endophytic microorganisms. *J. Nat. Prod.,* 67**,** 257-268.

STROBEL, G., DAISY, B., CASTILLO, U. AND HARPER, J. J. 2004a. Natural Products from Endophytic Microorganisms. *Natural Product Reports,* 24**,** 87-108.

STROBEL, G., DAISY, B., CASTILLO, U. AND HARPER, J. J. 2004b. Natural Products from Endophytic Microorganisms. *Natural products,* 67**,** 257-268.

STROBEL, G., YANG, X., SEARS, J., KRAMER, R., SIDHU, R. S. & HESS, W. M. 1996. Taxol from *Pestalotiopsis microspora,* an endophytic fungus of *Taxus wallachiana*. *Microbiology,* 142 (Pt 2)**,** 435-40.

STROBEL, G. A. 2002a. Rainforest endophytes and bioactive natural products. *Critical Reviews in Biotechnology,* 22**,** 315-333.

SUNKAR, S. & NACHIYAR, C. V. 2011. Isolation and characterization of antimicrobial compounds produced by endophytic fungus *Aspergillus* sp. isolated from *Writhtia tintorica*. *J. Pharm. Res.,* 4**,** 1136-1137.

TACHIBANA, M., MATSUI, C., TAKEUCHI, Y., SUZUKI, E. & UMEZAWA, K. 2008. Inhibition of NF-kappa B activation by penicillic acid and dihydropenicillic acid isolated from fungi. *Heterocycles,* 76**,** 1561-1569.

TAKAGI, M., MOTOHASHI, K. & SHIN-YA, K. 2010. Isolation of 2 new metabolites, JBIR-74 and JBIR-75, from the sponge-derived *Aspergillus* sp. fS14. *J. Antibiot.,* 63**,** 393-395.

TAN, R. X., AND ZOU, W. X. 2001. Endophyts: A rich source of functional metabolites. *Natural Product Reports,* 18**,** 448-459.

TANG, X., YI, Z. & LI, N. 2012. *Cytotoxic compound secalonic acid F-producing deep-sea Penicillium F11*.

TANTANGMO, F., LENTA, B. N., BOYOM, F. F., NGOUELA, S., KAISER, M., TSAMO, E., WENIGER, B., ROSENTHAL, P. J. & VONTHRON-SENECHEAU, C. 2010. Antiprotozoal activities of some constituents of *Markhamia tomentosa* (Bignoniaceae). *Ann. Trop. Med. Parasitol.*, 104**,** 391-398.

TAWFIKE, A., VIEGELMANN, C. & EDRADA-EBEL, R. 2013. Metabolomics and Dereplication Strategies in Natural Products. *In:* ROESSNER, U. & DIAS, D. A. (eds.) *Metabolomics Tools for Natural Product Discovery.* Humana Press.

TOKURA, K. & KAGAWA, S. 1995. *Anticancer agents containing chebulanin from Terminalia chebula*.

TOMASSINI, J. E., DAVIES, M. E., HASTINGS, J. C., LINGHAM, R., MOJENA, M., RAGHOOBAR, S. L., SINGH, S. B., TKACZ, J. S. & GOETZ, M. A. 1996. A novel antiviral agent which inhibits the endonuclease of influenza viruses. *Antimicrob. Agents Chemother.,* 40**,** 1189-1193.

UEDA, H., NAKAJIMA, H., HORI, Y., FUJITA, T., NISHIMURA, M., GOTO, T., OKUHARA, M. 1994. FR901228, a novel antitumor bicyclic depsipeptide produced by *Chromobacterium violaceum* No. 968. I. Taxonomy, fermentation, isolation, physico-chemical and biological properties, and antitumor activity. *Journal of Antibiotic,* 47**,** 301-310.

VALSARAJ, R., PUSHPANGADAN, P., SMITT, U. W., ADSERSEN, A., CHRISTENSEN, S. B., SITTIE, A., NYMAN, U., NIELSEN, C. & OLSEN, C. E. 1997. New Anti-HIV-1, Antimalarial, and Antifungal Compounds from *Terminalia bellerica*. *J. Nat. Prod.,* 60**,** 739-742.

VAN DEN BOOGAARD, J., KIBIKI, G. S., KISANGA, E. R., BOEREE, M. J. & AARNOUTSE, R. E. 2009. New drugs against tuberculosis: problems, progress, and evaluation of agents in clinical development. *Antimicrob. Agents Chemother.,* 53**,** 849-862.

VENKATASUBBAIAH, P. & CHILTON, W. S. 1990. Phytotoxins of plant pathogens. Part IV. Phytotoxins of *Botryosphaeria obtusa*. *J. Nat. Prod.,* 53**,** 1628-30.

VERMA, A., AHMED, B., UPADHYAY, R. & SONI, N. 2012. Nymphasterol, a new steroid from *Nymphaea stellata*. *Med. Chem. Res.,* 21**,** 783-787.

WANG, C., WU, J. & MEI, X. 2001. Enhancement of taxol production and excretion in *Taxus chinensis* cell culture by fungal elicitation and medium renewal. *Appl. Microbiol. Biotechnol.,* 55**,** 404-410.

WANI, M. A., SANJANA, K., KUMAR, D. M. & LAL, D. K. 2010. GC – MS analysis reveals production of 2 – Phenylethanol from *Aspergillus niger* endophytic in rose. *Journal of Basic Microbiology,* 50**,** 110-114.

WANI, M. C., TAYLOR, H. L., WALL, M. E., COGGON, P. & MCPHAIL, A. T. 1971. Plant antitumor agents. VI. The isolation and structure of taxol, a novel antileukemic and antitumor agent from *Taxus brevifolia*. *J Am Chem Soc,* 93**,** 2325-7.

WANSI, J. D., LALLEMAND, M.-C., CHIOZEM, D. D., TOZE, F. A. A., MBAZE, L. M. A., NAHARKHAN, S., IQBAL, M. C., TILLEQUIN, F., WANDJI, J. & FOMUM, Z. T. 2007. α-Glucosidase inhibitory constituents from stem bark of *Terminalia superba* (Combretaceae). *Phytochemistry (Elsevier),* 68**,** 2096-2100.

WHO 1998. Control and surveillance of African trypanosomiasis. Report of a WHO Expert Committee. *World Health Organ Tech Rep Ser,* 881**,** I-VI, 1-114.

XU, Y., LU, C. & ZHENG, Z. 2012. A new 3,4-dihydroisocoumarin isolated from *Botryosphaeria* sp. F00741. *Chem. Nat. Compd.,* 48**,** 205-207.

YOSHIDA, T., KATO, T., KAWAMURA, Y., MATSUMOTO, K. & ITAZAKI, H. 1993. *Aldose reductase inhibitors manufacture with Chaetomella*.

YUAN, J., HE, Z., ZHU, X. & WU, J. 2010. Potent anti-breast cancer effects of a novel secalonic acid D analog D69 derived from marine microbes. *Guangdong Yaoxueyuan Xuebao,* 26**,** 519-523.

YULIANA, N. D., JAHANGIR, M., VERPOORTE, R. & CHOI, Y. H. 2013. Metabolomics for the rapid dereplication of bioactive compounds from natural sources. *Phytochem. Rev.,* 12**,** 293-304.

YULIANA, N. D., KHATIB, A., CHOI, Y. H. & VERPOORTE, R. 2011. Metabolomic for bioactivity assessment of natural products. *Phytother. Res.,* 25**,** 157-169.

YURCHENKO, A. N., SMETANINA, O. F., KALINOVSKY, A. I., PIVKIN, M. V., DMITRENOK, P. S. & KUZNETSOVA, T. A. 2010. A new meroterpenoid from the marine fungus *Aspergillus versicolor* (Vuill.) Tirab. *Russ. Chem. Bull.,* 59**,** 852-856.

ZHANG, C.-L., ZHENG, B.-Q., LAO, J.-P., MAO, L.-J., CHEN, S.-Y., KUBICEK, C. P. & LIN, F.-C. 2008a. Clavatol and patulin formation as the antagonistic principle of *Aspergillus clavatonanicus*, an endophytic fungus of *Taxus mairei*. *Appl. Microbiol. Biotechnol.,* 78**,** 833-840.

ZHANG, H.-C., MA, Y.-M., LIU, R. & ZHOU, F. 2012. Endophytic fungus *Aspergillus tamarii* from *Ficus carica* L., a new source of indolyl diketopiperazines. *Biochem. Syst. Ecol.,* 45**,** 31-33.

ZHANG, H.-W., ZHANG, J., HU, S., ZHANG, Z.-J., ZHU, C.-J., NG, S. W. & TAN, R.-X. 2010. Ardeemins and cytochalasins from *Aspergillus terreus* residing in *Artemisia annua*. *Planta Med.,* 76**,** 1616-1621.

ZHANG, H. W., SONG, Y. C., AND TAN, R. X. 2006. Biology and chemistry of endophytes. *Natural Product Reports,* 23**,** 753-771.

ZHANG, J.-Y., TAO, L.-Y., LIANG, Y.-J., YAN, Y.-Y., DAI, C.-L., XIA, X.-K., SHE, Z.-G., LIN, Y.-C. & FU, L.-W. 2009a. Secalonic acid D induced leukemia cell apoptosis and cell cycle arrest of G1 with involvement of GSK-3β/β-catenin/c-Myc pathway. *Cell Cycle,* 8**,** 2444-2450.

ZHANG, P., ZHOU, P.-P. & YU, L.-J. 2009b. An endophytic taxol-producing fungus from *Taxus* x *media*, *Aspergillus candidus* MD3. *FEMS Microbiol. Lett.,* 293**,** 155-159.

ZHANG, W., KROHN, K., ZIA, U., FLORKE, U., PESCITELLI, G., DI BARI, L., ANTUS, S., KURTAIN, T., RHEINHEIMER, J., DRAEGER, S. & SCHULZ, B. 2008b. New mono- and dimeric members of the secalonic acid family: blennolides A-G isolated from the fungus *Blennoria* sp. *Chem. - Eur. J.*, 14**,** 4913-4923.

ZHANG, X., CAMBRAI, A., MIESCH, M., ROUSSI, S., RAUL, F., AOUDE-WERNER, D. & MARCHIONI, E. 2006. Separation of Δ5- and Δ7-phytosterols by adsorption chromatography and semipreparative reversed phase high-performance liquid chromatography for quantitative analysis of phytosterols in foods. *J. Agric. Food Chem.,* 54**,** 1196-1202.

ZHAO, K., PING, W., LI, Q., HAO, S., ZHAO, L., GAO, T. & ZHOU, D. 2009. Aspergillus niger var. taxi, a new species variant of taxol-producing fungus isolated from Taxus cuspidata in China. *J. Appl. Microbiol.,* 107**,** 1202-1207.

ZHOU, F., ZHANG, H., LIU, R. & ZHANG, D. 2013. Isolation and biological evaluation of secondary metabolites of the endophytic fungus *Aspergillus fumigatus* from Astragalus membranaceus. *Chem. Nat. Compd.,* 49**,** 568-570.

ZHOU, G.-B., ZHANG, P.-F. & PAN, Y.-J. 2005. A novel method for synthesis of arylacetic acids from aldehydes, N-(2,3,4,6-tetra-O-pivaloylated-d-glucopyranosyl)amine and trimethylsilylcyanide. *Tetrahedron,* 61**,** 5671-5677.

ZHOU, X., WANG, Z., JIANG, K., WEI, Y., LIN, J., SUN, X. & TANG, K. 2007. Screening of taxol-producing endophytic fungi from *Taxus chinensis* var. mairei. *Prikl Biokhim Mikrobiol,* 43**,** 490-4.

Appendices

7. Appendix I: Molecular Biology GenBank Blast Search Results

Aspergillus aculeatus

>Terminalia-yLF1b-PCR=ITS4_A10_2011-02-22 EDIT Reverse Complement

cTTCCGTAGGTGAACCTGCGGAAGGATCATTACCGAGTGCTGGGTCCTTCGGGGCCCAACCTCCCACCCGTGCT
TACCGTACCCTGTTGCTTCGGCGGGCCCGCCTTCGGGCGGCCCGGGGCCTGCCCCCGGGACCGCGCCCGCCGGAGACC
CCAATGGAACACTGTCTGAAAGCGTGCAGTCTGAGTCGATTGATACCAATCAGTCAAAACTTTCAACAATGGATCTCT
TGGTTCCGGCATCGATGAAGAACGCAGCGAAATGCGATAACTAATGTGAATTGCAGAATTCAGTGAATCATCGAGTCT
TTGAACGCACATTGCGCCCCCTGGTATTCCGGGGGGCATGCCTGTCCGAGCGTCATTTCTCCCCTCCAGCCCCGCTGG
TTGTTGGGCCGCGCCCCCCCGGGGGCGGGCCTCGAGAGAAACGGCGGCACCGTCCGGTCCTCGAGCGTATGGGGCTCT
GTCACCCGCTCTATGGGCCCGGCCGGGGCTTGCCTCGACCCCCAATCcTTctCagAt

gb|EU645733.1| Aspergillus aculeatus strain JO6 18S ribosomal RNA gene, partial
sequence; internal transcribed spacer 1, 5.8S ribosomal
RNA gene, and internal transcribed spacer 2, complete sequence;
and 28S ribosomal RNA gene, partial sequence
Length=546

Score = 959 bits (519), Expect = 0.0
Identities = 519/519 (100%), Gaps = 0/519 (0%)
Strand=Plus/Plus

```
Query  2    TTCCGTAGGTGAACCTGCGGAAGGATCATTACCGAGTGCTGGGTCCTTCGGGGCCCAACC  61
            ||||||||||||||||||||||||||||||||||||||||||||||||||||||||||||
Sbjct  27   TTCCGTAGGTGAACCTGCGGAAGGATCATTACCGAGTGCTGGGTCCTTCGGGGCCCAACC  86

Query  62   TCCCACCCGTGCTTACCGTACCCTGTTGCTTCGGCGGGCCCGCCTTCGGGCGGCCCGGGG  121
            ||||||||||||||||||||||||||||||||||||||||||||||||||||||||||||
Sbjct  87   TCCCACCCGTGCTTACCGTACCCTGTTGCTTCGGCGGGCCCGCCTTCGGGCGGCCCGGGG  146

Query  122  CCTGCCCCCGGGACCGCGCCCGCCGGAGACCCCAATGGAACACTGTCTGAAAGCGTGCAG  181
            ||||||||||||||||||||||||||||||||||||||||||||||||||||||||||||
Sbjct  147  CCTGCCCCCGGGACCGCGCCCGCCGGAGACCCCAATGGAACACTGTCTGAAAGCGTGCAG  206

Query  182  TCTGAGTCGATTGATACCAATCAGTCAAAACTTTCAACAATGGATCTCTTGGTTCCGGCA  241
            ||||||||||||||||||||||||||||||||||||||||||||||||||||||||||||
Sbjct  207  TCTGAGTCGATTGATACCAATCAGTCAAAACTTTCAACAATGGATCTCTTGGTTCCGGCA  266

Query  242  TCGATGAAGAACGCAGCGAAATGCGATAACTAATGTGAATTGCAGAATTCAGTGAATCAT  301
            ||||||||||||||||||||||||||||||||||||||||||||||||||||||||||||
Sbjct  267  TCGATGAAGAACGCAGCGAAATGCGATAACTAATGTGAATTGCAGAATTCAGTGAATCAT  326

Query  302  CGAGTCTTTGAACGCACATTGCGCCCCCTGGTATTCCGGGGGGCATGCCTGTCCGAGCGT  361
            ||||||||||||||||||||||||||||||||||||||||||||||||||||||||||||
Sbjct  327  CGAGTCTTTGAACGCACATTGCGCCCCCTGGTATTCCGGGGGGCATGCCTGTCCGAGCGT  386
```

Clustalw alignment & Boxshade

```
gi|194371458|gb|EU645733.1|      1 ATCATTACCGAGTGCTGGGTCCTTCGGGGCCCAACCTCCCACCCGTGCTTACCGTACCCT
Terminalia-yLF1b-PCR=ITS4_A10_   1 ATCATTACCGAGTGCTGGGTCCTTCGGGGCCCAACCTCCCACCCGTGCTTACCGTACCCT

gi|194371458|gb|EU645733.1|     61 GTTGCTTCGGCGGGCCCGCCTTCGGGCGGCCCGGGGCCTGCCCCCGGGACCGCGCCCGCC
Terminalia-yLF1b-PCR=ITS4_A10_  61 GTTGCTTCGGCGGGCCCGCCTTCGGGCGGCCCGGGGCCTGCCCCCGGGACCGCGCCCGCC

gi|194371458|gb|EU645733.1|    121 GGAGACCCCAATGGAACACTGTCTGAAAGCGTGCAGTCTGAGTCGATTGATACCAATCAG
Terminalia-yLF1b-PCR=ITS4_A10_ 121 GGAGACCCCAATGGAACACTGTCTGAAAGCGTGCAGTCTGAGTCGATTGATACCAATCAG

gi|194371458|gb|EU645733.1|    181 TCAAAACTTTCAACAATGGATCTCTTGGTTCCGGCATCGATGAAGAACGCAGCGAAATGC
Terminalia-yLF1b-PCR=ITS4_A10_ 181 TCAAAACTTTCAACAATGGATCTCTTGGTTCCGGCATCGATGAAGAACGCAGCGAAATGC
```

```
gi|194371458|gb|EU645733.1|     241 GATAACTAATGTGAATTGCAGAATTCAGTGAATCATCGAGTCTTTGAACGCACATTGCGC
Terminalia-yLF1b-PCR=ITS4_A10_  241 GATAACTAATGTGAATTGCAGAATTCAGTGAATCATCGAGTCTTTGAACGCACATTGCGC

gi|194371458|gb|EU645733.1|     301 CCCCTGGTATTCCGGGGGGCATGCCTGTCCGAGCGTCATTTCTCCCCTCCAGCCCCGCTG
Terminalia-yLF1b-PCR=ITS4_A10_  301 CCCCTGGTATTCCGGGGGGCATGCCTGTCCGAGCGTCATTTCTCCCCTCCAGCCCCGCTG

gi|194371458|gb|EU645733.1|     361 GTTGTTGGGCCGCGCCCCCCCGGGGGCGGGCCTCGAGAGAAACGGCGGCACCGTCCGGTC
Terminalia-yLF1b-PCR=ITS4_A10_  361 GTTGTTGGGCCGCGCCCCCCCGGGGGCGGGCCTCGAGAGAAACGGCGGCACCGTCCGGTC

gi|194371458|gb|EU645733.1|     421 CTCGAGCGTATGGGGCTCTGTCACCCGCTCTATGGGCCCGGCCGGGGCTTGCCTCGACCC
Terminalia-yLF1b-PCR=ITS4_A10_  421 CTCGAGCGTATGGGGCTCTGTCACCCGCTCTATGGGCCCGGCCGGGGCTTGCCTCGACCC

gi|194371458|gb|EU645733.1|     481 CCAATCTTCTCAGATT
Terminalia-yLF1b-PCR=ITS4_A10_  481 CCAATCTTCTCAGAT-
```

Curvularia sp.

> TL-F2A=ITS1_G12_2011-02-25.Edit

tatGAAGGCTGCACCGCCaACAGGCGGCAAGGCTGGAGTATTTTATTACCCTTGTCTTTTGCGCACTTGTTGTT
TCCTGGGCGGGTTCGCCCGCCTCCAGGACCACATGATAAACCTTTTTTATGCAGTTGCAATCAGCGTCAGTACAACAA
ATGTAAATCATTTACAACTTTCAACAACGGATCTCTTGGTTCTGGCATCGATGAAGAACGCAGCGAAATGCGATACGT
AGTGTGAATTGCAGAATTCAGTGAATCATCGAATCTTTGAACGCACATTGCGCCCTTTGGTATTCCAAAGGGCATGCC
TGTTCGAGCGTCATTTGTACCCTCAAGCTTTGCTTGGTGTTGGGCGTTTTTTGTCTTTGGTTTTGTCCAAAGACTCGC
CTTAAAACGATTGGCAGCCGGCCTACTGGTTTCGCAGCGCAGCACATTTTTGCGCTTGCAATCAGCAAAAGAGGACGG
CACTCCATCAAGACTCTATATCACTTTTGACCTCGGATCAGGTAGGGATACCCGCTGAACTTAAGCATATCAATAAGC
GGAGGaa

>gb|HQ631061.1| Curvularia sp. TMS-2011 voucher SC16d1p11-2 18S ribosomal RNA
gene, partial sequence; internal transcribed spacer 1, 5.8S
ribosomal RNA gene, and internal transcribed spacer 2, complete
sequence; and 28S ribosomal RNA gene, partial sequence
Length=629

 Score = 1014 bits (549), Expect = 0.0
 Identities = 549/549 (100%), Gaps = 0/549 (0%)
 Strand=Plus/Plus

```
Query  1    TATGAAGGCTGCACCGCCAACAGGCGGCAAGGCTGGAGTATTTTATTACCCTTGTCTTTT  60
            ||||||||||||||||||||||||||||||||||||||||||||||||||||||||||||
Sbjct  81   TATGAAGGCTGCACCGCCAACAGGCGGCAAGGCTGGAGTATTTTATTACCCTTGTCTTTT  140

Query  61   GCGCACTTGTTGTTTCCTGGGCGGGTTCGCCCGCCTCCAGGACCACATGATAAACCTTTT  120
            ||||||||||||||||||||||||||||||||||||||||||||||||||||||||||||
Sbjct  141  GCGCACTTGTTGTTTCCTGGGCGGGTTCGCCCGCCTCCAGGACCACATGATAAACCTTTT  200

Query  121  TTATGCAGTTGCAATCAGCGTCAGTACAACAAATGTAAATCATTTACAACTTTCAACAAC  180
            ||||||||||||||||||||||||||||||||||||||||||||||||||||||||||||
Sbjct  201  TTATGCAGTTGCAATCAGCGTCAGTACAACAAATGTAAATCATTTACAACTTTCAACAAC  260

Query  181  GGATCTCTTGGTTCTGGCATCGATGAAGAACGCAGCGAAATGCGATACGTAGTGTGAATT  240
            ||||||||||||||||||||||||||||||||||||||||||||||||||||||||||||
Sbjct  261  GGATCTCTTGGTTCTGGCATCGATGAAGAACGCAGCGAAATGCGATACGTAGTGTGAATT  320

Query  241  GCAGAATTCAGTGAATCATCGAATCTTTGAACGCACATTGCGCCCTTTGGTATTCCAAAG  300
            ||||||||||||||||||||||||||||||||||||||||||||||||||||||||||||
Sbjct  321  GCAGAATTCAGTGAATCATCGAATCTTTGAACGCACATTGCGCCCTTTGGTATTCCAAAG  380

Query  301  GGCATGCCTGTTCGAGCGTCATTTGTACCCTCAAGCTTTGCTTGGTGTTGGGCGTTTTTT  360
            ||||||||||||||||||||||||||||||||||||||||||||||||||||||||||||
Sbjct  381  GGCATGCCTGTTCGAGCGTCATTTGTACCCTCAAGCTTTGCTTGGTGTTGGGCGTTTTTT  440

Query  361  GTCTTTGGTTTTGTCCAAAGACTCGCCTTAAAACGATTGGCAGCCGGCCTACTGGTTTCG  420
            ||||||||||||||||||||||||||||||||||||||||||||||||||||||||||||
Sbjct  441  GTCTTTGGTTTTGTCCAAAGACTCGCCTTAAAACGATTGGCAGCCGGCCTACTGGTTTCG  500
```

```
Query  421  CAGCGCAGCACATTTTTGCGCTTGCAATCAGCAAAAGAGGACGGCACTCCATCAAGACTC  480
            ||||||||||||||||||||||||||||||||||||||||||||||||||||||||||||
Sbjct  501  CAGCGCAGCACATTTTTGCGCTTGCAATCAGCAAAAGAGGACGGCACTCCATCAAGACTC  560

Query  481  TATATCACTTTTGACCTCGGATCAGGTAGGGATACCCGCTGAACTTAAGCATATCAATAA  540
            ||||||||||||||||||||||||||||||||||||||||||||||||||||||||||||
Sbjct  561  TATATCACTTTTGACCTCGGATCAGGTAGGGATACCCGCTGAACTTAAGCATATCAATAA  620

Query  541  GCGGAGGAA  549
            |||||||||
Sbjct  621  GCGGAGGAA  629
```

Clustalw alignment & Boxshade

```
gi|317383382|gb|HQ631061.1|       1 ACCTGCGGAGGGATCATTACACAATAAACATATGAAGGCTGCACCGCCAACAGGCGGCAA
TL-F2A=ITS1_G12_2011-02-25.Edi    1 ------------------------------TATGAAGGCTGCACCGCCAACAGGCGGCAA

gi|317383382|gb|HQ631061.1|      61 GGCTGGAGTATTTTATTACCCTTGTCTTTTGCGCACTTGTTGTTTCCTGGGCGGGTTCGC
TL-F2A=ITS1_G12_2011-02-25.Edi   31 GGCTGGAGTATTTTATTACCCTTGTCTTTTGCGCACTTGTTGTTTCCTGGGCGGGTTCGC

gi|317383382|gb|HQ631061.1|     121 CCGCCTCCAGGACCACATGATAAACCTTTTTTATGCAGTTGCAATCAGCGTCAGTACAAC
TL-F2A=ITS1_G12_2011-02-25.Edi   91 CCGCCTCCAGGACCACATGATAAACCTTTTTTATGCAGTTGCAATCAGCGTCAGTACAAC

gi|317383382|gb|HQ631061.1|     181 AAATGTAAATCATTTACAACTTTCAACAACGGATCTCTTGGTTCTGGCATCGATGAAGAA
TL-F2A=ITS1_G12_2011-02-25.Edi  151 AAATGTAAATCATTTACAACTTTCAACAACGGATCTCTTGGTTCTGGCATCGATGAAGAA

gi|317383382|gb|HQ631061.1|     241 CGCAGCGAAATGCGATACGTAGTGTGAATTGCAGAATTCAGTGAATCATCGAATCTTTGA
TL-F2A=ITS1_G12_2011-02-25.Edi  211 CGCAGCGAAATGCGATACGTAGTGTGAATTGCAGAATTCAGTGAATCATCGAATCTTTGA

gi|317383382|gb|HQ631061.1|     301 ACGCACATTGCGCCCTTTGGTATTCCAAAGGGCATGCCTGTTCGAGCGTCATTTGTACCC
TL-F2A=ITS1_G12_2011-02-25.Edi  271 ACGCACATTGCGCCCTTTGGTATTCCAAAGGGCATGCCTGTTCGAGCGTCATTTGTACCC

gi|317383382|gb|HQ631061.1|     361 TCAAGCTTTGCTTGGTGTTGGGCGTTTTTTGTCTTTGGTTTTGTCCAAAGACTCGCCTTA
TL-F2A=ITS1_G12_2011-02-25.Edi  331 TCAAGCTTTGCTTGGTGTTGGGCGTTTTTTGTCTTTGGTTTTGTCCAAAGACTCGCCTTA

gi|317383382|gb|HQ631061.1|     421 AAACGATTGGCAGCCGGCCTACTGGTTTCGCAGCGCAGCACATTTTTGCGCTTGCAATCA
TL-F2A=ITS1_G12_2011-02-25.Edi  391 AAACGATTGGCAGCCGGCCTACTGGTTTCGCAGCGCAGCACATTTTTGCGCTTGCAATCA

gi|317383382|gb|HQ631061.1|     481 GCAAAAGAGGACGGCACTCCATCAAGACTCTATATCACTTTTGACCTCGGATCAGGTAGG
TL-F2A=ITS1_G12_2011-02-25.Edi  451 GCAAAAGAGGACGGCACTCCATCAAGACTCTATATCACTTTTGACCTCGGATCAGGTAGG

gi|317383382|gb|HQ631061.1|     541 GATACCCGCTGAACTTAAGCATATCAATAAGCGGAGGAA
TL-F2A=ITS1_G12_2011-02-25.Edi  511 GATACCCGCTGAACTTAAGCATATCAATAAGCGGAGGAA
```

Aspergillus oryzae

>DRAC-FROZ_PCR=ITS1_A12_2011-03-03

GGTTCCTAGCGAGCCCAACCTCCCACCCGTGTTTACTGTACCTTAGTTGCTTCGGCGGGCCCGCCATTCATGGC
CGCCGGGGGCTCTCAGCCCCGGGCCCGCGCCCGCCGGAGACACCACGAACTCTGTCTGATCTAGTGAAGTCTGAGTTG
ATTGTATCGCAATCAGTTAAAACTTTCAACAATGGATCTCTTGGTTCCGGCATCGATGAAGAACGCAGCGAAATGCGA
TAACTAGTGTGAATTGCAGAATTCCGTGAATCATCGAGTCTTTGAACGCACATTGCGCCCCCTGGTATTCCGGGGGGC
ATGCCTGTCCGAGCGTCATTGCTGCCCATCAAGCACGGCTTGTGTGTTGGGTCGTCGTCCCCTCTCCGGGGGGGGACGG
GCCCCAAAGGCAGCGGCGGCACCGCGTCCGATCCTCGAGCGTATGGGGCTTTGTCACCCGCTCTGTAGGCCCGGCCGG
CGCTTGCCGAACGCAAATCAATCTTTTTCCAGGTTGACCTCGGATCAGGTAGGGATACCCGCTGAACTTAAgCATATC
AATAagCGGA

> TLF1=ITS1_E12_2011-02-25.ab1 edited

GGGtTCctaGcGAGCCCAACCTCCCACCCGTGTTTACTGTACCTTAGTTGCTTCGGCGGGCCCGCCATTCATGG
CCGCCGGGGGCTCTCAGCCCCGGGCCCGCGCCCGCCGGAGACACCACGAACTCTGTCTGATCTAGTGAAGTCTGAGTT
GATTGTATCGCAATCAGTTAAAACTTTCAACAATGGATCTCTTGGTTCCGGCATCGATGAAGAACGCAGCGAAATGCG
ATAACTAGTGTGAATTGCAGAATTCCGTGAATCATCGAGTCTTTGAACGCACATTGCGCCCCCTGGTATTCCGGGGGG
CATGCCTGTCCGAGCGTCATTGCTGCCCATCAAGCACGGCTTGTGTGTTGGGTCGTCGTCCCCTCTCCGGGGGGGACG

GGCCCCAAAGGCAGCGGCGGCACCGCGTCCGATCCTCGAGCGTATGGGGCTTTGTCACCCGCTCTGTAGGCCCGGCCG
GCGCTTGCCGAACGCAAATCAATCTTTTCCAGGTTGACCTCGGATCAGGTAGGGATACCCGCTGAACTTAAGCATATC
AATAAGCGgAgGAA

> Ter-AL-F2B_PCR=ITS1_E12_2011-03-03.ab1-edited

tGtAGGgTTCCTAGCGAGCCCaaCCTCCCACCCGTGTTTACTGTACCTTAGTTGCTTCGGCGGGCCCGCCATTC
ATGGCCGCCGGGGGCTCTCAGCCCCGGGCCCGCGCCCGCCGGAGACACCACGAACTCTGTCTGATCTAGTGAAGTCTG
AGTTGATTGTATCGCAATCAGTTAAAACTTTCAACAATGGATCTCTTGGTTCCGGCATCGATGAAGAACGCAGCGAAA
TGCGATAACTAGTGTGAATTGCAGAATTCCGTGAATCATCGAGTCTTTGAACGCACATTGCGCCCCCTGGTATTCCGG
GGGGCATGCCTGTCCGAGCGTCATTGCTGCCCATCAAGCACGGCTTGTGTGTTGGGTCGTCGTCCCCTCTCCGGGGGGG
GACGGGCCCCAAAGGCAGCGGCGGCACCGCGTCCGATCCTCGAGCGTATGGGGCTTTGTCACCCGCTCTGTAGGCCCG
GCCGGCGCTTGCCGAACGCAAATCAATCTTTTCCAGGTTGACCTCGGATCAGGTAGGGATACCCGCTGAACTTAAGCA
TATCAATAAGCGGA

>gb|HQ340103.1| Aspergillus flavus culture-collection MUM:10.202 18S ribosomal
RNA gene, partial sequence; internal transcribed spacer 1,
5.8S ribosomal RNA gene, and internal transcribed spacer 2,
complete sequence; and 28S ribosomal RNA gene, partial sequence
Length=912

Score = 1027 bits (556), Expect = 0.0
Identities = 556/556 (100%), Gaps = 0/556 (0%)
Strand=Plus/Plus

```
Query  7    TGTAGGGTTCCTAGCGAGCCCAACCTCCCACCCGTGTTTACTGTACCTTAGTTGCTTCGG  66
            ||||||||||||||||||||||||||||||||||||||||||||||||||||||||||||
Sbjct  160  TGTAGGGTTCCTAGCGAGCCCAACCTCCCACCCGTGTTTACTGTACCTTAGTTGCTTCGG  219

Query  67   CGGGCCCGCCATTCATGGCCGCCGGGGGCTCTCAGCCCCGGGCCCGCGCCCGCCGGAGAC  126
            ||||||||||||||||||||||||||||||||||||||||||||||||||||||||||||
Sbjct  220  CGGGCCCGCCATTCATGGCCGCCGGGGGCTCTCAGCCCCGGGCCCGCGCCCGCCGGAGAC  279

Query  127  ACCACGAACTCTGTCTGATCTAGTGAAGTCTGAGTTGATTGTATCGCAATCAGTTAAAAC  186
            ||||||||||||||||||||||||||||||||||||||||||||||||||||||||||||
Sbjct  280  ACCACGAACTCTGTCTGATCTAGTGAAGTCTGAGTTGATTGTATCGCAATCAGTTAAAAC  339

Query  187  TTTCAACAATGGATCTCTTGGTTCCGGCATCGATGAAGAACGCAGCGAAATGCGATAACT  246
            ||||||||||||||||||||||||||||||||||||||||||||||||||||||||||||
Sbjct  340  TTTCAACAATGGATCTCTTGGTTCCGGCATCGATGAAGAACGCAGCGAAATGCGATAACT  399

Query  247  AGTGTGAATTGCAGAATTCCGTGAATCATCGAGTCTTTGAACGCACATTGCGCCCCCTGG  306
            ||||||||||||||||||||||||||||||||||||||||||||||||||||||||||||
Sbjct  400  AGTGTGAATTGCAGAATTCCGTGAATCATCGAGTCTTTGAACGCACATTGCGCCCCCTGG  459

Query  307  TATTCCGGGGGGCATGCCTGTCCGAGCGTCATTGCTGCCCATCAAGCACGGCTTGTGTGT  366
            ||||||||||||||||||||||||||||||||||||||||||||||||||||||||||||
Sbjct  460  TATTCCGGGGGGCATGCCTGTCCGAGCGTCATTGCTGCCCATCAAGCACGGCTTGTGTGT  519

Query  367  TGGGTCGTCGTCCCCCTCTCCGGGGGGGGACGGGCCCCAAAGGCAGCGGCGGCACCGCGTCC  426
            ||||||||||||||||||||||||||||||||||||||||||||||||||||||||||||
Sbjct  520  TGGGTCGTCGTCCCCCTCTCCGGGGGGGGACGGGCCCCAAAGGCAGCGGCGGCACCGCGTCC  579

Query  427  GATCCTCGAGCGTATGGGGCTTTGTCACCCGCTCTGTAGGCCCGGCCGGCGCTTGCCGAA  486
            ||||||||||||||||||||||||||||||||||||||||||||||||||||||||||||
Sbjct  580  GATCCTCGAGCGTATGGGGCTTTGTCACCCGCTCTGTAGGCCCGGCCGGCGCTTGCCGAA  639

Query  487  CGCAAATCAATCTTTTCCAGGTTGACCTCGGATCAGGTAGGGATACCCGCTGAACTTAAG  546
            ||||||||||||||||||||||||||||||||||||||||||||||||||||||||||||
Sbjct  640  CGCAAATCAATCTTTTCCAGGTTGACCTCGGATCAGGTAGGGATACCCGCTGAACTTAAG  699

Query  547  CATATCAATAAGCGGA  562
            ||||||||||||||||
Sbjct  700  CATATCAATAAGCGGA  715
```

>gb|HQ285588.1| Aspergillus oryzae strain YI-A7 18S ribosomal RNA gene, partial
sequence; internal transcribed spacer 1, 5.8S ribosomal RNA
gene, and internal transcribed spacer 2, complete sequence;

```
and 28S ribosomal RNA gene, partial sequence
Length=597

 Score = 1027 bits (556),  Expect = 0.0
 Identities = 556/556 (100%), Gaps = 0/556 (0%)
 Strand=Plus/Plus

Query  7    TGTAGGGTTCCTAGCGAGCCCAACCTCCCACCCGTGTTTACTGTACCTTAGTTGCTTCGG  66
            ||||||||||||||||||||||||||||||||||||||||||||||||||||||||||||
Sbjct  38   TGTAGGGTTCCTAGCGAGCCCAACCTCCCACCCGTGTTTACTGTACCTTAGTTGCTTCGG  97

Query  67   CGGGCCCGCCATTCATGGCCGCCGGGGGCTCTCAGCCCCGGGCCCGCGCCCGCCGGAGAC  126
            ||||||||||||||||||||||||||||||||||||||||||||||||||||||||||||
Sbjct  98   CGGGCCCGCCATTCATGGCCGCCGGGGGCTCTCAGCCCCGGGCCCGCGCCCGCCGGAGAC  157

Query  127  ACCACGAACTCTGTCTGATCTAGTGAAGTCTGAGTTGATTGTATCGCAATCAGTTAAAAC  186
            ||||||||||||||||||||||||||||||||||||||||||||||||||||||||||||
Sbjct  158  ACCACGAACTCTGTCTGATCTAGTGAAGTCTGAGTTGATTGTATCGCAATCAGTTAAAAC  217

Query  187  TTTCAACAATGGATCTCTTGGTTCCGGCATCGATGAAGAACGCAGCGAAATGCGATAACT  246
            ||||||||||||||||||||||||||||||||||||||||||||||||||||||||||||
Sbjct  218  TTTCAACAATGGATCTCTTGGTTCCGGCATCGATGAAGAACGCAGCGAAATGCGATAACT  277

Query  247  AGTGTGAATTGCAGAATTCCGTGAATCATCGAGTCTTTGAACGCACATTGCGCCCCCTGG  306
            ||||||||||||||||||||||||||||||||||||||||||||||||||||||||||||
Sbjct  278  AGTGTGAATTGCAGAATTCCGTGAATCATCGAGTCTTTGAACGCACATTGCGCCCCCTGG  337

Query  307  TATTCCGGGGGGGCATGCCTGTCCGAGCGTCATTGCTGCCCATCAAGCACGGCTTGTGTGT  366
            ||||||||||||||||||||||||||||||||||||||||||||||||||||||||||||
Sbjct  338  TATTCCGGGGGGGCATGCCTGTCCGAGCGTCATTGCTGCCCATCAAGCACGGCTTGTGTGT  397

Query  367  TGGGTCGTCGTCCCCTCTCCGGGGGGGGACGGGCCCCAAAGGCAGCGGCGGCACCGCGTCC  426
            ||||||||||||||||||||||||||||||||||||||||||||||||||||||||||||
Sbjct  398  TGGGTCGTCGTCCCCTCTCCGGGGGGGGACGGGCCCCAAAGGCAGCGGCGGCACCGCGTCC  457

Query  427  GATCCTCGAGCGTATGGGGCTTTGTCACCCGCTCTGTAGGCCCGGCCGGCGCTTGCCGAA  486
            ||||||||||||||||||||||||||||||||||||||||||||||||||||||||||||
Sbjct  458  GATCCTCGAGCGTATGGGGCTTTGTCACCCGCTCTGTAGGCCCGGCCGGCGCTTGCCGAA  517

Query  487  CGCAAATCAATCTTTTCCAGGTTGACCTCGGATCAGGTAGGGATACCCGCTGAACTTAAG  546
            ||||||||||||||||||||||||||||||||||||||||||||||||||||||||||||
Sbjct  518  CGCAAATCAATCTTTTCCAGGTTGACCTCGGATCAGGTAGGGATACCCGCTGAACTTAAG  577

Query  547  CATATCAATAAGCGGA  562
            ||||||||||||||||
Sbjct  578  CATATCAATAAGCGGA  593
```

Boxshade

```
DRAC-FROZ_PCR=ITS1_A12_2011-03     1 -----GGTTCCTAGCGAGCCCAACCTCCCACCCGTGTTTACTGTACCTTAGTTGCTTCGG
TLF1=ITS1_E12_2011-02-25.ab1       1 ----GGGTTCCTAGCGAGCCCAACCTCCCACCCGTGTTTACTGTACCTTAGTTGCTTCGG
Ter-AL-F2B_PCR=ITS1_E12_2011-0     1 TGTAGGGTTCCTAGCGAGCCCAACCTCCCACCCGTGTTTACTGTACCTTAGTTGCTTCGG


DRAC-FROZ_PCR=ITS1_A12_2011-03    56 CGGGCCCGCCATTCATGGCCGCCGGGGGCTCTCAGCCCCGGGCCCGCGCCCGCCGGAGAC
TLF1=ITS1_E12_2011-02-25.ab1      57 CGGGCCCGCCATTCATGGCCGCCGGGGGCTCTCAGCCCCGGGCCCGCGCCCGCCGGAGAC
Ter-AL-F2B_PCR=ITS1_E12_2011-0    61 CGGGCCCGCCATTCATGGCCGCCGGGGGCTCTCAGCCCCGGGCCCGCGCCCGCCGGAGAC


DRAC-FROZ_PCR=ITS1_A12_2011-03   116 ACCACGAACTCTGTCTGATCTAGTGAAGTCTGAGTTGATTGTATCGCAATCAGTTAAAAC
TLF1=ITS1_E12_2011-02-25.ab1     117 ACCACGAACTCTGTCTGATCTAGTGAAGTCTGAGTTGATTGTATCGCAATCAGTTAAAAC
Ter-AL-F2B_PCR=ITS1_E12_2011-0   121 ACCACGAACTCTGTCTGATCTAGTGAAGTCTGAGTTGATTGTATCGCAATCAGTTAAAAC


DRAC-FROZ_PCR=ITS1_A12_2011-03   176 TTTCAACAATGGATCTCTTGGTTCCGGCATCGATGAAGAACGCAGCGAAATGCGATAACT
TLF1=ITS1_E12_2011-02-25.ab1     177 TTTCAACAATGGATCTCTTGGTTCCGGCATCGATGAAGAACGCAGCGAAATGCGATAACT
Ter-AL-F2B_PCR=ITS1_E12_2011-0   181 TTTCAACAATGGATCTCTTGGTTCCGGCATCGATGAAGAACGCAGCGAAATGCGATAACT


DRAC-FROZ_PCR=ITS1_A12_2011-03   236 AGTGTGAATTGCAGAATTCCGTGAATCATCGAGTCTTTGAACGCACATTGCGCCCCCTGG
TLF1=ITS1_E12_2011-02-25.ab1     237 AGTGTGAATTGCAGAATTCCGTGAATCATCGAGTCTTTGAACGCACATTGCGCCCCCTGG
Ter-AL-F2B_PCR=ITS1_E12_2011-0   241 AGTGTGAATTGCAGAATTCCGTGAATCATCGAGTCTTTGAACGCACATTGCGCCCCCTGG


DRAC-FROZ_PCR=ITS1_A12_2011-03   296 TATTCCGGGGGGGCATGCCTGTCCGAGCGTCATTGCTGCCCATCAAGCACGGCTTGTGTGT
TLF1=ITS1_E12_2011-02-25.ab1     297 TATTCCGGGGGGGCATGCCTGTCCGAGCGTCATTGCTGCCCATCAAGCACGGCTTGTGTGT
Ter-AL-F2B_PCR=ITS1_E12_2011-0   301 TATTCCGGGGGGGCATGCCTGTCCGAGCGTCATTGCTGCCCATCAAGCACGGCTTGTGTGT
```

```
DRAC-FROZ_PCR=ITS1_A12_2011-03  356 TGGGTCGTCGTCCCCTCTCCGGGGGGGACGGGCCCCAAAGGCAGCGGCGGCACCGCGTCC
TLF1=ITS1_E12_2011-02-25.ab1    357 TGGGTCGTCGTCCCCTCTCCGGGGGGGACGGGCCCCAAAGGCAGCGGCGGCACCGCGTCC
Ter-AL-F2B_PCR=ITS1_E12_2011-0  361 TGGGTCGTCGTCCCCTCTCCGGGGGGGACGGGCCCCAAAGGCAGCGGCGGCACCGCGTCC


DRAC-FROZ_PCR=ITS1_A12_2011-03  416 GATCCTCGAGCGTATGGGGCTTTGTCACCCGCTCTGTAGGCCCGGCCGGCGCTTGCCGAA
TLF1=ITS1_E12_2011-02-25.ab1    417 GATCCTCGAGCGTATGGGGCTTTGTCACCCGCTCTGTAGGCCCGGCCGGCGCTTGCCGAA
Ter-AL-F2B_PCR=ITS1_E12_2011-0  421 GATCCTCGAGCGTATGGGGCTTTGTCACCCGCTCTGTAGGCCCGGCCGGCGCTTGCCGAA


DRAC-FROZ_PCR=ITS1_A12_2011-03  476 CGCAAATCAATCTTTTTCCAGGTTGACCTCGGATCAGGTAGGGATACCCGCTGAACTTAA
TLF1=ITS1_E12_2011-02-25.ab1    477 CGCAAATCAATCTTTT-CCAGGTTGACCTCGGATCAGGTAGGGATACCCGCTGAACTTAA
Ter-AL-F2B_PCR=ITS1_E12_2011-0  481 CGCAAATCAATCTTTT-CCAGGTTGACCTCGGATCAGGTAGGGATACCCGCTGAACTTAA


DRAC-FROZ_PCR=ITS1_A12_2011-03  536 GCATATCAATAAGCGGA----
TLF1=ITS1_E12_2011-02-25.ab1    536 GCATATCAATAAGCGGAGGAA
Ter-AL-F2B_PCR=ITS1_E12_2011-0  540 GCATATCAATAAGCGGA----
```

>DF-BT2=BT2A

GGAACTCCTCAAAAGCATGATCTCGGATGTGTCCtGTTATATCTGCCACATGTTTGCTAACAACTTTGCAGGCA
AACCATCTCTGGCGAGCACGGCCTTGACGGCTCCGGTGTGTAAGTACAGCCTGTATACACCTCGAACGAACGACGACC
ATATGGCATTAGAAGTTGGAATGGATCTGACGGCAAGGATAGTTACAATGGCTCCTCCGATCTCCAGCTGGAGCGTAT
GAACGTCTACTTCAACGAGGTGCGTACCTCAAAATTTCAGCATCTATGAAAACGCTTTGCAACTCCTGACCGCTTCTC
CAGGCCAGCGGAAACAAGTATGTCCCTCGTGCCGTCCTCGTTGATCTTGAGCCTGGTACCATGGACGCCGTCCGTGCC
GGTCCCTTCGGTCAGCTCTTCCGTCCCGACAACTTCGTTTTCGGCCAGTCCGGTGCTGGTAACAACTGGGCCAAGGg

>TF1-BT2=BT2A

tatgcTTTGgAccaagGAACTCCTCAAAAGCATGATCTCGGATGTGTCCTGTTATATCTGCCACATGTTTGCTA
ACAACTTTGCAGGCAAACCATCTCTGGCGAGCACGGCCTTGACGGCTCCGGTGTGTAAGTACAGCCTGTATACACCTC
GAACGAACGACGACCATATGGCATTAGAAGTTGGAATGGATCTGACGGCAAGGATAGTTACAATGGCTCCTCCGATCT
CCAGCTGGAGCGTATGAACGTCTACTTCAACGAGGTGCGTACCTCAAAATTTCAGCATCTATGAAAACGCTTTGCAAC
TCCTGACCGCTTCTCCAGGCCAGCGGAAACAAGTATGTCCCTCGTGCCGTCCTCGTTGATCTTGAGCCTGGTACCATG
GACGCCGTCCGTGCCGGTCCCTTCGGTCAGCTCTTCCGTCCCGACAACTTCGTTTTCGGCCAGTCCGGTGCTGGTAAC
AACTGGGCCAAGGG

>TF2B-BT2=BT2A

gCTttgGAcCaaGGAACTCCTCAAAAGCATGATCTCGGATGTGTCCTGTTATATCTGCCACATGTTTGCTAACA
ACTTTGCAGGCAAACCATCTCTGGCGAGCACGGCCTTGACGGCTCCGGTGTGTAAGTACAGCCTGTATACACCTCGAA
CGAACGACGACCATATGGCATTAGAAGTTGGAATGGATCTGACGGCAAGGATAGTTACAATGGCTCCTCCGATCTCCA
GCTGGAGCGTATGAACGTCTACTTCAACGAGGTGCGTACCTCAAAATTTCAGCATCTATGAAAACGCTTTGCAACTCC
TGACCGCTTCTCCAGGCCAGCGGAAACAAGTATGTCCCTCGTGCCGTCCTCGTTGATCTTGAGCCTGGTACCATGGAC
GCCGTCCGTGCCGGTCCCTTCGGTCAGCTCTTCCGTCCCGACAACTTCGTTTTCGGCCAGTCCGGTGCTGGTAACAAC
TGGGCCAAGGGTCACTACACTGAGgg

Boxshade

http://www.ch.embnet.org/software/BOX_form.htmL

```
DF-BT2=BT2A       1 ----------------GGAACTCCTCAAAAGCATGATCTCGGATGTGTCCTGTTATATCTG
TF1-BT2=BT2A      1 TATGCTTTGGACCAAGGAACTCCTCAAAAGCATGATCTCGGATGTGTCCTGTTATATCTG
TF2B-BT2=BT2A     1 ---GCTTTGGACCAAGGAACTCCTCAAAAGCATGATCTCGGATGTGTCCTGTTATATCTG


DF-BT2=BT2A      46 CCACATGTTTGCTAACAACTTTGCAGGCAAACCATCTCTGGCGAGCACGGCCTTGACGGC
TF1-BT2=BT2A     61 CCACATGTTTGCTAACAACTTTGCAGGCAAACCATCTCTGGCGAGCACGGCCTTGACGGC
TF2B-BT2=BT2A    58 CCACATGTTTGCTAACAACTTTGCAGGCAAACCATCTCTGGCGAGCACGGCCTTGACGGC


DF-BT2=BT2A     106 TCCGGTGTGTAAGTACAGCCTGTATACACCTCGAACGAACGACGACCATATGGCATTAGA
TF1-BT2=BT2A    121 TCCGGTGTGTAAGTACAGCCTGTATACACCTCGAACGAACGACGACCATATGGCATTAGA
TF2B-BT2=BT2A   118 TCCGGTGTGTAAGTACAGCCTGTATACACCTCGAACGAACGACGACCATATGGCATTAGA


DF-BT2=BT2A     166 AGTTGGAATGGATCTGACGGCAAGGATAGTTACAATGGCTCCTCCGATCTCCAGCTGGAG
TF1-BT2=BT2A    181 AGTTGGAATGGATCTGACGGCAAGGATAGTTACAATGGCTCCTCCGATCTCCAGCTGGAG
TF2B-BT2=BT2A   178 AGTTGGAATGGATCTGACGGCAAGGATAGTTACAATGGCTCCTCCGATCTCCAGCTGGAG


DF-BT2=BT2A     226 CGTATGAACGTCTACTTCAACGAGGTGCGTACCTCAAAATTTCAGCATCTATGAAAACGC
TF1-BT2=BT2A    241 CGTATGAACGTCTACTTCAACGAGGTGCGTACCTCAAAATTTCAGCATCTATGAAAACGC
TF2B-BT2=BT2A   238 CGTATGAACGTCTACTTCAACGAGGTGCGTACCTCAAAATTTCAGCATCTATGAAAACGC


DF-BT2=BT2A     286 TTTGCAACTCCTGACCGCTTCTCCAGGCCAGCGGAAACAAGTATGTCCCTCGTGCCGTCC
```

```
TF1-BT2=BT2A   301 TTTGCAACTCCTGACCGCTTCTCCAGGCCAGCGGAAACAAGTATGTCCCTCGTGCCGTCC
TF2B-BT2=BT2A  298 TTTGCAACTCCTGACCGCTTCTCCAGGCCAGCGGAAACAAGTATGTCCCTCGTGCCGTCC

DF-BT2=BT2A    346 TCGTTGATCTTGAGCCTGGTACCATGGACGCCGTCCGTGCCGGTCCCTTCGGTCAGCTCT
TF1-BT2=BT2A   361 TCGTTGATCTTGAGCCTGGTACCATGGACGCCGTCCGTGCCGGTCCCTTCGGTCAGCTCT
TF2B-BT2=BT2A  358 TCGTTGATCTTGAGCCTGGTACCATGGACGCCGTCCGTGCCGGTCCCTTCGGTCAGCTCT

DF-BT2=BT2A    406 TCCGTCCCGACAACTTCGTTTTCGGCCAGTCCGGTGCTGGTAACAACTGGGCCAAGGG--
TF1-BT2=BT2A   421 TCCGTCCCGACAACTTCGTTTTCGGCCAGTCCGGTGCTGGTAACAACTGGGCCAAGGG--
TF2B-BT2=BT2A  418 TCCGTCCCGACAACTTCGTTTTCGGCCAGTCCGGTGCTGGTAACAACTGGGCCAAGGGTC

DF-BT2=BT2A        -------------
TF1-BT2=BT2A       -------------
TF2B-BT2=BT2A  478 ACTACACTGAGGG
```

Clustalw Alignment of *A. flavus and A. oryzae* PCR products

>A.Flavus_Tubulin_430bp_PCR_product

GCCATCTTTCCTCCTTCTCTCTTCTCCTCTTCCTTTTACCTACTCCCCGTCGACTGTCTCCCCCAGTCTATCCA
ACAACCCTTCTCCAACGACCTCTTCGCCGTTTTCAAACCCACCTTTTCCTACCAACAACGCCAAAATCCCCTCCACAA
TGCGTGAGATCGTATGTTGCTCCCTACCCCCGGTGGGGGGAGAAGTCTGCTCAAAAAGCCCTATCCCCCCCCCCCTGAT
AGGGACCCCACCCGTTCTCCAATACTACAAGGTTGCTGACGGAGTTTGTTTCATCATATAGGTTCACCTTCAGACCGG
CCAGTGTGTAAGTTCGACTATGATTTGATGTCTAGCAGGACCATGGCGACGGATACTAAACGTATGTTGGTGATAGGG
TAACCAAATAGGTGCCGCTTTCTGGTATGTCTCAATGCCTTCGA

>A.Oryzae_Tubulin_431bp_PCR_product

GCCATCTTTCCTCCTTCTCTCTTCTCCTCTTCCTTTTACCTACTCCCCGTCGACTGTCTCCCCCAGTCTATCCA
ACAACCCTTCTCCAACGACCTCTTCGCCGTTTTCAAACCCACCTTTTCCTACCAACAACGCCAATATCCCCTCCACAA
TGCGTGAGATCGTATGTTGCTCCCTACCCCCGGTCCCCCCTCTTCAGACGCGTTTTTCGGGGATACCCCCCCCCCTGA
TAGGGACCCCACCCGTTCTCCAATACTACAAGGTTGCTGACGGAGTTTGTTTCATCATATAGGTTCACCTTCAGACCG
GCCAGTGTGTAAGTTCGACTACGATTTGACGTCTAGCAGGACCATGGCGACGGATACTAAACGTATGTTGGTGATAGG
GTAACCAAATAGGTGCCGCTTTCTGGTATGTCTCAATGCCTTCGA

```
A.Flavus_Tubulin_430bp_PCR_pro    1 GCCATCTTTCCTCCTTCTCTCTTCTCCTCTTCCTTTTACCTACTCCCCGTCGACTGTCTC
A.Oryzae_Tubulin_431bp_PCR_pro    1 GCCATCTTTCCTCCTTCTCTCTTCTCCTCTTCCTTTTACCTACTCCCCGTCGACTGTCTC

A.Flavus_Tubulin_430bp_PCR_pro   61 CCCCAGTCTATCCAACAACCCTTCTCCAACGACCTCTTCGCCGTTTTCAAACCCACCTTT
A.Oryzae_Tubulin_431bp_PCR_pro   61 CCCCAGTCTATCCAACAACCCTTCTCCAACGACCTCTTCGCCGTTTTCAAACCCACCTTT

A.Flavus_Tubulin_430bp_PCR_pro  121 TCCTACCAACAACGCCAAAATCCCCTCCACAATGCGTGAGATCGTATGTTGCTCCCTACC
A.Oryzae_Tubulin_431bp_PCR_pro  121 TCCTACCAACAACGCCAAATATCCCCTCCACAATGCGTGAGATCGTATGTTGCTCCCTACC

A.Flavus_Tubulin_430bp_PCR_pro  181 CCCGGTGGGG-------GGAGAAGTCTGCTCAAAAAGCCCTATCCCCCCCCCCTGATAGG
A.Oryzae_Tubulin_431bp_PCR_pro  181 CCGGGTCCCCCCTCTTCAGACGCGTTT-TTCGGGGA----TA-CCCCCCCCCTGATAGG

A.Flavus_Tubulin_430bp_PCR_pro  234 GACCCCACCCGTTCTCCAATACTACAAGGTTGCTGACGGAGTTTGTTTCATCATATAGGT
A.Oryzae_Tubulin_431bp_PCR_pro  235 GACCCCACCCGTTCTCCAATACTACAAGGTTGCTGACGGAGTTTGTTTCATCATATAGGT

A.Flavus_Tubulin_430bp_PCR_pro  294 TCACCTTCAGACCGGCCAGTGTGTAAGTTCGACTATGATTTGATGTCTAGCAGGACCATG
A.Oryzae_Tubulin_431bp_PCR_pro  295 TCACCTTCAGACCGGCCAGTGTGTAAGTTCGACTACGATTTGACGTCTAGCAGGACCATG

A.Flavus_Tubulin_430bp_PCR_pro  354 GCGACGGATACTAAACGTATGTTGGTGATAGGGTAACCAAATAGGTGCCGCTTTCTGGTA
A.Oryzae_Tubulin_431bp_PCR_pro  355 GCGACGGATACTAAACGTATGTTGGTGATAGGGTAACCAAATAGGTGCCGCTTTCTGGTA

A.Flavus_Tubulin_430bp_PCR_pro  414 TGTCTCAATGCCTTCGA
A.Oryzae_Tubulin_431bp_PCR_pro  415 TGTCTCAATGCCTTCGA
```

Using specifically designed AT1 primers

>DF-AT1=AT1FOR_A01_2011-03-31 - EDIT
GtcTCCCCCaGTCTATCcaAcaACCCTTCTCCAACGACCTCTTCGCCGTT
TTCAAACCCACCTTTTCCTACCAACAACGCCAATATCCCCTCCACAATGC
GTGAGATCGTATGTTGCTCcCTACccccGGTCccccCTCTTCAGACGCGT
ttttCGgggATAccCcccCccc

BLAST results

ref|NW_001884677.1| Aspergillus oryzae RIB40 contig SC038
dbj|AP007169.1| Aspergillus oryzae RIB40 DNA, SC038
Length=1725576

Features in this part of subject sequence:
tubulin alpha-1 chain

Score = 318 bits (172), Expect = 6e-84
Identities = 172/172 (100%), Gaps = 0/172 (0%)
Strand=Plus/Minus

```
Query  1       GTCTCCCCCAGTCTATCCAACAACCCTTCTCCAACGACCTCTTCGCCGTTTTCAAACCCA  60
               ||||||||||||||||||||||||||||||||||||||||||||||||||||||||||||
Sbjct  832392  GTCTCCCCCAGTCTATCCAACAACCCTTCTCCAACGACCTCTTCGCCGTTTTCAAACCCA  832333

Query  61      CCTTTTCCTACCAACAACGCCAATATCCCCTCCACAATGCGTGAGATCGTATGTTGCTCC  120
               ||||||||||||||||||||||||||||||||||||||||||||||||||||||||||||
Sbjct  832332  CCTTTTCCTACCAACAACGCCAATATCCCCTCCACAATGCGTGAGATCGTATGTTGCTCC  832273

Query  121     CTACCCCCGGTCCCCCCTCTTCAGACGCGTTTTTCGGGGATACCCCCCCCCC  172
               ||||||||||||||||||||||||||||||||||||||||||||||||||||
Sbjct  832272  CTACCCCCGGTCCCCCCTCTTCAGACGCGTTTTTCGGGGATACCCCCCCCCC  832221
```

>gb|L49386.1|ASNBT Aspergillus parasiticus beta-tubulin gene, exons 1-8, complete
cds
Length=2076

Score = 276 bits (149), Expect = 3e-71
Identities = 164/171 (96%), Gaps = 2/171 (1%)
Strand=Plus/Plus

```
Query  1    GTCTCCCCCAGTCTATCCAACAACCCTTCTCCAACGACCTCTTCGCCGTTTTCAAACCCA  60
            |||||| |||||||||||||||| |||||||||||||||||| ||||||||||||
Sbjct  6    GTCTCCTCCAGTCTATCCAACAACCCCTCTCCAACGACCTCTTCGCCTTTTTCAAACCCA  65

Query  61   CCTTTTCCTACCAACAACGCCAATATCCCCTCCACAATGCGTGAGATCGTATGTTGCTCC  120
            ||||||||||||||||||||||| |||||||||||||||||||||||||||||||||||
Sbjct  66   CCTTTTCCTACCAACAACGCCAATATTCCCTCCACAATGCGTGAGATCGTATGTTGCTCC  125

Query  121  CTACCCCC--GGTCCCCCCTCTTCAGACGCGTTTTTCGGGGATACCCCCCC  169
            ||||||||  |||||||||||||||||| ||||||||||||||||||||
Sbjct  126  CTACCCCCCCGGTCCCCCCTCTTCAGACGAGTTTTTCGGGGATACCCCCCC  176
```

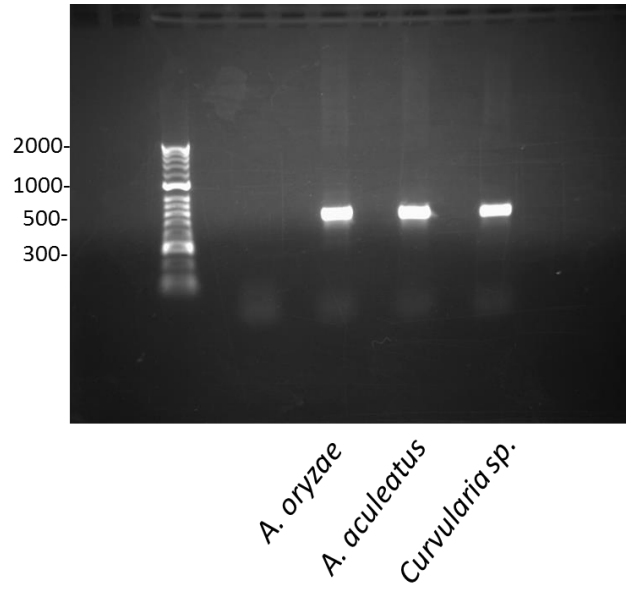

Fig.221 DNA image for A. oryzae, A. aculeatus and Curvularia sp.

Aspergillus flocculus or A. ochraceopetaliformis

>MF1 ITS4 Reverse complement

gGCGGgccCGCCGTTCGCGCGGCCGCCGGGGGGGAACCCCTCCCCCCGGGCGAGCGCCCGCCGGAGACCCCAAC
GTGAACACTGTCTGAAGTTTTGTCGTCTGAGTTCGATTGTATCGCAATCAGTTAAAACTTTCAACAATGGATCTCTTG
GTTCCGGCATCGATGAAGAACGCAGCGAAATGCGATAATTAATGTGAATTGCAGAATTCAGTGAATCATCGAGTCTTT
GAACGCACATTGCACCCCCTGGTATTCCGGGGGGTATGCCTGTCCGAGCGTCATTGCTGCCCTCAAGCCCGGCTTGTG
TGTTGGGTCCTCGTCCCCCCCGGGGGACGGGCCCGAAAGGCAGCGGCGGCACCGCGTCC

>gb|FJ491571.1| Aspergillus flocculosus strain CBS 112784 internal
transcribed
spacer 1, partial sequence; 5.8S ribosomal RNA gene, complete
sequence; and internal transcribed spacer 2, partial sequence
Length=497

 Score = 678 bits (367), Expect = 0.0
 Identities = 367/367 (100%), Gaps = 0/367 (0%)
 Strand=Plus/Plus

```
Query  1    GGCGGGCCCGCCGTTCGCGCGGCCGCCGGGGGGGAACCCCTCCCCCCGGGCGAGCGCCCG  60
            ||||||||||||||||||||||||||||||||||||||||||||||||||||||||||||
Sbjct  35   GGCGGGCCCGCCGTTCGCGCGGCCGCCGGGGGGGAACCCCTCCCCCCGGGCGAGCGCCCG  94

Query  61   CCGGAGACCCCAACGTGAACACTGTCTGAAGTTTTGTCGTCTGAGTTCGATTGTATCGCA  120
            ||||||||||||||||||||||||||||||||||||||||||||||||||||||||||||
Sbjct  95   CCGGAGACCCCAACGTGAACACTGTCTGAAGTTTTGTCGTCTGAGTTCGATTGTATCGCA  154

Query  121  ATCAGTTAAAACTTTCAACAATGGATCTCTTGGTTCCGGCATCGATGAAGAACGCAGCGA  180
            ||||||||||||||||||||||||||||||||||||||||||||||||||||||||||||
Sbjct  155  ATCAGTTAAAACTTTCAACAATGGATCTCTTGGTTCCGGCATCGATGAAGAACGCAGCGA  214

Query  181  AATGCGATAATTAATGTGAATTGCAGAATTCAGTGAATCATCGAGTCTTTGAACGCACAT  240
            ||||||||||||||||||||||||||||||||||||||||||||||||||||||||||||
Sbjct  215  AATGCGATAATTAATGTGAATTGCAGAATTCAGTGAATCATCGAGTCTTTGAACGCACAT  274
```

```
Query  241  TGCACCCCCTGGTATTCCGGGGGGTATGCCTGTCCGAGCGTCATTGCTGCCCTCAAGCCC  300
            ||||||||||||||||||||||||||||||||||||||||||||||||||||||||||||
Sbjct  275  TGCACCCCCTGGTATTCCGGGGGGTATGCCTGTCCGAGCGTCATTGCTGCCCTCAAGCCC  334

Query  301  GGCTTGTGTGTTGGGTCCTCGTCCCCCCCGGGGGACGGGCCCGAAAGGCAGCGGCGGCAC  360
            ||||||||||||||||||||||||||||||||||||||||||||||||||||||||||||
Sbjct  335  GGCTTGTGTGTTGGGTCCTCGTCCCCCCCGGGGGACGGGCCCGAAAGGCAGCGGCGGCAC  394

Query  361  CGCGTCC  367
            |||||||
Sbjct  395  CGCGTCC  401


>gb|FJ571434.1|  Aspergillus sp. OY10607 18S ribosomal RNA gene, partial
sequence;
internal transcribed spacer 1, 5.8S ribosomal RNA gene,
and internal transcribed spacer 2, complete sequence; and 28S
ribosomal RNA gene, partial sequence
Length=568

 Score =  678 bits (367),  Expect = 0.0
 Identities = 367/367 (100%), Gaps = 0/367 (0%)
 Strand=Plus/Plus

Query  1    GGCGGGCCCGCCGTTCGCGCGGCCGCCGGGGGGGAACCCCTCCCCCCGGGCGAGCGCCCG  60
            ||||||||||||||||||||||||||||||||||||||||||||||||||||||||||||
Sbjct  65   GGCGGGCCCGCCGTTCGCGCGGCCGCCGGGGGGGAACCCCTCCCCCCGGGCGAGCGCCCG  124

Query  61   CCGGAGACCCCAACGTGAACACTGTCTGAAGTTTTGTCGTCTGAGTTCGATTGTATCGCA  120
            ||||||||||||||||||||||||||||||||||||||||||||||||||||||||||||
Sbjct  125  CCGGAGACCCCAACGTGAACACTGTCTGAAGTTTTGTCGTCTGAGTTCGATTGTATCGCA  184

Query  121  ATCAGTTAAAACTTTCAACAATGGATCTCTTGGTTCCGGCATCGATGAAGAACGCAGCGA  180
            ||||||||||||||||||||||||||||||||||||||||||||||||||||||||||||
Sbjct  185  ATCAGTTAAAACTTTCAACAATGGATCTCTTGGTTCCGGCATCGATGAAGAACGCAGCGA  244

Query  181  AATGCGATAATTAATGTGAATTGCAGAATTCAGTGAATCATCGAGTCTTTGAACGCACAT  240
            ||||||||||||||||||||||||||||||||||||||||||||||||||||||||||||
Sbjct  245  AATGCGATAATTAATGTGAATTGCAGAATTCAGTGAATCATCGAGTCTTTGAACGCACAT  304

Query  241  TGCACCCCCTGGTATTCCGGGGGGTATGCCTGTCCGAGCGTCATTGCTGCCCTCAAGCCC  300
            ||||||||||||||||||||||||||||||||||||||||||||||||||||||||||||
Sbjct  305  TGCACCCCCTGGTATTCCGGGGGGTATGCCTGTCCGAGCGTCATTGCTGCCCTCAAGCCC  364

Query  301  GGCTTGTGTGTTGGGTCCTCGTCCCCCCCGGGGGACGGGCCCGAAAGGCAGCGGCGGCAC  360
            ||||||||||||||||||||||||||||||||||||||||||||||||||||||||||||
Sbjct  365  GGCTTGTGTGTTGGGTCCTCGTCCCCCCCGGGGGACGGGCCCGAAAGGCAGCGGCGGCAC  424

Query  361  CGCGTCC  367
            |||||||
Sbjct  425  CGCGTCC  431


>gb|EF661432.1|  Aspergillus ochraceopetaliformis isolate NRRL 35668 internal
transcribed spacer 1, 5.8S ribosomal RNA gene, and internal
transcribed spacer 2, complete sequence; and 28S ribosomal RNA
gene, partial sequence
Length=1151

 Score =  678 bits (367),  Expect = 0.0
 Identities = 367/367 (100%), Gaps = 0/367 (0%)
 Strand=Plus/Plus

Query  1    GGCGGGCCCGCCGTTCGCGCGGCCGCCGGGGGGGAACCCCTCCCCCCGGGCGAGCGCCCG  60
            ||||||||||||||||||||||||||||||||||||||||||||||||||||||||||||
Sbjct  61   GGCGGGCCCGCCGTTCGCGCGGCCGCCGGGGGGGAACCCCTCCCCCCGGGCGAGCGCCCG  120

Query  61   CCGGAGACCCCAACGTGAACACTGTCTGAAGTTTTGTCGTCTGAGTTCGATTGTATCGCA  120
            ||||||||||||||||||||||||||||||||||||||||||||||||||||||||||||
Sbjct  121  CCGGAGACCCCAACGTGAACACTGTCTGAAGTTTTGTCGTCTGAGTTCGATTGTATCGCA  180

Query  121  ATCAGTTAAAACTTTCAACAATGGATCTCTTGGTTCCGGCATCGATGAAGAACGCAGCGA  180
            ||||||||||||||||||||||||||||||||||||||||||||||||||||||||||||
```

```
Sbjct  181  ATCAGTTAAAACTTTCAACAATGGATCTCTTGGTTCCGGCATCGATGAAGAACGCAGCGA  240

Query  181  AATGCGATAATTAATGTGAATTGCAGAATTCAGTGAATCATCGAGTCTTTGAACGCACAT  240
            ||||||||||||||||||||||||||||||||||||||||||||||||||||||||||||
Sbjct  241  AATGCGATAATTAATGTGAATTGCAGAATTCAGTGAATCATCGAGTCTTTGAACGCACAT  300

Query  241  TGCACCCCCTGGTATTCCGGGGGGTATGCCTGTCCGAGCGTCATTGCTGCCCTCAAGCCC  300
            ||||||||||||||||||||||||||||||||||||||||||||||||||||||||||||
Sbjct  301  TGCACCCCCTGGTATTCCGGGGGGTATGCCTGTCCGAGCGTCATTGCTGCCCTCAAGCCC  360

Query  301  GGCTTGTGTGTTGGGTCCTCGTCCCCCCCGGGGGACGGGCCCGAAAGGCAGCGGCGGCAC  360
            ||||||||||||||||||||||||||||||||||||||||||||||||||||||||||||
Sbjct  361  GGCTTGTGTGTTGGGTCCTCGTCCCCCCCGGGGGACGGGCCCGAAAGGCAGCGGCGGCAC  420

Query  361  CGCGTCC  367
            |||||||
Sbjct  421  CGCGTCC  427
```

Clustalw alignment & Boxshade

```
gi|256259281|gb|FJ491582.1|    1 GCGCGGCCGCCGGGGGGGAACCCTCCCCCCGGGCGAGCGCCCGCCGGAGACCCCAACGT
MF1                            1 GCGCGGCCGCCGGGGGGGAACCCTCCCCCCGGGCGAGCGCCCGCCGGAGACCCCAACGT

gi|256259281|gb|FJ491582.1|   61 GAACACTGTCTGAAGTTTTGTCGTCTGAGTTCGATTGTATCGCAATCAGTTAAAACTTTC
MF1                           61 GAACACTGTCTGAAGTTTTGTCGTCTGAGTTCGATTGTATCGCAATCAGTTAAAACTTTC

gi|256259281|gb|FJ491582.1|  121 AACAATGGATCTCTTGGTTCCGGCATCGATGAAGAACGCAGCGAAATGCGATAATTAATG
MF1                          121 AACAATGGATCTCTTGGTTCCGGCATCGATGAAGAACGCAGCGAAATGCGATAATTAATG

gi|256259281|gb|FJ491582.1|  181 TGAATTGCAGAATTCAGTGAATCATCGAGTCTTTGAACGCACATTGCACCCCCTGGTATT
MF1                          181 TGAATTGCAGAATTCAGTGAATCATCGAGTCTTTGAACGCACATTGCACCCCCTGGTATT

gi|256259281|gb|FJ491582.1|  241 CCGGGGGGTATGCCTGTCCGAGCGTCATTGCTGCCCTCAAGCCCGGCTTGTGTGTTGGGT
MF1                          241 CCGGGGGGTATGCCTGTCCGAGCGTCATTGCTGCCCTCAAGCCCGGCTTGTGTGTTGGGT

gi|256259281|gb|FJ491582.1|  301 CCTCGTCCCCCCCGGGGGACGGGCCCGAAAGGCAGCGGCGGCACCGCGTCCGGTCCTCGA
MF1                          301 CCTCGTCCCCCCCGGGGGACGGGCCCGAAAGGCAGCGGCGGCACCGCGTCC---------

gi|256259281|gb|FJ491582.1|  361 GCGTATGGGGCTTTGTCACACCGCTCTCGTAGGCCCGGCCGGCGCTGGCCGACGCTGAAA
MF1                              ------------------------------------------------------------

gi|256259281|gb|FJ491582.1|  421 AGCAACCATTATTCTCCAGGTGACCTC
MF1                              ---------------------------
```

Syncephalastrum racemosum

>AT-1-MF3A-ITS=ITS1_E09_2011-05-19_copy

TCTCTCaaTTCTCATTCATTTGGGGATTGAGGGGAAAGAATTGGAATTCACCCAGTCTATTGCAACGATTCCTG
GGTTAACAAAGAATGGATTTTCATTTAAAACATTTTTAAATCAAACAATACCAATTGATTCTTAATTGAATTGAAGAA
GTAAAAAAGAAAAAAGCTCTCAATTGAGACTTTGGACTTTTTAAACAACTTTAAGCAATGGATCTCTTGGCTCTCGCA
TCGATGAAGAGCGTAgCAAATTGCGATAATTAgTGCGATCTGCATTCTGCgAATCATCgAGTTCTTGAACGCACCTTG
CACCCTTTGGCTTGTCCTTGGGGTATGCTTGTtTgcaGTACAACTATAAACCCACAAATGAcaTTTttTTTTTTT

gb|HQ285713.1| Syncephalastrum racemosum strain HS-A2 18S ribosomal RNA gene,
partial sequence; internal transcribed spacer 1, 5.8S ribosomal
RNA gene, and internal transcribed spacer 2, complete
sequence; and 28S ribosomal RNA gene, partial sequence
Length=645

```
 Score =  521 bits (282),  Expect = 1e-144
 Identities = 336/360 (93%), Gaps = 12/360 (3%)
 Strand=Plus/Plus

Query  26   ATTGAGGGGAAAGAA-TTGGAATTCACCCAGTCTATTGCAACGATTCCTGGGTTAACAAA  84
            ||||||  |||||||| ||||  ||||||||||||||||||||||||||||||||||||
Sbjct  53   ATTGAGAGGAAAGAATTTGGTATTCACCCAGTCTATTGCAACGATTCCTGGGTTAACAAA  112

Query  85   GAATGGATTTTC-ATTTAAAACATTTTTAAATCAAACAATACCAATTGATTCTTAATTGA  143
            |||||||||||| ||| ||||||||||   |   | | ||||||||||||||||||||||
Sbjct  113  GAATGGATTTTCAATTAAAAACATTTTT---TTTTA-ATTACCAATTGATTCTTAATTGA  168

Query  144  ATTGAAG-A-AGTAAAAAAGAAA-AAAGCTCTCAATTGAGACTTTGGAC--TTTTTAAAC  198
            |||||||  | |  |||||||||| || ||||||||||||||||||||  |||||||||
Sbjct  169  ATTGAAGTATAAAAAAAAAGAAAGAAGGCTCTCAATTGAGACTTTGGACTTTTTTTAAAC  228

Query  199  AACTTTAAGCAATGGATCTCTTGGCTCTCGCATCGATGAAGAGCGTAGCAAATTGCGATA  258
            |||||||||||||||||||||||||||||||||||||||||| ||||||||||||||||||
Sbjct  229  AACTTTAAGCAATGGATCTCTTGGCTCTCGCATCGATGAAAAGCGTAGCAAATTGCGATA  288

Query  259  ATTAGTGCGATCTGCATTCTGCGAATCATCGAGTTCTTGAACGCACCTTGCACCCTTTGG  318
            ||||||||||||||||||||||||||||||||||||||||||||||||||||||||||||
Sbjct  289  ATTAGTGCGATCTGCATTCTGCGAATCATCGAGTTCTTGAACGCACCTTGCACCCTTTGG  348

Query  319  CTTGTCCTTGGGGTATGCTTGTTTGCAGTACAACTATAAACCCACAAATGACATTTTTTT  378
            ||||||||||||||||||||||| |||||| ||||||||||||||||||||||||||||||
Sbjct  349  CTTGTCCTTGGGGTATGCTTGTTT-CAGTACGACTATAAACCCACAAATGACATTTTTTT  407
```

Clustalw alignment & Boxshade

```
AT-1-MF3A-ITS=ITS1_E09_2011-05    1 GGATTGAGGGGAAAGAATT-GGAATTCACCCAGTCTATTGCAACGATTCCTGGGTTAACA
gi|329458521|gb|HQ285713.1|       1 TCATTGAGAGGAAAGAATTTGGTATTCACCCAGTCTATTGCAACGATTCCTGGGTTAACA

AT-1-MF3A-ITS=ITS1_E09_2011-05   60 AAGAATGGATTTTCATTTAAAA-CATTTTTAAATCAAACAATACCAATTGATTCTTAATT
gi|329458521|gb|HQ285713.1|      61 AAGAATGGATTTTCAATTAAAAACATTTTT--TTTTAAT--TACCAATTGATTCTTAATT

AT-1-MF3A-ITS=ITS1_E09_2011-05  119 GAATTGAAG---AAGTAAAAAAGAAAAAAGCTCTCAATTGAGACTTTGGACTTTTT--AA
gi|329458521|gb|HQ285713.1|     117 GAATTGAAGTATAAAAAAAAAGAAAGAAGCTCTCAATTGAGACTTTGGACTTTTTTAA

AT-1-MF3A-ITS=ITS1_E09_2011-05  174 ACAACTTTAAGCAATGGATCTCTTGGCTCTCGCATCGATGAAGAGCGTAGCAAATTGCGA
gi|329458521|gb|HQ285713.1|     177 ACAACTTTAAGCAATGGATCTCTTGGCTCTCGCATCGATGAAAAGCGTAGCAAATTGCGA

AT-1-MF3A-ITS=ITS1_E09_2011-05  234 TAATTAGTGCGATCTGCATTCTGCGAATCATCGAGTTCTTGAACGCACCTTGCACCCTTT
gi|329458521|gb|HQ285713.1|     237 TAATTAGTGCGATCTGCATTCTGCGAATCATCGAGTTCTTGAACGCACCTTGCACCCTTT

AT-1-MF3A-ITS=ITS1_E09_2011-05  294 GGCTTGTCCTTGGGGTATGCTTGTTTGCAGTACAACTATAAACCCACAAATGACATTTTT
gi|329458521|gb|HQ285713.1|     297 GGCTTGTCCTTGGGGTATGCTTGTTT-CAGTACGACTATAAACCCACAAATGACATTTTT

AT-1-MF3A-ITS=ITS1_E09_2011-05  354 TT------------------------------------------------------------
gi|329458521|gb|HQ285713.1|     356 TTATTGAAATGTCCATTGGGATTGGGATGTCAAAGGGAAACCTTTCATCCTGAAAATGAG

AT-1-MF3A-ITS=ITS1_E09_2011-05  356 -------------------------TTTTT-----------------------------
gi|329458521|gb|HQ285713.1|     416 TCCATAGGATTAAAAATCAATTGAGGTTTTTTTTCCTTTGCATCAAATTTTTTTCAATT

AT-1-MF3A-ITS=ITS1_E09_2011-05      ------------------------------------------------------------
gi|329458521|gb|HQ285713.1|     476 AAAAAAAAAGCAATTGGGAAAAAAGGATCCAATTCTTCAAACTCGTTGTCTGAAATCAAG

AT-1-MF3A-ITS=ITS1_E09_2011-05      ------------------------------------------------------------
gi|329458521|gb|HQ285713.1|     536 TAGGATTACCCGCTGAACTTAAGCATATCAATAAGCGGAGGAGTTTTATCTCCCGCTATA
```

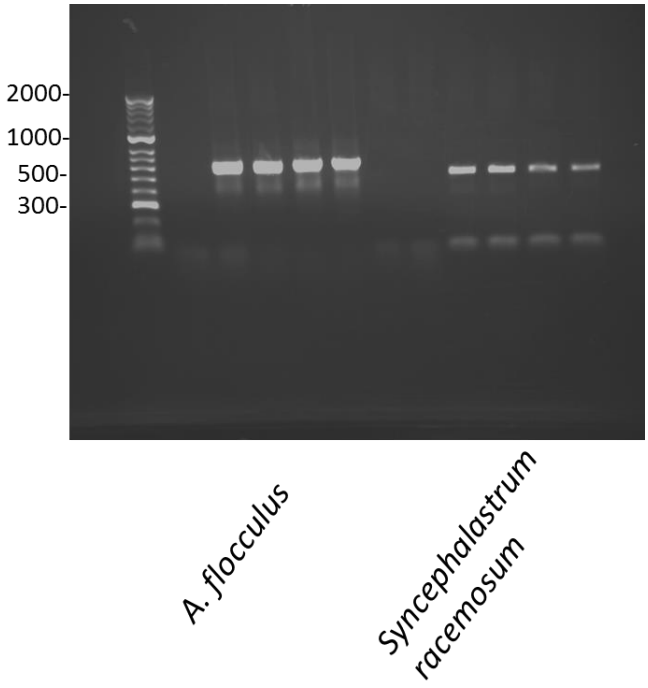

Fig.222 DNA image of A. flocculus and Syncephalastrum racemosum

8. Appendix II: Bioactivity Charts Of Anticancer Active Compounds

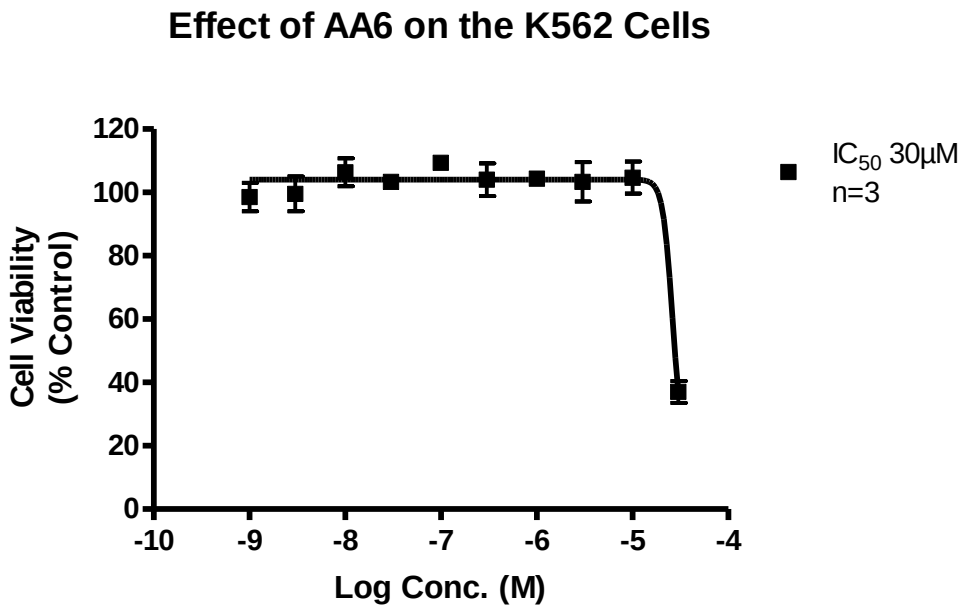

Effect of AA7 on the K562 Cells

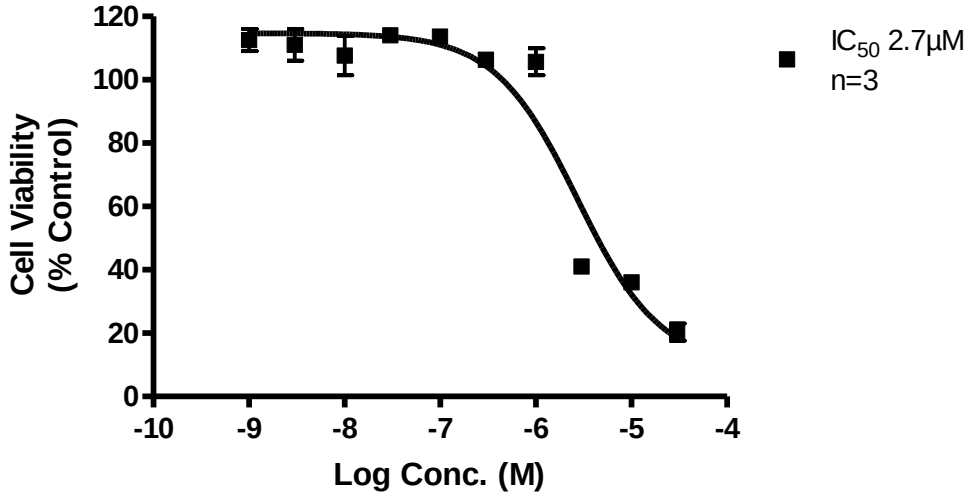

Effect of AA8 on the K562 Cells

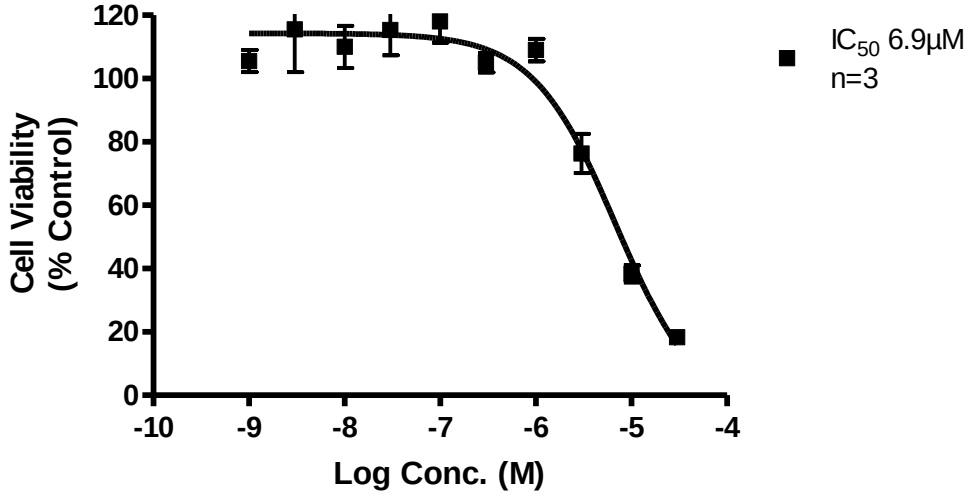

Effect of AA9 on the K562 Cells

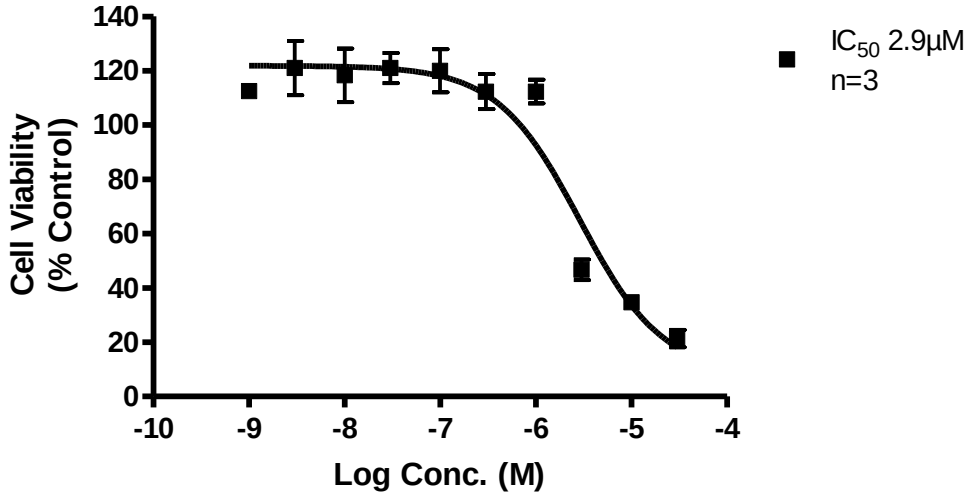

Effect of AA10 on the K562 Cells

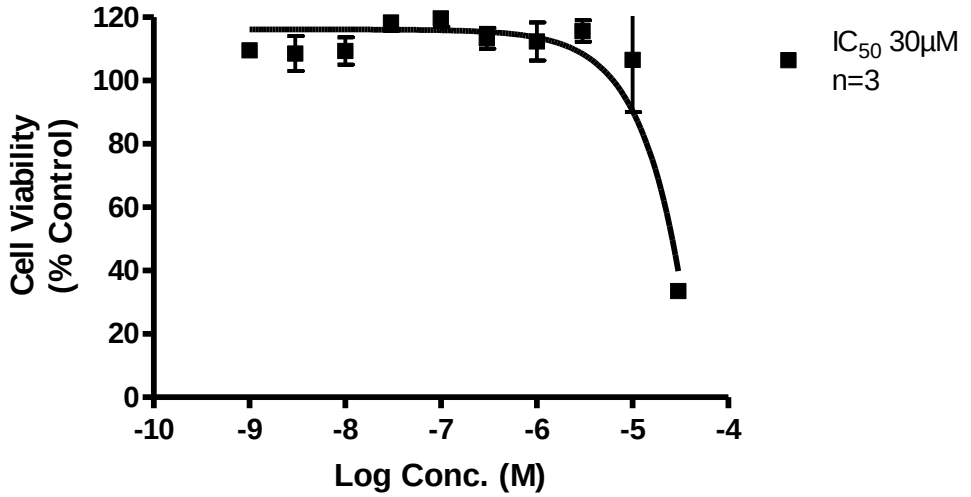

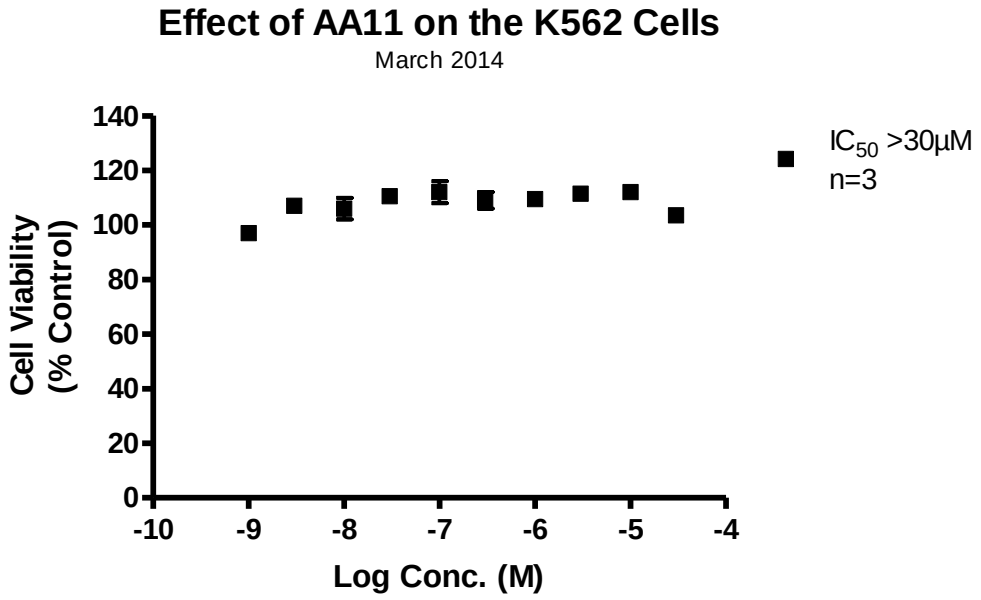
Effect of AA11 on the K562 Cells
March 2014
Cell Viability (% Control)
140
120
100
80
60
40
20
0
-10
-9
-8
-7
-6
-5
-4
Log Conc. (M)
IC50 >30µM
n=3

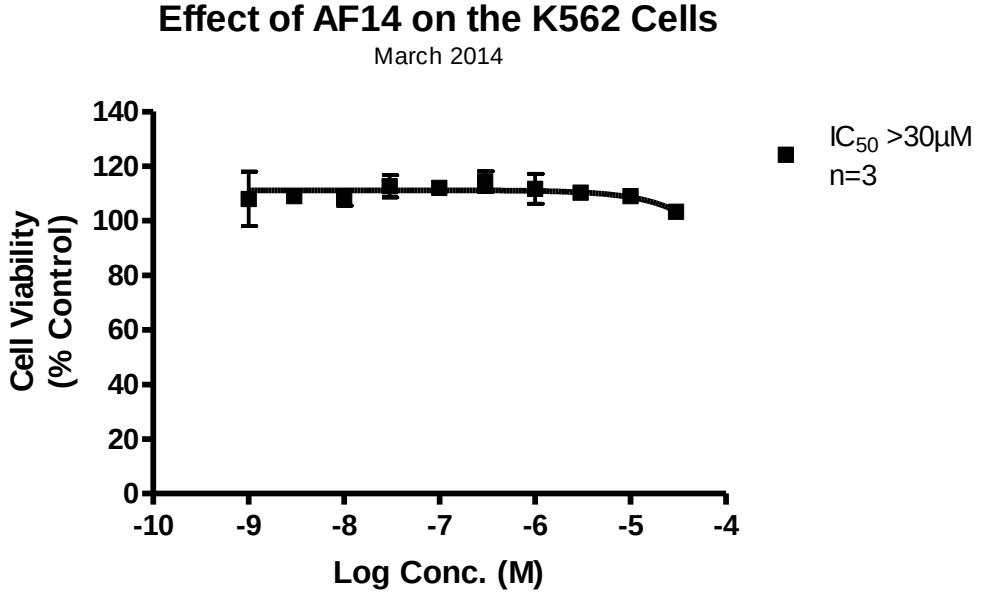
Effect of AF14 on the K562 Cells
March 2014
Cell Viability (% Control)
140
120
100
80
60
40
20
0
-10
-9
-8
-7
-6
-5
-4
Log Conc. (M)
IC50 >30µM
n=3

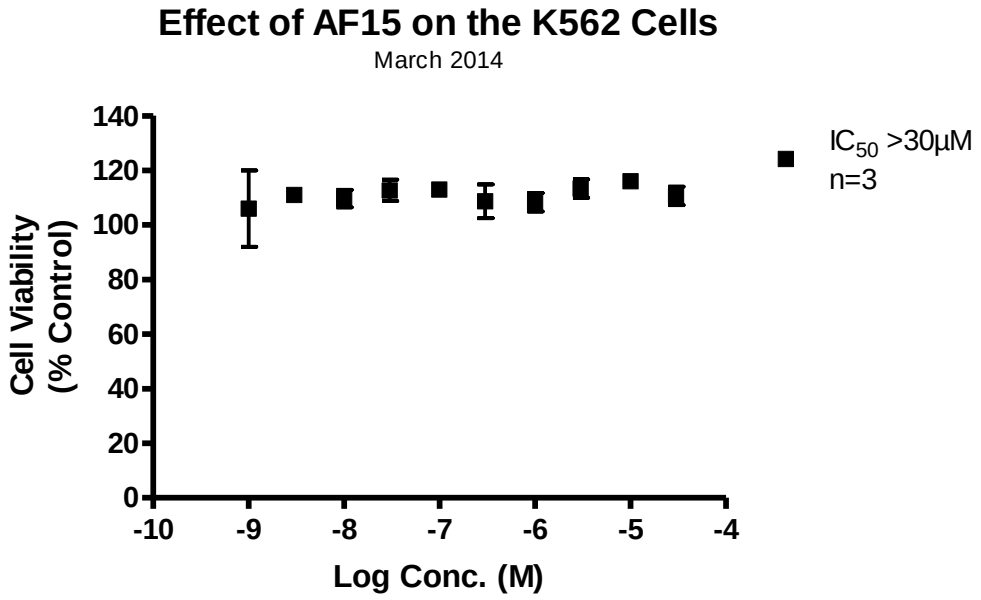
Effect of AF15 on the K562 Cells
March 2014
Cell Viability (% Control)
140
120
100
80
60
40
20
0
-10
-9
-8
-7
-6
-5
-4
Log Conc. (M)
IC50 >30µM
n=3

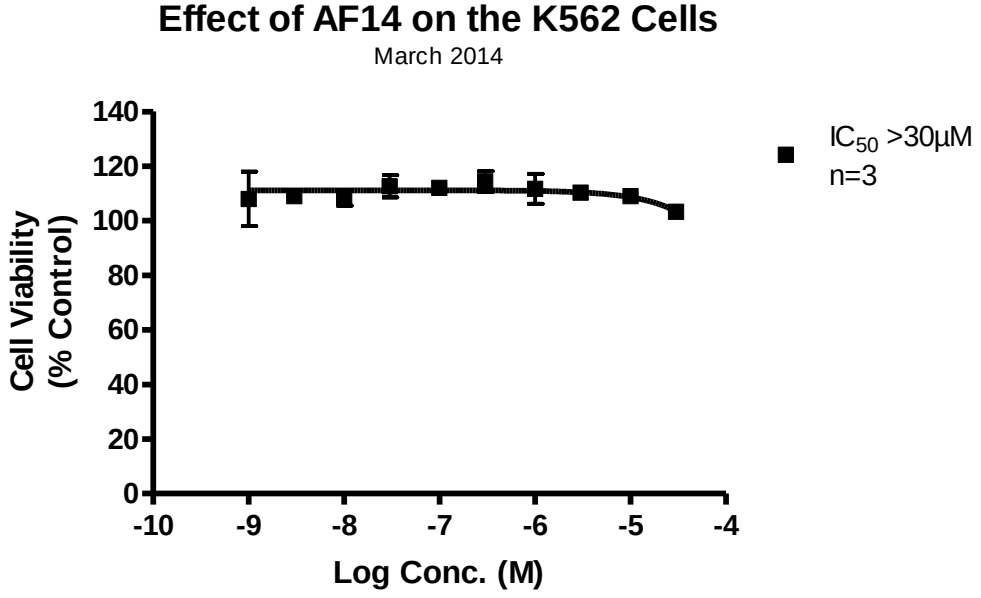
Effect of AF14 on the K562 Cells
March 2014
Cell Viability (% Control)
140
120
100
80
60
40
20
0
-10
-9
-8
-7
-6
-5
-4
Log Conc. (M)
IC50 >30µM
n=3

Effect of AF14 on the K562 Cells

March 2014

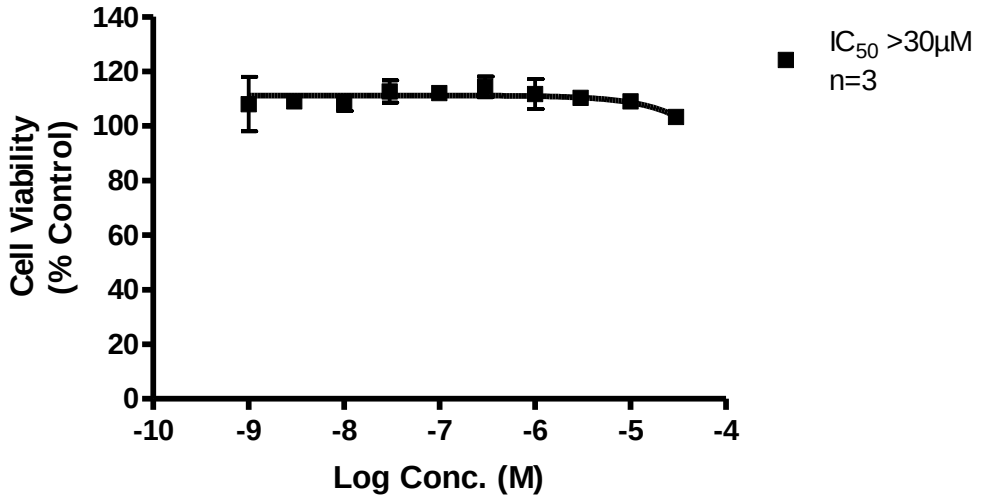

Effect of AF16 on the K562 Cells

March 2014

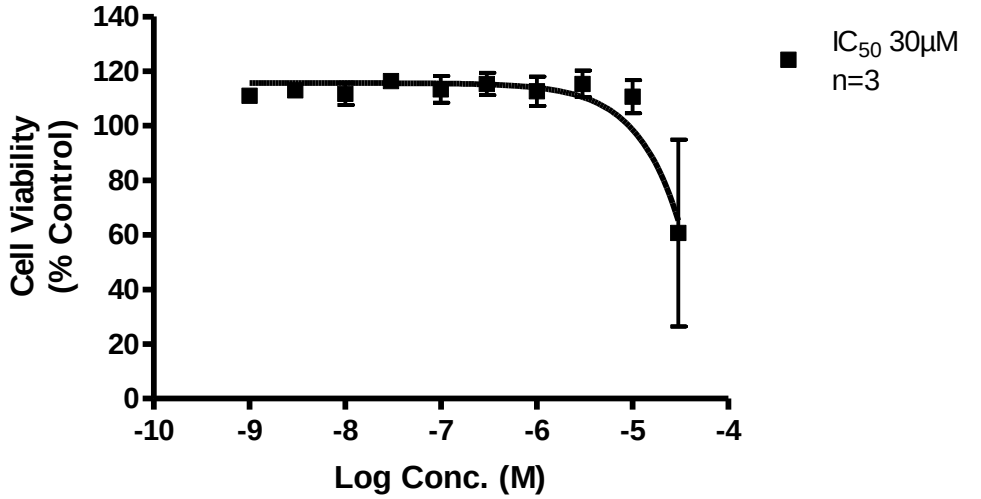

Effect of AF17 on the K562 Cells

March 2014

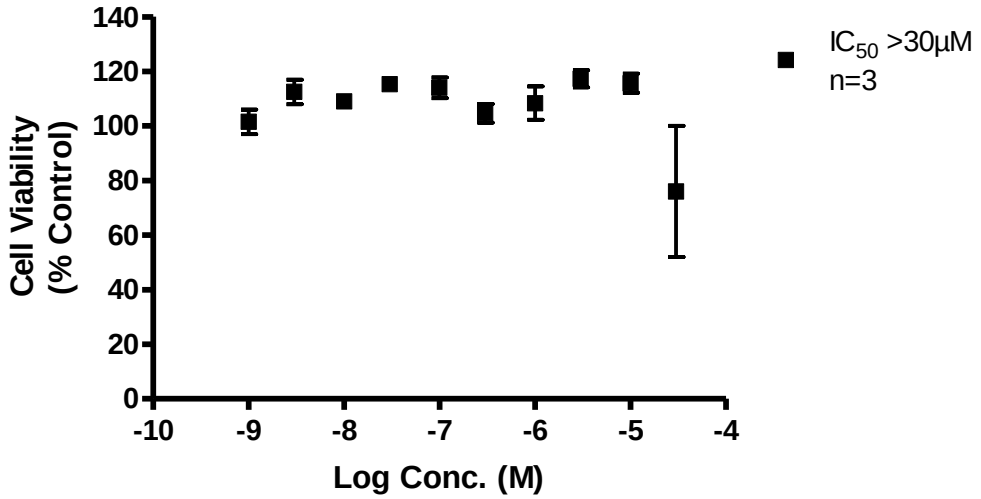

AF17 in the NFκB Assay

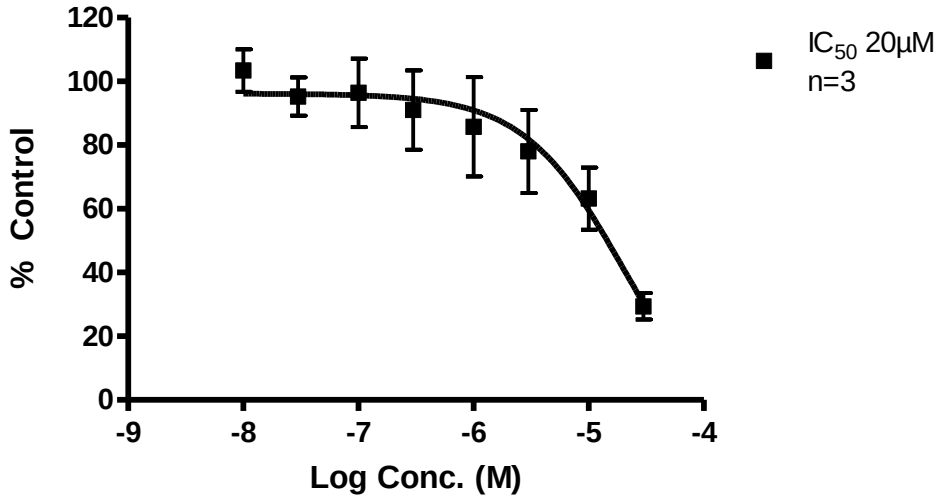

CV7 in the NFκB Assay

February 2014

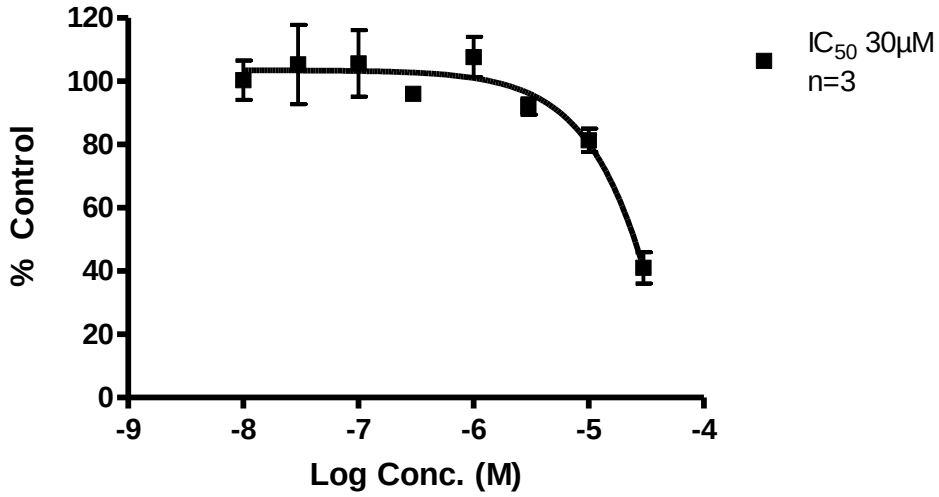

Effect of CV9 on the K562 Cells

March 2014

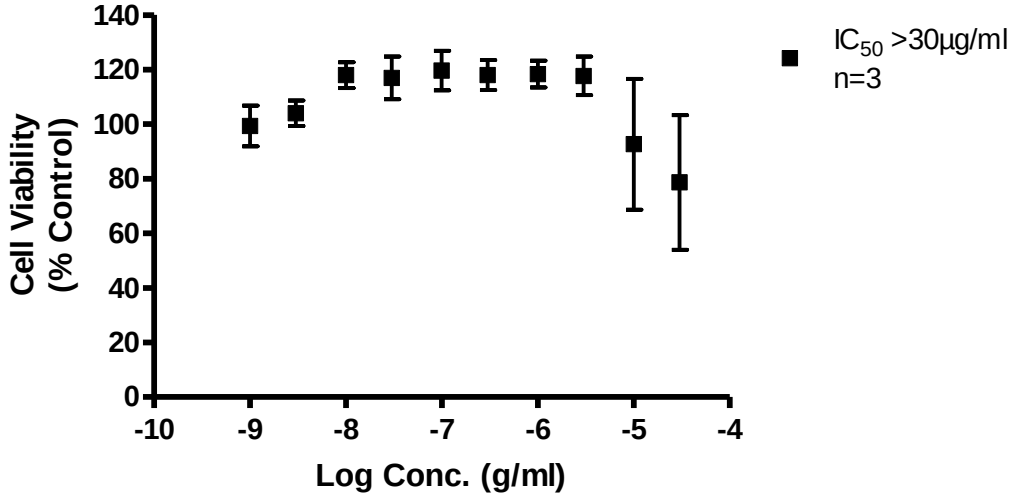

Effect of CV10 on the K562 Cells

March 2014

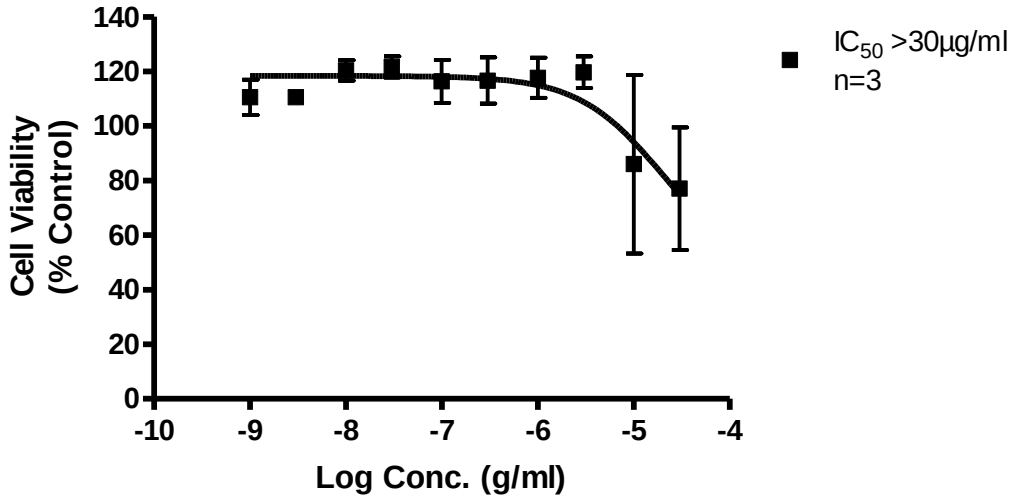

Effect of CV11 on the K562 Cells

March 2014